

UNIVERSITAT ROVIRA I VIRGILI

GOLD(I)-CATALYZED ASYMMETRIC CYCLIZATIONS AND CYCLOADDITIONS OF HETEROATOM-SUBSTITUTED ALKYNES WITH ALKENES

Andrea Cataffo

UNIVERSITAT ROVIRA I VIRGILI

GOLD(I)-CATALYZED ASYMMETRIC CYCLIZATIONS AND CYCLOADDITIONS OF HETEROATOM-SUBSTITUTED ALKYNES WITH ALKENES

Andrea Cataffo

Andrea Cataffo

Gold(I)-Catalyzed Asymmetric Cyclizations and Cycloadditions of Heteroatom-Substituted Alkynes with Alkenes

DOCTORAL THESIS

Supervised by Prof. Antonio M. Echavarren

Institut Català d'Investigació Química (ICIQ)



Tarragona 2024

UNIVERSITAT ROVIRA I VIRGILI

GOLD(I)-CATALYZED ASYMMETRIC CYCLIZATIONS AND CYCLOADDITIONS OF HETEROATOM-SUBSTITUTED ALKYNES WITH ALKENES

Andrea Cataffo



UNIVERSITAT ROVIRA I VIRGILI

I STATE that the present study, entitled “*Gold(I)-Catalyzed Asymmetric Cyclizations and Cycloadditions of Heteroatom-Substituted Alkynes with Alkenes*”, presented by Andrea Cataffo to award the degree of Doctor, has been carried out under my supervision at the Institut Català d'Investigació Química (ICIQ).

Tarragona, May 30, 2024

A handwritten signature in blue ink, consisting of several loops and a long horizontal stroke at the end.

Prof. Antonio M. Echavarren

Doctoral Thesis Supervisor

UNIVERSITAT ROVIRA I VIRGILI

GOLD(I)-CATALYZED ASYMMETRIC CYCLIZATIONS AND CYCLOADDITIONS OF HETEROATOM-SUBSTITUTED ALKYNES WITH ALKENES

Andrea Cataffo

To my Family, for supporting me so far

To my Labmates, for being there during the process

UNIVERSITAT ROVIRA I VIRGILI

GOLD(I)-CATALYZED ASYMMETRIC CYCLIZATIONS AND CYCLOADDITIONS OF HETEROATOM-SUBSTITUTED ALKYNES WITH ALKENES

Andrea Cataffo

“There is nothing like looking, if you want to find something.

You certainly usually find something if you look, but is not always quite the something you were after.”

J. R. R. Tolkien

UNIVERSITAT ROVIRA I VIRGILI

GOLD(I)-CATALYZED ASYMMETRIC CYCLIZATIONS AND CYCLOADDITIONS OF HETEROATOM-SUBSTITUTED ALKYNES WITH ALKENES

Andrea Cataffo

Acknowledgments

I would like to thank Prof. **Antonio M. Echavarren** for accepting me as PhD student in his research group at the Institut Català d'Investigació Química (ICIQ) back in 2020. Thank you for guiding me through the intricate world of organic chemistry while always trusting me and letting me free to explore.

I would also like to thank **Sonia Gavaldà** and Dr. **Imma Escofet** for the incredible technical support you provided during these four years. The group wouldn't be working this well without you.

I would like to express my gratitude to **Bas de Bruin** for hosting me in his research group during nearly 4 months at the University of Amsterdam, supervising me in the exciting synthesis of 8-membered-ring compounds. I also want to thank the other people of the Homkat group: **Minghui**, for guiding me so well in the tough project we shared, what an adventure! **Demi** for being so fun and kind, **Felix** for the interesting talks, **Daniel** for the great Chinese lunches, and then **Eva**, **Rens**, **Jasslie**, **Lotte**, **Marie** and all the others for making me feel at home.

I then want to thank the research support units at ICIQ for their help: **NMR**, **X-Ray Diffraction**, **HRMS**, **CHROMTAE** and **CRTU**.

I would like then to acknowledge all of my colleagues, which I had the pleasure to share these amazing years with:

Thank you **Isabel**, for being who you are and letting me be who I am, from the beginning: transparency is the quality I value the most in a friend. Thank you for inspiring me with all the things you know and do (apart from being a chemist) while growing up together, among beautiful, but also very tough moments. The world deserves more people like you: keep shining.

Thank you **Eduardo**, the PhD would have definitely been more boring without you and your dances in the lab. Thank you for helping me in the crazy project we shared. Whatever you will end up doing next, I suggest you to keep doing it with the same enthusiasm which characterized you over these years, that's a precious super-power.

Thank you **Pablo** and **Eric**, for all the Wednesday dinners which made the week lighter, for the trips together that made the months exciting and for the laughs that made these years unique. Thank you because you taught me that sometimes it's ok to take life less seriously.

Thank you **Anna S.**, I feel so lucky that my path crossed with such a genuinely nice person and a great scientist like you. Thank you for your support, in every kind of situation. The afternoons spent bouldering or watching movies with you and **Miquel** made me feel like having a second family, thank you!

Thank you **Gala**, for your innate kindness, always ready to help the next person: that's something that I've seen in very few people, keep it! Thank you **Àlex** for being a good friend and always available for sharing advices and opinions on chemistry: you are on the right path to become an excellent scientist.

Thank you **Tania** for making us all laugh with your acute sense of humor during dinners, hikings, but especially everyday in the kitchen of 2.2/2.3, where it's most important keeping the moral high. Thank you **Laura** for always being sweet and caring about how I was doing: I have now learned how to receive hugs from people a bit more.

Thank you **Leo**, for being the person who followed me during the first, critical, month of my PhD, when I didn't speak Spanish and I felt lost for so many reasons. All the laughs we shared in labs with Edu and Isabel and the parties in your terrace made the first weird "pandemic" year way smoother. Thank you **Alba**, for the reassuring words (and clothes appreciation), **Ana** for the fun moments (nunca olvidaré el coche horizontal) and **Inma** for your "buenos días corazón" that made my mornings brighter. Thank you **Nicolás** for the useful chemistry discussion and for always bringing delicious cakes to ICIQ (I still advice you, in case you get tired of chemistry, to open a pastry shop). Thank you **Ali** for being so genuine and fun, thank you **Paul** for all the laughs, my last year in 2.2 was definitely more fun thanks to you and your swearing. Moltes gracies **Arnau**, for the "flash" Catalan lessons and the short stories on Barcelona and its architecture. Thank you **Xiaoqing** for your kindness, I really admire what you have accomplished with patience and dedication in your PhD project! Thank you **Fede** for the motivated Monobloc afternoons, **Anders** for the beers outside the lab, **Elena** for being always nice and available and **Anna A.** and **Riccardo P.** for working hard on the projects we shared.

My thanks go also to all the other people I had the pleasure to cross my path with at the very beginning of my PhD: **Margherita** and **Giuseppe**, with which I had the opportunity to collaborate with, **Joan**, always being around with positive attitude, **Marc**, for the useful advices, and then also **Otilia**, **Helena**, **Mauro**, **Franco**, **Ulysse**, **Remi**.

I then want to thank my friends in Napoli who always made me impatient to come back home during my holidays to spend the best time together during these four years. Thank you **Elena**, **Carmine**, **Simone**, **Steven**, **Rita**, **Carolina**, **Cesare**, **Flavia**, **Luca**, **Boris**, **Cristiano** and **Filippo** for being an essential part of my growth.

A final, Italian, Thank You, goes to my family. Grazie **Mamma**, **Papa'** e **Marco**, per aver sempre avuto fiducia in tutto cio' che faccio. La tranquillità di sapere che siete sempre al mio fianco fa si che io possa sempre realizzare tutto quello che voglio.

We thank the MCIN/AEI/10.13039/501100011033 (PID2019-104815GB-I00 and CEX2019-000925-S), the European Research Council (Advanced Grant 835080), the AGAUR (2021 SGR 01256), and CERCA Program/Generalitat de Catalunya for financial support.



European Research Council

Established by the European Commission



UNIVERSITAT ROVIRA I VIRGILI

GOLD(I)-CATALYZED ASYMMETRIC CYCLIZATIONS AND CYCLOADDITIONS OF HETEROATOM-SUBSTITUTED ALKYNES WITH ALKENES

Andrea Cataffo

At the moment of writing this Doctoral Thesis, the results presented herein have been published in:

Synthesis of Cyclobutanones by Gold(I)-Catalyzed [2 + 2] Cycloaddition of Ynol Ethers with Alkenes

Zanini M., Cataffo A., Echavarren A.M., *Org. Lett.*, **2021**, 23(22), 8989–8993.

Chiral Auxiliary Approach for Gold(I)-Catalyzed Cyclizations

Cataffo A., Peña-Lopéz M., Pedrazzani R., Echavarren A. M., *Angew. Chem. Int. Ed.* **2023**, 62, e202312874.

In addition, other results that are not related to the topic of this Doctoral Thesis have been published in:

Between T and Y: Asymmetry in the Interaction of LAu(I) with Bipy and β -Diiminate-like Ligands

Cataffo A., Haas T., Ehm C., Budzelaar P. H. M., *Eur. J. Inorg. Chem.*, **2021**, 314– 320.

* *Denotes equal contribution*

UNIVERSITAT ROVIRA I VIRGILI

GOLD(I)-CATALYZED ASYMMETRIC CYCLIZATIONS AND CYCLOADDITIONS OF HETEROATOM-SUBSTITUTED ALKYNES WITH ALKENES

Andrea Cataffo

Table of Contents

Prologue	21
Abbreviations and Acronyms	23
Abstract	25
General Objectives	27
General Introduction	29
Historical Perspective of Gold(I) Catalysis.....	32
Relativistic Effects in Gold Chemistry.....	33
Bonding Situation in Gold(I) Species, Alkynophilicity and General Reactivity.....	35
Intramolecular Reactivity: Gold(I)-Catalyzed Cycloisomerization of 1, <i>n</i> -Enynes.....	38
Gold(I)-Catalyzed Intermolecular Reactions of Alkynes with Alkenes.....	44
Asymmetric Gold(I) Catalysis.....	48
Chapter I: Chiral Auxiliary Approach for Gold(I)-Catalyzed Cyclizations	59
Introduction.....	61
<i>Ynamides in Gold(I) Catalysis</i>	61
<i>Chiral Auxiliaries in Asymmetric Synthesis</i>	68
Objectives.....	75
Results and Discussion.....	76
<i>1,5-Enyne Cascade Cyclization</i>	76
<i>1,6-Enyne Alkoxy cyclization</i>	86
<i>Towards the Total Synthesis of Hernandulcin</i>	105
<i>Intermolecular Trials</i>	110
Conclusions.....	112
Experimental Part.....	113
<i>General Information</i>	113
<i>Synthetic Procedures and Characterization Data</i>	114
<i>Crystallographic Data</i>	176
<i>DFT Calculations</i>	179

Chapter II: Synthesis of Cyclobutanones by Gold(I)-Catalyzed [2+2] Cycloaddition of Ynol Ethers with Alkenes	183
Introduction.....	185
<i>Ynol Ethers in Gold(I) Catalysis</i>	185
<i>Synthesis of Cyclobutanones</i>	189
Objectives.....	196
Results and Discussion.....	197
<i>[2+2] Cycloaddition of Ynol Ethers with Alkenes</i>	197
<i>Product Derivatization: Access to Cyclobutanones</i>	204
<i>Reaction Mechanism</i>	208
<i>Towards the Asymmetric [2+2] Cycloaddition</i>	110
Conclusions.....	218
Experimental Part.....	113
<i>General Information</i>	113
<i>Synthetic Procedures and Characterization Data</i>	114
Chapter III: Enantioselective Cyclizations of Bromoenynes: A New Mechanistic Understanding of Gold(I)-Catalyzed Alkoxy cyclizations	243
Introduction.....	245
<i>Haloalkynes in Gold(I) Catalysis</i>	246
<i>1,2-H Shift in Gold(I) Catalysis</i>	254
<i>Enantioselective Alkoxy cyclizations of Enynes</i>	256
Objectives.....	261
Results and Discussion.....	262
<i>Reaction Optimization, Scope and Product Diversification</i>	262
<i>Experimental Mechanistic Studies</i>	268
<i>Computational Studies</i>	277
Conclusions.....	291
Experimental Part.....	292
<i>General Information</i>	292
<i>Synthetic Procedures and Characterization Data</i>	292
<i>Crystallographic Data</i>	307
<i>DFT Calculations</i>	308
General Conclusions	313

UNIVERSITAT ROVIRA I VIRGILI

GOLD(I)-CATALYZED ASYMMETRIC CYCLIZATIONS AND CYCLOADDITIONS OF HETEROATOM-SUBSTITUTED ALKYNES WITH ALKENES

Andrea Cataffo

UNIVERSITAT ROVIRA I VIRGILI

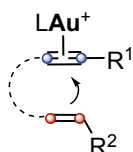
GOLD(I)-CATALYZED ASYMMETRIC CYCLIZATIONS AND CYCLOADDITIONS OF HETEROATOM-SUBSTITUTED ALKYNES WITH ALKENES

Andrea Cataffo

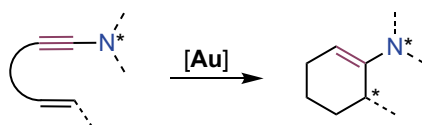
Prologue

This Doctoral Thesis manuscript has been divided into five main parts: a general introduction on gold(I) catalysis, three research chapters, and general conclusions. The numbering of the compounds as well as the one of scheme, tables, figures and references is organized by chapter.

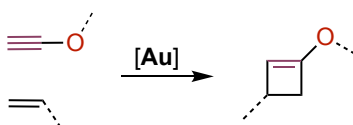
The **General Introduction** covers the basic principles of homogeneous gold(I) catalysis and gives an overview on the intramolecular cycloisomerization of enynes, on the intermolecular reactions of alkynes with alkenes and finally on asymmetric gold(I)-catalysis.



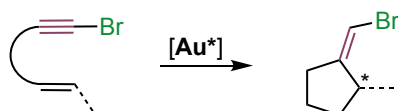
Chapter I focuses on the gold(I)-catalyzed asymmetric cyclization of *N*-substituted alkynes (ynamides) with alkenes through the implementation of chiral auxiliaries. This work was conducted in collaboration with Dr. Miguel Peña-López and Dr. Riccardo Pedrazzani, and, therefore, their results are presented to give a complete picture of the research project discussed in the chapter. This work has been published in *Angew. Chem. Int. Ed.* **2023**, 62, e202312874.



Chapter II comprehends our studies on the gold(I)-catalyzed [2+2] cycloaddition/hydrolysis sequence of *O*-substituted alkynes (ynol ethers) with alkenes to form cyclobutanones and the efforts towards its asymmetric version. This work was conducted in collaboration with Dr. Margherita Zanini, and some of her results are presented for coherence. This work has been published in *Org. Lett.*, **2021**, 23 (22), 8989–8993.



Chapter III presents the gold(I)-catalyzed enantioselective alkoxy cyclization of 1-*Br*-1,6-enynes. Through both experimental and theoretical mechanistic studies, the origin of an unexpected racemization process could be unveiled and a first accurate model for enyne alkoxy cyclization could be proposed. The theoretical work was done in collaboration with Dr. Eduardo García-Padilla and his results are herein presented for gaining a full understanding. This work has been submitted for publication.



UNIVERSITAT ROVIRA I VIRGILI

GOLD(I)-CATALYZED ASYMMETRIC CYCLIZATIONS AND CYCLOADDITIONS OF HETEROATOM-SUBSTITUTED ALKYNES WITH ALKENES

Andrea Cataffo

Abbreviations and Acronyms

In this manuscript, the abbreviations and acronyms most commonly used in organic and organometallic chemistry have been used following the recommendations of “Guidelines of Authors” of the Journal of Organic Chemistry.

Additional abbreviations and acronyms used in this manuscript are listed below:

ACN	Acetonitrile
APCI	atmospheric pressure chemical ionization
BAr ₄ ^{F-}	tetrakis[3,5-bis(trifluoromethyl)phenylborate]
<i>dr</i>	diastereomeric ratio
ESI	electrospray ionization
JohnPhos	(2-biphenyl)di- <i>tert</i> -butylphosphine
IMes	1,3-bis(2,4,6-trimethylphenyl)imidazol-2-ylidene
Int	intermediate
IPr	1,3-bis(2,6-diisopropylphenyl)imidazol-2-ylidene
L	ligand
MALDI	matrix assisted laser desorption ionization
Mes	2,4,6-trimethylphenyl
MS	mass spectrometry/molecular sieves
MW	microwave irradiation
NTf ₂ ⁻	bis(trifluoromethyl)imideate
OTf	triflate
ORTEP	oak ridge thermal ellipsoid plot
<i>t</i> BuXPhos	2-(di- <i>tert</i> -butylphosphino)-2',4',6'-triisopropyl-1,1'-biphenyl
TS	transition state
equiv	equivalent(s)

UNIVERSITAT ROVIRA I VIRGILI

GOLD(I)-CATALYZED ASYMMETRIC CYCLIZATIONS AND CYCLOADDITIONS OF HETEROATOM-SUBSTITUTED ALKYNES WITH ALKENES

Andrea Cataffo

Abstract

Gold(I)-catalyzed transformations have been widely used for constructing complex molecular structures under mild reaction conditions. In this context, our group has been focused on finding new ways of activating triple bonds towards both intramolecular and intermolecular reactions with alkenes. In this Doctoral Thesis, we focused on the use of polarized heteroatom-substituted alkynes for both racemic and asymmetric reactions.

We developed two distinct strategies for stereoselective gold(I)-catalyzed cyclizations of 1,*n*-enynes utilizing, for the first time, a chiral auxiliary approach. Firstly, a stereoselective cascade cyclization of 1,5-enynamides was achieved through the use of commercially available [JohnPhosAu(MeCN)SbF₆] catalyst using the Oppolzer camphorsultam as a chiral auxiliary. This approach involved a one-pot cyclization-hydrolysis sequence, resulting in the direct formation of enantioenriched spirocyclic ketones. Secondly, the stereoselective alkoxy cyclization of 1,6-enynamides was directed by an Evans-type oxazolidinone. A reduction-hydrolysis sequence was employed to remove the auxiliary, yielding enantioenriched β-tetralones. DFT studies furnished insights over the experimentally observed diastereoselectivity by disclosing that the cyclization would occur preferentially through the *Si* face of the alkene, due to the steric clash of the *Re* face with the chiral auxiliary.

Cyclobutenes and cyclobutanone derivatives are scaffolds of great interest since they constitute common motifs within natural products and they are useful intermediates in organic synthesis. We developed a new synthetic method that allows the direct access to cyclobutenyl ethers, with good yields and excellent regioselectivities, via a gold(I)-catalyzed [2+2] cycloaddition of alkenes with terminal ynol ethers. These functionalized alkynes can be considered as stable equivalents of ketenes, which are usually difficult to handle. Hydrolysis or bromination of the [2+2] products led to cyclobutanones.

The development of the first enantioselective gold(I)-catalyzed alkoxy cyclization of 1-bromo-1,6-enynes was accomplished through the use of a modified JohnPhos ligand featuring a distal C₂-2,5-diarylpyrrolidine moiety affording enantioenriched 5-membered-ring vinyl bromides, which can be easily further functionalized through Pd-catalysis. Interestingly, both experimental and theoretical investigations of the reaction mechanism revealed the occurrence of an in-cycle racemization process, which was demonstrated to occur through an unprecedented reversible 1,2-H shift. These findings contribute to a new general understanding of gold(I)-catalyzed alkoxy cyclizations, for which an accurate model has been herein described for the first time.

UNIVERSITAT ROVIRA I VIRGILI

GOLD(I)-CATALYZED ASYMMETRIC CYCLIZATIONS AND CYCLOADDITIONS OF HETEROATOM-SUBSTITUTED ALKYNES WITH ALKENES

Andrea Cataffo

General Objectives

The objective of this Doctoral Thesis was the development of new gold(I)-catalyzed cycloadditions of heteroatom-substituted alkynes with alkenes. In particular we focused on:

- The development of the first methodology that relies on chiral auxiliaries for the asymmetric gold(I)-catalyzed cyclization of enynes.
- The gold(I)-catalyzed synthesis of cyclobutanones through reaction of ynol ethers with alkenes.
- The detailed mechanistic description of gold(I)-catalyzed alkoxy cyclizations through the enantioselective cyclization of bromoenynes.

Each chapter of this manuscript presents an additional, more detailed, objective section.

UNIVERSITAT ROVIRA I VIRGILI

GOLD(I)-CATALYZED ASYMMETRIC CYCLIZATIONS AND CYCLOADDITIONS OF HETEROATOM-SUBSTITUTED ALKYNES WITH ALKENES

Andrea Cataffo

General Introduction

UNIVERSITAT ROVIRA I VIRGILI

GOLD(I)-CATALYZED ASYMMETRIC CYCLIZATIONS AND CYCLOADDITIONS OF HETEROATOM-SUBSTITUTED ALKYNES WITH ALKENES

Andrea Cataffo

Historical Perspective of Gold(I) Catalysis

Midas was a wealthy king ruling over Phrygia, in Asia Minor, with a lavish palace and a beautiful daughter. Despite his immense riches, his insatiable greed for gold consumed him. He spent his days counting his coins and adorning himself with golden ornaments, believing that his happiness laid in the accumulation of wealth. One day, the god Dionysus passed through Midas's kingdom who kindly hosted his old schoolmaster, satyr Sylenus, in his palace. Grateful for Midas's hospitality, Dionysus offered to grant him a wish. Without hesitation, Midas wished for everything he touched to turn into gold. Dionysus warned Midas to reconsider his wish, but the king remained resolute. Granting his request, Dionysus made everything Midas touched transform into gold. Initially ecstatic, Midas soon realized the consequences of his wish when even his food turned into gold, making it impossible to eat. Overcome with despair, he pleaded with Dionysus to remove the curse and save him from starvation. Taking pity on Midas, Dionysus instructed him to wash his hands in the river Pactolus. As Midas obeyed, the river's waters turned into gold, and everything Midas had touched returned to normal. Grateful and humbled by the experience, Midas became a benevolent ruler, sharing his wealth with his people and living a life of gratitude and generosity until his death.^{1,2}



Figure 1. In Nathaniel Hawthorne's version of the Midas myth, the king's daughter also turns into a golden statue when he touches her. Illustration by Walter Crane for the 1893 edition.

¹ Ovid, *Metamorphoses* 11.136-141.

² Niece, S. L. *Gold*; Harvard University Press, 2009.

The legend of King Midas of Phrygia first written by the roman poet Ovidius (43 a.C. - 17 d.C.) in his renowned “Metamorphoses”, might have evolved as an explanation for the actual richness of the river Pactolus during the 400 BC in western Turkey.^{2,3} While gold is believed to have originated from supernova nucleosynthesis and the collisions of neutron stars,⁴ on earth, gold is commonly found in ores within rock formations (often forming an alloy with silver),² and in oceans.⁵ The oldest gold artifacts in the world are from Bulgaria and are dating back to the 5th millennium BC (4600 BC to 4200 BC)^{Error! Bookmark not defined.}, and since then, its use as a symbol of power⁶ as well its occurrence in religion have been reported widely.⁷

Within the chemical community, for a significant period, gold was widely perceived as unreactive and ineffective as a catalyst compared to other transition metals, to the extent that it was labeled as "catalytically dead".⁸ In 1931, AuCl₃ was described to promote the chlorination of arenes in a stoichiometric fashion (Scheme 1a)⁹ but only in 1986 Ito and Hayashi described the first gold(I)-catalyzed transformation reporting the asymmetric nucleophilic attack of isocyanide to aldehydes (Scheme 1b).¹⁰ However, this groundbreaking research stood alone in the field for nearly a decade until Teles and colleagues reported in 1998 the synthesis of acetals through the addition of alcohols to alkynes catalyzed by gold(I) complexes featuring a phosphine ligand (Scheme 1c).¹¹ Subsequently, employing the same gold(I) complex activated by protonolysis, Tanaka and collaborators achieved the Markovnikov-type hydration of alkynes to produce ketones and aldehydes (Scheme 1c).¹²

Over the years, gold catalysis has found applications in various fields of organic synthesis, including natural product synthesis,¹³ pharmaceutical chemistry,¹⁴ and material science.¹⁵

³ Strabo, *Geography* 13.1.23, 13.4.5; cf. Philostratus, *Life of Apollonius* 6.37.

⁴ Seeger, P. A.; Fowler, W. A.; Clayton, D. D., Nucleosynthesis of Heavy Elements by Neutron Capture., *Astrophys. J. Suppl. Ser.* **1965**, *11*, 121.

⁵ Kenison Falkner, K.; Edmond, J. M. Gold in Seawater, *Earth Planet. Sci. Lett.* **1990**, *98*, 208–221.

⁶ Bernstein, P. L. *The Power of Gold: The History of an Obsession*; Wiley, **2004**.

⁷ a) Daly, K. N. *Greek and Roman Mythology, A to Z*; Infobase Publishing, **2009**. b) Moors, A. Wearing Gold, Owning Gold: The Multiple Meanings of Gold Jewelry, **2013**. c) Alborn, T. The Greatest Metaphor Ever Mixed: Gold in the British Bible, 1750–1850, *J. Hist. Ideas* **2017**, *78*, 427–447.

⁸ Schmidbaur, H., Gold-Chemie: Ein Eldorado., Gold-Chemie: Ein Eldorado. *Naturwissenschaftliche Rundschau*, 1995, *48*, 443–451.

⁹ Kharasch, M. S.; Isbell, H. S. THE CHEMISTRY OF ORGANIC GOLD COMPOUNDS. III. DIRECT INTRODUCTION OF GOLD INTO THE AROMATIC NUCLEUS (PRELIMINARY COMMUNICATION), *J. Am. Chem. Soc.* **1931**, *53*, 3053–3059.

¹⁰ Ito, Y.; Sawamura, M.; Hayashi, T. Catalytic asymmetric aldol reaction: reaction of aldehydes with isocyanoacetate catalyzed by a chiral ferrocenylphosphine-gold(I) complex, *J. Am. Chem. Soc.* **1986**, *108*, 6405–6406.

¹¹ Teles, J. H.; Brode, S.; Chabanas, M. Cationic Gold(I) Complexes: Highly Efficient Catalysts for the Addition of Alcohols to Alkynes, *Angew. Chem. Int. Ed.* **1998**, *37*, 1415–14184, *Angew. Chem.* **1998**, *110*, 1475–1478.

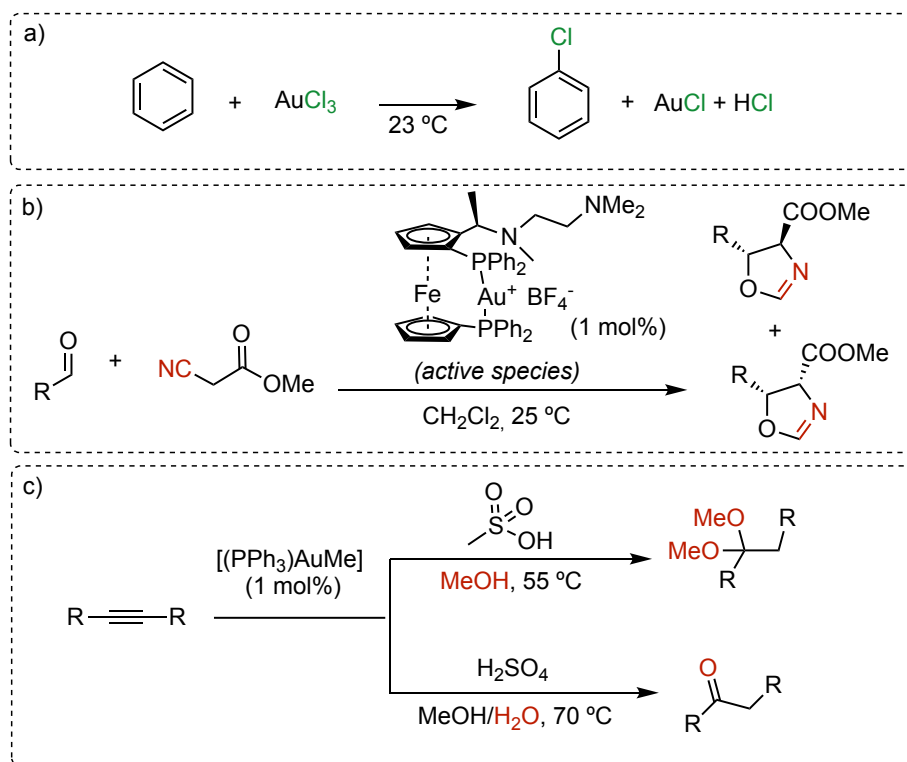
¹² Mizushima, E.; Sato, K.; Hayashi, T.; Tanaka, M. Highly Efficient Au^I-Catalyzed Hydration of Alkynes, *Angew. Chem. Int. Ed.* **2002**, *41*, 4563–45656, *Angew. Chem.* **2002**, *114*, 4745–4747.

¹³ a) De, S.; Dan, A. K.; Sahu, R.; Parida, S.; Das, D., Total Synthesis of Natural Products Using Gold Catalysis, *Chem. – Asian J.* **2022**, *17*, e202200896. b) Lin, B.; Liu, T.; Luo, T. Gold-Catalyzed Cyclization and Cycloaddition in Natural Product Synthesis, *Nat. Prod. Rep.* **2024**, Advance article.

¹⁴ Shen, H. C.; Graham, T. H. Gold-Catalyzed Formation of Heterocycles – an Enabling New Technology for Medicinal Chemistry, *Drug Discov. Today Technol.* **2013**, *10*, e3–e149.

¹⁵ Hendrich, C. M.; Sekine, K.; Koshikawa, T.; Tanaka, K.; Hashmi, A. S. K. Homogeneous and Heterogeneous Gold Catalysis for Materials Science, *Chem. Rev.* **2021**, *121*, 9113–9163.

Its versatility and ability to access complex molecular architectures with high levels of stereo- and regioselectivity have made it a valuable tool for synthetic chemists worldwide.¹⁶



Scheme 1. First examples of the use of gold complexes in organic synthesis: a) Chlorination of benzene through the use of AuCl_3 . b) Gold(I)-catalyzed enantioselective isocyanide addition to aldehydes c) Gold(I)-catalyzed methanol and water addition to alkynes.

Relativistic Effects

One of the key features of gold catalysis is its unique ability to facilitate transformations under mild reaction conditions, often at room temperature and atmospheric pressure. This mildness is attributed to the relatively low oxidation state of gold, which allows for the activation of substrates without requiring harsh reaction conditions.

The unique behavior of gold as a catalyst can be attributed in part to relativistic effects.¹⁷ The theoretical basis for relativistic effects stems from the integration of quantum mechanics and special relativity. Schrödinger's equation, introduced in 1926, accurately predicts the energy levels of hydrogen atoms but fails to explain the fine structure of the hydrogen atomic spectrum, where spectral bands split.

¹⁶ a) Hashmi, A. S. K.; Hutchings, G. J. *Gold Catalysis*, *Angew. Chem. Int. Ed.* **2006**, *45*, 7896–793611, *Angew. Chem.* **2006**, *118*, 8064–8105. b) Fensterbank, L.; Malacria, M. Molecular Complexity from Polyunsaturated Substrates: The Gold Catalysis Approach, *Acc. Chem. Res.* **2014**, *47*, 953–965. c) Dorel, R.; Echavarren, A. M. Gold(I)-Catalyzed Activation of Alkynes for the Construction of Molecular Complexity, *Chem. Rev.* **2015**, *115*, 9028–9072.

¹⁷ a) Pyykkö, P., Theoretical Chemistry of Gold, *Angew. Chem. Int. Ed.* **2004**, *43*, 4412–4456., *Angew. Chem.* **2004**, *116*, 4512–4557. b) Gorin, D. J.; Toste, F. D. Relativistic Effects in Homogeneous Gold Catalysis, *Nature* **2007**, *446*, 395–403.

To address this, Dirac developed a new equation in 1928 that incorporates special relativity, allowing for solutions in systems where electrons approach significant velocities, relative to the speed of light (c).¹⁸

The radial speed of electrons in atoms is proportional to the atomic number. For heavy atoms, such as those with filled 4f and 5d orbitals like Pt, Au, and Hg, the increase in mass and therefore electron speed near the nucleus is substantial. This increase in mass leads to a contraction of the Bohr radius of electron orbits, as it is inversely proportional to mass. This contraction affects not only the 1s orbitals but also all s and p orbitals. The contracted internal orbitals shield the electrons in the d and f orbitals more effectively, resulting in a weaker nucleus attraction. Consequently, the external d and f orbitals become highly diffuse. While a simpler treatment suffices for lighter atoms, the relativistic contraction of internal orbitals and expansion of external ones become significant for heavy atoms with filled 4f and 5d orbitals, reaching a maximum in gold (Figure 2).¹⁹

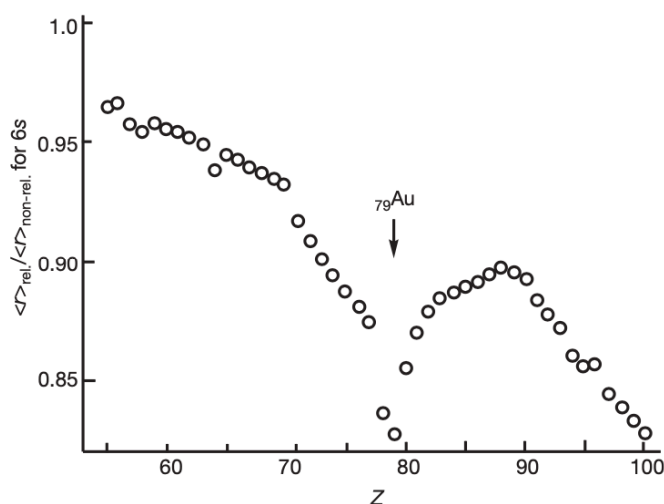


Figure 2. Calculated relativistic contraction of the 6s orbitals from Cs ($Z = 55$) to Fm ($Z = 100$).²⁰

Relativistic effects explain various experimental observations, including the golden color of Au attributed to 5d electron excitation to the Fermi level, absorbing blue visible light, contrasting with silver's larger bandgap, which absorbs no visible light. This smaller bandgap in Au results from relativistic contraction of 6s and 6p orbitals and expansion of 5d orbitals. Secondly, the strong relativistic contraction of the 6s orbital in gold facilitates efficient overlap with ligand orbitals, favoring, efficient s/p and s/d orbital hybridization, enhancing metal-ligand bonding and stabilizing low-coordinate gold complexes.

¹⁸ a) Pitzer, K. S. Relativistic Effects on Chemical Properties, *Acc. Chem. Res.* **1979**, *12*, 271–276. b) Pyykko, P.; Desclaux, J. P. Relativity and the Periodic System of Elements, *Acc. Chem. Res.* **1979**, *12*, 276–281.

¹⁹ Autschbach, J.; Siekierski, S.; Seth, M.; Schwerdtfeger, P.; Schwarz, W. H. E. Dependence of Relativistic Effects on Electronic Configuration in the Neutral Atoms of D- and f-Block Elements, *J. Comput. Chem.* **2002**, *23*, 804–813.

²⁰ Graphic taken from ref. 17b.

This characteristic, coupled with a generally lower nucleophilicity compared to other coinage metals, rationalizes the reluctance of gold(I) complexes towards oxidative addition, a fundamental step in redox catalytic cycles. Apart from practical considerations, such as the ability to conduct gold(I)-catalyzed reactions in air and a broad functional group tolerance, the redox stability of gold(I) complexes enables the exploration of activation modes typically inaccessible to other transition metals. In addition to the well-documented robust Au-L bond strengths, experimental evidence supporting the unique electronic structure is found in the concept of 'aurophilicity'.²¹ This phenomenon denotes the inclination for Au-Au interactions to exhibit stabilizing effects akin to hydrogen bonds. Finally, the enhanced Lewis acidity and electronegativity of gold(I) species compared to other Group 11 metals can also be attributed to the relativistic contraction of the valence s and p orbitals of Au, which result in a low-lying LUMO and therefore an enhanced electrophilicity.

Bonding Situation in Gold(I) Species, Alkynophilicity and General Reactivity

The high electronegativity and Lewis acidity in gold(I) species results in a very high degree of covalency in bonding and for this reason ligands play a crucial role in altering the electronic properties of the gold atom significantly.²²

Among the different species encountered in gold catalysis, gold-carbenes have been often proposed as the key intermediates in many gold-catalyzed transformations. Toste and Goddard introduced an elucidation of the bonding mechanism of gold carbenes in 2009.²³ According to their proposition, both the ligand L and carbene are capable of donating their electron pairs to gold, resulting in the formation of a three-center four-electron σ -hyperbond (Figure 3).²⁴ Additionally, the gold center can engage in the formation of two π -bonds by back-donating its electrons from two filled 5d orbitals to vacant π -acceptors on the ligand and carbene.

Given this particular bonding situation, widely discussed over the years,²⁵ and strongly dependent on the ancillary ligands, gold carbenes display a specific behavior that distinguishes them within the

²¹ a) Scherbaum, F.; Grohmann, A.; Huber, B.; Krüger, C.; Schmidbaur, H. "Aurophilicity" as a Consequence of Relativistic Effects: The Hexakis(Triphenylphosphaneaurio)Methane Dication [(Ph₃PAu)₆C]²⁺, *Angew. Chem. Int. Ed. Engl.* **1988**, *27*, 1544–1546, *Angew. Chem.* **1988**, *100*, 1602–1604. b) Schmidbaur, H.; Schier, A. A Briefing on Aurophilicity, *Chem. Soc. Rev.* **2008**, *37*, 1931–1951. c) Penney, A. A.; Sizov, V. V.; Grachova, E. V.; Krupenya, D. V.; Gurzhiy, V. V.; Starova, G. L.; Tunik, S. P. Aurophilicity in Action: Fine-Tuning the Gold(I)–Gold(I) Distance in the Excited State To Modulate the Emission in a Series of Dinuclear Homoleptic Gold(I)–NHC Complexes, *Inorg. Chem.* **2016**, *55*, 4720–4732.

²² a) Gorin, D. J.; Sherry, B. D.; Toste, F. D. Ligand Effects in Homogeneous Au Catalysis, *Chem. Rev.* **2008**, *108*, 3351–3378. b) Chintawar, C. C.; Yadav, A. K.; Kumar, A.; Sancheti, S. P.; Patil, N. T. Divergent Gold Catalysis: Unlocking Molecular Diversity through Catalyst Control, *Chem. Rev.* **2021**, *121*, 8478–8558.

²³ Benitez, D.; Shapiro, N. D.; Tkatchouk, E.; Wang, Y.; Goddard, W. A.; Toste, F. D., A Bonding Model for Gold(I) Carbene Complexes, *Nat. Chem.* **2009**, *1*, 482–486.

²⁴ a) Bancroft, G. M.; Chan, T. Role of the Au 5d Orbitals in Bonding: Photoelectron Spectra of [AuMe(PMe₃)], *Inorg. Chem.* **1982**, *21*, 8, 2946–2949. b) Marrazzini, G.; Gabbiani, C.; Ciancaleoni, G. Interplay between Gold(I)-Ligand Bond Components and Hydrogen Bonding: A Combined Experimental/Computational Study, *ACS Omega* **2019**, *4*, 1344–1353.

²⁵ a) Fürstner, A.; Morency, L. On the Nature of the Reactive Intermediates in Gold-Catalyzed Cycloisomerization Reactions, *Angew. Chem. Int. Ed.* **2008**, *47*, 5030–5033, *Angew. Chem.* **2008**, *120*, 5108–5111. b) Hashmi, A. S. K. "High Noon" in Gold Catalysis: Carbene versus Carbocation Intermediates. *Angew. Chem. Int. Ed.* **2008**, *47*, 6754–6756, *Angew. Chem.* **2008**,

broader category of Fischer carbenes.²⁶ In general, the employment of phosphite ligands tends to yield complexes with a carbocation-like character, often characterized by high reactivity and electrophilicity (Figure 3). Conversely, the utilization of strongly σ -donating NHC ligands increases the carbene character of gold complexes, resulting in diminished electrophilicity, lower reactivity but enhanced selectivity. Phosphine ligands and in particular Buchwald-type ligands²⁷ exhibit an intermediate behavior between these two extremes.²⁸

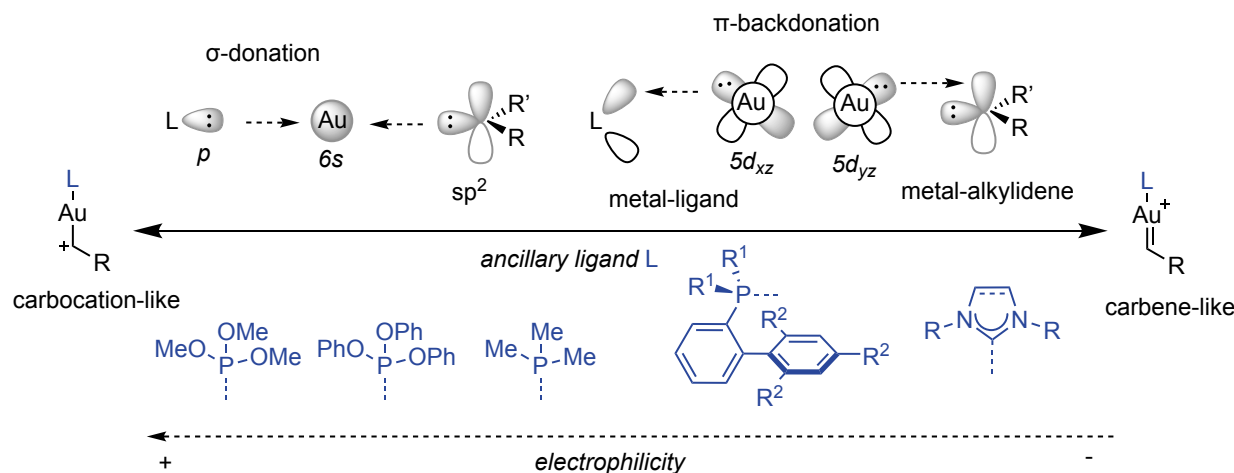


Figure 3. Bonding description and ancillary ligand influence in gold(I)-complexes.

Gold(I) coordination to alkynes can be partially rationalized by the Dewar-Chatt-Duncanson model²⁹: a σ -interaction arises from the donation of electron density from the π -bond of the alkyne to the empty 6s orbital of the metal. In contrast to the classic model, the backdonation cannot happen towards the antibonding π^* orbital of the alkyne, since the 5p orbitals of Au result too low (due to the aforementioned relativistic effects) for significant overlap, so the backbonding π -interaction consists instead in the donation to the non-bonding p orbitals of the alkyne.^{17b} This observation may have implications for the Lewis acidity of Au(I): the absence of a strong backbonding from Au(I) into π -ligands could render the unsaturated substrates more electron deficient, thereby facilitating nucleophilic addition.

120, 6856–6858. c) Seidel, G.; Mynott, R.; Fürstner, A. Elementary Steps of Gold Catalysis: NMR Spectroscopy Reveals the Highly Cationic Character of a “Gold Carbenoid.” *Angew. Chem. Int. Ed.* **2009**, *48*, 2510–2513, *Angew. Chem.* **2009**, *121*, 2548–2551. d) Echavarren, A. M. Carbene or Cation? *Nat. Chem.* **2009**, *1*, 431–433. e) Wang, Y.; Muratore, M. E.; Echavarren, A. M. Gold Carbene or Carbenoid: Is There a Difference? *Chem. Eur. J.* **2015**, *21*, 7332–7339. f) Escofet, I.; Armengol-Relats, H.; Bruss, H.; Besora, M.; Echavarren, A. M. On the Structure of Intermediates in Enyne Gold(I)-Catalyzed Cyclizations: Formation of Trans-Fused Bicyclo[5.1.0]Octanes as a Case Study. *Chem. Eur. J.* **2020**, *26*, 15738–15745. g) García-Padilla, E.; Escofet, I.; Maseras, F.; Echavarren, A. M. Puzzling Structure of the Key Intermediates in Gold(I)-Catalyzed Cyclization Reactions of Enynes and Allenenes. *ChemPlusChem*, **2023**, e202300502.

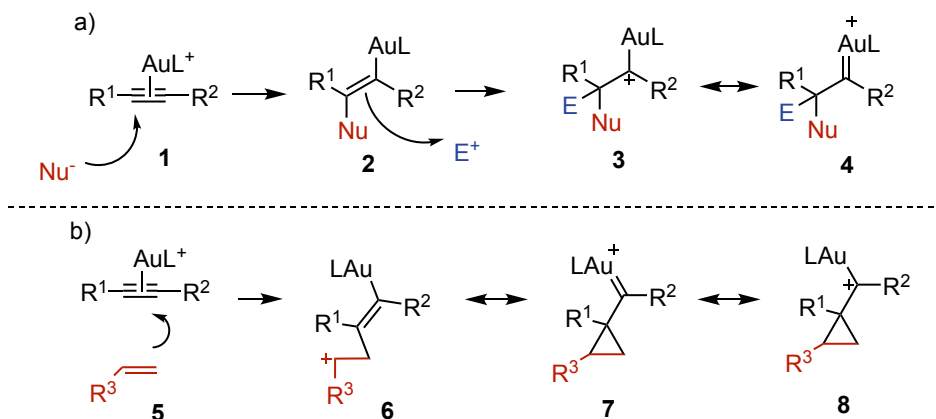
²⁶ Crabtree, R. H. *The Organometallic Chemistry of the Transition Metals*; John Wiley & Sons, **2009**.

²⁷ Wolfe, J. P.; Buchwald, S. L., A Highly Active Catalyst for the Room-Temperature Amination and Suzuki Coupling of Aryl Chlorides, *Angew. Chem. Int. Ed.* **1999**, *38*, 2413–2416, *Angew. Chem.* **1999**, *111*, 2570–2573.

²⁸ Zuccarello, G.; Zanini, M.; Echavarren, A. M., Buchwald-Type Ligands on Gold(I) Catalysis, *Isr. J. Chem.* **2020**, *60*, 360–372.

²⁹ a) Dewar, J. S., A review of the pi-complex theory. *Bull. Soc. Chim. Fr.* **1951**, *18*, C71–C79. b) Chatt, J., Duncanson, L. A., Olefin co-ordination compounds. 3. Infra-red spectra and structure - attempted preparation of acetylene complexes. *J. Chem. Soc.* **1953**, 2939–2947. c) Salvi, N.; Belpassi, L.; Tarantelli, F., On the Dewar–Chatt–Duncanson Model for Catalytic Gold(I) Complexes, *Chem. Eur. J.* **2010**, *16*, 7231–7240.

In many instances of gold-catalyzed reactions, a competitive scenario can emerge, where both an alkyne and an alkene coexist in the reaction mixture. The preferential activation of alkynes over alkenes presents a curious phenomenon, given that gold has been demonstrated to form stronger bonds with alkenes.³⁰ This intriguing behavior finds its roots in kinetics, where the activated alkyne LUMOs exhibit relatively lower energy levels compared to their alkene counterparts.³¹ Consequently, this disparity in energy levels leads to a favored nucleophilic attack on alkynes, elucidating the observed "alkynophilicity." Typically, this attack proceeds in an anti-fashion with respect to activated species **1** via an outer-sphere mechanism, with Markovnikov selectivity (Scheme 2a).³² Various carbon and heteronucleophiles, including arenes, heteroarenes, alcohols, thiols, amines, imines, sulfoxides, and *N*-oxides, can participate in this process.³³ The resulting trans-alkenyl gold species **2** can subsequently undergo further transformations (typically reaction with an electrophile) to yield the corresponding products.¹⁶ In the case of alkene nucleophiles, a homoallylic carbocation **6** is generated (Scheme 2b). This carbocation is in resonance³⁴ with one of the hallmark intermediates in gold(I) catalysis: the cyclopropyl gold(I) carbene **7-8**.³⁵



Scheme 2. Reactivity of alkynes with nucleophiles under gold(I)-catalysis.

³⁰ a) Nechaev, M. S.; Rayón, V. M.; Frenking, G. Energy Partitioning Analysis of the Bonding in Ethylene and Acetylene Complexes of Group 6, 8, and 11 Metals: (CO)₅TM-C₂H_x and Cl₄TM-C₂H_x (TM = Cr, Mo, W), (CO)₄TM-C₂H_x (TM = Fe, Ru, Os), and TM⁺-C₂H_x (TM = Cu, Ag, Au), *J. Phys. Chem. A* **2004**, *108*, 3134–3142. b) Brown, T. J.; Dickens, M. G.; Widenhoefer, R. A., Syntheses and X-Ray Crystal Structures of Cationic, Two-Coordinate Gold(I) π -Alkene Complexes That Contain a Sterically Hindered *o*-Biphenylphosphine Ligand, *Chem. Commun.* **2009**, No. 42, 6451–6453. c) Brooner, R. E. M.; Widenhoefer, R. A. Cationic, Two-Coordinate Gold π Complexes. *Angew. Chem. Int. Ed.* **2013**, *52*, 11714–11724, *Angew. Chem.* **2013**, *125*, 11930–11941.

³¹ García-Mota, M.; Cabello, N.; Maseras, F.; Echavarren, A. M.; Pérez-Ramírez, J.; Lopez, N. Selective Homogeneous and Heterogeneous Gold Catalysis with Alkynes and Alkenes: Similar Behavior, Different Origin, *ChemPhysChem* **2008**, *9*, 1624–1629.

³² Fürstner, A. Gold and Platinum Catalysis - a Convenient Tool for Generating Molecular Complexity. *Chem. Soc. Rev.* **2009**, *38*, 3208–3221.

³³ a) Debrouwer, W.; Heugebaert, T. S. A.; Roman, B. I.; Stevens, C. V. Homogeneous Gold-Catalyzed Cyclization Reactions of Alkynes with *N*- and *S*-Nucleophiles. *Adv. Synth. Catal.* **2015**, *357*, 2975–3006. b) Echavarren, A. M.; Muratore, M. E.; López-Carrillo, V.; Escribano-Cuesta, A.; Huguet, N.; Obradors, C. Gold-Catalyzed Cyclizations of Alkynes with Alkenes and Arenes, *Organic Reactions*, **2017**, 1–288.

³⁴ There's been debates on the nature of this resonance, which sometimes has been defined as equilibrium (ref. 25 f,g).

³⁵ Dorel, R.; Echavarren, A. M., Gold-Catalyzed Reactions via Cyclopropyl Gold Carbene-like Intermediates, *J. Org. Chem.* **2015**, *80*, 7321–7332.

Catalytically active cationic gold(I) complexes are typically formed in situ from their neutral precursors through either protolysis of [LAuMe] or chloride abstraction in [LAuCl] with AgX. However, the use of silver salts in gold(I) catalysis has been associated with the formation of less active chloride-bridged digold complexes, leading to the so called “silver effect” which might affect the reactivity and selectivity of transformations.³⁶

Intramolecular Reactivity: Gold(I)-Catalyzed Cycloisomerization of 1,*n*-Enynes

When dealing with enynes, the alkene functionality is in close proximity to the alkyne moiety and, as it can be imagined, gold(I),^{16,37} as platinum(II),^{32,38} revealed to be an excellent promoter for intramolecular cycloadditions, namely cycloisomerizations, of these species. In this context, 1,6-enynes were the most studied substrates so far (Scheme 3).³⁹

The activation of the alkyne functionality by gold(I) leads to the formation of a (η^2 -alkyne)–metal complex **9** which, after nucleophilic attack from the alkene, produces cyclopropyl gold(I) carbene-like intermediates **10** or **16** through either *anti*-5-*exo*-*dig* (the *syn*-*exo*-*dig* pathway was discarded⁴⁰) or 6-*endo*-*dig* cyclizations.⁴¹ As anticipated (Scheme 2b), these carbene intermediates were demonstrated to have partial carbocationic character.^{25f,40a,42}

³⁶ a) Wang, D.; Cai, R.; Sharma, S.; Jirak, J.; Thummanapelli, S. K.; Akhmedov, N. G.; Zhang, H.; Liu, X.; Petersen, J. L.; Shi, X., “Silver Effect” in Gold(I) Catalysis: An Overlooked Important Factor, *J. Am. Chem. Soc.* **2012**, *134*, 9012–9019. b) Homs, A.; Escofet, I.; Echavarren, A. M., On the Silver Effect and the Formation of Chloride-Bridged Digold Complexes, *Org. Lett.* **2013**, *15*, 5782–5785.

³⁷ Obradors, C.; Echavarren, A. M. Gold-Catalyzed Rearrangements and Beyond, *Acc. Chem. Res.* **2014**, *47*, 902–912.

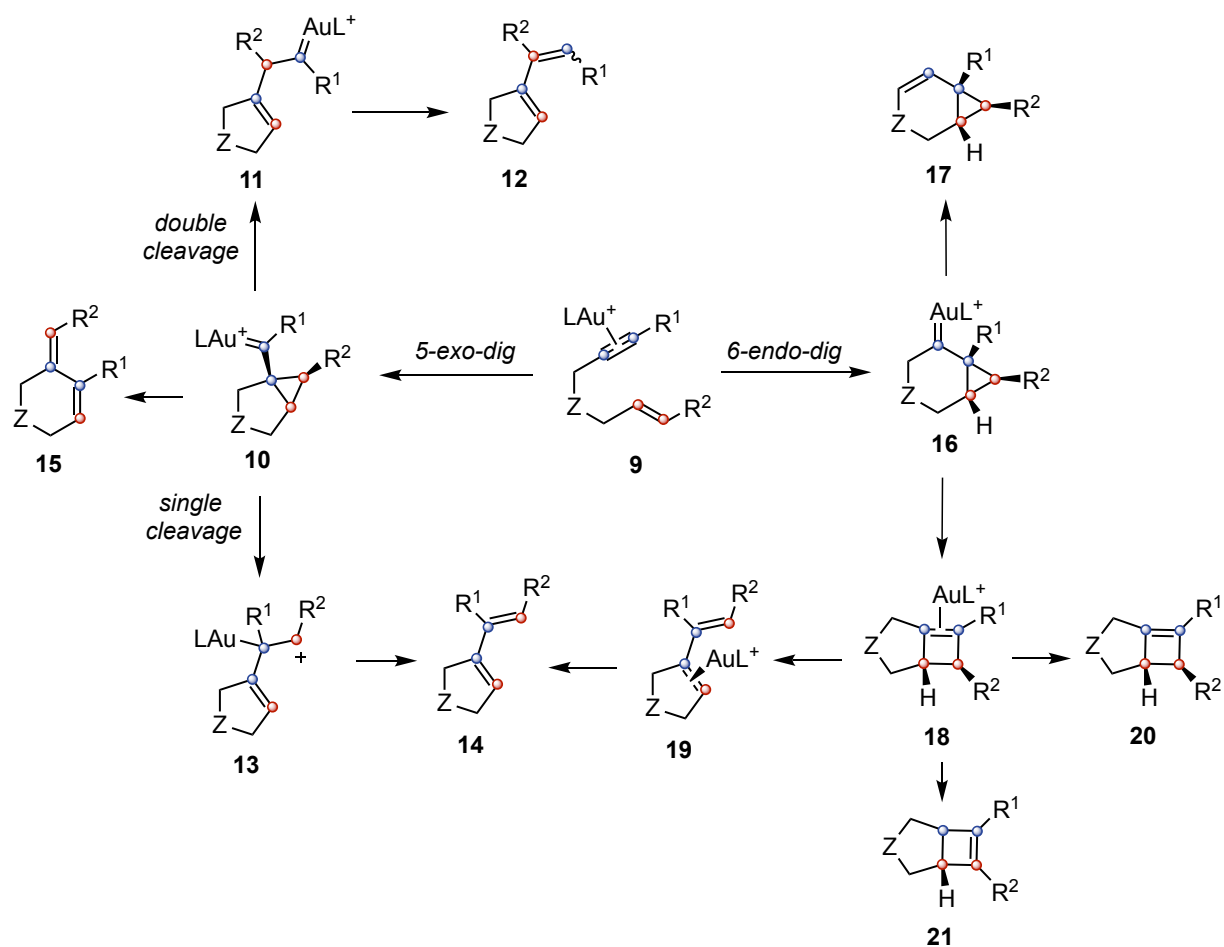
³⁸ a) Fürstner, A.; Stelzer, F.; Szillat, H. Platinum-Catalyzed Cycloisomerization Reactions of Enynes. *J. Am. Chem. Soc.* **2001**, *123*, 11863–11869. b) Muñoz, M. P.; Méndez, M.; Nevado, C.; Cárdenas, D. J.; Echavarren, A. M. Hydroxy- and Alkoxy-cyclizations of Enynes Catalyzed by Platinum(II) Chloride. *Synthesis* **2003**, *2003*, 2898–2902. c) Zhang, L.; Sun, J.; Kozmin, S. A. Gold and Platinum Catalysis of Enyne Cycloisomerization. *Adv. Synth. Catal.* **2006**, *348*, 2271–2296. d) Vasu, D.; Das, A.; Liu, R.-S. Platinum-Catalyzed Cycloisomerization of 1,4-Enynes via Activation of a Sp³-Hybridized C–H Bond. *Chem. Commun.* **2010**, *46*, 4115–4117. e) Sato, T.; Onuma, T.; Nakamura, I.; Terada, M. Platinum-Catalyzed Cycloisomerization of 1,4-Enynes via 1,2-Alkenyl Rearrangement. *Org. Lett.* **2011**, *13*, 4992–4995.

³⁹ Mattalia, J.-M.; Nava, P. Gold-Catalyzed Cycloisomerizations of 1,6-Enynes. A Computational Study, *J. Organomet. Chem.* **2014**, *749*, 335–342.

⁴⁰ a) Nieto-Oberhuber, C.; López, S.; Muñoz, M. P.; Cárdenas, D. J.; Buñuel, E.; Nevado, C.; Echavarren, A. M. Divergent Mechanisms for the Skeletal Rearrangement and [2+2] Cycloaddition of Enynes Catalyzed by Gold, *Angew. Chem. Int. Ed.* **2005**, *44*, 6146–6148, *Angew. Chem.* **2005**, *117*, 6302–6304. b) Escribano-Cuesta, A.; Pérez-Galán, P.; Herrero-Gómez, E.; Sekine, M.; Braga, A. A. C.; Maseras, F.; Echavarren, A. M. The Role of Cyclobutenes in Gold(I)-Catalysed Skeletal Rearrangement of 1,6-Enynes, *Org. Biomol. Chem.* **2012**, *10*, 6105–6111.

⁴¹ Nieto-Oberhuber, C.; Muñoz, M. P.; Buñuel, E.; Nevado, C.; Cárdenas, D. J.; Echavarren, A. M. Cationic Gold(I) Complexes: Highly Alkynophilic Catalysts for the Exo- and Endo-Cyclization of Enynes. *Angew. Chem. Int. Ed.* **2004**, *43*, 2402–2406, *Angew. Chem.* **2004**, *116*, 2456–2460.

⁴² Fürstner, A.; Davies, P. W. Catalytic Carbophilic Activation: Catalysis by Platinum and Gold π Acids, *Angew. Chem. Int. Ed.* **2007**, *46*, 3410–3449, *Angew. Chem.* **2007**, *119*, 3478–3519.



Scheme 3. Mechanistic pathways in gold(I)-catalyzed cycloisomerizations of 1,6-enynes. Z = C, N or O tether.

Intermediates **10** can further evolve to generate rearranged carbenes **11** through the formal insertion of the terminal alkene carbon into the alkyne carbons to eventually yield double-cleavage rearrangement products **12** after α -proton elimination. While products with both configurations have been observed in this rearrangement, compounds with a *Z* configuration ($R^2 = H$) are often favored. Alternatively, **10** can also undergo single-cleavage rearrangement.^{40a} This process entails the migration of the terminal carbon of the alkene to the terminal carbon of the alkyne, effectively representing a formal cleavage of the alkene. The resulting homoallyl carbocation **13** subsequently converts to single-cleavage rearrangement product **14** in a stereospecific manner, preserving the configuration of the alkene in the *exo*-double bond of the product. The outcome of whether intermediate **10** undergoes single or double cleavage hinges on the nature of the substituents attached to the alkyne. Electron-withdrawing substituents tend to encourage the double-cleavage rearrangement, whereas electron-donating groups typically favor the formation of the single-cleavage diene. In addition to these products, six-membered ring compounds **15** can also be generated from **10** through an alternative *endo*-type single-cleavage rearrangement, wherein the internal carbon of the double bond migrates toward C1 of the alkyne.⁴³

⁴³ Cabello, N.; Jiménez-Núñez, E.; Buñuel, E.; Cárdenas, D. J.; Echavarren, A. M., On the Mechanism of the Puzzling “Endocyclic” Skeletal Rearrangement of 1,6-Enynes, *Eur. J. Org. Chem.* **2007**, 2007, 4217–4223.

On the other hand, intermediates **16** resulting from *6-endo-dig* cyclization can give rise to bicyclo[4.1.0]hept-2-ene derivatives **17** through α -proton elimination.⁴⁴ Alternatively, ring expansion of the cyclopropane ring in **16** yields (η^2 -cyclobutene)-gold(I) complexes **18**. The opening of these complexes can form precursors **19** of 1,3-dienes **14**, the same products of the single-cleavage rearrangement of **10**.^{40b} Apart from few cases reported where the highly strained cyclobutenes **20** product of a formal [2+2] cycloaddition, have been isolated starting from 1,6-enynes,⁴⁵ the more stable isomer **21** are usually encountered.^{44a,46}

Cyclizations of 1,5-enynes also involve species that lie intermediate between an open carbocation and a cyclopropyl gold(I) carbene.⁴⁷ The latter is highly electrophilic, enabling it to undergo formal C–H insertion reactions at β -C–H bonds, resulting in the formation of new cyclopropanes.⁴⁸ 1,7-enynes, which have been less studied, typically undergo single cleavage rearrangement via both *endo*- and *exo*-cyclopropyl gold(I) carbenes.⁴⁹ When coming to higher order 1,*n* enynes, formal [2+2] products of type **20** can easily be formed thanks to the reduced ring strain.^{40a,50} The pathway followed by a particular enyne among all the ones illustrated in Scheme 3 is highly dependent on its substitution pattern and can vary in some cases depending on the ligand chosen for the gold(I) catalyst.

When an external nucleophile is present in the reaction mixture, cyclopropyl gold(I) carbene **10/16** (Scheme 3) can be trapped to generate additional products. In the case of alcohol nucleophiles, the alkoxy cyclization products **24/26** form from 1,6-enynes **23/25** in a stereospecific fashion: *E* alkenes afford selectively *anti* products and *Z* alkenes afford *syn* products (Scheme 4a).^{41,44a} Moreover, these processes always follow the Markovnikov regiochemistry, as it can be seen from reaction of **27/30** to respectively form products **29/32**, where MeOH always attacks the most substituted carbon in intermediates **28/31** (Scheme 4b).^{44a}

⁴⁴ a) Nieto-Oberhuber, C.; Muñoz, M. P.; López, S.; Jiménez-Núñez, E.; Nevado, C.; Herrero-Gómez, E.; Raducan, M.; Echavarren, A. M. Gold(I)-Catalyzed Cyclizations of 1,6-Enynes: Alkoxy cyclizations and Exo/Endo Skeletal Rearrangements, *Chem. Eur. J.* **2006**, *12*, 1677–1693. b) Lee, Y. T.; Kang, Y. K.; Chung, Y. K. Au(I)-Catalyzed Cycloisomerization Reaction of Amide- or Ester-Tethered 1,6-Enynes to Bicyclo[3.2.0]Hept-6-En-2-Ones, *J. Org. Chem.* **2009**, *74*, 7922–7934.

⁴⁵ a) Brooner, R. E. M.; Brown, T. J.; Widenhofer, R. A. Direct Observation of a Cationic Gold(I)-Bicyclo[3.2.0]Hept-1(7)-Ene Complex Generated in the Cycloisomerization of a 7-Phenyl-1,6-Enyne, *Angew. Chem. Int. Ed.* **2013**, *52*, 6259–6261, *Angew. Chem.* **2013**, *125*, 6379–6381. b) Lee, S. I.; Kim, S. M.; Choi, M. R.; Kim, S. Y.; Chung, Y. K.; Han, W.-S.; Kang, S. O. Au(I)-Catalyzed Cyclization of Enynes Bearing an Olefinic Cycle, *J. Org. Chem.* **2006**, *71*, 9366–9372.

⁴⁶ Kim, N.; Brooner, R. E. M.; Widenhofer, R. A., Unexpected Skeletal Rearrangement in the Gold(I)/Silver(I)-Catalyzed Conversion of 7-Aryl-1,6-Enynes to Bicyclo[3.2.0]Hept-6-Enes via Hidden Brønsted Acid Catalysis, *Organometallics* **2017**, *36*, 673–678.

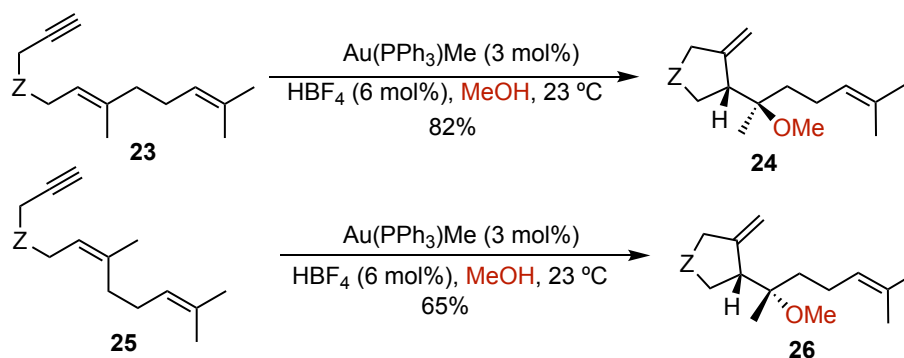
⁴⁷ López-Carrillo, V.; Huguet, N.; Mosquera, Á.; Echavarren, A. M., Nature of the Intermediates in Gold(I)-Catalyzed Cyclizations of 1,5-Enynes, *Chem. Eur. J.* **2011**, *17*, 10972–10978.

⁴⁸ Horino, Y.; Yamamoto, T.; Ueda, K.; Kuroda, S.; Toste, F. D., Au(I)-Catalyzed Cycloisomerizations Terminated by Sp³ C–H Bond Insertion, *J. Am. Chem. Soc.* **2009**, *131*, 2809–2811.

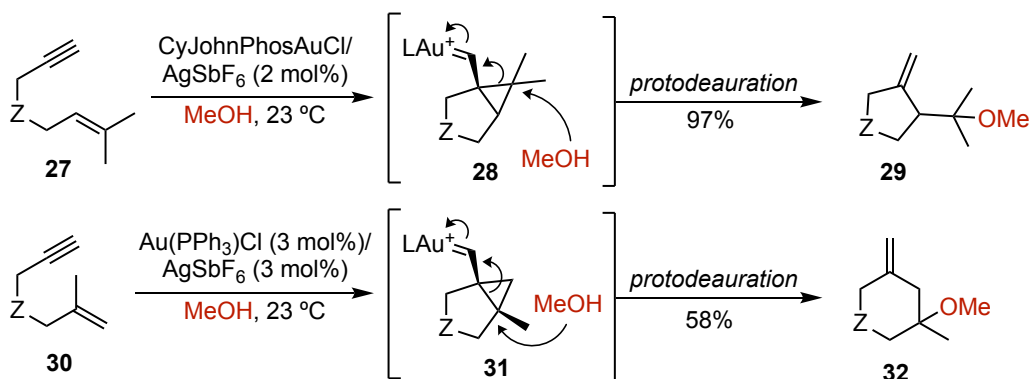
⁴⁹ a) Cabello, N.; Rodríguez, C.; Echavarren, A. M. Gold-Catalyzed Cyclizations of 1,7-Enynes, *Synlett* **2007**, *2007*, 1753–1758. b) Huang, C.; Kothandaraman, P.; Koh, B. Q.; Chan, P. W. H., Study of Substrate Dependence on the Chemoselectivity of the Gold-Catalysed Cycloisomerisation of Aryl Substituted 1,7-Enynes, *Org. Biomol. Chem.* **2012**, *10*, 9067–9078.

⁵⁰ a) Odabachian, Y.; Gagosz, F. Cyclobutenes as Isolable Intermediates in the Gold(I)-Catalysed Cycloisomerisation of 1,8-Enynes, *Adv. Synth. Catal.* **2009**, *351*, 379–386. b) Obradors, C.; Leboeuf, D.; Aydin, J.; Echavarren, A. M. Gold(I)-Catalyzed Macrocyclization of 1,*n*-Enynes, *Org. Lett.* **2013**, *15*, 1576–1579.

a) Stereospecificity



b) Regioselectivity



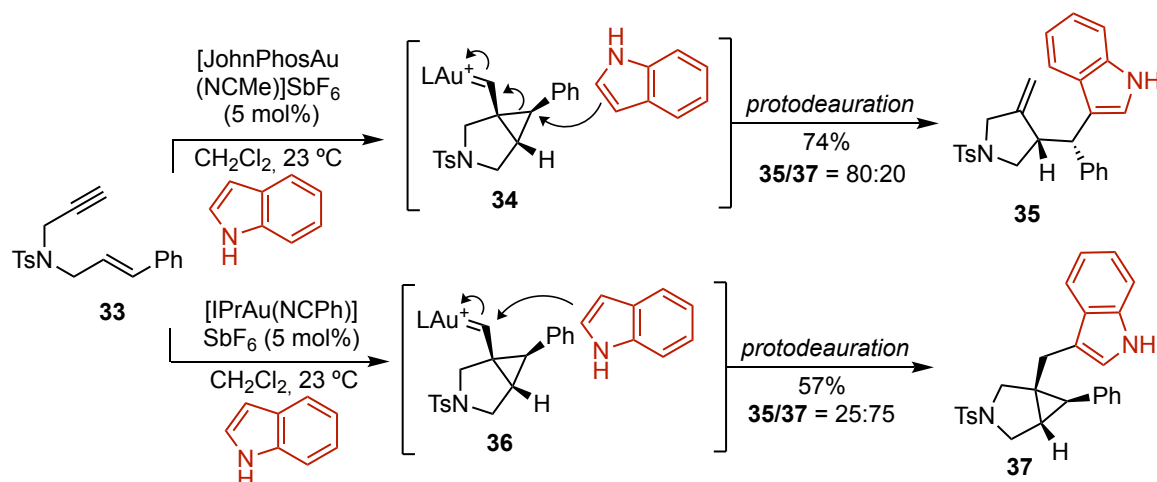
Scheme 4. Stereospecificity and regioselectivity of gold(I)-catalyzed alkoxymercuration reactions. $Z = \text{CO}_2\text{Me}$.

Nitrogen-⁵¹ and carbon-⁵² containing nucleophiles have also found extensive application as external nucleophiles. When it comes to the latter, whether the site of attack is on the cyclopropyl ring or the carbenic carbon, it depends on the ancillary ligand. For instance, when using a phosphine-based ligand in the reaction of nitrogen-tethered 1,6-enyne **33** with indole, the cyclopropyl gold(I) carbene **34** is predominantly attacked on the benzylic carbon, while with a carbene ligand (IPr) the attack on the carbene carbon becomes favored (Scheme 5).^{52b} Very recently, the groups of Bandini and López addressed chemoselectivity to be linked to the barriers of the rate-determining protodeauration step happening after nucleophilic attack.⁵³

⁵¹ a) Leseurre, L.; Toullec, P. Y.; Genêt, J.-P.; Michelet, V., Gold-Catalyzed Hydroamination/Cycloisomerization Reaction of 1,6-Enynes, *Org. Lett.* **2007**, *9*, 4049–4052. b) Miller, R.; Carreras, J.; Muratore, M. E.; Gaydou, M.; Camponovo, F.; Echavarren, A. M., Broad Scope Aminocyclization of Enynes with Cationic JohnPhos–Gold(I) Complex as the Catalyst, *J. Org. Chem.* **2016**, *81*, 1839–1849.

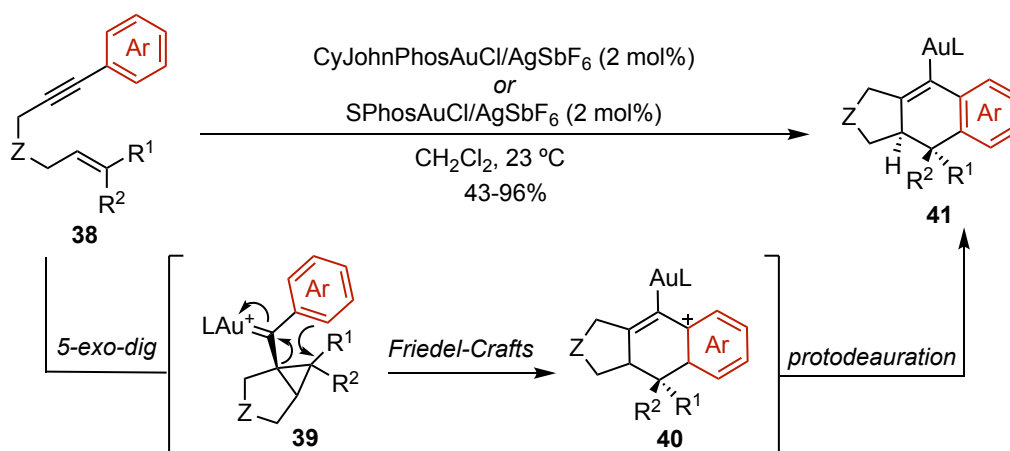
⁵² a) Amijs, C. H. M.; Ferrer, C.; Echavarren, A. M., Gold(I)-Catalysed Arylation of 1,6-Enynes: Different Site Reactivity of Cyclopropyl Gold Carbenes, *Chem. Commun.* **2007**, No. 7, 698–700. b) Amijs, C. H. M.; López-Carrillo, V.; Raducan, M.; Pérez-Galán, P.; Ferrer, C.; Echavarren, A. M., Gold(I)-Catalyzed Intermolecular Addition of Carbon Nucleophiles to 1,5- and 1,6-Enynes, *J. Org. Chem.* **2008**, *73*, 7721–7730.

⁵³ Pedrazzani, R.; Kiriakidi, S.; Monari, M.; Lazzarini, I.; Bertuzzi, G.; López, C. S.; Bandini, M., Fluorinated Biphenyl Phosphine Ligands for Accelerated [Au(I)]-Catalysis, *ACS Catal.* **2024**, *14*, 6128–6136.



Scheme 5. Nucleophilic attack of indoles to NTs-tethered 1,6-enynes.

Aryl rings can also serve as internal nucleophiles when having internal 1,6-enynes of the type **38**, leading to a formal [4+2] cycloaddition to afford tricyclic products **41** under gold(I)-catalysis (Scheme 6).⁵⁴ The reaction commences with a *5-exo-dig* cyclization of the enyne to form cyclopropyl gold(I) carbene **39**, followed by the trapping and ring-expansion of the cyclopropyl ring via a Friedel-Crafts-type reaction to generate **40**. Finally, re-aromatization and protodeauration furnish the desired product **41**.



Scheme 6. First gold(I)-catalyzed [4+2] cycloaddition described starting from 1,6-enynes **38**. Z = CO₂Me.

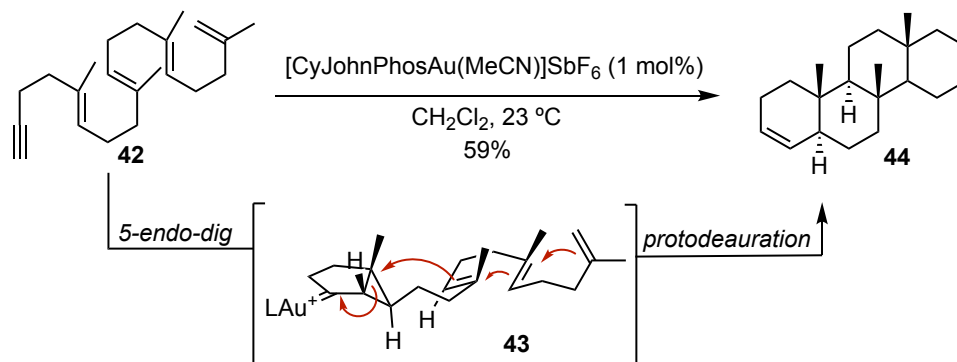
Similarly, gold(I)-catalyzed polyenyne cascade cyclizations involve the intramolecular participation of multiple double bonds upon alkyne activation. With pioneer work performed by Michelet⁵⁵ and Toste,⁵⁶

⁵⁴ a) Nieto-Oberhuber, C.; López, S.; Echavarren, A. M., Intramolecular [4 + 2] Cycloadditions of 1,3-Enynes or Arylalkynes with Alkenes with Highly Reactive Cationic Phosphine Au(I) Complexes, *J. Am. Chem. Soc.* **2005**, *127*, 6178–6179. b) Nieto-Oberhuber, C.; Pérez-Galán, P.; Herrero-Gómez, E.; Lauterbach, T.; Rodríguez, C.; López, S.; Bour, C.; Rosellón, A.; Cárdenas, D. J.; Echavarren, A. M., Gold(I)-Catalyzed Intramolecular [4+2] Cycloadditions of Arylalkynes or 1,3-Enynes with Alkenes: Scope and Mechanism, *J. Am. Chem. Soc.* **2008**, *130*, 269–279.

⁵⁵ Toullec, P. Y.; Blarrie, T.; Michelet, V., Mimicking Polyolefin Carbocyclization Reactions: Gold-Catalyzed Intramolecular Phenoxycyclization of 1,5-Enynes, *Org. Lett.* **2009**, *11*, 2888–2891.

⁵⁶ Sethofer, S. G.; Mayer, T.; Toste, F. D., Gold(I)-Catalyzed Enantioselective Polycyclization Reactions, *J. Am. Chem. Soc.* **2010**, *132*, 8276–8277.

describing the simultaneous formation of two to three C–C bonds, our group reported the formation of steroid-like tetracyclic compound **44** involving the formation of four new C–C bonds under gold(I) catalysis (Scheme 7), and extended the transformation to previously unexplored bromoalkynes (as also mentioned in the Introduction of Chapter III).



Scheme 7. Gold(I)-promoted cascade cyclization of polyenyne **42** to yield tetracyclic **44**.

Gold(I)-Catalyzed Intermolecular Reactions of Alkynes with Alkenes

In comparison to the plethora of gold(I)-catalyzed intramolecular transformations, the scope of intermolecular reactions involving alkynes and alkenes to forge new C–C bonds is relatively constrained.⁵⁷ Apart from having two distinct and independent moieties with similar affinities for coordination with the metal's binding site, a possibility for gold(I)-promoted dimerizations or polymerizations⁵⁸ might also constitute a problem which is minimized in intramolecular transformations. Moreover, electron-rich alkenes, which are ideally suited for reactivity with gold(I)-activated alkynes, would tend to preferentially coordinate with gold(I),³⁰ thereby diminishing the concentration of the active (η^2 -alkyne)–gold(I) complex.

The first example of gold(I)-catalyzed intermolecular reactivity between alkynes and alkenes was reported by Hashmi in 2006, (who previously also described the intramolecular version⁵⁹) with an isolated example of phenylacetylene **45** reacting with 2,5-dimethylfuran **46** using a bimetallic phosphine gold(I) complex (Scheme 8).⁶⁰ Once formed cyclopropyl gold(I) carbene **47**, this opens to

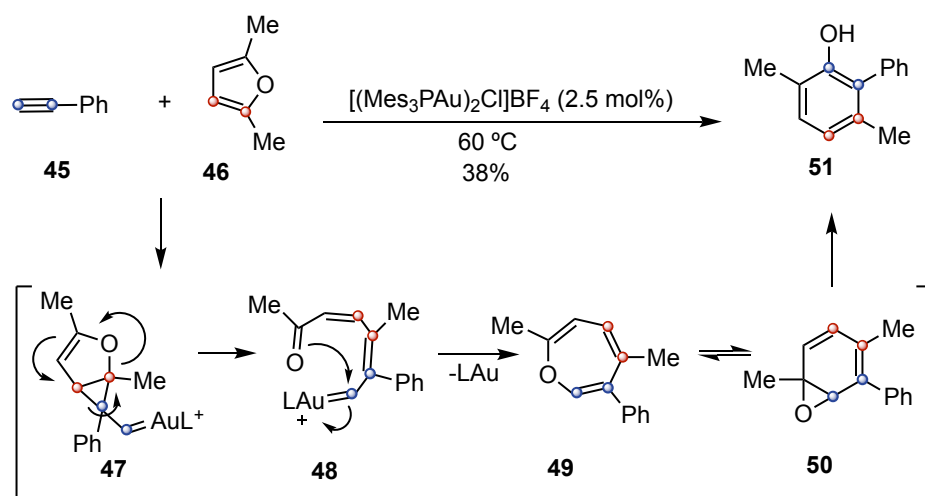
⁵⁷ a) Muratore, M. E.; Homs, A.; Obradors, C.; Echavarren, A. M., Meeting the Challenge of Intermolecular Gold(I)-Catalyzed Cycloadditions of Alkynes and Allenes, *Chem. Asian J.* **2014**, *9*, 3066–3082. b) García-Morales, C.; Echavarren, A. M., From Straightforward Gold(I)-Catalyzed Enyne Cyclizations to More Demanding Intermolecular Reactions of Alkynes with Alkenes, *Synlett* **2018**, *29*, 2225–2237.

⁵⁸ a) Urbano, J.; Hormigo, A. J.; Frémont, P. de; Nolan, S. P.; Díaz-Requejo, M. M.; Pérez, P. J., Gold-Promoted Styrene Polymerization, *Chem. Commun.* **2008**, No. 6, 759–761. b) Nzulu, F.; Bontemps, A.; Robert, J.; Barbazanges, M.; Fensterbank, L.; Goddard, J.-P.; Malacria, M.; Ollivier, C.; Petit, M.; Rieger, J.; Stoffelbach, F., Gold-Catalyzed Polymerization Based on Carbene Polycyclopropanation, *Macromolecules* **2014**, *47*, 6652–6656.

⁵⁹ Brown, T. J.; Dickens, M. G.; Widenhofer, R. A., Syntheses and X-Ray Crystal Structures of Cationic, Two-Coordinate Gold(I) π -Alkene Complexes That Contain a Sterically Hindered *o*-Biphenylphosphine Ligand, *Chem. Commun.* **2009**, No. 42, 6451–6453.

⁶⁰ Hashmi, A. S. K.; Blanco, M. C.; Kurpejović, E.; Frey, W.; Bats, J. W., Gold Catalysis: First Applications of Cationic Binuclear Gold(I) Complexes and the First Intermolecular Reaction of an Alkyne with a Furan, *Adv. Synth. Catal.* **2006**, *348*, 709–713.

generate ketone **48**, which after intramolecular trapping yields oxepine **49**, in a tautomeric equilibrium with arene-oxide **50**. Finally, the latter, rearranges to the more stable phenol **51**. A few years later, our group expanded the scope of this reaction, implementing the synthesis of indenenes.⁶¹



Scheme 8. Intermolecular gold(I)-catalyzed cyclization of furans with alkynes.

The gold(I)-catalyzed [2+2] cycloaddition of alkynes with alkenes was first described by our group in 2010 to regioselectively generate cyclobutenes (Scheme 9),⁶² valuable intermediate in synthesis⁶³ and precursors of useful cyclobutane scaffolds which find use in medicinal chemistry⁶⁴ and are present in many natural products.⁶⁵⁻⁶⁶ While the reaction was initially reported only for aryl- and cyclopropyl-alkynes with alkenes,⁶² the scope was later expanded to 1,3-diynes,⁶⁷ 1,3-enynes⁶⁸ and 1,3-dienes.⁶⁸

⁶¹ Huguet, N.; Lebœuf, D.; Echavarren, A. M., Intermolecular Gold(I)-Catalyzed Cyclization of Furans with Alkynes: Formation of Phenols and Indenes, *Chem. Eur. J.* **2013**, *19*, 6581–6585.

⁶² López-Carrillo, V.; Echavarren, A. M., Gold(I)-Catalyzed Intermolecular [2+2] Cycloaddition of Alkynes with Alkenes, *J. Am. Chem. Soc.* **2010**, *132*, 9292–9294.

⁶³ a) Lee-Ruff, E.; Mladenova, G., Enantiomerically Pure Cyclobutane Derivatives and Their Use in Organic Synthesis, *Chem. Rev.* **2003**, *103*, 1449–1484. b) Namyslo, J. C.; Kaufmann, D. E., The Application of Cyclobutane Derivatives in Organic Synthesis, *Chem. Rev.* **2003**, *103*, 1485–1538. c) Fürstner, A.; Aïssa, C., PtCl_2 -Catalyzed Rearrangement of Methylene-cyclopropanes, *J. Am. Chem. Soc.* **2006**, *128*, 6306–6307. d) Fumagalli, G.; Stanton, S.; Bower, J. F., Recent Methodologies That Exploit C–C Single-Bond Cleavage of Strained Ring Systems by Transition Metal Complexes, *Chem. Rev.* **2017**, *117*, 9404–9432.

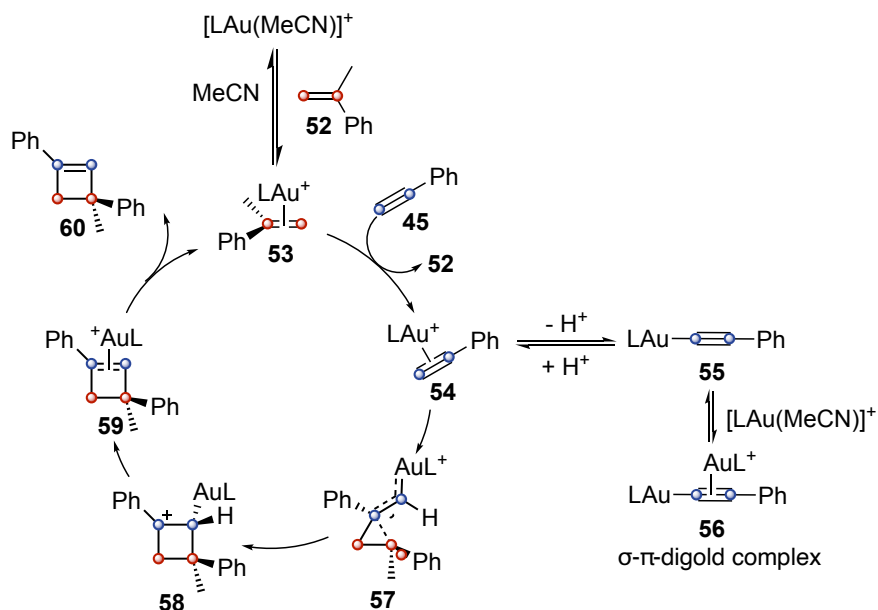
⁶⁴ a) Wishart, D. S.; Feunang, Y. D.; Guo, A. C.; Lo, E. J.; Marcu, A.; Grant, J. R.; Sajed, T.; Johnson, D.; Li, C.; Sayeeda, Z.; Assempour, N.; Iynkkaran, I.; Liu, Y.; Maciejewski, A.; Gale, N.; Wilson, A.; Chin, L.; Cummings, R.; Le, D.; Pon, A.; Knox, C.; Wilson, M., DrugBank 5.0: A Major Update to the DrugBank Database for 2018, *Nucleic Acids Res.* **2018**, *46*, D1074–D1082. b) van der Kolk, M. R.; Janssen, M. A. C. H.; Rutjes, F. P. J. T.; Blanco-Ania, D., Cyclobutanes in Small-Molecule Drug Candidates, *ChemMedChem* **2022**, *17*, e202200020.

⁶⁵ a) Dembitsky, V. M., Naturally Occurring Bioactive Cyclobutane-Containing (CBC) Alkaloids in Fungi, Fungal Endophytes, and Plants, *Phytomedicine* **2014**, *21*, 1559–1581. b) Li, J.; Gao, K.; Bian, M.; Ding, H., Recent Advances in the Total Synthesis of Cyclobutane-Containing Natural Products, *Org. Chem. Front.* **2019**, *7*, 136–154.

⁶⁶ The properties of four-membered ring compounds are discussed more in depth in the Introduction of Chapter II.

⁶⁷ De Orbe, M. E.; Amenós, L.; Kirillova, M. S.; Wang, Y.; López-Carrillo, V.; Maseras, F.; Echavarren, A. M., Cyclobutene vs 1,3-Diene Formation in the Gold-Catalyzed Reaction of Alkynes with Alkenes: The Complete Mechanistic Picture, *J. Am. Chem. Soc.* **2017**, *139*, 10302–10311.

⁶⁸ De Orbe, M. E.; Echavarren, A. M., Broadening the Scope of the Gold-Catalyzed [2+2] Cycloaddition Reaction: Synthesis of Vinylcyclobutenes and Further Transformations, *Eur. J. Org. Chem.* **2018**, *2018*, 2740–2752.



Scheme 9. Catalytic cycle for the gold(I)-catalyzed [2+2] cycloaddition of alkynes with alkenes.

The catalytic cycle was described based on previous theoretical work performed on enynes:⁴⁰ as anticipated, gold(I) favors coordination with alkenes over alkynes,³⁰ so the first complex formed can be considered to be **53**, starting from generic $[\text{LAu}(\text{MeCN})]^+$ and α -methyl styrene **52**. Then, ligand exchange with phenylacetylene **45** to form $(\eta^2\text{-alkyne})\text{gold(I)}$ complex **54** is followed by nucleophilic attack from the alkene, which constitutes the rate-determining step. Cyclopropyl gold(I) carbene **57** is therefore formed and subsequently ring expansion takes place, leading to the formation of benzylic carbocation **58**, which upon demetallation yields cyclobutene **60** releasing the cationic gold(I) complex and regenerating the catalytic cycle. In the course of this pathway, complex **54** can form σ - π digold complexes **56** which were demonstrated to be poor catalysts for enyne cycloisomerizations⁶⁹ and completely unproductive for [2+2] cycloadditions.⁷⁰ By changing the counteranion from SbF_6^- to the bulkier and softer $\text{BAR}_4^{\text{F}-}$ it was noticed how the reaction yield and rate increased along with a higher concentration of catalytically active species **53** and **54**. This trend was attributed to the increased basicity $\text{BAR}_4^{\text{F}-}$ anion given the lower stability of the bulkier conjugated acid, which would therefore form less alkynyl gold **55** (and digold complex **56**) starting from η^2 -gold complex **54**.

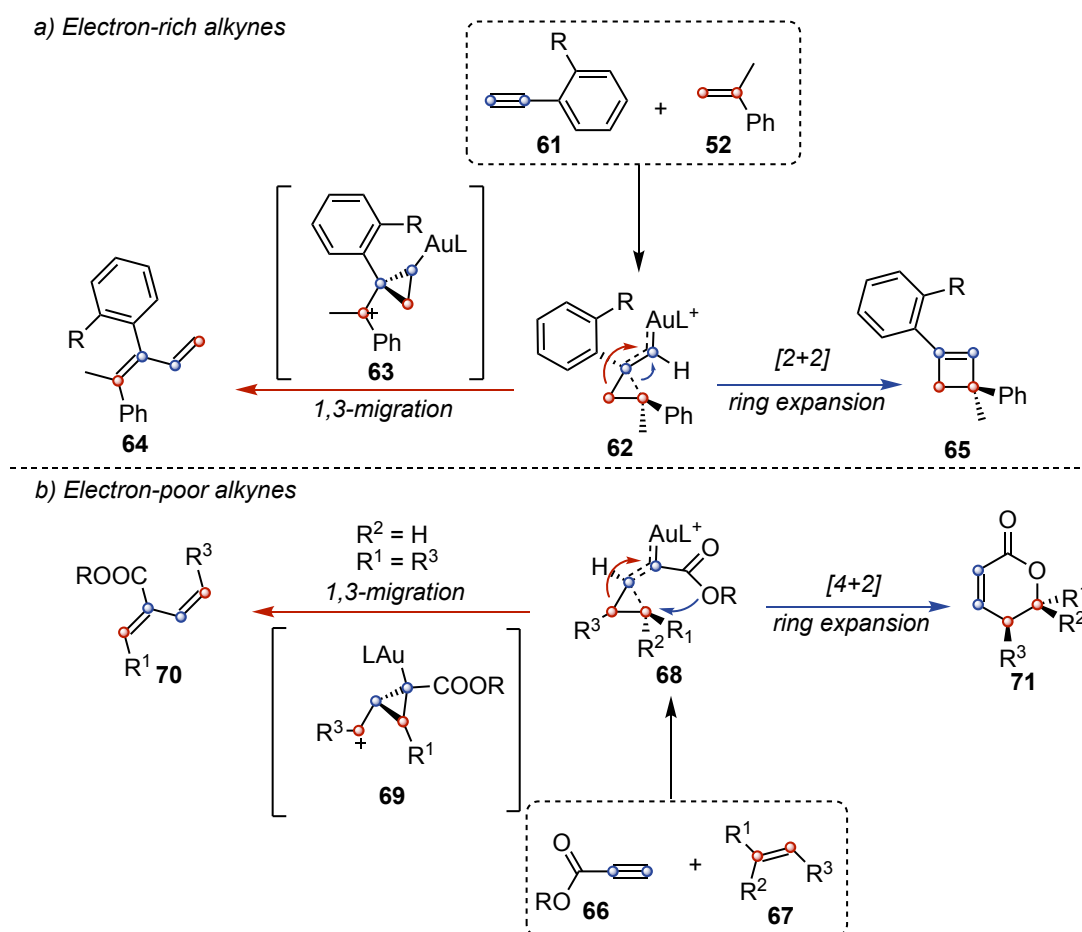
The same phenomenon was also observed in the intermolecular gold(I)-catalyzed [2+2+2] cycloaddition of alkynes with oxoalkenes to yield 8-oxabicyclo[3.2.1]oct-3-enes, in which two C–C and one C–O bonds are formed.⁷¹

⁶⁹ Ferrer, S.; Echavarren, A. M., Role of σ , π -Digold(I) Alkyne Complexes in Reactions of Enynes, *Organometallics* **2018**, *37*, 781–786.

⁷⁰ Homs, A.; Obradors, C.; Leboeuf, D.; Echavarren, A. M., Dissecting Anion Effects in Gold(I)-Catalyzed Intermolecular Cycloadditions, *Adv. Synth. Catal.* **2014**, *356*, 221–228.

⁷¹ Obradors, C.; Echavarren, A. M., Intermolecular Gold-Catalyzed Cycloaddition of Alkynes with Oxoalkenes, *Chem. Eur. J.* **2013**, *19*, 3547–3551.

When working with electron-rich *ortho*-substituted phenylacetylenes **61**, cyclopropyl gold(I) carbene **62**, formed through interaction of the alkene with the more substituted carbon of the alkyne, was shown to be a common intermediate for the expected [2+2] product **65** and for the cross-metathesis product **64**, result of a 1,3-migration through TS **63** (Scheme 10a).⁶⁷ When switching to electron-poor propiolic acid derivatives **66**, the group of Shin reported that cyclopropyl gold carbene **68**, which in contrast to **62**, was formed via interaction of the alkene with the terminal alkyne carbon, can again evolve stereospecifically into 1,3-dienes **70** through TS **69**, similar to **63**, when having 1,2-disubstituted alkenes (Scheme 9b).⁷² In the case of 1,1 di- or trisubstituted alkynes, ring expansion selectively affords α,β -unsaturated δ -lactones **71**, product of formal [4+2] cycloaddition (Scheme 10b).



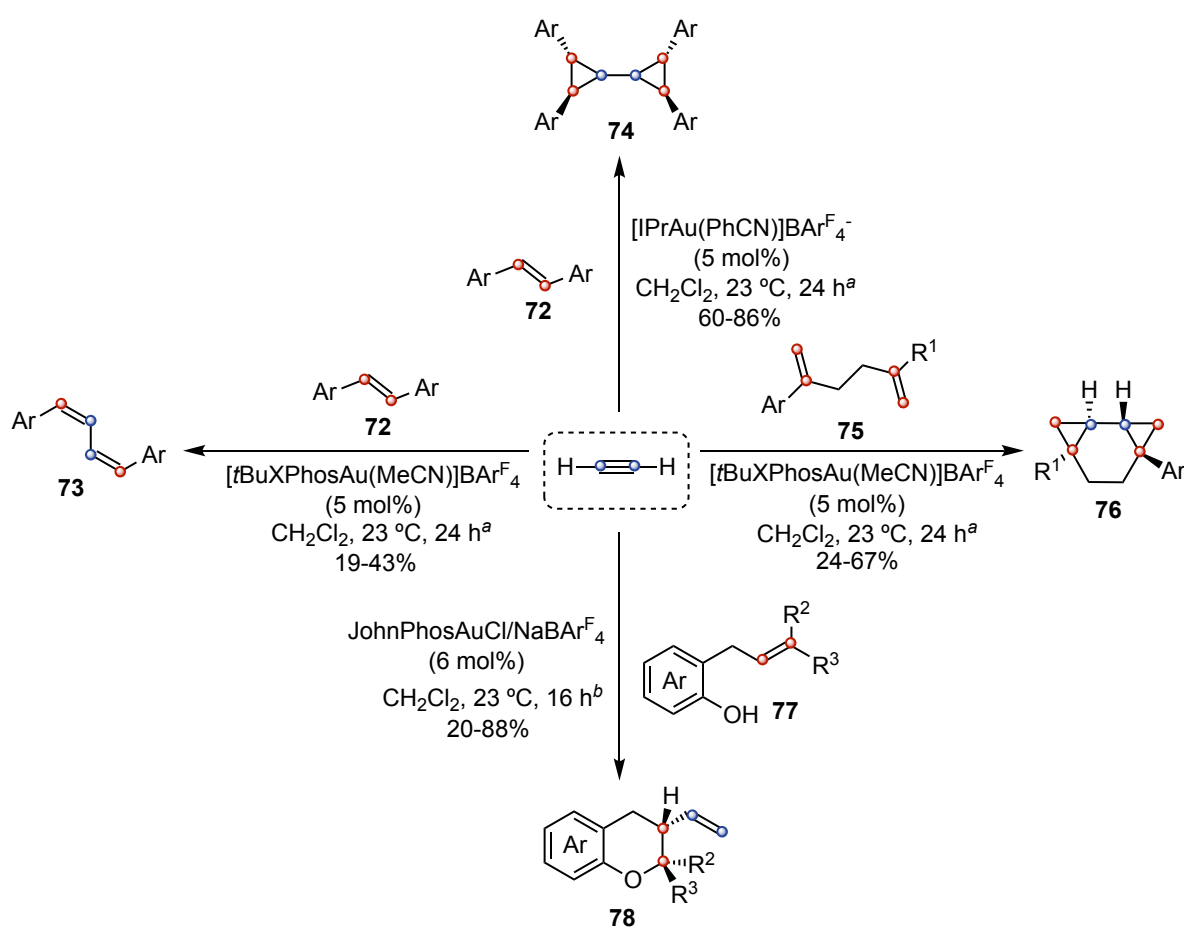
Scheme 10. Gold(I)-catalyzed metathesis vs ring expansion in electron rich (a) and electron poor (b) alkynes.

Always on the topic of intermolecular reactivity, our group has recently developed gold(I)-catalyzed transformations involving acetylene gas (Scheme 11). In the presence of stilbenes **72**, depending on the catalyst used, *Z,Z*-dienes **73** or bicyclopropanes **74** may be formed.⁷³

⁷² Yeom, H.-S.; Koo, J.; Park, H.-S.; Wang, Y.; Liang, Y.; Yu, Z.-X.; Shin, S., Gold-Catalyzed Intermolecular Reactions of Propiolic Acids with Alkenes: [4 + 2] Annulation and Enyne Cross Metathesis, *J. Am. Chem. Soc.* **2012**, *134*, 208–211.

⁷³ Schamagel, D.; Escofet, I.; Armengol-Relats, H.; de Orbe, M. E.; Korber, J. N.; Echavarren, A. M., Acetylene as a Dicarbene Equivalent for Gold(I) Catalysis: Total Synthesis of Waitzicuminone in One Step, *Angew. Chem. Int. Ed.* **2020**, *59*, 4888–489, *Angew. Chem.* **2020**, *132*, 4918–4921.

In the first case, oligomers, result of competing reactions with additional acetylene molecules, were also detected. In the context of the same work, intramolecular biscyclopropanation of 1,5-dienes **75** to form tricyclo[5.1.0.0^{2,4}]octanes **76** as single diastereomers could be achieved, in analogy with previous results obtained using phenylacetylene.⁶² This last transformation could also be applied to the first total synthesis of waitziacuminone,⁷⁴ formed in just one step starting from geranyl acetone. More recently, the use of acetylene was extended to the gold(I)-catalyzed aryloxycyclization of *o*-allylphenols **77** to stereospecifically afford chromanes **78**.⁷⁵ This reaction constitute an intermolecular version of 1,*n*-enyne alkoxycyclizations, introduced above. In this case, the newly formed terminal vinyl groups are less reactive towards acetylene, minimizing the problems associated to oligomerizations. In all the cases mentioned it can be seen how the bulky BARF₄⁻ counteranion was selected to have better results.^{67,70}



Scheme 11. Gold(I)-catalyzed reactions of acetylene gas. ^aAcetylene source: CaC₂ and water. ^bAcetylene introduced at 1.0 bar pressure.

⁷⁴ Jakupovic, J.; Schuster, A.; Bohlmann, F.; King, R. M.; Haegit, L., Labdane Derivatives and Other Constituents from *Waitzia Acuminata*, *Phytochemistry* **1989**, *28*, 1943–1948.

⁷⁵ Medina-Gil, T.; Sadurní, A.; Hammarback, L. A.; Echavarrén, A. M., Gold(I)-Catalyzed Intermolecular Aryloxyvinylolation with Acetylene Gas, *ACS Catal.* **2023**, *13*, 10751–10755.

Asymmetric Gold(I) Catalysis

Accessing optically active chemical compounds has always presented a significant challenge in organic chemistry. In the field of asymmetric catalysis, the four main strategies that have emerged over the years are listed in Figure 4 and they vary depending on where the chiral information is placed among the different reaction components.

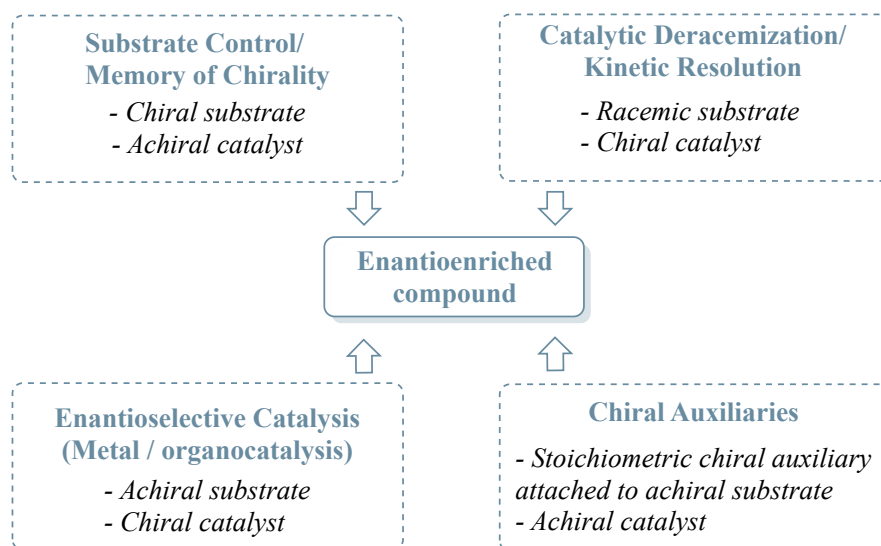


Figure 4. Different strategies to access enantiomerically enriched compounds via asymmetric catalysis.

The substrate control approach envisions an asymmetric reaction where a stereocenter present on a molecule directs the stereoselectivity in the formation of a second chiral center.⁷⁶ When the chirality is preserved even if the stereocenter is broken at some point in the reaction and re-formed in the same or another part of the molecule, the concept of memory of chirality (MOC) comes into play.⁷⁷ In the case of gold(I) catalysis the main cases of MOC are reported for direct nucleophilic addition to C–C bonds or reactions involving migrating groups.⁷⁸ As an example, in 2008 the group of Liu disclosed the regioselective hydrative carbocyclization of enantioenriched allenynes of the type **79** to afford **82**, where through transition state **80**, the preexistent chirality situated on the allene moiety is completely preserved in the final product (Scheme 12a).⁷⁹ The first example of MOC in gold(I)-catalyzed reactions involving migrating groups was described by Nakamura and co-workers, with the carbothiolyation of alkyne **83** which, after gold(I)-catalyzed *5-endo-dig* cyclization, forms zwitterionic species **84**,

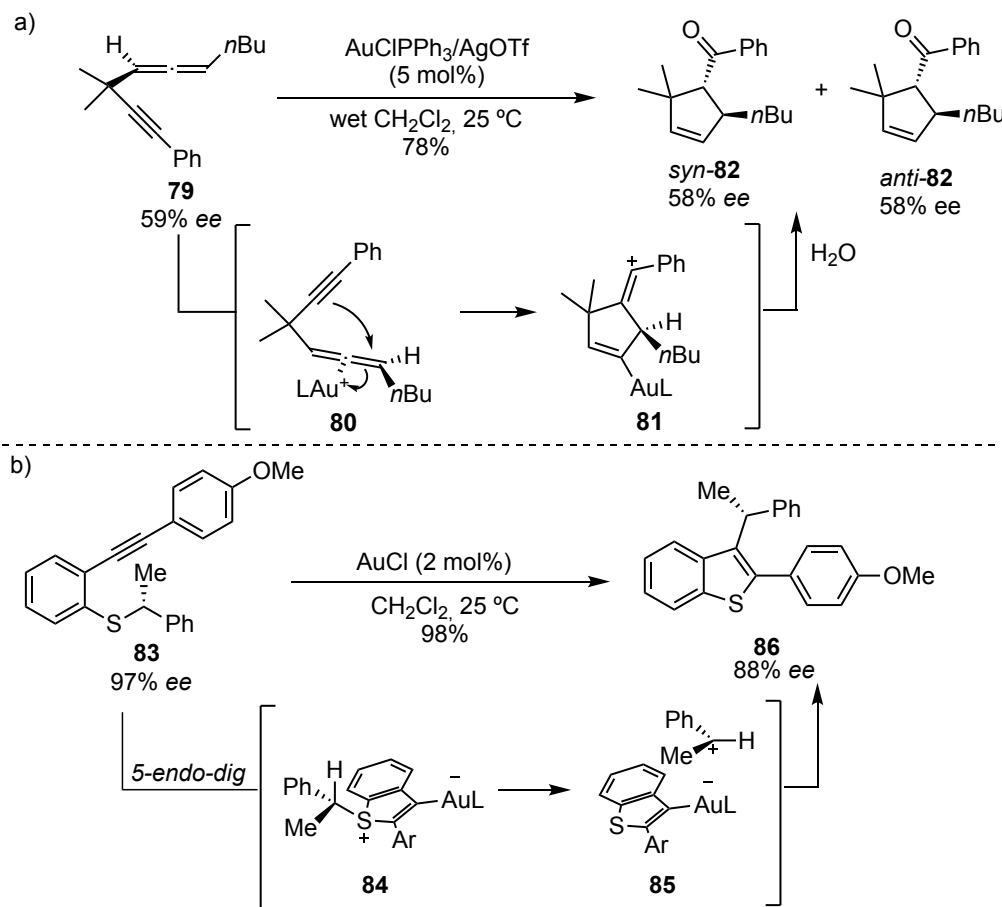
⁷⁶ a) Paek, S.-M.; Jeong, M.; Jo, J.; Heo, Y. M.; Han, Y. T.; Yun, H., Recent Advances in Substrate-Controlled Asymmetric Induction Derived from Chiral Pool α -Amino Acids for Natural Product Synthesis, *Molecules* **2016**, *21*, 951. b) Bhadra, S.; Yamamoto, H., Substrate Directed Asymmetric Reactions, *Chem. Rev.* **2018**, *118*, 3391–3446.

⁷⁷ Kawabata, T.; Yahiro K.; Fuji K., Memory of Chirality: Enantioselective Alkylation Reactions at an Asymmetric Carbon Adjacent to a Carbonyl Group, *J. Am. Chem. Soc.* **1991**, *113*, 9694–9696. b) Zhao, H.; Hsu, D. C.; Carlier, P. R., Memory of Chirality: An Emerging Strategy for Asymmetric Synthesis, *Synthesis* **2005**, *1*, 1–16. c) Hardwick, T.; Ahmed, N., Memory of Chirality as a Prominent Pathway for the Synthesis of Natural Products through Chiral Intermediates, *ChemistryOpen* **2018**, *7*, 484–487.

⁷⁸ Patil, N. T., Chirality Transfer and Memory of Chirality in Gold-Catalyzed Reactions, *Chem. Asian J.* **2012**, *7*, 2186–2194.

⁷⁹ Yang, C.-Y.; Lin, G.-Y.; Liao, H.-Y.; Datta, S.; Liu, R.-S., Gold-Catalyzed Hydrative Carbocyclization of 1,5- and 1,7-Allenynes Mediated by π -Allene Complex: Mechanistic Evidence Supported by the Chirality Transfer of Allenyne Substrates, *J. Org. Chem.* **2008**, *73*, 4907–4914.

precursor of the tight ion pair **85**.⁸⁰ The latter eventually affords the [1,3] migration product **86** with slightly eroded *ee* (Scheme 12b).



Scheme 12. Chirality transfer in: a) gold(I)-catalyzed hydrative carbocyclization of 1,5-allenynes, b) gold(I)-catalyzed carbothioloxylation of *o*-alkynylphenyl 1-arylethyl sulfides.

When having a chiral substrate but in a racemic form, catalytic deracemization approaches can be applied.⁸¹ Given the scarce applications found in gold(I) catalysis, these will not be dealt with in the present introduction.

The most popular strategy to build enantioenriched compounds relies on the use of chiral catalysts. Transition metal catalysis can both rely on chiral-at-metal complexes⁸² or on chiral ligands. In the case of gold(I), its linear coordination geometry places the ligand, which contains the chiral information, and substrate, in opposite positions, precluding the use of conventional chelating ligands and enabling free rotation around L-Au and Au-substrate bonds. Furthermore, gold(I)-catalyzed reactions proceed through outer-sphere activation.

⁸⁰ Nakamura, I.; Sato, T.; Terada, M.; Yamamoto, Y., Chirality Transfer in Gold-Catalyzed Carbothiolation of *o*-Alkynylphenyl 1-Arylethyl Sulfides, *Org. Lett.* **2008**, *10*, 2649–2651.

⁸¹ Huang, M.; Pan, T.; Jiang, X.; Luo, S., Catalytic Deracemization Reactions, *J. Am. Chem. Soc.* **2023**, *145*, 10917–10929.

⁸² Steinlandt, P. S.; Zhang, L.; Meggers, E., Metal Stereogenicity in Asymmetric Transition Metal Catalysis, *Chem. Rev.* **2023**, *123*, 4764–4794.

All of these factors, make the design of effective chiral ligands for asymmetric gold(I) catalysis, challenging (Figure 5).⁸³

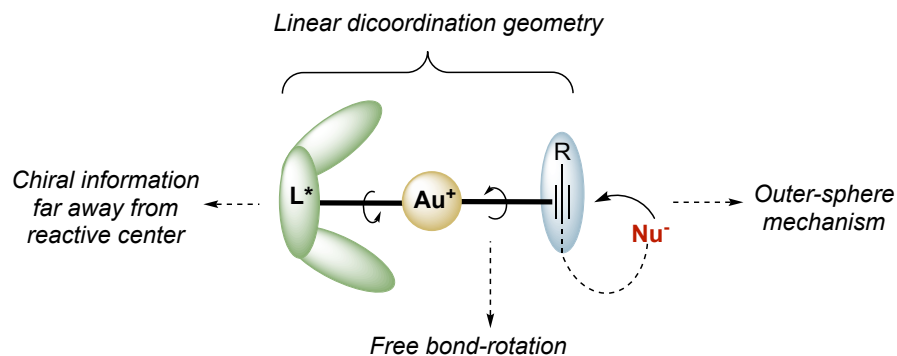


Figure 5. Main limitations of asymmetric gold(I) catalysis.

Three main strategies have been developed so far which rely on different ligand design (Figure 6). The most popular and widely used chiral gold complexes are axially chiral binuclear gold(I) complexes (phosphines or diaminocarbene⁸⁴) which are active for different kind of annulations, including 1,*n* enyne cycloisomerizations (Figure 6a).⁸⁵ In the context of diphosphine ligands, in 2017 our group developed the enantioselective version of the [2+2] cycloaddition of alkynes with alkenes previously introduced,⁶² via the use of non-*C*₂-chiral Josiphos digold(I) complexes.⁸⁶

⁸³ a) Wang, Y.-M.; Lackner, A. D.; Toste, F. D., Development of Catalysts and Ligands for Enantioselective Gold Catalysis, *Acc. Chem. Res.* **2014**, *47*, 889–901. b) Zi, W.; Toste, F. D., Recent Advances in Enantioselective Gold Catalysis, *Chem. Soc. Rev.* **2016**, *45*, 4567–4589. c) Li, Y.; Li, W.; Zhang, J., Gold-Catalyzed Enantioselective Annulations, *Chem. Eur. J.* **2017**, *23*, 467–512. d) Zuccarello, G.; Escofet, I.; Caniparoli, U.; Echavarren, A. M., New-Generation Ligand Design for the Gold-Catalyzed Asymmetric Activation of Alkynes, *ChemPlusChem* **2021**, *86*, 1283–1296. e) Wu, Y.; Yang, H.; Gao, H.; Huang, X.; Geng, L.; Zhang, R., Advances in Versatile Chiral Ligands for Asymmetric Gold Catalysis, *Catalysts* **2023**, *13*, 1294. f) Gade, A. B.; Urvashi; Patil, N. T., Asymmetric Gold Catalysis Enabled by Specially Designed Ligands, *Org. Chem. Front.* **2024**, *11*, 1858–1895.

⁸⁴ a) Bartolomé, C.; García-Cuadrado, D.; Ramiro, Z.; Espinet, P., Synthesis and Catalytic Activity of Gold Chiral Nitrogen Acyclic Carbenes and Gold Hydrogen Bonded Heterocyclic Carbenes in Cyclopropanation of Vinyl Arenes and in Intramolecular Hydroalkoxylation of Allenes, *Inorg. Chem.* **2010**, *49*, 9758–9764. b) Wang, Y.-M.; Kuzniewski, C. N.; Rauniyar, V.; Hoong, C.; Toste, F. D., Chiral (Acyclic Diaminocarbene)Gold(I)-Catalyzed Dynamic Kinetic Asymmetric Transformation of Propargyl Esters, *J. Am. Chem. Soc.* **2011**, *133*, 12972–12975. c) Niemeyer, Z. L.; Pindi, S.; Khrakovsky, D. A.; Kuzniewski, C. N.; Hong, C. M.; Joyce, L. A.; Sigman, M. S.; Toste, F. D., Parameterization of Acyclic Diaminocarbene Ligands Applied to a Gold(I)-Catalyzed Enantioselective Tandem Rearrangement/Cyclization, *J. Am. Chem. Soc.* **2017**, *139*, 12943–12946. d) Vosáhl, P.; Franc, M.; Harmach, P.; Schulz, J.; Štěpnička, P., Synthesis of Gold(I) Diaminocarbene Complexes by the Addition of Amines across Coordinated Isocyanoferrrocene, *J. Organomet. Chem.* **2023**, *1000*, 122874.

⁸⁵ a) Muñoz, M. P.; Adrio, J.; Carretero, J. C.; Echavarren, A. M., Ligand Effects in Gold- and Platinum-Catalyzed Cyclization of Enynes: Chiral Gold Complexes for Enantioselective Alkoxycyclization, *Organometallics* **2005**, *24*, 1293–1300. b) Chao, C.-M.; Vitale, M. R.; Toullec, P. Y.; Genêt, J.-P.; Michelet, V., Asymmetric Gold-Catalyzed Hydroarylation/Cyclization Reactions, *Chem. Eur. J.* **2009**, *15*, 1319–1323. c) Chao, C.-M.; Beltrami, D.; Toullec, P. Y.; Michelet, V., Asymmetric Au(I)-Catalyzed Synthesis of Bicyclo[4.1.0]Heptene Derivatives via a Cycloisomerization Process of 1,6-Enynes, *Chem. Commun.* **2009**, No. 45, 6988–6990. d) Gawade, S. A.; Bhunia, S.; Liu, R.-S., Intermolecular Gold-Catalyzed Diastereo- and Enantioselective [2+2+3] Cycloadditions of 1,6-Enynes with Nitrones, *Angew. Chem. Int. Ed.* **2012**, *51*, 7835–7838, *Angew. Chem.* **2012**, *124*, 7955–7958.

⁸⁶ García-Morales, C.; Ranieri, B.; Escofet, I.; López-Suarez, L.; Obradors, C.; Konovalov, A. I.; Echavarren, A. M., Enantioselective Synthesis of Cyclobutenes by Intermolecular [2+2] Cycloaddition with Non-*C*₂ Symmetric Digold Catalysts, *J. Am. Chem. Soc.* **2017**, *139*, 13628–13631.

A second class of gold(I) complexes envisions monodentate phosphoramidites⁸⁷ mainly used in allenene cyclizations with pioneer work by Toste and co-workers⁸⁸ or phosphonite ligands such as the one introduced by Alcarazo for the synthesis of helicenes starting from diyines⁸⁹ (Figure 6b). Finally, non-chiral gold(I) complexes with chiral counteranions, in particular phosphate species, constitutes another strategy in enantioselective gold catalysis, first introduced by Toste in 2007 (Figure 6c).⁹⁰

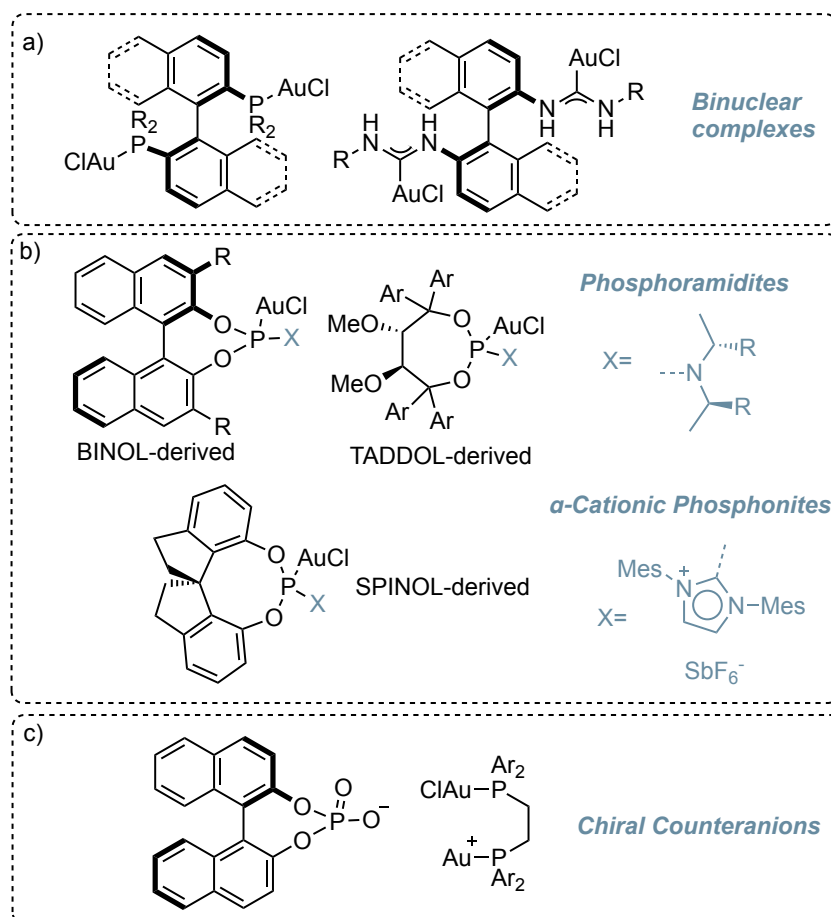


Figure 6. Different ligand design approaches for asymmetric gold(I) catalysis.

⁸⁷ a) Teller, H.; Corbet, M.; Mantilli, L.; Gopakumar, G.; Goddard, R.; Thiel, W.; Fürstner, A., One-Point Binding Ligands for Asymmetric Gold Catalysis: Phosphoramidites with a TADDOL-Related but Acyclic Backbone, *J. Am. Chem. Soc.* **2012**, *134*, 15331–15342. b) Alonso, I.; Trillo, B.; López, F.; Montserrat, S.; Ujaque, G.; Castedo, L.; Lledós, A.; Mascareñas, J. L., Gold-Catalyzed [4C+2C] Cycloadditions of Allenedienes, Including an Enantioselective Version with New Phosphoramidite-Based Catalysts: Mechanistic Aspects of the Divergence between [4C+3C] and [4C+2C] Pathways, *J. Am. Chem. Soc.* **2009**, *131*, 13020–13030.

⁸⁸ a) Luzung, M. R.; Mauleón, P.; Toste, F. D., Gold(I)-Catalyzed [2+2]-Cycloaddition of Allenenes, *J. Am. Chem. Soc.* **2007**, *129*, 12402–12403. b) González, A. Z.; Benitez, D.; Tkatchouk, E.; Goddard, W. A.; Toste, F. D., Phosphoramidite Gold(I)-Catalyzed Diastereo- and Enantioselective Synthesis of 3,4-Substituted Pyrrolidines, *J. Am. Chem. Soc.* **2011**, *133*, 5500–5507.

⁸⁹ González-Fernández, E.; Nicholls, L. D. M.; Schaaf, L. D.; Farès, C.; Lehmann, C. W.; Alcarazo, M., Enantioselective Synthesis of [6]Carbohelicenes, *J. Am. Chem. Soc.* **2017**, *139*, 1428–1431.

⁹⁰ Hamilton, G. L.; Kang, E. J.; Mba, M.; Toste, F. D., A Powerful Chiral Counterion Strategy for Asymmetric Transition Metal Catalysis, *Science* **2007**, *317*, 496–499.

While for years mainly reactions with allenes were described,⁹¹ and neutral gold(I) complexes presenting chiral phosphate ligands were demonstrated to be inactive in enyne cyclizations,⁹² our group recently disclosed an H-bonded counterion-directed strategy which combines an achiral phosphinourea Au(I) chloride complex with a BINOL-derived phosphoramidate Ag(I) salt allowing the use of chiral counteranions for the challenging asymmetric alkyne functionalization.⁹³ Shortly after, the use of chiral gold complexes in combination with chiral counteranion in a matched ion pair fashion was also described for highly enantioselective alkoxy cyclizations of 1,6-enynes.⁹⁴

In the context of asymmetric gold(I)-catalyzed alkyne activation, monophosphines and monodentate NHC have seen more application than the previously mentioned ligands (Figure 7). Just to mention some relevant examples, the groups of Voiturez and Marinetti applied the use of helically chiral phosphaelicenes functionalized with chiral menthyl substituent (named HelPhos) to the cycloisomerization of *N*-tethered 1,6-enynes (Figure 7a).⁹⁵ The use of monophosphines presenting a remote basic group that assists alkyne deprotonation (WangPhos-type ligands)⁹⁶ or stabilizes α -oxo-gold carbene intermediates in oxidative enyne cyclizations (DalPhos type-ligands)⁹⁷ was introduced by the group of Zhang (Figure 7b). Finally, in the context of monodentate NHC ligands,⁹⁸ recently, Autschbach, Crassous, Bastin, and César introduced a novel design for a chiral NHC-gold complex, featuring a configurationally stable pentahelicenic unit attached to the C5 position of an imidazo[1,5-*a*]pyridinium bicycle which exhibits central, axial, and helical chirality (Figure 7c).⁹⁹ The complex was applied in the gold(I)-catalyzed cycloisomerization of *N*-tethered 1,6-enynes, yielding cycloadducts with remarkable enantioselectivities.

⁹¹ LaLonde, R. L.; Wang, Z. J.; Mba, M.; Lackner, A. D.; Toste, F. D., Gold(I)-Catalyzed Enantioselective Synthesis of Pyrazolidines, Isoxazolidines, and Tetrahydrooxazines, *Angew. Chem. Int. Ed.* **2010**, *49*, 598–601, *Angew. Chem.* **2010**, *122*, 608–611. b) Zi, W.; Toste, F. D., Gold(I)-Catalyzed Enantioselective Desymmetrization of 1,3-Diols through Intramolecular Hydroalkoxylation of Allenes, *Angew. Chem. Int. Ed.* **2015**, *54*, 14447–14451, *Angew. Chem.* **2015**, *127*, 14655–14659. c) Pedrazzani, R.; An, J.; Monari, M.; Bandini, M., New Chiral BINOL-Based Phosphates for Enantioselective [Au(I)]-Catalyzed Dearomatization of β -Naphthols with Allenamides, *Eur. J. Org. Chem.* **2021**, *2021*, 1732–1736.

⁹² Raducan, M.; Moreno, M.; Bour, C.; Echavarren, A. M., Phosphate Ligands in the Gold(I)-Catalysed Activation of Enynes, *Chem. Commun.* **2011**, *48*, 52–54.

⁹³ a) Franchino, A.; Martí, À.; Echavarren, A. M., H-Bonded Counterion-Directed Enantioselective Au(I) Catalysis, *J. Am. Chem. Soc.* **2022**, *144*, 3497–3509. b) Martí, À.; Montesinos-Magraner, M.; Echavarren, A. M.; Franchino, A., H-Bonded Counterion-Directed Catalysis: Enantioselective Gold(I)-Catalyzed Addition to 2-Alkynyl Enones as a Case Study, *Eur. J. Org. Chem.* **2022**, *2022*, e202200518.

⁹⁴ Martí, À.; Ogalla, G.; Echavarren, A. M., Hydrogen-Bonded Matched Ion Pair Gold(I) Catalysis, *ACS Catal.* **2023**, *13*, 10217–10223.

⁹⁵ Yavari, K.; Aillard, P.; Zhang, Y.; Nuter, F.; Retailleau, P.; Voiturez, A.; Marinetti, A., Helicenes with Embedded Phosphole Units in Enantioselective Gold Catalysis, *Angew. Chem. Int. Ed.* **2014**, *53*, 861–865, *Angew. Chem.* **2014**, *126*, 880–884.

⁹⁶ Wang, Y.; Wang, Z.; Li, Y.; Wu, G.; Cao, Z.; Zhang, L., A General Ligand Design for Gold Catalysis Allowing Ligand-Directed Anti-Nucleophilic Attack of Alkynes, *Nat. Commun.* **2014**, *5*, 3470.

⁹⁷ Ji, K.; Zheng, Z.; Wang, Z.; Zhang, L., Enantioselective Oxidative Gold Catalysis Enabled by a Designed Chiral P,N-Bidentate Ligand, *Angew. Chem. Int. Ed.* **2015**, *54*, 1245–1249, *Angew. Chem.* **2015**, *127*, 1261–1265.

⁹⁸ a) Banerjee, D.; Buzas, A. K.; Besnard, C.; Kündig, E. P., Chiral *N*-Heterocyclic Carbene Gold Complexes: Synthesis, Properties, and Application in Asymmetric Catalysis, *Organometallics* **2012**, *31*, 8348–8354. b) Michalak, M.; Kośnik, W., Chiral *N*-Heterocyclic Carbene Gold Complexes: Synthesis and Applications in Catalysis, *Catalysts* **2019**, *9*, 890.

⁹⁹ Pallova, L.; Abella, L.; Jean, M.; Vanthuynne, N.; Barthes, C.; Vendier, L.; Autschbach, J.; Crassous, J.; Bastin, S.; César, V., Helical Chiral *N*-Heterocyclic Carbene Ligands in Enantioselective Gold Catalysis, *Chem. Eur. J.* **2022**, *28*, e202200166.

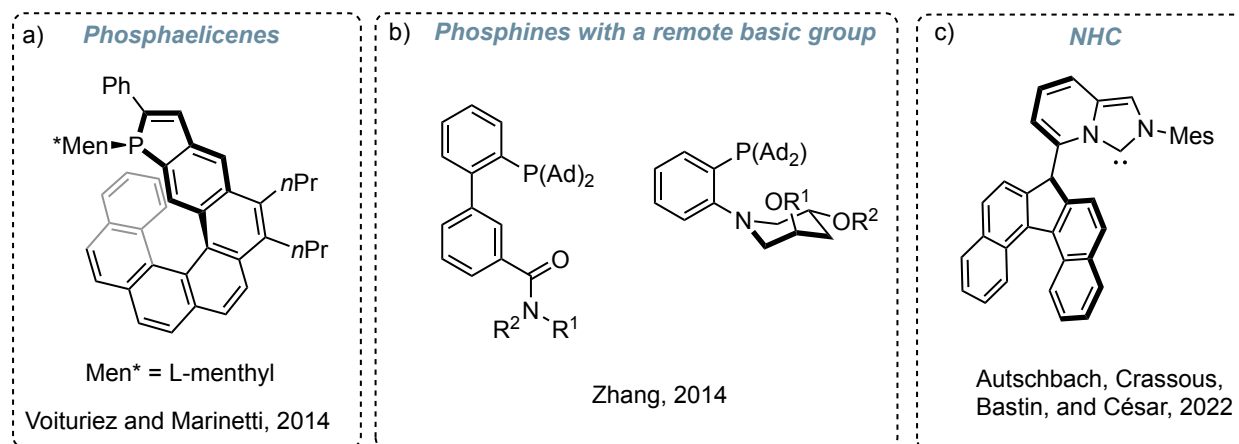


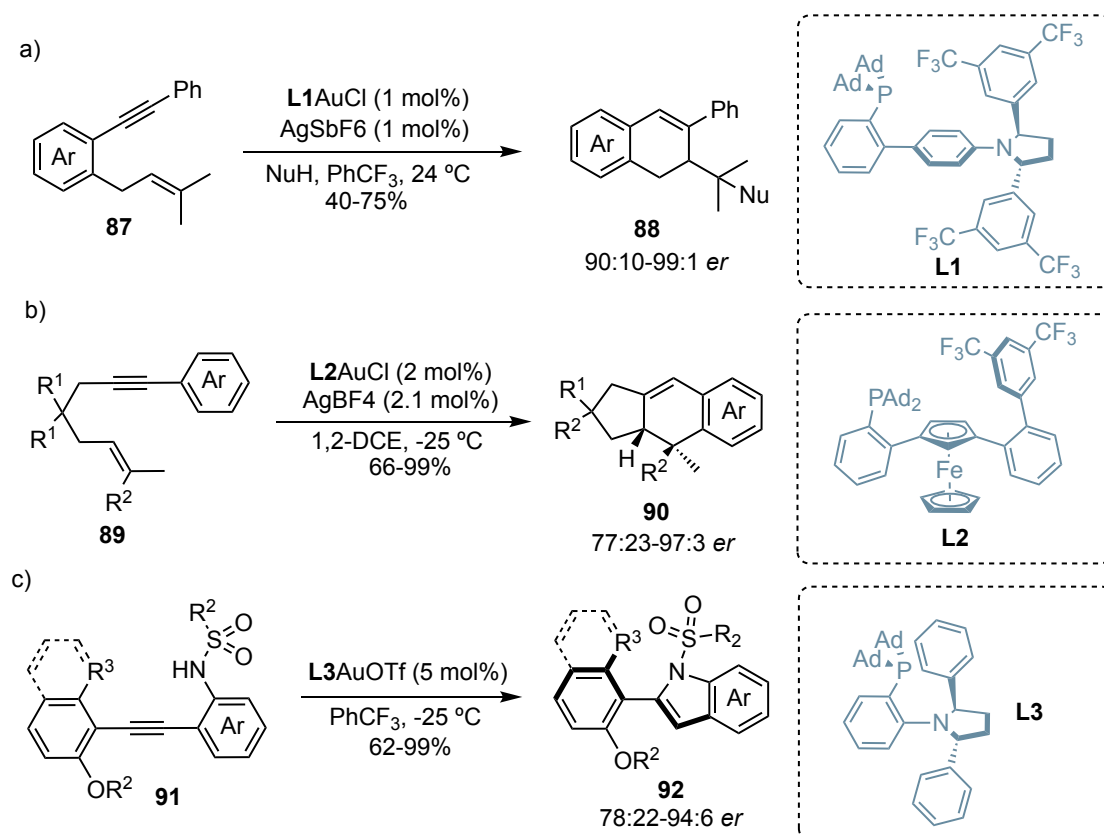
Figure 7. Chiral monophosphines and monodentate NHC used in asymmetric gold(I)-catalyzed alkyne activation.

Our group has recently introduced a novel series of customized JohnPhos-type ligands featuring a C_2 -symmetric chiral diaryl pyrrolidine moiety positioned at the para position of the biphenyl scaffold (Scheme 13).¹⁰⁰ These complexes were tested, showing excellent levels of enantioinduction, in different 1,6-enyne cyclizations including [4+2] cycloadditions, synthesis of azabicyclo[4.1.0]hept-4-enes and alkoxy cyclizations, the latter being applied to the total synthesis of different members of the carexane natural product family derived from **88** (Scheme 13a). DFT calculations revealed that non-covalent π - π interactions between the enynes and the ligand are key for the selective encapsulation of substrates in the chiral pocket of the gold(I) complex. Inspired by this design, shortly after, planar monodentate chiral 1,3-disubstituted ferrocene phosphine ligands were introduced, which could be synthesized in fewer steps compared to the pyrrolidine antecedents and were also applied to highly enantioselective [4+2] cycloadditions of 1,6-enynes **89** to afford tricyclic scaffolds **90** (Scheme 13b).¹⁰¹ Finally, shorter analogues of the aforementioned pyrrolidine ligands were developed and used in the atroposelective cyclization of diarylacetylenes **91** to afford axially chiral indoles **92** (Scheme 13c).¹⁰²

¹⁰⁰ Zuccarello, G.; Mayans, J. G.; Escofet, I.; Scharnagel, D.; Kirillova, M. S.; Pérez-Jimeno, A. H.; Calleja, P.; Boothe, J. R.; Echavarren, A. M., Enantioselective Folding of Enynes by Gold(I) Catalysts with a Remote C_2 -Chiral Element, *J. Am. Chem. Soc.* **2019**, *141*, 11858–11863.

¹⁰¹ Caniparoli, U.; Escofet, I.; Echavarren, A. M., Planar Chiral 1,3-Disubstituted Ferrocenyl Phosphine Gold(I) Catalysts, *ACS Catal.* **2022**, *12*, 3317–3322.

¹⁰² Zuccarello, G.; Nannini, L. J.; Arroyo-Bondía, A.; Fincias, N.; Arranz, I.; Pérez-Jimeno, A. H.; Peeters, M.; Martín-Torres, I.; Sadurní, A.; García-Vázquez, V.; Wang, Y.; Kirillova, M. S.; Montesinos-Magraner, M.; Caniparoli, U.; Núñez, G. D.; Maseras, F.; Besora, M.; Escofet, I.; Echavarren, A. M., Enantioselective Catalysis with Pyrrolidinyl Gold(I) Complexes: DFT and NEST Analysis of the Chiral Binding Pocket, *JACS Au* **2023**, *3*, 1742–1754.



Scheme 13. Chiral monophosphine ligands for gold(I)-catalyzed cyclizations recently designed in our group.

When instead of a metal center, a chiral organic molecule is used as a catalyst, it is the case of organocatalysis.¹⁰³ Even if organocatalysis by definition doesn't require the use of metals, merging it with gold(I) catalysis has brought to a) extending the organocatalysts scope to alkyne chemistry and b) providing an alternative, compared to the traditional and challenging ligand design, for inducing enantioselectivity in gold(I)-catalyzed transformation.¹⁰⁴

As a key example, in 2009, Krause and Alexakis developed an one-pot Michael addition-tandem acetalization/cyclization envisioning the use of achiral PPh_3AuCl and a chiral pyrrolidine (Scheme 14a).¹⁰⁵ Initially, isovaleraldehyde **94** reacts via Michael addition with nitroenyne **93** in the presence of chiral pyrrolidine catalyst **95**, resulting in the formation of aldehyde **96** with high diastereoselectivity (up to 97:3 *dr* for *syn:anti*) and enantioselectivity (up to >99% *ee*).

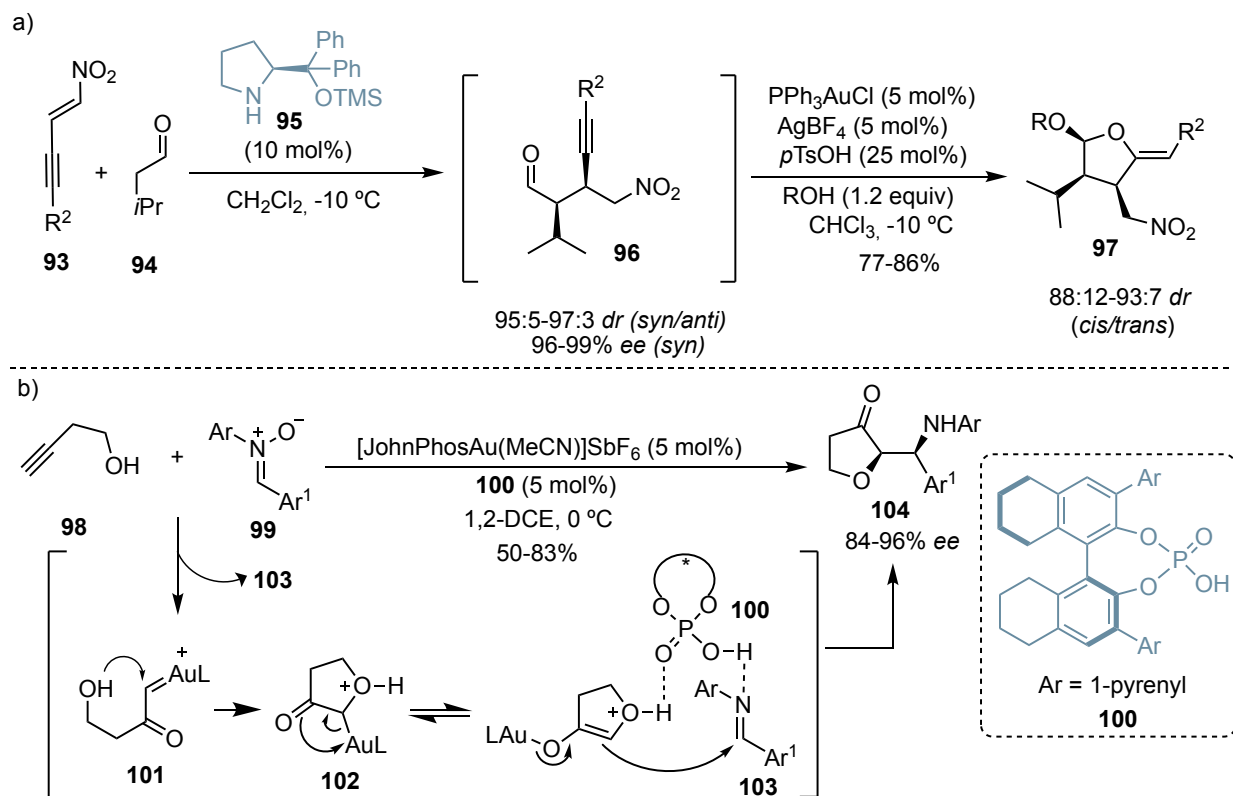
¹⁰³ a) Xiang, S.-H.; Tan, B., Advances in Asymmetric Organocatalysis over the Last 10 Years, *Nat. Commun.* **2020**, *11*, 3786. b) Han, B.; He, X.-H.; Liu, Y.-Q.; He, G.; Peng, C.; Li, J.-L., Asymmetric Organocatalysis: An Enabling Technology for Medicinal Chemistry, *Chem. Soc. Rev.* **2021**, *50*, 1522–1586. c) Melnyk, N.; Iribarren, I.; Mates-Torres, E.; Trujillo, C., Theoretical Perspectives in Organocatalysis, *Chem. Eur. J.* **2022**, *28*, e202201570. d) García Mancheño, O.; Waser, M., Recent Developments and Trends in Asymmetric Organocatalysis, *Eur. J. Org. Chem.* **2023**, *26*, e202200950.

¹⁰⁴ a) Hashmi, A. S. K.; Hubbert, C., Gold and Organocatalysis Combined, *Angew. Chem. Int. Ed.* **2010**, *49*, 1010–1012. b) Loh, C. C. J.; Enders, D., Merging Organocatalysis and Gold Catalysis - A Critical Evaluation of the Underlying Concepts, *Chem. Eur. J.* **2012**, *18*, 10212–10225. c) Pegu, C.; Paroi, B.; Patil, N. T., Enantioselective Merged Gold/Organocatalysis, *Chem. Commun.* **2024**, *60*, 3607–3623.

¹⁰⁵ Belot, S.; Vogt, K. A.; Besnard, C.; Krause, N.; Alexakis, A. Enantioselective One-Pot Organocatalytic Michael Addition/Gold-Catalyzed Tandem Acetalization/Cyclization. *Angew. Chem. Int. Ed.* **2009**, *48*, 8923–8926, *Angew. Chem.* **2009**, *121*, 9085–9088.

Subsequently, the newly formed aldehyde undergoes gold-catalyzed tandem acetalization/cyclization in the presence of alcohols, affording tetrahydrofuranyl ether **97** with yields ranging from 77% to 86% and up to 93 :7 *dr* for *cis/trans* isomers.

Apart from chiral amines, also chiral Brønsted acids were widely used in combination with gold catalysis.¹⁰⁶ In contrast to the previously mentioned chiral counteranion strategy, in this case gold, is not always strictly involved in the enantiodetermining step. Hu and Xu in 2018 reported the enantioselective Mannich-type reaction of 3-butynol and nitrones operated through cooperative catalysis between the [JohnPhosAu(MeCN)]SbF₆ complex and chiral Brønsted acid **100** (Scheme 14b).¹⁰⁷ After gold-catalyzed oxidation of **98** in the presence of **99**, with concomitant elimination of imine **103**, intramolecular attack of the tethered hydroxyl group on the gold carbene species **101** yields the gold-oxonium ylide **102**. The enolate form of the latter species undergoes a Mannich-type addition with the eliminated **103** under enantioselective catalysis operated by **100** through dual H-bonding, resulting in the formation of enantioenriched **104**.



Scheme 14. Use of organocatalysts in combination with gold(I) catalysis.

¹⁰⁶ Inamdar, S. M.; Konala, A.; Patil, N. T., When Gold Meets Chiral Brønsted Acid Catalysts: Extending the Boundaries of Enantioselective Gold Catalysis, *Chem. Commun.* **2014**, 50, 15124–15135.

¹⁰⁷ Wei, H.; Bao, M.; Dong, K.; Qiu, L.; Wu, B.; Hu, W.; Xu, X. Enantioselective Oxidative Cyclization/Mannich Addition Enabled by Gold(I)/Chiral Phosphoric Acid Cooperative Catalysis. *Angew. Chem. Int. Ed.* **2018**, 57, 17200–17204, *Angew. Chem.* **2018**, 130, 17446–17450.

A last widely affirmed strategy to access chiral molecules, similar in concept to organocatalysis, sees the use of chiral auxiliaries. In this case, the chiral moiety, added in a stoichiometric amount, has to be previously attached to the achiral substrate and then removed after having achieved the target stereoselective transformation.¹⁰⁸ There are very few examples of chiral auxiliaries used in combination with gold(I) catalysis: the topic will be object of the following chapter.

¹⁰⁸ a) Christmann, M., Bräse, S., *Asymmetric Synthesis: The Essentials*, Eds.; Wiley-VCH: Weinheim, **2007**. b) Diaz-Muñoz, G.; Miranda, I. L.; Sartori, S. K.; De Rezende, D. C.; Alves Nogueira Diaz, M., Use of Chiral Auxiliaries in the Asymmetric Synthesis of Biologically Active Compounds: A Review, *Chirality* **2019**, *31*, 776–812.

UNIVERSITAT ROVIRA I VIRGILI

GOLD(I)-CATALYZED ASYMMETRIC CYCLIZATIONS AND CYCLOADDITIONS OF HETEROATOM-SUBSTITUTED ALKYNES WITH ALKENES

Andrea Cataffo

UNIVERSITAT ROVIRA I VIRGILI

GOLD(I)-CATALYZED ASYMMETRIC CYCLIZATIONS AND CYCLOADDITIONS OF HETEROATOM-SUBSTITUTED ALKYNES WITH ALKENES

Andrea Cataffo

Chapter I

Chiral Auxiliary Approach for Gold(I)-Catalyzed Cyclizations

UNIVERSITAT ROVIRA I VIRGILI

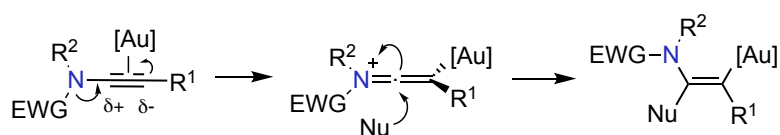
GOLD(I)-CATALYZED ASYMMETRIC CYCLIZATIONS AND CYCLOADDITIONS OF HETEROATOM-SUBSTITUTED ALKYNES WITH ALKENES

Andrea Cataffo

Introduction

Ynamides in Gold(I)-Catalysis

Nitrogen-substituted alkynes, ynamines, and their electron-deficient version, ynamides, present an intrinsic polarization of the *N*-lone pair electrons which makes the α -carbon electrophilic and the β -carbon nucleophilic. This yields opportunities for addressing regio- and chemoselectivity challenges in the development of unconventional synthetic transformations.¹ In the presence of gold(I) catalysts, ynamides form a polarized keteniminium intermediate which favors the attack of nucleophiles to the α -position (Scheme 1.1).² Conversely, ynamines lacking an electron-withdrawing group on the nitrogen atom have seen limited use in synthesis due to challenges associated with their preparation and handling (notably sensitive to hydrolysis and exhibiting high reactivity).



Scheme 1.1. Reactivity of ynamides under gold(I) catalysis.

Many examples of direct attack of *O*- and *N*-nucleophiles to ynamides in the presence of gold(I) catalysts have been reported so far (Scheme 1.2). As representative examples, the group of Sueda reported in 2013 the bimetallic Ag/Au approach to catalyze alcohol addition to *N*-substituted triple bonds to give β -regioselective carbonylation products **1.1**.³ The carboxylation of ynamides through formal [4+3] cycloaddition of epoxides⁴ and [4+2] cycloaddition of oxetanes⁵ described by the group of Liu led to valuable oxygen-containing cyclic enamines **1.2** and **1.3**. As for nitrogen containing nucleophiles, anilines could be successfully used to form imines **1.4** via gold(I)-catalyzed hydroamination of ynamides.⁶

¹ a) DeKorver, K. A.; Li, H.; Lohse, A. G.; Hayashi, R.; Lu, Z.; Zhang, Y.; Hsung, R. P., Ynamides: A Modern Functional Group for the New Millennium, *Chem. Rev.* **2010**, *110*, 5064–5106. b) Evano, G.; Coste, A.; Jouvin, K., Ynamides: Versatile Tools in Organic Synthesis, *Angew. Chem. Int. Ed.* **2010**, *49*, 2840–2859, *Angew. Chem.* **2010**, *122*, 2902–2921. c) Lynch, C. C.; Sripada, A.; Wolf, C., Asymmetric Synthesis with Ynamides: Unique Reaction Control, Chemical Diversity and Applications, *Chem. Soc. Rev.* **2020**, *49*, 8543–8583. d) Luo, J.; Chen, G.-S.; Chen, S.-J.; Yu, J.-S.; Li, Z.-D.; Liu, Y.-L., Exploiting Remarkable Reactivities of Ynamides: Opportunities in Designing Catalytic Enantioselective Reactions, *ACS Catal.* **2020**, *10*, 13978–13992. e) Chen, Y.-B.; Qian, P.-C.; Ye, L.-W., Brønsted Acid-Mediated Reactions of Ynamides, *Chem. Soc. Rev.* **2020**, *49*, 8897–8909. f) Hu, Y.-C.; Zhao, Y.; Wan, B.; Chen, Q.-A., Reactivity of Ynamides in Catalytic Intermolecular Annulations, *Chem. Soc. Rev.* **2021**, *50*, 2582–2625.

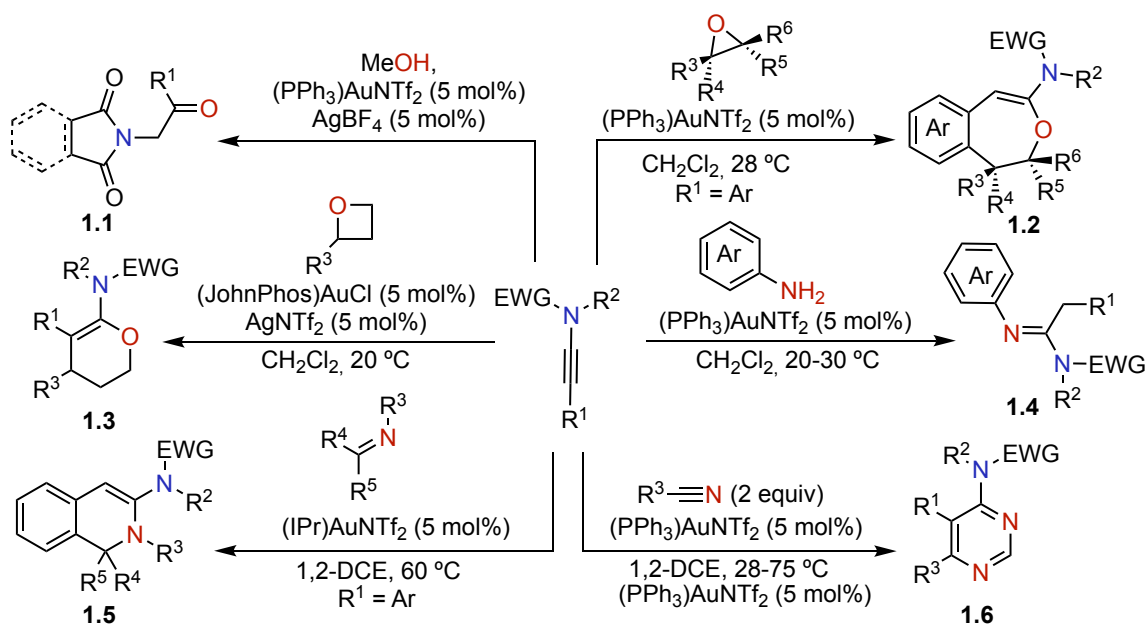
² a) Shandilya, S.; Protim Gogoi, M.; Dutta, S.; Sahoo, A. K., Gold-Catalyzed Transformation of Ynamides, *Chem. Rec.* **2021**, *21*, 4123–4149. b) Campeau, D.; León Rayo, D. F.; Mansour, A.; Muratov, K.; Gagosz, F., Gold-Catalyzed Reactions of Specially Activated Alkynes, Allenes, and Alkenes, *Chem. Rev.* **2021**, *121*, 8756–8867.

³ Sueda, T.; Kawada, A.; Urashi, Y.; Teno, N., Ag- and Au-Catalyzed Addition of Alcohols to Ynamides: β -Regioselective Carbonylation and Production of Oxazoles, *Org. Lett.* **2013**, *15*, 1560–1563.

⁴ Karad, S. N.; Bhunia, S.; Liu, R.-S., Retention of Stereochemistry in Gold-Catalyzed Formal [4+3] Cycloaddition of Epoxides with Arenynamides, *Angew. Chem. Int. Ed.* **2012**, *51*, 8722–8726, *Angew. Chem.* **2012**, *124*, 8852–8856.

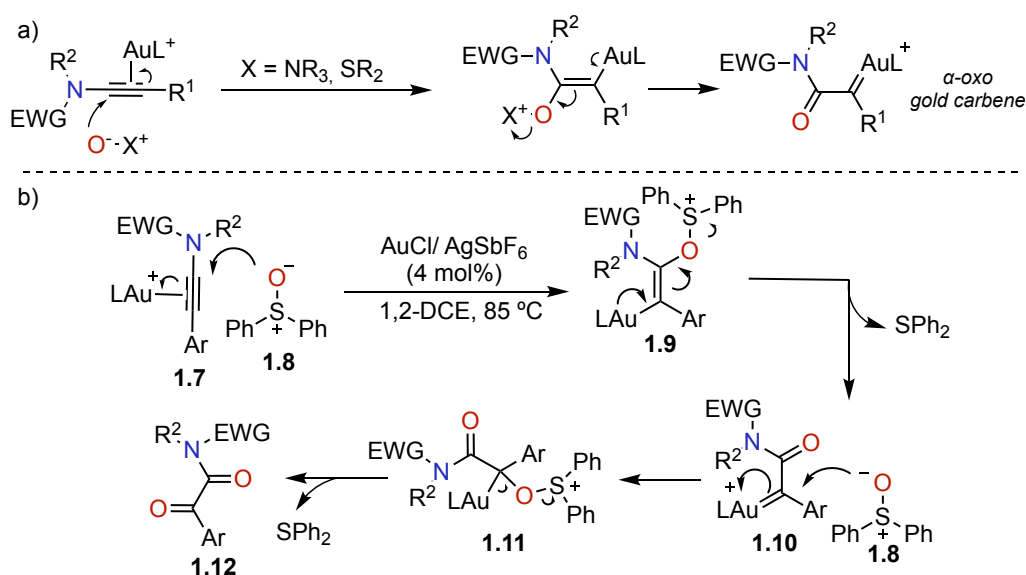
⁵ Pawar, S. K.; Vasu, D.; Liu, R.-S., Gold- and Silver-Catalyzed [4+2] Cycloadditions of Ynamides with Oxetanes and Azetidines, *Adv. Synth. Catal.* **2014**, *356*, 2411–2416.

⁶ Kramer, S.; Dooleweerd, K.; Lindhardt, A. T.; Rottländer, M.; Skrydstrup, T., Highly Regioselective Au(I)-Catalyzed Hydroamination of Ynamides and Propiolic Acid Derivatives with Anilines, *Org. Lett.* **2009**, *11*, 4208–4211.



Scheme 1.2. Intermolecular gold(I)-catalyzed reactions of ynamides with *O*- and *N*- nucleophiles.

Imines⁷ and nitriles⁸ were also described to respectively form dihydroisoquinolines **1.5** and pyrimidines **1.6** under gold(I) catalysis and heating. Another mood of reactivity of ynamides with gold(I) sees the formation of α -oxo (Scheme 1.3a) and α -imino (Scheme 1.4a) gold(I) carbene intermediates when using respectively *N*-oxide/sulfoxide derivatives or nitrene-transfer reagents.



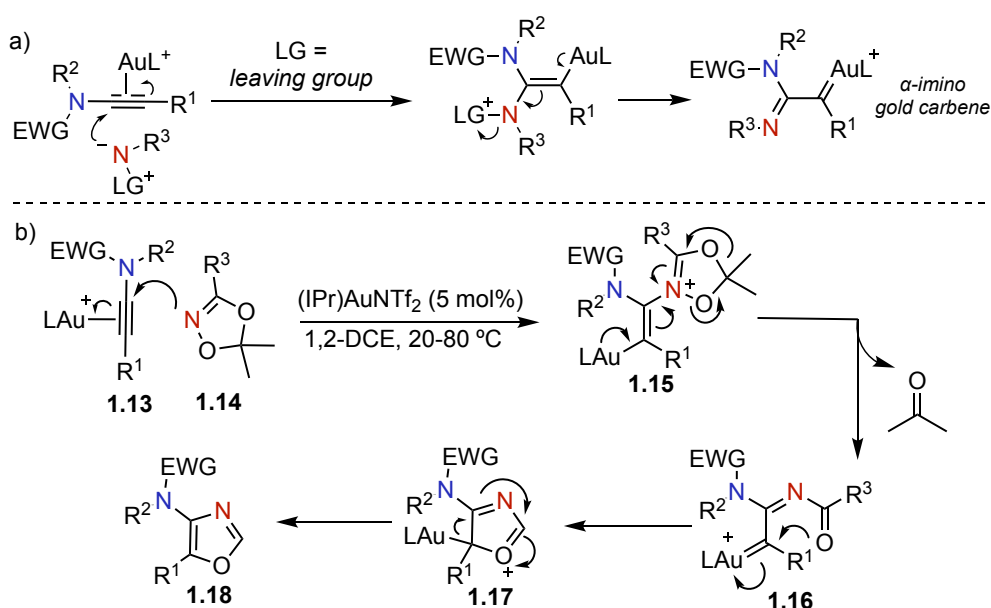
Scheme 1.3. a) Generation of α -oxo gold carbenes starting from ynamides. b) Oxidation of ynamides to 1,2-dicarbonyl derivatives through the use of sulfoxides.

⁷ Xin, Z.; Kramer, S.; Overgaard, J.; Skrydstrup, T., Access to 1,2-Dihydroisoquinolines through Gold-Catalyzed Formal [4+2] Cycloaddition, *Chem. Eur. J.* **2014**, *20*, 7926–7930.

⁸ Karad, S. N.; Liu, R.-S., Regiocontrolled Gold-Catalyzed [2+2+2] Cycloadditions of Ynamides with Two Discrete Nitriles to Construct 4-Aminopyrimidine Cores, *Angew. Chem. Int. Ed.* **2014**, *53*, 9072–9076, *Angew. Chem.* **2014**, *126*, 9218–9222.

As an example, the group of Li reported that in the presence of diphenyl sulfoxide **1.8**, ynamide **1.7** could be converted to α -oxo carbene intermediate **1.10**, which, attacked by a second molecule of **1.8** affords 1,2-dicarbonyl derivatives **1.12** through the elimination of SPh_2 (Scheme 1.3b).⁹

As for nitrene-transfer reactions through α -imino gold carbenes, among the many cases reported in literature, it is worth to mention the report from the group of Liu (Scheme 1.4b).¹⁰ Dioxazoles **1.14** could be reacted with ynamides **1.13** to generate iminium ion **1.15** which, after ring fragmentation and acetone elimination, forms α -imino gold-carbene **1.16**. Notably, acetone was generated quantitatively and detectable in the crude reaction mixture. Subsequently, nucleophilic attack of the acyl oxygen in **1.16** onto the gold-carbene occurs, followed by elimination of the gold catalyst, ultimately leading to the formation of oxazole products **1.18**.



Scheme 1.4. a) Generation of α -imino gold carbenes starting from ynamides. b) Use of dioxazoles as nitrene equivalents for the synthesis of oxazoles.

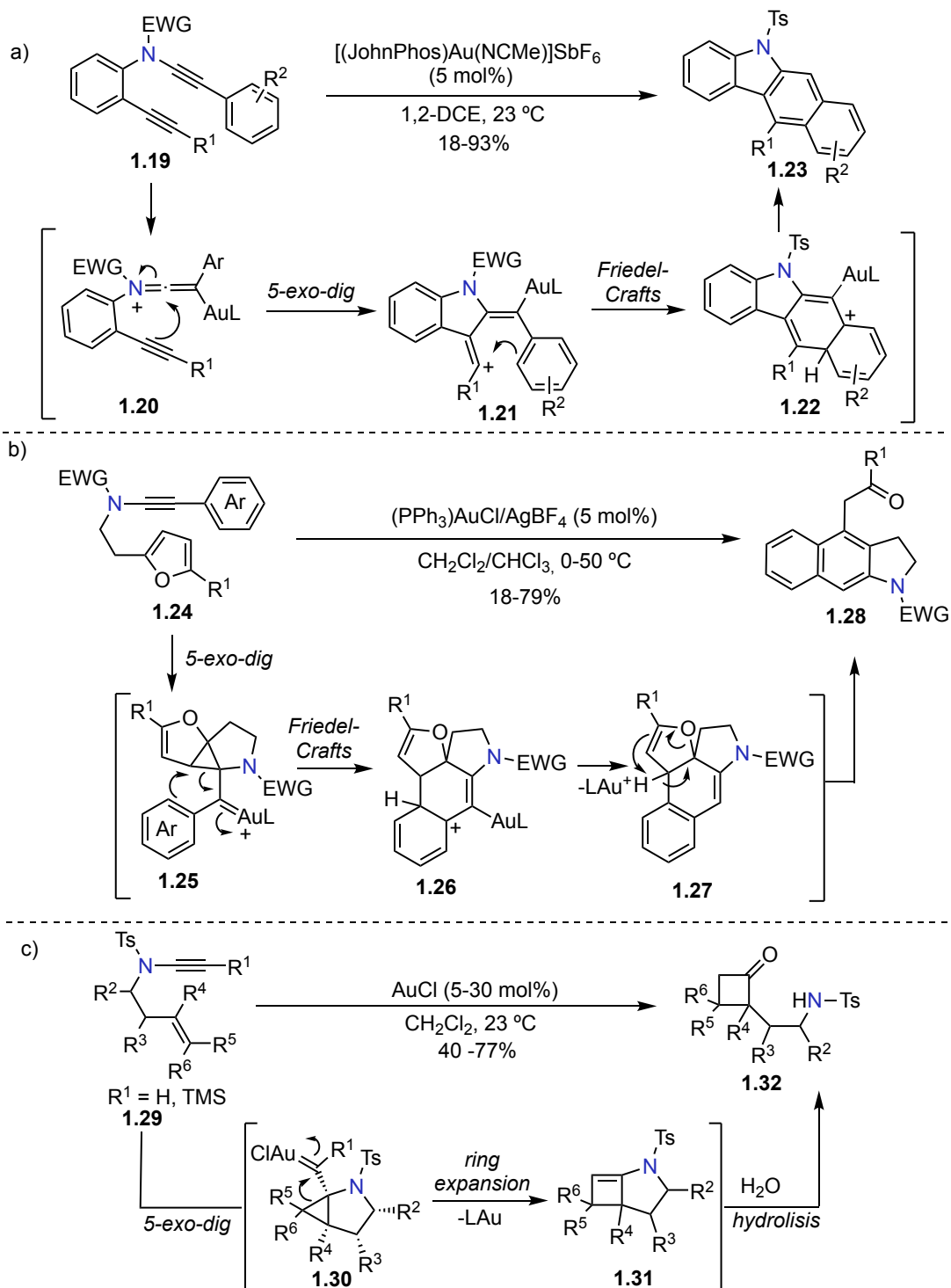
As far as concerns reactivity with carbon nucleophiles, several gold(I)-catalyzed alkyne, aryl and alkene additions to the triple bond of ynamides were described over the years. Alkyne-tethered ynamides **1.19** were reported to react through an intramolecular dehydro-Diels-Alder under gold(I)-catalysis via keteniminium ion **1.20**, which, after a *5-exo-dig*/Friedel-Crafts/protodeauration sequence, affords benzocarbazoles **1.23** in moderate to excellent yields (Scheme 1.5a).¹¹ The group of Hashmi studied the *5-exo-dig* cyclization of furan-ynamides **1.24** followed by a Friedel-Crafts type addition in **1.25** to form

⁹ Xu, C.-F.; Xu, M.; Jia, Y.-X.; Li, C.-Y., Gold-Catalyzed Synthesis of Benzil Derivatives and α -Keto Imides via Oxidation of Alkynes, *Org. Lett.* **2011**, *13*, 1556–1559.

¹⁰ Chen, M.; Sun, N.; Chen, H.; Liu, Y., Dioxazoles, a New Mild Nitrene Transfer Reagent in Gold Catalysis: Highly Efficient Synthesis of Functionalized Oxazoles, *Chem. Commun.* **2016**, *52*, 6324–6327.

¹¹ Xu, W.; Wang, G.; Xie, X.; Liu, Y., Gold(I)-Catalyzed Formal Intramolecular Dehydro-Diels-Alder Reaction of Ynamide-Ynes: Synthesis of Functionalized Benzo[*b*]Carbazoles, *Org. Lett.* **2018**, *20*, 3273–3277.

1.26 which, after rearrangement and protodeauration, delivers polycyclic heterocycles **1.28** (Scheme 1.5b).¹²



Scheme 1.5. a) Formal tetrahydro-Diels–Alder of alkyne tethered ynamides to form benzocarbazoles. b) Gold(I)-catalyzed furan-ynamide cycloisomerization. c) Gold(I)-catalyzed cycloisomerization of 1,6-enynamides followed by hydrolysis.

¹² Hashmi, A. S. K.; Pankajakshan, S.; Rudolph, M.; Enns, E.; Bander, T.; Rominger, F.; Frey, W., Gold Catalysis: Anellated Heterocycles and Dependency of the Reaction Pathway on the Tether Length, *Adv. Synth. Catal.* **2009**, 351, 2855–2875.

Always starting from 1,6-enynes, Cossy and co-workers described the AuCl-catalyzed cycloisomerization of ene-ynamides **1.29**, which, through 5-*exo-dig* cyclization to form cyclopropyl gold(I) carbene **1.30** and subsequent ring expansion, yields cyclobutene **1.31** (Scheme 1.5c).¹³ This species, in the presence of the residual water present in the solvent, spontaneously evolves into cyclobutanones of the type **1.32**.

While the intramolecular examples with unsaturated carbon nucleophiles reported in literature are numerous,¹⁴ less are the cases of intermolecular reactivity. Ynamides were described to behave both as electrophiles and nucleophiles in the gold(I)-catalyzed homodimerization reaction described by Gagosz and Skrydstrup (Scheme 1.6a).¹⁵ After the attack of a unit of **1.33** to another, to form keteniminium **1.34**, a 1,5-H shift brings to intermediate **1.35** which undergoes a metalla-Nazarov¹⁶ reaction leading to **1.36**. Finally, a 1,2-H shift/gold(I) catalyst regeneration brings to cyclopentadiene products of the type **1.37**. In the context of alkyne-alkyne reactivity, the group of Haberhauer recently described that, in the presence of terminal acetylenes, regio- and stereoselective synthesis of ynenamides can be achieved through gold(I)-catalyzed hydroalkynylation of ynamides (Scheme 1.6b).¹⁷ Through DFT and deuterium labeling studies, it was demonstrated that a dual gold(I) catalysis mediates the process: σ

¹³ Couty, S.; Meyer, C.; Cossy, J., Diastereoselective Gold-Catalyzed Cycloisomerizations of Ene-Ynamides, *Angew. Chem. Int. Ed.* **2006**, *45*, 6726–6730, *Angew. Chem.* **2006**, *118*, 6878–6882.

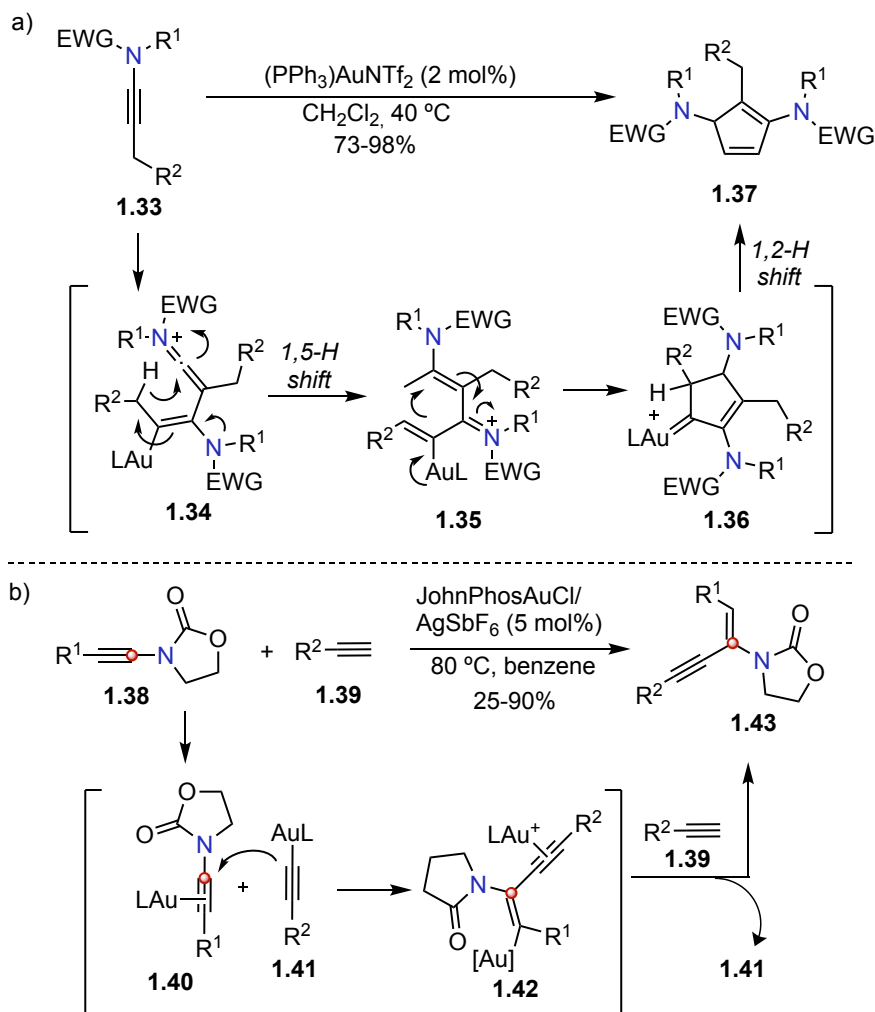
¹⁴ For more examples see: a) Buzas, A.; Istrate, F.; Le Goff, X. F.; Odabachian, Y.; Gagosz, F., Gold(I)-Catalyzed [4+2] Cycloaddition of *N*-(Hex-5-Enynyl) *Tert*-Butyloxycarbamates, *J. Organomet. Chem.* **2009**, *694*, 515–519. b) Zheng, N.; Chang, Y.-Y.; Zhang, L.-J.; Gong, J.-X.; Yang, Z., Gold-Catalyzed Intramolecular Tandem Cyclization of Indole-Ynamides: Diastereoselective Synthesis of Spirocyclic Pyrrolidinoindolines, *Chem. Asian J.* **2016**, *11*, 371–375. c) Zhong, C.-Z.; Tung, P.-T.; Chao, T.-H.; Yeh, M.-C. P., Gold-Catalyzed Stereoselective Synthesis of Bicyclic Lactams and Ketones from *N*-Tosylynamidomethyl-Tethered Cyclohexenes, *J. Org. Chem.* **2017**, *82*, 481–501. d) Chen, X.; Merrett, J. T.; Hong Chan, P. W., Gold-Catalyzed Formal [4 + 2] Cycloaddition of 5-(Ethylnylamino)Pent-2-Yn-1-Yl Esters to 1,2,3,5-Tetrahydrobenzo[*g*]Quinolines, *Org. Lett.* **2018**, *20*, 1542–1545. e) Morita, T.; Fukuhara, S.; Fuse, S.; Nakamura, H., Gold(I)-Catalyzed Intramolecular S_E Ar Reaction: Efficient Synthesis of Isoxazole-Containing Fused Heterocycles, *Org. Lett.* **2018**, *20*, 433–436. f) Zhao, Q.; León Rayo, D. F.; Campeau, D.; Daenen, M.; Gagosz, F., Gold-Catalyzed Formal Dehydro-Diels–Alder Reactions of Ene-Ynamide Derivatives Bearing Terminal Alkyne Chains: Scope and Mechanistic Studies, *Angew. Chem. Int. Ed.* **2018**, *57*, 13603–13607, *Angew. Chem.* **2018**, *130*, 13791–13795. g) Wang, H.-F.; Wang, S.-Y.; Qin, T.-Z.; Zi, W., Dual Gold-Catalyzed Formal Tetrahydro-Diels–Alder Reactions for the Synthesis of Carbazoles and Indolines, *Chem. Eur. J.* **2018**, *24*, 17911–17914. h) Liu, C.; Sun, Z.; Xie, F.; Liang, G.; Yang, L.; Li, Y.; Cheng, M.; Lin, B.; Liu, Y., Gold(I)-Catalyzed Pathway-Switchable Tandem Cycloisomerizations to Indolizino[8,7-*b*]Indole and Indolo[2,3-*a*]Quinolizine Derivatives, *Chem. Commun.* **2019**, *55*, 14418–14421. i) Liu, J.; Chakraborty, P.; Zhang, H.; Zhong, L.; Wang, Z.-X.; Huang, X., Gold-Catalyzed Atom-Economic Synthesis of Sulfone-Containing Pyrrolo[2,1-*a*]Isoquinolines from Dinamides: Evidence for Consecutive Sulfonyl Migration, *ACS Catal.* **2019**, *9*, 2610–2617. j) Matsuoka, J.; Kumagai, H.; Inuki, S.; Oishi, S.; Ohno, H., Construction of the Pyrrolo[2,3-*d*]Carbazole Core of Spiroindoline Alkaloids by Gold-Catalyzed Cascade Cyclization of Ynamide, *J. Org. Chem.* **2019**, *84*, 9358–9363. k) Zhu, B.; Zhu, L.; Xia, J.; Huang, S.; Huang, X., Gold-Catalyzed Cycloisomerization of Enynamides: Regio- and Stereoselective Approach to Tetracyclic Spiroindolines, *Tetrahedron* **2020**, *76*, 131056. l) Fabian León Rayo, D.; Hong, Y. J.; Campeau, D.; Tantillo, D. J.; Gagosz, F., On the Mechanism of Au-Catalyzed Enynamide-Yne Dehydro-Diels–Alder Reactions: An Experimental and Computational Study, *Chem. Eur. J.* **2021**, *27*, 10637–10648.

¹⁵ Kramer, S.; Odabachian, Y.; Overgaard, J.; Rottländer, M.; Gagosz, F.; Skrydstrup, T., Taking Advantage of the Ambivalent Reactivity of Ynamides in Gold Catalysis: A Rare Case of Alkyne Dimerization, *Angew. Chem. Int. Ed.* **2011**, *50*, 5090–5094, *Angew. Chem.* **2011**, *123*, 5196–5200.

¹⁶ a) Lin, G.-Y.; Li, C.-W.; Hung, S.-H.; Liu, R.-S., Diversity in Gold- and Silver-Catalyzed Cycloisomerization of Epoxide–Alkyne Functionalities, *Org. Lett.* **2008**, *10*, 5059–5062. b) Lemièrre, G.; Gandon, V.; Cariou, K.; Hours, A.; Fukuyama, T.; Dhiman, A.-L.; Fensterbank, L.; Malacria, M., Generation and Trapping of Cyclopentenylidene Gold Species: Four Pathways to Polycyclic Compounds, *J. Am. Chem. Soc.* **2009**, *131*, 2993–3006.

¹⁷ Siera, H.; Kreuzahler, M.; Wölper, C.; Haberhauer, G., Regio- and Stereoselective Synthesis of Ynenamides through Gold(I)-Catalyzed Hydroalkynylation of Ynamides, *Eur. J. Org. Chem.* **2022**, *2022*, e202200591.

complex **1.41** attacks π -activated **1.40** at the carbon attached to the nitrogen, then, protodeauration of **1.42** mediated from another molecule of **1.39** brings to **1.43** regenerating the catalytic cycle.



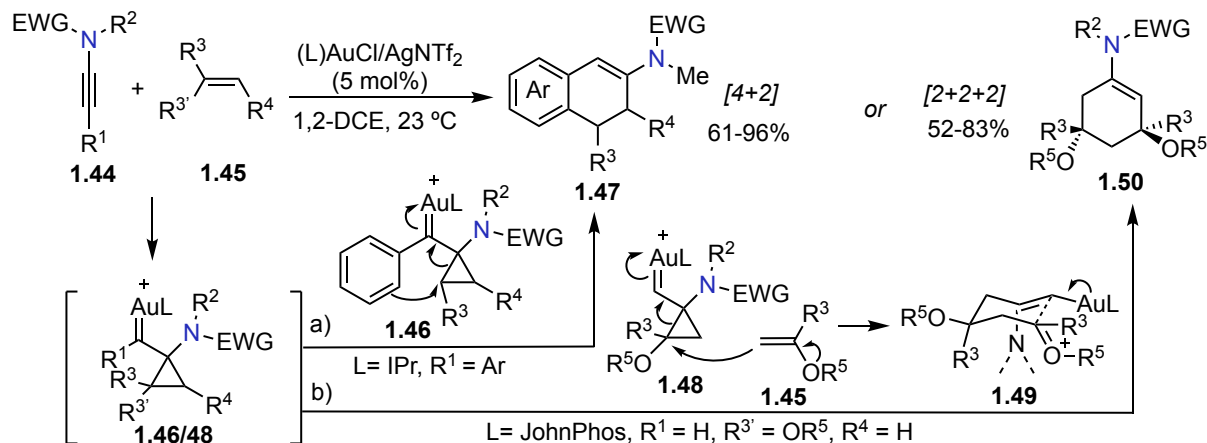
Scheme 1.6. a) Gold(I)-catalyzed homodimerization of ynamides. b) Gold(I)-catalyzed hydroalkynylation of ynamides. The carbon highlighted in red represents ¹³C labeling.

As for gold(I)-catalyzed intermolecular reactivity of ynamides with double bonds, apart from the hydroarylation of ynamides with indoles described by Rossi and co-workers,¹⁸ only two transformations have been reported so far with alkenes, by the group of Liu, which see as intermediate cyclopropyl gold(I) carbene **1.46/48** (Scheme 1.7).¹⁹ When using an IPrAu(I) complex and arylynamides in combination with electron rich alkenes, a [4+2] cycloaddition occurs, resulting from the Friedel-Crafts type trapping of cyclopropyl **1.46**, followed by protodeauration (Scheme 1.7a). When having enol ethers as nucleophiles, products **1.47** spontaneously convert into their naphthalene derivatives upon alcohol loss (not shown in Scheme 1.7). With terminal ynamides, the best performing ligand for gold was found to be JohnPhos. Interestingly, in this case, only enol ethers could be reacted as nucleophiles, affording

¹⁸ Pirovano, V.; Negrato, M.; Abbiati, G.; Dell'Acqua, M.; Rossi, E., Gold-Catalyzed *Cis*-Hydroarylation of Ynamides with Indoles: Regio- and Stereoselective Synthesis of a Class of 2-Vinylindoles, *Org. Lett.* **2016**, *18*, 4798–4801.

¹⁹ Dateer, R. B.; Shaibu, B. S.; Liu, R.-S., Gold-Catalyzed Intermolecular [4+2] and [2+2+2] Cycloadditions of Ynamides with Alkenes, *Angew. Chem. Int. Ed.* **2012**, *51*, 113–117. *Angew. Chem.* **2012**, *124*, 117–121.

the [2+2+2] products **1.50** (Scheme 1.7b). After the generation of cyclopropyl gold(I) carbene **1.48** in fact, a second molecule of nucleophile **1.45** can attack it to generate chair-like transition state **1.49**, which constitutes the least hindered conformation and therefore justifies the observed stereoselectivity in the product.



Scheme 1.7. Gold-catalyzed intermolecular [4+2] and [2+2+2] cycloadditions of ynamides with alkenes.

It is interesting to see how, in both cases described above, only alkenes presenting electron-donating substituents could be reacted in an intermolecular fashion with ynamides, which highlights the intrinsic electron rich nature of ynamides compared to non-substituted alkynes.

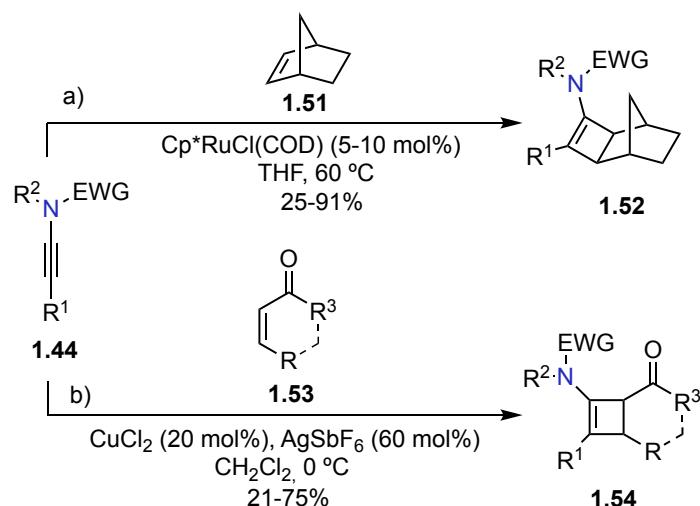
There are only a few examples in literature which describe the intermolecular [2+2] between ynamides and alkenes: in 2005 Tam described the reaction to happen exclusively with norbornenes **1.51** at 60 °C using a ruthenium catalyst (Scheme 1.8a).²⁰ A higher temperature was required for this reaction with respect to when having electron poorer alkynes which reacted under Ru catalysis at room temperature.²¹ Later, Hsung and co-workers reported the copper-catalyzed Ficini [2+2] cycloaddition of ynamides and α,β -unsaturated ketones, where ynamides **1.44** were proposed to act as nucleophilic partners towards the β position of **1.53** (Scheme 1.8b).²² Shortly after, the enantioselective versions of these reactions were also developed.²³

²⁰ Riddell, N.; Villeneuve, K.; Tam, W., Ruthenium-Catalyzed [2 + 2] Cycloadditions of Ynamides, *Org. Lett.* **2005**, *7*, 3681–3684.

²¹ a) Jordan, R. W.; Tam, W., Ruthenium-Catalyzed [2 + 2] Cycloadditions of 2-Substituted Norbornenes, *Org. Lett.* **2000**, *2*, 3031–3034. b) Villeneuve, K.; Riddell, N.; Jordan, R. W.; Tsui, G. C.; Tam, W., Ruthenium-Catalyzed [2 + 2] Cycloadditions between Bicyclic Alkenes and Alkynyl Halides, *Org. Lett.* **2004**, *6*, 4543–4546.

²² Li, H.; Hsung, R. P.; DeKorver, K. A.; Wei, Y., Copper-Catalyzed Ficini [2 + 2] Cycloaddition of Ynamides, *Org. Lett.* **2010**, *12*, 3780–3783.

²³ a) Schotes, C.; Mezzetti, A., Enantioselective Ficini Reaction: Ruthenium/PNNP-Catalyzed [2+2] Cycloaddition of Ynamides with Cyclic Enones, *Angew. Chem. Int. Ed.* **2011**, *50*, 3072–3074, *Angew. Chem.* **2011**, *123*, 3128–3130. b) Enomoto, K.; Oyama, H.; Nakada, M., Highly Enantioselective Catalytic Asymmetric [2+2] Cycloadditions of Cyclic α -Alkylidene β -Oxo Imides with Ynamides, *Chem. Eur. J.* **2015**, *21*, 2798–2802.



Scheme 1.8. Intermolecular [2+2] cycloaddition of ynamides with alkenes catalyzed by other transition metals.

Chiral Auxiliaries in Asymmetric Synthesis

Among the different strategies developed over the years for the synthesis of enantiomerically enriched compounds, the chiral auxiliary approach has gained a certain degree of popularity thanks to its reliability and usually simple applicability in a wide number of transformations.²⁴ The concept behind this strategy is to use, most of the time, cheap commercially available or readily accessible chiral scaffolds that can be easily attached to and removed from the target achiral substrate: once incorporated, the chiral auxiliary directs the stereoselectivity of the reaction and provides an enantiomerically enriched product, and, after cleavage of the auxiliary, it can be ideally re-used (Figure 1.1a).

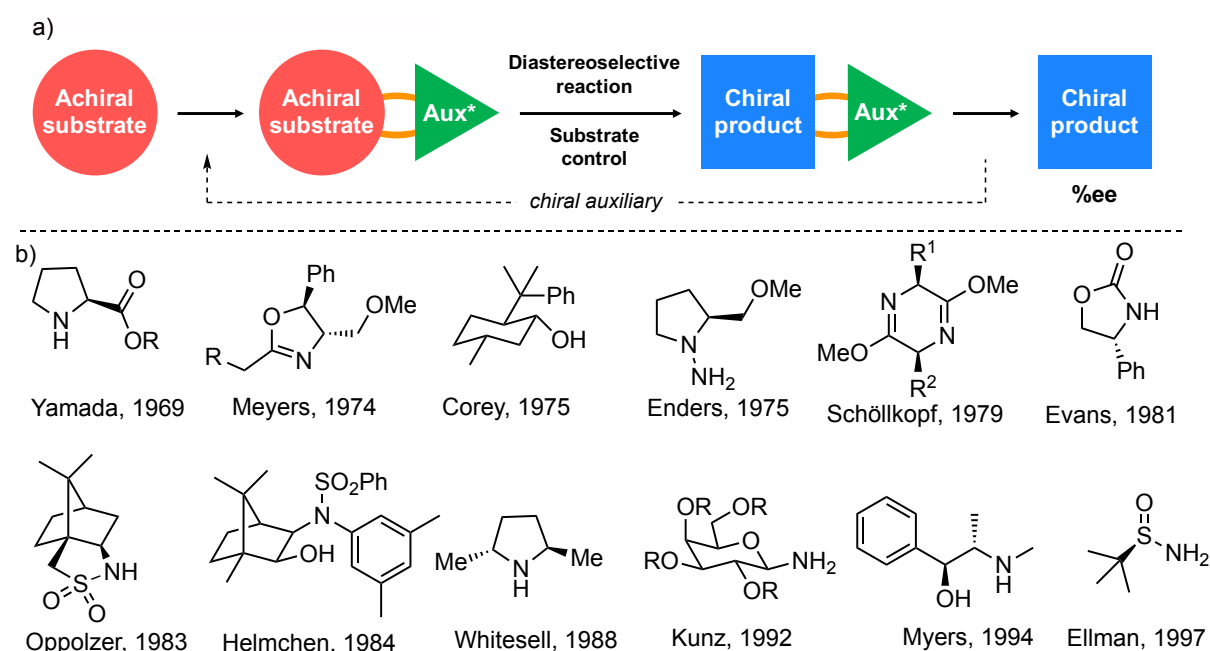
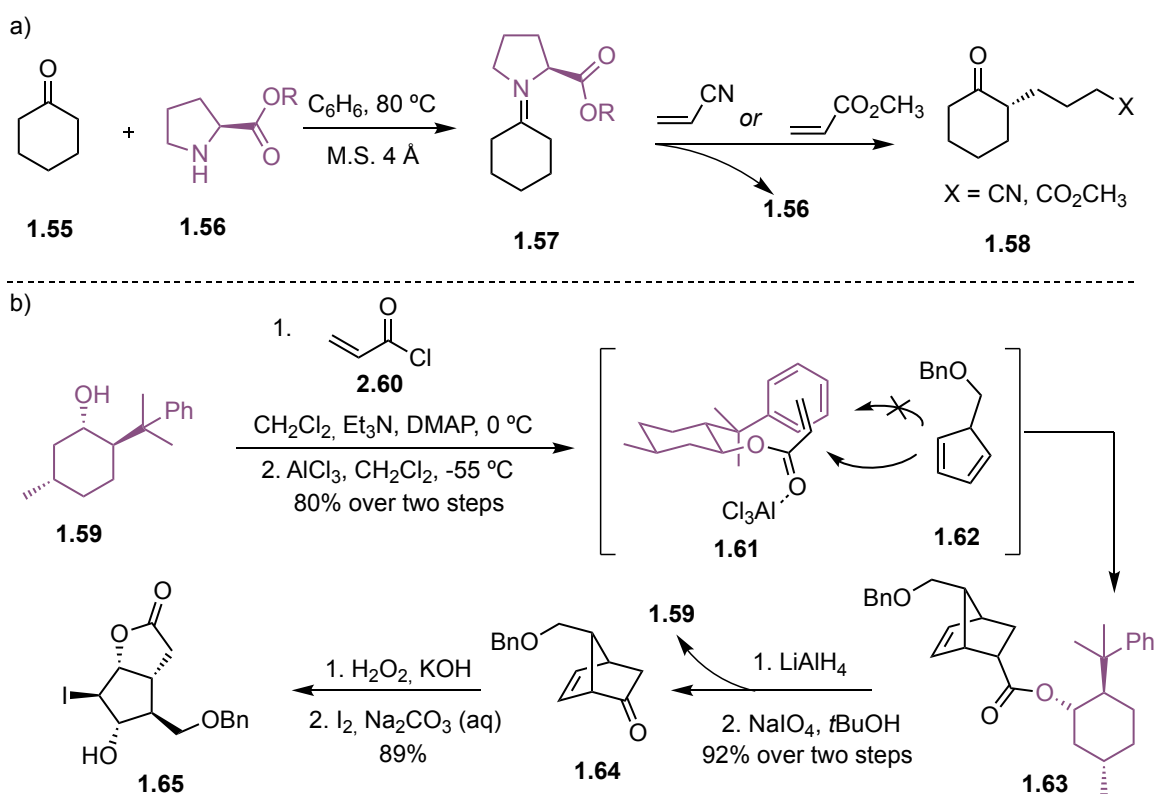


Figure 1.1. The chiral auxiliary approach in asymmetric synthesis.

²⁴ Christmann, M., Bräse, S., *Asymmetric Synthesis: The Essentials*, Eds.; Wiley-VCH: Weinheim, 2007.

Clearly, one of the challenges associated to this procedure is that the conditions used to cleave the auxiliary might be harsh enough to racemize the enantioenriched product. Many chiral auxiliaries have been developed over the years especially during the 70s and the 80s (Figure 1.1b), the first example being Yamada's (*L*)-proline derived ester **1.56** for α -alkylation of cyclohexanone **1.55** which relies on the formation and subsequent hydrolysis of enamine **1.57** to form enantioenriched **1.58** (Scheme 1.9a).²⁵ Shortly after, Corey reported the use of (-)-8-phenylmenthol **1.59** to synthesize Prostaglandin precursor **1.63** through asymmetric Diels-Alder between acrylate ester **1.61** furnished with the chiral auxiliary, and diene **1.62** (Scheme 1.9b).²⁶ Full recovery of the auxiliary **1.59** was possible through cleavage with LiAlH_4 .



Scheme 1.9. First examples of the use chiral auxiliaries in asymmetric synthesis: a) Yamada's *L*-proline, b) Corey's (-)-8-phenylmenthol.

²⁵ Yamada, S.; Hiroi, K.; Achiwa, K. Asymmetric Synthesis with Amino Acid I Asymmetric Induction in the Alkylation of Keto-Enamine. *Tetrahedron Lett.* **1969**, *10*, 4233–4236.

²⁶ Corey, E. J.; Ensley, H. E. Preparation of an Optically Active Prostaglandin Intermediate via Asymmetric Induction. *J. Am. Chem. Soc.* **1975**, *97*, 6908–6909.

Among the different auxiliaries, Evans oxazolidinones²⁷ emerged as an excellent option when it came to a wide number of reactions, starting with the originally designed aldol reactions,²⁸ alkylations,²⁹ and Diels-Alder cycloadditions.³⁰ In the context of asymmetric aldol reactions, from chiral imide **1.66**, under kinetic conditions using the boron reagent *n*Bu₂BOTf in the presence of *i*Pr₂NEt, the (*Z*)-enolate **1.67** forms (Scheme 1.10a). The *syn* vs *anti* diastereoselectivity can be explained looking at the Zimmermann–Traxler model³¹ of the six-membered transition states **1.68–70**, where the approaching aldehyde accommodates the R² substituent in equatorial position, vs **1.72** where R² presents disfavoured 1,3-diaxial interactions with the other axial substituents. To obtain the *anti* diastereomer, the reaction should be performed starting from the (*E*)-enolate. While the diastereoselectivity model is substrate-dependent and it is valid regardless of the presence of a chiral auxiliary, the enantioselectivity, which in this case represents the discrimination among the two *syn* diastereomers **1.69** and **1.71**, depends on the face of the enolate to which the aldehyde is approaching. Therefore, in the case of using a chiral oxazolidinone attached to the substrate, the enantioselectivity can also be directed. Again, looking at the chair-like transition states it is possible to see that in **1.70** the R group of the chiral auxiliary would clash with one of the butyl substituents of the boron species, making **1.68** the energetically favoured TS for the aldol reaction, which leads to the so-called “Evans *syn*” product **1.69**. Once isolated, many ways to remove the auxiliary have been established, each bringing to different functionalities (Scheme 1.10b): carboxylic acids **1.74** can be accessed in the presence of LiOH and H₂O₂, esters **1.75** in the presence of (TiOBn)₄, alcohols **1.76** by reduction with LiBH₄ or LiAlH₄ and finally amides **1.77** by treatment with NH(OMe)Me in the presence of AlMe₃.

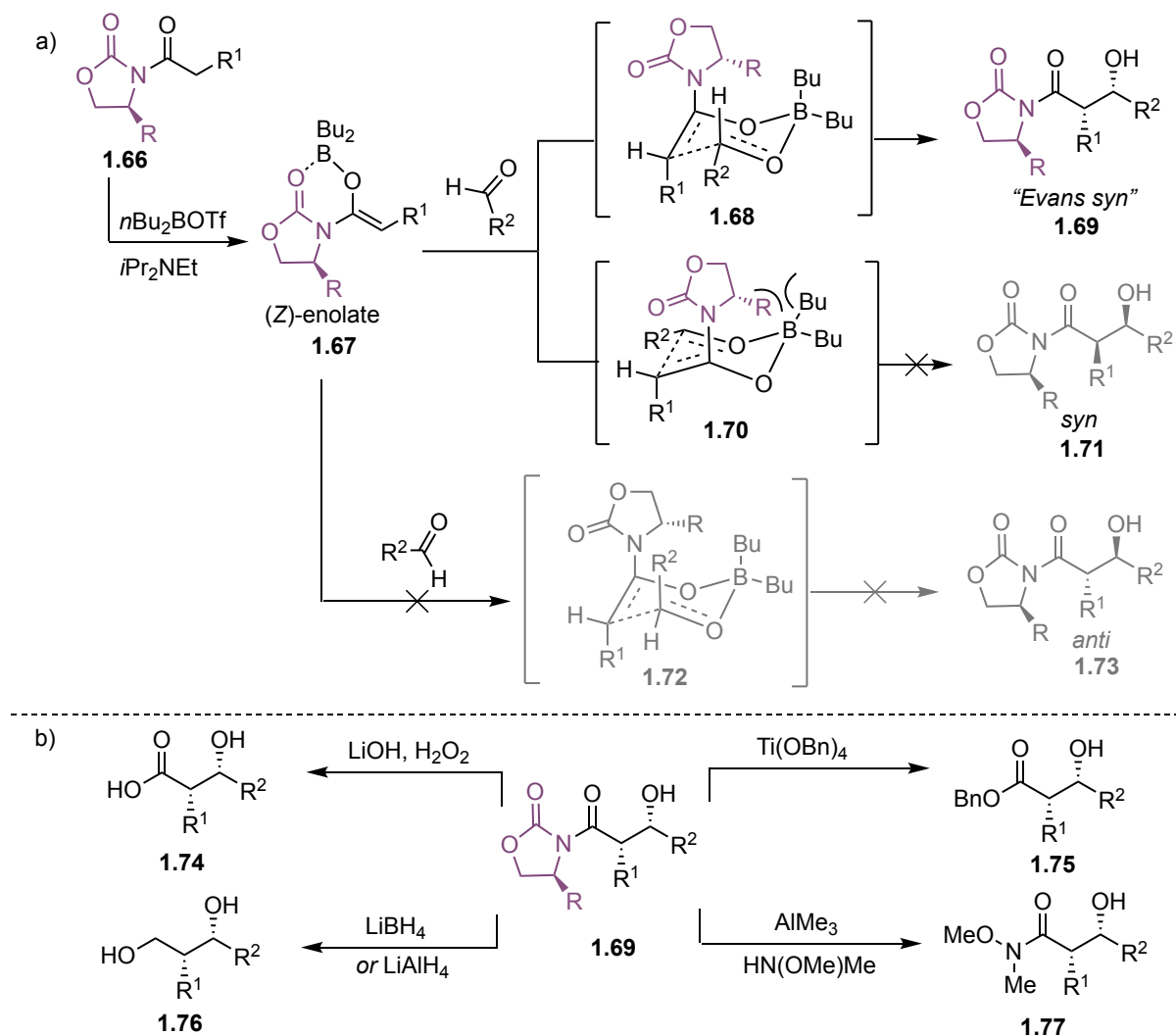
²⁷ a) Heravi, M. M.; Zadsirjan, V., Oxazolidinones as Chiral Auxiliaries in Asymmetric Aldol Reactions Applied to Total Synthesis, *Tetrahedron Asymmetry* **2013**, *24*, 1149–1188. b) Bhamboo, P.; Bera, S.; Mondal, D., TiCl₄-Promoted Asymmetric Aldol Reaction of Oxazolidinones and Its Sulphur-Congeners for Natural Product Synthesis, *Asian J. Org. Chem.* **2021**, *10*, 2763–2819. c) Nazari, A.; Heravi, M. M.; Zadsirjan, V., Oxazolidinones as Chiral Auxiliaries in Asymmetric Aldol Reaction Applied to Natural Products Total Synthesis, *J. Organomet. Chem.* **2021**, *932*, 121629. d) Morales-Monarca, G. H.; Gnecco, D.; Terán, J. L., Diastereoselective Functionalization of Chiral N-Acyl-1,3-Oxazolidines and Their Applications in the Synthesis of Bioactive Molecules, *Eur. J. Org. Chem.* **2022**, *2022*, e202200267. e) Chen, L.; Huang, P., Evans’ Chiral Auxiliary-Based Asymmetric Synthetic Methodology and Its Modern Extensions, *Eur. J. Org. Chem.* **2024**, *27*, e202301131.

²⁸ a) Evans, D. A.; Bartroli, J.; Shih, T. L. Enantioselective aldol condensations. 2. Erythro-selective chiral aldol condensations via boron enolates, *J. Am. Chem. Soc.* **1981**, *103*, 8, 2127–2129. b) Evans, D. A., Studies in Asymmetric Synthesis. The Development of Practical Chiral Enolate Synthons, *Aldrichimica Acta*, *15*, **1982**, *15*, 23–32.

²⁹ Evans, D. A.; Ennis, M. D.; Mathre, D. J. Asymmetric alkylation reactions of chiral imide enolates. A practical approach to the enantioselective synthesis of alpha-substituted carboxylic acid derivatives, *J. Am. Chem. Soc.* **1982**, *104*, 6, 1737–1739.

³⁰ Evans, D. A.; Chapman, K. T.; Bisaha, J. New asymmetric Diels-Alder cycloaddition reactions. Chiral alpha,beta-unsaturated carboximides as practical chiral acrylate and crotonate dienophile synthons. *J. Am. Chem. Soc.* **1984**, *106*, 15, 4261–4263.

³¹ a) Zimmermann, H. E.; Traxler M. D., The Stereochemistry of the Ivanov and Reformatsky Reactions. I, *J. Am. Chem. Soc.* **1957**, *79*, 8, 1920–1923. b) Arya, P.; Qin, H., Advances in Asymmetric Enolate Methodology, *Tetrahedron* **2000**, *56*, 917–947.

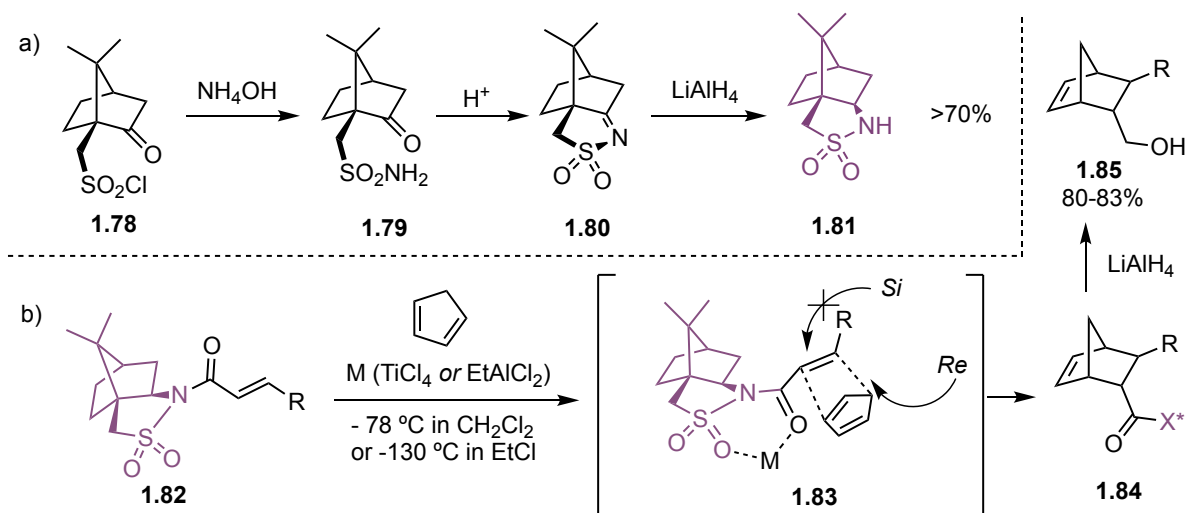


Scheme 1.10. a) Zimmerman-Traxler model for the stereoselectivity of asymmetric aldol reaction using Evans oxazolidinones. b) Oxazolidinone removal strategies.

Another cyclic nitrogen-based auxiliary that had remarkable success over the years is the Oppolzer sultam³² synthesized in 1984 starting from camphorsulfonyl chloride **1.78** (Scheme 1.11a), and used in the first place to direct the stereoselectivity of the Diels-Alder reaction of **1.82** with cyclopentadiene through the discrimination of the *Re* face of the dienophile in **1.83** (Scheme 1.11b).³³ Once obtained bicyclic alkene **1.84**, the removal of the chiral auxiliary could be achieved via the use of LiAlH₄.

³² Heravi, M. M.; Zadsirjan, V. Recent Advances in the Application of the Oppolzer Camphorsultam as a Chiral Auxiliary. *Tetrahedron Asymmetry* **2014**, *25*, 1061–1090.

³³ a) Oppolzer, W.; Chapuis, C.; Bernardinelli, G. Camphor-Derived N-Acryloyl and N-Crotonoyl Sultams: Practical Activated Dienophiles in Asymmetric Diels-Alder Reactions. Preliminary Communication. *Helv. Chim. Acta* **1984**, *67*, 1397–1401. b) Oppolzer, W. Camphor as a Natural Source of Chirality in Asymmetric Synthesis. *Pure Appl. Chem.* **1990**, *62*, 1241–1250.



Scheme 1.11. Oppolzer sultam synthesis and first application in an asymmetric Diels-Alder reaction. X* = chiral auxiliary.

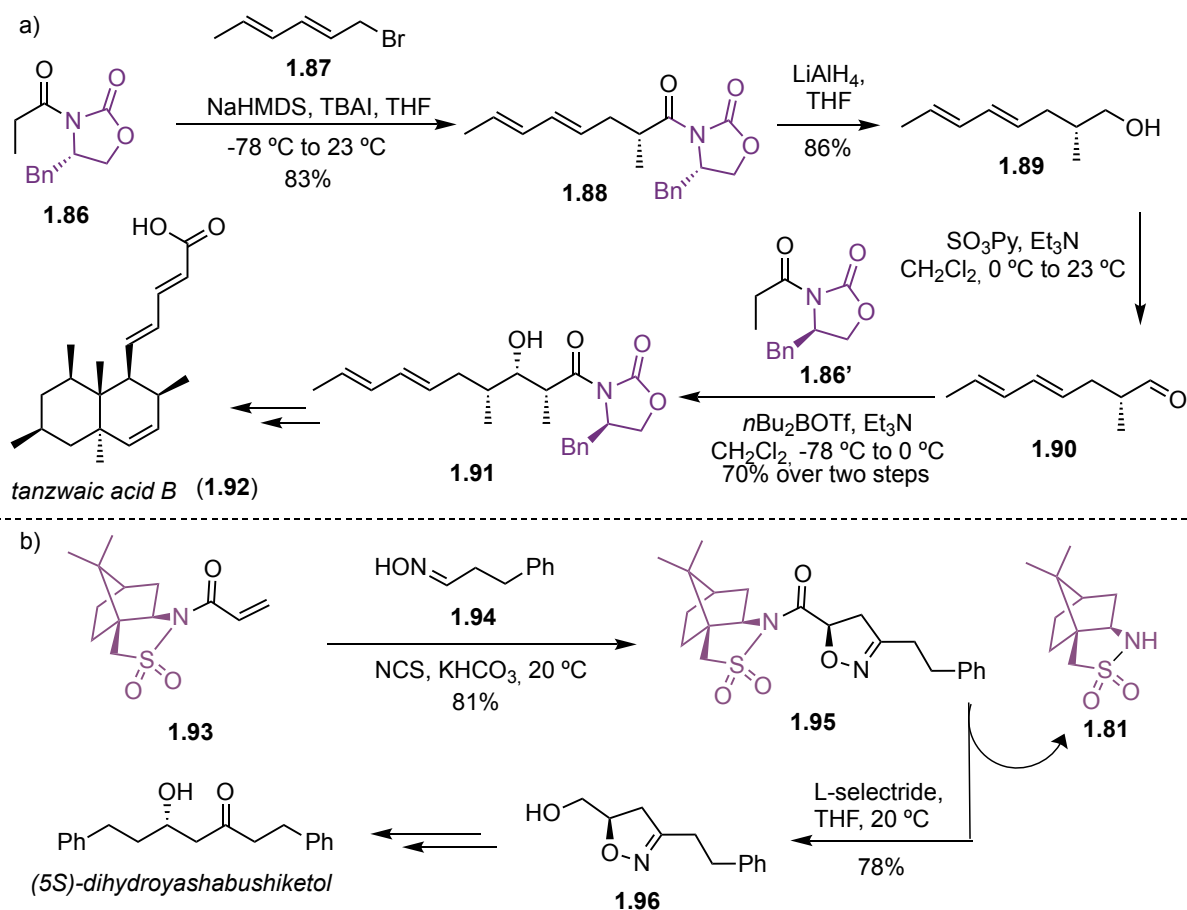
As it can be imagined, one of the main and first applications of chiral auxiliaries could be found in total synthesis of enantiomerically enriched natural products or pharmacologically relevant compounds and, still today they constitute a valid strategy for introducing chiral centers in complex molecules.³⁴ As an example, the recently described first total synthesis of tanzawaic acid B (**1.92**), a natural polyketide presenting antifungal and antimalarial activity, starts from the asymmetric alkylation of the Evans oxazolidinone-functionalised amide **1.86** with 1-bromohexa-2,4-diene **1.87** to form **1.88** (Scheme 1.12a).³⁵ After subsequent reduction and oxidation to form aldehyde **1.90**, a second asymmetric reaction, this time an aldol, using the enantiomer of **1.86**, **1.86'**, affords enantioenriched **1.91** which eventually will deliver tanzawaic acid B.

Polyketide (5*S*)-dihydroyashabushiketol (**1.97**), first isolated from Japanese yashabushi flowers (*Alnus firma*) in 1970, could be synthesized in 2011 by the diastereoselective 1,3-dipolar additions of camphorsultam derivative **1.93** with nitrile oxide **1.94** to form **1.95** (Scheme 1.12b).³⁶ Cleavage and recovery of the auxiliary through treatment with L-selectride affords dihydroisoxazole derivative **1.96**, precursor of (5*S*)-dihydroyashabushiketol **1.97**.

³⁴ Diaz-Muñoz, G.; Miranda, I. L.; Sartori, S. K.; de Rezende, D. C.; Alves Nogueira Diaz, M. Use of Chiral Auxiliaries in the Asymmetric Synthesis of Biologically Active Compounds: A Review. *Chirality* **2019**, *31*, 776–812.

³⁵ Murata, T.; Tsutsui, H.; Yoshida, T.; Kubota, H.; Hiraishi, S.; Natsukawa, H.; Suzuki, Y.; Hiraga, D.; Mori, T.; Maekawa, Y.; Tateyama, S.; Toyoyama, K.; Ito, K.; Suzuki, K.; Yonekura, K.; Shibata, N.; Sato, T.; Tasaki, Y.; Inohana, T.; Takano, A.; Egashira, N.; Honda, M.; Umezaki, Y.; Shiina, I. First Total Synthesis of Tanzawaic Acid B. *ACS Omega* **2023**, *8*, 27703–27709.

³⁶ Romanski, J.; Nowak, P.; Chapuis, C.; Jurczak, J. Total Synthesis of (5*S*)-Dihydroyashabushiketol. *Tetrahedron Asymmetry* **2011**, *22*, 787–790.



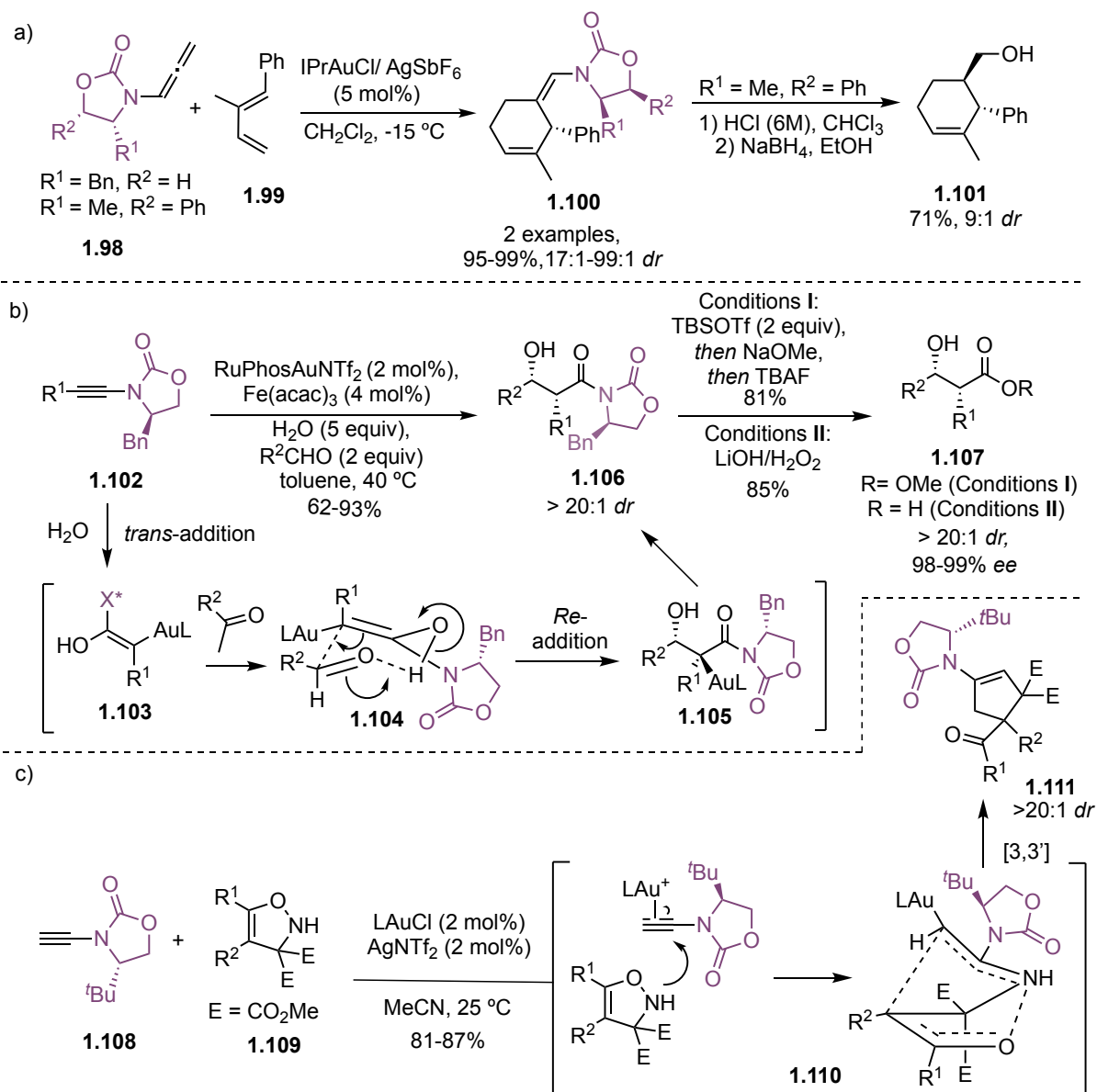
Scheme 1.12 a) Application of Evans oxazolidinones in the total synthesis of tanzwaic acid B through consecutive asymmetric alkylation and aldol reactions. b) Application of Oppolzer sultam in the total synthesis of (5*S*)-dihydroyashabushiketol through asymmetric 1,3-dipolar addition.

When we started to explore the use of chiral auxiliaries in gold(I) catalysis, aiming to provide an alternative to the time-consuming ligand design approach, only one example was present in literature: the group of Mascareñas described, in 2011, the gold(I)-catalyzed Diels-Alders reaction of allenamides with dienes (Scheme 1.13a).³⁷ In this context, a couple of examples were reported using a chiral oxazolidinone at the allenamide nitrogen, which afforded the two enamines **1.100** in moderate to excellent *dr*. After treatment under acidic conditions followed by NaBH₄ reduction, enantioenriched alcohol **1.101** could also be isolated. Last year, a Au(I)/Fe(III)-catalyzed hydrative aldol reaction (HAR) using again Evans oxazolidinone-substituted ynamides **1.102** was described by the group of Shi (Scheme 1.13b).³⁸ The reaction, which requires the use of a Fe(III) co-catalyst to prevent C-Au protonation in **1.104**, proceeds via gold(I)-catalyzed water *trans*-addition to **1.102** to form **1.103**, which, through the aforementioned chair-like TS **1.104**, selectively affords the *Re*-face addition product **1.106** in excellent diastereoselectivities. Different removal strategies were then developed to afford enantioenriched β-

³⁷Faustino, H.; López, F.; Castedo, L.; Mascareñas, J. L., Gold(I)-Catalyzed Intermolecular (4 + 2) Cycloaddition of Allenamides and Acyclic Dienes, *Chem. Sci.* **2011**, *2*, 633–637.

³⁸ Yuan, T.; Radefeld, K.; Shan, C.; Wegner, C.; Nichols, E.; Ye, X.; Tang, Q.; Wojtas, L.; Shi, X., Asymmetric Hydrative Aldol Reaction (HAR) via Vinyl-Gold Promoted Intermolecular Ynamide Addition to Aldehydes, *Angew. Chem. Int. Ed.* **2023**, *62*, e202305810, *Angew. Chem.* **2023**, *135*, e202305810.

hydroxy esters and carboxylic acids **1.107**. To conclude, this year, Anderson and co-workers described the intermolecular diastereoselective [3,3']-sigmatropic rearrangement between gold(I)-activated ynamides **1.108** presenting Evans oxazolidinones and NH-isoxazolines **1.109** that proceeds via concerted transition state **1.110** (Scheme 1.13c).³⁹ However, the oxazolidinone moiety cannot really be considered an auxiliary in this case, since it was not removed after the stereoselective transformation.



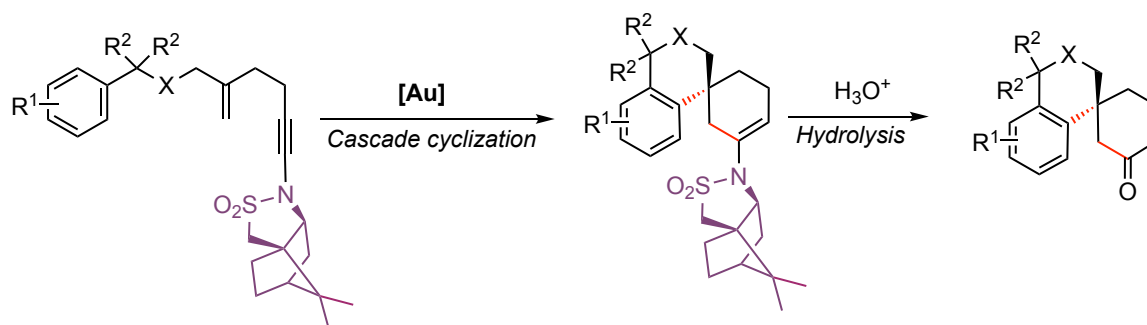
Scheme 1.13. Use of chiral auxiliaries in gold(I)-catalysis: a) Diels-Alder between allenamides and dienes, b) Hydrative aldol reaction of ynamides, c) [3,3']-Sigmatropic rearrangement of NH-isoxazolines with ynamides.

Even considering these most recent advances, there's no example so far of a methodology for asymmetric gold(I)-catalyzed cyclizations of alkynes with alkenes which relies on chiral auxiliaries.

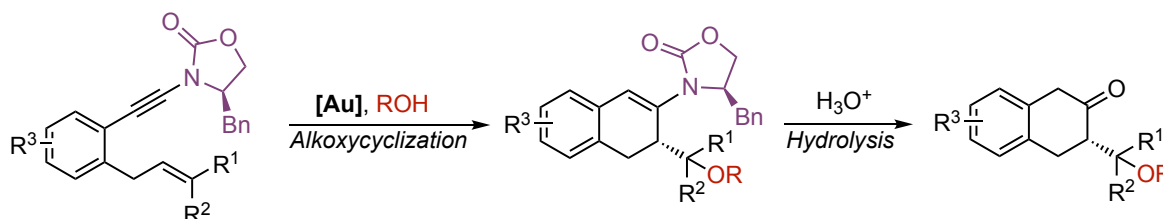
³⁹ Alshreimi, A. S.; Zhang, G.; Shim, E. J.; Wink, D. J.; Anderson, L. L., Gold-Catalyzed *N*-Alkenylation of Isoxazolines and the Use of Alkenyl Gold Intermediates in the Synthesis of 2-Amino-1-Pyrrolines, *ACS Catal.* **2024**, *14*, 2229–2234.

Objectives

Given the difficulties encountered in enantioselective gold(I)-catalysis posed by the linear dicoordination of gold(I) catalysts, our objective is to develop the first gold(I)-catalyzed stereoselective cyclizations starting from *N*-substituted alkynes bearing chiral auxiliaries. Based on our previous report which described racemic polyenyne cyclizations,⁴⁰ a stereoselective cascade cyclization of 1,5-enynes is herein designed using the Oppolzer camphorsultam as chiral auxiliary.⁴¹



Then, given the familiarity and primate in our group on asymmetric gold(I)-catalyzed alkoxy cyclizations,⁴² the stereoselective alkoxy cyclization of 1,6-enynes mediated by an Evans-type oxazolidinone will also be explored.^{43,44}



Finally, efforts towards the application of chiral auxiliaries in gold(I)-catalyzed reactions of alkynes with alkenes in the context of the total synthesis of sesquiterpene hernandulcin,⁴⁵ and the extension of this methodology to intermolecular cycloadditions, will be reported.

⁴⁰ Rong, Z.; Echavarren, A. M., Broad Scope Gold(I)-Catalysed Polyenyne Cyclisations for the Formation of up to Four Carbon–Carbon Bonds, *Org. Biomol. Chem.* **2017**, *15*, 2163–2167.

⁴¹ Work performed in collaboration with Miguel Peña-López.

⁴² Muñoz, M. P.; Adrio, J.; Carretero, J. C.; Echavarren, A. M., Ligand Effects in Gold- and Platinum-Catalyzed Cyclization of Enynes: Chiral Gold Complexes for Enantioselective Alkoxy cyclization, *Organometallics* **2005**, *24*, 1293–1300.

⁴³ Work performed in collaboration with Riccardo Pedrazzani.

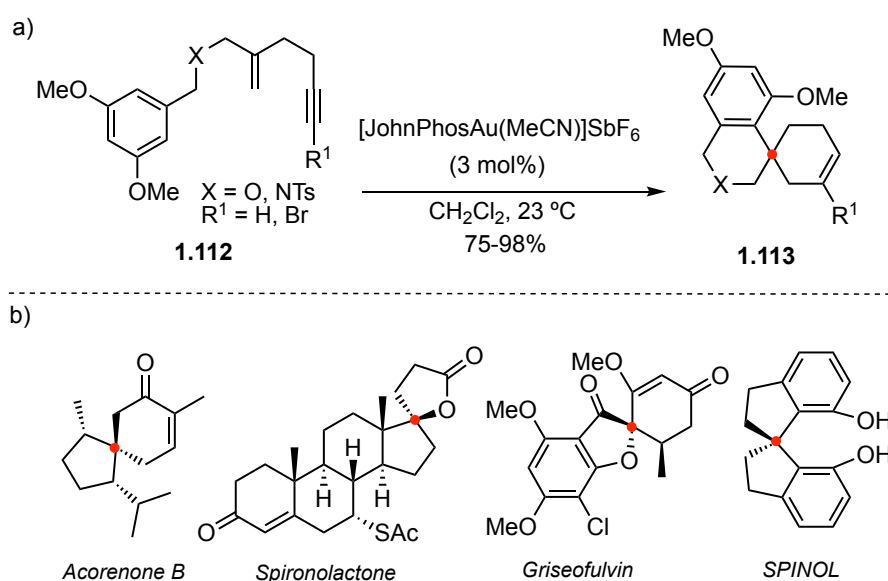
⁴⁴ More information can be found in the associated publication: Cataffo, A.; Peña-López, M.; Pedrazzani, R.; Echavarren, A. M., Chiral Auxiliary Approach for Gold(I)-Catalyzed Cyclizations, *Angew. Chem. Int. Ed.* **2023**, *62*, e202312874.

⁴⁵ Work performed in collaboration with Marc Paul Beller and Luyu Cai.

Results and Discussion

1,5-Enyne Cascade Cyclization⁴¹

As mentioned, in 2017 our group developed the gold(I)-catalyzed cyclization of 1,5-enynes, where the activation of terminal alkynes or bromoalkynes initiates a cascade cyclization to produce spirocyclic compounds in a racemic manner (Scheme 1.14a).⁴⁰ The spiro motif is prevalent in numerous biologically active natural,⁴⁶ synthetic⁴⁷ products, and chiral ligands.⁴⁸ Despite being less common compared to flat aromatic scaffolds, spirocyclic compounds are gaining importance in modern drug discovery (Scheme 1.14b).⁴⁹



Scheme 1.14 a) Gold(I)-catalyzed cascade cyclization of 1,5-enynes to access spirocyclic compounds. b) Valuable examples of spirocyclic compounds.

Despite advancements, the synthesis of chiral spirocycles remains relatively underdeveloped. Moreover, in contrast to 1,6-enynes, there have been very few examples on enantioselective cyclizations involving 1,5-enynes so far, with none describing cascade cyclizations.⁵⁰ To perform our studies, we considered auxiliaries **X**₁₋₈ and gold(I)-catalysts **1.A-M** (Figure 1.2).

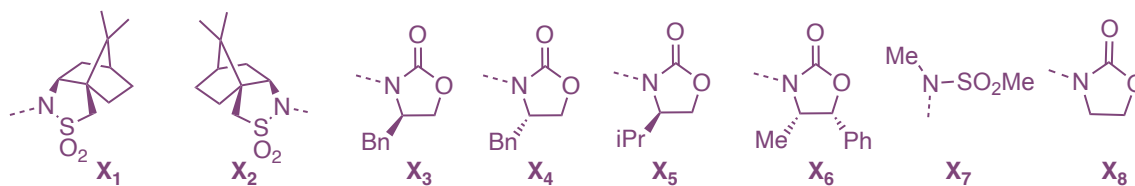
⁴⁶ a) K. Smith, L.; R. Baxendale, I., Total Syntheses of Natural Products Containing Spirocarbocycles, *Org. Biomol. Chem.* **2015**, *13*, 9907–9933. b) Chupakhin, E.; Babich, O.; Prosekov, A.; Asyakina, L.; Krasavin, M., Spirocyclic Motifs in Natural Products, *Molecules* **2019**, *24*, 4165.

⁴⁷ a) D'yakonov, V. A.; Trapeznikova, O. A.; De Meijere, A.; Dzhemilev, U. M., Metal Complex Catalysis in the Synthesis of Spirocarbocycles, *Chem. Rev.* **2014**, *114*, 5775–5814. b) Gilles, L.; Antoniotti, S., Spirocyclic Compounds in Fragrance Chemistry: Synthesis and Olfactory Properties, *ChemPlusChem* **2022**, *87*, e202200227.

⁴⁸ Ding, K.; Han, Z.; Wang, Z., Spiro Skeletons: A Class of Privileged Structure for Chiral Ligand Design, *Chem. Asian J.* **2009**, *4*, 32–41.

⁴⁹ a) Zheng, Y.; Tice, C. M.; Singh, S. B., The Use of Spirocyclic Scaffolds in Drug Discovery, *Bioorg. Med. Chem. Lett.* **2014**, *24*, 3673–3682. b) Hiesinger, K.; Dar'in, D.; Proschak, E.; Krasavin, M., Spirocyclic Scaffolds in Medicinal Chemistry, *J. Med. Chem.* **2021**, *64*, 150–183.

⁵⁰ a) Zheng, H.; Felix, R. J.; Gagné, M. R., Gold-Catalyzed Enantioselective Ring-Expanding Cycloisomerization of Cyclopropylidene Bearing 1,5-Enynes, *Org. Lett.* **2014**, *16*, 2272–2275. b) Wu, Z.; Retailleau, P.; Gandon, V.; Voituriez, A.; Marinetti, A., Use of Planar Chiral Ferrocenyl-phosphine-Gold(I) Complexes in the Asymmetric Cycloisomerization of 3-Hydroxylated 1,5-Enynes, *Eur. J. Org. Chem.* **2016**, *2016*, 70–75. c) Han, X.; Retailleau, P.; Gandon, V.; Voituriez, A., Enantioselective Gold(I)-Catalyzed Cyclization/Intermolecular Nucleophilic Additions of 1,5-Enyne Derivatives, *Chem. Commun.* **2020**, *56*, 9457–9460.

Chiral auxiliaries **X**:

Gold(I) catalysts:

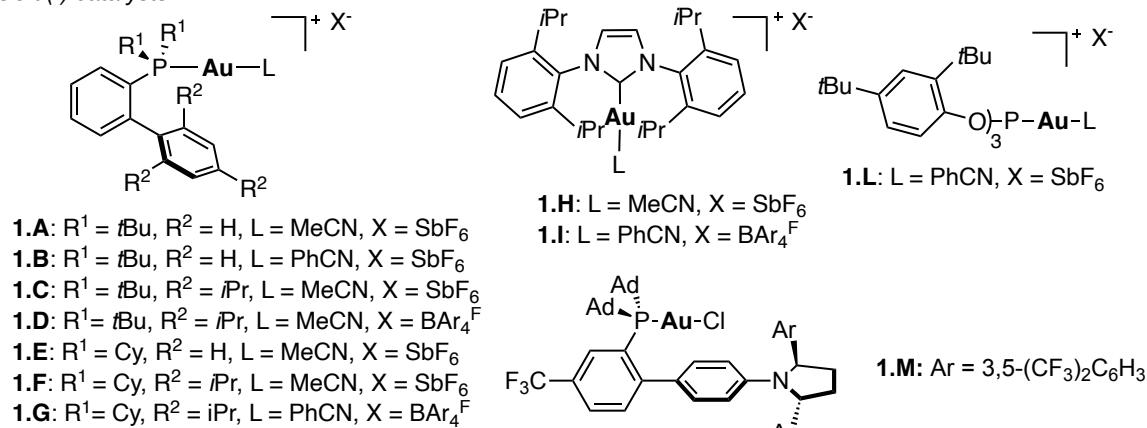
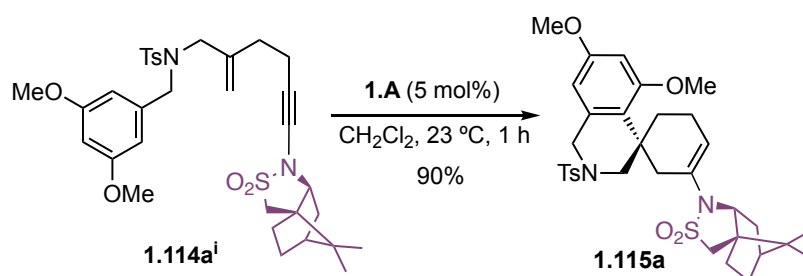


Figure 1.2 Chiral auxiliaries and gold(I) catalysts used in our intramolecular studies.

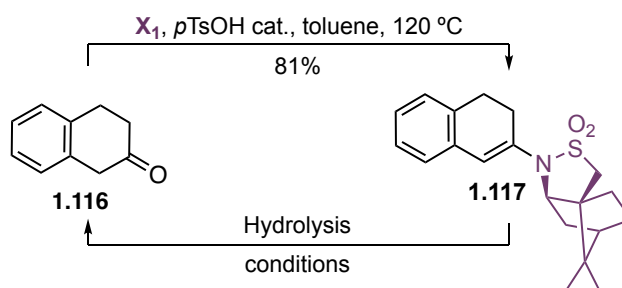
We first subjected 1,5-enynamide **1.114aⁱ** equipped with Oppolzer's sultam **X₁** as the chiral auxiliary to catalyst **1.A** and we could satisfactorily isolate **1.115a** in 90% yield (Scheme 1.15).



Scheme 1.15 First trial in the cascade cyclization of **1.114aⁱ** employing **1.A** as a catalyst⁵¹

Then, we were interested in removing the chiral auxiliary, so we performed a screening of different conditions on the model substrate **1.117** synthesized by condensation of the chiral auxiliary with β -tetralone **1.116** as shown in Table 1.1. First, hydrolysis with 10% aqueous HCl was tested overnight at 23 °C in different solvents as methanol, ethanol, dichloromethane and methanol/dichloromethane, obtaining the best result in THF (Table 1.1, entries 1-5). The use of neutral conditions (H₂O/THF) as well as other acidic media as *p*-toluenesulfonic acid, camphorsulfonic acid or acetic acid did not provide better results in any case (Table 1.1, entries 6-9). In addition, shorter reaction times involved a significant decrease of the yield.

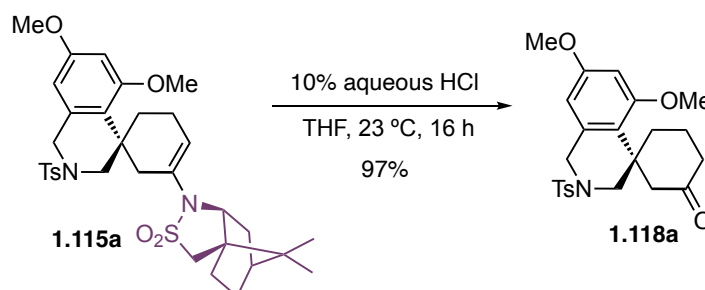
⁵¹ Work performed by Miguel Peña-López.

Table 1.1 Optimization for the hydrolysis of chiral auxiliary **X₁** in model substrate **1.117**.⁵¹

Entry	Hydrolysis conditions	Yield (%) ^a
1	10% aq. HCl, MeOH, 23 °C, 16 h	80
2	10% aq. HCl, EtOH, 23 °C, 16 h	41
3	10% aq. HCl, CH ₂ Cl ₂ , 23 °C, 16 h	19
4	10% aq. HCl, MeOH/CH ₂ Cl ₂ , 23 °C, 16 h	91
5	10% aq. HCl, THF, 23 °C, 16 h	99
6	H ₂ O/THF, 23 °C, 16 h	n.d.
7	<i>p</i> TsOH, H ₂ O/THF, 23 °C, 16 h	23
8	CSA, H ₂ O/THF, 23 °C, 16 h	17
9	AcOH, H ₂ O/THF, 23 °C, 16 h	n.d.

^a NMR yield using durene as internal standard. n.d.: not detected.

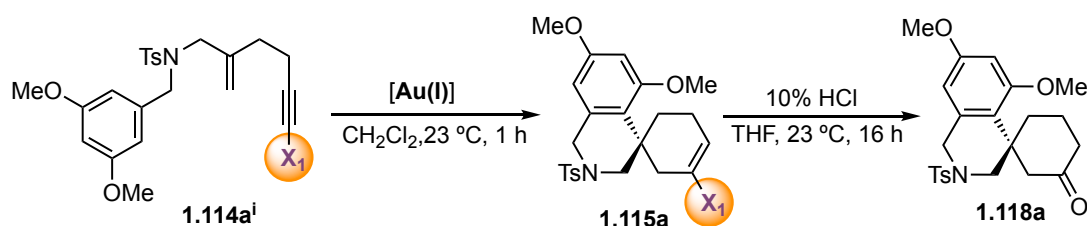
We then treated, a solution of compound **1.115a** (0.100 mmol) in THF (3 mL) with 10% aqueous HCl (1.5 mL) for 16 h at 23 °C, obtaining the desired ketone **1.118a** in 97% yield. (Scheme 1.16).



Scheme 1.16. Optimized hydrolysis conditions applied to substrate **1.115a** to obtain spirocyclic ketone **1.118a**.⁵¹

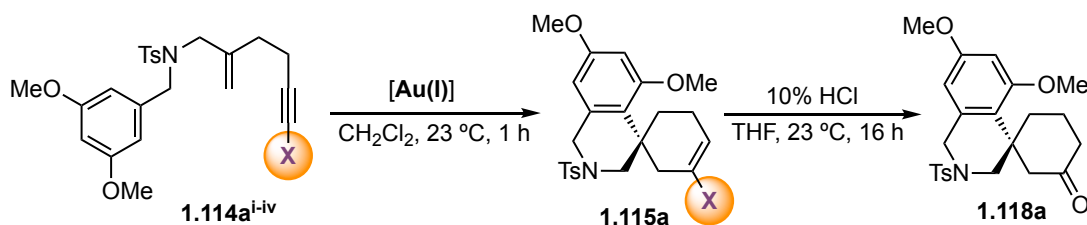
We therefore hypothesized that a two-step sequence involving gold(I)-catalyzed cyclization followed by acid-catalyzed hydrolysis with the aforementioned optimized conditions would provide access to enantioenriched chiral spirocyclic ketones **1.118** in a more practical manner. Cationic gold(I) complexes **1.A-F** and **1.H-L** equipped with JohnPhos, XPhos, NHC, and phosphite type ligands, furnished spirocyclic ketone **1.118a** in good yield and enantiomeric ratios, with catalyst **1.A** exhibiting the best performance (98%, 93:7 *er*) (Table 1.2, entries 1 and 2-9).

After selecting **1.A** as best catalyst, we were interested in varying the parameters of the reaction conditions and testing the effect of using different chiral auxiliaries on the final *er* of **1.118a** (Table 1.3).

Table 1.2 Catalyst screening for the gold(I)-catalyzed cascade cyclization of 1,5-enamides using chiral auxiliaries.⁵¹

Entry	[Au(I)]	Yield 1.115a (%) ^a	Yield 1.118a (%) ^b	<i>er</i> 1.118a
1	1.A (5 mol%)	91	98	93:7
2	1.B (5 mol%)	88	96	93:7
3	1.C (5 mol%)	81	95	90:10
4	1.D (5 mol%)	82	88	92:8
5	1.E (5 mol%)	29	98	88:12
6	1.F (5 mol%)	81	91	89:11
7	1.H (5 mol%)	85	93	93:7
8	1.I (5 mol%)	73	93	93:7
9	1.L (5 mol%)	19	89	77:23

^a NMR yield using durene or 1,1,2,2-tetrachloroethane as internal standard. ^b Overall isolated yield for the two-step sequence starting from **1.114aⁱ** (after the gold(I)-catalyzed cyclization, the solvent was evaporated and the crude product was treated with 1:3 10% HCl:THF 0.03 M).

Table 1.3 Chiral auxiliary screening for the gold(I)-catalyzed cascade cyclization of 1,5-enamides.⁴¹

Entry	X	[Au(I)]	Yield 1.115a (%) ^a	Yield 1.118a (%) ^b	<i>er</i> 1.118a
1	X ₁	1.A (3 mol%)	95(94) ^c	96	94:6
2 ^d	X ₁	1.A (3 mol%)	65	72	96:4
3	X ₂	1.A (3 mol%)	91	88	6:94
4	X ₃	1.A (3 mol%)	86	92	12:88
5	X ₆	1.A (3 mol%)	88	89	89:11
6	X ₇	1.A (3 mol%)	93	91	51:49
7 ^e	X ₇	1.M (3 mol%)	85	64	51:49
8 ^e	X ₁	1.M (3 mol%)	/	52	70:30
9 ^e	X ₂	1.M (3 mol%)	/	34	40:60

^a NMR yield using durene or 1,1,2,2-tetrachloroethane as internal standard. ^b Overall isolated yield for the two-step sequence starting from **1.114a**. ^c In parenthesis, isolated yield. ^d Reaction at -20 °C for 24 h. ^e AgSbF₆ (3 mol%) was used to activate **1.M**.

First, we noticed that lowering the catalyst loading to 3 mol% yielded **1.118a** in 96% yield with a slightly improved 94:6 *er* compared to when using 5 mol% (Table 1.3, entry 1). Lowering the temperature to -20 °C for 24 h enhanced the *er* to 96:4 but resulted in a lower yield (Table 1.3, entry 2). The opposite enantiomer of **1.118a** was efficiently obtained (88%, 6:94 *er*) using the enantiomeric camphorsultam **X₂** (Table 1.3, entry 3). Other chiral auxiliaries such as Evans-type oxazolidinones **X₃** and **X₆** provided **1.118a** with lower enantioselectivity (Table 1.3, entries 4-5). As a control, achiral *N*-methyl methanesulfonamide **X₇** yielded racemic **1.118a** in 91% yield (Table 1.3, entry 6). The achiral substrate presenting **X₇** was also subjected to chiral catalyst **1.M**, which had been previously optimized in our group for 1,6-enyne cyclizations,⁵² to compare the enantioselective approach with the chiral auxiliary one: in this case, essentially racemic **1.118a** was obtained in 64% yield (Table 1.3, entry 7). We then combined chiral catalyst **1.M** with chiral substrates bearing the Oppolzer sultam **X₁** and its enantiomer **X₂** to see whether there could be any enantioselectivity amplification but in both cases the *er* was lower than when using achiral catalysts (Table 1.3, entries 8-9). The poor enantioselectivities encountered when using **1.M** (Table 1.3, entries 7-9) are not a surprise, given the fact that the substrate is a 1,5-enyne, while the chiral catalyst used was optimized for 1,6-enyne cyclizations.⁵² In an unpublished work from our group⁵³ a screening of chiral catalysts for the 1,5-enyne cascade cyclization was performed following conditions previously optimized by Toste for enantioselective polycyclization of 1,6-enynes,⁵⁴ but scarce results were obtained, demonstrating the lack of alternatives so far to achieve this transformation with a satisfactory *er*.

The absolute configurations of **1.115a** and **1.118a** were confirmed as *S* by single crystal X-ray diffraction (Scheme 1.17). Importantly, following the hydrolysis, Oppolzer's sultam (**X₁**) was recovered enantiomerically pure in an excellent 96% yield, which combined with the formation of no by-products makes this process atom-efficient and environmentally benign. This sequence likely proceeds with the initial formation of a gold(I)-keteniminium intermediate,⁵⁵ which triggers a cascade process to form the polycyclic compound (Scheme 1.17). After alkyne activation, a *6-endo-dig* cyclization with the terminal alkene occurs to furnish a distorted cyclopropyl gold(I)-carbene/gold(I)-stabilized carbocation **1.120**. Following the intramolecular attack of the aryl ring, succeeded by a rearomatization step, the alkenyl-gold(I) species **1.121** is formed together with a second new C–C bond, leading to the formation of the

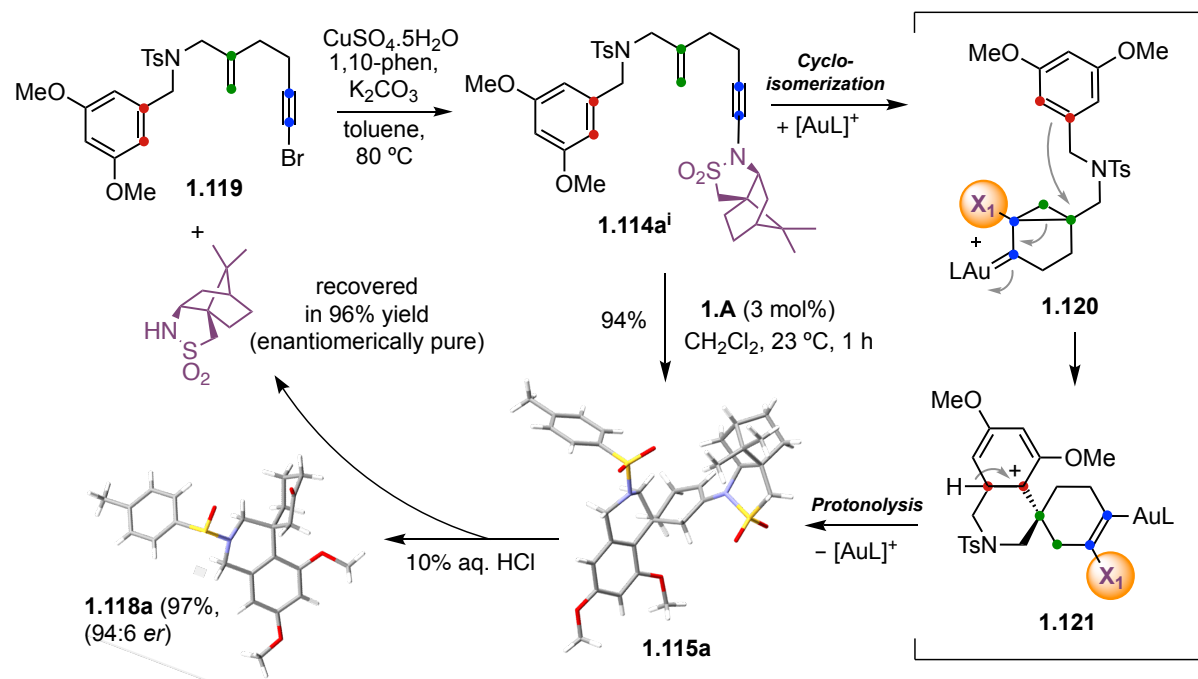
⁵² a) Zuccarello, G.; Mayans, J. G.; Escofet, I.; Scharnagel, D.; Kirillova, M. S.; Pérez-Jimeno, A. H.; Calleja, P.; Boothe, J. R.; Echavarren, A. M., Enantioselective Folding of Enynes by Gold(I) Catalysts with a Remote C₂-Chiral Element, *J. Am. Chem. Soc.* **2019**, *141*, 11858–11863. b) Zuccarello, G.; Nannini, L. J.; Arroyo-Bondía, A.; Fincias, N.; Arranz, I.; Pérez-Jimeno, A. H.; Peeters, M.; Martín-Torres, I.; Sadurní, A.; García-Vázquez, V.; Wang, Y.; Kirillova, M. S.; Montesinos-Magraner, M.; Caniparoli, U.; Núñez, G. D.; Maseras, F.; Besora, M.; Escofet, I.; Echavarren, A. M., Enantioselective Catalysis with Pyrrolidinyl Gold(I) Complexes: DFT and NEST Analysis of the Chiral Binding Pocket, *JACS Au* **2023**, *3*, 1742–1754.

⁵³ Rong Z, Gold(I)-Catalyzed Stereoselective Polycyclizations, *PhD Thesis*, **2017**, Universitat Rovira I Virgili, ICIQ (<https://www.tdx.cat/handle/10803/440512#page=1>).

⁵⁴ Sethofer, S. G.; Mayer, T.; Toste, F. D., Gold(I)-Catalyzed Enantioselective Polycyclization Reactions, *J. Am. Chem. Soc.* **2010**, *132*, 8276–8277.

⁵⁵ a) Evano, G.; Lecomte, M.; Thilmany, P.; Theunissen, C., Ketiminium Ions: Unique and Versatile Reactive Intermediates for Chemical Synthesis, *Synthesis* **2017**, *49*, 3183–3214. b) Chen, Y.-B.; Qian, P.-C.; Ye, L.-W., Brønsted Acid-Mediated Reactions of Ynamides, *Chem. Soc. Rev.* **2020**, *49*, 8897–8909.

stereocenter under the influence of the chiral auxiliary within the substrate. Ultimately, protodeauration facilitates the formation of **1.115a**.

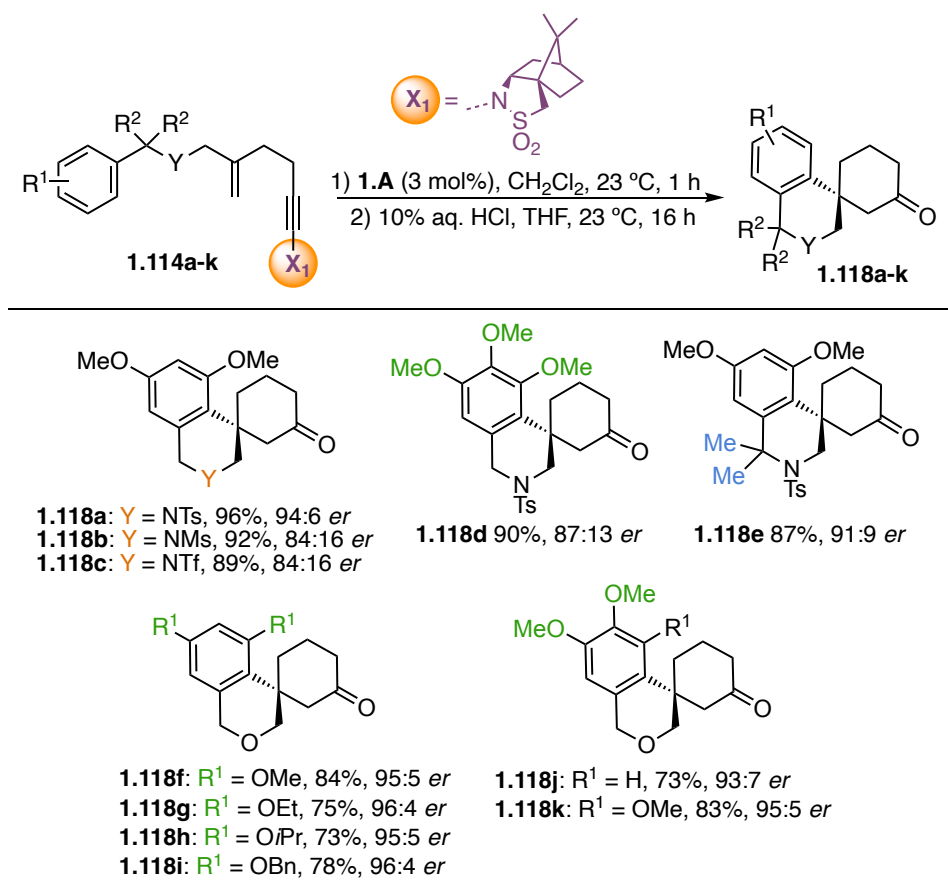


Scheme 1.17. Introduction/recovery of the chiral auxiliary starting from bromoenyne **1.119** through Cu-catalyzed C–N coupling⁵⁶ and determination of absolute configuration for **1.115a** and **1.118** by X-ray diffraction. Reaction pathway of stereoselective gold(I)-catalyzed cyclization of 1,5-enynes using Oppolzer's sultam as chiral auxiliary.

The investigation of the reaction scope was conducted under the optimized conditions (Table 1.4). Ketones **1.118b** and **1.118c**, featuring other electron-withdrawing substituents at the *N*-tether, were obtained in good yields, albeit with slightly lower enantiomeric ratios (89-92%, 84:16 *er*). Enynamides **1.114d** with 3,4,5-trimethoxybenzene and **1.114e** with benzylic gem-dimethyl substituents could be converted to ketones **1.118d** and **1.118e** in good yields and enantiomeric ratios (87-90%, 87:13 to 91:9 *er*). We also explored the formation of analogous oxo-spirocyclic ketones. Various OR groups at positions 3 and 5 on the aromatic moiety provided ketones **1.118f-i** in good yields and excellent enantioselectivities (73-84%, 95:5 to 96:4 *er*). The reaction proceeded smoothly with 3,4-dimethoxybenzene- and 3,4,5-trimethoxybenzene-containing 1,5-enynamides **1.114j** and **1.114k**, yielding ketones **1.118j** and **1.118k** in 73 and 83% yield and 93:7 and 95:5 *er*, respectively.

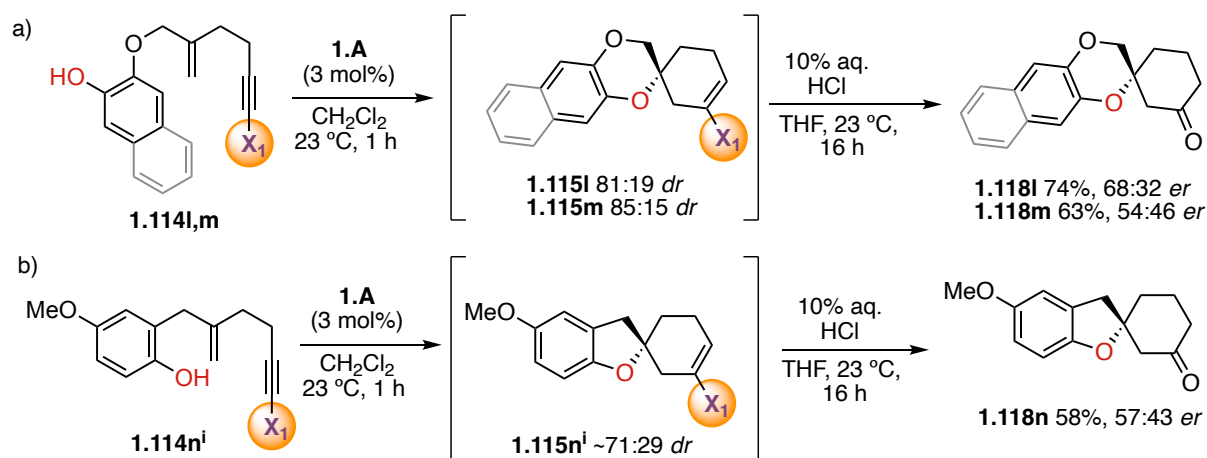
Our protocol was also applied to substituted phenols, where the hydroxy group served as a nucleophile in attacking the intermediate cyclopropyl gold(I)-carbene species, leading to the formation of a new C–O bond (Scheme 1.18).⁴⁰

⁵⁶ Fujino, D.; Yorimitsu, H.; Osuka, A., Regiocontrolled Palladium-Catalyzed Arylative Cyclizations of Alkynols, *J. Am. Chem. Soc.* **2014**, *136*, 6255–6258.

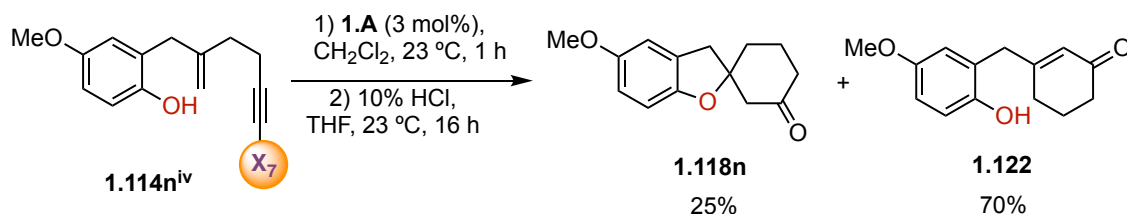
Table 1.4. Substrate scope for gold(I)-catalyzed cascade cyclization of 1,5-enynamides **1.114a-k**.^{4,51}

^aIsolated yields for the one-pot two-step sequence. After the gold(I)-catalyzed cyclization, the solvent was evaporated and the crude product was treated with 1:3 10% HCl:THF 0.03 M.

Although reasonable yields were obtained for the formation of heterocyclic structures **1.118l-m** and **1.118n**, the enantioselectivities were low (68:32 *er* for **1.118l**, 54:46 *er* for **1.118m**, and 57:43 *er* for **1.118n**) (Scheme 1.18). To rationalize the low encountered values, we measured the *dr* of the enamine intermediates with the Oppolzer auxiliary on the crude reaction mixtures before performing the acidic hydrolysis, which resulted to be 81:19 for **1.115l**, 85:15 for **1.115m**, and 71:29 for **1.115n**ⁱ.

**Scheme 1.18.** Gold(I)-catalyzed cyclizations of 1,5-enynamides bearing phenols.⁴¹

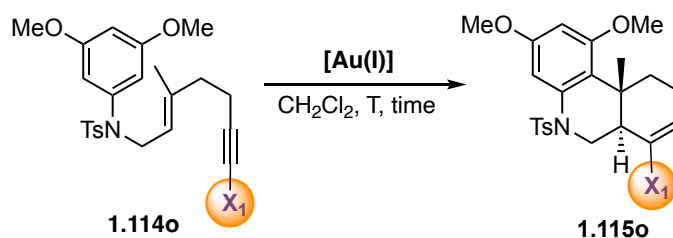
The higher *dr* values encountered suggested partial racemization happening during the hydrolysis step, hypothesis which was further supported when subjecting substrate **1.114n^{iv}** bearing achiral sulfonamide **X₇** to the standard reaction conditions (Scheme 1.19). In fact, when performing the one-pot two-steps sequence, together with **1.118n**, side product **1.122** was isolated in 70% yield.



Scheme 1.19. Gold(I)-catalyzed cyclization of 1,5-enynamide **1.114n^{iv}** bearing achiral **X₇**.⁵¹

We then contemplated the application of the same conditions to the structurally different substrate **1.114o**, presenting an internal alkene, which would result in the formation of two new stereogenic carbons (Table 1.5). Since performing the reaction, as in the previous cases, with 3 mol% of **1.A** during 1 h led to moderate 46% yield (Table 1.5 entry 1), we first focused on improving this yield by changing the catalyst loading, time and temperature of the reaction (Table 1.5 entries 2-7). A satisfactory yield of 71% was obtained when using 10 mol% of **1.A** over 1 h at 23 °C, however, when changing the catalyst to **1.H** (Table 1.5, entry 8), and finally to **1.I**, the yield went up to 79% over 5 h at 23 °C (Table 1.5, entry 9).

Table 1.5. Optimization for the gold(I)-catalyzed cyclization of internal alkene **1.114o**.⁵¹

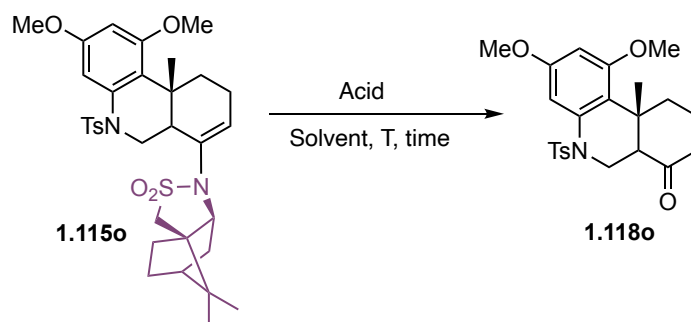


Entry	Au catalyst	Time (h)	T (°C)	Yield 1.115o (%) ^a
1	1.A (3 mol%)	1	23	46
2	1.A (3 mol%)	16	23	60
3	1.A (5 mol%)	1	23	54
3	1.A (5 mol%)	5	23	65
4	1.A (5 mol%)	16	23	57
5	1.A (10 mol%)	1	23	71
6	1.A (10 mol%)	16	23	56
7	1.A (5 mol%)	5	40	61
8	1.H (5 mol%)	5	23	78
9	1.I (5 mol%)	5	23	79

^aIsolated yields.

We then moved to finding appropriate conditions to remove chiral auxiliary **X₁** (Table 1.6) since the previously applied conditions to obtain the enantioenriched ketone, did not work (Table 1.6, entry 1). Screening HCl and *p*TsOH at high temperature always afforded **1.118** with a consistent amount of unreacted starting material or unidentified impurities (Table 1.6, entries 2-5 and entries 7-11). When using 37% aq. HCl in THF at 80 °C however, the only product forming together with **1.118** (isolated in 83% yield) was 1,4-butanediol formed via ring-opening of THF (Table 1.6, entry 6).

Table 1.6. Optimization for the acidic hydrolysis of enamine **1.115o**.⁵¹

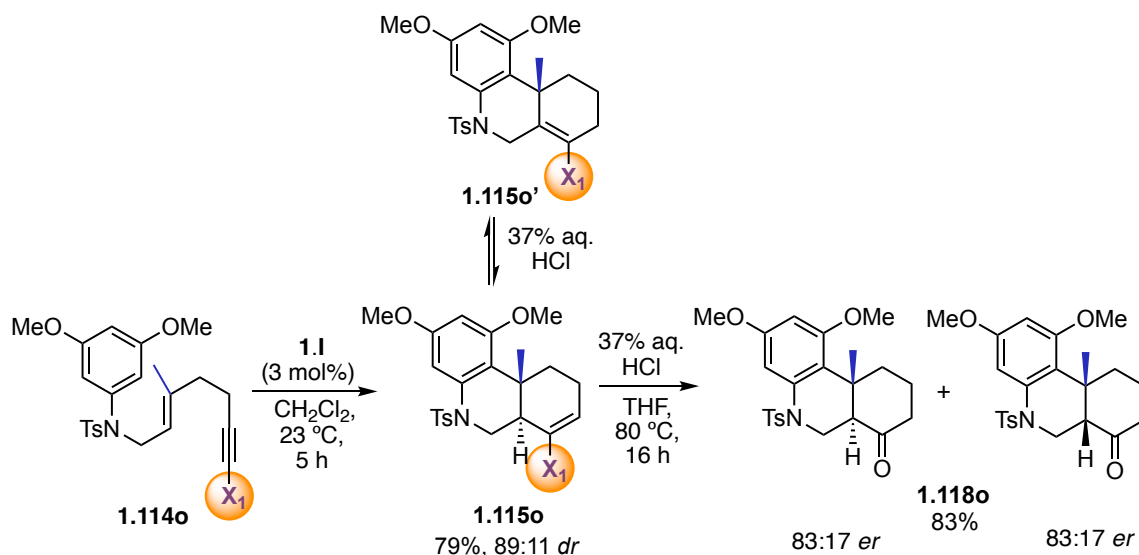


Entry	Acid (1:3 with THF)	Solvent (0.03 M)	T (°C)	Time (h)	Products
1	10% aq. HCl	THF	23	16	1.115o
2	10% aq. HCl	THF	80	5	1.115o + impurity
3	10% aq. HCl	THF	80	16	1.115o + impurity
4	20% aq. HCl	MeOH/CH ₂ Cl ₂	80	16	1.115o + 1.118o
5	37% aq. HCl	THF	23	16	1.115o + 1.118o ^a
6	37% aq. HCl	THF	80	16	1.118o (83%) ^{a,b}
7	37% aq. HCl	MeOH/CH ₂ Cl ₂	23	16	1.115o
8	37% aq. HCl	EtOH	80	16	1.118o + impurity
9	37% aq. HCl	toluene	80	16	1.118o + impurity
10	<i>p</i> TsOH.H ₂ O (3 equiv)	CH ₂ Cl ₂	50	16	1.115o + 1.118o + impurity
11	<i>p</i> TsOH.H ₂ O (5 equiv)	1,2-DCE	80	16	1.118o + impurity

^a1,4-Butanediol formed via ring-opening of THF. ^b Isolated yield.

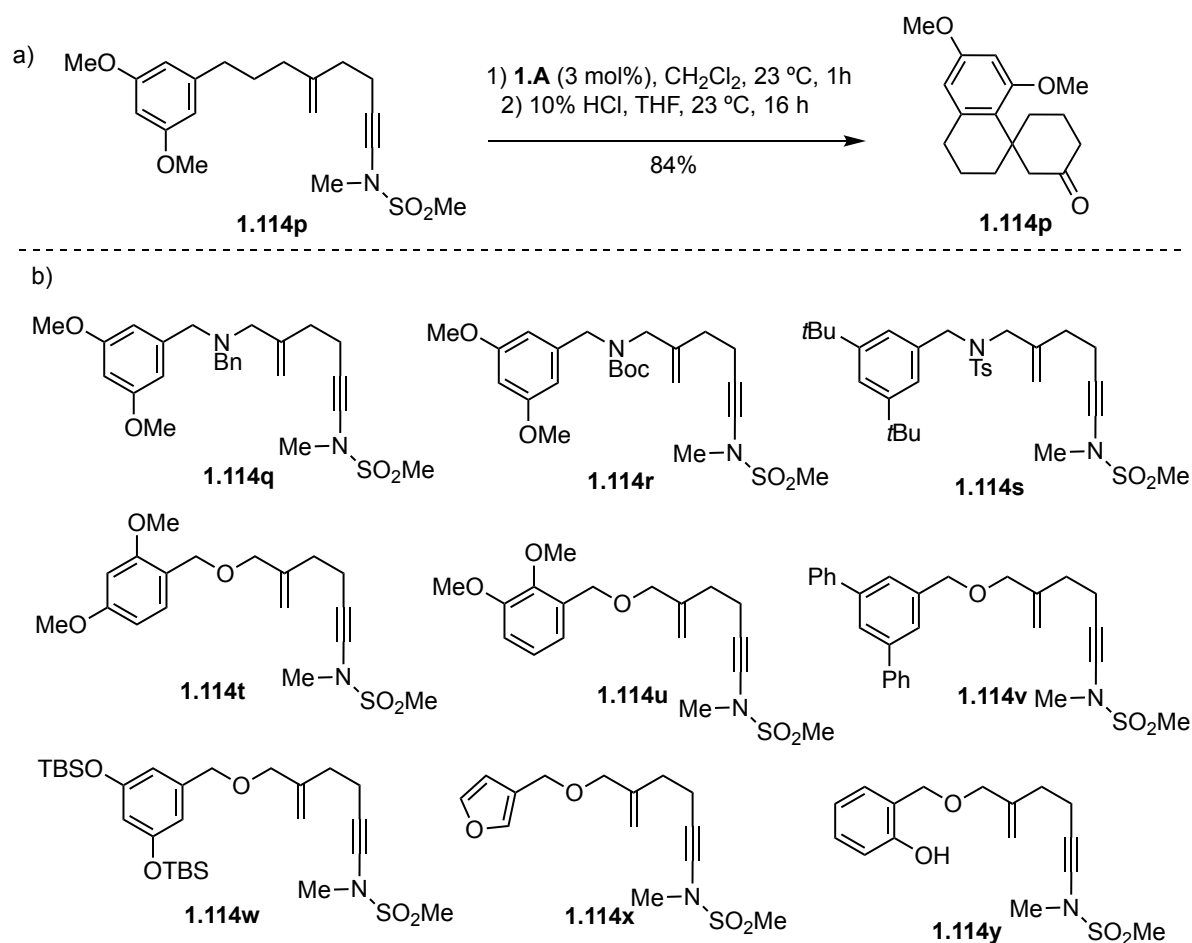
Nevertheless, these conditions caused the epimerization of one of the stereogenic centers formed during the polycyclization through isomerization of the enamine **1.115o** to **1.115o'**, resulting in a 1.9:1 ratio of diastereomers of **1.118o**, each exhibiting an 83:17 *er* (Scheme 1.20).

As for the substrates that did not afford the desired products, **1.114p** reacted when bearing the achiral sulfonamide **X₇** to give racemic **1.118p** in 84% isolated yield (Scheme 1.21a), but when we tried to synthesize the chiral version of **1.114p** bearing **X₁**, no reaction occurred.



Scheme 1.20. Gold(I)-catalyzed cyclization/hydrolysis of 1,5-enynamide **1.114o** presenting an internal alkene and epimerization of **1.115o** to **1.115o'**.⁵¹

Additionally, substrates **1.114q-y** did not provide any product under the optimized reaction conditions (Scheme 1.21b).

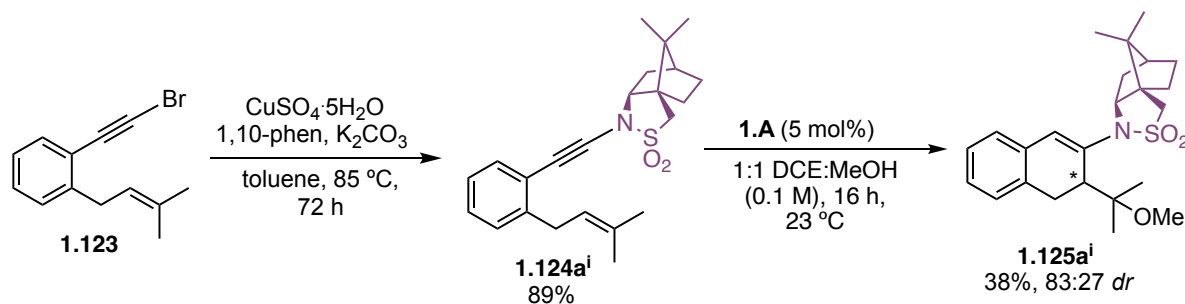


Scheme 1.21 Unsuccessful substrates for the gold(I)-catalyzed cascade cyclization of 1,5-enynamides. a) Cyclization of racemic **1.114p**. b) Unreactive substrates.

1,6-Enyne Alkoxy cyclization

We then moved to applying the chiral auxiliary approach to gold(I)-catalyzed alkoxy cyclizations, a class of reactions which, as mentioned in the **General Introduction** and as it will be discussed more in detail in **Chapter III**, was first developed in 2005 by our group in an enantioselective manner,⁴² and then more recently vastly improved by efficiently designing chiral catalysts.^{52,57}

Due to the promising outcomes demonstrated by Oppolzer's sultam **X**₁ as a chiral auxiliary in the 1,5-enynamides cascade cyclization, our initial focus was on investigating the alkoxy cyclization of 1,6-enynamide **1.124a**ⁱ featuring **X**₁ (Scheme 1.22) This substrate could be synthesized starting from 1-bromo-1,6-enyne **1.123** through the same Cu-catalyzed C–N coupling strategy used for the 1,5-enynamides described above (Scheme 1.17).⁵⁶ Employing gold(I)-catalyzed cyclization in the presence of MeOH at 23 °C using catalyst **1.A** yielded the 6-*endo-dig* product **1.125a**ⁱ in a 38% yield and 83:27 diastereomeric ratio (Scheme 1.22). No 5-*exo-dig* product was detected.

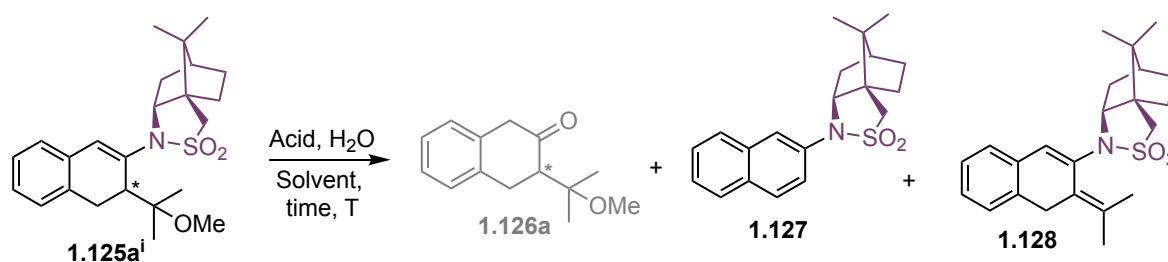


Scheme 1.22. Gold(I)-catalyzed alkoxy cyclization of 1,6-enynamide **1.124a**ⁱ. ^a DCE: 1,2-dichloroethane

Despite several attempts to hydrolyse enamine **1.125a**ⁱ under acidic conditions to obtain the resulting enantioenriched ketone **1.126** before proceeding with the optimization of reaction conditions, no success was encountered (Table 1.7). Side products deriving by the formal elimination of an acetone molecule resulting in naphthalene derivative **1.127**, or the alcohol loss product **1.128** were instead detected most of the times.

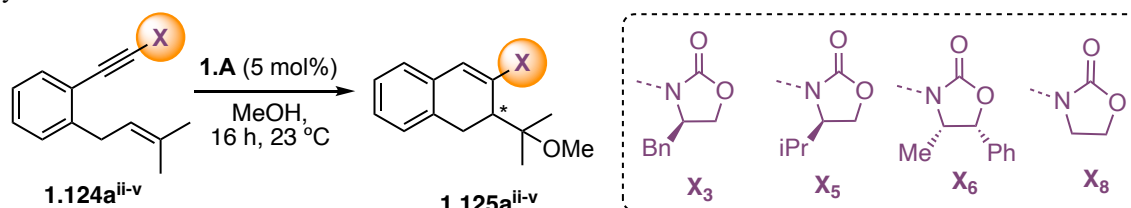
Consequently, Evans-type auxiliaries were considered (Table 1.8). Among the three different auxiliaries screened using **1.A** as a catalyst in a 1:1 MeOH:1,2-DCE solution, **X**₅ performed the best (97% yield, 96:4 *dr*, Table 1.8, entry 2). Also in this case, we performed the reaction with **1.124a**^v presenting achiral oxazolidinone **X**₈ using chiral catalyst **1.M** which afforded **1.125a**^v in 88% yield and good 91:9 *er*. This improved result in terms of enantioselectivities compared to when using **1.M** with 1,5-enynamides was expected, being **1.124a**^v a 1,6-enyne.⁵²

⁵⁷ a) Martín-Torres, I.; Ogalla, G.; Yang, J.-M.; Rinaldi, A.; Echavarren, A. M., Enantioselective Alkoxy cyclization of 1,6-Enynes with Gold(I)-Cavitands: Total Synthesis of Mafaicheenaminc C, *Angew. Chem. Int. Ed.* **2021**, *60*, 9339–9344, *Angew. Chem.* **2021**, *133*, 9425–9430. b) Franchino, A.; Martí, À.; Echavarren, A. M., H-Bonded Counterion-Directed Enantioselective Au(I) Catalysis, *J. Am. Chem. Soc.* **2022**, *144*, 3497–3509. c) Martí, À.; Ogalla, G.; Echavarren, A. M., Hydrogen-Bonded Matched Ion Pair Gold(I) Catalysis, *ACS Catal.* **2023**, *13*, 10217–10223.

Table 1.7. Hydrolysis attempts of enamine **1.125aⁱ** under acidic conditions.

Entry	Acidic medium and solvent	T (°C)	Time (h)	Detected products ^a
1	<i>p</i> TsOH (1 equiv) in H ₂ O:THF (1:3)	23	24	/
2	<i>p</i> TsOH (1 equiv) in H ₂ O:THF (1:3)	80	16	1.127
4	10% aq. HCl in THF (1:2)	23	24	/
5	10% aq. HCl in THF (1:2)	60	3	1.127^a
6	10% aq. HCl:THF (1:3)	80	16	1.127^a
7	conc. HCl in THF (1:2)	23	3	/
8	conc. HCl:THF (1:1)	23	3	1.127^a
9	conc. HCl:1,2-DCE:MeOH (1:1:1)	23	16	1.127 + 1.128
10	conc. HCl:1,2-DCE (1:2)	23	16	1.128
11	2:1:1 H ₂ O:THF :TFA	23	16	/
12	conc. H ₂ SO ₄ in 1,2-DCE (1:3)	23	16	1.128

^a1,4-Butanediol formed via ring-opening of THF.

Table 1.8. Screening of Evans-type chiral auxiliaries for the gold(I)-catalyzed alkoxy cyclization of 1,6-enynamides.^a

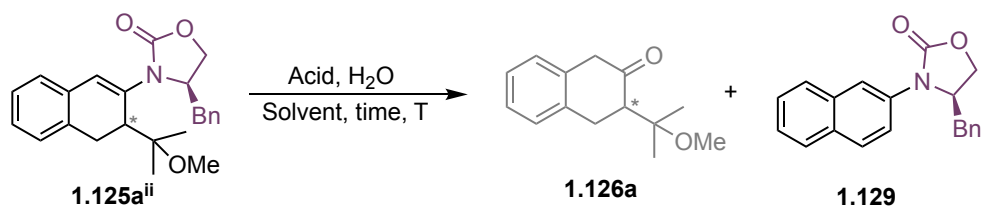
Entry	X	[Au(I)]	MeOH	Yield 1.125a (%) ^b	<i>dr</i> 1.125a ^c
1	X₃	1.A (5 mol%)	1:1 with 1,2-DCE	97	93:7
2	X₅	1.A (5 mol%)	1:1 with 1,2-DCE	97	96:4
3	X₆	1.A (5 mol%)	1:1 with 1,2-DCE	99	88:22
4 ^d	X₈	1.M (3 mol%)	1:1 with CH ₂ Cl ₂	88	91:9 (<i>er</i>)

^aAll the reactions were performed at 0.1 M concentration and at 23 °C, unless otherwise stated. ^bNMR yield using trichloroethylene as internal standard. ^c*dr* measured at ¹H NMR and confirmed by LC-MS analysis. ^dAgSbF₆ (3 mol%) was used to activate **M**.

We therefore subjected **1.125aⁱⁱ** and **1.125aⁱⁱⁱ** to acidic conditions to test whether we could respectively remove oxazolidinones **X₃** and **X₅**. While for **1.125aⁱⁱⁱ** only starting material was recovered with different

conditions, in the case of **1.125aⁱⁱ** also decomposition product **1.129** was detected when increasing the temperature (Table 1.9).

Table 1.9 Hydrolysis attempts of enamine **1.125aⁱⁱ** under acidic conditions.



Entry	Acidic medium and solvent	T (°C)	Time (h)	Detected products ^a
1	10% aq. HCl:THF (1:2)	23	16	/
2	10% aq. HCl:THF (1:2)	60	16	1.129
3	conc. HCl:THF (1:2)	80	7	1.129
4	conc. HCl:EtOH (1:2)	80	6	Unidentified mixture
5	<i>p</i> TsOH (1.2 equiv) in THF	23	16	/

We then envisioned a different protocol to remove the chiral oxazolidinones, which considered the use of LiAlH₄ to reduce the cyclic carbamate to alcohol,⁵⁸ followed by hydrolysis of the derived acyclic enamine with *p*TsOH. This destructive methodology would not allow, however, the recovery of the chiral auxiliary. We first tested these conditions on racemic **1.125a^v** bearing **X₈**, and we obtained the racemic product **1.126a** in 30% isolated yield, together with **1.130**, which formed after treatment of the reaction crude in silica (Scheme 1.23). We observed this product also when dissolving the sample in CDCl₃ for NMR analysis: it seems that this new class of 2-tetralones is particularly prone to eliminate the alcohol functionality under acidic conditions unfortunately bringing to loss of the chiral center. Nevertheless, we were interested in improving this protocol since 2-tetralones are reported to be valuable frameworks in organic synthesis⁵⁹ and pharmacologically relevant intermediates⁶⁰ such as antidepressants⁶¹ or benzomorphan analgesics.⁶²

⁵⁸ Huo, H.-H.; Zhang, H.-K.; Xia, X.-E.; Huang, P.-Q., A Formal Enantioselective Total Synthesis of FR901483, *Org. Lett.* **2012**, *14*, 4834–4837.

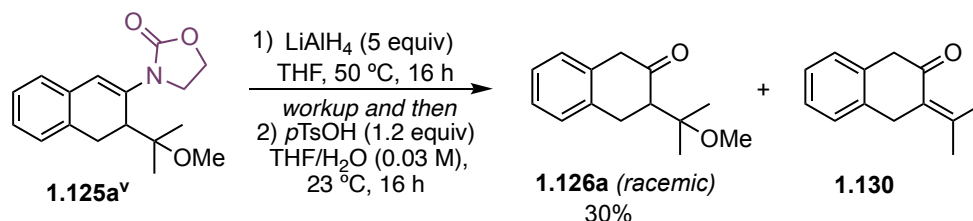
⁵⁹ a) Shner, V. F.; Przhiyaglovskaya, N. M., COMPOUNDS OF THE β-TETRALONE SERIES, *Russ. Chem. Rev.* **1966**, *35*, 523. b) Jensen, B. L.; Chockalingam, K. Total Synthesis of 4,5,7a,8-Tetrahydro-1,2-Dimethoxyphenanthro[10,1-Bc]-Azepin-6(7H)-One: A Photochemical Approach. *J. Heterocycl. Chem.* **1986**, *23*, 343–347. c) Covarrubias-Zúñiga, A.; Cantú, F.; Maldonado, L. A. A Total Synthesis of the Racemic Sesquiterpene Parvifoline. *J. Org. Chem.* **1998**, *63*, 2918–2921.

⁶⁰ a) Ye, B.; Yao, Z.-J.; Burke, T. R. Synthesis of a New Tyrosine Analogue Having X1 and X2 Angles Constrained to Values Observed for an SH2 Domain-Bound Phosphotyrosyl Residue. *J. Org. Chem.* **1997**, *62*, 5428–5431. b) Brewster, W. K.; Nichols, D. E.; Riggs, R. M.; Mottola, D. M.; Lovenberg, T. W.; Lewis, M. H.; Mailman, R. B. Trans-10,11-dihydroxy-5,6,6a,7,8,12b-hexahydrobenzo[a]phenanthridine: a highly potent selective dopamine D1 full agonist. *J. Med. Chem.* **1990**, *33*, 1756–1764.

⁶¹ Wentland M. P.; Bailey D. M.; Alexander E. J.; Castaldi M. J.; Ferrari R. A.; Haubrich D. R.; Luttinger D. A.; Perrone M. H., Synthesis and antidepressant properties of novel 2-substituted 4,5-dihydro-1H-imidazole derivatives, *J. Med. Chem.* **1987**, *30*, 1482–1489.

⁶² a) Bartrop, J. A., 81. Syntheses in the Morphine Series. Part I. Derivatives of Bicyclo[3 : 3 : 1]-2-Azanonane, *J. Chem. Soc. Resumed* **1947**, No. 0, 399–401. b) Bartrop, J. A.; Saxton, J. E., 184. Syntheses in the Morphine Series. Part III. Further Experiments with β-Tetralone, *J. Chem. Soc. Resumed* **1952**, No. 0, 1038–1041.

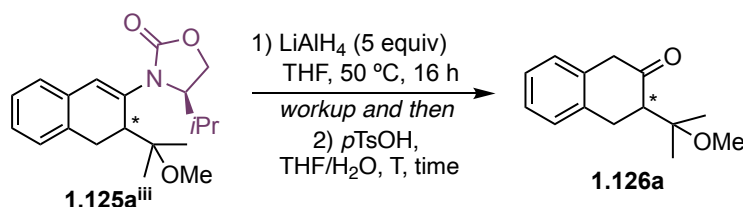
Furthermore, there aren't currently many strategies devoted to the synthesis of these scaffolds,⁶³ especially in an enantioenriched manner.⁶⁴



Scheme 1.23. Oxazolidinone reduction-hydrolysis protocol applied to racemic enamine **1.125a^v** presenting auxiliary **X₈**.

We then applied the newly developed protocol to **1.125aⁱⁱⁱ** and the yield of the one-pot two-steps process was measured on the reaction crude by NMR integration, to deduct the efficiency of the reactions before decomposition of the product on silica. After performing the first reduction step at 50 °C and checking by TLC that all the starting material was consumed, we left the reaction overnight with *p*TsOH at 23 °C as we did for racemic **1.125a^v**, but only traces of **1.126a** were spotted in the reaction crude (Table 1.10, entry 1). Increasing the number of equivalents of *p*TsOH and the concentration gave **1.126a** in 11% yield (Table 1.10, entry 2) while increasing the reaction time to 40 h resulted in 27% NMR yield (Table 1.10, entry 3). Finally, by performing the hydrolysis step at 68 °C, full starting material conversion was achieved after 3 h but only 30% of **1.126a** was detected (Table 1.10, entry 4).

Table 1.10. Oxazolidinone reduction-hydrolysis protocol applied to enamine **1.125aⁱⁱⁱ** presenting auxiliary **X₅**.



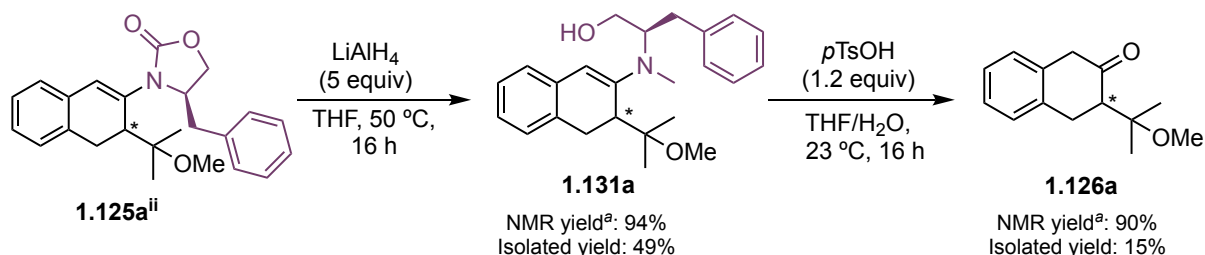
Entry	<i>p</i> TsOH (equiv)	C in 2:1 THF:H ₂ O	T (°C)	Time (h)	Yield 1.126a (%) ^[a]
1	1.2	0.03 M	23	16	traces
2	2.0	0.06 M	23	24	11
3	1.2	0.03 M	23	40	27
4	1.2	0.03 M	68	3	30

^aYield calculated by ¹H NMR integration using trichloroethylene as internal standard.

⁶³ a) Jensen, B. L.; Michaud, D. P. An Improved Enamine-Alkylation Procedure. Synthesis of 1-Benzyl-2-Indanones and 1-Benzyl-2-Tetralones. *Synthesis* **1977**, *1977*, 848–849. b) Jensen, B. L.; Slobodzian, S. V. A Concise Synthesis of 1-Substituted-2-Tetralones by Selective Diol Dehydration Leading to Ketone Transposition. *Tetrahedron Lett.* **2000**, *41*, 6029–6033.

⁶⁴ Liu, Y.; Deng, Y.; Zavalij, P. Y.; Liu, R.; Doyle, M. P. An Efficient Route to Highly Enantioenriched Tetrahydroazulenes and β-Tetralones by Desymmetrization Reactions of δ,δ-Diaryldiazoacetate-Acetates. *Chem. Commun.* **2014**, *51*, 565–568.

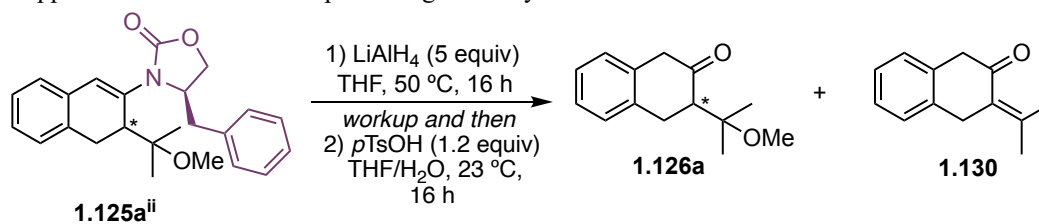
Given the low conversion to **1.126a** from **1.125aⁱⁱⁱ**, we shifted our focus to enamine **1.125aⁱⁱ** bearing (*R*)-4-benzyloxazolidin-2-one **X₃** hoping to observe better results. This time, we monitored the NMR yield and then isolated the intermediate open-form enamine **1.131a** (Scheme 1.24). When performing the reduction at 50 °C using 5 equiv of LiAlH₄, and then the hydrolysis step at 23 °C overnight, while both **1.131a** and **1.126a** partially decomposed in silica bringing to low isolated yields, the NMR yields were excellent, indicating a high efficiency of both reactions under the reported conditions, in contrast to what seen for **1.125aⁱⁱⁱ** (Table 1.10).



Scheme 1.24. Oxazolidinone reduction-hydrolysis protocol applied to enamine **1.125aⁱⁱ** presenting auxiliary **X₃**. ^aYield calculated by ¹H NMR integration using trichloroethylene as internal standard.

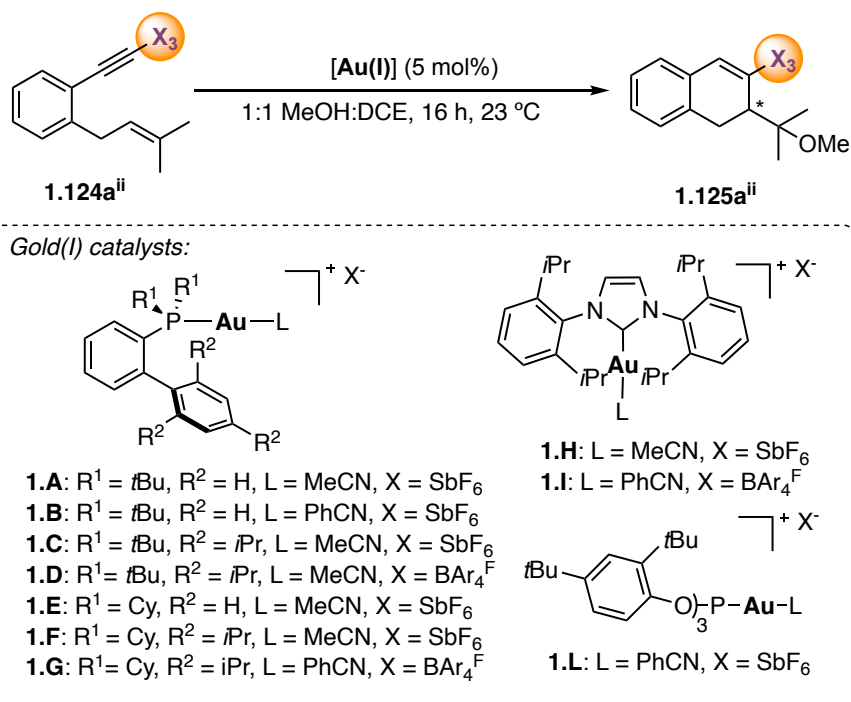
Having in hand an optimal set of conditions for the reduction-hydrolysis sequence of **1.125aⁱⁱ**, we focused on optimizing the purification strategy for a one-pot two steps protocol which would minimize the loss of yield given by decomposition (Table 1.11). When working with silica (whether activated or pre-treated with triethylamine) or with neutral alumina, the isolated yield was never superior to 28% (Table 1.11, entries 1-3). Finally, using basic alumina, **1.126a** could be isolate in an 40% yield over two steps (Table 1.11, entry 4).

Table 1.11. Optimization of the purification techniques used for the one-pot two-step reduction-hydrolysis protocol applied to enamine **1.125aⁱⁱ** presenting auxiliary **X₃**.



Entry	Purification technique	Isolated yield 1.126a (%)
1	Silica or neutral alumina column	25
2	Silica column pre-treated with pure TEA	25
3	Silica column pre-trated with 3% TEA	28
4	Basic alumina column	40

Once assessed that chiral auxiliary **X₃** could be removed with a higher efficiency compared to **X₅**, we decided to bring on our optimization of the gold(I)-catalyzed cyclization using substrate **1.124aⁱⁱ** bearing **X₃**. Catalyst screening of complexes **1.A-L** (5 mol%) revealed that **1.A** was already the best option in terms of yields and diastereoselectivity (Table 1.12).

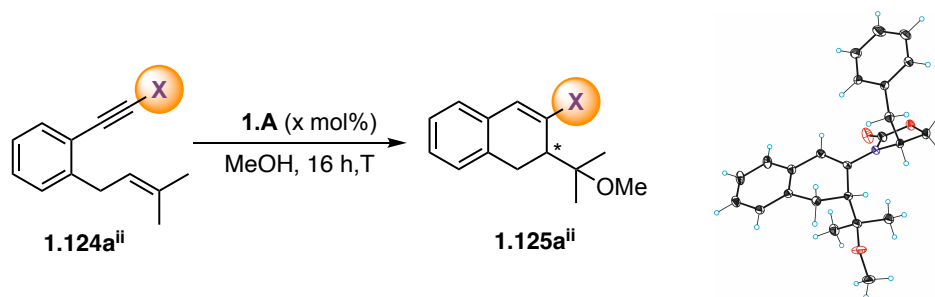
Table 1.12. Catalyst screening for the gold(I)-catalyzed alkoxycyclization of 1,6-enynamide **1.124aⁱⁱ**.^a

Entry	[Au(I)]	Yield 1.125aⁱⁱ (%)	<i>dr</i> 1.125aⁱⁱ
1	1.A	97	93:7
2	1.B	96	93:7
3	1.C	94	92:8
4	1.D	97	91:9
5	1.E	95	87:23
6	1.F	92	92:8
7	1.G	96	92:8
8	1.H	99	90:10
9	1.I	90	89:11
10	1.L	88	91:9

^aAll the reactions were performed at 0.1 M concentration. DCE = 1,2-dichloroethane. ^bNMR yield using trichloroethylene as internal standard. ^c*dr* measured at ¹H NMR and confirmed by LC-MS analysis.

We then proceeded to vary the remaining reaction parameters: increasing the quantity of nucleophile had a beneficial impact on the diastereomeric ratio (Table 1.13, comparing entries 1 and 2). Ultimately, lowering the temperature to -20°C resulted in full conversion and a *dr* of 99:1 after 16 hours (Table 1.13, entry 3). Moreover, the catalyst loading could be reduced to 3% without any drop in yield and just a slightly lower diastereomeric ratio (Table 1.13, entry 4). The configuration of the new stereocenter of **1.125aⁱⁱ** was determined as *R* by X-ray diffraction which also confirmed the product being result of a *6-endo-dig* cyclization. Under the optimized conditions, the reaction with the (*S*)-benzoxazolidinone auxiliary **X₄** yielded the enantiomer of **1.125aⁱⁱ** in 99% yield and a *dr* of 1:99. (Table 1.13, entry 5).

Table 1.13. Catalyst loading, equivalents of alcohol and temperature variation in the gold(I)-catalyzed alkoxy cyclization of 1,6-enynamide **1.124aⁱⁱ**.^a Determination of absolute configuration for **1.125aⁱⁱ** by X-Ray diffraction.



Entry	X	1.A (x mol%)	Solvent	T	Yield 1.125aⁱⁱ (%) ^b	<i>dr</i> 1.125aⁱⁱ ^c
1	X ₃	5 mol%	10 equiv of MeOH in 1,2-DCE	23 °C	97	92:8
2	X ₃	5 mol%	MeOH	23 °C	99	94:6
3	X ₃	5 mol%	MeOH	-20 °C	99 (95)	>99:1
4	X ₃	3 mol%	MeOH	-20 °C	99	99:1
5	X ₄	3 mol%	MeOH	-20 °C	99	1:99

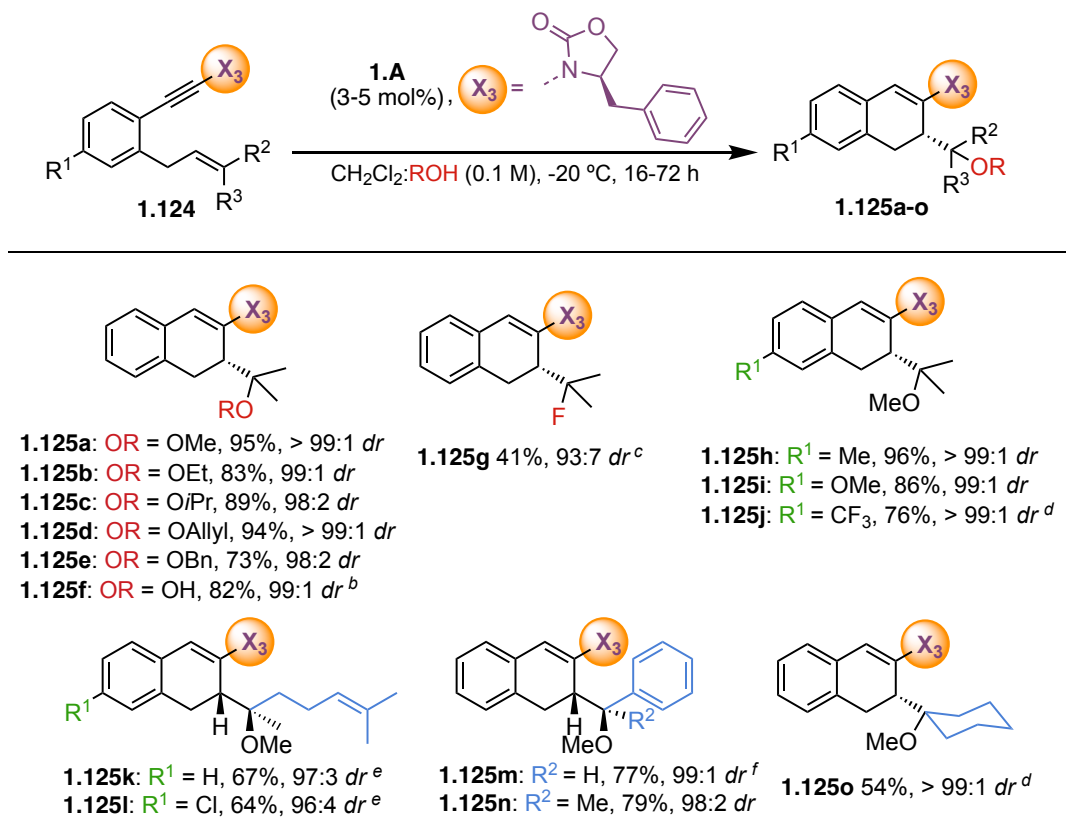
^aAll the reactions were performed at 0.1 M concentration. ^bNMR yield using trichloroethylene as internal standard. In parentheses, isolated yields. ^c*dr* measured at ¹H NMR and confirmed by LC-MS analysis.

Once having optimized the reaction conditions, the scope of the diastereoselective *6-endo-dig* cyclization of 1,6-enynamides was investigated in the presence of various alcohols (Table 1.14). Substrate **1.124aⁱⁱ** afforded **1.125a-e** in good to excellent yields and diastereoselectivities (ranging from 98:2 *dr* to >99:1 *dr*). Additionally, water acted as a nucleophile, yielding **1.125f** in 82% yield and a surprising 99:1 *dr* even if the reaction was conducted at room temperature. When HF-pyridine was used as a source of F⁻, product **1.125g** was obtained with a 41% yield and a lower 93:7 *dr*, which was not surprising given the previous results obtained in our group when using this nucleophile.^{57b} Both electron-withdrawing and electron-donating substituents at the aryl moiety led to the corresponding adducts **1.125h** (96%, >99:1 *dr*), **1.125i** (86%, 99:1 *dr*) and **1.125j** (76%, >99:1 *dr*) without any loss in diastereoselectivity, however, the least reactive *p*-CF₃ derivative required an increased (10 mol%) catalyst loading. We then moved to modifying the alkene chain: geranyl substituted enynamide brought to **1.125k** (67%, 97:3 *dr*) and **1.125l** (64%, 96:4 *dr*) in good yields and high *dr*. In these cases, as in the case of **1.125m** (77%, 99:1 *dr*) and **1.125n** (79%, 98:2 *dr*), we assume the major diastereomers to be the ones reported in Table 1.14, on the basis of literature reports which show that the cyclizations starting from *E* alkenes usually afford in a stereospecific manner the *anti* products (as discussed in the **General Introduction**).⁶⁵

⁶⁵ a) Nieto-Oberhuber, C.; Muñoz, M. P.; Buñuel, E.; Nevado, C.; Cárdenas, D. J.; Echavarren, A. M. Cationic Gold(I) Complexes: Highly Alkynophilic Catalysts for the Exo- and Endo-Cyclization of Enynes. *Angew. Chem. Int. Ed.* **2004**, *43*, 2402–2406, *Angew. Chem.* **2004**, *116*, 2456–2460. b) Nieto-Oberhuber, C.; Muñoz, M. P.; López, S.; Jiménez-Núñez, E.; Nevado, C.; Herrero-Gómez, E.; Raducan, M.; Echavarren, A. M., Gold(I)-Catalyzed Cyclizations of 1,6-Enynes: Alkoxy cyclizations and Exo/Endo Skeletal Rearrangements, *Chem. Eur. J.* **2006**, *12*, 1677–1693.

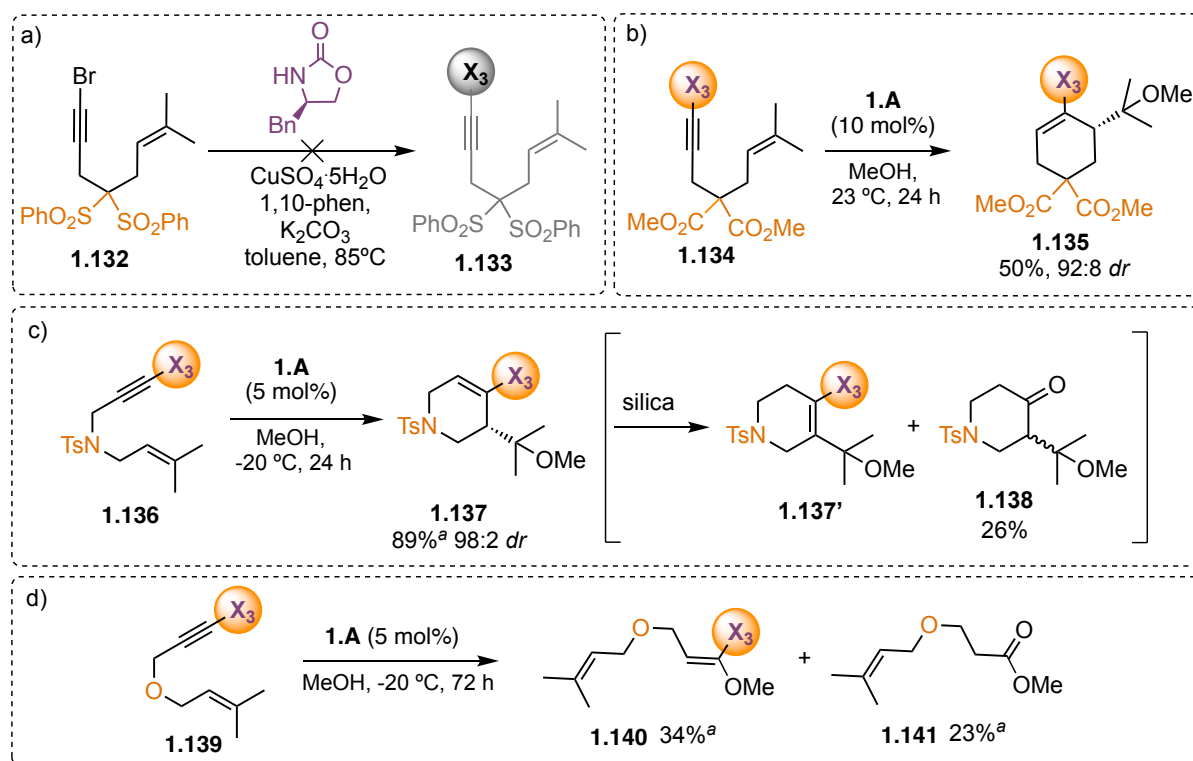
Finally, by using 10 mol% of catalyst, **1.125o** could be isolated in excellent >99:1 *dr*, although with a lower 54% yield, probably due to the steric bulk of the cyclohexyl group.

Table 1.14. Alcohol and substrate scope for the gold(I)-catalyzed alkoxy cyclization of 1,6-enamides.^{a, 43}



^a Yields of isolated products and the *dr* determined by both ¹H NMR integration and LC-MS analysis after column chromatography. The specific reaction times are reported in the experimental section. Unless stated differently, 5 mol% of **1.A** was used and CH₂Cl₂ : ROH = 1:3. ^b The reaction was conducted at 23 °C. ^c HF-pyridine (3 equiv) was used in this case as a F⁻ source. ^d Reactions performed with 10 mol% of **1.A**. ^e The reported yields and *dr* are referred to two of the four possible diastereomers which formed during the reaction. ^f Three of the four possible diastereomers were isolated in 11:3:1 ratio and the reported yield refers to the major one, together with its *dr* with respect to the fourth diastereomer which was not isolated.

To verify whether the methodology was limited to aryl-tethered enynes, we synthesized 1,6-enamides **1.134**, **1.136** and **1.139**, while the coupling from **1.132** to form sulphone-tethered enynamide **1.133** did not work (Scheme 1.25a). **1.135** could be obtained in a 50% yield and 92:8 *dr* from the poorly reactive malonate-tethered **1.134** only when working at room temperature and with 10% of catalyst loading (Scheme 1.25b). When we tried to hydrolyze enamine **1.135** under acidic conditions (by using HCl or *p*TsOH) to obtain the corresponding ketone, methanol elimination was observed. Nevertheless, *N*-tosyl derivative **1.136** readily reacted at -20°C to afford heterocyclic **1.137** in excellent NMR yield (89%) and diastereoselectivities (98:2 *dr*). However, when subjecting the latter to silica gel for purification, a mixture of isomerized enamine **1.137'** and presumably epimerized ketone **1.138** formed (Scheme 1.25c). Finally, oxygen-tethered **1.139** only gave products **1.140** and **1.141** of direct methanol addition to the triple bond (Scheme 1.25d).



Scheme 1.25. Tether scope for the gold(I)-catalyzed alkoxy cyclization of 1,6-enynes. All the reactions were performed in 1:3 CH₂Cl₂:MeOH. Isolated yields unless specified otherwise. ^a The yield was determined by ¹H NMR using 1,1,2,2-tetrachloroethane as internal standard.

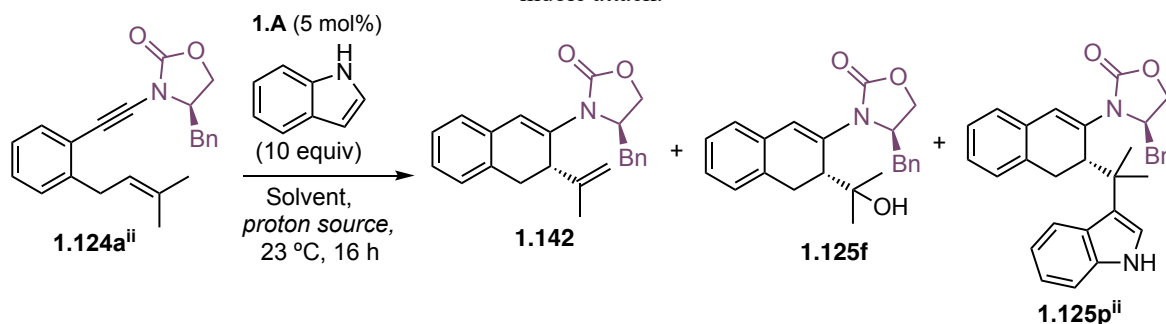
When attempting the addition of indoles as carbon nucleophiles^{57c,66} with 1,6-enynes **1.124** under the same conditions utilized for the addition of alcohols, we only recovered starting material (Table 1.15, entry 1), despite efforts by increasing temperature, nucleophile equivalents, or catalyst loading. We suspected then that in the absence of alcohol, the reaction would not proceed, as it is well-established that proton sources facilitate the protodeauration step in gold(I) catalysis.⁶⁷ The reaction was performed again in the presence of pyridinium *p*-toluenesulfonate (PPTS) to provide a proton source to the system and the desired product **1.125p**ⁱⁱ was indeed isolated but just in 25% yield (Table 1.15, entry 2). The low yield can be attributed to the formation of the cycloisomerization and water attack by-products **1.142** and **1.125f**. To disfavour the water attack, the reaction was run in the glovebox using dry PPTS in dry CH₂Cl₂, and since the elimination of a proton from the isopropyl methyl is

⁶⁶ a) Toullec, P. Y.; Genin, E.; Leseurre, L.; Genêt, J.-P.; Michelet, V., Room-Temperature Au(I)-Catalyzed C–C Bond Formation through a Tandem Friedel–Crafts-Type Addition/Carbocyclization Reaction, *Angew. Chem. Int. Ed.* **2006**, *45*, 7427–7430, *Angew. Chem.* **2006**, *118*, 7587–7590. b) Amijs, C. H. M.; Ferrer, C.; Echavarren, A. M., Gold(I)-Catalysed Arylation of 1,6-Enynes: Different Site Reactivity of Cyclopropyl Gold Carbenes, *Chem. Commun.* **2007**, No. 7, 698–700. c) Amijs, C. H. M.; López-Carrillo, V.; Raducan, M.; Pérez-Galán, P.; Ferrer, C.; Echavarren, A. M., Gold(I)-Catalyzed Intermolecular Addition of Carbon Nucleophiles to 1,5- and 1,6-Enynes, *J. Org. Chem.* **2008**, *73*, 7721–7730.

⁶⁷ The effect of acids on protodeauration has been demonstrated by the isolation and protonation of the vinylgold intermediate: a) Liu, L.-P.; Xu, B.; Mashuta, M. S.; Hammond, G. B., Synthesis and Structural Characterization of Stable Organogold(I) Compounds. Evidence for the Mechanism of Gold-Catalyzed Cyclizations, *J. Am. Chem. Soc.* **2008**, *130*, 17642–17643. See also: b) Zhu, Y.; Yu, B., Characterization of the Isochromen-4-Yl-Gold(I) Intermediate in the Gold(I)-Catalyzed Glycosylation of Glycosyl Ortho-Alkynylbenzoates and Enhancement of the Catalytic Efficiency Thereof, *Angew. Chem. Int. Ed.* **2011**, *50*, 8329–8332, *Angew. Chem.* **2011**, *123*, 8479–8482. c) Barrio, P.; Kumar, M.; Lu, Z.; Han, J.; Xu, B.; Hammond, G. B., Acidic Co-Catalysts in Cationic Gold Catalysis, *Chem. Eur. J.* **2016**, *22*, 16410–16414 d) Lu, Z.; Li, T.; Mudshinge, S. R.; Xu, B.; Hammond, G. B., Optimization of Catalysts and Conditions in Gold(I) Catalysis - Counterion and Additive Effects, *Chem. Rev.* **2021**, *121*, 8452–8477.

likely to be operated by the *p*-toluenesulfonate anion of PPTS, this time a catalytic amount of the acid was used (Table 1.15, entry 3) but no product was visible at ¹H NMR. The quantity of PPTS was then raised to 0.3 equiv (Table 1.15, entry 4): in this case, the product was isolated in 21% yield, no water attack was observed and less elimination product was formed, but a lot of starting material was still recovered. Subsequently, *p*-toluenesulfonic acid (PTSA) and camphorsulfonic acid (CSA) were also tested: given the weaker ionic character compared to PPTS, the percentage of observed elimination product was, as hoped, lower (Table 1.15, compare entries 5-6 with entry 2), but in the first case, even if the PTSA was previously dried through azeotropic distillation in toluene, it appears that the water molecules trapped in the lattice were sufficient to form product **1.125f**. To provide a proton source to the system that would not act as a base or as a nucleophile, the reaction was conducted using hexafluoroisopropanol (HFIP) as a solvent (Table 2.15, entry 7) which was previously dried to avoid any interference with water attack. Delightfully, the desired product **1.125pⁱⁱ** was obtained in 67% isolated yield and >99:1 *dr*. When using only 5 equiv of HFIP in dry CH₂Cl₂, only traces of the desired product were detected, together with some elimination product **1.142** (Table 2.15, entry 8).

Table 1.15. Screening of proton sources for the gold(I)-catalyzed *6-endo-dig* cyclization of **1.124aⁱⁱ** followed by indole attack.



Entry	Solvent	Proton Source	Yield 1.142 (%)	Yield 1.125f (%)	Yield 1.125pⁱⁱ (%)
1 ^b	CH ₂ Cl ₂	/	/	/	/
2	CH ₂ Cl ₂	PPTS (1 equiv)	42	29	25
3	dry CH ₂ Cl ₂	dry PPTS (0.05 equiv)	/	/	/
4	dry CH ₂ Cl ₂	dry PPTS (0.3 equiv)	25	/	21
5	dry CH ₂ Cl ₂	PTSA (1 equiv)	18	36	18
6	dry CH ₂ Cl ₂	dry CSA (1 equiv)	28	/	12
7	dry HFIP	/	/	/	67^c
8	dry CH ₂ Cl ₂	dry HFIP (5 equiv)	traces	/	traces

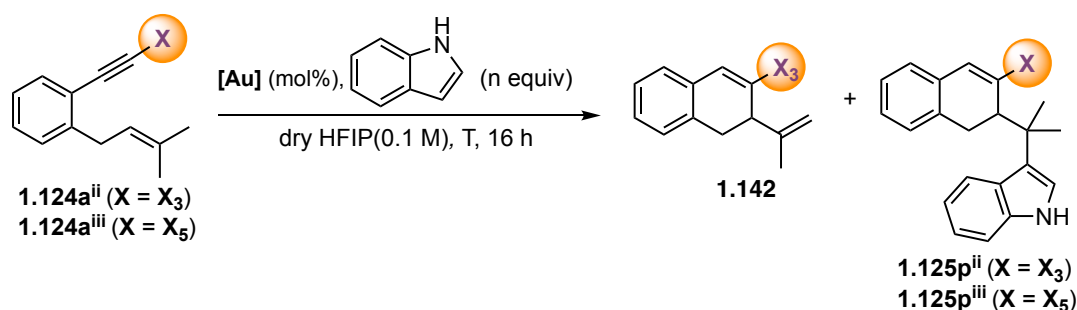
^aIsolated yields. ^bThe reaction was also performed at 80 °C, 20 equiv of indole and with 10 mol% of catalyst.

^c*dr* > 99:1

Apart from serving as proton shuttle for the protoedauration step, as elaborated further in the mechanistic studies section, this solvent might also kinetically favor the reaction by stabilizing the cationic species involved.⁶⁸

The reaction conditions were therefore investigated further (Table 1.16). When lowering the quantity of nucleophile from 10 to 5 or 1.2 equiv, partial formation of the elimination product **1.142** was also observed (Table 1.16, entries 2-3). Lowering the temperature only brought to lower conversion (Table 1.16, entry 4) while changing the chiral auxiliary to (*R*)-4-isopropylloxazolidin-2-one **X₅** lead to **1.125pⁱⁱⁱ** with the same *dr* but lower yields (50%, >99:1 *dr*, Table 2.16, entry 5). The catalyst loading could be lowered to 3 mol% (Table 1.16, entry 6) which afforded the product in 75% yield and *dr* > 99:1 (after purification).

Table 1.16. Screening of conditions for the gold(I)-catalyzed *6-endo-dig* cyclization of **1.124aⁱⁱ⁻ⁱⁱⁱ** followed by indole attack.



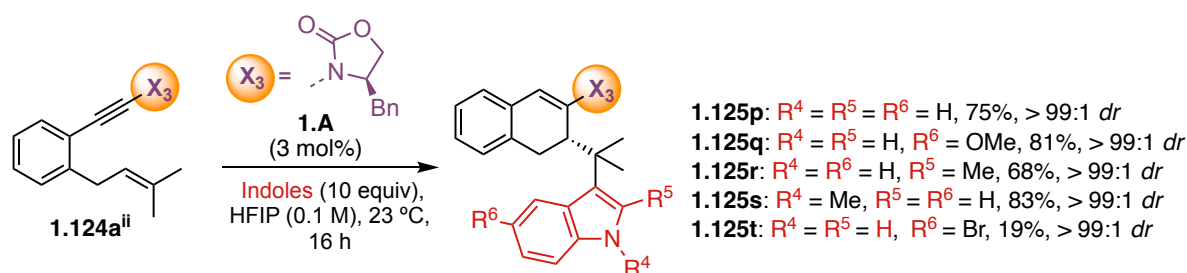
Entry	[Au]	X	T	Indole (equiv)	Product ^a
1	1.A (5 mol%)	X ₃	23 °C	10	1.125pⁱⁱ : 67%, <i>dr</i> = 95:5 (>99:1) ^b , traces of 1.142
2	1.A (5 mol%)	X ₃	23 °C	1.2	1.142 : 1.125pⁱⁱ = 1:6, 1.125pⁱⁱ : 56%
3	1.A (5 mol%)	X ₃	0 °C	5	1.142 : 1.125pⁱⁱ = 1:2, 1.125pⁱⁱ : 28%
4	1.A (5 mol%)	X ₃	23 °C	10	1.124aⁱⁱ : 1.125pⁱⁱ = 1.2 : 1
5	1.A (5 mol%)	X ₅	23 °C	10	1.125pⁱⁱⁱ : 50%, <i>dr</i> = 95:5 (>99:1) ^b
6	1.A (3 mol%)	X ₃	23 °C	10	1.125pⁱⁱ : 75%, <i>dr</i> = 95:5 (>99:1) ^b , traces of 1.142
7	1.A (3 mol%)	X ₃	23 °C	15	1.142 : 1.125pⁱⁱ = 1:28, formation of a side product
8	JohnPhosAuC 1 (3 mol%)	X ₃	23 °C	10	1.125pⁱⁱ : 70%, <i>dr</i> = 95:5 (>99:1) ^b
9	/	X ₃	23 °C	10	/

^aIsolated yields. ^bDiastereomeric ratio measured first on the crude and then after purification (in parenthesis) by LC-MS.

⁶⁸ a) Bégué, J.-P.; Bonnet-Delpon, D.; Crousse, B., Fluorinated Alcohols: A New Medium for Selective and Clean Reaction, *Synlett* **2004**, 1, 18–29. b) Pozhydaiev, V.; Power, M.; Gandon, V.; Moran, J.; Lebœuf, D., Exploiting Hexafluoroisopropanol (HFIP) in Lewis and Brønsted Acid-Catalyzed Reactions, *Chem. Commun.* **2020**, 56, 11548–11564.

Increasing the quantity of nucleophile to 15 equiv to avoid the formation of **1.142** traces did not increase the yield since the formation of an unidentified side product was detected (Table 1.16, entry 7). Product **1.125pⁱⁱ** could also be isolated in 70% yield and >99:1 *dr* using JohnphosAuCl as a catalyst, confirming that HFIP can also activate gold(I)-chloride precursors, as recently reported by Nolan and Vougioukalakis (Table 1.16, entry 8).⁶⁹ Finally, a control experiment without gold confirmed that the reaction is not HFIP catalyzed (Table 1.16, entry 9).

Having optimized the reaction conditions, **1.124aⁱⁱ** was cyclized in the presence electron rich indoles, to afford **1.125p-s** in high yields (68-83%) and excellent diastereoselectivities (*dr* ≥ 99:1 in every case). (Scheme 1.26). Electron poorer **1.125t** presenting a Br substituent on the aryl ring of the indole was isolated in modest 19% yield but still with excellent *dr* > 99:1.



Scheme 1.26. Scope of indoles in the gold(I)-catalyzed *6-endo-dig* cyclization of **1.124aⁱⁱ** followed by nucleophilic attack. The reported *dr* were calculated at LC-MS after purification by column chromatography.

When we tested cyano-substituted indole and other carbon nucleophiles previously used for gold(I)-catalyzed *6-endo-dig* cyclizations followed by nucleophilic attack,^{66c} no reaction was observed (Figure 1.3).

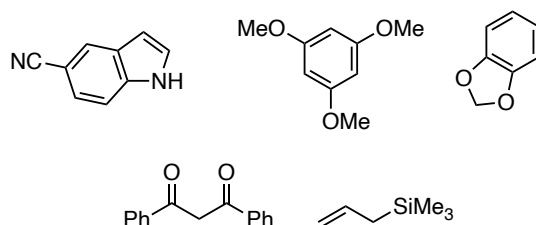


Figure 1.3. Unreactive C-nucleophiles in the gold(I)-catalyzed *6-endo-dig* cyclization of **1.124aⁱⁱ** followed by nucleophilic attack.

Anilines were also reported to be suitable nucleophiles in gold(I)-catalyzed enyne cyclizations.⁷⁰ When combining the benzene-tethered enyne **1.124aⁱⁱ** with 5 equiv of aniline in CH₂Cl₂, formation of the desired product **1.125u** was obtained in 44% isolated yield, together with a 40% of the undesired

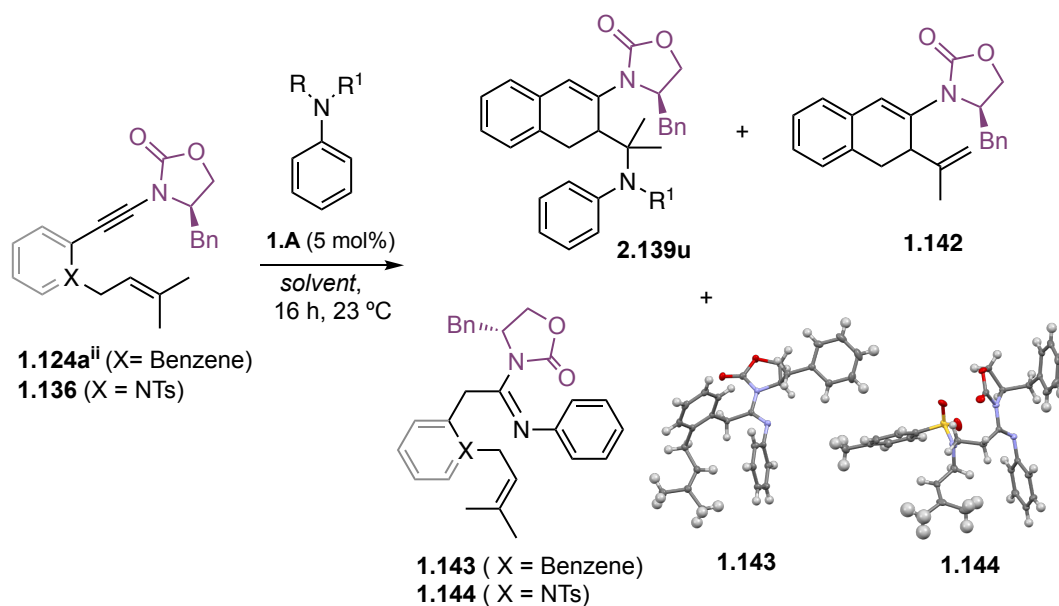
⁶⁹ a) Tzouras, N. V.; Gobbo, A.; Pozsoni, N. B.; Chalkidis, S. G.; Bhandary, S.; Van Hecke, K.; Vougioukalakis, G. C.; Nolan, S. P., Hydrogen Bonding-Enabled Gold Catalysis: Ligand Effects in Gold-Catalyzed Cycloisomerizations in Hexafluoroisopropanol (HFIP), *Chem. Commun.* **2022**, 58, 8516–8519. b) Tzouras, N. V.; Zorba, L. P.; Kaplanai, E.; Tsoureas, N.; Nelson, D. J.; Nolan, S. P.; Vougioukalakis, G. C., Hexafluoroisopropanol (HFIP) as a Multifunctional Agent in Gold-Catalyzed Cycloisomerizations and Sequential Transformations, *ACS Catal.* **2023**, 13, 8845–8860.

⁷⁰ a) Leseurre, L.; Toullec, P. Y.; Genêt, J.-P.; Michelet, V., Gold-Catalyzed Hydroamination/Cycloisomerization Reaction of 1,6-Enynes, *Org. Lett.* **2007**, 9, 4049–4052. b) Miller, R.; Carreras, J.; Muratore, M. E.; Gaydou, M.; Camponovo, F.; Echavarren, A. M., Broad Scope Aminocyclization of Enynes with Cationic JohnPhos–Gold(I) Complex as the Catalyst, *J. Org. Chem.* **2016**, 81, 1839–1849.

amidine **1.143**, for which X-Rays confirmed the structure (Table 1.17, entry 1). Furthermore, compound **1.125u** decomposes over time even if stored at low temperatures. Unfortunately, lowering the equiv of aniline to favour the cyclization of the enyne prior to the direct nucleophilic attack of the aniline to the alkyne was not useful, since not all the starting material was consumed and furthermore only by-products **1.142** and **1.143** were detected in this case (Table 1.17, entry 2). To avoid amidine formation, *N*-methylaniline was combined with the benzene-tethered enyne but no reaction was observed when using 5 equiv of nucleophile in CH₂Cl₂ (Table 1.17, entry 3) and partial formation of the elimination product **1.142** was observed when performing the reaction in HFIP (Table 1.17, entry 4).

When using the NTs-tethered enyne **1.136** in CH₂Cl₂ with 2.5 equiv of aniline, selective formation of the amidine product **1.144** was observed (Table 1.17, entry 5). X-Rays allowed the structure determination for this compound too. Lowering the quantity of nucleophile to 1.2 equiv again was not productive (Table 1.17, entry 6). Given all the difficulties encountered with *N*-nucleophiles we decided to move forward without further trials.

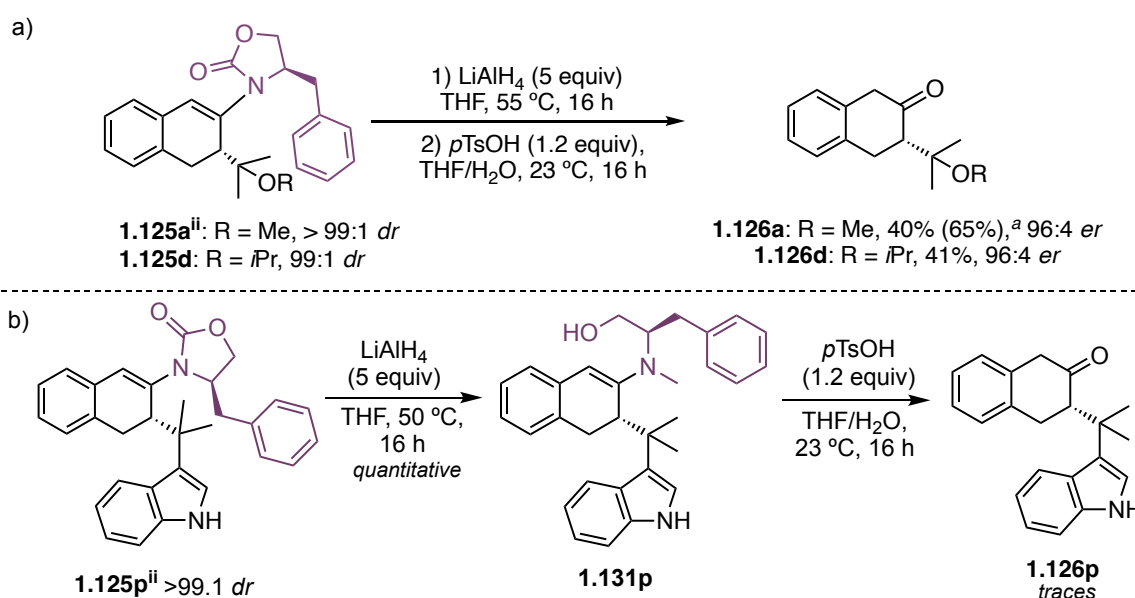
Table 1.17 Screening of conditions for the gold(I)-catalyzed *6-endo-dig* cyclization of **1.124aⁱⁱ** and **1.136** followed by aniline attack.^a



Entry	Tether (X)	R, R ¹	Solvent	Aniline (equiv)	Detected Products
1	benzene	H, H	CH ₂ Cl ₂	5	1.125u (44%), 1.143 (40%)
2	benzene	H, H	CH ₂ Cl ₂	2.5	1.142 , 1.143 ,
3	benzene	H, Me	CH ₂ Cl ₂	5	/
4	benzene	H, Me	HFIP	5	1.142
5	NTs	H, H	CH ₂ Cl ₂	2.5	1.144 (quantitative)
6	NTs	H, H	CH ₂ Cl ₂	1.2	1.144 (quantitative)

^aIsolated yields

Once explored the alkoxy cyclization scope, we devoted our efforts in functionalizing the highly enantioenriched enamine products obtained with the newly developed methodology. Applying the reduction-hydrolysis sequence discussed above (Table 1.11) to **1.125aⁱⁱ** (*dr* > 99:1) and **1.125d** (*dr* = 99:1) afforded (*S*)-2-tetralones **1.126a** and **1.126d** in 40–41% yields and slightly eroded 96:4 *er* (Scheme 1.27a). As commented previously the low isolated yield can be attributed to the formation, during purification in basic alumina, of by-product **1.130** (Table 1.11). With the hope of forming a more stable species, also product **1.125pⁱⁱ**, presenting a C–C bond instead of the more labile C–O one, was subjected to the same conditions (Scheme 1.27b). Unfortunately, the newly formed ketone was recovered only in traces. By analyzing the crude of the reaction between the two steps, it was possible to determine that while the reduction worked perfectly, the hydrolysis brought to main decomposition of the product.



Scheme 1.27. a) Reduction-hydrolysis of enantioenriched enamines **1.125a,d** to afford β -tetralones **1.126a,d**. ^aIn parenthesis, the NMR yield calculated using 1,1,2,2-tetrachloroethane as internal standard. b) Reduction-hydrolysis of enantioenriched enamine **1.125p** to afford β -tetralone **1.126p**.

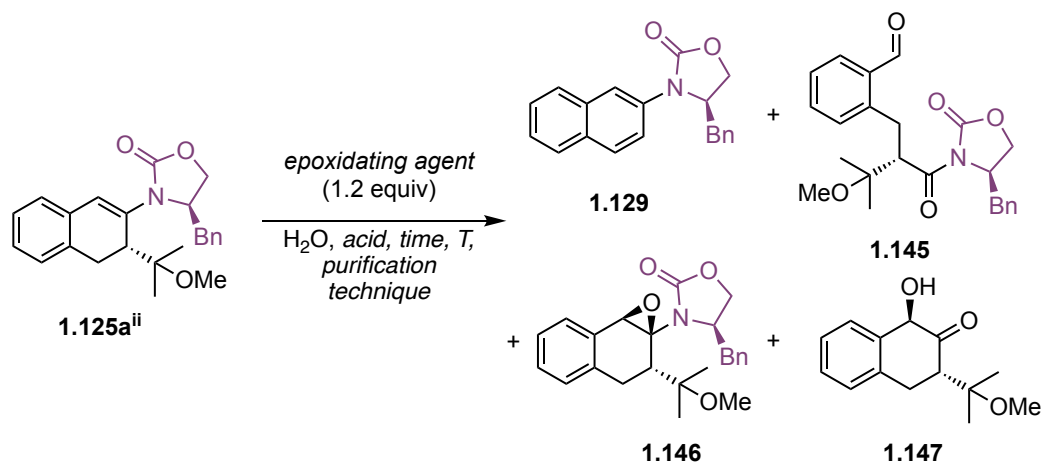
As anticipated, given the scarce reports of strategies developed so far to synthesize 2-tetralones, especially substituted⁶³ or enantioenriched⁶⁴ ones, we were interested in developing other transformations originating from enantioenriched **1.125aⁱⁱ**. We envisioned whether we could isolate 1-hydroxy-2-tetralone **1.147**, using an epoxidation-hydrolysis sequence of enamine **1.125aⁱⁱ** (Table 1.18). A first trial with *m*CPBA afforded oxidative fragmentation product **1.145**, as reported for similar compounds described in literature (Table 1.18, entry 1).⁷¹ When conducting the reaction in DMDO (0.065 M in acetone),⁷² epoxide **1.146** was observed together with traces of target **1.147** (Table 1.18, entry 2). If after reaction with DMDO, the solution was treated with HCl during 1 h, mainly naphthalene decomposition product **1.129** formed (Table 1.18, entry 3). If the hydrolysis was instead conducted

⁷¹ Xiong, H.; Hsung, R. P.; Shen, L.; Hahn, J. M. Chiral Enamide. Part 1: Epoxidations of Chiral Enamides. A Viable Approach to Chiral Nitrogen Stabilized Oxyallyl Cations in [4+3] Cycloadditions. *Tetrahedron Lett.* **2002**, *43*, 4449–4453.

⁷² Taber D. F.; DeMatteo P. W.; Hassan R. A. Simplified Preparation of Dimethyldioxirane (DMDO). *Org. Synth.* **2013**, *90*, 3501.

using during 1 h using *p*TsOH, **1.147** formed and it was isolated in 35% yield using silica gel for purification (Table 1.18, entry 4). Changing purification conditions was not productive (Table 1.19, entries 5-7), while increasing the hydrolysis step time to 16 h allowed to isolate the product in 54% yield (Table 1.18, entry 8).

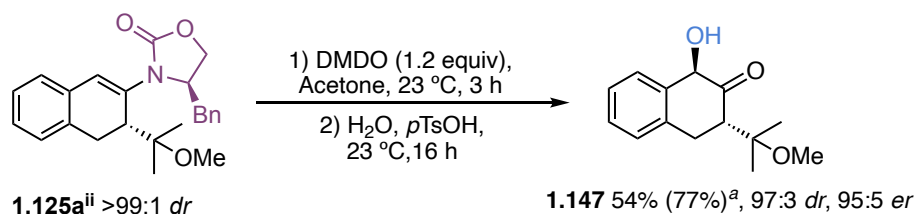
Table 1.18. Optimization for the epoxidation-hydrolysis sequence of **1.125aⁱⁱ** to afford **1.147**



Entry	Epoxidating agent	Acid	T (°C)	Time	Purification	Product ^a
1	<i>m</i> CPBA ^b	/	0	3 h	Silica	1.145 (32%)
2	DMDO ^c	/	23	16 h	Silica	1.146 (20 %) + 1.147 (traces)
3	DMDO ^c	HCl ^d	23	3 h + 1 h	Silica	Mainly 1.129
4	DMDO ^c	<i>p</i> TsOH ^e	23	3 h + 1 h	Silica	1.147 (35 %)
5	DMDO ^c	<i>p</i> TsOH ^e	23	3 h + 1 h	Neutral alumina	No separation
6	DMDO ^c	<i>p</i> TsOH ^e	23	3 h + 1 h	Silica pre-treated with 3% TEA	No separation
7	DMDO ^c	<i>p</i> TsOH ^e	23	3 h + 1 h	Basic alumina	1.147 (traces)
8	DMDO^c	<i>p</i>TsOH^e	23	3 h + 16 h	Silica	1.147 (54%)

^aIsolated yields. ^bReaction in CH₂Cl₂ (0.1M). ^cDMDO in Acetone (0.065M). ^d1:2 HCl 10% : DMDO in Acetone (0.065 M). ^e1.5 equiv of *p*TsOH directly poured after 3 hours of reaction in DMDO in Acetone (0.065 M) together with H₂O (1:2 H₂O: DMDO in Acetone (0.065 M)).

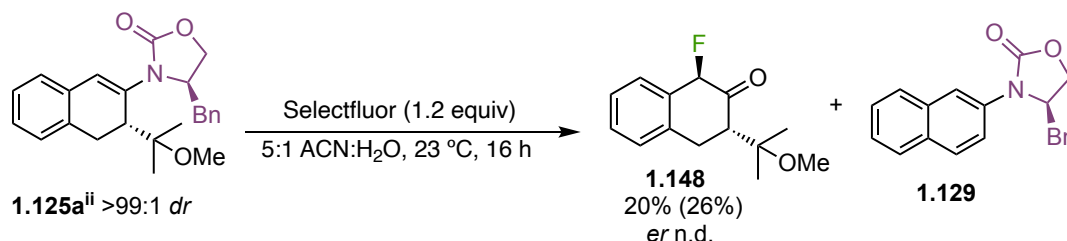
Also in this case, the conversion measured by NMR was consistently higher (77%) than the isolated yield, sign of product decomposition during the purification step (Scheme 1.28).



Scheme 1.28. Optimized conditions for the epoxidation-hydrolysis sequence of enantioenriched enamine **1.125aⁱⁱ** to afford 1-hydroxy-2-tetralone **1.147**. ^a In parenthesis, the NMR yield calculated using 1,1,2,2-tetrachloroethane as internal standard.

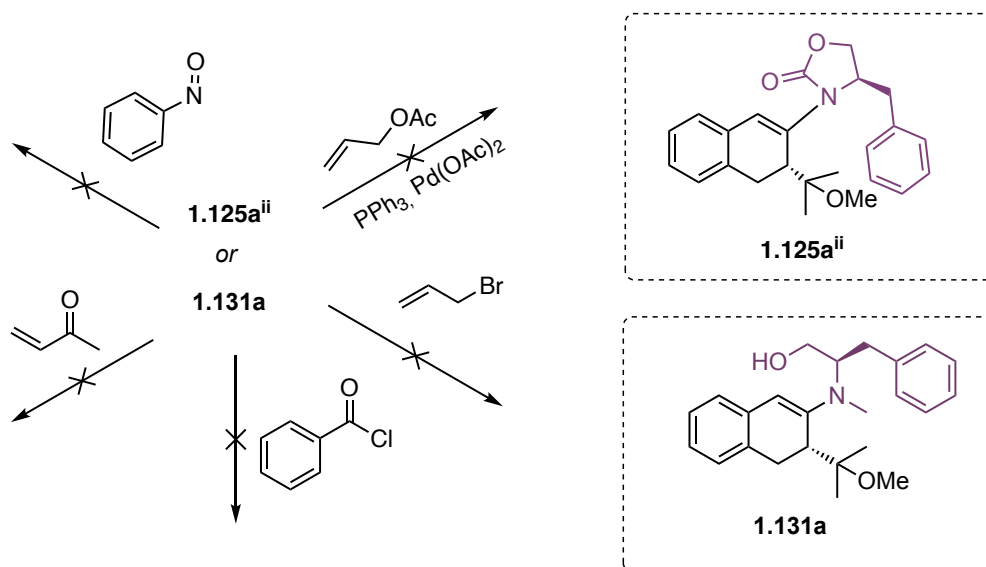
Delightfully the *er* after application of the reported conditions remained high (95:5 *er*), and the *dr* with respect to the newly created chiral center (which configuration was assigned through 2D NMR) also results excellent (97:3 *dr*).

Treatment of **1.125aⁱⁱ** with Selectfluor in an acetonitrile/water mixture delivered **1.148** in only 26% NMR yield: formation of **1.129** revealed to be the main obstacle (Scheme 1.29). Since we could not optimize the reaction further and we also faced problems in isolating the racemic ketone, we moved on with different trials.



Scheme 1.29. Treatment of **1.125aⁱⁱ** with Selectfluor to afford 1-fluoro-2 tetralone **2.162**.

Allylation, both Pd-catalyzed using allyl acetate⁷³ and simply in reflux with allyl bromide⁷⁴, were attempted, but only starting material was recovered when leaving the reaction overnight (Scheme 1.30). The same outcome was observed when attempting acylation with benzoyl chloride⁷⁴, annulation with methyl vinyl ketone⁷⁴ and α -oxygenation with nitrosobenzene.⁷⁵ Trials using the open adduct **1.131a** were also performed, hoping that the reason for the scarce reactivity observed with **1.125aⁱⁱ**, was due to the electron-poor character of the carbamate enamine. Unfortunately, no desired product was observed even in these cases.



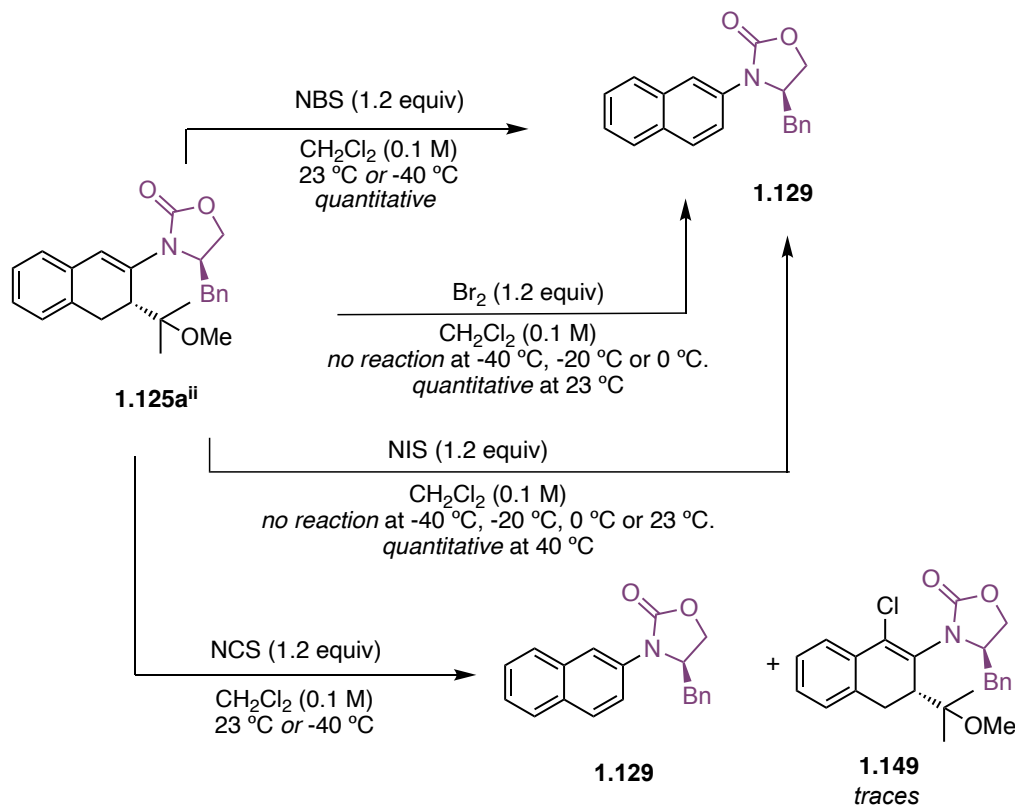
Scheme 1.30. Testing enamine **1.125aⁱⁱ** reactivity with electrophiles

⁷³ Tsuji, J. Organic Synthesis by Means of Noble Metal Compounds. L. Palladium Catalyzed Reactions of Enamines with Butadiene and Allyl Acetate. *Bull. Chem. Soc. Jpn.* **1973**, *46*, 1896–1897.

⁷⁴ Stork, Gilbert.; Brizzolara, A.; Landesman, H.; Szmuszkowicz, J.; Terrell, R. The Enamine Alkylation and Acylation of Carbonyl Compounds. *J. Am. Chem. Soc.* **1963**, *85*, 207–222.

⁷⁵ Mukherjee, S.; Yang, J. W.; Hoffmann, S.; List, B. Asymmetric Enamine Catalysis. *Chem. Rev.* **2007**, *107*, 5471–5569.

When subjecting **1.125aⁱⁱ** to halogen sources⁷⁵, the major product observed was always naphthalene **1.129** (Scheme 1.31). The only case where a small percentage of different product **1.149** was observed was when using NCS, but since it was detected only in traces through LC-MS, no hydrolysis to obtain the target ketone was attempted.

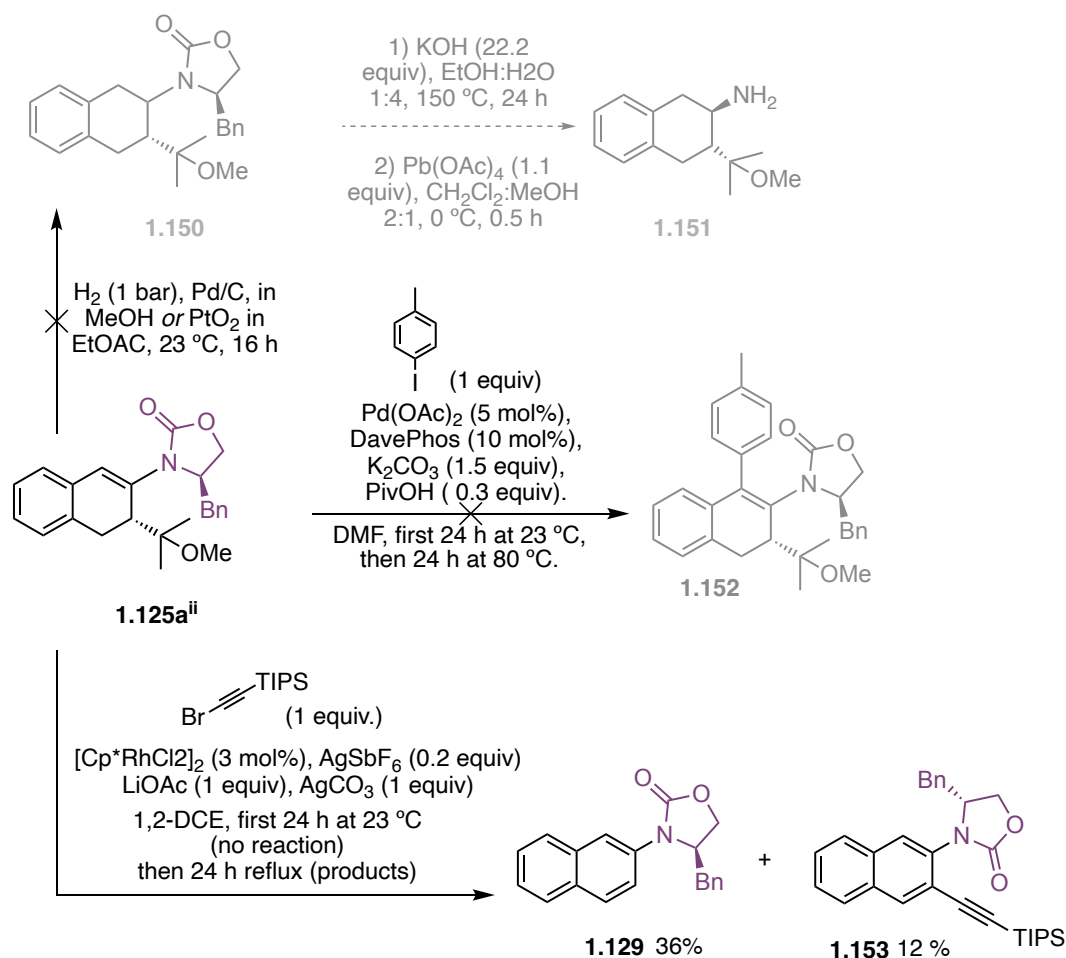


Scheme 1.31. Testing enamine's **1.125aⁱⁱ** reactivity with halogen sources.

When attempting the heterogeneous hydrogenation of the enamine bond with H_2 on Pd/C or PtO_2 , which was planned to eventually get to amine **1.151** from **1.150**, only starting material was recovered (Scheme 1.32). $\text{Csp}^2\text{-H}$ arylation to afford **1.152**⁷⁶ and alkynylation⁷⁷ trials following literature procedures, failed, even though in the latter case, when leaving the reaction at reflux overnight, the alkynylation product **1.153** was isolated (12%), derived from the C–H activation of the less sterically hindered aromatic proton of the usual decomposition product **1.129**. It is interesting to notice that this product would originate from the rhodium center forming a 6-membered-ring transition state with the directing group (the carbamate's carbonyl), when in the case reported in literature,⁷⁷ a 5-membered-ring is involved instead.

⁷⁶ Livendahl, M.; Echavarren, A. M. Palladium-Catalyzed Arylation Reactions: A Mechanistic Perspective. *Isr. J. Chem.* **2010**, *50*, 630–651.

⁷⁷ Tan, E.; Quinonero, O.; Elena de Orbe, M.; Echavarren, A. M. Broad-Scope Rh-Catalyzed Inverse-Sonogashira Reaction Directed by Weakly Coordinating Groups. *ACS Catal.* **2018**, *8*, 2166–2172.



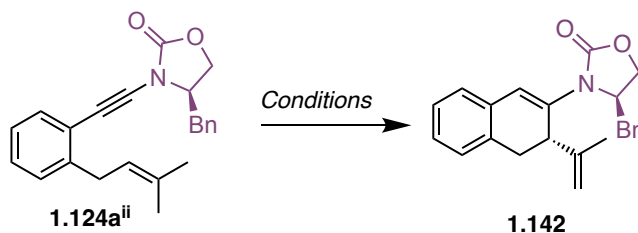
Scheme 1.32. Attempted hydrogenation, C–H arylation and alkylation of enamine **1.125aⁱⁱ**.

We then moved to gain a deeper understanding of the alkoxy cyclization reaction mechanism through control experiments (Table 1.19). Notably, in the absence of nucleophiles, full recovery of the starting material was observed (Table 1.19, entry 1). To understand why the substrate fails to yield cycloisomerization product **1.142**, the reaction was repeated in the presence of a stoichiometric amount of anhydrous pyridinium *p*-toluenesulfonate (PPTS) to determine if, under standard conditions, the alcohol might act as a proton shuttle for the protodeauration step⁷⁸ (Table 1.19, entry 2). In these conditions, conversion of **1.124aⁱⁱ** into the cycloisomerization product **1.142** (91:9 *dr*) was observed. Reducing the amount of PPTS to 5 mol% yielded the same result (Table 1.19, entry 3). To rule out the possibility of proton-catalyzed processes, we conducted the reaction in the sole presence of a stoichiometric amount of PPTS, but only starting material was recovered (Table 1.19, entry 4). Furthermore, the reaction was performed in the presence of NaOTs to assess whether the tosylate anion, which may potentially deprotonate one of the two terminal methyls, could act as the shuttle for protodeauration. However, no product was observed under anhydrous conditions (Table 1.19, entry 6), indicating that the presence of pyridinium as a Brønsted acid is essential for facilitating the

⁷⁸ Navarro, M.; Alferez, M. G.; de Sousa, M.; Miranda-Pizarro, J.; Campos, J. Dicoordinate Au(I)–Ethylene Complexes as Hydroamination Catalysts. *ACS Catal.* **2022**, *12*, 4227–4241.

protodemetalation step. These findings suggest that while the transformation is indeed gold(I)-catalyzed, the presence of a proton shuttle is necessary to facilitate protodemetalation leading to the *6-endo-dig* product. Additionally, the reaction was conducted in the presence of the Lewis acid CeCl_3 to rule out the possibility of competition between the alkyne and the carbonyl group of the carbamate in the gold coordination step (Table 1.19, entry 7). Once again, no reactivity was observed. These results confirm our initial hypothesis the catalyst turnover-determining step is protodeauration, consistent with observations of some cases in gold catalysis.^{67,78,79}

Table 1.19. Control experiments in the cyclization of **1.124aⁱⁱ** to form **1.142**.^a



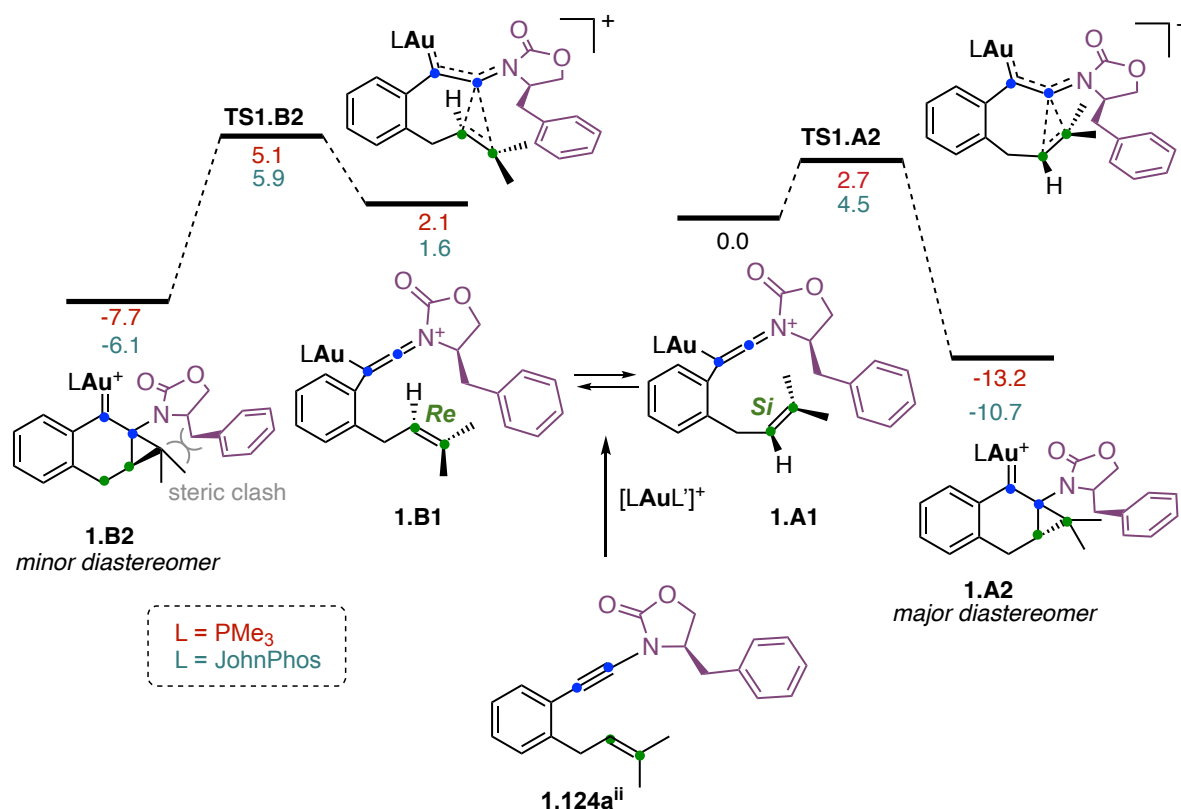
Entry	[Au(I)]	Additive	Product
1	1.A (5 mol%)	/	/
2	1.A (5 mol%)	PPTS (1 equiv)	1.142 (65%) ^b
3	1.A (5 mol%)	PPTS (5 mol%)	1.142 (62%) ^b
4	/	PPTS (1 equiv)	/
5	1.A (5 mol%)	NaOTs (1 equiv), 15-crown-5 (1 equiv) ^c	1.142 (42%) ^d + 1.125f (21%) ^d
6	1.A (5 mol%)	NaOTs (1 equiv), 15-crown-5 (1 equiv) ^c , molecular sieves (4Å)	/
7	1.A (5 mol%)	CeCl_3 (5 mol%)	/

^a Reactions were performed in the at 23 °C during 24 h using dry CH_2Cl_2 (0.1 M). ^b Isolated yields. ^c The crown ether was used to dissolve NaOTs in CH_2Cl_2 . Since the first trial performed with wet 15-crown-5 afforded the elimination product **1.142** together with the hydroxycyclization one (**1.125f**), we repeated the experiment in the presence of molecular sieves to operate in the total absence of water that would serve itself as a proton shuttle. ^d NMR yield using 1,1,2,2-tetrachloroethane as internal standard.

To conclude, the origin of the selectivity during the cyclization step through the *Re* and *Si* face of the alkene was elucidated by DFT calculations, which were preliminarily performed with $\text{L} = \text{PMe}_3$ (Scheme 1.33, red values). The system was modeled first by optimizing the structure of **1.A2** starting from the X-Ray structure of the cyclized product **1.125aⁱⁱ**. From **1.A2** it was possible to find **TS1.A2** and, after relaxation, the gold(I)-keteniminium **1.A1**. Once calculated also **TS1.B2**, it was possible to assess that, due to the steric clash of the chiral auxiliary's benzyl moiety, the overall barrier to convert **1.A1** into the cyclopropyl gold carbene **1.B2** is 2.4 $\text{Kcal}\cdot\text{mol}^{-1}$ higher than the one for converting it into

⁷⁹ a) Stylianakis, I.; Faza, O. N.; López, C. S.; Kolocouris, A. The Key Role of Protodeauration in the Gold-Catalyzed Reaction of 1,3-Diynes with Pyrrole and Indole to Form Complex Heterocycles. *Org. Chem. Front.* **2020**, *7*, 997–1005. b) Gubler, J.; Radić, M.; Stöferle, Y.; Chen, P. 2-Aminoalkylgold Complexes: The Putative Intermediate in Au-Catalyzed Hydroamination of Alkenes Does Not Protodemetalate. *Chem. Eur. J.* **2022**, *28*, e202200332. c) Pedrazzani, R.; Kiriakidi, S.; Monari, M.; Lazzarini, I.; Bertuzzi, G.; López, C. S.; Bandini, M., Fluorinated Biphenyl Phosphine Ligands for Accelerated [Au(I)]-Catalysis, *ACS Catal.* **2024**, *14*, 6128–6136.

1.A2, which results to be $5.6 \text{ Kcal}\cdot\text{mol}^{-1}$ more stable than **1.B2**. We then switched to the real system, with $L = \text{JohnPhos}$ (Scheme 1.33, light blue values). The barrier that must be overcome to afford the more stable cyclopropyl gold(I)-carbene intermediate **1.A2** starting from **1.A1** is $4.5 \text{ Kcal}\cdot\text{mol}^{-1}$, lower than the overall $\text{Kcal}\cdot\text{mol}^{-1}$ barrier that is needed to first interconvert **1.A1** to **1.B1** and then to afford **1.B2** through the gold(I)-catalyzed cyclization. As expected, the steric clash between the chiral auxiliary and the *Re* face of the alkene accounts for the experimentally observed diastereoselectivity making **TS1.A2** the stereodetermining step.



Scheme 1.33. Origin of the diastereoselectivity in the gold(I)-catalyzed 6-endo-dig cyclization of enynamide **1.124aⁱⁱ**. DFT calculations performed with B3LYP/6-31G(d) (C, H, P, O), LANL2DZ (Br) and SDD (Au) in CH_2Cl_2 (PCM). Free energies in $\text{Kcal}\cdot\text{mol}^{-1}$. $L = \text{PMe}_3$ or **JohnPhos**. In the experimental section the pathway calculated with PMe_3 will be labeled as follow: **1.A1'**, **1.A2'**...

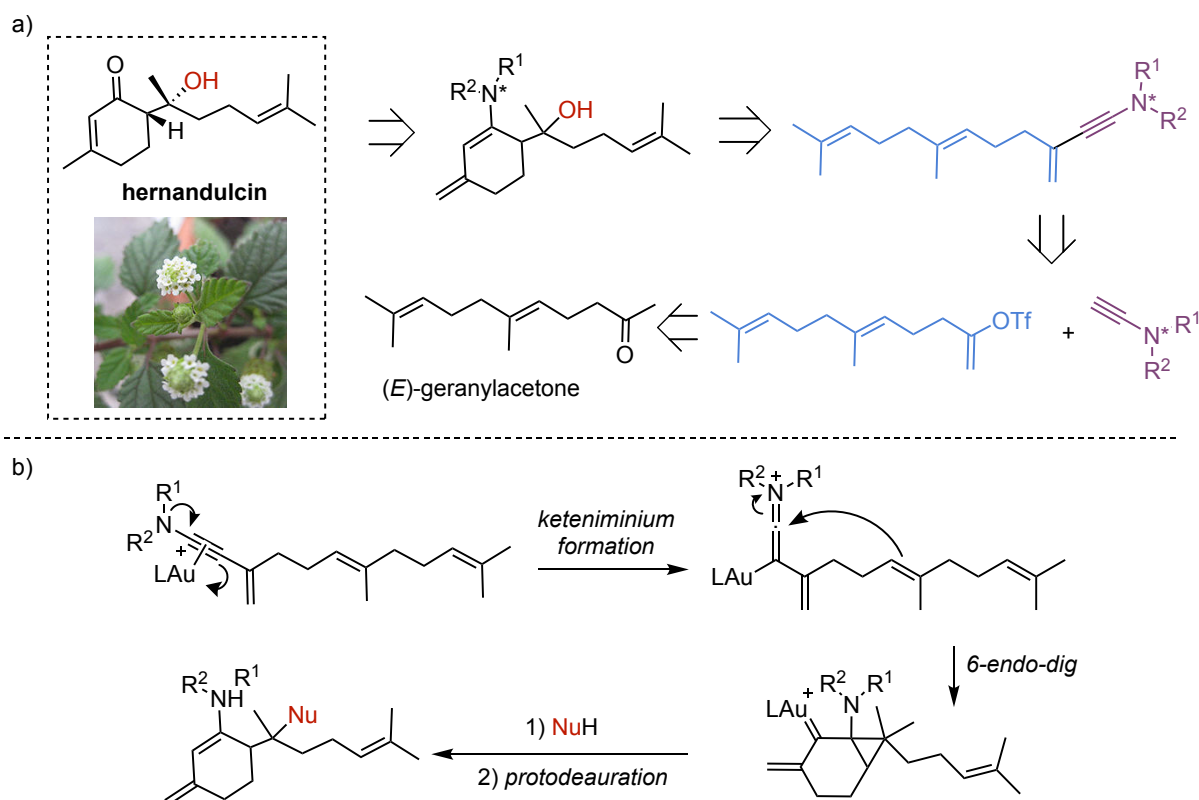
Towards the Total Synthesis of Hernandulcin⁴⁵

Once developed gold(I)-catalyzed alkoxy cyclizations of enynamides using chiral auxiliaries, we were interested in applying our methodology to total synthesis. Hernandulcin is an intensely sweet compound isolated from the plant *Lippia dulcis* found in Mexico and belonging to the family of sesquiterpenes.⁸⁰ So far, previous reports describe long synthesis difficultly applicable to an industrial scale.⁸¹

⁸⁰ Compadre, C. M.; Pezzuto, J. M.; Kinghorn, A. D.; Kamath, S. K., Hernandulcin: An Intensely Sweet Compound Discovered by Review of Ancient Literature, *Science* **1985**, *227*, 417–419.

⁸¹ a) Mori, K.; Kato, M., Synthesis of (6s,1's)-(+)-Hernandulcin, a Sweetener, and Its Stereoisomers, *Tetrahedron* **1986**, *42*, 5895–5900. b) Kim, J. H.; Lim, H. J.; Cheon, S. H., Synthesis of (+)-Hernandulcin and (+)-Epihernandulcin, *Tetrahedron Lett.* **2002**, *43*, 4721–4722. c) Rigamonti, M. G.; Gatti, F. G., Stereoselective Synthesis of Hernandulcin, Peroxyliplidulcine A, Lippidulcines A, B and C and Taste Evaluation, *Beilstein J. Org. Chem.* **2015**, *11*, 2117–2124.

Our aim is to develop a concise synthesis of hernandulcin envisioning as key step the gold(I)-catalyzed alkoxy cyclization of a 1,6-enyne derived from geranyl acetone (Scheme 1.34a). To induce enantioselectivity, the use of *N*-containing chiral auxiliaries seems ideal since the cyclization product, an enamine, could then be converted, through hydrolysis, to the desired final ketone. Furthermore, the use of enynamides (*N*-substituted enynes) should favour the formation of the *6-endo-dig* cyclization product over the competing *5-exo-dig* one, due to the formation of the gold(I) keteniminium intermediate (Scheme 1.34b), as in the case of **1.124**. Ideally, water would be directly used in the nucleophilic addition step, to directly obtain the target alcohol functionality present in hernandulcin, without needing further deprotection steps.

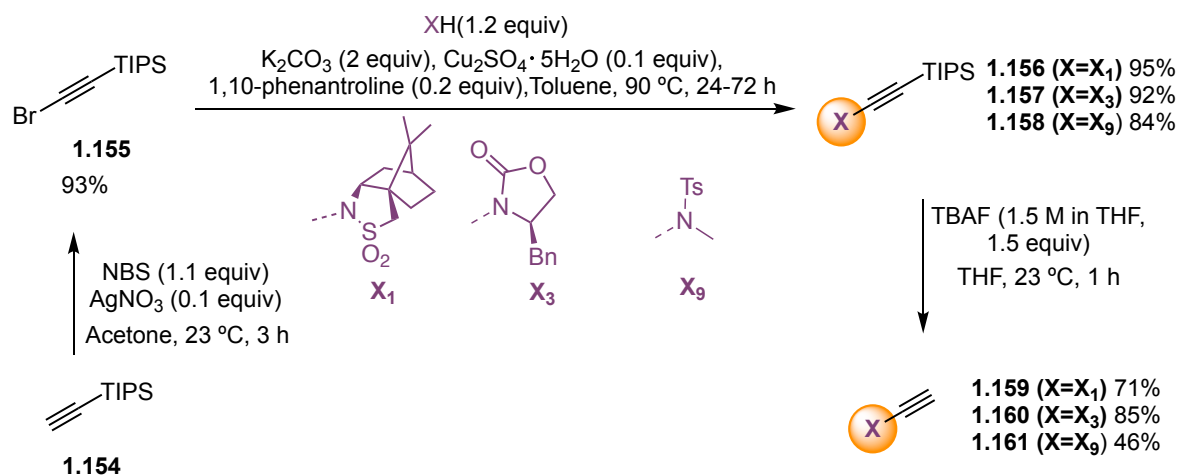


Scheme 1.34. a) Retrosynthetic analysis of hernandulcin envisioning gold(I)-catalyzed alkoxy cyclization of 1,6-enynamides. *Lippia dulcis* plant shown below hernandulcin's structure. b) Proposed mechanism for formation of the enamine precursor for hernandulcin synthesis.

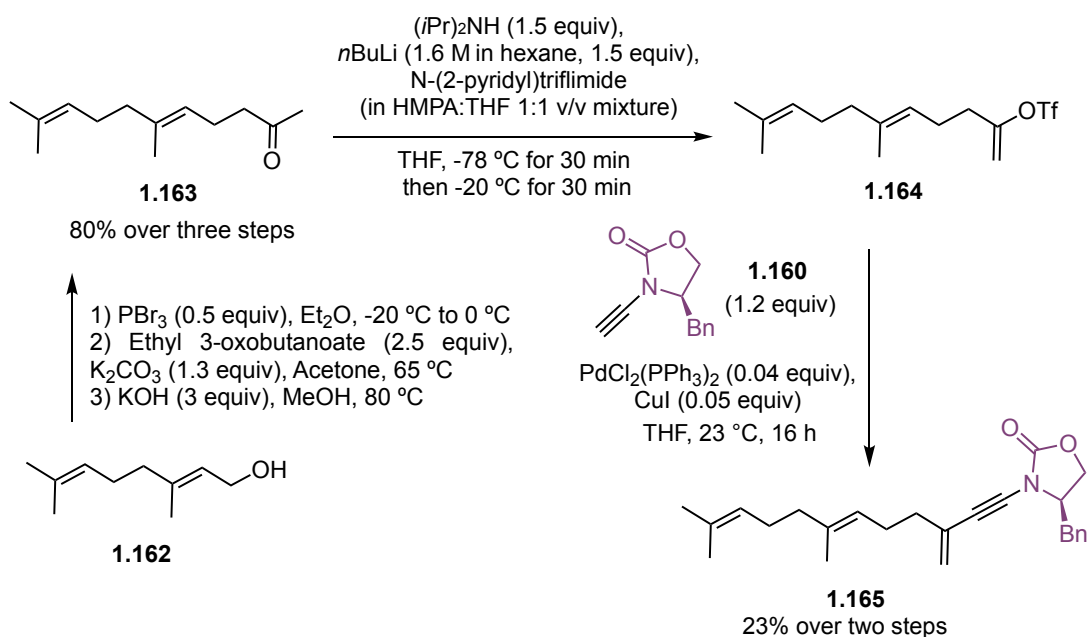
We prepared **1.159**, **1.160** and **1.161** following modified literature procedures^{19,82} which start from commercially available TIPS-acetylene **1.154**, followed by NBS bromination to form **1.155** and Cu-catalyzed C–N coupling to yield TIPS-protected **1.156-158** (Scheme 1.35). Finally, TBAF deprotection allows to isolate the terminal ynamides which constitute one of the two coupling partners for the construction of the target enynamide (Scheme 1.34a). The other part of the molecule was assembled starting from (*E*)-geranylacetone **1.163**, which, even if commercially available, was synthesized starting

⁸² Frederick, M. O.; Mulder, J. A.; Tracey, M. R.; Hsung, R. P.; Huang, J.; Kurtz, K. C. M.; Shen, L.; Douglas, C. J., A Copper-Catalyzed C–N Bond Formation Involving Sp-Hybridized Carbons. A Direct Entry to Chiral Ynamides via N-Alkynylation of Amides, *J. Am. Chem. Soc.* **2003**, *125*, 2368–2369.

from geraniol **1.162**⁸³ to avoid impurities of (*Z*)-geranylacetone, often present in commercial samples. **1.163** was converted to triflate **1.164**⁸⁴ through the use of *N*-(2-pyridyl)triflimide⁸⁵ following a recently developed procedure (Scheme 1.36).⁸⁶ Given the promising results obtained by using Evans oxazolidinones in gold(I)-catalyzed alkoxy cyclizations⁴⁴, we were interested in testing first ynamide **1.160**. Given the low stability of **1.164**, the subsequent Sonogashira reaction was performed on the crude, affording **1.165** in 23% isolated yield over two steps. (Scheme 1.36).



Scheme 1.35. Synthesis of ynamide precursors **1.159-1.161**.



Scheme 1.36. Triflation followed by Pd-catalyzed coupling of ynamide **1.160** on (*E*)-geranylacetone.

⁸³ Snyder, S. A.; Treitler, D. S.; Brucks, A. P., Simple Reagents for Direct Halonium-Induced Polyene Cyclizations, *J. Am. Chem. Soc.* **2010**, *132*, 14303–14314.

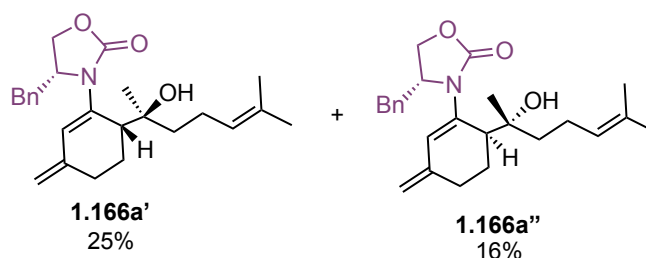
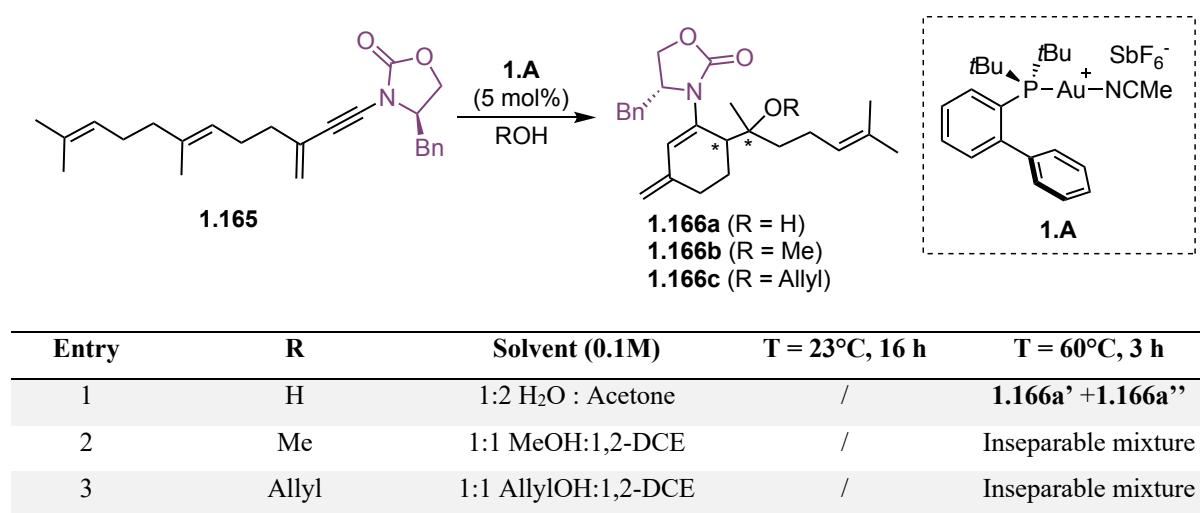
⁸⁴ Miller, M. W.; Johnson, C. R., Sonogashira Coupling of 2-Iodo-2-Cycloalkenones: Synthesis of (+)- and (–)-Harveynone and (–)-Tricholomenyn A, *J. Org. Chem.* **1997**, *62*, 1582–1583.

⁸⁵ Comins, D. L.; Dehghani, A., Pyridine-Derived Triflating Reagents: An Improved Preparation of Vinyl Triflates from Metallo Enolates., *Tetrahedron Lett.* **1992**, *33*, 6299–6302.

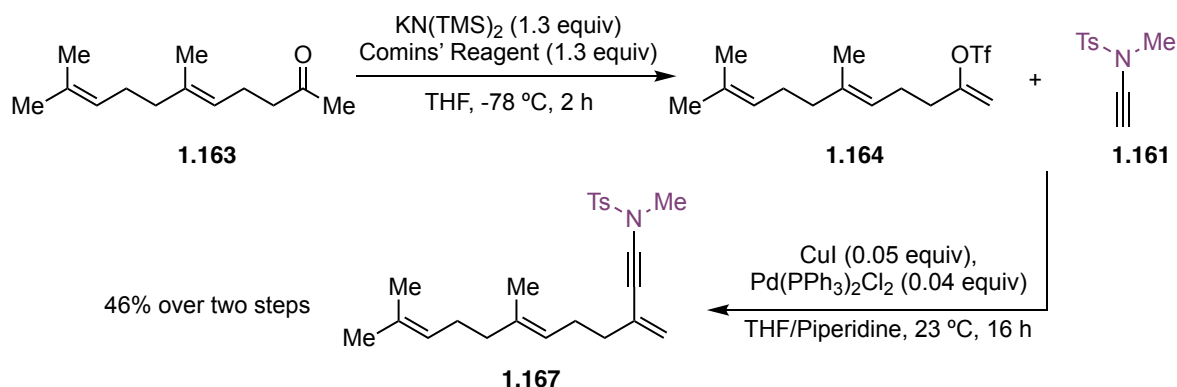
⁸⁶ Borra, S.; Kumar, M.; McNulty, J.; Baidilov, D.; Hudlicky, T., Chemoenzymatic Synthesis of the Antifungal Compound (–)-Pestynol by a Convergent, Sonogashira Construction of the Central Yne-Diene, *Eur. J. Org. Chem.* **2019**, *2019*, 77–79.

The first trials for gold(I)-catalyzed alkoxy cyclization of **1.165** were performed using water, methanol, and allyl alcohol as nucleophiles (Table 1.20) in the presence of the commercially available [JohnPhosAu(MeCN)]SbF₆ (**1.A**). Since all the cases no reactivity was observed when operating at room temperature or at 45 °C, the reactions were repeated at 60 °C. The starting material was in these cases consumed within 3 h. While it was not possible to rationalize the results obtained when using methanol or allyl alcohol as nucleophiles (Table 1.20, entries 2-3) in the case of hydroxycyclization, two possible diastereomers of **1.166a** were isolated and identified by NMR analysis and mass (Table 1.20, entry 1). The diastereomers were assigned considering it was shown that cyclizations starting from *E* alkenes should afford in a stereospecific manner the *anti* products.⁶⁵ Furthermore, the relative isolated yields of **1.166a'** (25%) and **1.166a''** (16%) were assigned based on the enantioinduction that the chiral auxiliary should provide discriminating one of the two faces of the approaching alkene.

Table 1.20. Gold(I)-catalyzed alkoxy cyclization of geranyol-derived enamide **1.164**.

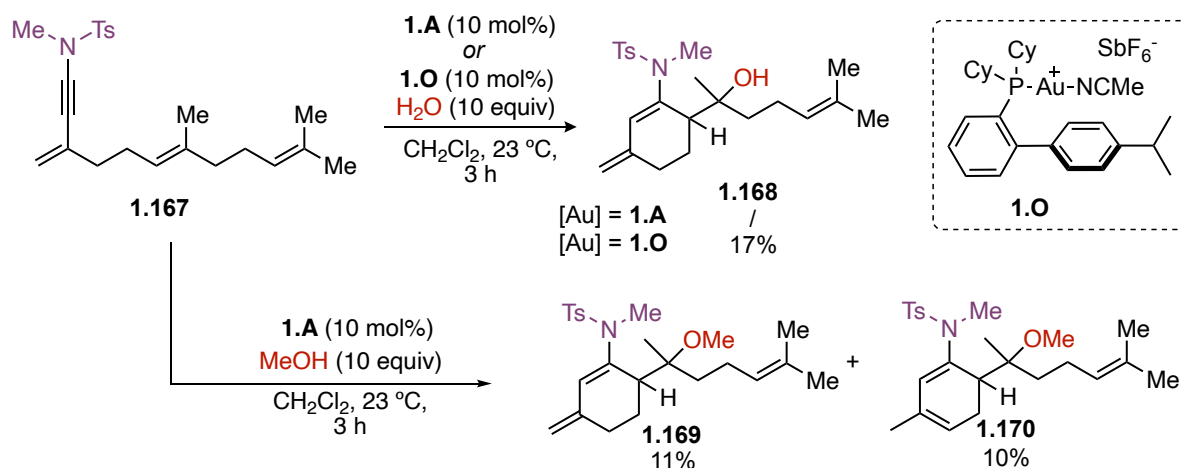


Since we could not isolate clean fractions of **1.166a**, which seemed contaminated by other by-products, we decided to move to structurally simpler **1.167**. (Scheme 1.37). This enamide was synthesized in a more satisfying yield compared to **1.165** by applying small changes to the reaction conditions reported before, and being achiral it would not form complex diastereomeric mixtures.



Scheme 1.37 Triflation followed by Pd-catalyzed coupling of ynamide **1.161** on (*E*)-geranylacetone.⁴⁵

With the new substrate in hand, we tested its reactivity under gold(I)-catalysis. When using 10 mol% of **1.A** and water as a nucleophile, full consumption of the starting material was achieved at room temperature over 3 h (Scheme 1.39). However, the main product of the reaction was not clearly identified. When changing the catalyst to **1.O**, the desired alkoxy cyclization product **1.168** was recovered in 17% yield. We then performed the reaction in the presence of methanol and catalyst **1.A** which afforded the desired product **1.169** and its isomer **1.170**, albeit low yields (~10%).

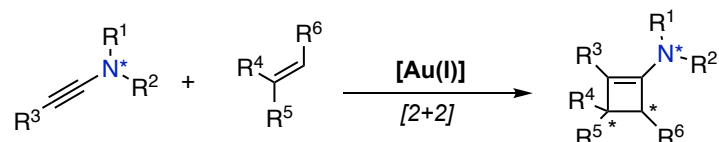


Scheme 1.39. Gold(I)-catalyzed alkoxy cyclizations of achiral enamide **1.167**.⁴⁵

Given the preliminary results obtained with substrate **1.167**, efforts will be made to optimize the reaction with water with the objective of selectively forming **1.168**. Synthesis of the chiral enamide derived from ynamide **1.159** bearing the electronically similar Oppolzer sultam sulfonamide as chiral auxiliary would then be an obvious continuation to develop the asymmetric version of these transformations.

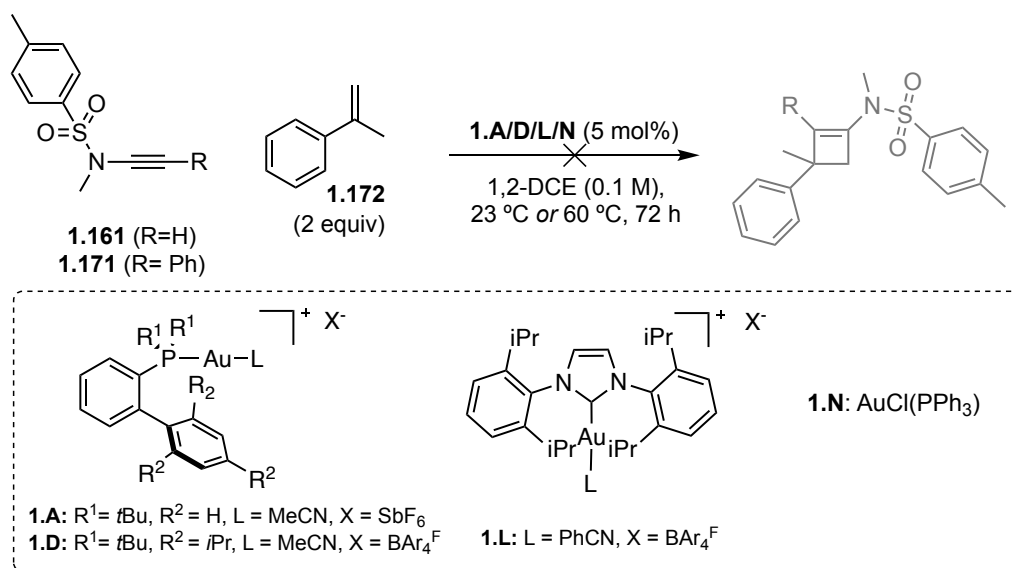
Intermolecular Trials

The only reported examples in literature so far of intermolecular reactivity of ynamides with alkenes under gold(I)-catalysis are [4+2] and [2+2+2] cycloadditions with electron-rich alkenes (Scheme 1.7).¹⁹ We wondered whether we could extend our chiral auxiliary approach to intermolecular [2+2] cycloadditions of terminal or internal *N*-substituted alkynes with alkenes, to afford enantioenriched four-membered enamines (Scheme 1.40). These species, as reported in intramolecular reactions (Scheme 5c),¹³ may then be easily hydrolyzed to interesting cyclobutanone scaffolds.



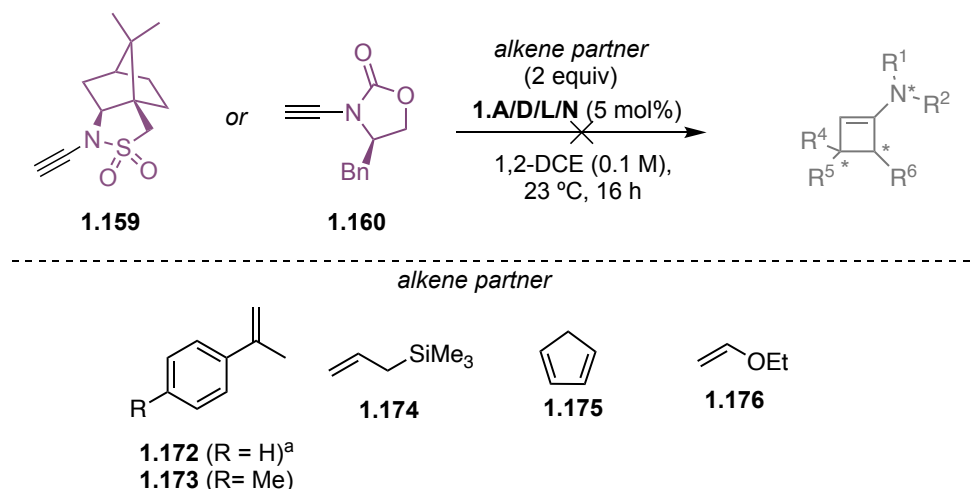
Scheme 1.40. Hypothesized stereoselective gold(I)-catalyzed intermolecular [2+2] cycloaddition of ynamides bearing chiral auxiliaries with alkenes.

We first tested achiral terminal ynamide **1.161** and internal ynamide **1.171**¹⁹ in the presence of the gold(I) catalysts **1.A/D/L/N** and α -methylstyrene under the conditions depicted in Scheme 1.41. No reaction was observed in any case, working at room temperature or at 60 °C.



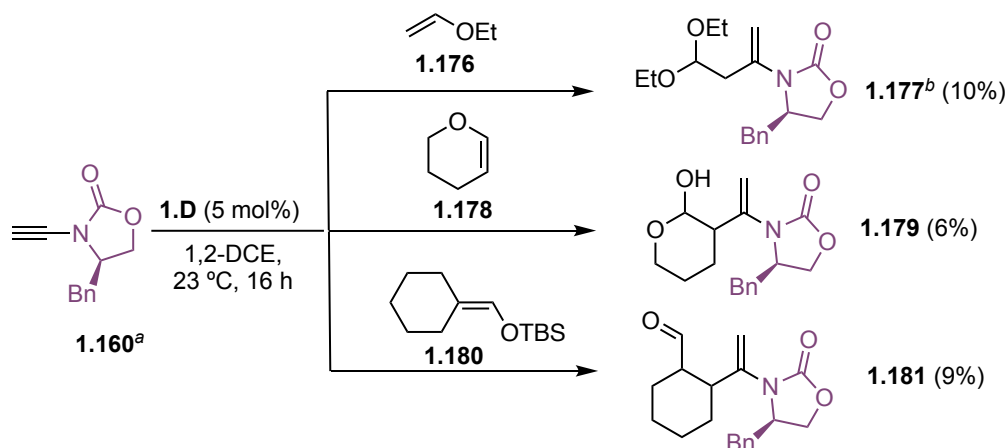
Scheme 1.41. First attempts for [2+2] cycloadditions of achiral ynamides **1.161** and **1.171** with alkenes.

We then decided to test ynamides **1.159** and **1.160**. Screening different alkenes **1.172-175** with the aforementioned catalysts **1.A/D/L/N** resulted in most cases in no reactivity (Scheme 1.42).



Scheme 1.42. Failed reactions between chiral ynamides **1.159** and **1.160** with alkenes. ^aThe reaction was also performed at 60 °C.

When using enol ether **1.176** though, a product could be spotted together with the unreacted starting materials. Enol ethers were reported previously as the only alkenes which would engage the gold(I)-catalyzed [2+2+2] cycloadditions with ynamides¹⁹ probably given their electron rich nature. We therefore repeated the reaction on a bigger scale, combining **1.160** with enol ethers **1.176**, **1.178** and **1.180**, isolating in low yields respectively **1.177**, **1.179** and **1.181** (Scheme 1.43). It looks like, after a first nucleophilic addition step, the newly formed carbocation on the alkene gets trapped by external nucleophiles (alcohol, water) which quench further reactivity with the alkenyl-gold(I) system.



Scheme 1.43 Gold(I)-catalyzed addition of enol ethers to ynamide **1.160**. ^aAlkyne:alkene = 2:1. ^b **1.A** was used in this case.

Conclusions

The development of a stereoselective gold(I)-catalyzed cyclizations using chiral auxiliaries represents a significant advancement in asymmetric synthesis. This approach offers a cost-effective and time-efficient alternative to conventional ligand optimization-based enantioselective synthesis, which, given the linear geometry of gold(I) species still constitutes a big challenge.

The cascade cyclization-hydrolysis sequence of 1,5-enynes to produced spirocyclic ketones, employing Oppolzer's sultam as a chiral auxiliary, enabling the simultaneous formation of two C–C bonds and a chiral spiro center with high yields and enantioselectivities. The utilization of a readily available gold(I) catalyst, along with the recovery of the chiral auxiliary, ensures the efficiency and practicality of this process.

The highly diastereoselective gold(I)-catalyzed alkoxy cyclization of 1,6-enynes using Evans-type oxazolidinones was also achieved. This methodology provided access to a new class enantiomerically enriched β -tetralones and offered a deeper understanding of the mode of action of chiral auxiliaries in gold(I)-catalyzed reactions.

The newly developed methodology was tested on the total synthesis of the sesquiterpene hernandulcin, for which an achiral precursor could be synthesized and afforded, so far in low yields, the target enamine.

Trials in intermolecular reactions of *N*-substituted alkynes with alkenes were unsuccessful, therefore, on this matter, we will shift our focus to *O*-substituted alkynes (**Chapter II**).

Experimental Part

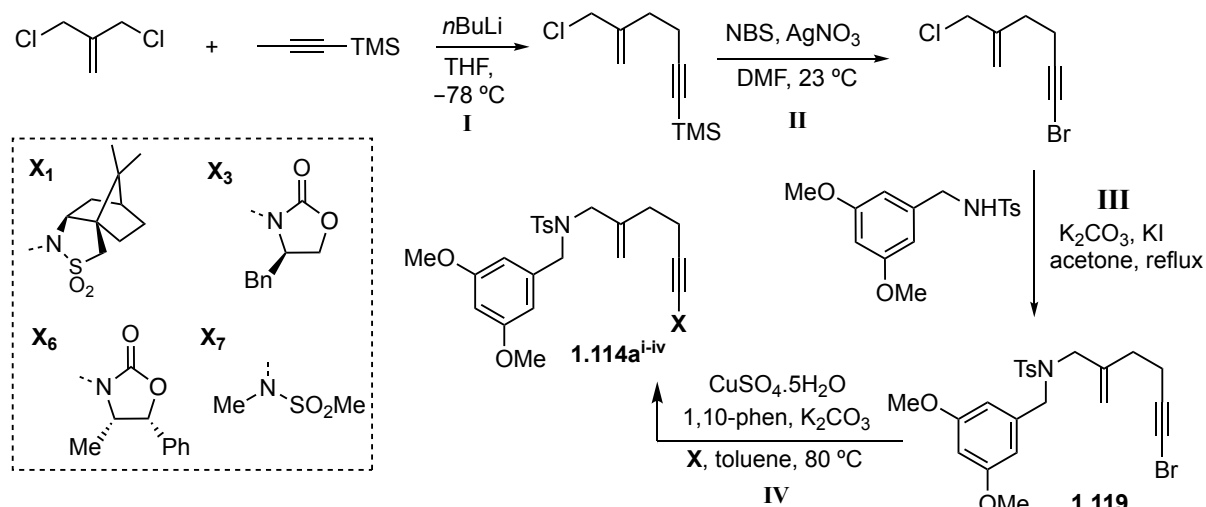
General information

Anhydrous reactions were performed under nitrogen or argon in solvents dried by passing through an activated alumina column on a PureSolv™ solvent purification system (Innovative Technologies, Inc., MA). Analytical thin layer chromatography was carried out using TLC-aluminium sheets with 0.2 mm of silica gel (Merck GF234) using UV light as the visualizing agent, and an acidic solution of vanillin in ethanol or a basic aqueous solution of KMnO_4 as the developing agent. Flash column chromatography (FCC) was carried out manually using PanReac Silica Gel 60 (40–63 μm) or employing the automated flash column chromatographer CombiFlash Companion with disposable pre-packed normal phase silica gel columns (Teledyne Isco). Preparative TLC was performed on 20 cm \times 20 cm silica gel plates (2.0 mm or 1.0 mm silica thickness, Analtech). Melting points were measured using a Mettler Toledo MP70 Melting Point apparatus. NMR spectra were recorded on Bruker Ultrashield 300, 400 or 500 MHz spectrometers using the residual solvent signal as internal standard [for ^1H NMR: CDCl_3 at 7.26 ppm, CD_2Cl_2 at 5.31 ppm, C_6D_6 at 7.16 ppm, for ^{13}C NMR: CDCl_3 at 77.16 ppm, CD_2Cl_2 at 54.00 ppm, C_6D_6 at 128.06 ppm]. All measurements were carried out at room temperature unless otherwise stated, and in some cases DEPT was used to assign carbon types. The following abbreviations were used to explain multiplicities: s = singlet, d = doublet, t = triplet, q = quartet, p = pentet, m = multiplet, br s = broad singlet. Coupling constants (J) are reported in Hertz (Hz). Infrared spectra were recorded on a Bruker ALPHA FTIR-ATR TR0 spectrometer with ATR module on a thin film (the sample was dissolved in a volatile solvent, then the solvent evaporated). The most intense absorption bands (ν) are listed in wavenumbers (cm^{-1}). Mass spectra were recorded on a Waters LCT Premier Spectrometer (ESI and APCI) or on an Autoflex Broker Daltonics (MALDI and LDI). Optical rotations were recorded using a Jasco P-1030 polarimeter equipped with a PMT detector using a 2 mL, 10 cm long cell. $[\alpha]_{\text{D}}^{\text{T}}$ values, reported in $\text{deg mL g}^{-1} \text{dm}^{-1}$, are calculated on the average value of at least ten consecutive readings. Concentrations (c) are quoted in g/100 mL (*i.e.* 10 mg/mL). HPLC analyses were performed on an Agilent Technologies 1200 series instrument. SFC analyses were performed on an Agilent Technologies 1260 Infinity II or on a Waters ACQUITY UPC2 instrument. Chiral GC analysis was performed on an Agilent 6890N coupled with a mass selective detector 5973 Inert. X-Ray data were collected on a Kappa APEX II DUO diffractometer equipped with an APPEX 2 4K CCD area detector, a Microsource with MoK_α radiation and an Oxford Cryostream 700 low temperature device. All reagents were used as purchased, with no further purification. While gold(I) complexes **1.A** and **1.C** are commercially available, **1.B** and **1.D-L** were synthesized according to previously reported procedures.⁸⁷ The NMR data are in agreement with the ones reported in the literature.

⁸⁷ Synthesis of gold(I) complexes – Complexes **1.B**, **G**: These complexes were prepared in situ following the procedures described in reference: Nieto-Oberhuber, M. P. Muñoz, S. López, E. Jiménez-Núñez, C. Nevado, E. Herrero-Gómez, M. Raducan, A. M. Echavarren *Chem. Eur. J.* **2006**, 12, 1677 – 1693; Complex **1.D**: M. E. de Orbe, A. M. Echavarren, *Org. Synth.* **2016**, 93, 115-126; Complexes **1.E**, **F**: V. López-Carrillo, A.M. Echavarren, *J. Am. Chem. Soc.* **2010**, 132, 27, 9292–9294; Complex **1.H** = J. S. Johnson, E. Chong, K. N. Tu, S. A. Blum, *Organometallics* **2016**, 35, 5, 655–662; Complex **1.I** = N. Huguet, D. Leboeuf, A. M. Echavarren, *Chem. Eur. J.* **2013**, 19, 6581; Complex **1.L**: C. H. M. Amijs, V. López-Carrillo, M. Raducan, P. Pérez-Galán, C. Ferrer, A. M. Echavarren, *J. Org. Chem.* **2008**, 73, 19, 7721–7730;

Synthetic Procedures and Characterization Data

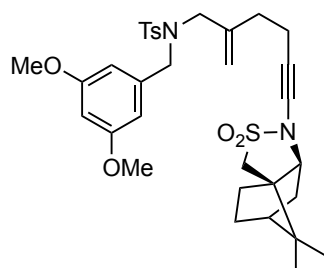
General procedure A for the synthesis of 1,5-enynamides **1.114a^{i-iv}**



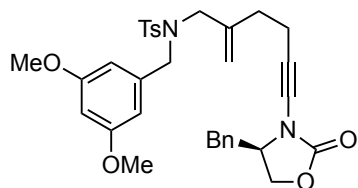
Step I-III: Compound **1.119** was synthesized as reported in the scheme according to literature procedure⁴⁰, all the spectral data were fully consistent with those previously reported.

Step IV: Compounds **1.114a^{i-iv}** were synthesized as reported below, following a literature procedure for the copper-catalyzed cross-coupling formation of the carbon-nitrogen bond.⁵⁶

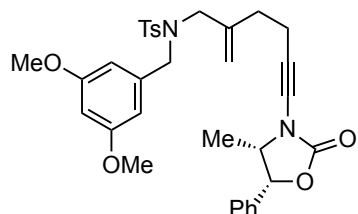
***N*-(3,5-Dimethoxybenzyl)-*N*-(6-((3*aS*,6*R*,7*aS*)-8,8-dimethyl-2,2-dioxidotetrahydro-3*H*-3*a*,6-methanobenzo[*c*]isothiazol-1(4*H*)-yl)-2-methylenehex-5-yn-1-yl)-4-methylbenzenesulfonamide (1.114aⁱ)**



Copper sulphate pentahydrate (11.8 mg, 0.047 mmol), 1,10-phenanthroline hydrate (18.7 mg, 0.094 mmol), potassium carbonate (131 mg, 0.945 mmol) and (1*R*)-(+)-2,10-camphosultam (102 mg, 0.472 mmol) were placed under inert atmosphere. Then, toluene (1 mL) and a solution of **1.119** (233 mg, 0.472 mmol) in toluene (3 mL) were sequentially added. After stirring at 80 °C overnight, the mixture was passed through Celite pad and concentrated under reduced pressure. The resulting residue was purified by column chromatography on silica gel (15-20% EtOAc/cyclohexane) to give **1.114aⁱ** (246 mg, 0.392 mmol, 83%) as colorless oil. ¹H NMR (400 MHz, CDCl₃) δ 7.76 – 7.69 (m, 2H), 7.36 – 7.28 (m, 2H), 6.31 (t, *J* = 2.3 Hz, 1H), 6.27 (d, *J* = 2.3 Hz, 2H), 4.93 (s, 1H), 4.85 (s, 1H), 4.27 (s, 2H), 3.72 (s, 2H), 3.70 (s, 6H), 3.48 (dd, *J* = 8.1, 4.2 Hz, 1H), 3.19 (s, 2H), 2.42 (s, 3H), 2.32 (t, *J* = 7.2 Hz, 2H), 2.12 – 2.07 (m, 2H), 1.98 – 1.80 (m, 3H), 1.71 (dd, *J* = 13.3, 8.1 Hz, 1H), 1.45 – 1.35 (m, 1H), 1.34 – 1.21 (m, 1H), 1.08 (s, 3H), 0.92 (s, 3H); ¹³C NMR (101 MHz, CDCl₃) δ 160.9, 143.4, 141.7, 138.4, 137.6, 129.8, 127.4, 115.5, 106.5, 100.1, 71.7, 68.4, 67.2, 55.4, 52.0, 51.0, 50.9, 49.6, 48.0, 44.5, 34.6, 32.4, 31.7, 27.2, 21.6, 20.3, 20.1, 17.2.; HRMS (ESI⁺): *m/z*: calculated for C₃₃H₄₂N₂NaO₆S₂: 649.2376 [M+Na]⁺; found: 649.2376.

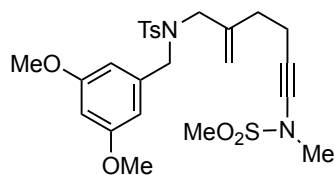
(*R*)-*N*-(6-(4-Benzyl-2-oxooxazolidin-3-yl)-2-methylenehex-5-yn-1-yl)-*N*-(3,5-dimethoxybenzyl)-4-methylbenzenesulfonamide (1.114ⁱⁱ)

Copper sulphate pentahydrate (6.0 mg, 0.024 mmol), 1,10-phenantroline hydrate (9.5 mg, 0.048 mmol), potassium carbonate (66.1 mg, 0.478 mmol) and (*R*)-4-benzyloxazolidin-2-one (42.4 mg, 0.239 mmol) were placed under inert atmosphere. Then, toluene (1 mL) and a solution of **1.119** (117.7 mg, 0.239 mmol) in toluene (3 mL) were sequentially added. After stirring at 80 °C for 68 hours, the mixture was passed through Celite pad and concentrated under reduced pressure. The resulting residue was purified by column chromatography on silica gel (20-25% EtOAc/cyclohexane) to give **1.114ⁱⁱ** (57.3 mg, 0.097 mmol, 41%) as colorless oil. ¹H NMR (500 MHz, CDCl₃) δ 7.75 – 7.69 (m, 2H), 7.36 – 7.23 (m, 5H), 7.21 – 7.14 (m, 2H), 6.31 (t, *J* = 2.3 Hz, 1H), 6.25 (d, *J* = 2.3 Hz, 2H), 4.97 (s, 1H), 4.89 (s, 1H), 4.30 – 4.23 (m, 3H), 4.18 (tdd, *J* = 8.3, 5.8, 3.9 Hz, 1H), 4.06 (dd, *J* = 8.7, 5.8 Hz, 1H), 3.81 – 3.69 (m, 2H), 3.67 (s, 6H), 3.16 (dd, *J* = 13.9, 3.9 Hz, 1H), 2.88 (dd, *J* = 13.9, 8.3 Hz, 1H), 2.45 – 2.38 (m, 5H), 2.18 (t, *J* = 7.2 Hz, 2H); ¹³C NMR (126 MHz, CDCl₃) δ 160.9, 156.2, 143.5, 142.1, 138.3, 137.5, 134.5, 129.9, 129.5, 129.1, 127.5, 127.3, 115.3, 106.5, 100.0, 72.5, 69.8, 67.3, 58.4, 55.4, 52.3, 51.1, 37.8, 32.2, 21.6, 17.1; HRMS (ESI⁺): *m/z*: calculated for C₃₃H₃₆N₂NaO₆S: 611.2186 [M+Na]⁺; found: 611.2213.

***N*-(3,5-Dimethoxybenzyl)-4-methyl-*N*-(6-((4*S*,5*R*)-4-methyl-2-oxo-5-phenyloxazolidin-3-yl)-2-methylenehex-5-yn-1-yl)benzenesulfonamide (1.114ⁱⁱⁱ)**

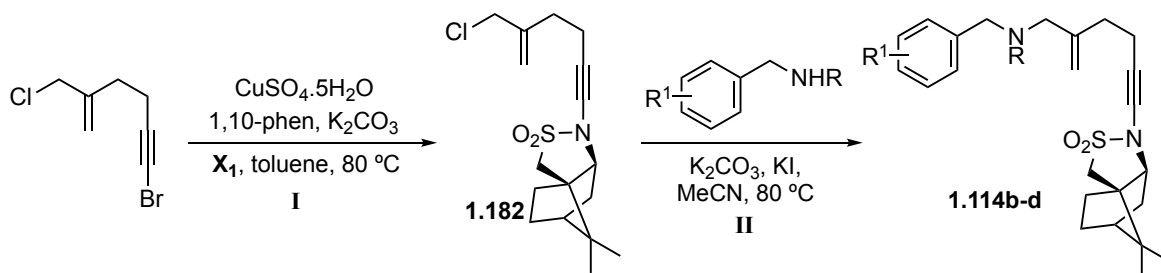
Copper sulphate pentahydrate (7.3 mg, 0.029 mmol), 1,10-phenantroline hydrate (11.6 mg, 0.058 mmol), potassium carbonate (81 mg, 0.584 mmol) and (4*S*,5*R*)-4-methyl-5-phenyloxazolidin-2-one (51.8 mg, 0.292 mmol) were placed under inert atmosphere. Then, toluene (1 mL) and a solution of **1.119** (143.9 mg, 0.292 mmol) in toluene (3 mL) were sequentially added. After stirring at 80 °C for 72 hours, the mixture was passed through Celite pad and concentrated under reduced pressure. The resulting residue was purified by column chromatography on silica gel (15-20% EtOAc/cyclohexane) to give **1.114ⁱⁱⁱ** (96.8 mg, 0.164 mmol, 56%) as colorless oil. ¹H NMR (500 MHz, CDCl₃) δ 7.74 – 7.69 (m, 2H), 7.38 (ddd, *J* = 11.0, 7.8, 6.0 Hz, 3H), 7.30 (d, *J* = 8.0 Hz, 2H), 7.27 – 7.22 (m, 2H), 6.31 (t, *J* = 2.3 Hz, 1H), 6.25 (d, *J* = 2.2 Hz, 2H), 5.66 (d, *J* = 8.1 Hz, 1H), 4.93 (s, 1H), 4.86 (s, 1H), 4.30 – 4.22 (m, 3H), 3.79 – 3.68 (m, 2H), 3.68 (s, 6H), 2.42 (s, 3H), 2.37 (t, *J* = 7.2 Hz, 2H), 2.14 (t, *J* = 7.3 Hz, 2H), 0.89 (d, *J* = 6.7 Hz, 3H); ¹³C NMR (126 MHz, CDCl₃) δ 160.8, 155.9, 143.4, 142.0, 138.2, 137.4, 134.1, 129.7, 128.9, 128.7, 127.24, 126.0, 115.2, 106.4, 99.9, 79.5, 71.2, 69.8, 58.0, 55.3, 52.1, 51.0, 32.1, 21.5, 17.0, 14.8. HRMS (ESI⁺): *m/z*: calculated for C₃₃H₃₆N₂NaO₆S: 611.2186 [M+Na]⁺; found: 611.2176.

***N*-(3,5-Dimethoxybenzyl)-4-methyl-*N*-(2-methylene-6-(*N*-methylmethanesulfonamido)hex-5-yn-1-yl)benzenesulfonamide (1.114a^{iv})**

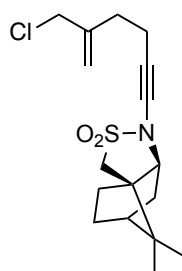


Copper sulphate pentahydrate (7.61 mg, 0.030 mmol), 1,10-phenantroline hydrate (12.1 mg, 0.061 mmol), potassium carbonate (84.2 mg, 0.609 mmol) and *N*-methylmethanesulfonamide (28 mL, 0.305 mmol) were placed under inert atmosphere. Then, toluene (1 mL) and a solution of **1.119** (150 mg, 0.305 mmol) in toluene (3 mL) were sequentially added. After stirring at 80 °C overnight, the mixture was passed through Celite pad and concentrated under reduced pressure. The resulting residue was purified by column chromatography on silica gel to give **1.114a^{iv}** (139.6 mg, 0.268 mmol, 88%) as colorless oil. ¹H NMR (500 MHz, CDCl₃) δ 7.74 – 7.68 (m, 2H), 7.33 – 7.27 (m, 2H), 6.30 (t, *J* = 2.3 Hz, 1H), 6.23 (d, *J* = 2.3 Hz, 2H), 4.92 (s, 1H), 4.86 (s, 1H), 4.24 (s, 2H), 3.73 (s, 2H), 3.67 (s, 6H), 3.12 (s, 3H), 3.00 (s, 3H), 2.41 (s, 3H), 2.32 (t, *J* = 7.2 Hz, 2H), 2.12 (t, *J* = 7.2 Hz, 2H); ¹³C NMR (126 MHz, CDCl₃) δ 160.8, 143.5, 142.2, 138.3, 137.5, 129.8, 127.3, 115.2, 106.5, 99.9, 75.0, 68.4, 55.3, 52.2, 51.1, 39.2, 36.0, 32.2, 21.6, 16.9. HRMS (ESI⁺): *m/z*: calculated for C₂₅H₃₂N₂NaO₆S₂: 543.1594 [M+Na]⁺; found: 543.1611.

General procedure B for the synthesis 1,5-enynes 1.114b-d



Step I: (3*aS*,6*R*,7*aS*)-1-(5-(Chloromethyl)hex-5-en-1-yn-1-yl)-8,8-dimethylhexahydro-3*H*-3*a*,6-methanobenzo[*c*]isothiazole 2,2-dioxide (1.182)⁵⁶

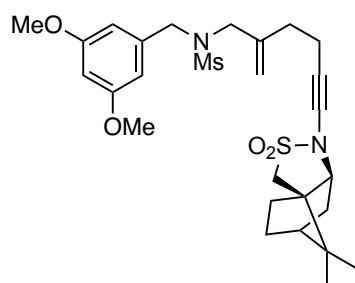


Copper sulphate pentahydrate (48.1 mg, 0.193 mmol), 1,10-phenantroline hydrate (76 mg, 0.386 mmol), potassium carbonate (533 mg, 3.86 mmol) and (1*R*)-(+)-2,10-camphosultam (456 mg, 2.12 mmol) were placed under inert atmosphere. Then, toluene (2 mL) and a solution of 6-bromo-2-(chloromethyl)hex-1-en-5-yne (400 mg, 1.93 mmol) in toluene (3 mL) were sequentially added. After stirring at 80 °C for 16 hours, the mixture was passed through Celite pad and concentrated under reduced pressure. The residue was purified by column chromatography on silica gel (15-20% EtOAc/cyclohexane) to give **1.182** (533.6 mg, 1.56 mmol, 81%) as colorless oil. ¹H NMR (500 MHz, CDCl₃) δ 5.18 (q, *J* = 0.9 Hz, 1H), 5.03 (q, *J* = 1.2 Hz, 1H), 4.06 (d, *J* = 1.0 Hz, 2H), 3.50 (dd, *J* = 8.1, 4.2 Hz, 1H), 3.21 (s, 2H), 2.50 (td, *J* = 7.1, 1.1 Hz, 2H), 2.41 (td, *J* = 6.8, 1.4 Hz, 2H), 2.15 (dtd, *J* = 13.4, 4.0, 2.8 Hz, 1H), 1.97 – 1.81 (m, 3H), 1.72 (dd, *J* = 13.3, 8.2 Hz, 1H), 1.45 – 1.37 (m, 1H), 1.35

– 1.25 (m, 1H), 1.09 (s, 3H), 0.93 (s, 3H) ; ^{13}C NMR (126 MHz, CDCl_3) δ 143.6 115.8, 71.5, 68.5, 67.2, 51.1, 49.7, 48.2, 44.5, 34.6, 32.5, 31.8, 27.2, 20.3, 20.1, 17.6. HRMS (ESI+): m/z : calculated for $\text{C}_{17}\text{H}_{25}\text{ClNO}_2\text{S}$: 342.1289 $[\text{M}+\text{H}]^+$; found: 342.1289.

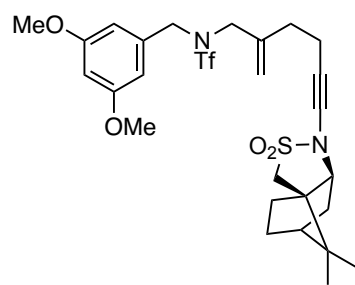
Step II: to a solution of **1.182** (1.0 equiv) and the corresponding *N*-protected benzylamine (1.2 equiv) in MeCN was added potassium carbonate (1.2 equiv) and potassium iodide (0.1 equiv) at 23 °C. A condenser was attached and the mixture was heated at 80 °C overnight. The solvent was evaporated and the residue was taken up in Et_2O , washed sequentially with water, brine, dried over anhydrous Na_2SO_4 , filtered and concentrated. The residue was purified by column chromatography on silica gel (EtOAc/cyclohexane) to give **1.114b-d** in the reported yields.

(3a*S*,6*R*,7a*S*)-1-(5-(Chloromethyl)hex-5-en-1-yn-1-yl)-8,8-dimethylhexahydro-3*H*-3a,6-methanobenzo[*c*]isothiazole 2,2-dioxide (1.114b)



Using the general procedure, reaction of **1.182** with *N*-(3,5-dimethoxybenzyl)methanesulfonamide⁸⁸ afforded compound **1.114b** (72,6 mg, 0.132 mmol, 73%) as colorless oil. ^1H NMR (500 MHz, CDCl_3) δ 6.49 (d, $J = 2.3$ Hz, 2H), 6.38 (t, $J = 2.3$ Hz, 1H), 5.10 (s, 1H), 5.08 (s, 1H), 4.31 (s, 2H), 3.78 (s, 2H), 3.78 (s, 6H), 3.51 – 3.44 (m, 1H), 3.19 (s, 2H), 2.81 (s, 3H), 2.47 (t, $J = 7.1$ Hz, 2H), 2.28 – 2.21 (m, 2H), 2.17 – 2.10 (m, 1H), 1.95 – 1.82 (m, 3H), 1.71 (dd, $J = 13.3, 8.1$ Hz, 1H), 1.44 – 1.36 (m, 1H), 1.33 – 1.23 (m, 1H), 1.07 (s, 3H), 0.91 (s, 3H). ^{13}C NMR (126 MHz, CDCl_3) δ 161.1, 141.8, 138.0, 115.4, 107.0, 100.0, 71.6, 68.7, 67.2, 55.5, 51.2, 51.0, 50.2, 49.6, 48.0, 44.5, 40.1, 34.6, 32.5, 31.7, 27.1, 20.3, 20.0, 17.3. HRMS (ESI+): m/z : calculated for $\text{C}_{27}\text{H}_{38}\text{N}_2\text{NaO}_6\text{S}_2$: 573.2063 $[\text{M}+\text{Na}]^+$; found: 573.2067.

***N*-(3,5-Dimethoxybenzyl)-*N*-(6-((3a*S*,6*R*,7a*S*)-8,8-dimethyl-2,2-dioxido-tetrahydro-3*H*-3a,6-methanobenzo[*c*]isothiazol-1(4*H*)-yl)-2-methylenehex-5-yn-1-yl)-1,1,1-trifluoromethanesulfonamide (1.114c)**



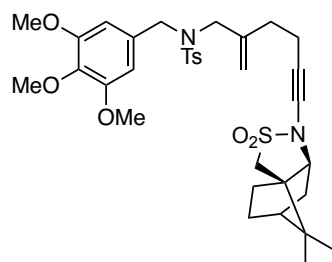
Using the general procedure, reaction of **1.182** with *N*-(3,5-dimethoxybenzyl)-1,1,1-trifluoromethanesulfonamide⁸⁹ afforded compound **1.114c** (93.0 mg, 0.154 mmol, 87%) as colorless oil. ^1H NMR δ 6.45 (d, $J = 2.3$ Hz, 2H), 6.40 (t, $J = 2.3$ Hz, 1H), 5.13 (s, 1H), 5.00 (s, 1H), 4.44 (s, 2H), 3.86 (s, 2H), 3.77 (s, 6H), 3.51 – 3.43 (m, 1H), 3.19 (s, 2H), 2.42 (t, $J = 7.0$ Hz, 2H), 2.17 (t, $J = 7.0$ Hz, 2H), 2.15 – 2.10 (m, 1H), 1.95 – 1.80 (m, 3H), 1.70 (dd, $J = 13.3, 8.1$ Hz, 1H), 1.41 – 1.36 (m, 1H), 1.33 – 1.25

⁸⁸ Benzyl amine preparation: O'Sullivan, S.; Doni, E.; Tuttle, T.; Murphy, J. A. Metal-Free Reductive Cleavage of C–N and S–N Bonds by Photoactivated Electron Transfer from a Neutral Organic Donor. *Angew. Chem. Int. Ed.* **2014**, *53*, 474–4781, *Angew. Chem.* **2013**, *125*, 2295–2298.

⁸⁹ Benzyl amine preparation: Ma, R.; White, M. C. C–H to C–N Cross-Coupling of Sulfonamides with Olefins. *J. Am. Chem. Soc.* **2018**, *140*, 3202–3205.

(m, 1H), 1.07 (s, 3H), 0.92 (s, 3H); ^{13}C NMR (126 MHz, CDCl_3) δ 161.2, 139.8, 136.2, 120.1 (q, $J = 323$ Hz), 116.4, 106.8, 100.5, 71.2, 68.9, 67.2, 55.5, 52.2, 51.5, 51.0, 49.6, 48.0, 44.5, 34.5, 32.2, 31.7, 27.1, 20.2, 20.0, 17.2.; ^{19}F NMR (471 MHz, CDCl_3) δ -75.3. HRMS (ESI+): m/z : calculated for $\text{C}_{27}\text{H}_{35}\text{F}_3\text{N}_2\text{NaO}_6\text{S}_2$: 627.1781 $[\text{M}+\text{Na}]^+$; found: 627.1793.

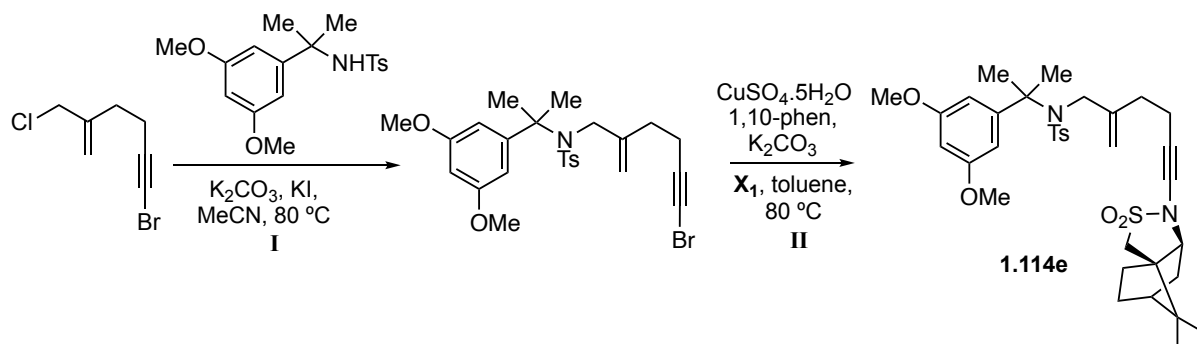
***N*-(6-((3*aS*,6*R*,7*aS*)-8,8-Dimethyl-2,2-dioxidotetrahydro-3*H*-3*a*,6-methanobenzo[*c*]isothiazol-1(4*H*)-yl)-2-methylenehex-5-yn-1-yl)-4-methyl-*N*-(3,4,5-trimethoxybenzyl)benzenesulfonamide (1.114d)**



Using the general procedure, reaction of **1.182** with 4-methyl-*N*-(3,4,5-trimethoxybenzyl)benzenesulfonamide⁹⁰ gave compound **1.114d** (93.7 mg, 0.143 mmol, 85%) as colorless oil. ^1H NMR (500 MHz, CDCl_3) δ 7.75 – 7.69 (m, 2H), 7.33 – 7.28 (m, 2H), 6.32 (s, 2H), 4.96 (s, 1H), 4.87 (s, 1H), 4.28 (s, 2H), 3.80 (s, 3H), 3.72 (s, 2H), 3.71 (s, 6H), 3.50 – 3.43 (m, 1H), 3.19 (s, 2H), 2.41 (s, 3H), 2.33 (t, $J = 7.1$ Hz, 2H), 2.17 – 2.08

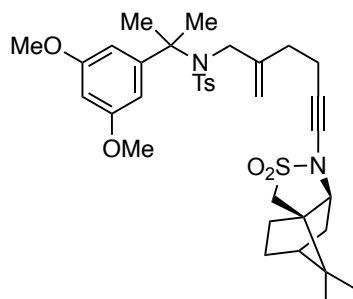
(m, 3H), 1.95 – 1.79 (m, 3H), 1.70 (dd, $J = 13.3, 8.1$ Hz, 1H), 1.42 – 1.35 (m, 1H), 1.31 – 1.24 (m, 1H), 1.07 (s, 3H), 0.91 (s, 3H); ^{13}C NMR (126 MHz, CDCl_3) δ 153.2, 143.4, 141.8, 137.9, 137.5, 131.6, 129.9, 127.3, 115.4, 105.8, 71.6, 68.5, 67.2, 61.0, 56.1, 51.8, 51.0, 50.9, 49.6, 48.0, 44.5, 34.6, 32.4, 31.7, 27.1, 21.6, 20.3, 20.0, 17.2. HRMS (ESI+): m/z : calculated for $\text{C}_{34}\text{H}_{44}\text{N}_2\text{NaO}_7\text{S}_2$: 679.2482 $[\text{M}+\text{Na}]^+$; found: 679.2490.

Procedure C for the synthesis of 1,5-enyne 1.114e



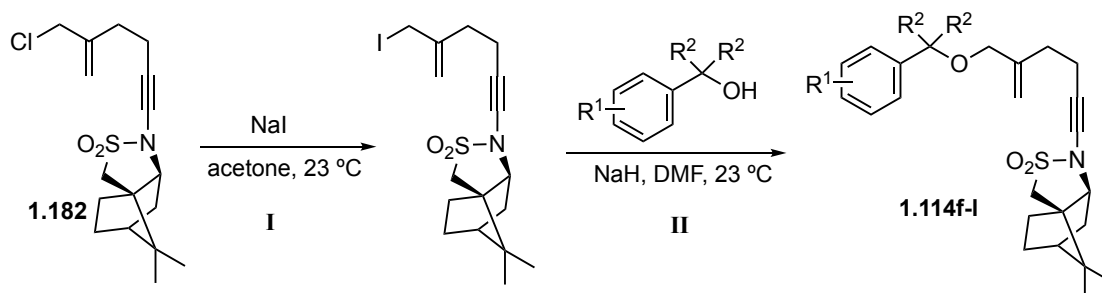
⁹⁰ Benzyl amine preparation: Plamont, R.; Graux, L. V.; Clavier, H. Highly Selective Syn Addition of 1,3-Diones to Internal Ynamides Catalyzed by Zinc Iodide. *Eur. J. Org. Chem.* **2018**, 2018, 1372–1376.

***N*-(2-(3,5-Dimethoxyphenyl)propan-2-yl)-*N*-(6-((3*aS*,6*R*,7*aS*)-8,8-dimethyl-2,2-dioxidotetrahydro-3*H*-3*a*,6-methanobenzo[*c*]isothiazol-1(4*H*)-yl)-2-methylenehex-5-yn-1-yl)-4-methylbenzenesulfonamide (1.114e)**



The previously described procedure had to be inverted to access the substrate **1.114e**. Using the same reaction conditions, compound **1.114e** (58.5 mg, 0.089 mmol, 37%, 2 steps) was obtained as colorless oil.⁹¹ ¹H NMR (500 MHz, CDCl₃) δ 7.59 – 7.51 (m, 2H), 7.24 – 7.17 (m, 2H), 6.36 (d, *J* = 2.2 Hz, 2H), 6.30 (t, *J* = 2.2 Hz, 1H), 5.01 (d, *J* = 1.4 Hz, 1H), 4.93 (q, *J* = 1.3 Hz, 1H), 3.92 (s, 2H), 3.69 (s, 6H), 3.52 – 3.44 (m, 1H), 3.19 (s, 2H), 2.40 (s, 3H), 2.39 (t, *J* = 7.2 Hz, 2H), 2.23 (t, *J* = 7.2 Hz, 2H), 1.96 – 1.80 (m, 4H), 1.72 (dd, *J* = 13.4, 8.2 Hz, 1H), 1.67 (s, 7H), 1.43 – 1.36 (m, 1H), 1.34 – 1.25 (m, 1H), 1.08 (s, 3H), 0.92 (s, 3H).; ¹³C NMR (126 MHz, CDCl₃) δ 160.5, 148.4, 145.2, 142.8, 140.6, 129.3, 127.4, 113.0, 105.0, 98.9, 71.9, 68.2, 67.3, 64.8, 55.3, 52.5, 51.0, 49.6, 48.0, 44.5, 34.6, 33.0, 31.7, 29.6, 27.2, 21.6, 20.3, 20.1, 17.4. HRMS (ESI+): *m/z*: calculated for C₃₅H₄₆N₂NaO₆S₂: 677.2689 [M+Na]⁺; found: 677.2696.

General procedure D for the synthesis of 1,5-enynes 1.114f-k



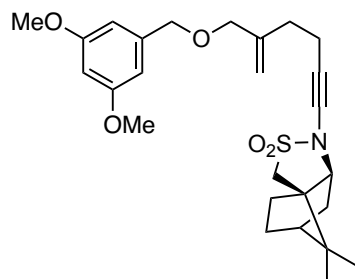
Step I: Sodium iodide (3.0 equiv) was added to a solution of **1.182** (1.0 equiv) in acetone and the reaction mixture was stirred overnight at 23 °C. The mixture was diluted with water and extracted with Et₂O. The combined organic layer was sequentially washed with saturated Na₂S₂O₃, brine, dried over anhydrous Na₂SO₄, filtered and the solvent was evaporated. The obtained crude was filtered through a small column on silica gel (30% Et₂O/pentane) to give the corresponding allyl iodide which was concentrated until the theoretical weight and used directly for the next step.

Step II: Sodium hydride (1.2 equiv, 60% in mineral oil) was added to a solution of the corresponding benzyl alcohol (1.2 equiv) in DMF at 0 °C and the mixture was kept at this temperature for 20 minutes. Then, a solution of the allyl iodide previously prepared (1.0 equiv) in DMF was added via cannula and the reaction mixture was stirred overnight at room temperature. After that time, water was added, the aqueous phase was extracted 3 x Et₂O, and the combined organic extracts were washed with water,

⁹¹ Benzyl amine preparation: Schneider, C.; Broda, E.; Snieckus, V. Directed Ortho-Metalation–Cross-Coupling Strategies. One-Pot Suzuki Reaction to Biaryl and Heterobiaryl Sulfonamides. *Org. Lett.* **2011**, *13*, 3588–3591.

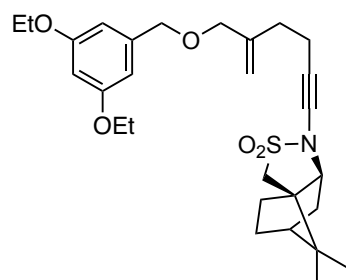
brine, dried over anhydrous Na_2SO_4 , filtered and concentrated under reduced pressure. The residue was purified by column chromatography on silica gel (EtOAc/cyclohexane) affording **1.114f-l** in the reported yields.

(3a*S*,6*R*,7a*S*)-1-(5-(((3,5-Dimethoxybenzyl)oxy)methyl)hex-5-en-1-yn-1-yl)-8,8-dimethylhexahydro-3*H*-3a,6-methanobenzo[*c*]isothiazole 2,2-dioxide (1.114f)



Using the general procedure, compound **1.114f** (35.0 mg, 0.074 mmol, 54%) was obtained as colorless oil. $^1\text{H NMR}$ (500 MHz, CDCl_3) δ 6.50 (d, $J = 2.3$ Hz, 2H), 6.38 (t, $J = 2.3$ Hz, 1H), 5.10 (s, 1H), 4.99 (s, 1H), 4.43 (s, 2H), 3.96 (s, 2H), 3.79 (s, 6H), 3.51 – 3.44 (m, 1H), 3.20 (s, 2H), 2.48 (t, $J = 7.2$ Hz, 2H), 2.32 (t, $J = 7.3$ Hz, 2H), 2.19 – 2.10 (m, 1H), 1.95 – 1.80 (m, 3H), 1.70 (dd, $J = 13.3, 8.1$ Hz, 1H), 1.44 – 1.36 (m, 1H), 1.34 – 1.23 (m, 1H), 1.08 (s, 3H), 0.92 (s, 3H); $^{13}\text{C NMR}$ (126 MHz, CDCl_3) δ 161.0, 144.3, 140.9, 113.3, 105.4, 99.8, 73.0, 71.9, 72.0, 68.2, 67.2, 55.5, 51.0, 49.6, 48.0, 44.5, 34.5, 32.7, 31.7, 27.1, 20.3, 20.1, 17.6. **HRMS** (ESI+): m/z : calculated for $\text{C}_{26}\text{H}_{36}\text{NO}_5\text{S}$: 474.2309 $[\text{M}+\text{H}]^+$; found: 474.2314.

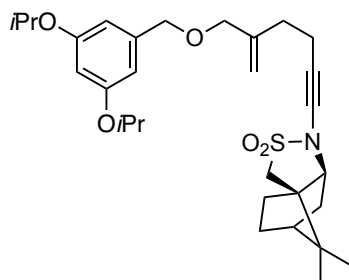
(3a*S*,6*R*,7a*S*)-1-(5-(((3,5-Diethoxybenzyl)oxy)methyl)hex-5-en-1-yn-1-yl)-8,8-dimethylhexahydro-3*H*-3a,6-methanobenzo[*c*]isothiazole 2,2-dioxide (1.114g)



Using the general procedure, compound **1.114g** (40.2 mg, 0.080 mmol, 47%) was obtained as colorless oil.⁹² $^1\text{H NMR}$ (500 MHz, CDCl_3) δ 6.48 (d, $J = 2.3$ Hz, 2H), 6.36 (t, $J = 2.3$ Hz, 1H), 5.09 (d, $J = 1.7$ Hz, 1H), 5.01 – 4.97 (m, 1H), 4.41 (s, 2H), 4.01 (q, $J = 7.0$ Hz, 4H), 3.95 (s, 2H), 3.48 (dd, $J = 8.1, 4.1$ Hz, 1H), 3.20 (s, 2H), 2.48 (t, $J = 7.2$ Hz, 2H), 2.31 (t, $J = 7.3$ Hz, 2H), 2.19 – 2.10 (m, 1H), 1.95 – 1.80 (m, 3H), 1.70 (dd, $J = 13.3, 8.1$ Hz, 1H), 1.39 (t, $J = 7.0$ Hz, 6H), 1.33 – 1.22 (m, 2H), 1.08 (s, 3H), 0.92 (s, 3H); $^{13}\text{C NMR}$ (126 MHz, CDCl_3) δ 160.3, 144.4, 140.8, 113.2, 106.0, 100.7, 73.0, 72.0, 68.2, 67.3, 63.6, 51.0, 49.6, 48.1, 44.5, 34.6, 32.8, 31.7, 27.2, 20.3, 20.1, 17.7, 15.0. **HRMS** (ESI+): m/z : calculated for $\text{C}_{28}\text{H}_{40}\text{NO}_5\text{S}$: 502.2622 $[\text{M}+\text{H}]^+$; found: 502.2626.

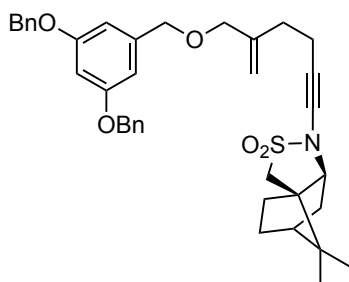
⁹² Benzyl alcohol preparation: Yu, C.; Zhang, X.; Zhang, J.; Shen, Z. Total Synthesis of Dysidavarone A. *Tetrahedron* **2016**, *72*, 4337–4345.

(3a*S*,6*R*,7a*S*)-1-(5-(((3,5-Diisopropoxybenzyl)oxy)methyl)hex-5-en-1-yn-1-yl)-8,8-dimethylhexahydro-3*H*-3a,6-methanobenzo[*c*]isothiazole 2,2-dioxide (1.114h)



Using the general procedure, compound **1.114h** (43.2 mg, 0.082 mmol, 26%) was obtained as colorless oil.⁹³ ¹H NMR (500 MHz, CDCl₃) δ 6.45 (d, *J* = 2.3 Hz, 2H), 6.34 (t, *J* = 2.3 Hz, 1H), 5.09 (s, 1H), 4.99 (s, 1H), 4.52 (p, *J* = 6.1 Hz, 2H), 4.40 (s, 2H), 3.95 (s, 2H), 3.48 (dd, *J* = 8.1, 4.2 Hz, 1H), 3.20 (s, 2H), 2.48 (t, *J* = 7.2 Hz, 2H), 2.32 (t, *J* = 7.3 Hz, 2H), 2.18 – 2.11 (m, 1H), 1.95 – 1.82 (m, 3H), 1.70 (dd, *J* = 13.3, 8.1 Hz, 1H), 1.43 – 1.36 (m, 1H), 1.32 (d, *J* = 6.1 Hz, 12H), 1.29 – 1.25 (m, 1H), 1.08 (s, 3H), 0.92 (s, 3H); ¹³C NMR (126 MHz, CDCl₃) 159.3, 144.4, 140.8, 113.2, 107.2, 103.1, 73.0, 72.0, 72.0, 70.0, 68.2, 67.2, 51.0, 49.6, 48.0, 44.5, 34.6, 32.7, 31.7, 27.2, 22.2, 20.3, 20.1, 17.6; HRMS (ESI⁺): *m/z*: calculated for C₃₀H₄₄NO₅S: 530.2935 [M+H]⁺; found: 530.2934.

(3a*S*,6*R*,7a*S*)-1-(5-(((3,5-Bis(benzyloxy)benzyl)oxy)methyl)hex-5-en-1-yn-1-yl)-8,8-dimethylhexahydro-3*H*-3a,6-methanobenzo[*c*]isothiazole 2,2-dioxide (1.114i)

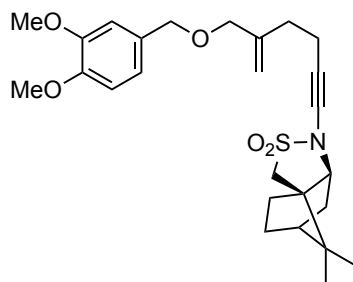


Using the general procedure, compound **1.114i** (44.1 mg, 0.071 mmol, 42%) was obtained as colorless oil.⁹⁴ ¹H NMR (500 MHz, CDCl₃) δ 7.44 – 7.41 (m, 4H), 7.41 – 7.36 (m, 4H), 7.35 – 7.30 (m, 2H), 6.61 (d, *J* = 2.3 Hz, 2H), 6.55 (t, *J* = 2.3 Hz, 1H), 5.09 (s, 1H), 5.04 (s, 4H), 5.00 (s, 1H), 4.43 (s, 2H), 3.96 (s, 2H), 3.47 (dd, *J* = 8.1, 4.2 Hz, 1H), 3.19 (s, 2H), 2.48 (t, *J* = 7.3 Hz, 2H), 2.32 (d, *J* = 14.6 Hz, 1H), 2.18 – 2.11 (m, 1H), 1.94 – 1.81 (m, 3H), 1.69 (dd, *J* = 13.4, 8.1 Hz, 1H), 1.42 – 1.35 (m, 1H), 1.31 – 1.23 (m, 1H), 1.08 (s, 3H), 0.91 (s, 3H). ¹³C NMR (126 MHz, CDCl₃) δ 160.2, 144.2, 141.0, 137.1, 128.7, 128.1, 127.7, 113.3, 106.6, 101.5, 73.0, 72.0, 71.9, 70.2, 68.2, 67.2, 51.0, 49.6, 48.0, 44.5, 34.5, 32.7, 31.7, 27.1, 20.3, 20.0, 17.6. HRMS (ESI⁺): *m/z*: calculated for C₃₈H₄₄NO₅S: 626.2935 [M+H]⁺; found: 626.2936.

⁹³ Benzyl alcohol preparation: St. John, S. E.; Jensen, K. C.; Kang, S.; Chen, Y.; Calamini, B.; Mesecar, A. D.; Lipton, M. A. Design, Synthesis, Biological and Structural Evaluation of Functionalized Resveratrol Analogues as Inhibitors of Quinone Reductase 2. *Bioorg. Med. Chem.* **2013**, *21*, 6022–6037.

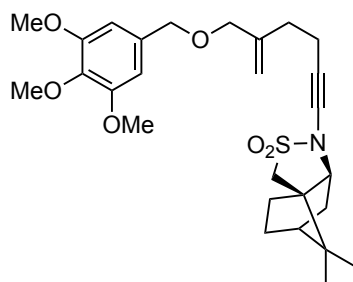
⁹⁴ Benzyl alcohol preparation: Wan, X.; Wang, X.-B.; Yang, M.-H.; Wang, J.-S.; Kong, L.-Y. Dimerization of Piceatannol by *Momordica Charantia* Peroxidase and α -Glucosidase Inhibitory Activity of the Biotransformation Products. *Bioorg. Med. Chem.* **2011**, *19*, 5085–5092.

(3*aS*,6*R*,7*aS*)-1-(5-(((3,4-Dimethoxybenzyl)oxy)methyl)hex-5-en-1-yn-1-yl)-8,8-dimethylhexahydro-3*H*-3*a*,6-methanobenzo[*c*]isothiazole 2,2-dioxide (1.114j)



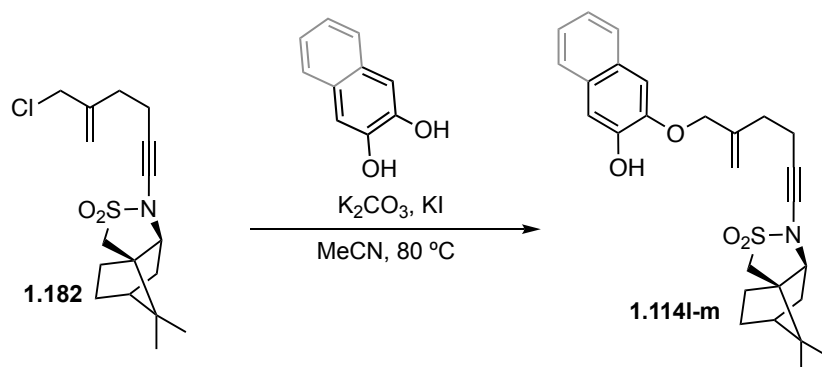
Using the general procedure, compound **1.114j** (40.1 mg, 0.085 mmol, 48%) was obtained as colorless oil. $^1\text{H NMR}$ (500 MHz, CDCl_3) δ 6.92 – 6.80 (m, 3H), 5.09 (s, 1H), 4.99 (s, 1H), 4.41 (s, 2H), 3.95 (d, $J = 1.2$ Hz, 2H), 3.88 (s, 3H), 3.87 (s, 3H), 3.47 (dd, $J = 8.2, 4.2$ Hz, 1H), 3.19 (s, 2H), 2.47 (t, $J = 7.5$ Hz, 2H), 2.32 (d, $J = 14.7$ Hz, 1H), 2.17 – 2.10 (m, 1H), 1.94 – 1.82 (m, 3H), 1.69 (dd, $J = 13.3, 8.1$ Hz, 1H), 1.44 – 1.36 (m, 1H), 1.32 – 1.23 (m, 1H), 1.07 (s, 3H), 0.91 (s, 3H); $^{13}\text{C NMR}$ (126 MHz, CDCl_3) δ 149.1, 148.7, 144.4, 131.0, 120.4, 113.2, 111.2, 111.0, 72.8, 71.9, 71.9, 68.2, 67.2, 56.0, 56.0, 51.0, 49.6, 48.0, 44.5, 34.5, 32.8, 31.7, 27.1, 20.3, 20.0, 17.6. **HRMS** (ESI⁺): m/z : calculated for $\text{C}_{26}\text{H}_{36}\text{NO}_5\text{S}$: 474.2309 $[\text{M}+\text{H}]^+$; found: 474.2311.

(3*aS*,6*R*,7*aS*)-8,8-Dimethyl-1-(5-(((3,4,5-trimethoxybenzyl)oxy)methyl)hex-5-en-1-yn-1-yl)hexahydro-3*H*-3*a*,6-methanobenzo[*c*]isothiazole 2,2-dioxide (1.114k)



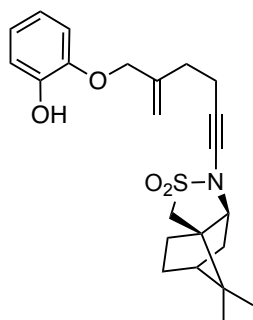
Using the general procedure, compound **1.114k** (51.5 mg, 0.102 mmol, 60%) was obtained as colorless oil. $^1\text{H NMR}$ (500 MHz, CDCl_3) δ 6.57 (s, 2H), 5.10 (s, 1H), 5.00 (s, 1H), 4.41 (s, 2H), 3.98 (s, 2H), 3.86 (s, 6H), 3.83 (s, 3H), 3.47 (dd, $J = 8.0, 4.2$ Hz, 1H), 3.19 (s, 2H), 2.49 (t, $J = 7.6$ Hz, 2H), 2.33 (d, $J = 14.7$ Hz, 1H), 2.17 – 2.10 (m, 1H), 1.94 – 1.82 (m, 3H), 1.69 (dd, $J = 13.3, 8.1$ Hz, 1H), 1.41 – 1.36 (m, 1H), 1.32 – 1.25 (m, 1H), 1.07 (s, 3H), 0.91 (s, 3H); $^{13}\text{C NMR}$ (126 MHz, CDCl_3) δ 153.4, 144.3, 137.4, 134.2, 113.4, 104.7, 73.2, 72.1, 71.9, 68.2, 67.2, 60.9, 56.2, 51.0, 49.6, 48.0, 44.5, 34.5, 32.8, 31.7, 27.1, 20.3, 20.0, 17.7; **HRMS** (ESI⁺): m/z : calculated for $\text{C}_{27}\text{H}_{38}\text{NO}_6\text{S}$: 504.2414 $[\text{M}+\text{H}]^+$; found: 504.2420.

General procedure E for the synthesis of phenol-substituted 1,5-enynes 1.114l-m



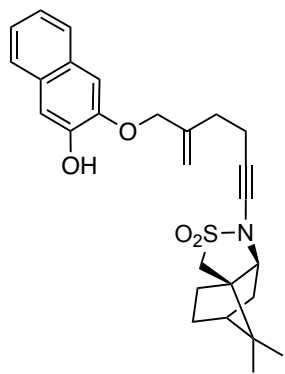
To a solution of **1.182** (1.0 equiv) and the corresponding diol (1.2 equiv) in MeCN was added potassium carbonate (1.2 equiv) and potassium iodide (0.1 equiv) at 23 °C. A condenser was attached and the mixture was heated at 80 °C overnight. The solvent was evaporated and the residue was taken up in Et₂O, washed sequentially with water, brine, dried over anhydrous Na₂SO₄, filtered and concentrated. The residue was purified by column chromatography on silica gel (EtOAc/cyclohexane) to give **1.114l-m** in the reported yields.

(3a*S*,6*R*,7a*S*)-1-(5-((2-Hydroxyphenoxy)methyl)hex-5-en-1-yn-1-yl)-8,8-dimethylhexahydro-3*H*-3a,6-methanobenzo[*c*]isothiazole 2,2-dioxide (1.114l)

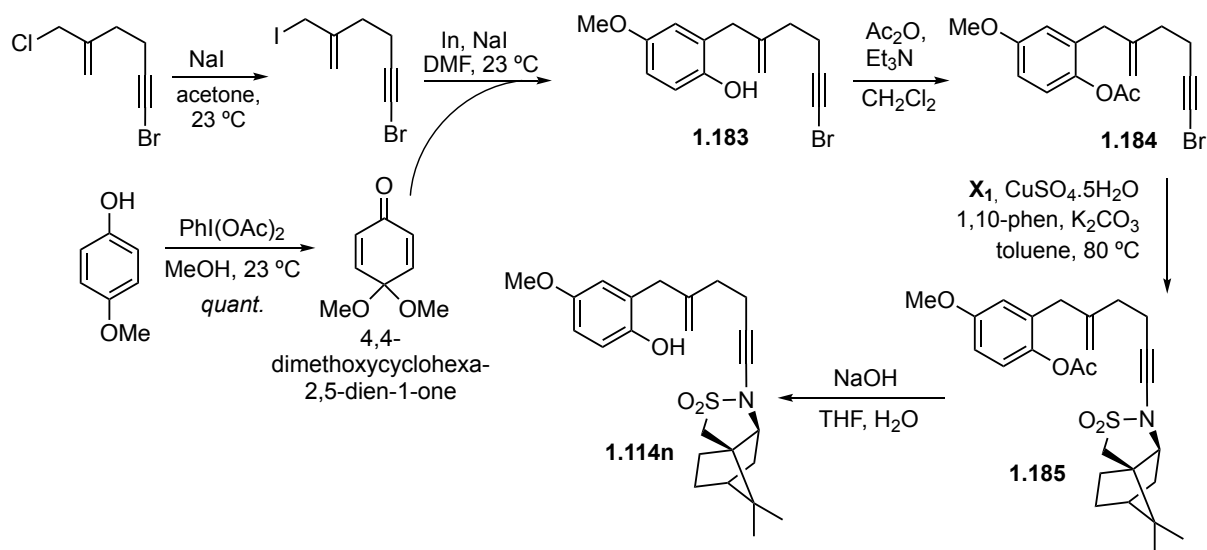


Using the general procedure, reaction of **1.182** with catechol afforded compound **1.114l** (74.1 mg, 0.178 mmol, 76%) as colorless oil. ¹H NMR (500 MHz, CDCl₃) δ 6.93 (dd, *J* = 8.0, 1.7 Hz, 1H), 6.90 – 6.84 (m, 2H), 6.84 – 6.77 (m, 1H), 5.70 (s, 1H), 5.20 (s, 1H), 5.12 – 5.08 (m, 1H), 4.57 (s, 2H), 3.47 (dd, *J* = 8.1, 4.1 Hz, 1H), 3.21 (s, 2H), 2.53 (t, *J* = 7.3 Hz, 2H), 2.41 – 2.35 (m, 1H), 2.17 – 2.10 (m, 1H), 1.95 – 1.82 (m, 3H), 1.69 (dd, *J* = 13.3, 8.1 Hz, 1H), 1.42 – 1.36 (m, 1H), 1.32 – 1.24 (m, 1H), 1.08 (s, 3H), 0.92 (s, 3H); ¹³C NMR (126 MHz, CDCl₃) δ 146.0, 145.8, 142.9, 121.8, 120.2, 114.8, 114.3, 112.4, 71.7, 71.6, 68.7, 67.2, 51.0, 49.6, 48.0, 44.5, 34.5, 32.5, 31.7, 27.1, 20.3, 20.0, 17.8; HRMS (ESI⁺): *m/z*: calculated for C₂₃H₂₈NO₄S: 414.1745 [M+H]⁺; found: 414.1730.

(3a*S*,6*R*,7a*S*)-1-(5-(((3-Hydroxynaphthalen-2-yl)oxy)methyl)hex-5-en-1-yn-1-yl)-8,8-dimethylhexahydro-3*H*-3a,6-methanobenzo[*c*]isothiazole 2,2-dioxide (1.114m)



Using the general procedure, reaction of **1.182** with naphthalene-2,3-diol afforded compound **1.114m** (56.6 mg, 0.122 mmol, 52%) as colorless oil. ¹H NMR (500 MHz, CDCl₃) δ 7.66 (ddd, *J* = 8.6, 5.2, 1.8 Hz, 2H), 7.34 – 7.27 (m, 2H), 7.27 (s, 1H), 7.16 (s, 1H), 6.00 (s, 1H), 5.28 (s, 1H), 5.16 (s, 1H), 4.72 (q, *J* = 12.2 Hz, 2H), 3.39 (dd, *J* = 8.1, 4.2 Hz, 1H), 3.19 (s, 2H), 2.57 (t, *J* = 7.2 Hz, 2H), 2.43 (t, *J* = 7.1 Hz, 2H), 2.14 – 2.06 (m, 1H), 1.89 – 1.76 (m, 3H), 1.66 – 1.59 (m, 1H), 1.32 – 1.26 (m, 1H), 1.25 – 1.17 (m, 1H), 1.06 (s, 3H), 0.90 (s, 3H); ¹³C NMR (126 MHz, CDCl₃) δ 146.5, 145.9, 142.6, 129.8, 129.0, 126.7, 126.4, 124.5, 123.9, 114.9, 109.6, 107.2, 71.7, 71.5, 68.8, 67.2, 51.0, 49.6, 48.0, 44.5, 34.5, 32.6, 31.6, 27.1, 20.3, 20.0, 18.0; HRMS (ESI⁺): *m/z*: calculated for C₂₇H₃₀NO₄S: 464.1901 [M+H]⁺; found: 464.1909.

Procedure F for the synthesis of phenol-substituted 1,5-enyne 1.114n**2-(6-Bromo-2-methylenehex-5-yn-1-yl)-4-methoxyphenol (1.183)**

1) Sodium iodide (1.008 g, 6.72 mmol) was added to a solution of 6-bromo-2-(chloromethyl)hex-1-en-5-yne (465 mg, 2.24 mmol) in acetone (6 mL) and the reaction mixture was stirred overnight at 23 °C. The mixture was diluted with water (10 mL) and extracted with Et₂O (3 x 15 mL). The combined organic layer was sequentially washed with saturated Na₂S₂O₃ (20 mL), brine (20 mL), dried over anhydrous Na₂SO₄, filtered and the solvent was evaporated. The obtained crude was filtered through a small column on silica gel (100% pentane) to give compound allyl iodide which was concentrated until the theoretical weight and used directly for the next step. 2) On the other hand, 4-methoxyphenol (200 mg, 1.61 mmol) was dissolved in methanol (6 mL) at 23 °C and (diacetoxyiodo)benzene (623 mg, 1.93 mmol) was added.⁹⁵ After 1 hour at 23 °C, the solution was diluted with saturated NaHCO₃ (10 mL) and extracted with Et₂O (3x15 mL). The combined organic layer was washed with brine (20 mL), dried over anhydrous Na₂SO₄, filtered and the solvent was evaporated (temperature below 20 °C). The obtained crude was purified by column chromatography on silica gel (30% Et₂O/pentane) to give 4,4-dimethoxycyclohexa-2,5-dien-1-one which was concentrated until the theoretical weight and used directly for the next step. 3) Indium (169 mg, 1.47 mmol) and sodium iodide (221 mg, 1.47 mmol) were poured into DMF (4 mL) at 23 °C and a solution of the allyl iodide (649 mg, 2.17 mmol) in DMF (4 mL) was added via cannula. After 30 minutes at 23 °C, a solution of freshly prepared 4,4-dimethoxycyclohexa-2,5-dien-1-one (216 mg, 1.40 mmol) in DMF (4 mL) was also added and the reaction was stirred overnight at 23 °C.⁹⁶ The solution was diluted with water slightly acidified with 10% HCl and the aqueous phase was extracted with Et₂O (3x15 mL). The combined organic layer was washed with water (20 mL), brine (20 mL), dried over

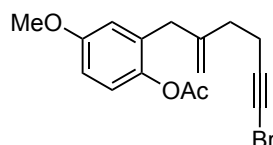
⁹⁵ Mitchell, A. S.; Russell, R. A. Oxidation with Hypervalent Iodine Reagents. Part II: Novel Cyclohexadienones as Precursors for the Synthesis of Anthraquinones. *Tetrahedron* **1997**, *53*, 4387–4410.

⁹⁶ Mal, D.; Pahari, P.; Senapati, B. K. A Room Temperature Alternative of the Claisen Rearrangement Route to *Ortho* Allylated Phenols: Unique Reactivity Pattern of Allylindium Reagents. *Tetrahedron Lett.* **2005**, *46*, 2097–2100.

anhydrous Na₂SO₄, filtered and the solvent was evaporated. The obtained crude was purified by column chromatography on silica gel (5-10% EtOAc/cyclohexane) to give **1.183** (293 mg, 0.993 mmol, 71%, 2 steps) as colorless oil.

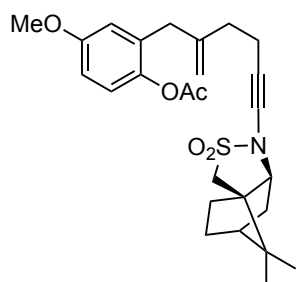
¹H NMR (500 MHz, CDCl₃) δ 6.76 (d, *J* = 8.6 Hz, 1H), 6.72 – 6.65 (m, 2H), 4.96 (q, *J* = 1.1 Hz, 1H), 4.91 (tt, *J* = 1.5, 0.8 Hz, 1H), 4.82 (s, 1H), 3.76 (s, 3H), 3.36 (s, 2H), 2.39 (td, *J* = 7.3, 0.8 Hz, 2H), 2.29 – 2.22 (m, 2H). ¹³C NMR (126 MHz, CDCl₃) δ 153.83, 148.45, 146.10, 125.89, 116.87, 116.55, 113.00, 112.83, 79.63, 55.84, 38.84, 38.09, 34.04, 18.61. HRMS (ESI+): *m/z*: calculated for C₁₄H₁₄BrO₂: 293.0183 [M+H]⁺; found: 293.0180.

2-(6-Bromo-2-methylenehex-5-yn-1-yl)-4-methoxyphenyl acetate (**1.184**)



Acetic anhydride (0.105 mL, 1.08 mmol) and Et₃N (0.300 mL, 2.16 mmol) were sequentially added to a solution of **1.183** (159 mg, 0.539 mmol) in CH₂Cl₂ (4 mL) at 0 °C. After 15 minutes at that temperature, the reaction mixture was stirred overnight at 23 °C. Then, saturated NH₄Cl (15 mL) was added, the aqueous layer was extracted with CH₂Cl₂ (3 x 15 mL) and the combined organic layer was washed with brine (20 mL), dried over anhydrous Na₂SO₄, filtered and the solvent was evaporated. The obtained crude was purified by column chromatography on silica gel (5-10% EtOAc/cyclohexane) to give compound **1.184** (167 mg, 0.495 mmol, 92%) as colorless oil. ¹H NMR (500 MHz, CDCl₃) δ 6.95 (d, *J* = 8.6 Hz, 1H), 6.80 – 6.73 (m, 2H), 4.90 (dd, *J* = 1.4, 0.8 Hz, 1H), 4.81 (dd, *J* = 1.5, 0.8 Hz, 1H), 3.78 (s, 3H), 3.25 (s, 2H), 2.33 (td, *J* = 7.4, 0.7 Hz, 2H), 2.27 (s, 3H), 2.21 – 2.15 (m, 2H).; ¹³C NMR (126 MHz, CDCl₃) δ 169.8, 157.5, 145.3, 142.9, 132.3, 123.3, 116.1, 112.9, 112.6, 79.8, 55.7, 38.5, 37.6, 34.0, 21.0, 18.6. HRMS (ESI+): *m/z*: calculated for C₁₆H₁₇BrNaO₃: 359.0253 [M+Na]⁺; found: 359.0252.

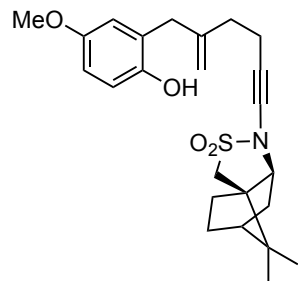
2-(6-(((3a*S*,6*R*,7a*S*)-8,8-Dimethyl-2,2-dioxidotetrahydro-3*H*-3a,6-methanobenzo[*c*]isothiazol-1(4*H*)-yl)-2-methylenehex-5-yn-1-yl)-4-methoxyphenyl acetate (**1.185**)⁵⁶



Copper sulphate pentahydrate (12.1 mg, 0.048 mmol), 1,10-phenanthroline hydrate (19.2 mg, 0.097 mmol), potassium carbonate (134 mg, 0.966 mmol) and (1*R*)-(+)-2,10-camphosultam (114 mg, 0.531 mmol) were placed under inert atmosphere. Then, toluene (2 mL) and a solution of **1.184** (163 mg, 0.483 mmol) in toluene (3 mL) were sequentially added. After stirring at 80 °C overnight, the mixture was passed through Celite pad and concentrated under reduced pressure. The resulting residue was purified by column chromatography on silica gel (20% EtOAc/cyclohexane) to give **1.185** (207 mg, 0.440 mmol, 91%) as a yellow oil. ¹H NMR (500 MHz, CDCl₃) δ 6.97 – 6.91 (m, 1H), 6.79 – 6.74 (m, 2H), 4.89 (s, 1H), 4.76 (s, 1H), 3.78 (s, 3H), 3.49 (dd, *J* = 7.7, 3.9 Hz, 1H), 3.23 (s, 2H), 3.20 (s, 2H), 2.43 (t, *J* = 7.4 Hz, 2H), 2.26 (s, 3H), 2.19 (t, *J* = 7.4 Hz, 2H), 2.19 – 2.11 (m, 1H), 1.95 – 1.80 (m, 3H), 1.71 (dd, *J* = 13.4, 8.1 Hz, 1H), 1.45 – 1.37 (m, 1H), 1.34 – 1.28 (m, 1H), 1.08 (s, 3H), 0.92 (s, 3H).; ¹³C NMR (126 MHz, CDCl₃) δ 169.9, 157.4, 145.6, 142.9, 132.4, 123.2, 116.1, 112.8, 112.6, 71.9, 68.2, 67.3, 55.7, 51.0, 49.6, 48.0, 44.5, 37.4, 34.9,

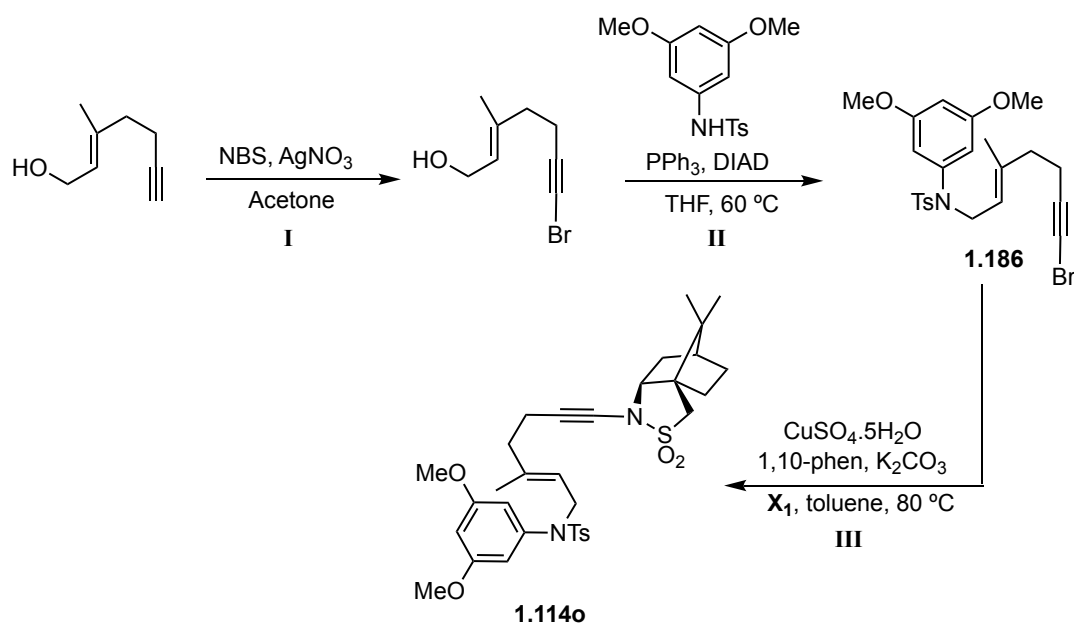
34.6, 31.7, 27.2, 21.0, 20.3, 20.1, 17.6. **HRMS** (ESI⁺): *m/z*: calculated for C₂₆H₃₃NNaO₅S: 494.1972 [M+Na]⁺; found: 494.1985.

(3*a*S,6*R*,7*a*S)-1-(5-(2-Hydroxy-5-methoxybenzyl)hex-5-en-1-yn-1-yl)-8,8-dimethylhexahydro-3*H*-3*a*,6-methanobenzo[*c*]isothiazole 2,2-dioxide (1.114*n*)



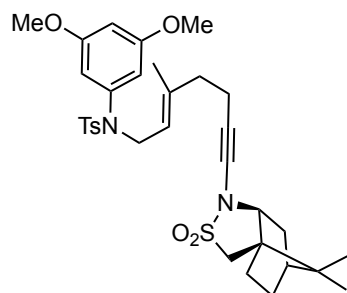
A solution of sodium hydroxide (97 mg, 2.42 mmol) in H₂O (3 mL) was added to a solution of **1.185** (228 mg, 0.483 mmol) in THF (3 mL). The mixture was stirred overnight protected of the air at 23 °C. After that time, saturated NH₄Cl (15 mL) was added, the aqueous layer was extracted with EtOAc (3 x 15 mL) and the combined organic layer was washed with brine (20 mL), dried over anhydrous Na₂SO₄, filtered and the solvent was evaporated. The obtained crude was purified by column chromatography on silica gel (20% EtOAc/cyclohexane) to give compound **1.114n** (175 mg, 0.406 mmol, 84%) as a yellow oil. **¹H NMR** (500 MHz, CDCl₃) δ 6.76 (dd, *J* = 8.4, 0.7 Hz, 1H), 6.71 – 6.64 (m, 2H), 4.96 (d, *J* = 1.3 Hz, 1H), 4.95 (s, 1H), 4.87 (d, *J* = 1.5 Hz, 1H), 3.75 (s, 3H), 3.50 (dd, *J* = 8.1, 4.2 Hz, 1H), 3.36 (s, 2H), 3.21 (s, 2H), 2.48 (t, *J* = 7.2 Hz, 2H), 2.29 – 2.22 (m, 2H), 2.19 – 2.11 (m, 1H), 1.95 – 1.80 (m, 3H), 1.75 – 1.69 (m, 1H), 1.45 – 1.37 (m, 1H), 1.33 – 1.25 (m, 1H), 1.08 (s, 3H), 0.92 (s, 3H); **¹³C NMR** (126 MHz, CDCl₃) δ 153.8, 148.6, 146.3, 126.1, 117.0, 116.4, 112.9, 112.8, 71.8, 68.5, 67.3, 55.8, 51.0, 49.6, 48.0, 44.5, 38.0, 34.8, 34.5, 31.7, 27.1, 20.3, 20.0, 17.8. **HRMS** (ESI⁺): *m/z*: calculated for C₂₄H₃₁NNaO₄S: 452.1866 [M+Na]⁺; found: 452.1858.

Procedure G for the synthesis of internal 1,5-enyne 1.114o



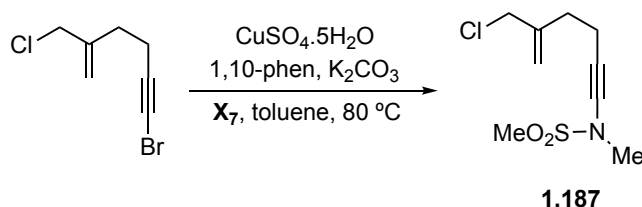
Step I-II: Compound **1.186** was synthesized as reported in the scheme according to literature procedure.⁴⁰ All the spectral data were fully consistent with those previously reported.

***N*-(3,5-Dimethoxyphenyl)-*N*-((*E*)-7-((3*aR*,6*S*,7*aS*)-8,8-dimethyl-2,2-dioxidotetrahydro-3*H*-3*a*,6-methanobenzo[*c*]isothiazol-1(4*H*)-yl)-3-methylhept-2-en-6-yn-1-yl)-4-methylbenzenesulfonamide (1.114o)⁵⁶**



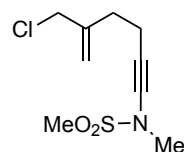
Copper sulfate pentahydrate (12,2 mg, 0,049 mmol), 1,10-phenanthroline hydrate (19,3 mg, 0,097 mmol), potassium carbonate (135 mg, 0,975 mmol) and (*1R*)-(+)-2,10-camphosultam (105 mg, 0,487 mmol) were placed under inert atmosphere. To the flask, toluene (1 mL) and a solution of **1.186** (240 mg, 0,487 mmol) in toluene (3 mL) were sequentially added. After stirring at 70 °C overnight, the mixture was passed through Celite pad and concentrated under reduced pressure. The resulting residue was purified by column chromatography on silica gel (20% EtOAc/cyclohexane) to give **1.114o** (270 mg, 0,487 mmol, 88%) as a yellow oil. ¹H NMR (400 MHz, CDCl₃) δ 7.58 – 7.50 (m, 2H), 7.26 – 7.22 (m, 2H), 6.35 (t, *J* = 2.3 Hz, 1H), 6.17 (d, *J* = 2.3 Hz, 2H), 5.13 (tt, *J* = 5.5, 1.4 Hz, 1H), 4.11 (d, *J* = 6.8 Hz, 2H), 3.69 (s, 6H), 3.48 (dd, *J* = 8.1, 4.2 Hz, 1H), 3.19 (s, 2H), 2.41 (s, 3H), 2.29 – 2.20 (m, 2H), 2.17 – 2.05 (m, 3H), 1.97 – 1.81 (m, 3H), 1.72 (dd, *J* = 13.3, 8.1 Hz, 1H), 1.51 (d, *J* = 1.3 Hz, 3H), 1.45 – 1.35 (m, 1H), 1.35 – 1.26 (m, 1H), 1.06 (s, 3H), 0.91 (s, 3H); ¹³C NMR (101 MHz, CDCl₃) δ 160.6, 143.4, 141.3, 138.8, 135.9, 129.5, 127.9, 120.1, 107.0, 100.2, 71.8, 68.2, 67.2, 55.5, 51.0, 49.6, 48.7, 48.0, 44.5, 38.9, 34.5, 31.7, 27.1, 21.6, 20.3, 20.0, 17.9, 16.2. HRMS (ESI⁺): *m/z*: calculated for C₃₃H₄₂N₂NaO₆S₂ [M+Na]⁺: 649.2380; found: 649.2372.

General procedure H for the synthesis of racemic products



To determine the enantiopurity of the products by chiral HPLC, 1,5-enynes **1.114b-o** bearing *N*-methylmethanesulfonamide as chiral auxiliary were prepared to access the ketones **1.118b-o** as racemic mixtures. For this purpose, the previously described experimental procedures were reproduced starting from precursor **1.187** with **X₇** or introducing the achiral sulfonamide moiety by copper-catalyzed reaction from the corresponding bromoalkynes.

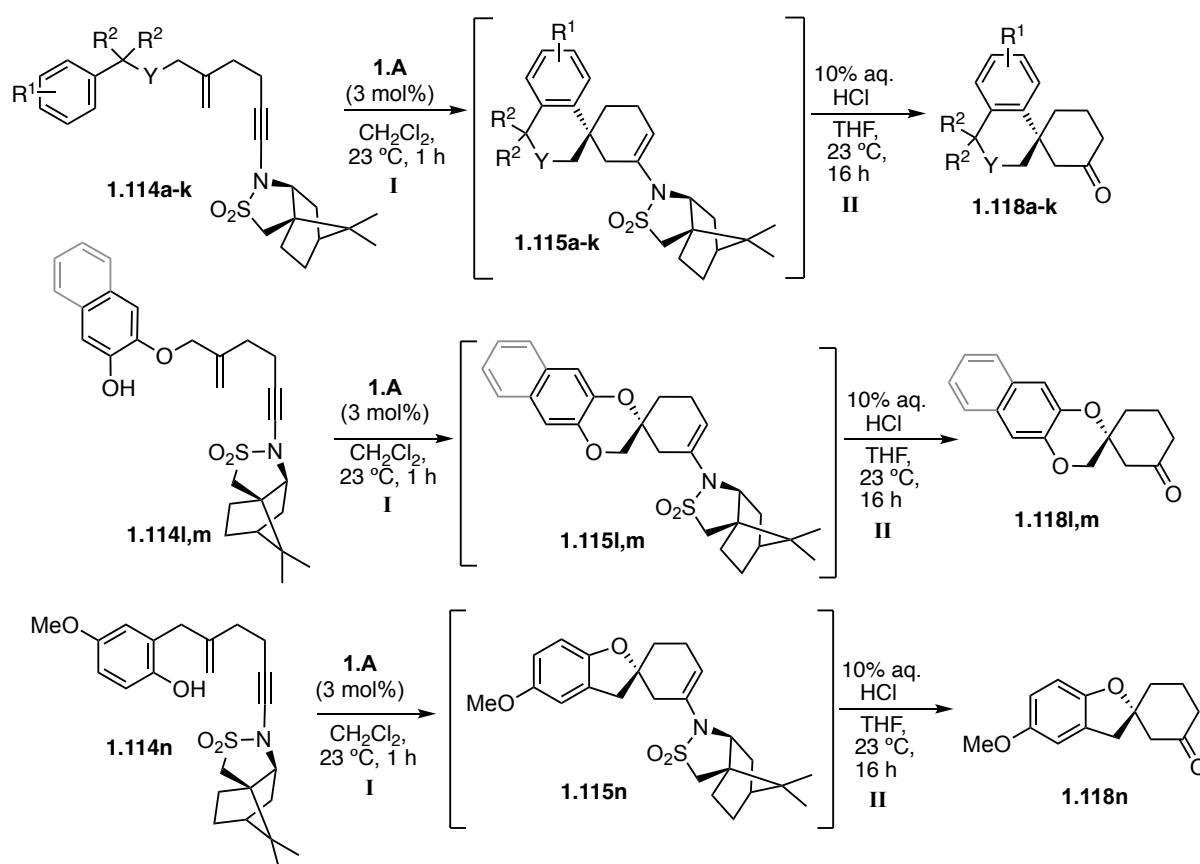
***N*-(5-(Chloromethyl)hex-5-en-1-yn-1-yl)-*N*-methylmethanesulfonamide (1.187)⁵⁶**



Copper sulphate pentahydrate (48.1 mg, 0.193 mmol), 1,10-phenanthroline hydrate (76 mg, 0.386 mmol), potassium carbonate (533 mg, 3.86 mmol) and *N*-methylmethanesulfonamide (0.195 mL, 2.12 mmol) were placed under inert atmosphere. Then, toluene (2 mL) and a solution of 6-bromo-2-(chloromethyl)hex-1-en-5-yne (400 mg, 1.93 mmol) in toluene (3 mL) were sequentially added. After stirring at 80 °C for 16

hours, the mixture was passed through Celite pad and concentrated under reduced pressure. The resulting residue was purified by column chromatography on silica gel (15-20% EtOAc/cyclohexane) to give **1.187** (302 mg, 1.28 mmol, 67%) as slightly yellow oil. $^1\text{H NMR}$ (500 MHz, CDCl_3) δ 5.20 (q, $J = 0.9$ Hz, 1H), 5.06 – 5.01 (m, 1H), 4.07 (q, $J = 0.9$ Hz, 2H), 3.16 – 3.12 (m, 3H), 3.04 – 3.00 (m, 3H), 2.49 (tq, $J = 6.9, 1.2$ Hz, 2H), 2.44 – 2.37 (m, 2H); $^{13}\text{C NMR}$ (126 MHz, CDCl_3) δ 143.7, 115.8, 75.2, 68.2, 48.1, 39.3, 36.2, 32.4, 17.2. **HRMS** (ESI $^+$): m/z : calculated for $\text{C}_9\text{H}_{14}\text{NCINaO}_2\text{S}$: 258.0326 $[\text{M}+\text{Na}]^+$; found: 258.0325.

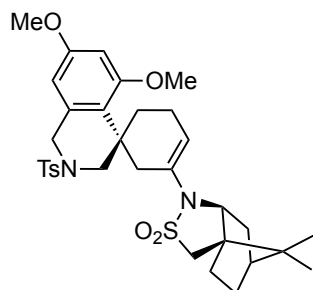
General procedure I for the gold(I)-catalyzed cyclization of 1,5-enynes 1.114a-n followed by hydrolysis.



To a solution of the corresponding 1,5-enyne in CH_2Cl_2 (2 mL, 0.05 M) under argon atmosphere, catalyst **1.A** (3 mol%) was added and the mixture was stirred for 1 hour at room temperature. After that time, few drops of triethylamine were added, and the solvent was removed under reduced pressure. The products of type **1.115** were subjected to the next step without further purification (in the case of **1.115l-n**, the *dr* of the enamine intermediate was measured before proceeding with the next step). The crude was dissolved in THF (3 mL) and treated with 10% aqueous HCl (1.5 mL) at room temperature overnight. Then, the mixture was poured into water and extracted with CH_2Cl_2 (3 x 10 mL). The combined organic extracts were washed with brine, dried over Na_2SO_4 , filtered, and concentrated under reduced pressure. The crude was purified by flash column chromatography on silica gel to afford, after

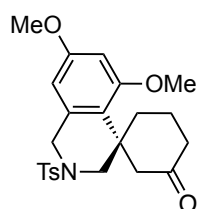
concentration and high-vacuum drying, the corresponding ketones in the reported yields. In cases where the chiral auxiliary was difficult to separate from the desired product, the crude was treated with 5% NaOH solution and extracted with Et₂O.

(3a*R*,6*R*,7a*S*)-1-((*S*)-5',7'-Dimethoxy-2'-tosyl-2',3'-dihydro-1'*H*-spiro[cyclohexane-1,4'-isoquinolin]-3-en-3-yl)-8,8-dimethylhexahydro-3*H*-3a,6-methanobenzo[*c*]isothiazole 2,2-dioxide (1.115a)

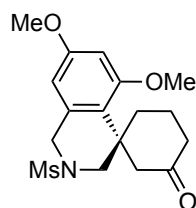


Following the general procedure, the intermediate polycyclic compound **1.115a** was isolated by column chromatography on silica gel (10% EtOAc/cyclohexane) as a white solid (63.0 mg, 0.100 mmol, 94%). **M.p.** 192-194 °C; **¹H NMR** (400 MHz, CDCl₃) δ 7.75 – 7.67 (m, 2H), 7.39 – 7.29 (m, 2H), 6.31 (d, *J* = 2.6 Hz, 1H), 6.11 (d, *J* = 2.5 Hz, 1H), 5.46 (dt, *J* = 5.0, 2.4 Hz, 1H), 4.11 – 3.94 (m, 2H), 3.78 (s, 3H), 3.73 (s, 3H), 3.51 (dd, *J* = 7.7, 4.5 Hz, 1H), 3.43 – 3.33 (m, 1H), 3.27 – 3.14 (m, 2H), 3.11 (d, *J* = 11.8 Hz, 1H), 3.01 (d, *J* = 11.9 Hz, 1H), 2.63 (ddd, *J* = 13.4, 11.5, 6.6 Hz, 1H), 2.43 (s, 3H), 2.26 – 2.15 (m, 1H), 2.10 (dt, *J* = 12.9, 3.3 Hz, 1H), 2.04 (d, *J* = 17.3 Hz, 1H), 1.95 – 1.85 (m, 3H), 1.70 (dd, *J* = 13.0, 7.8 Hz, 1H), 1.56 – 1.48 (m, 1H), 1.48 – 1.37 (m, 1H), 1.29 (dd, *J* = 17.1, 10.7 Hz, 2H), 1.17 (s, 3H), 0.93 (s, 3H); **¹³C NMR** (101 MHz, CDCl₃) δ 159.8, 159.0, 143.8, 134.4, 132.9, 131.1, 129.8, 128.1, 121.9, 117.7, 102.4, 98.7, 64.6, 55.4, 52.3, 50.8, 50.1, 49.4, 48.0, 44.7, 37.8, 36.1, 34.0, 32.4, 27.3, 27.1, 21.8, 21.7, 20.6, 20.2. **HRMS** (ESI⁺): *m/z*: calculated for C₃₃H₄₂N₂NaO₆S₂: 649.2376 [M+Na]⁺; found: 649.2391.

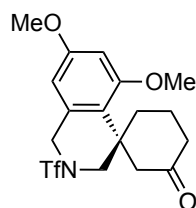
(*S*)-5',7'-Dimethoxy-2'-tosyl-2',3'-dihydro-1'*H*-spiro[cyclohexane-1,4'-isoquinolin]-3-one (1.118a)



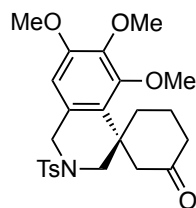
Following the general procedure, the ketone **1.118a** was isolated by column chromatography on silica gel (20% EtOAc/cyclohexane) as a white solid (44.1 mg, 0.103 mmol, 96% from **1.114a**) with 94:6 *er*. **M.p.** 163-165 °C; **¹H NMR** (400 MHz, CDCl₃) δ 7.74 – 7.68 (m, 2H), 7.38 – 7.32 (m, 2H), 6.31 (d, *J* = 2.5 Hz, 1H), 6.14 (d, *J* = 2.4 Hz, 1H), 4.51 (dd, *J* = 14.8, 1.7 Hz, 1H), 3.74 (s, 3H), 3.71 (s, 3H), 3.74 – 3.63 (m, 2H), 3.21 (d, *J* = 15.5 Hz, 1H), 2.43 (s, 3H), 2.39 (dd, *J* = 7.5, 5.9 Hz, 2H), 2.31 (dd, *J* = 11.9, 1.2 Hz, 1H), 2.20 (ddd, *J* = 14.5, 8.9, 5.6 Hz, 1H), 2.09 – 1.99 (m, 1H), 1.98 – 1.87 (m, 3H). **¹³C NMR** (101 MHz, CDCl₃) δ 210.9, 159.2, 158.8, 144.0, 133.7, 132.9, 130.0, 127.9, 121.6, 102.3, 98.3, 55.4, 54.5, 53.9, 49.2, 48.7, 40.8, 40.4, 31.9, 21.7, 20.9. **IR (selected frequency)**: 1708 cm⁻¹. **HRMS** (ESI⁺): *m/z*: calculated for C₂₃H₂₇NNaO₅S: 452.1502 [M+Na]⁺; found: 452.1511; **Chiral HPLC** (IA column, 90:10 Hex:*i*PrOH, 1.0 mL/min): 24.665 min (94), 39.697 min (6). **[α]_D²⁶** (*c* = 0.150 in CHCl₃) = -65.5 °.

(S)-5',7'-Dimethoxy-2'-(methylsulfonyl)-2',3'-dihydro-1'H-spiro[cyclohexane-1,4'-isoquinolin]-3-one (1.118b)

Following the general procedure, the ketone **1.118b** was isolated by column chromatography on silica gel (40% EtOAc/cyclohexane) as a white solid (41.7 mg, 0.118 mmol, 92%) with 84:16 *er*. **M.p.** 147-149 °C; **¹H NMR** (500 MHz, CDCl₃) δ 6.35 (d, *J* = 2.5 Hz, 1H), 6.19 (d, *J* = 2.5 Hz, 1H), 4.53 (dt, *J* = 14.8, 1.1 Hz, 1H), 4.14 (d, *J* = 14.7 Hz, 1H), 3.75 (d, *J* = 12.4 Hz, 6H), 3.61 (dd, *J* = 12.1, 1.7 Hz, 1H), 3.26 (dd, *J* = 15.4, 1.0 Hz, 1H), 2.87 (s, 3H), 2.75 (dd, *J* = 12.1, 1.1 Hz, 1H), 2.43 – 2.35 (m, 2H), 2.28 – 2.21 (m, 1H), 2.08 – 2.02 (m, 1H), 1.95 – 1.86 (m, 3H); **¹³C NMR** (126 MHz, CDCl₃) δ 210.9, 159.4, 159.0, 133.6, 121.4, 102.4, 98.5, 55.4, 54.6, 53.7, 49.0, 48.6, 40.9, 40.4, 35.0, 31.7, 20.9; **HRMS** (ESI⁺): *m/z*: calculated for C₁₇H₂₃NNaO₅S: 376.1189 [M+Na]⁺; found: 376.1181; **Chiral HPLC** (IA column, 90:10 Hex:*i*PrOH, 1.0 mL/min): 40.300 min (84), 67.707 min (16); [α]_D²⁶ (*c* = 0.150 in CHCl₃) = -43.8 °.

(S)-5',7'-Dimethoxy-2'-((trifluoromethyl)sulfonyl)-2',3'-dihydro-1'H-spiro[cyclohexane-1,4'-isoquinolin]-3-one (1.118c)

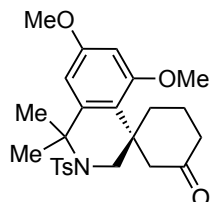
Following the general procedure, the ketone **1.118c** was isolated by column chromatography on silica gel (40% EtOAc/cyclohexane) as a white solid (54.9 mg, 0.135 mmol, 89%) with 84:16 *er*. **M.p.** 59-61 °C; **¹H NMR** (500 MHz, CDCl₃) δ 6.37 (d, *J* = 2.5 Hz, 1H), 6.20 – 6.16 (m, 1H), 4.72 (d, *J* = 15.6 Hz, 1H), 4.45 (d, *J* = 15.6 Hz, 1H), 3.86 – 3.78 (m, 1H), 3.77 (s, 3H), 3.72 (s, 3H), 3.17 (dd, *J* = 15.8, 1.1 Hz, 1H), 3.13 – 3.02 (m, 1H), 2.47 – 2.32 (m, 2H), 2.18 (br. s, 1H), 2.02 (d, *J* = 15.8 Hz, 1H), 1.94 – 1.84 (m, 3H); **¹³C NMR** (126 MHz, CDCl₃) δ 209.7, 159.6, 158.9, 132.3, 121.0, 120.4 (q, *J* = 324.2 Hz), 101.9, 98.8, 55.5, 54.5, 54.2, 48.8, 48.1, 40.1, 40.1, 31.9, 20.6; **¹⁹F NMR** (471 MHz, CDCl₃) δ -74.3; **HRMS** (ESI⁺): *m/z*: calculated for C₁₇H₂₀F₃NNaO₅S: 430.0906 [M+Na]⁺; found: 430.0902; **Chiral HPLC** (IA column, 90:10 Hex:*i*PrOH, 1.0 mL/min): 8.630 min (84), 11.292 min (16); [α]_D²⁶ (*c* = 0.155 in CHCl₃) = -55.6 °.

(S)-5',6',7'-Trimethoxy-2'-tosyl-2',3'-dihydro-1'H-spiro[cyclohexane-1,4'-isoquinolin]-3-one (1.118d)

Following the general procedure, the ketone **1.118d** was isolated by column chromatography on silica gel (50% EtOAc/cyclohexane) as a white solid (39.3 mg, 0.086 mmol, 90%) with 87:13 *er*. **M.p.** 153-155 °C; **¹H NMR** (500 MHz, CDCl₃) δ 7.72 – 7.67 (m, 2H), 7.35 (d, *J* = 1.4 Hz, 1H), 6.29 (s, 1H), 4.47 (ddd, *J* = 14.4, 1.7, 0.8 Hz, 1H), 3.88 (s, 3H), 3.79 (s, 3H), 3.77 (s, 3H), 3.68 (dd, *J* = 14.4, 1.0 Hz, 1H), 3.64 (dd, *J* = 12.0, 1.7 Hz, 1H), 3.36 (dd, *J* = 15.2, 0.8 Hz, 1H), 2.43 (s, 3H), 2.41 (dd, *J* = 5.4, 2.5 Hz, 2H), 2.31 (dd, *J* = 11.9, 1.1 Hz, 1H), 2.15 (td, *J* = 9.9, 5.2 Hz, 1H), 2.09 – 1.89 (m, 4H); **¹³C NMR** (126

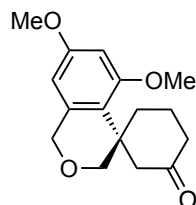
MHz, CDCl₃) δ 210.5, 152.9, 152.7, 144.1, 141.2, 132.7, 130.0, 127.9, 127.2, 125.6, 104.8, 60.7, 60.6, 56.0, 53.1, 49.0, 48.8, 41.8, 40.6, 32.7, 21.7, 21.0; **HRMS** (ESI⁺): m/z : calculated for C₂₄H₂₉NNaO₆S: 482.1608 [M+Na]⁺; found: 482.1618; **Chiral HPLC** (IA column, 93:7 Hex:*i*PrOH, 1.0 mL/min): 32.586 min (87), 34.772 min (13); $[\alpha]_D^{26}$ ($c = 0.180$ in CHCl₃) = -48.5 °.

(S)-5',7'-Dimethoxy-1',1'-dimethyl-2'-tosyl-2',3'-dihydro-1'H-spiro[cyclohexane-1,4'-isoquinolin]-3-one (1.118e)



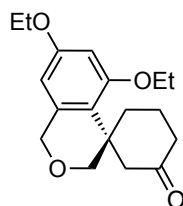
Following the general procedure, the ketone **1.118e** was isolated by column chromatography on silica gel (20-40% EtOAc/cyclohexane) as a white solid (36.5 mg, 0.080 mmol, 87%) with 91:9 *er*. **M.p.** 75-77 °C; **¹H NMR** (500 MHz, CDCl₃) δ 7.82 – 7.76 (m, 2H), 7.33 – 7.27 (m, 2H), 6.31 (dd, $J = 17.2, 2.4$ Hz, 2H), 3.77 (s, 3H), 3.65 (s, 3H), 3.60 (d, $J = 13.1$ Hz, 1H), 2.97 (d, $J = 13.1$ Hz, 1H), 2.91 – 2.84 (m, 1H), 2.42 (s, 3H), 2.37 – 2.27 (m, 1H), 2.24 (dt, $J = 16.7, 5.5$ Hz, 1H), 2.01 – 1.91 (m, 2H), 1.93 (s, 3H), 1.66 (s, 3H), 1.72 – 1.50 (m, 3H); **¹³C NMR** (126 MHz, CDCl₃) δ 210.1, 159.1, 157.7, 146.4, 143.5, 138.7, 129.6, 128.0, 122.1, 103.4, 97.0, 63.1, 55.4, 54.2, 52.6, 48.8, 40.2, 40.0, 32.4, 31.9, 27.3, 21.7, 20.5; **HRMS** (ESI⁺): m/z : calculated for C₂₅H₃₁NNaO₅S: 480.1815 [M+Na]⁺; found: 480.1823; **Chiral HPLC** (IA column, 90:10 Hex:*i*PrOH, 1.0 mL/min): 18.072 min (91), 23.728 min (9); $[\alpha]_D^{26}$ ($c = 0.150$ in CHCl₃) = -69.6 °.

(S)-5',7'-Dimethoxyspiro[cyclohexane-1,4'-isochroman]-3-one (1.118f)



Following the general procedure, the ketone **1.118f** was isolated by column chromatography on silica gel (20% EtOAc/cyclohexane) as a white solid (20.0 mg, 0.072 mmol, 84%) with 95:5 *er*. **M.p.** 62-64 °C; **¹H NMR** (400 MHz, CDCl₃) δ 6.33 (d, $J = 2.5$ Hz, 1H), 6.11 (d, $J = 2.5$ Hz, 1H), 4.72 (s, 2H), 3.81 – 3.78 (m, 1H), 3.77 (s, 3H), 3.73 (s, 3H), 3.45 (dd, $J = 11.4, 0.9$ Hz, 1H), 2.97 (dd, $J = 15.6, 1.1$ Hz, 1H), 2.43 – 2.20 (m, 3H), 2.03 (d, $J = 15.7$ Hz, 1H), 1.96 – 1.77 (m, 1H); **¹³C NMR** (101 MHz, CDCl₃) δ 211.2, 159.2, 158.8, 136.7, 121.5, 100.1, 97.9, 74.9, 69.4, 55.4, 54.4, 47.1, 40.5, 38.2, 32.3, 21.0; **HRMS** (ESI⁺): m/z : calculated for C₁₆H₂₀NaO₄: 299.1254 [M+Na]⁺; found: 299.1256; **Chiral HPLC** (IA column, 98:2 Hex:*i*PrOH, 1.0 mL/min): 35.006 min (5), 36.828 min (95); $[\alpha]_D^{26}$ ($c = 0.125$ in CHCl₃) = -56.8 °.

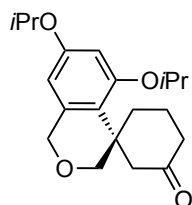
(S)-5',7'-Diethoxyspiro[cyclohexane-1,4'-isochroman]-3-one (1.118g)



Following the general procedure, the ketone **1.118g** was isolated by column chromatography on silica gel (10% EtOAc/cyclohexane) as a white solid (17.8 mg, 0.058 mmol, 75%) with 96:4 *er*. **M.p.** 71-73 °C; **¹H NMR** (500 MHz, CDCl₃) δ 6.33 (d, $J = 2.4$ Hz, 1H), 6.08 (d, $J = 2.2$ Hz, 1H), 4.73 – 4.63 (m, 2H), 4.04 (q, $J = 7.0$ Hz, 2H), 4.01 – 3.94 (m, 2H), 3.79 (d, $J = 11.6$ Hz, 1H), 3.47 (dd, $J = 11.6, 1.1$ Hz, 1H), 3.34 (d, $J = 15.4$ Hz, 1H), 2.49 – 2.35 (m, 3H), 2.14 – 2.07 (m, 1H), 2.02 – 1.92 (m, 1H), 1.90 – 1.76 (m, 2H), 1.44 (t, $J = 7.0$ Hz, 3H), 1.39 (t, $J = 7.0$ Hz, 3H); **¹³C NMR** (126 MHz, CDCl₃) δ 212.1, 158.4,

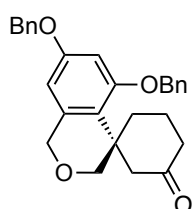
158.2, 136.9, 120.8, 100.5, 99.0, 74.3, 69.7, 63.6, 63.5, 47.4, 40.8, 38.9, 31.0, 21.3, 15.0, 14.8; **HRMS** (ESI+): m/z : calculated for $C_{18}H_{24}NaO_4$: 327.1567 $[M+Na]^+$; found: 327.1570; **Chiral HPLC** (IA column, 98:2 Hex:*i*PrOH, 1.0 mL/min): 26.841 min (96), 29.614 min (4); $[\alpha]_D^{26}$ ($c = 0.114$ in $CHCl_3$) = -59.2° .

(S)-5',7'-Diisopropoxyspiro[cyclohexane-1,4'-isochroman]-3-one (1.118h)



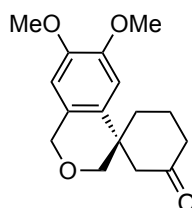
Following the general procedure, the ketone **1.118h** was isolated by column chromatography on silica gel (15% EtOAc/cyclohexane) as a white solid (19.9 mg, 0.060 mmol, 73%) with 95:5 *er*. **M.p.** 77-79 °C; **¹H NMR** (500 MHz, $CDCl_3$) δ 6.31 (d, $J = 2.4$ Hz, 1H), 6.06 (d, $J = 2.4$ Hz, 1H), 4.71 – 4.62 (m, 2H), 4.64 – 4.57 (m, 1H), 4.47 (p, $J = 6.1$ Hz, 1H), 3.78 (d, $J = 11.6$ Hz, 1H), 3.50 – 3.47 (m, 1H), 3.47 – 3.44 (m, 1H), 2.54 – 2.44 (m, 1H), 2.38 (dd, $J = 8.8, 4.8$ Hz, 2H), 2.11 (d, $J = 15.2$ Hz, 1H), 2.02 – 1.93 (m, 1H), 1.88 – 1.75 (m, 2H), 1.40 (d, $J = 5.9$ Hz, 3H), 1.36 (d, $J = 6.1$ Hz, 3H), 1.33 (d, $J = 1.9$ Hz, 3H), 1.31 (d, $J = 1.8$ Hz, 3H); **¹³C NMR** (126 MHz, $CDCl_3$) δ 212.5, 157.3, 157.1, 137.1, 120.7, 101.5, 100.5, 74.0, 69.9, 69.8, 69.6, 47.5, 41.0, 39.2, 30.5, 22.3, 22.3, 22.2, 21.9, 21.4; **HRMS** (ESI+): m/z : calculated for $C_{20}H_{29}O_4$: 333.2060 $[M+H]^+$; found: 333.2062; **Chiral HPLC** (IA column, 99.7:0.3 Hex:*i*PrOH, 1.0 mL/min): 52.165 min (5), 56.719 min (95); $[\alpha]_D^{26}$ ($c = 0.160$ in $CHCl_3$) = -41.3° .

(S)-5',7'-Bis(benzyloxy)spiro[cyclohexane-1,4'-isochroman]-3-one (1.118i)



Following the general procedure, the ketone **1.118i** was isolated by column chromatography on silica gel (10-15% EtOAc/cyclohexane) as a white solid (22.8 mg, 0.053 mmol, 78%) with 96:4 *er*. **M.p.** 96-98 °C; **¹H NMR** (500 MHz, $CDCl_3$) δ 7.45 – 7.28 (m, 10H), 6.49 (d, $J = 2.4$ Hz, 1H), 6.22 (d, $J = 2.4$ Hz, 1H), 5.04 (s, 2H), 4.98 (s, 2H), 4.69 (d, $J = 2.3$ Hz, 2H), 3.78 (d, $J = 11.6$ Hz, 1H), 3.49 (dd, $J = 11.6, 1.0$ Hz, 1H), 3.37 (dd, $J = 15.1, 1.0$ Hz, 1H), 2.48 (td, $J = 12.7, 3.7$ Hz, 1H), 2.29 – 2.21 (m, 1H), 2.15 – 2.10 (m, 1H), 2.12 – 2.04 (m, 1H), 1.94 – 1.70 (m, 3H); **¹³C NMR** (126 MHz, $CDCl_3$) δ 211.8, 158.3, 158.3, 137.2, 136.8, 136.6, 128.9, 128.8, 128.4, 128.3, 127.8, 127.7, 121.2, 101.6, 99.8, 74.2, 70.4, 70.3, 69.7, 47.3, 40.6, 39.3, 30.9, 21.4; **HRMS** (ESI+): m/z : calculated for $C_{28}H_{29}O_4$: 429.2060 $[M+H]^+$; found: 429.2062; **Chiral HPLC** (IA column, 95:5 Hex:*i*PrOH, 1.0 mL/min): 35.577 min (4), 43.211 min (96); $[\alpha]_D^{26}$ ($c = 0.150$ in $CHCl_3$) = -30.8° .

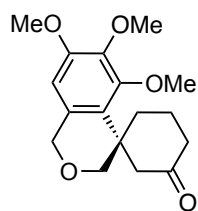
(S)-6',7'-Dimethoxyspiro[cyclohexane-1,4'-isochroman]-3-one (1.118j)



Following the general procedure, the ketone **1.118j** was isolated by column chromatography on silica gel (30% EtOAc/cyclohexane) as a white solid (16.5 mg, 0.060 mmol, 73%) with 93:7 *er*. **M.p.** 55-57 °C; **¹H NMR** (500 MHz, $CDCl_3$) δ 6.77 (s, 1H), 6.46 (s, 1H), 4.73 (s, 2H), 3.87 (s, 3H), 3.84 (s, 3H), 3.74 (d, $J = 11.5$ Hz, 1H), 3.59 (d, $J = 11.5$ Hz, 1H), 2.65 (d, $J = 14.3$ Hz, 1H), 2.52 – 2.37 (m, 3H), 2.13 – 1.94 (m, 3H), 1.89 (dtt, $J = 17.9, 11.3, 5.4$ Hz, 1H). **¹³C NMR** (126 MHz, $CDCl_3$) δ 211.0, 148.1, 148.1, 132.2, 126.3, 108.9, 107.1, 72.2, 68.6, 56.3, 56.0, 50.1, 41.2, 40.8, 34.6, 21.8; **HRMS** (ESI+):

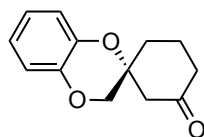
m/z : calculated for $C_{16}H_{20}NaO_4$: 299.1254 $[M+Na]^+$; found: 299.1258; **Chiral HPLC** (IA column, 95:5 Hex:*i*PrOH, 1.0 mL/min): 31.621 min (7), 36.930 min (93); $[\alpha]_D^{26}$ ($c = 0.160$ in $CHCl_3$) = -8.3° .

(S)-5',6',7'-Trimethoxyspiro[cyclohexane-1,4'-isochroman]-3-one (1.118k)



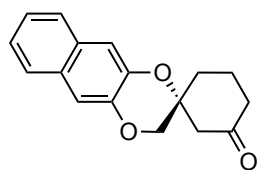
Following the general procedure, the ketone **1.118k** was isolated by column chromatography on silica gel (20% EtOAc/cyclohexane) as a colorless oil (25.2 mg, 0.082 mmol, 83%) with 95:5 *er.* **¹H NMR** (500 MHz, $CDCl_3$) δ 6.25 (s, 1H), 4.69 (d, $J = 0.9$ Hz, 2H), 3.90 (s, 3H), 3.81 (s, 3H), 3.80 (s, 3H), 3.75 (d, $J = 11.5$ Hz, 1H), 3.47 (dd, $J = 11.6, 0.8$ Hz, 1H), 3.05 (dd, $J = 15.5, 1.2$ Hz, 1H), 2.50 – 2.39 (m, 1H), 2.39 – 2.32 (m, 1H), 2.23 (ddd, $J = 13.7, 10.7, 3.5$ Hz, 1H), 2.11 (dt, $J = 15.4, 1.2$ Hz, 1H), 1.98 – 1.77 (m, 2H). **¹³C NMR** (126 MHz, $CDCl_3$) δ 210.6, 152.8, 152.6, 140.8, 130.1, 125.5, 102.5, 74.3, 69.2, 60.7, 60.4, 56.0, 47.4, 40.7, 39.0, 32.9, 21.0; **HRMS** (ESI+): m/z : calculated for $C_{17}H_{23}O_5$: 307.1540 $[M+Na]^+$; found: 307.1543; **Chiral HPLC** (IA column, 98:2 Hex:*i*PrOH, 1.0 mL/min): 25.421 min (5), 27.821 min (95); $[\alpha]_D^{26}$ ($c = 0.226$ in $CHCl_3$) = -42.5° .

(R)-3H-Spiro[benzo[b][1,4]dioxine-2,1'-cyclohexan]-3'-one (1.118l)

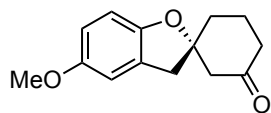


Following the general procedure, the ketone **1.118l** was isolated by column chromatography on silica gel (15% EtOAc/cyclohexane) as a white solid (28.3 mg, 0.130 mmol, 74%) with 68:32 *er.* **M.p.** 77-78 $^\circ C$; **¹H NMR** (500 MHz, $CDCl_3$) δ 6.90 – 6.81 (m, 4H), 4.00 (d, $J = 11.2$ Hz, 1H), 3.91 (d, $J = 11.2$ Hz, 1H), 2.63 (dt, $J = 14.7, 2.1$ Hz, 1H), 2.56 – 2.47 (m, 1H), 2.43 (dt, $J = 14.7, 0.9$ Hz, 1H), 2.42 – 2.33 (m, 1H), 2.19 – 2.06 (m, 2H), 1.97 – 1.87 (m, 1H), 1.85 – 1.75 (m, 1H). **¹³C NMR** (126 MHz, $CDCl_3$) δ 207.5, 142.3, 141.5, 122.2, 121.6, 117.9, 117.1, 76.4, 70.4, 47.6, 41.0, 30.2, 20.1; **HRMS** (ESI+): m/z : calculated for $C_{13}H_{14}NaO_3$: 241.0835 $[M+Na]^+$; found: 214.0838; **Chiral HPLC** (IA column, 99.5:0.5 Hex:*i*PrOH, 1.0 mL/min): 38.477 min (68), 41.709 min (32). $[\alpha]_D^{26}$ ($c = 0.290$ in $CHCl_3$) = 0.8° .

(R)-3'H-Spiro[cyclohexane-1,2'-naphtho[2,3-b][1,4]dioxin]-3-one (1.118m)



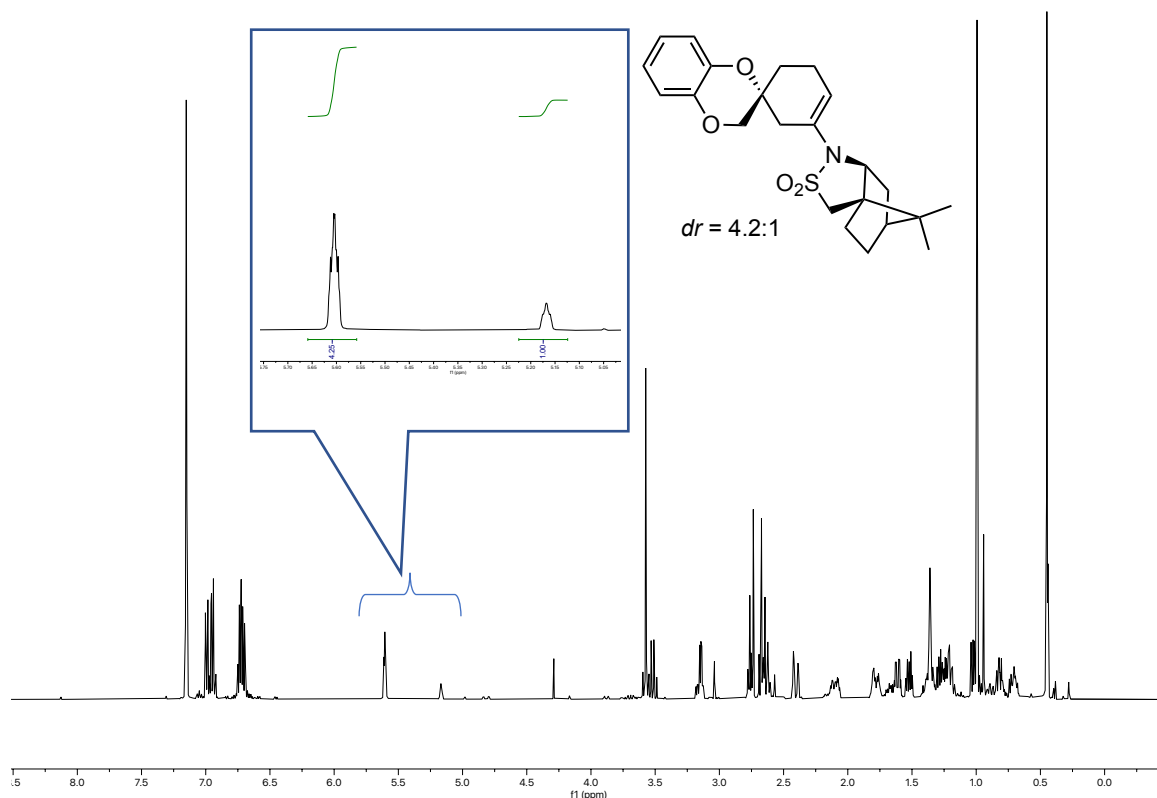
Following the general procedure, the ketone **1.118m** was isolated by column chromatography on silica gel (15-20% EtOAc/cyclohexane) as a white solid (40.7 mg, 0.152 mmol, 63%) with 54:46 *er.* **M.p.** 140-142 $^\circ C$; **¹H NMR** (500 MHz, $CDCl_3$) δ 7.64 (ddt, $J = 9.8, 7.0, 3.5$ Hz, 2H), 7.33 – 7.26 (m, 2H), 7.25 (s, 1H), 4.11 (d, $J = 11.2$ Hz, 1H), 4.03 (d, $J = 11.2$ Hz, 1H), 2.69 (dt, $J = 14.7, 2.1$ Hz, 1H), 2.55 (dddd, $J = 14.8, 6.1, 4.3, 2.2$ Hz, 1H), 2.49 (d, $J = 14.7$ Hz, 1H), 2.40 (dddd, $J = 14.9, 11.2, 6.2, 1.0$ Hz, 1H), 2.22 – 2.11 (m, 2H), 1.94 (dddd, $J = 13.4, 10.6, 6.8, 3.9$ Hz, 1H), 1.89 – 1.82 (m, 1H); **¹³C NMR** (126 MHz, $CDCl_3$) δ 207.3, 142.6, 141.8, 130.0, 129.7, 126.6, 126.6, 124.5, 124.5, 113.4, 112.5, 70.5, 47.7, 41.0, 30.4, 20.1; **HRMS** (ESI+): m/z : calculated for $C_{17}H_{16}NaO_3$: 291.0992 $[M+Na]^+$; found: 291.0992; **Chiral HPLC** (IA column, 99:1 Hex:*i*PrOH, 1.0 mL/min): 58.719 min (54), 66.967 min (46). $[\alpha]_D^{26}$ ($c = 0.175$ in $CHCl_3$) = 8.7°

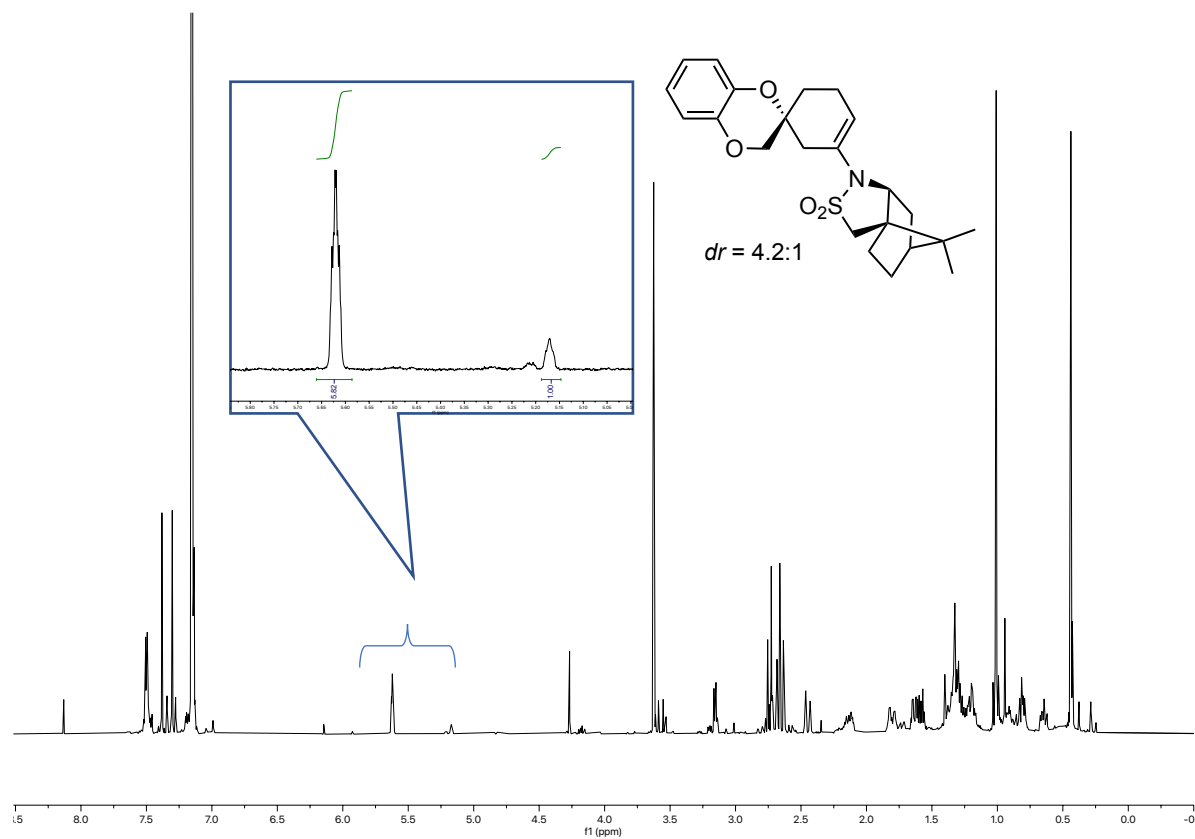
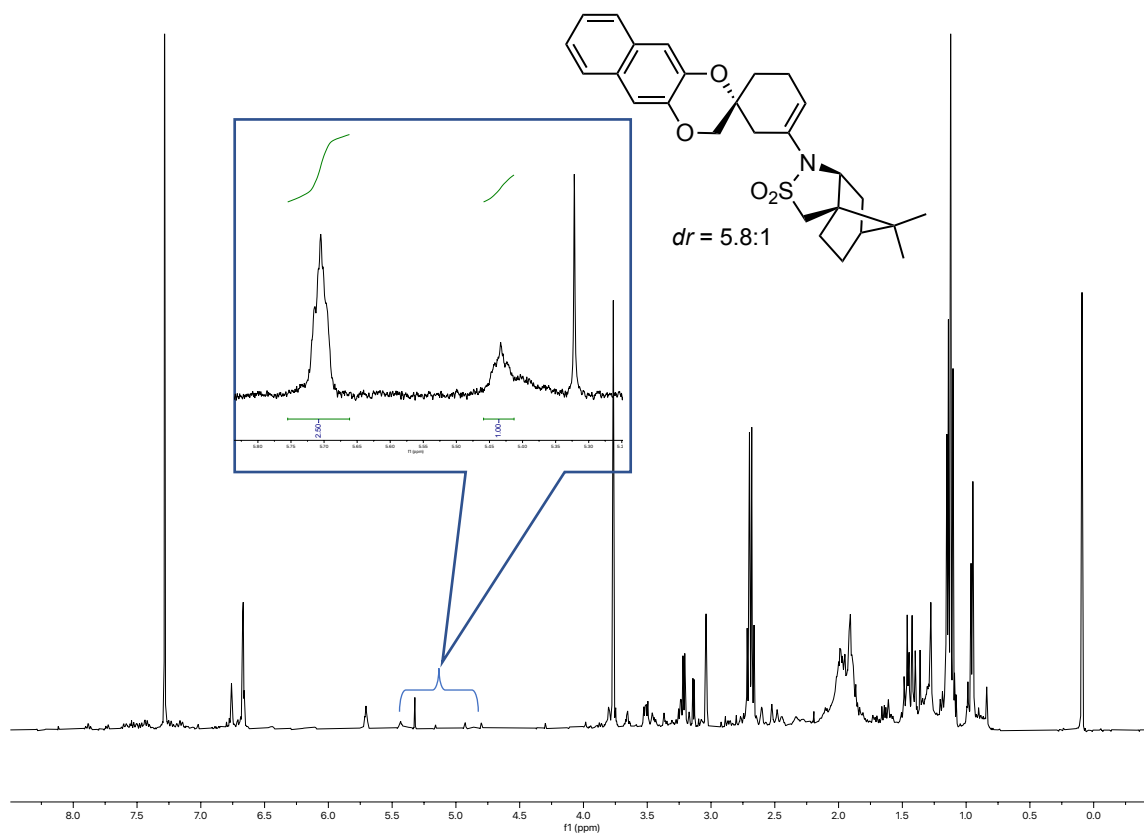
(S)-5-Methoxy-3H-spiro[benzofuran-2,1'-cyclohexan]-3'-one (1.118n)

Following the general procedure, the ketone **1.118n** was isolated by column chromatography on silica gel (30% Et₂O/pentane) as a brownish solid (31.7 mg, 0.136 mmol, 58%) with 57:43 *er*. **M.p.** 80-82 °C; **¹H NMR** (500 MHz, CDCl₃) δ 6.72 (dd, *J* = 2.3, 1.1 Hz, 1H), 6.68 – 6.60 (m, 2H), 3.74 (s, 3H), 3.05 (d, *J* = 15.6 Hz, 1H), 2.97 (d, *J* = 15.6 Hz, 1H), 2.73 (dt, *J* = 14.2, 1.8 Hz, 1H), 2.56 (dt, *J* = 14.2, 1.2 Hz, 1H), 2.50 – 2.41 (m, 1H), 2.40 – 2.30 (m, 1H), 2.22 – 2.06 (m, 2H), 1.98 – 1.82 (m, 2H). **¹³C NMR** (126 MHz, CDCl₃) δ 208.4, 154.3, 152.5, 126.8, 113.3, 111.6, 109.9, 89.9, 56.2, 52.5, 41.8, 40.6, 35.7, 21.2; **HRMS** (ESI⁺): *m/z*: calculated for C₁₄H₁₆NaO₃: 255.0992 [M+Na]⁺; found: 255.0985; **Chiral HPLC** (IA column, 98:2 Hex:*i*PrOH, 1.0 mL/min): 21.940 min (57), 28.813 min (43). **[α]_D²⁶** (*c* = 0.05 in CHCl₃) = 29.3 °

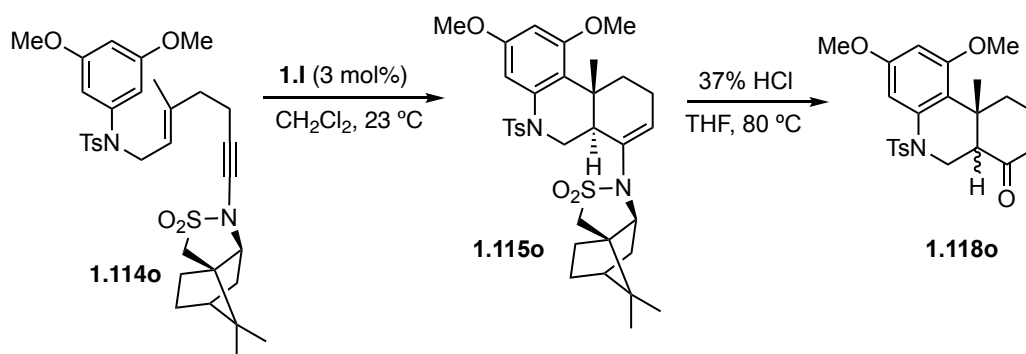
Experimental data for the racemisation under acidic conditions of enamines 1.118l-n

Crude **¹H NMR** of **1.115l**

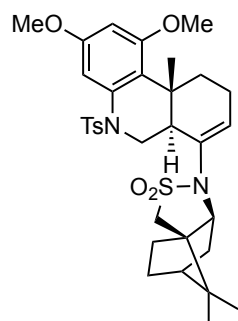


Crude ^1H NMR of **1.115m**Crude ^1H NMR of **1.115n**

Procedure J for the gold(I)-catalyzed cyclization of internal 1,5-enyne **1.114o** followed by hydrolysis.

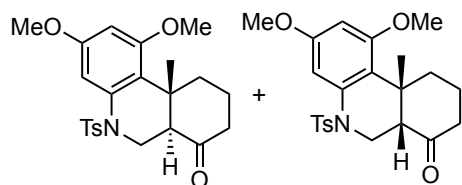


(3a*S*,6*R*,7a*S*)-1-((6a*R*,10a*R*)-1,3-Dimethoxy-10a-methyl-5-tosyl-5,6,6a,9,10,10a-hexahydrophenanthridin-7-yl)-8,8-dimethylhexahydro-3*H*-3a,6-methanobenzo[*c*]isothiazole 2,2-dioxide (1.115o)



To a solution of **1.115o** (50.3 mg, 0.080 mmol) in CH₂Cl₂ (1 mL) under argon atmosphere, catalyst **1.I** (3 mol%) was added and the mixture was stirred for 5 hours at 23 °C. After that time, few drops of triethylamine were added, the solvent was removed under reduced pressure and the crude was purified by column chromatography on silica gel (20% EtOAc/cyclohexane) to afford **1.115o** as a 89:11 mixture of diastereomers (39.4 mg, 0.062 mmol, 78%). ¹H NMR (500 MHz, CDCl₃) δ 7.75 – 7.69 (m, 2H), 7.25 – 7.20 (m, 2H), 6.93 (d, *J* = 2.5 Hz, 1H), 6.15 (d, *J* = 2.5 Hz, 1H), 5.72 – 5.68 (m, 1H), 4.79 (dd, *J* = 11.7, 4.5 Hz, 1H), 3.70 (d, *J* = 0.7 Hz, 6H), 3.52 (dd, *J* = 7.9, 5.1 Hz, 1H), 3.28 – 3.17 (m, 3H), 3.06 (ddd, *J* = 13.3, 5.4, 2.5 Hz, 1H), 2.74 – 2.67 (m, 1H), 2.36 (s, 3H), 2.27 – 2.21 (m, 2H), 1.96 – 1.84 (m, 4H), 1.79 – 1.72 (m, 1H), 1.69 (dd, *J* = 13.0, 7.8 Hz, 1H), 1.56 – 1.48 (m, 1H), 1.29 (s, 1H), 1.25 (s, 3H), 0.96 (s, 3H), 0.90 (s, 3H); ¹³C NMR (126 MHz, CDCl₃) δ 159.1, 158.3, 143.6, 137.9, 137.2, 130.4, 129.7, 127.5, 124.3, 118.5, 99.1, 95.5, 65.7, 55.5, 55.4, 49.7, 49.2, 47.8, 46.3, 44.4, 43.5, 36.5, 35.6, 32.6, 31.2, 27.1, 23.1, 21.7, 20.6, 20.3, 17.2. HRMS (ESI⁺): *m/z*: calculated for C₃₃H₄₂N₂NaO₆S₂ [M+Na]⁺: 649.2380; found: 649.2375.

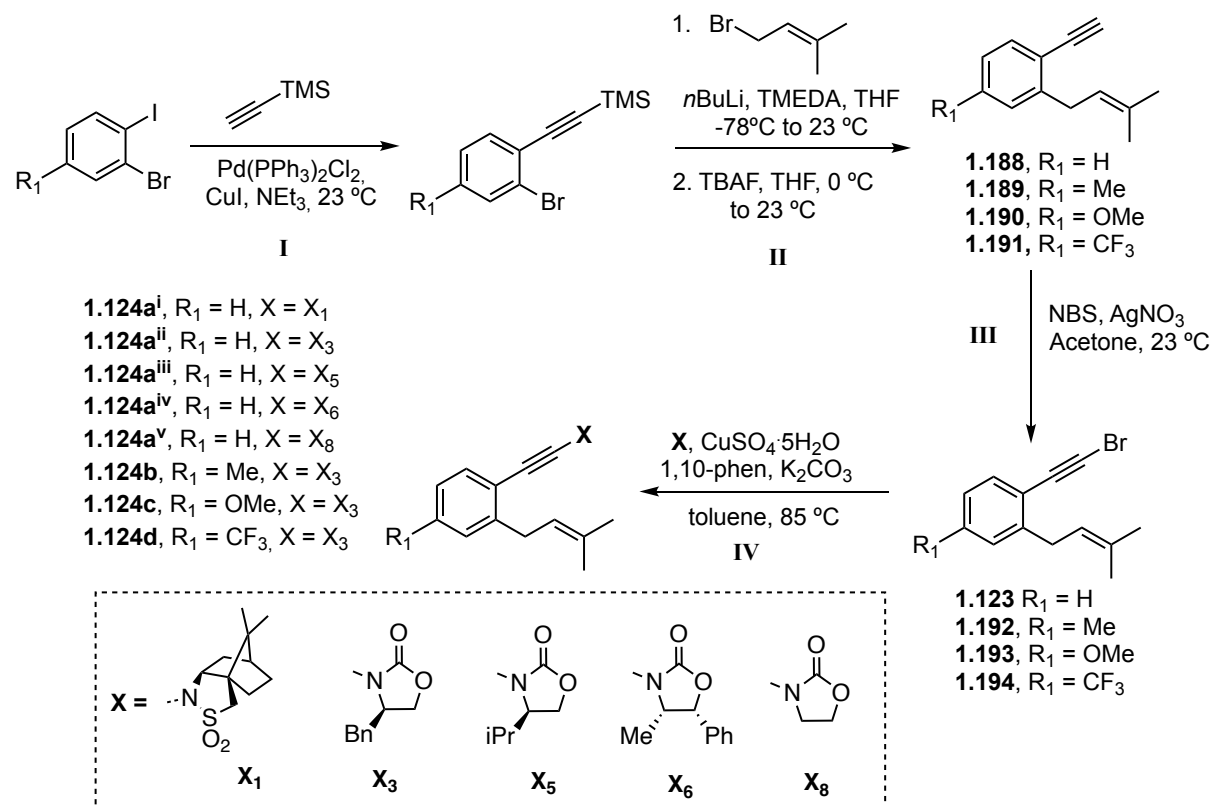
(10a*R*)-1,3-Dimethoxy-10a-methyl-5-tosyl-6,6a,8,9,10,10a-hexahydrophenanthridin-7(5*H*)-one (1.118o)



37% HCl (1.5 mL) was added to a solution of **1.115o** (33.0 mg, 0.053 mmol) in THF (3 mL) and the solution was left to stir at 80 °C overnight. Then, the mixture was poured into water and extracted with CH₂Cl₂ (3 x 10 mL). The combined organic extracts were washed with brine, dried over Na₂SO₄, filtered and concentrated under reduced pressure. The crude was purified by column chromatography on silica gel (20% EtOAc/cyclohexane) to afford **1.118o** as a 1.9:1 mixture of diastereomers, with 83:17 *er* (transparent oil, 18.2 mg, 0.044 mmol, 83%). ¹H NMR (500 MHz, CDCl₃) δ 7.61 – 7.51 (m, 3H, Md + md), 7.30 – 7.21 (m, 3H, Md + md), 7.09 – 7.02 (m, 1.5H, Md + md), 6.30 (s, 1.5H, Md + md), 4.39 (dd, *J* = 14.2, 2.7 Hz, 0.5H, md),

4.11 (dd, $J = 13.5, 3.5$ Hz, 1H, Md), 3.80 (s, 3H, Md), 3.80 (s, 1.5H, md), 3.76 (s, 1.5H, md), 3.75 (s, 3H, Md), 3.72 – 3.64 (m, 1.5H, Md + md), 3.23 (dd, $J = 14.2, 11.6$ Hz, 0.5H, md), 3.00 (d, $J = 13.6$ Hz, 0.5H, md), 2.40 (s, 1.5H, md), 2.37 (s, 3H, Md), 2.29 (m, $J = 9.7, 5.0$ Hz, 2.5H, Md + md), 2.27 – 2.21 (m, 1H, Md), 2.17 – 2.11 (m, 1H, md), 2.10 – 2.06 (m, 1H, Md), 2.06 – 1.98 (m, 0.5H, md), 1.95 – 1.86 (m, 2H, Md), 1.70 (m, $J = 10.5, 8.4, 4.3$ Hz, 2H, Md + md), 0.97 (s, 1.5H md), 0.97 (s, 3H, Md). ^{13}C NMR (126 MHz, CDCl_3) δ 210.4 (Md), 210.2 (md), 159.3 (md), 159.3 (Md), 158.5 (md), 158.5 (Md), 144.0 (Md), 144.0 (md), 137.6 (md), 137.5 (Md), 136.9 (md), 136.7 (Md), 129.8 (md), 129.8 (Md), 127.6 (Md), 127.4 (md), 118.8 (md), 118.1 (Md), 101.5 (md), 101.3 (Md), 97.7 (Md), 97.2 (md), 56.4 (Md), 55.6 (Md), 55.5 (md), 55.4 (md), 55.3 (Md), 54.2 (md), 45.0 (Md), 41.7 (md), 41.2 (md), 40.6 (md), 40.1 (Md), 39.3 (Md), 34.6 (md), 32.0 (Md), 29.8 (md), 24.4 (Md), 22.1 (md), 21.7 (Md), 21.0 (Md), 18.8 (md). **Chiral HPLC** (IA column, 90:10 Hex:*i*PrOH, 1.0 mL/min): 17.540 min (6), 19.537 min (28), 23.600 min (55), 24.526 min (11). **HRMS** (ESI⁺): m/z : calculated for $\text{C}_{23}\text{H}_{27}\text{NO}_5\text{S}$: 430.1683 $[\text{M}+\text{H}]^+$; found: 430.1700. $[\alpha]_{\text{D}}^{26}$ ($c = 0.175$ in CHCl_3) = -56.3°

General procedure **K** for the synthesis of 1,6-enynes **1.124a^{i-v}-d**

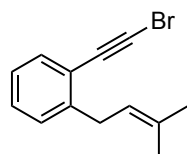


Compounds **1.188-1.191** were synthesized as shown in the scheme, according to literature procedure.^{97,98} All the spectral data were fully consistent with those previously reported.^{57a}

Step III: Compounds **1.123, 1.192-1.194** were synthesized by dissolving the precursors in acetone (0.05 M) and the resulting solutions were then treated with NBS (1.1 equiv) and AgNO₃ (0.2 equiv).⁴⁰ and left to stir for 2 h at 23 °C. After completeness, the reaction mixtures were poured into water, extracted with hexane (x2) and washed with brine. Finally, the organic phase was dried over anhydrous Na₂SO₄ and the solvent was evaporated under reduced pressure. The products were purified by flash column chromatography in pentane.

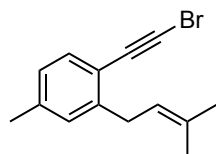
Step IV⁵⁶: Copper sulphate pentahydrate (0.1 equiv), 1,10-phenanthroline hydrate (0.2 equiv), potassium carbonate (2 equiv) and auxiliary **X** (1.2 equiv) were placed under inert atmosphere. Then, and a solution of **1.192-1.194** (1 equiv) in toluene (0.1 M) was added to the vial which was subsequently degassed. After stirring at 85 °C, over 72 h under a N₂ atmosphere, the mixture was passed through Celite pad and concentrated under reduced pressure. The resulting residue was purified by flash column chromatography to afford **1.124a^{i-v}-d**.

1-(Bromoethynyl)-2-(3-methylbut-2-en-1-yl)benzene (**1.123**)



Compound **1.123** was synthesized following the general procedure. After column chromatography (pentane), the product was isolated as a transparent oil (1.02 g, 4.09 mmol, 78%). ¹H NMR (500 MHz, C₆D₆) δ 7.35 (dd, *J* = 7.7, 1.4 Hz, 1H), 7.04 (ddd, *J* = 7.8, 1.4, 0.7 Hz, 1H), 6.98 (td, *J* = 7.5, 1.4 Hz, 1H), 6.82 (td, *J* = 7.5, 1.4 Hz, 1H), 5.30 (tdq, *J* = 7.3, 2.9, 1.5 Hz, 1H), 3.52 (s, 1H), 3.51 (s, 1H), 1.61 (d, *J* = 1.3 Hz, 3H), 1.58 (d, *J* = 1.4 Hz, 3H); ¹³C NMR (126 MHz, C₆D₆) δ 144.8, 133.1, 132.8, 129.1, 128.9, 126.1, 122.8, 122.6, 79.8, 53.4, 33.4, 25.8, 17.9. HRMS (APCI+): *m/z*: calculated for C₁₃H₁₄Br: 249.0273 [M+H]⁺; found: 249.0270.

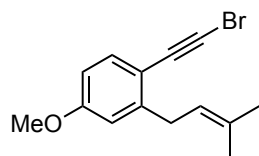
1-(Bromoethynyl)-4-methyl-2-(3-methylbut-2-en-1-yl)benzene (**1.192**)



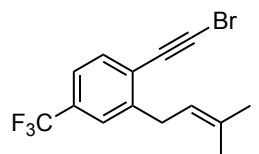
Compound **1.192** was synthesized following the general procedure. After column chromatography (pentane), the product was isolated as a transparent oil (984 mg, 3.74 mmol, 66%). ¹H NMR (400 MHz, CDCl₃) δ 7.40 – 7.33 (m, 1H), 7.04 (t, *J* = 2.1 Hz, 1H), 6.98 (d, *J* = 7.7 Hz, 1H), 5.33 (ddtq, *J* = 8.6, 5.6, 2.6, 1.4 Hz, 1H), 3.52 (d, *J* = 7.3 Hz, 2H), 2.36 (s, 3H), 1.84 – 1.78 (m, 6H); ¹³C NMR (101 MHz, CDCl₃) δ 144.4, 139.1, 132.8, 132.7, 129.4, 126.7, 122.5, 119.2, 79.4, 51.9, 33.1, 25.9, 21.6, 18.1. HRMS (APCI+): *m/z*: calculated for C₁₄H₁₄Br: 261.0273 [M-H]⁺; found: 261.0274.

⁹⁷ Hou, H.; Xu, Y.; Yang, H.; Chen, X.; Yan, C.; Shi, Y.; Zhu, S. Visible-Light Mediated Hydrosilylative and Hydrophosphorylative Cyclizations of Enynes and Dienes. *Org. Lett.* **2020**, *22*, 1748–1753.

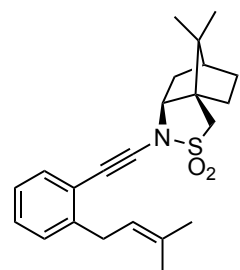
⁹⁸ In step II-2, previous deprotection instead of direct bromination of the TMS-alkynes (Nishikawa, T.; Shibuya, S.; Hosokawa, S.; Isobe, M. One Pot Synthesis of Haloacetylenes from Trimethylsilylacetylenes. *Synlett* **1994**, *1994*, 485–486.) afforded overall higher yields.

1-(Bromoethynyl)-4-methoxy-2-(3-methylbut-2-en-1-yl)benzene (1.193)

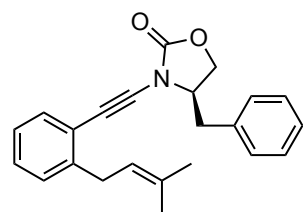
Compound **1.193** was synthesized following the general procedure. After column chromatography (pentane), the product was isolated as a transparent oil (402 mg, 2.14 mmol, 67%). $^1\text{H NMR}$ (400 MHz, CDCl_3) δ 7.38 (d, $J = 8.5$ Hz, 1H), 6.75 (d, $J = 2.7$ Hz, 1H), 6.69 (dd, $J = 8.5, 2.7$ Hz, 1H), 5.36 – 5.26 (m, 1H), 3.81 (s, 3H), 3.49 (d, $J = 7.4$ Hz, 2H), 1.79 (s, 3H), 1.77 (s, 3H); $^{13}\text{C NMR}$ (101 MHz, CDCl_3) δ 160.1, 146.4, 134.1, 133.3, 122.1, 114.5, 114.4, 111.1, 79.1, 55.3, 51.0, 33.2, 25.9, 18.1. **HRMS** (APCI+): m/z : calculated for $\text{C}_{14}\text{H}_{16}\text{BrO}$: 279.0379 $[\text{M}+\text{H}]^+$; found: 279.0368.

1-(Bromoethynyl)-2-(3-methylbut-2-en-1-yl)-4-(trifluoromethyl)benzene (1.194)

Compound **1.194** was synthesized following the general procedure. After column chromatography (pentane), the product was isolated as a transparent oil (290 mg, 2.41 mmol, 65%). $^1\text{H NMR}$ (400 MHz, CDCl_3) δ 7.52 (d, $J = 8.0$ Hz, 1H), 7.45 – 7.42 (m, 1H), 7.39 (dd, $J = 8.2, 1.9$ Hz, 1H), 5.27 (ddp, $J = 8.8, 5.8, 1.4$ Hz, 1H), 3.54 (d, $J = 7.3$ Hz, 2H), 1.78 (d, $J = 1.3$ Hz, 3H), 1.75 (s, 3H). $^{13}\text{C NMR}$ (101 MHz, CDCl_3) δ 145.4, 134.4, 133.1, 130.6 (q, $J = 32.3$ Hz), 125.9 (d, $J = 1.5$ Hz), 125.4 (q, $J = 3.7$ Hz), 122.7 (q, $J = 3.8$ Hz), 121.1, 78.1, 56.0, 33.0, 25.9, 18.1; $^{19}\text{F NMR}$ (376 MHz, CDCl_3) δ -62.92; **HRMS** (APCI+): m/z : calculated for $\text{C}_{14}\text{H}_{13}\text{BrF}_3$: 317.0147 $[\text{M}+\text{H}]^+$; found: 317.0146.

(3aR,6S,7aS)-8,8-Dimethyl-1-((2-(3-methylbut-2-en-1-yl)phenyl)ethynyl)hexahydro-3H-3a,6-methanobenzo[c]isothiazole 2,2-dioxide (1.124aⁱ)

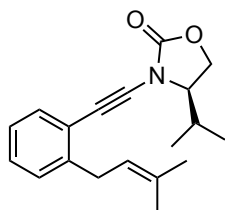
Compound **1.124aⁱ** was synthesized following the general procedure. After column chromatography (10:1 cyclohexane:EtOAc), the product was isolated as a white solid 200 mg, 0.521 mmol, 89%). **M.p.** 65-71 °C; $^1\text{H NMR}$ (400 MHz, CDCl_3) δ 7.40 (dd, $J = 7.7, 1.4$ Hz, 1H), 7.25 – 7.13 (m, 2H), 7.11 (td, $J = 7.3, 1.8$ Hz, 1H), 5.35 (tp, $J = 7.3, 1.4$ Hz, 1H), 3.69 (dd, $J = 8.1, 4.2$ Hz, 1H), 3.48 (d, $J = 7.3$ Hz, 2H), 3.29 (s, 2H), 2.30 (dtd, $J = 13.4, 4.0, 2.6$ Hz, 1H), 2.02 – 1.84 (m, 3H), 1.81 (dd, $J = 13.4, 8.2$ Hz, 1H), 1.74 (s, 3H), 1.71 (s, 3H), 1.52 – 1.41 (m, 1H), 1.39 – 1.30 (m, 1H), 1.16 (s, 3H), 0.96 (s, 3H); $^{13}\text{C NMR}$ (101 MHz, CDCl_3) δ 143.5, 133.0, 132.3, 128.3, 128.1, 125.7, 122.4, 122.1, 80.6, 71.7, 67.4, 51.4, 50.0, 48.1, 44.6, 34.6, 33.1, 31.8, 27.2, 25.9, 20.3, 20.1, 18.1. **HRMS** (ESI+): m/z : calculated for $\text{C}_{23}\text{H}_{29}\text{NNaO}_2\text{S}$: 406.1811 $[\text{M}+\text{Na}]^+$; found: 406.1810.

(R)-4-Benzyl-3-((2-(3-methylbut-2-en-1-yl)phenyl)ethynyl)oxazolidin-2-one (1.124aⁱⁱ)

Compound **1.124aⁱⁱ** was synthesized following the general procedure. After column chromatography (5:1 cyclohexane:EtOAc), the product was isolated as a brown solid (257 mg, 0.744 mmol, 60%). **M.p.** 38-42 °C; $^1\text{H NMR}$ (500 MHz, CDCl_3) δ 7.47 (dd, $J = 7.6, 1.4$ Hz, 1H), 7.38 – 7.33 (m, 2H), 7.32 – 7.28 (m, 1H), 7.27 – 7.21 (m, 4H), 7.17 (td, $J = 7.4, 1.6$ Hz, 1H), 5.39 (tdq, $J = 7.2, 2.9, 1.4$ Hz, 1H), 4.41 – 4.31 (m, 2H), 4.23 – 4.13 (m, 1H), 3.56 (d, $J = 7.2$ Hz,

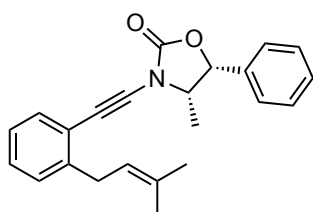
2H), 3.30 (dd, $J = 14.0, 3.4$ Hz, 1H), 3.08 – 2.99 (m, 1H), 1.75 (d, $J = 1.3$ Hz, 3H), 1.74 (s, 3H); ^{13}C NMR (126 MHz, CDCl_3) δ 155.5, 143.6, 134.3, 133.2, 132.4, 129.5, 129.2, 128.6, 128.5, 127.7, 125.9, 122.4, 121.7, 81.7, 72.3, 67.5, 58.8, 38.1, 33.2, 25.9, 18.1; HRMS (ESI+): m/z : calculated for $\text{C}_{23}\text{H}_{23}\text{NNaO}_2$: 368.1621 $[\text{M}+\text{Na}]^+$; found: 368.1616.

(*R*)-4-Isopropyl-3-((2-(3-methylbut-2-en-1-yl)phenyl)ethynyl)oxazolidin-2-one (1.124aⁱⁱⁱ)



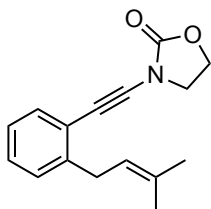
Compound **1.124aⁱⁱⁱ** was synthesized following the general procedure. After column chromatography (7:1 cyclohexane:EtOAc), the product was isolated as a transparent oil (213 mg, 0.716 mmol, 70%). ^1H NMR (400 MHz, CDCl_3) δ 7.46 – 7.39 (m, 1H), 7.26 – 7.16 (m, 2H), 7.16 – 7.10 (m, 1H), 5.33 (tdt, $J = 7.2, 2.9, 1.4$ Hz, 1H), 4.42 (t, $J = 8.9$ Hz, 1H), 4.20 (dd, $J = 9.0, 5.8$ Hz, 1H), 4.05 (ddd, $J = 8.8, 5.8, 4.1$ Hz, 1H), 3.50 (d, $J = 7.2$ Hz, 2H), 2.30 (hd, $J = 6.9, 4.1$ Hz, 1H), 1.74 (d, $J = 1.4$ Hz, 3H), 1.72 (s, 3H), 1.03 (d, $J = 5.0$ Hz, 3H), 1.02 (d, $J = 5.2$ Hz, 3H); ^{13}C NMR (101 MHz, CDCl_3) δ 156.0, 143.5, 133.0, 132.3, 128.5, 128.4, 125.8, 122.4, 121.8, 82.2, 71.3, 64.8, 62.2, 33.1, 29.4, 25.8, 18.0, 17.4, 15.2; HRMS (ESI+): m/z : calculated for $\text{C}_{19}\text{H}_{23}\text{NNaO}_2$: 320.1621 $[\text{M}+\text{Na}]^+$; found: 320.1620.

(4*S*,5*R*)-4-Methyl-3-((2-(3-methylbut-2-en-1-yl)phenyl)ethynyl)-5-phenyloxazolidin-2-one (1.124a^{iv})

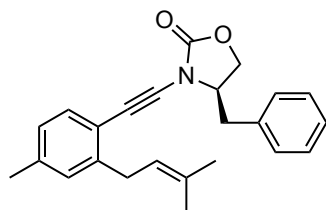


Compound **1.124a^{iv}** was synthesized following the general procedure. After column chromatography (5:1 cyclohexane:EtOAc), the product was isolated as a transparent oil (75.4 mg, 0.218 mmol, 73%). ^1H NMR (400 MHz, CDCl_3) δ 7.45 – 7.32 (m, 4H), 7.31 – 7.23 (m, 2H), 7.26 – 7.14 (m, 2H), 7.11 (td, $J = 7.4, 1.7$ Hz, 1H), 5.74 (d, $J = 8.0$ Hz, 1H), 5.31 (tp, $J = 7.2, 1.4$ Hz, 1H), 4.43 (dq, $J = 8.1, 6.6$ Hz, 1H), 3.49 (d, $J = 7.3$ Hz, 2H), 1.71 (d, $J = 1.4$ Hz, 3H), 1.69 (s, 3H), 0.99 (d, $J = 6.7$ Hz, 3H); ^{13}C NMR (101 MHz, CDCl_3) δ 155.3, 143.5, 134.0, 133.0, 132.3, 129.1, 128.8, 128.4, 128.4, 126.1, 125.8, 122.3, 121.7, 81.9, 79.8, 71.1, 58.4, 33.1, 25.8, 18.0, 15.0. HRMS (ESI+): m/z : calculated for $\text{C}_{23}\text{H}_{23}\text{NNaO}_2$: 368.1621 $[\text{M}+\text{Na}]^+$; found: 368.1610.

3-((2-(3-Methylbut-2-en-1-yl)phenyl)ethynyl)oxazolidin-2-one (1.124a^v)



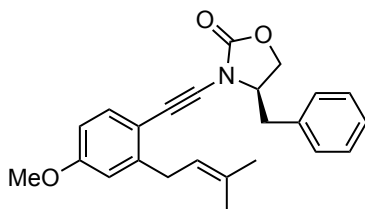
Compound **1.124a^v** was synthesized following the general procedure. After column chromatography (3:1 cyclohexane:EtOAc), the product was isolated as a transparent oil (147 mg, 0.576 mmol, 72%). ^1H NMR (400 MHz, CDCl_3) δ 7.41 (dt, $J = 7.6, 0.9$ Hz, 1H), 7.27 – 7.16 (m, 2H), 7.15 – 7.09 (m, 1H), 5.33 (tdt, $J = 7.3, 2.9, 1.4$ Hz, 1H), 4.50 – 4.41 (m, 2H), 4.02 – 3.93 (m, 2H), 3.50 (d, $J = 7.3$ Hz, 2H), 1.74 (d, $J = 1.1$ Hz, 3H), 1.72 (s, 3H); ^{13}C (101 MHz, CDCl_3) δ 155.9, 143.5, 133.0, 132.1, 128.4, 128.4, 125.7, 122.3, 121.5, 82.7, 70.1, 63.1, 47.1, 33.0, 25.8, 18.0; HRMS (ESI+): m/z : calculated for $\text{C}_{16}\text{H}_{18}\text{NO}_2$: 256.1332 $[\text{M}+\text{H}]^+$; found: 256.1331.

(R)-4-Benzyl-3-((4-methyl-2-(3-methylbut-2-en-1-yl)phenyl)ethynyl)oxazolidin-2-one (1.124b)

Compound **1.124b** was synthesized following the general procedure.

After column chromatography (5:1 cyclohexane:EtOAc), the product was isolated as a white solid (664 mg, 1.85 mmol, 67%). **M.p.** = 83-87 °C; **¹H NMR** (400 MHz, CDCl₃) δ 7.42 – 7.21 (m, 6H), 7.08 – 7.03 (m, 1H), 7.03 – 6.96 (m, 1H), 5.39 (dddt, *J* = 7.2, 5.7, 2.9, 1.4 Hz, 1H), 4.41

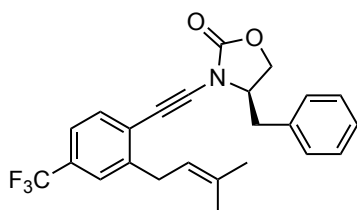
– 4.29 (m, 2H), 4.22 – 4.11 (m, 1H), 3.56 (d, *J* = 7.2 Hz, 2H), 3.33 – 3.24 (m, 1H), 3.08 – 2.98 (m, 1H), 2.36 (s, 3H), 1.76 (dt, *J* = 2.5, 1.2 Hz, 6H); **¹³C NMR** (101 MHz, CDCl₃) δ 155.4, 143.4, 138.6, 134.3, 132.8, 132.3, 129.4, 129.2, 129.0, 127.5, 126.6, 122.5, 118.5, 81.0, 72.1, 67.3, 58.5, 37.8, 33.1, 25.8, 21.5, 18.0; **HRMS** (ESI+): *m/z*: calculated for C₂₄H₂₆NO₂: 360.1958 [M+H]⁺; found: 360.1954.

(R)-4-Benzyl-3-((4-methoxy-2-(3-methylbut-2-en-1-yl)phenyl)ethynyl)oxazolidin-2-one (1.124c)

Compound **1.124c** was synthesized following the general procedure.

After column chromatography (5:1 cyclohexane:EtOAc), the product was isolated as a white solid (258 mg, 0.687 mmol, 69%). **M.p.** = 136-141 °C; **¹H NMR** (500 MHz, CDCl₃) δ 7.41 (d, *J* = 8.5 Hz, 1H), 7.38 – 7.32 (m, 2H), 7.31 – 7.27 (m, 1H), 7.25 – 7.22 (m, 2H), 6.76 (d, *J* =

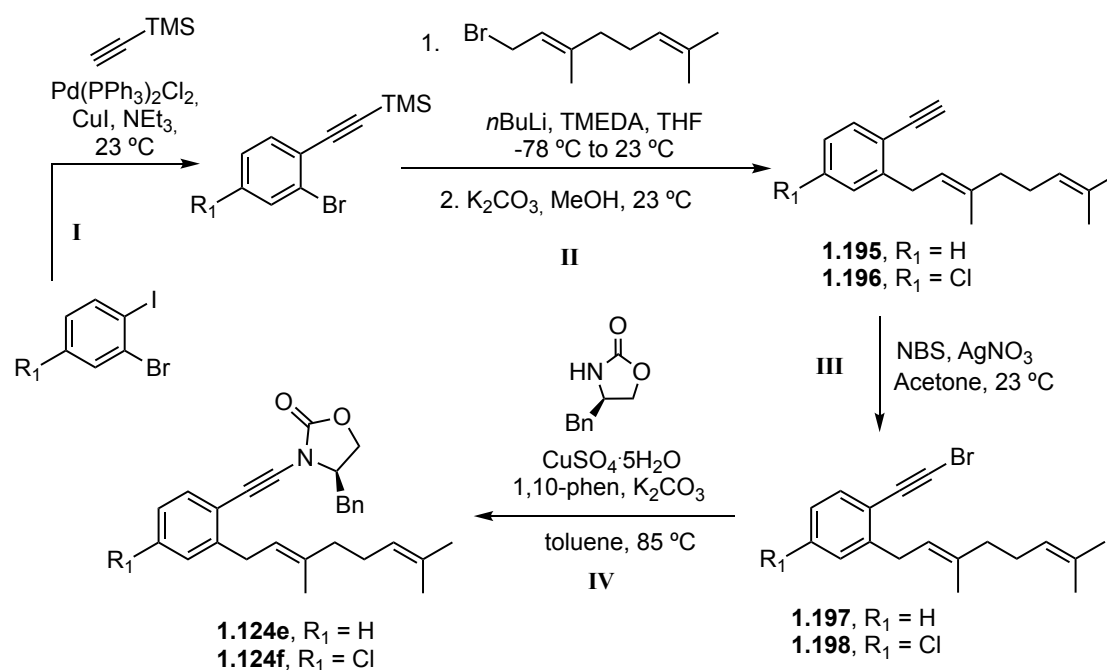
2.7 Hz, 1H), 6.71 (dd, *J* = 8.5, 2.7 Hz, 1H), 5.36 (ddq, *J* = 8.6, 5.8, 1.4 Hz, 1H), 4.39 – 4.28 (m, 2H), 4.20 – 4.13 (m, 1H), 3.81 (s, 3H), 3.53 (d, *J* = 7.2 Hz, 2H), 3.34 – 3.24 (m, 1H), 3.07 – 2.96 (m, 1H), 1.75 (d, *J* = 1.3 Hz, 3H), 1.72 (s, 3H); **¹³C NMR** (126 MHz, CDCl₃) δ 160.0, 155.6, 145.9, 134.4, 134.2, 133.4, 129.5, 129.1, 127.6, 122.1, 114.4, 113.8, 111.2, 80.3, 71.9, 67.4, 58.7, 55.3, 38.0, 33.3, 25.8, 18.1. **HRMS** (ESI+): *m/z*: calculated for C₂₄H₂₆NO₃: 376.1907 [M+H]⁺; found: 376.1908.

(R)-4-Benzyl-3-((2-(3-methylbut-2-en-1-yl)-4-(trifluoromethyl)phenyl)ethynyl)oxazolidin-2-one (1.124d)

Compound **1.124d** was synthesized following the general procedure.

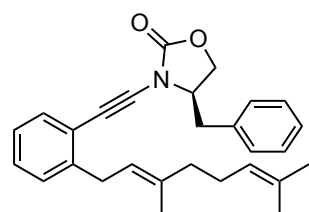
After column chromatography (5:1 cyclohexane:EtOAc), the product was isolated as a white solid (130 mg, 0.314 mmol, 34%). **M.p.** = 78-80 °C; **¹H NMR** (500 MHz, CDCl₃) δ 7.51 (d, *J* = 8.0 Hz, 1H), 7.46 (d, *J* = 1.9 Hz, 1H), 7.41 (dd, *J* = 8.1, 1.9 Hz, 1H), 7.39 – 7.34 (m, 2H),

7.33 – 7.29 (m, 1H), 7.27 – 7.23 (m, 2H), 5.36 (dddd, *J* = 7.2, 5.7, 2.9, 1.4 Hz, 1H), 4.46 – 4.35 (m, 2H), 4.25 – 4.15 (m, 1H), 3.58 (d, *J* = 7.2 Hz, 2H), 3.35 – 3.25 (m, 1H), 3.05 (ddd, *J* = 14.1, 6.2, 2.0 Hz, 1H), 1.77 (d, *J* = 1.3 Hz, 3H), 1.73 (s, 3H); **¹³C NMR** (126 MHz, CDCl₃) δ 155.2, 143.9, 134.4, 134.1, 132.0, 130.0 (q, *J* = 32.3 Hz), 129.4, 129.2, 127.7, 125.7, 125.2 (q, *J* = 4.0 Hz), 123.0, 122.6 (q, *J* = 3.8 Hz), 121.1, 84.3, 71.5, 67.7, 58.6, 38.2, 33.0, 25.8, 18.1; **¹⁹F NMR** (471 MHz, CDCl₃) δ -62.58; **HRMS** (ESI+): *m/z*: calculated for C₂₄H₂₃F₃NO₂: 414.1675 [M+H]⁺; found: 414.1681.

General procedure L for the synthesis of 1,6-enynes **1.124e-f**

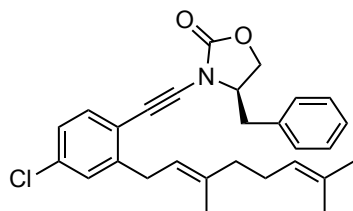
Compound **1.195** was synthesized as shown in the scheme, according to literature procedure and the spectral data were fully consistent with those previously reported.^{57a} Compound **1.196**, not reported before, was synthesized following the same route. Due to fast decomposition in silica of compounds **1.197-1.198**, step III and IV were performed without intermediate column chromatography, therefore, only the final products **1.124e** and **1.124f** were purified and fully characterised.

Step III-IV: See procedure K.

(*R,E*)-4-Benzyl-3-((2-(3,7-dimethylocta-2,6-dien-1-yl)phenyl)ethynyl)oxazolidin-2-one (1.124e)

Compound **1.124e** was synthesized following the general procedure. After column chromatography (3:1 cyclohexane:EtOAc), the product was isolated as a transparent oil (38.5 mg, 0.093 mmol, yield over two steps starting from **1.195**: 34%). ¹H NMR (400 MHz, CDCl₃) δ 7.45 (dd, *J* = 7.5, 1.4 Hz, 1H), 7.39 – 7.26 (m, 3H), 7.27 – 7.18 (m, 4H), 7.15 (td, *J* = 7.3, 1.7 Hz, 1H), 5.41 – 5.33 (m, 1H), 5.13 – 5.05 (m, 1H), 4.42 – 4.30 (m, 2H), 4.23 – 4.13 (m, 1H), 3.56 (d, *J* = 7.2 Hz, 2H), 3.31 (dd, *J* = 14.0, 3.4 Hz, 1H), 3.07 – 2.97 (m, 1H), 2.13 – 2.00 (m, 4H), 1.73 – 1.69 (m, 3H), 1.67 – 1.64 (m, 3H), 1.57 (s, 3H); ¹³C NMR (101 MHz, CDCl₃) δ 155.5, 143.5, 137.0, 134.3, 132.3, 131.6, 129.5, 129.2, 128.6, 128.4, 127.7, 125.8, 124.4, 122.1, 121.7, 81.8, 72.3, 67.5, 58.8, 39.9, 38.1, 32.9, 26.8, 25.8, 17.8, 16.4; HRMS (ESI⁺): *m/z*: calculated for C₂₈H₃₁NNaO₂: 436.2247 [M+Na]⁺; found: 436.2240.

(*R,E*)-4-Benzyl-3-((4-chloro-2-(3,7-dimethylocta-2,6-dien-1-yl)phenyl)ethynyl)oxazolidin-2-one
(1.124f)

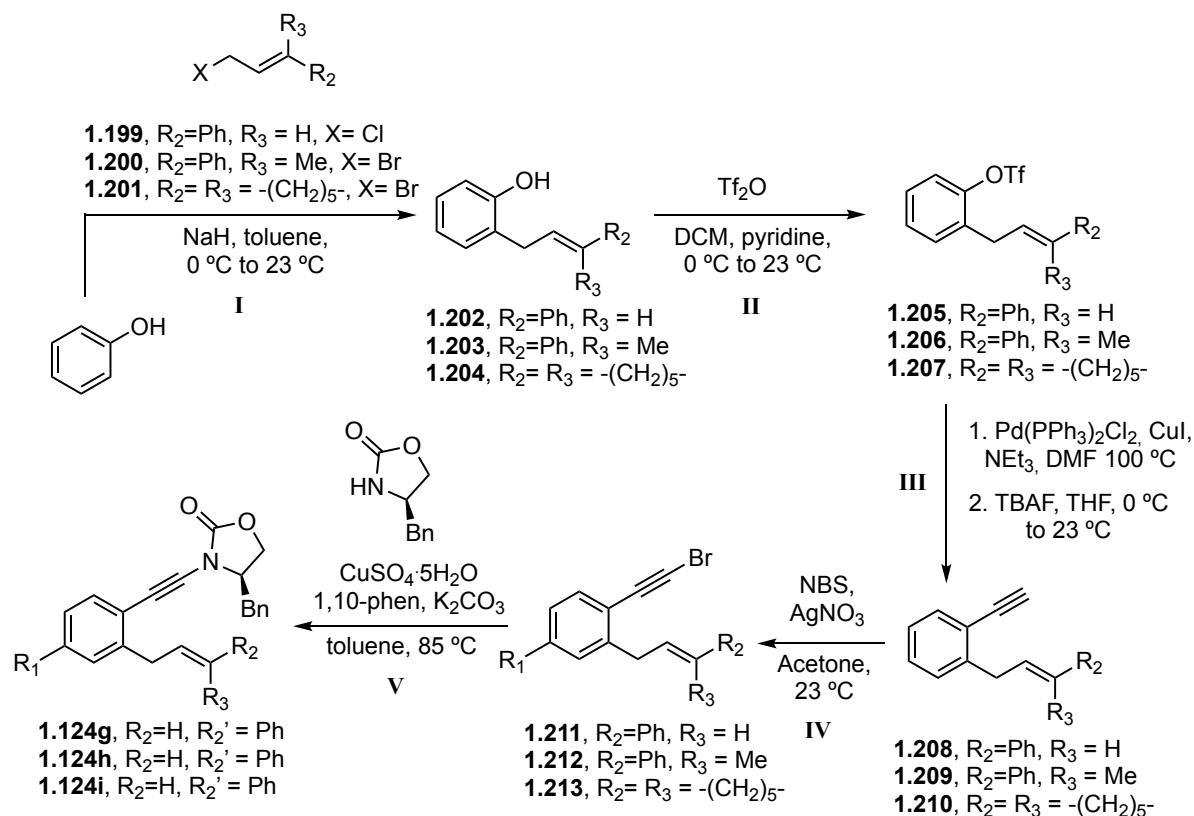


Compound **1.124f** was synthesized following the general procedure.

After preparative TLC (5:1 cyclohexane:EtOAc), the product was isolated as a yellow oil (28.6 mg, 0.064 mmol, yield over three steps starting from the precursor of **1.196**: 39%). ¹H NMR (500 MHz, CDCl₃) δ 7.38 – 7.31 (m, 3H), 7.33 – 7.26 (m, 1H), 7.26 – 7.20 (m,

2H), 7.18 (d, *J* = 2.1 Hz, 1H), 7.13 (dd, *J* = 8.2, 2.2 Hz, 1H), 5.33 (tq, *J* = 7.3, 1.3 Hz, 1H), 5.09 (dddd, *J* = 6.9, 5.6, 2.9, 1.5 Hz, 1H), 4.42 – 4.31 (m, 2H), 4.21 – 4.15 (m, 1H), 3.52 (d, *J* = 7.2 Hz, 2H), 3.33 – 3.26 (m, 1H), 3.05 – 2.97 (m, 1H), 2.08 (ddd, *J* = 16.8, 11.7, 5.2 Hz, 4H), 1.70 (s, 3H), 1.68 (d, *J* = 1.3 Hz, 3H), 1.59 (s, 3H); ¹³C NMR (126 MHz, CDCl₃) δ 155.4, 145.4, 137.9, 134.4, 134.2, 133.3, 131.8, 129.5, 129.2, 128.6, 127.8, 126.1, 124.2, 121.2, 120.3, 82.7, 71.4, 67.6, 58.7, 39.8, 38.2, 32.8, 26.7, 25.8, 17.9, 16.4; HRMS (ESI⁺): *m/z*: calculated for C₂₈H₃₀ClNNaO₂: 470.1857 [M+Na]⁺; found: 470.1863.

General procedure **M** for the synthesis of 1,6-enynes **1.124g-i**⁹⁹



⁹⁹ A different protocol was designed for these compounds since when following procedure **A**, the allylation step afforded mainly homocoupling products.

While compound **1.199** is commercially available, compounds **1.200-1.201** were synthesized according to literature procedure¹⁰⁰ and the spectral data were fully consistent with those previously reported.^{57b}

Step I: Following a modified literature procedure described for compound **1.202** which starts from the cinnamyl chloride **1.199**¹⁰¹, **1.203** and **1.204** were synthesized starting from the respective allyl bromide precursors: to a suspension of NaH (1.1 equiv) in toluene (0.5 M) at 0 °C, a solution of phenol (1 equiv) in toluene (1.8 M) was added dropwise. After 30 min, the allyl bromide (1.2 equiv) was added and the reaction was allowed to warm to 24 °C and maintained at this temperature for 24 hours. After complete consumption of phenol, the reaction was quenched with water, extracted, with ethyl acetate (x3), the combined organic phases dried over anhydrous Na₂SO₄ and the solvent was evaporated under reduced pressure. The resulting residue was purified by flash column chromatography to afford **1.203** and **1.204**.

Step II: **1.206** and **1.207** were synthesized following a literature procedure already described for **1.205**¹⁰²: The allyl phenol precursor (1.0 equiv) was dissolved in dichloromethane (0.2 M) under Ar atmosphere. Pyridine (0.72 mL, 8.9 mmol, 2.0 equiv) was added, and the reaction was cooled to 0°C. Trifluoromethanesulfonic anhydride (2.0 equiv) was added, the ice bath was removed, and the reaction was stirred for 15 hours at rt. The mixture was filtered through a pad of celite, eluting with ethyl acetate. The filtrate was concentrated in vacuo and the crude material was purified via flash column chromatography to afford the desired compounds.

Step III¹⁰³: To a DMF (0.5 M) solution of the corresponding aryl triflate (1.0 Eq), Pd(Ph₃P)₂Cl₂ (0.025 equiv), CuI (0.05 equiv) and triethylamine (2.5 equiv), ethynyltrimethylsilane (2 equiv) was slowly added and the reaction mixture was stirred at 100 °C until full consumption of the starting material. The mixture was diluted with water and washed with ethyl acetate (x2). The organic phase was washed then with water (x2), brine, and finally dried over anhydrous Na₂SO₄. The solvent was evaporated under reduced pressure and the crude was redissolved in THF (0.5 M) and directly subjected to the deprotection: TBAF (1.1 equiv, 1.0 M in THF) was added at 0°C and the solution was left to stir at 23°C for 2 hours before the addition of water. The solution was concentrated, extracted with diethyl ether, and chromatographed on a silica column to give **1.208-1.210**.

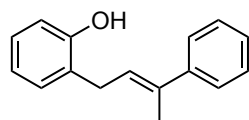
Step IV-V: See procedure **K**.

¹⁰⁰ Nguyen, T. N. T.; Thiel, N. O.; Pape, F.; Teichert, J. F. Copper(I)-Catalyzed Allylic Substitutions with a Hydride Nucleophile. *Org. Lett.* **2016**, *18*, 2455–2458.

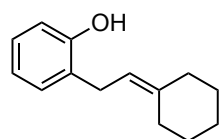
¹⁰¹ Denmark, S. E.; Kornfilt, D. J. P. Catalytic, Enantioselective, Intramolecular Sulfenofunctionalization of Alkenes with Phenols. *J. Org. Chem.* **2017**, *82*, 3192–3222.

¹⁰² White, D. R.; Hinds, E. M.; Bornowski, E. C.; Wolfe, J. P. Pd-Catalyzed Alkene Difunctionalization Reactions of Malonate Nucleophiles: Synthesis of Substituted Cyclopentanes via Alkene Aryl-Alkylation and Akenyl-Alkylation. *Org. Lett.* **2019**, *21*, 3813–3816.

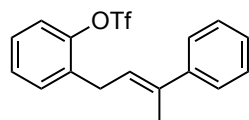
¹⁰³ For the first Sonogashira reactions of phenyl triflates: Chen, Q.-Y.; Yang, Z.-Y. Palladium-Catalyzed Reaction of Phenyl Fluoroalkanesulfonates with Alkynes and Alkenes. *Tetrahedron Lett.* **1986**, *27*, 1171–1174.

(E)-2-(3-Phenylbut-2-en-1-yl)phenol (1.203)

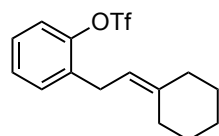
Compound **1.203** was synthesized following the general procedure. After column chromatography (10:1 *n*-hexane:EtOAc), the product was isolated as a yellow oil (1.23 g, 7.72 mmol, 71%). ¹H NMR (500 MHz, CDCl₃) δ 7.46 (dq, *J* = 6.8, 1.8 Hz, 2H), 7.36 (dtd, *J* = 9.2, 3.6, 1.7 Hz, 2H), 7.32 – 7.24 (m, 1H), 7.23 (dd, *J* = 6.8, 2.5 Hz, 1H), 7.20 – 7.12 (m, 1H), 6.94 (tq, *J* = 6.5, 1.7 Hz, 1H), 6.83 (d, *J* = 8.3 Hz, 1H), 6.01 (dddt, *J* = 7.3, 4.4, 3.0, 1.5 Hz, 1H), 5.12 – 5.02 (m, 1H), 3.62 (d, *J* = 7.4 Hz, 2H), 2.23 (s, 3H); ¹³C NMR (126 MHz, CDCl₃) δ 154.0, 143.4, 137.0, 130.1, 128.3, 127.7, 127.0, 126.8, 125.9, 125.6, 121.0, 115.7, 29.9, 16.1; HRMS (ESI⁺): *m/z*: calculated for C₁₆H₁₆NaO: 247.1093 [M+Na]⁺; found: 247.1092.

2-(2-Cyclohexylideneethyl)phenol (1.204)

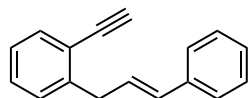
Compound **1.204** was synthesized following the general procedure. After column chromatography (12:1 *n*-hexane:EtOAc), the product was isolated as a colourless oil (1.95 g, 9.64 mmol, 64%). ¹H NMR (500 MHz, CDCl₃) δ 7.16 – 7.10 (m, 2H), 6.89 (td, *J* = 7.4, 1.2 Hz, 1H), 6.82 (dd, *J* = 8.4, 1.2 Hz, 1H), 5.34 – 5.27 (m, 2H, Csp²-H + O-H), 3.40 (d, *J* = 7.4 Hz, 2H), 2.33 (t, *J* = 5.3 Hz, 2H), 2.17 (t, *J* = 5.3 Hz, 2H), 1.67 – 1.48 (m, 6H); ¹³C NMR (126 MHz, CDCl₃) δ 154.5, 143.0, 130.1, 127.6, 127.0, 120.9, 118.5, 115.9, 37.3, 29.1, 28.8, 28.7, 27.8, 26.9; HRMS (ESI⁺): *m/z*: calculated for C₁₄H₁₆O: 203.1430 [M+H]⁺; found: 203.1430.

(E)-2-(3-Phenylbut-2-en-1-yl)phenyl trifluoromethanesulfonate (1.206)

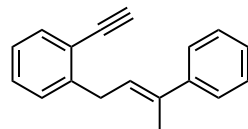
Compound **1.206** was synthesized following the general procedure. After column chromatography (50:1 to 20:1 *n*-hexane:EtOAc), the product was isolated as a colourless oil (1.47 g, 5.49 mmol, 75%). ¹H NMR (500 MHz, CDCl₃) δ 7.47 – 7.41 (m, 2H), 7.42 – 7.37 (m, 1H), 7.38 – 7.29 (m, 5H), 7.31 – 7.24 (m, 1H), 5.90 (dddt, *J* = 7.3, 5.8, 2.4, 1.3 Hz, 1H), 3.69 (d, *J* = 7.3 Hz, 2H), 2.25 – 2.02 (m, 3H); ¹³C NMR (126 MHz, CDCl₃) δ 148.2, 143.4, 137.8, 133.9, 128.6, 128.4, 128.1, 127.2, 125.9, 123.9, 121.5, 118.8 (q, *J* = 320.1 Hz), 29.1, 16.2; ¹⁹F NMR (376 MHz, CDCl₃) δ -73.83; HRMS (ESI⁺): *m/z*: calculated for C₁₇H₁₅F₃NaO₃S: 379.0586 [M+Na]⁺; found: 379.0573.

2-(2-Cyclohexylideneethyl)phenyl trifluoromethanesulfonate (1.207)

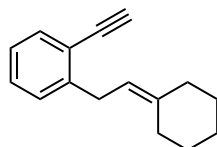
Compound **1.207** was synthesized following the general procedure. After column chromatography (50:1 to 20:1 *n*-hexane:EtOAc), the product was isolated as a colourless oil (2.81 g, 8.40 mmol, 87%). ¹H NMR (500 MHz, CDCl₃) δ 7.32 (tdt, *J* = 7.7, 5.8, 2.3 Hz, 2H), 7.29 – 7.22 (m, 2H), 5.21 (tt, *J* = 7.4, 1.3 Hz, 1H), 3.45 (d, *J* = 7.4 Hz, 2H), 2.25 – 2.19 (m, 2H), 2.15 (t, *J* = 5.5 Hz, 2H), 1.63 – 1.54 (m, 6H); ¹³C NMR (126 MHz, CDCl₃) δ 148.2, 142.8, 134.8, 131.2, 128.5, 127.7, 121.3, 118.8 (q, *J* = 320.0 Hz), 117.0, 28.9, 28.7, 27.9, 27.4, 27.0; ¹⁹F NMR (376 MHz, CDCl₃) δ -73.94; HRMS (ESI⁺): *m/z*: calculated for C₁₅H₁₇F₃NaO₃S: 357.0743 [M+Na]⁺; found: 357.0742.

1-Cinnamyl-2-ethynylbenzene (1.208)

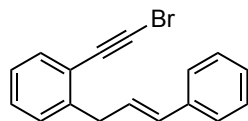
Compound **1.208** was synthesized following the general procedure. After column chromatography (pentane), the product was isolated as a yellow oil in a 6:1 *E:Z* isomeric ratio (194 mg, 0.889 mmol, 41%). ¹H NMR (400 MHz, CDCl₃) δ 7.58 (dt, *J* = 7.5, 1.8 Hz, 1.2H, *E+Z*), 7.43 – 7.39 (m, 2.4H, *E+Z*), 7.34 (ttdd, *J* = 7.5, 5.8, 3.4, 1.6 Hz, 4.8H, *E+Z*), 7.29 – 7.19 (m, 2.4H, *E+Z*), 6.53 (dt, *J* = 15.6, 1.7 Hz, 1.2H, *E+Z*), 6.44 (dtt, *J* = 15.7, 6.7, 1.9 Hz, 1.2H, *E+Z*), 3.82 – 3.78 (m, 2H, *E*), 3.66 (dd, *J* = 7.0, 1.8 Hz, 0.4H, *Z*), 3.37 (t, *J* = 1.7 Hz, 0.2H, *Z*), 3.35 (t, *J* = 1.7 Hz, 1H, *E*); ¹³C NMR (101 MHz, CDCl₃) δ 142.8 (*E*), 140.1 (*Z*), 139.7 (*Z*), 137.6 (*E*), 133.2 (*Z*), 133.1 (*E*), 131.6 (*Z*), 131.5 (*E*), 129.5 (*Z*), 129.2 (*E*), 129.0 (*E*), 129.0 (*Z*), 128.8 (*Z*), 128.6 (*Z*), 128.6 (*E*), 128.6 (*Z*), 128.3 (*E*), 127.2 (*E*), 126.9 (*Z*), 126.3 (*Z*), 126.3 (*E*), 124.9 (*E*), 121.8 (*E*), 120.5 (*Z*), 82.4 (*E*), 82.3 (*Z*), 81.8 (*Z*), 81.4 (*E*), 39.7 (*Z*), 37.8 (*E*); HRMS (APCI+): *m/z*: calculated for C₁₇H₁₅: 219.1168 [M+H]⁺; found: 219.1169.

(*E*)-1-Ethynyl-2-(3-phenylbut-2-en-1-yl)benzene (1.209)

Compound **1.209** was synthesized following the general procedure. After column chromatography (pentane), the product was isolated as a yellow oil (457 mg, 1.97 mmol, 48%). ¹H NMR (500 MHz, CDCl₃) δ 7.61 (dt, *J* = 7.7, 1.0 Hz, 1H), 7.53 – 7.49 (m, 2H), 7.43 – 7.38 (m, 2H), 7.38 – 7.34 (m, 2H), 7.34 – 7.30 (m, 1H), 7.26 (ddd, *J* = 7.6, 6.6, 2.2 Hz, 1H), 6.08 (tq, *J* = 7.4, 1.4 Hz, 1H), 3.86 (dd, *J* = 7.4, 1.1 Hz, 2H), 3.38 (s, 1H), 2.26 (dd, *J* = 1.5, 0.8 Hz, 3H); ¹³C NMR (126 MHz, CDCl₃) δ 143.7, 143.7, 136.1, 133.0, 129.1, 128.6, 128.3, 126.9, 126.0, 126.0, 125.9, 121.8, 82.5, 81.4, 33.6, 16.2; HRMS (APCI+): *m/z*: calculated for C₁₈H₁₇: 233.1325 [M+H]⁺; found: 233.1316.

1-(2-Cyclohexylideneethyl)-2-ethynylbenzene (1.210)

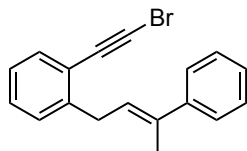
Compound **1.210** was synthesized following the general procedure. After column chromatography (pentane), the product was isolated as a transparent oil (673 mg, 3.20 mmol, 39%). ¹H NMR (400 MHz, CDCl₃) δ 7.51 (dd, *J* = 7.7, 1.4 Hz, 1H), 7.35 – 7.28 (m, 1H), 7.28 – 7.23 (m, 1H), 7.17 (td, *J* = 7.3, 1.3 Hz, 1H), 5.31 (tq, *J* = 7.4, 1.3 Hz, 1H), 3.59 (d, *J* = 7.5 Hz, 2H), 3.30 (d, *J* = 1.1 Hz, 1H), 2.30 (t, *J* = 5.4 Hz, 2H), 2.17 (t, *J* = 5.4 Hz, 2H), 1.64 – 1.54 (m, 6H); ¹³C NMR (101 MHz, CDCl₃) δ 144.7, 141.1, 132.9, 129.0, 128.5, 125.7, 121.6, 118.9, 82.6, 81.1, 37.3, 32.0, 29.0, 28.8, 28.0, 27.1; HRMS (APCI+): *m/z*: calculated for C₁₆H₁₉: 211.1481 [M+H]⁺; found: 211.1490.

1-(Bromoethyl)-2-cinnamylbenzene (1.211)

Compound **1.211** was synthesized following the general procedure. After column chromatography (pentane), the product was isolated as a yellow oil in a 7:1 *E:Z* isomeric ratio (209 mg, 0.703 mmol, 79%). ¹H NMR (400 MHz, CDCl₃) δ 7.60 – 7.49 (m, 1.3H, *E+Z*), 7.48-7.43 (m, 2.15H, *E+Z*), 7.42 – 7.19 (m, 7H, *E+Z*), 7.06-6.95 (m, 0.15H, *Z*), 6.62-6.51 (m, 1H, *E*), 6.55 – 6.46 (m, 0.15H, *Z*), 6.49 – 6.35 (m, 1H, *E*), 3.83-3.75 (m, 2H,

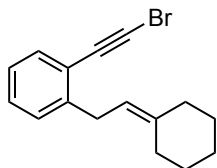
E), 3.72-3.65 (m, 0.3H, *Z*); ^{13}C NMR (101 MHz, CDCl_3) δ 142.9 (*E*), 140.0 (*Z*), 139.8 (*Z*), 137.6 (*E*), 133.1 (*Z*), 132.9 (*E*), 131.8 (*Z*), 131.7 (*E*), 129.5 (*Z*), 129.0 (*E*), 128.9 (*Z*), 128.8 (*E*), 128.6 (*Z*), 128.6 (*E*), 128.6 (*Z*), 128.1 (*E*), 127.2 (*E*), 126.9 (*Z*), 126.4 (*Z*), 126.3 (*E*), 126.3 (*E*), 124.9 (*E*), 122.4, 121.0, 79.0 (*E*), 78.9 (*Z*), 53.7 (*Z*), 53.4 (*E*), 39.6 (*Z*), 37.9 (*E*); HRMS (APCI⁺): *m/z*: calculated for $\text{C}_{17}\text{H}_{12}\text{Br}$: 295.0117 $[\text{M}-\text{H}]^+$; found: 295.0113.

(*E*)-1-(Bromoethynyl)-2-(3-phenylbut-2-en-1-yl)benzene (1.212)



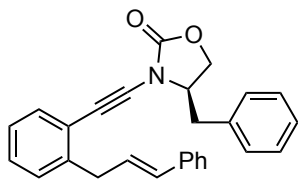
Compound **1.212** was synthesized following the general procedure. After column chromatography (pentane), the product was isolated as a yellow oil (164 mg, 0.527 mmol, 81%). ^1H NMR (500 MHz, CDCl_3) δ 7.56 (ddd, $J = 7.7, 1.5, 0.6$ Hz, 1H), 7.53 – 7.50 (m, 2H), 7.43 – 7.38 (m, 2H), 7.38 – 7.31 (m, 3H), 7.28 – 7.21 (m, 1H), 6.02 (tq, $J = 7.4, 1.4$ Hz, 1H), 3.83 (d, $J = 7.4$ Hz, 2H), 2.27 (dd, $J = 1.4, 0.8$ Hz, 3H); ^{13}C NMR (126 MHz, CDCl_3) δ 143.8, 143.7, 136.2, 132.9, 129.0, 128.7, 128.3, 126.9, 126.1, 125.9, 122.3, 111.9, 79.1, 53.3, 33.8, 16.2; HRMS (APCI⁺): *m/z*: calculated for $\text{C}_{18}\text{H}_{14}\text{Br}$: 309.0273 $[\text{M}-\text{H}]^+$; found: 309.0266.

1-(Bromoethynyl)-2-(2-cyclohexylideneethyl)benzene (1.213)



Compound **1.213** was synthesized following the general procedure. After column chromatography (pentane), the product was isolated as a yellow oil (678 mg, 2.34 mmol, 77%). ^1H NMR (400 MHz, CDCl_3) δ 7.46 (dd, $J = 7.7, 1.4$ Hz, 1H), 7.30 (td, $J = 7.5, 1.5$ Hz, 1H), 7.24 (ddd, $J = 7.8, 1.5, 0.7$ Hz, 1H), 7.16 (td, $J = 7.4, 1.5$ Hz, 1H), 5.27 (ddt, $J = 8.6, 7.4, 1.2$ Hz, 1H), 3.56 (d, $J = 7.4$ Hz, 2H), 2.31 (dd, $J = 6.8, 3.9$ Hz, 2H), 2.17 (t, $J = 5.3$ Hz, 2H), 1.67 – 1.54 (m, 6H); ^{13}C NMR (101 MHz, CDCl_3) δ 144.8, 141.2, 132.8, 128.9, 128.6, 125.8, 122.2, 118.9, 79.2, 52.9, 37.3, 32.1, 29.0, 28.8, 28.0, 27.1; HRMS (APCI⁺): *m/z*: calculated for $\text{C}_{16}\text{H}_{16}\text{Br}$: 287.0430 $[\text{M}-\text{H}]^+$; found: 287.0429.

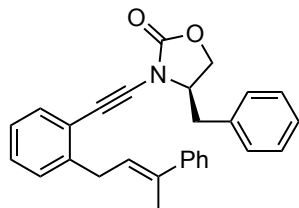
(*R*)-4-Benzyl-3-((2-cinnamylphenyl)ethynyl)oxazolidin-2-one (1.124g)



Compound **1.124g** was synthesized following the general procedure. After column chromatography (3:1 cyclohexane:EtOAc), the product was isolated as a brown solid in a 6:1 *E:Z* isomeric ratio (77.0 mg, 0.196 mmol, 58%). **M.p.** = 108-113 °C; ^1H NMR (400 MHz, CDCl_3) δ 7.57 – 7.42 (m, 1.2H, *E+Z*), 7.40 – 7.09 (m, 15.6H, *E+Z*), 7.01 (dt, $J = 15.8, 1.6$ Hz, 0.2H, *Z*), 6.57 – 6.36 (m, 2.2H, *E+Z*), 4.41 – 4.26 (m, 2.4H, *E+Z*), 4.22 – 4.09 (m, 1.2H, *E+Z*), 3.78 (dd, $J = 6.5, 1.2$ Hz, 2H, *E*), 3.61 (dd, $J = 7.0, 1.6$ Hz, 0.2H, *Z*), 3.26 (dt, $J = 13.7, 2.9$ Hz, 1.2H, *E+Z*), 3.05 – 2.89 (m, 1.2H, *E+Z*); ^{13}C NMR (101 MHz, CDCl_3) δ 155.5 (*E+Z*), 141.9 (*E*), 140.1 (*Z*), 139.0 (*Z*), 137.6 (*E*), 134.3 (*Z*), 134.2 (*E*), 132.5 (*Z*), 132.3 (*E*), 131.6 (*Z*), 131.5 (*E*), 129.5 (*Z*), 129.4 (*E*), 129.2 (*Z*), 129.1 (*E*), 129.1 (*E+Z*), 128.8 (*Z*), 128.6 (*E*), 128.6 (*E+Z*), 128.5 (*Z*), 128.3 (*E*), 127.6 (*Z*), 127.6 (*E*), 127.2 (*E*), 126.9 (*Z*), 126.3 (*E+Z*), 126.2 (*E*), 125.1 (*Z*), 122.0 (*E*), 120.6 (*Z*), 82.4 (*Z*), 82.0 (*E*), 72.1 (*Z*), 72.1 (*E*), 67.5 (*E*), 67.5

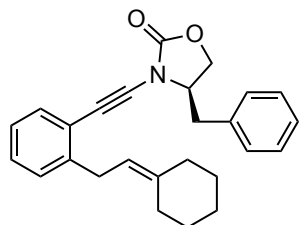
(*Z*), 58.6 (*E*), 58.5 (*Z*), 39.7 (*Z*), 38.1 (*E*), 38.1 (*E*), 38.0 (*Z*); **HRMS** (ESI⁺): *m/z*: calculated for C₂₇H₂₃NNaO₂: 416.1621 [M+Na]⁺; found: 416.1625.

(*R,E*)-4-Benzyl-3-((2-(3-phenylbut-2-en-1-yl)phenyl)ethynyl)oxazolidin-2-one (1.124h)



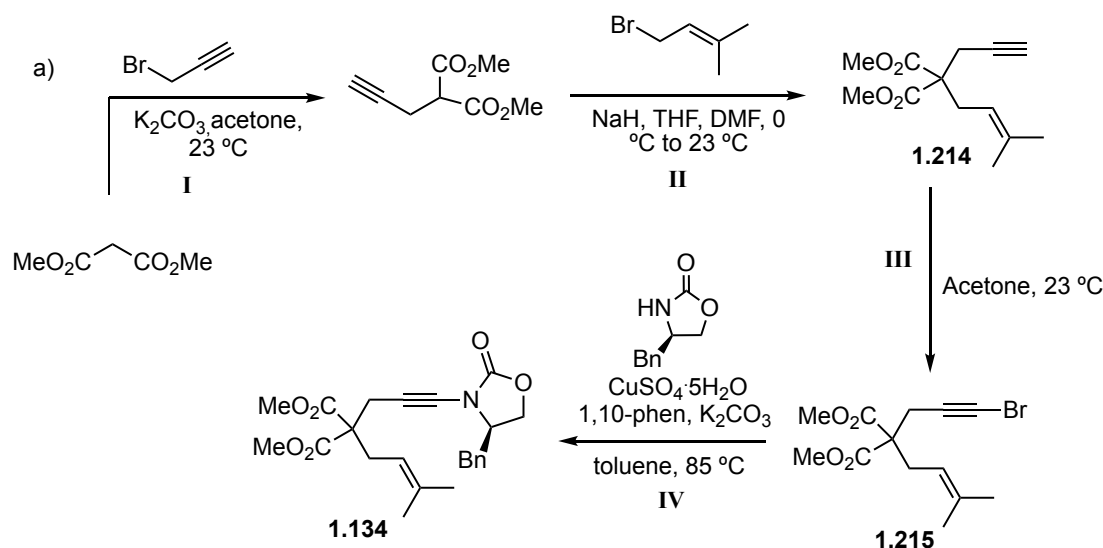
Compound **1.124h** was synthesized following the general procedure. After column chromatography (10:1 to 3:1 cyclohexane:EtOAc), the product was isolated as a brown oil (55.0 mg, 0.135 mmol, 28%). ¹H NMR (400 MHz, CDCl₃) δ 7.50 (dt, *J* = 7.5, 1.0 Hz, 1H), 7.46 – 7.38 (m, 2H), 7.35 – 7.26 (m, 7H), 7.25 – 7.15 (m, 4H), 6.03 (tq, *J* = 7.2, 1.4 Hz, 1H), 4.40 – 4.27 (m, 2H), 4.22 – 4.10 (m, 1H), 3.79 (d, *J* = 7.2 Hz, 2H), 3.27 (dd, *J* = 13.9, 3.5 Hz, 1H), 3.06 – 2.93 (m, 1H), 2.16 (d, *J* = 1.3 Hz, 3H); ¹³C NMR (101 MHz, CDCl₃) δ 155.5, 143.6, 142.8, 136.2, 134.2, 132.5, 129.5, 129.1, 128.7, 128.6, 128.3, 127.6, 126.9, 126.1, 126.1, 125.8, 121.9, 82.1, 72.2, 67.5, 58.6, 38.1, 33.9, 16.2; **HRMS** (ESI⁺): *m/z*: calculated for C₂₈H₂₅NNaO₂: 430.1777 [M+Na]⁺; found: 430.1779.

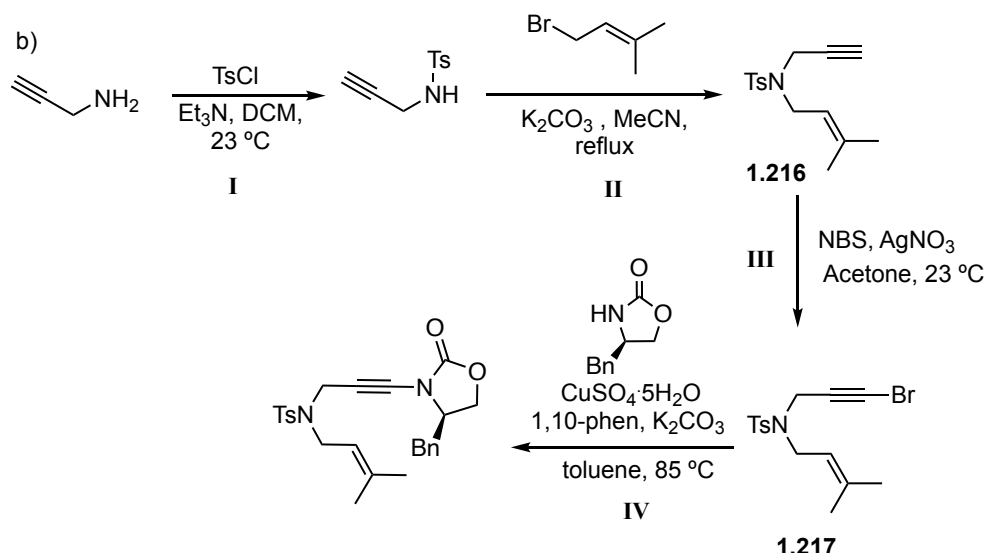
(*R*)-4-Benzyl-3-((2-(2-cyclohexylideneethyl)phenyl)ethynyl)oxazolidin-2-one (1.124i)



Compound **1.124i** was synthesized following the general procedure. After column chromatography (5:1 cyclohexane:EtOAc), the product was isolated as a yellow oil (506 mg, 1.31 mmol, 68%). ¹H NMR (400 MHz, CDCl₃) δ 7.52 – 7.44 (m, 1H), 7.40 – 7.29 (m, 3H), 7.34 – 7.20 (m, 4H), 7.17 (ddd, *J* = 7.6, 6.7, 2.1 Hz, 1H), 5.35 (tt, *J* = 7.3, 1.2 Hz, 1H), 4.35 (tdd, *J* = 8.1, 5.8, 4.2 Hz, 2H), 4.23 – 4.10 (m, 1H), 3.60 (d, *J* = 7.4 Hz, 2H), 3.28 (dd, *J* = 14.1, 3.3 Hz, 1H), 3.03 (ddt, *J* = 14.1, 8.8, 7.0 Hz, 1H), 2.27 (t, *J* = 5.4 Hz, 2H), 2.15 (d, *J* = 5.8 Hz, 2H), 1.66 – 1.48 (m, 6H); ¹³C NMR (101 MHz, CDCl₃) δ 155.4, 143.5, 141.1, 134.2, 132.1, 129.4, 129.0, 128.4, 128.3, 127.5, 125.7, 121.6, 118.7, 81.8, 72.1, 67.4, 58.5, 37.8, 37.1, 32.0, 28.8, 28.6, 27.8, 26.9; **HRMS** (ESI⁺): *m/z*: calculated for C₂₆H₂₇NNaO₂: 408.1934 [M+Na]⁺; found: 408.1938.

Procedure N a) and b) for the synthesis of 1,6-enynes 1.134 and 1.136





Compounds **1.214** and **1.216** were synthesized as reported in the scheme, according to literature procedure.⁹⁷ All the spectral data were fully consistent with those previously reported.

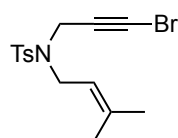
Step **III-IV**: See procedure **J**.

Dimethyl 2-(3-bromoprop-2-yn-1-yl)-2-(3-methylbut-2-en-1-yl)malonate (**1.215**)

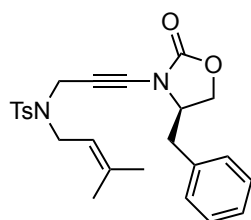
Compound **1.215** was synthesized following the general procedure. After column chromatography (10:1 to 5:1 cyclohexane:EtOAc), the product was isolated as a transparent oil (231 mg, 0.728 mmol, 51%). ¹H NMR (500 MHz, CDCl₃) δ 4.88 (tq, *J* = 7.7, 1.4 Hz, 1H), 3.73 (s, 6H), 2.79 (s, 2H), 2.76 (d, *J* = 7.7 Hz, 2H), 1.70 (s, 3H), 1.64 (s, 3H); ¹³C NMR (126 MHz, CDCl₃) δ 170.5, 137.2, 117.0, 75.4, 57.2, 52.9, 41.3, 31.1, 26.2, 23.9, 18.1.; HRMS (ESI⁺): *m/z*: calculated for C₁₃H₁₇BrNaO₄: 339.0202 [M+Na]⁺; found: 339.0199.

Dimethyl (R)-2-(3-(4-benzyl-2-oxooxazolidin-3-yl)prop-2-yn-1-yl)-2-(3-methylbut-2-en-1-yl)malonate (**1.134**)

Compound **1.134** was synthesized following the general procedure. After column chromatography (5:1 to 2:1 cyclohexane:EtOAc), the product was isolated as a yellow oil (157 mg, 0.380 mmol, 93%). ¹H NMR (500 MHz, CDCl₃) δ 7.38 – 7.31 (m, 2H), 7.31 – 7.25 (m, 1H), 7.22 – 7.16 (m, 2H), 4.94 (tp, *J* = 7.8, 1.5 Hz, 1H), 4.27 (dd, *J* = 8.7, 8.1 Hz, 1H), 4.17 (tdd, *J* = 8.2, 5.8, 3.6 Hz, 1H), 4.09 (dd, *J* = 8.7, 5.8 Hz, 1H), 3.74 (d, *J* = 1.4 Hz, 6H), 3.19 (dd, *J* = 13.8, 3.6 Hz, 1H), 2.97 (s, 2H), 2.89 (dd, *J* = 13.8, 8.6 Hz, 1H), 2.80 (d, *J* = 8.2 Hz, 2H), 1.71 (d, *J* = 1.4 Hz, 3H), 1.67 (s, 3H); ¹³C NMR (126 MHz, CDCl₃) δ 170.7, 155.8, 137.1, 134.4, 129.5, 129.2, 127.6, 117.1, 71.8, 68.5, 67.3, 58.5, 57.6, 52.9, 37.7, 31.2, 26.2, 22.9, 18.1.; HRMS (ESI⁺): *m/z*: calculated for C₂₃H₂₈NO₆: 414.1911 [M+H]⁺; found: 414.1911.

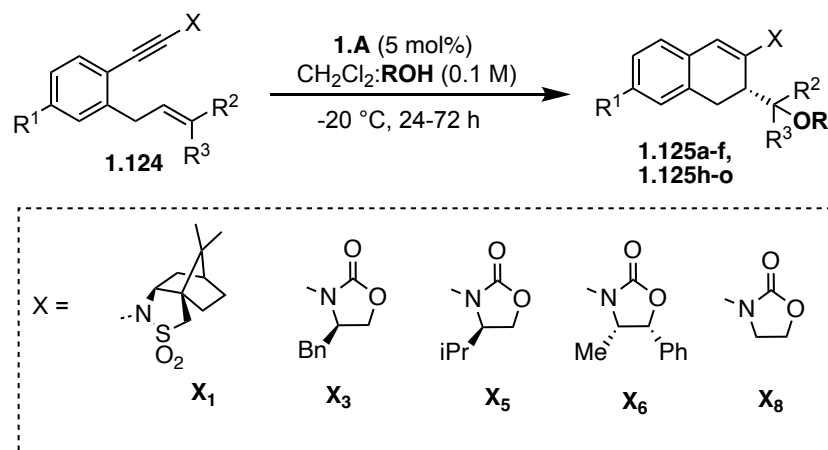
***N*-(3-Bromoprop-2-yn-1-yl)-4-methyl-*N*-(3-methylbut-2-en-1-yl)benzenesulfonamide (1.217)**

Compound **1.217** was synthesized following the general procedure. After column chromatography (5:1 pentane:EtOAc), the product was isolated as a white solid (657 mg, 1.84 mmol, 83%). **M.p.** = 92-95 °C; **¹H NMR** (500 MHz, CDCl₃) δ 7.38 – 7.31 (m, 2H), 7.31 – 7.25 (m, 1H), 7.22 – 7.16 (m, 2H), 4.94 (tp, *J* = 7.8, 1.5 Hz, 1H), 4.27 (dd, *J* = 8.7, 8.1 Hz, 1H), 4.17 (tdd, *J* = 8.2, 5.8, 3.6 Hz, 1H), 4.09 (dd, *J* = 8.7, 5.8 Hz, 1H), 3.74 (d, *J* = 1.4 Hz, 6H), 3.19 (dd, *J* = 13.8, 3.6 Hz, 1H), 2.97 (s, 2H), 2.89 (dd, *J* = 13.8, 8.6 Hz, 1H), 2.80 (d, *J* = 8.2 Hz, 2H), 1.71 (d, *J* = 1.4 Hz, 3H), 1.67 (s, 3H); **¹³C NMR** (126 MHz, CDCl₃) δ 143.6, 139.4, 135.8, 129.6, 127.9, 117.9, 73.4, 44.6, 44.3, 36.7, 26.0, 21.7, 18.0; **HRMS** (ESI⁺): *m/z*: calculated for C₁₅H₁₉BrNO₂S: 356.0314 [M+H]⁺; found: 356.0312.

***(R)*-*N*-(3-(4-Benzyl-2-oxooxazolidin-3-yl)prop-2-yn-1-yl)-4-methyl-*N*-(3-methylbut-2-en-1-yl)benzenesulfonamide (1.136)**

Compound **1.136** was synthesized following the general procedure. After column chromatography (4:1 to 3:1 cyclohexane:EtOAc), the product was isolated as a yellow oil (272 mg, 0.601 mmol, 60%). **¹H NMR** (500 MHz, CDCl₃) δ 7.79 – 7.71 (m, 2H), 7.34 – 7.22 (m, 5H), 7.12 – 7.04 (m, 2H), 5.11 (ddq, *J* = 8.7, 7.2, 1.5 Hz, 1H), 4.27 (s, 2H), 4.25 – 4.16 (m, 1H), 4.08 – 3.95 (m, 2H), 3.84 (d, *J* = 7.3 Hz, 2H), 2.92 (dd, *J* = 14.1, 3.6 Hz, 1H), 2.67 (dd, *J* = 13.9, 8.0 Hz, 1H), 2.30 (s, 2H), 1.71 (s, 3H), 1.69 (s, 3H); **¹³C NMR** (126 MHz, CDCl₃) δ 155.4, 143.4, 139.0, 136.4, 133.9, 129.6, 129.3, 129.0, 127.7, 127.6, 117.9, 74.0, 67.2, 67.0, 57.8, 44.1, 37.5, 35.9, 25.9, 21.4, 18.0; **HRMS** (ESI⁺): *m/z*: calculated for C₂₅H₂₈N₂NaO₄S: 475.1662 [M+Na]⁺; found: 475.1669.

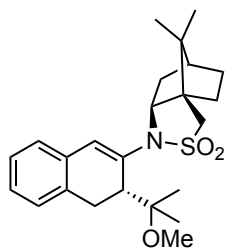
General procedure O for the gold(I)-catalyzed alkoxy cyclization of 1,6-enynes to afford 1.125a-f and 1.125h-o



The corresponding 1,6-enyne **1.124** was weighted in a microwave vial furnished with a magnet. Then, this vial was introduced in the glovebox together with a second vial containing catalyst **1.A** (5 mol%). The substrate was dissolved in ROH while the catalyst in CH₂Cl₂ (final volume = 0.1 M solution of 3:1

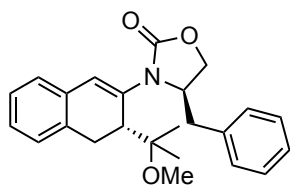
ROH:CH₂Cl₂). Then, the vials were sealed, taken out of the glovebox and brought to -20 °C (with the exception of products **1.125aⁱ**, **1.125aⁱⁱⁱ**, **1.125a^{iv}**, **1.125a^v** and **1.125f**, for which the reactions were conducted at 23 °C). Finally, the catalyst solution was added to the substrate one and the resulting mixture was left to stir at -20 °C. The reaction time varies depending on the substrate. After completion monitored by TLC, the reaction mixture was quenched with few drops of triethylamine, the solvent was evaporated and the crude was purified by flash column chromatography or preparative TLC. The *dr* were calculated before (when possible) and after the purification by ¹H NMR integration of the olefinic proton of the enamine (highlighted in the spectra) and LC-MS analysis. All the NMR spectra were integrated assigning only the major diastereomer's peaks. The relative configuration of **1.125aⁱⁱ** was assigned by X-Ray analysis and the other configurations were assigned by analogy.

(3a*R*,6*S*,7a*S*)-1-(*R*)-3-(2-Methoxypropan-2-yl)-3,4-dihydronaphthalen-2-yl)-8,8-dimethylhexahydro-3*H*-3a,6-methanobenzo[*c*]isothiazole 2,2-dioxide (1.125aⁱ)



Compound **1.125aⁱ** was synthesized following the general procedure but running the reaction at 23 °C for 16 h. The crude product in the crude has a *dr* = 83:27. After column chromatography (1:2 CH₂Cl₂:cyclohexane to pure CH₂Cl₂), the product was isolated as a white solid, single diastereomer (35 mg, 0.084 mmol, 39%). **M.p.** = 207-215 °C; ¹H NMR (400 MHz, CDCl₃) δ 7.20 – 7.05 (m, 3H), 7.01 – 6.94 (m, 1H), 6.11 (s, 1H), 3.69 (dd, *J* = 7.6, 4.8 Hz, 1H), 3.43 – 3.29 (m, 3H), 3.19 (s, 3H), 3.11 (d, *J* = 4.5 Hz, 2H), 2.07 – 1.85 (m, 5H), 1.51 (t, *J* = 9.3 Hz, 1H), 1.43 – 1.37 (m, 1H), 1.23 (s, 3H), 1.14 (s, 3H), 0.99 (s, 3H), 0.85 (s, 3H); ¹³C NMR (101 MHz, CDCl₃) δ 137.0, 135.3, 134.1, 129.2, 128.4, 127.2, 127.1, 126.2, 126.0, 78.7, 65.7, 51.9, 49.2, 48.7, 47.8, 44.8, 37.3, 33.3, 30.1, 27.2, 24.2, 24.2, 20.5, 20.4; **HRMS** (ESI⁺): *m/z*: calculated for C₂₄H₃₃NNaO₃S: 438.2073 [M+Na]⁺; found: 438.2073; [α]_D²⁶ (*c* = 0.2 in CHCl₃) = -40.2 °.

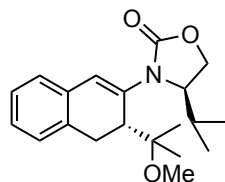
(*R*)-4-Benzyl-3-((*R*)-3-(2-methoxypropan-2-yl)-3,4-dihydronaphthalen-2-yl)oxazolidin-2-one (1.125aⁱⁱ)



Compound **1.125aⁱⁱ** was synthesized following the general procedure running the reaction for 16 h. Crude *dr* = 99:1. After column chromatography (20:1 CH₂Cl₂:EtOAc), the product was isolated as a white solid (59.0 mg, 0.156 mmol, 95%) with > 99:1 *dr*. **M.p.** = 117-121 °C; ¹H NMR (400 MHz, CDCl₃) δ 7.36 – 7.30 (m, 2H), 7.29 – 7.23 (m, 1H), 7.23 – 7.18 (m, 2H), 7.17 – 7.05 (m, 4H), 6.79 (s, 1H), 4.62 (tdd, *J* = 8.7, 5.7, 4.6 Hz, 1H), 4.27 (t, *J* = 8.5 Hz, 1H), 4.09 (dd, *J* = 8.7, 5.7 Hz, 1H), 3.21 (dd, *J* = 13.8, 4.6 Hz, 1H), 3.15 (s, 3H), 3.08 (d, *J* = 15.6 Hz, 1H), 3.02 – 2.92 (m, 1H), 2.92 (d, *J* = 8.2 Hz, 1H), 2.76 (dd, *J* = 13.8, 8.9 Hz, 1H), 1.06 (s, 3H), 0.98 (s, 3H); ¹³C NMR (101 MHz, CDCl₃) δ 155.8, 135.8, 134.4, 133.8, 133.5, 129.3, 129.0, 127.6, 127.3, 126.9, 126.5, 126.4, 123.9, 79.0, 66.6, 56.7, 49.0, 42.7, 39.2, 30.4, 22.8, 21.5; **HRMS** (ESI⁺): *m/z*: calculated for

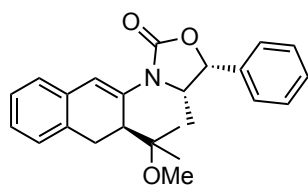
$C_{24}H_{27}NNaO_3$: 400.1883 $[M+Na]^+$; found: 400.1880; **LC-MS** (Column: EC-C18, 50ACN, 6 min, APCI): 1.952 min (99), 2.072 min (1); $[\alpha]_D^{26}$ ($c = 0.2$ in $CHCl_3$) = +336 °.

(R)-4-Isopropyl-3-((R)-3-(2-methoxypropan-2-yl)-3,4-dihydronaphthalen-2-yl)oxazolidin-2-one (1.125aⁱⁱⁱ)



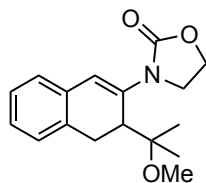
Compound **1.125aⁱⁱⁱ** was synthesized following the general procedure but running the reaction at 23 °C for 16 h. Crude *dr* = 96:4. After column chromatography (CH_2Cl_2), the product was isolated as a white solid (206 mg, 0.625 mmol, 87%) with 96:4 *dr*. **M.p.** = 147-149 °C. **¹H NMR** (400 MHz, $CDCl_3$) δ 7.15 – 7.04 (m, 4H), 6.84 (s, 1H), 4.32 – 4.23 (m, 2H), 4.18 – 4.09 (m, 1H), 3.19 – 3.12 (m, 1H), 3.15 (s, 3H), 3.10 – 3.02 (m, 1H), 2.63 (dd, $J = 8.0, 1.7$ Hz, 1H), 2.05 (pd, $J = 6.7, 3.1$ Hz, 1H), 1.03 (s, 3H), 1.00 (s, 3H), 0.96 (d, $J = 3.5$ Hz, 3H), 0.94 (d, $J = 3.3$ Hz, 3H); **¹³C NMR** (101 MHz, $CDCl_3$) δ 156.2, 134.0, 133.7, 133.7, 127.7, 126.9, 126.6, 126.6, 125.5, 79.1, 63.0, 59.5, 49.0, 43.4, 30.5, 29.8, 22.5, 21.4, 17.8, 15.1; **HRMS** (ESI+): *m/z*: calculated for $C_{20}H_{27}NNaO_3$: 352.1883 $[M+Na]^+$; found: 352.1887; **LC-MS** (InfinityLab Poroshell 120 EC-C18 (2.1x50mm, 1.9 μ m), Reverse phase 50% ACN, 0.5 mL/min): 1.517 min (96), 1.676 min (4); $[\alpha]_D^{26}$ ($c = 0.2$ in $CHCl_3$) = +340 °.

(4S,5R)-3-((S)-3-(2-Methoxypropan-2-yl)-3,4-dihydronaphthalen-2-yl)-4-methyl-5-phenyloxazolidin-2-one (1.125a^{iv})



Compound **1.125a^{iv}** was synthesized following the general procedure but running the reaction at 23 °C for 16 h. Crude *dr* = 88:22. After column chromatography (CH_2Cl_2), the product was isolated as a white solid (75.4 mg, 0.200 mmol, 94%) with 90:10 *dr*. **M.p.** = 98-109 °C. Major diastereomer: **¹H NMR** (400 MHz, $CDCl_3$) δ 7.46 – 7.31 (m, 5H), 7.17 – 7.05 (m, 4H), 6.78 (s, 1H), 5.65 (d, $J = 8.4$ Hz, 1H), 4.72 – 4.63 (m, 1H), 3.19 (s, 3H), 3.15 – 3.05 (m, 2H), 2.96 (d, $J = 7.4$ Hz, 1H), 1.05 (s, 3H), 1.03 (s, 3H), 0.84 (d, $J = 6.6$ Hz, 3H); **¹³C NMR** (101 MHz, $CDCl_3$) δ 155.3, 135.3, 134.4, 134.0, 133.6, 128.7, 127.7, 127.0, 126.6, 126.5, 126.3, 123.5, 78.9, 78.0, 55.8, 49.1, 42.7, 30.5, 22.8, 21.9, 15.1; **HRMS** (ESI+): *m/z*: calculated for $C_{24}H_{27}NNaO_3$: 400.1883 $[M+Na]^+$; found: 400.1881; **LC-MS** (InfinityLab Poroshell 120 EC-C18 (2.1x50mm, 1.9 μ m), Reverse phase 50% ACN, 0.5 mL/min): 2.154 min (90), 2.276 min (10); $[\alpha]_D^{26}$ ($c = 0.2$ in $CHCl_3$) = +274 °.

3-(3-(2-Methoxypropan-2-yl)-3,4-dihydronaphthalen-2-yl)oxazolidin-2-one (1.125a^v)

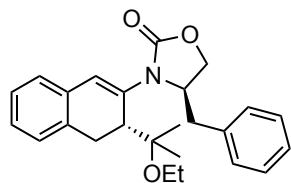


Compound **1.125a^v** was synthesized following the general procedure but running the reaction at 23 °C for 16 h. After column chromatography (30:1 CH_2Cl_2 :EtOAc), the product was isolated as a white solid (91.5 mg, 0.318 mmol, 88%). **M.p.** = 161-164 °C; **¹H NMR** (400 MHz, $CDCl_3$) δ 7.16 – 7.03 (m, 3H), 7.03 – 6.94 (m, 1H), 6.30 (s, 1H), 4.46 – 4.38 (m, 1H), 4.38 – 4.30 (m, 1H), 4.21 (q, $J = 9.0$ Hz, 1H), 3.82 (dd, $J = 8.0, 1.7$ Hz, 1H), 3.78 – 3.68 (m, 1H), 3.19 (s, 3H), 3.19 – 3.11 (m, 1H), 3.11 – 3.02 (m, 1H), 0.99 (s, 3H), 0.98 (s, 3H); **¹³C NMR** (101 MHz, $CDCl_3$) δ 155.6, 138.0, 134.3, 133.5, 127.3, 127.1,

126.4, 126.0, 117.3, 78.8, 61.7, 49.3, 46.7, 39.0, 30.1, 23.5, 22.5; **HRMS** (ESI⁺): *m/z*: calculated for C₁₇H₂₁NNaO₃: 310.1414 [M+Na]⁺; found: 310.1418.

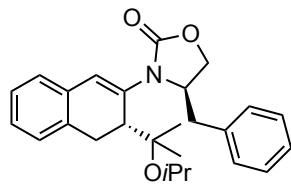
When performing the reaction with chiral catalyst **2.M** (Table 2.8, entry 4), the product was recovered in 88% yield and 91:9 *er*. **SFC** (OJ-3, CO₂:MeOH 90:10, 2 mL/min, 25 °C, BPR 2000 psi; 210 nm): 1.06 min (9), 1.50 min (91).

(R)-4-Benzyl-3-((R)-3-(2-ethoxypropan-2-yl)-3,4-dihydronaphthalen-2-yl)oxazolidin-2-one
(**1.125b**)

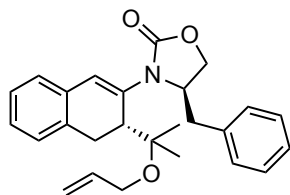


Compound **1.125b** was synthesized following the general procedure running the reaction for 24 h. Crude *dr* = 99:1. After column chromatography (CH₂Cl₂), the product was isolated as a white solid (32.5 mg, 0.083 mmol, 83%) with 99:1 *dr*. **M.p.** = 117-120 °C; **¹H NMR** (400 MHz, CDCl₃) δ 7.37 – 7.29 (m, 2H), 7.33 – 7.23 (m, 1H), 7.23 – 7.18 (m, 2H), 7.18 – 7.07 (m, 3H), 7.06 (d, *J* = 6.5 Hz, 1H), 6.81 (s, 1H), 4.68 (tdd, *J* = 8.7, 6.0, 4.5 Hz, 1H), 4.27 (t, *J* = 8.6 Hz, 1H), 4.07 (dd, *J* = 8.7, 6.0 Hz, 1H), 3.33 (q, *J* = 6.9 Hz, 2H), 3.23 – 3.14 (m, 1H), 3.07 (dd, *J* = 16.5, 1.7 Hz, 1H), 2.98 (dd, *J* = 16.5, 8.0 Hz, 1H), 2.85 (br. s, 1H), 2.78 (dd, *J* = 13.9, 8.8 Hz, 1H), 1.15 – 1.06 (m, 6H), 0.96 (s, 3H); **¹³C NMR** (101 MHz, CDCl₃) δ 155.8, 135.9, 134.5, 133.7, 133.7, 129.4, 129.0, 127.5, 127.3, 126.9, 126.6, 126.4, 124.3, 78.9, 66.5, 56.4, 56.1, 43.6, 39.3, 30.6, 23.5, 21.7, 16.2; **HRMS** (ESI⁺): *m/z*: calculated for C₂₅H₂₉NNaO₃: 414.2040 [M+Na]⁺; found: 414.2045; **LC-MS** (InfinityLab Poroshell 120 EC-C18 (2.1x50mm, 1.9 μm), Reverse phase 50% ACN, 0.5 mL/min): 2.446 min (99), 2.525 min (1); [**α**]_D²⁶ (*c* = 0.2 in CHCl₃) = +343 °.

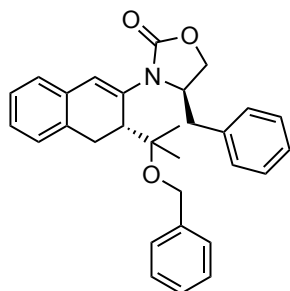
(R)-4-Benzyl-3-((R)-3-(2-isopropoxypropan-2-yl)-3,4-dihydronaphthalen-2-yl)oxazolidin-2-one
(**1.125c**)



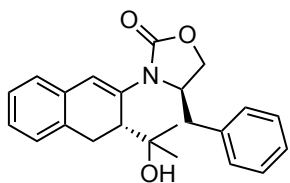
Compound **1.125c** was synthesized following the general procedure running the reaction for 24 h. The product in the crude as a *dr* = 98:2. After column chromatography (30:1 CH₂Cl₂:EtOAc), the product was isolated as a white solid (36.0 mg, 0.089 mmol, 89%) with 98:2 *dr*. **M.p.** = 125-128 °C. Major diastereomer: **¹H NMR** (400 MHz, CDCl₃) δ 7.37 – 7.28 (m, 2H), 7.26 (dt, *J* = 14.5, 1.4 Hz, 1H), 7.24 – 7.17 (m, 2H), 7.18 – 7.06 (m, 3H), 7.04 (d, *J* = 7.2 Hz, 1H), 6.88 (s, 1H), 4.72 (tt, *J* = 8.6, 4.9 Hz, 1H), 4.29 (t, *J* = 8.6 Hz, 1H), 4.09 (dd, *J* = 8.7, 5.3 Hz, 1H), 3.74 (p, *J* = 6.1 Hz, 1H), 3.16 (dd, *J* = 13.9, 4.6 Hz, 1H), 3.09 (dd, *J* = 16.5, 1.5 Hz, 1H), 2.94 (dd, *J* = 16.5, 8.2 Hz, 1H), 2.79 (dd, *J* = 13.9, 8.6 Hz, 1H), 2.74 – 2.67 (m, 1H), 1.09 (s, 3H), 1.05 (dd, *J* = 12.7, 6.1 Hz, 6H), 0.94 (s, 3H); **¹³C NMR** (101 MHz, CDCl₃) δ 155.6, 135.9, 134.2, 133.8, 133.6, 129.4, 129.0, 127.4, 127.3, 126.8, 126.6, 126.4, 124.1, 79.6, 66.2, 62.8, 56.3, 44.8, 39.5, 30.7, 25.5, 25.1, 24.1, 22.3; **HRMS** (ESI⁺): *m/z*: calculated for C₂₆H₃₁NNaO₃: 428.2196 [M+Na]⁺; found: 428.2205; **LC-MS** (InfinityLab Poroshell 120 EC-C18 (2.1x50mm, 1.9 μm), Reverse phase 50% ACN, 0.5 mL/min): 2.128 min (98), 2.374 min (2); [**α**]_D²⁶ (*c* = 0.2 in CHCl₃) = +347 °.

(R)-3-((R)-3-(2-(Allyloxy)propan-2-yl)-3,4-dihydronaphthalen-2-yl)-4-benzyloxazolidin-2-one**(1.125d)**

Compound **1.125d** was synthesized following the general procedure running the reaction for 24 h. Crude *dr* = 98:2. After column chromatography (CH₂Cl₂), the product was isolated as a white solid (37.8 mg, 0.094 mmol, 94%) with > 99:1 *dr*. **M.p.** = 95-98 °C. ¹H NMR (400 MHz, CDCl₃) δ 7.36 – 7.30 (m, 2H), 7.29 – 7.24 (m, 1H), 7.22 – 7.17 (m, 2H), 7.17 – 7.08 (m, 3H), 7.06 (d, *J* = 5.6 Hz, 1H), 6.81 (s, 1H), 5.88 (ddt, *J* = 17.2, 10.3, 5.6 Hz, 1H), 5.24 (dq, *J* = 17.2, 1.7 Hz, 1H), 5.11 (dq, *J* = 10.3, 1.4 Hz, 1H), 4.64 (tdd, *J* = 8.7, 5.7, 4.6 Hz, 1H), 4.25 (t, *J* = 8.5 Hz, 1H), 4.06 (dd, *J* = 8.6, 5.7 Hz, 1H), 3.84 (dt, *J* = 5.5, 1.5 Hz, 2H), 3.19 (dd, *J* = 13.8, 4.6 Hz, 1H), 3.11 – 2.91 (m, 2H), 2.77 (dd, *J* = 13.9, 8.8 Hz, 1H), 1.13 (s, 3H), 0.98 (s, 3H); ¹³C NMR (101 MHz, CDCl₃) δ 155.8, 136.1, 135.9, 134.5, 133.6, 129.4, 129.0, 127.6, 127.3, 126.9, 126.6, 126.4, 123.8, 116.1, 79.4, 66.5, 62.6, 56.5, 43.5, 39.2, 30.6, 23.6, 21.9; **HRMS** (ESI+): *m/z*: calculated for C₂₆H₃₀NO₃: 404.2220 [M+H]⁺; found: 404.2224; **LC-MS** (InfinityLab Poroshell 120 EC-C18 (2.1x50mm, 1.9 μm), Reverse phase 50% ACN, 0.5 mL/min): 2.653 min (99), 2.742 min (1); [α]_D²⁶ (*c* = 0.2 in CHCl₃) = +377 °.

(R)-4-Benzyl-3-((R)-3-(2-(benzyloxy)propan-2-yl)-3,4-dihydronaphthalen-2-yl)oxazolidin-2-one**(1.125e)**

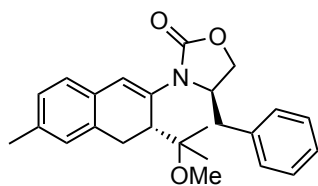
Compound **1.125e** was synthesized following the general procedure running the reaction for 36 h. Crude *dr* = n.d. After column chromatography (5:1 cyclohexane:EtOAc), the product was isolated as a transparent oil (33.3 mg, 0.073 mmol, 73%) with 98:2 *dr*. ¹H NMR (400 MHz, CDCl₃) δ 7.32 – 7.13 (m, 7H), 7.14 – 6.99 (m, 7H), 6.76 (s, 1H), 4.43 (tt, *J* = 8.9, 5.0 Hz, 1H), 4.28 (q, *J* = 10.3 Hz, 2H), 3.63 (dd, *J* = 8.6, 5.6 Hz, 1H), 3.51 (t, *J* = 8.5 Hz, 1H), 3.08 – 2.91 (m, 4H), 2.54 (dd, *J* = 13.9, 8.8 Hz, 1H), 1.21 (s, 3H), 0.99 (s, 3H); ¹³C NMR (101 MHz, CDCl₃) δ 155.7, 139.4, 135.9, 134.9, 133.8, 133.5, 129.3, 128.9, 128.4, 128.1, 127.5, 127.4, 127.2, 126.9, 126.7, 126.4, 122.8, 79.6, 66.0, 63.6, 56.4, 43.7, 38.9, 30.8, 23.7, 21.8; **HRMS** (ESI+): *m/z*: calculated for C₃₀H₃₁NNaO₃: 476.2196 [M+Na]⁺; found: 476.2202; **LC-MS** (InfinityLab Poroshell 120 EC-C18 (2.1x50mm, 1.9 μm), Reverse phase 50% ACN, 0.5 mL/min): 2.941 min (98), 2.998 min (2); [α]_D²⁶ (*c* = 0.1 in CHCl₃) = +260 °.

(R)-4-Benzyl-3-((R)-3-(2-hydroxypropan-2-yl)-3,4-dihydronaphthalen-2-yl)oxazolidin-2-one**(1.125f)**

Compound **1.125f** was synthesized following the general procedure but running the reaction at 23 °C for 16 h using 10 equivalents of water in CH₂Cl₂. Crude *dr* = 95:5. After column chromatography (5:1 cyclohexane:EtOAc), the product was isolated as a transparent oil (29.7 mg, 0.082 mmol, 82%) with 99:1 *dr*. ¹H NMR (500 MHz, CDCl₃) δ 7.37 – 7.30 (m, 2H), 7.31 – 7.23 (m,

1H), 7.25 – 7.18 (m, 2H), 7.18 – 7.04 (m, 4H), 6.72 (s, 1H), 4.62 (dddd, $J = 9.4, 8.3, 5.3, 4.4$ Hz, 1H), 4.29 (t, $J = 8.5$ Hz, 1H), 4.15 – 4.08 (m, 1H), 3.27 (dd, $J = 13.9, 4.3$ Hz, 1H), 3.10 – 2.94 (m, 3H), 2.79 (dd, $J = 13.9, 9.2$ Hz, 1H), 2.07 (br. s, 1H), 1.26 (s, 3H), 0.98 (s, 3H); $^{13}\text{C NMR}$ (101 MHz, CDCl_3) δ 156.1, 135.7, 134.6, 133.5, 133.4, 129.3, 129.1, 127.7, 127.4, 127.0, 126.7, 126.4, 122.5, 74.7, 66.6, 56.8, 44.0, 38.8, 31.3, 28.9, 26.5; **HRMS** (ESI+): m/z : calculated for $\text{C}_{23}\text{H}_{25}\text{NNaO}_3$: 386.1727 $[\text{M}+\text{Na}]^+$; found: 386.1730; **LC-MS** (InfinityLab Poroshell 120 EC-C18 (2.1x50mm, 1.9 μm), Reverse phase 50% ACN, 0.5 mL/min): 1.075 min (99), 1.321 min (1); $[\alpha]_{\text{D}}^{26}$ ($c = 0.2$ in CHCl_3) = +292 $^\circ$.

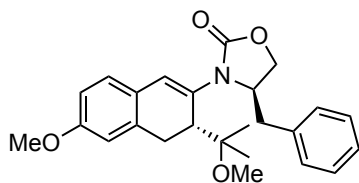
(R)-4-Benzyl-3-((R)-3-(2-methoxypropan-2-yl)-6-methyl-3,4-dihydronaphthalen-2-yl)oxazolidin-2-one (1.125h)



Compound **1.125h** was synthesized following the general procedure running the reaction for 16 h. Crude $dr = 98:2$. After column chromatography (20:1 CH_2Cl_2 :EtOAc), the product was isolated as a white solid (37.7 mg, 0.096 mmol, 96%) with $> 99:1$ dr . **M.p.** = 139-142

$^\circ\text{C}$; $^1\text{H NMR}$ (500 MHz, CDCl_3) δ 7.37 – 7.29 (m, 2H), 7.29 – 7.21 (m, 1H), 7.22 – 7.16 (m, 2H), 6.99 (d, $J = 7.6$ Hz, 1H), 6.97 – 6.92 (m, 1H), 6.90 (s, 1H), 6.75 (s, 1H), 4.59 (tdd, $J = 8.7, 5.8, 4.5$ Hz, 1H), 4.26 (t, $J = 8.5$ Hz, 1H), 4.08 (dd, $J = 8.7, 5.8$ Hz, 1H), 3.21 (dd, $J = 13.8, 4.5$ Hz, 1H), 3.15 (s, 3H), 3.07 – 3.00 (m, 1H), 2.99 – 2.86 (m, 2H), 2.74 (dd, $J = 13.8, 9.0$ Hz, 1H), 2.30 (s, 3H), 1.05 (s, 3H), 0.99 (s, 3H); $^{13}\text{C NMR}$ (101 MHz, CDCl_3) δ 155.9, 137.5, 135.9, 133.8, 133.3, 130.7, 129.3, 129.0, 127.9, 127.3, 127.1, 126.4, 124.1, 79.0, 66.7, 56.7, 49.0, 42.7, 39.2, 30.4, 22.8, 21.6, 21.5; **HRMS** (ESI+): m/z : calculated for $\text{C}_{25}\text{H}_{29}\text{NNaO}_3$: 414.2040 $[\text{M}+\text{Na}]^+$; found: 414.2046; **LC-MS** (InfinityLab Poroshell 120 EC-C18 (2.1x50mm, 1.9 μm), Reverse phase 50% ACN, 0.5 mL/min): 2.316 min (99), 2.426 min (1); $[\alpha]_{\text{D}}^{26}$ ($c = 0.2$ in CHCl_3) = +342 $^\circ$.

(R)-4-Benzyl-3-((R)-6-methoxy-3-(2-methoxypropan-2-yl)-3,4-dihydronaphthalen-2-yl)oxazolidin-2-one (1.125i)

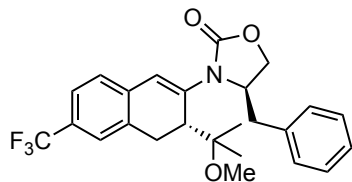


Compound **1.125i** was synthesized following the general procedure running the reaction for 24 h. Crude $dr = 96:4$. After column chromatography (3:1 cyclohexane:EtOAc), the product was isolated as a white solid (35.0 mg, 0.086 mmol, 86%) with $99:1$ dr . **M.p.** =

114-120 $^\circ\text{C}$; $^1\text{H NMR}$ (400 MHz, CDCl_3) δ 7.35 – 7.29 (m, 2H), 7.28 – 7.23 (m, 1H), 7.22 – 7.16 (m, 2H), 7.06 – 6.99 (m, 1H), 6.72 (s, 1H), 6.69 – 6.64 (m, 2H), 4.56 (tdd, $J = 8.7, 5.8, 4.5$ Hz, 1H), 4.26 (t, $J = 8.5$ Hz, 1H), 4.08 (dd, $J = 8.7, 5.8$ Hz, 1H), 3.79 (s, 3H), 3.20 (dd, $J = 13.8, 4.5$ Hz, 1H), 3.15 (s, 3H), 3.09 – 3.00 (m, 1H), 2.98 – 2.88 (m, 1H), 2.84 (d, $J = 8.1$ Hz, 1H), 2.74 (dd, $J = 13.8, 9.0$ Hz, 1H), 1.04 (s, 3H), 1.00 (s, 3H); $^{13}\text{C NMR}$ (101 MHz, CDCl_3) δ 159.4, 155.9, 135.9, 135.7, 131.8, 129.3, 129.0, 127.5, 127.3, 126.5, 124.1, 113.5, 111.0, 79.0, 66.7, 56.6, 55.4, 49.0, 42.5, 39.2, 30.7, 22.7, 21.6; **HRMS** (ESI+): m/z : calculated for $\text{C}_{25}\text{H}_{29}\text{NNaO}_4$: 430.1989 $[\text{M}+\text{Na}]^+$; found: 430.1984; **LC-MS**

(InfinityLab Poroshell 120 EC-C18 (2.1x50mm, 1.9 μm), Reverse phase 50% ACN, 0.5 mL/min): 1.813 min (99), 1.944 min (1); $[\alpha]_{\text{D}}^{26}$ ($c = 0.2$ in CHCl_3) = +261 $^\circ$.

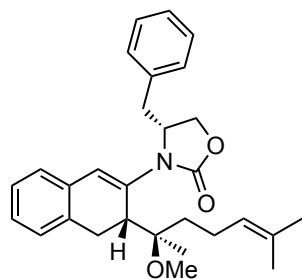
(R)-4-Benzyl-3-((R)-3-(2-methoxypropan-2-yl)-6-(trifluoromethyl)-3,4-dihydronaphthalen-2-yl)oxazolidin-2-one (1.125j)



Compound **1.125j** was synthesized following the general procedure but using 10% of catalyst loading and running the reaction for 24 h. Crude $dr = \text{n.d.}$ After preparative TLC (CH_2Cl_2), the product was isolated as a white solid (33.8 mg, 0.076 mmol, 76%) with $> 99:1$ dr . **M.p.** = 165-

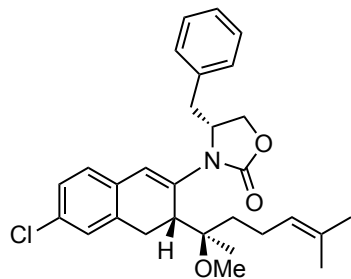
170 $^\circ\text{C}$; $^1\text{H NMR}$ (400 MHz, CDCl_3) δ 7.42 – 7.24 (m, 5H), 7.23 – 7.14 (m, 3H), 6.84 (s, 1H), 4.65 (td, $J = 8.5, 4.4$ Hz, 1H), 4.29 (t, $J = 8.5$ Hz, 1H), 4.10 (dd, $J = 8.7, 5.3$ Hz, 1H), 3.23 – 3.15 (m, 1H), 3.14 (s, 3H), 3.09 (d, $J = 16.1$ Hz, 1H), 2.99 – 2.84 (m, 2H), 2.79 (dd, $J = 13.8, 8.5$ Hz, 1H), 1.05 (s, 3H), 0.94 (s, 3H); $^{13}\text{C NMR}$ (101 MHz, CDCl_3) δ 155.6, 137.1, 137.1, 137.1, 135.7, 134.3, 129.4, 129.6 – 128.7 (m), 129.1, 127.5, 126.3, 125.7, 123.7 (q, $J = 4.0$ Hz), 123.5 (q, $J = 3.9$ Hz), 123.0, 122.0, 78.9, 66.7, 56.8, 49.0, 42.9, 39.5, 30.2, 22.9, 21.3; $^{19}\text{F NMR}$ (376 MHz, CDCl_3) δ -62.01. **HRMS** (ESI+): m/z : calculated for $\text{C}_{25}\text{H}_{27}\text{F}_3\text{NO}_3$: 446.1938 $[\text{M}+\text{H}]^+$; found: 446.1941; **LC-MS** (InfinityLab Poroshell 120 EC-C18 (2.1x50mm, 1.9 μm), Reverse phase 50% ACN, 0.5 mL/min): 2.491 min (99), 2.565 min (1); $[\alpha]_{\text{D}}^{26}$ ($c = 0.2$ in CHCl_3) = +313 $^\circ$.

(R)-4-Benzyl-3-((R)-3-((R)-2-methoxy-6-methylhept-5-en-2-yl)-3,4-dihydronaphthalen-2-yl)oxazolidin-2-one (1.125k)

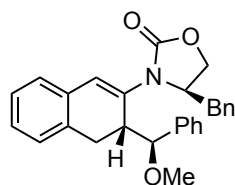


Compound **1.125k** was synthesized following the general procedure leaving the reaction during 72 h. Crude $dr = \text{n.d.}$ After consecutive preparative TLC (200:1 CH_2Cl_2 :EtOAc) and column chromatography (3:1 Cy:EA), the product was isolated as a transparent oil (11.9 mg, 0.027 mmol, 67%) with 97:3 dr . $^1\text{H NMR}$ (500 MHz, CDCl_3) δ 7.37 – 7.30 (m, 2H), 7.31 – 7.26 (m, 1H), 7.20 – 7.15 (m, 2H), 7.17 – 7.06 (m, 4H), 6.69 (s, 1H),

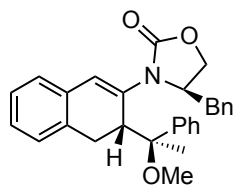
5.01 – 4.94 (m, 1H), 4.47 (tt, $J = 9.3, 4.8$ Hz, 1H), 4.26 (t, $J = 8.5$ Hz, 1H), 4.12 (dd, $J = 8.8, 5.3$ Hz, 1H), 3.29 (dd, $J = 13.7, 4.2$ Hz, 1H), 3.24 (d, $J = 16.4$ Hz, 1H), 3.19 (s, 3H), 3.13 (br. s, 1H), 2.99 (dd, $J = 16.4, 8.4$ Hz, 1H), 2.70 (dd, $J = 13.8, 9.7$ Hz, 1H), 2.01 – 1.86 (m, 1H), 1.64 (s, 3H), 1.61 – 1.56 (m, 1H), 1.48 – 1.35 (m, 1H), 1.48 – 1.35 (s, 3H), 0.91 (s, 3H); $^{13}\text{C NMR}$ (126 MHz, CDCl_3) δ 155.6, 135.8, 134.9, 133.2, 131.8, 129.2, 129.2, 128.1, 127.5, 127.1, 126.6, 126.5, 124.4, 80.4, 77.4, 66.7, 57.4, 57.4, 49.2, 39.6, 38.9, 35.4, 29.6, 25.8, 21.9, 20.2, 17.8; **HRMS** (ESI+): m/z : calculated for $\text{C}_{29}\text{H}_{35}\text{NNaO}_3$: 468.2509 $[\text{M}+\text{Na}]^+$; found: 468.2514; **LC-MS** (InfinityLab Poroshell 120 EC-C18 (2.1x50mm, 1.9 μm), Reverse phase 50% ACN, 0.5 mL/min): 2.873 min (3), 2.921 min (97); $[\alpha]_{\text{D}}^{26}$ ($c = 0.2$ in CHCl_3) = +201 $^\circ$.

(R)-4-Benzyl-3-((R)-6-chloro-3-((R)-2-methoxy-6-methylhept-5-en-2-yl)-3,4-dihydronaphthalen-2-yl)oxazolidin-2-one (1.125l)

Compound **1.125l** was synthesized following the general procedure leaving the reaction during 72 h. Crude *dr* = n.d. After column chromatography (3:1 Cy:EA), the product was isolated as a transparent oil (9.8 mg, 0.020 mmol, 64%) with 96:4 *dr*. ¹H NMR (400 MHz, CDCl₃) δ 7.36 – 7.27 (m, 3H), 7.20 – 7.09 (m, 2H), 7.14 – 7.07 (m, 2H), 7.04 – 6.97 (m, 1H), 6.65 (s, 1H), 5.02 – 4.91 (m, 1H), 4.47 (tt, *J* = 9.3, 4.9 Hz, 1H), 4.27 (t, *J* = 8.5 Hz, 1H), 4.12 (dd, *J* = 8.8, 5.2 Hz, 1H), 3.26 (dd, *J* = 13.7, 4.4 Hz, 1H), 3.18 (s, 2H), 3.16 (d, *J* = 2.6 Hz, 1H), 3.11 (d, *J* = 13.7 Hz, 1H), 2.88 (dd, *J* = 16.6, 8.4 Hz, 1H), 2.71 (dd, *J* = 13.7, 9.3 Hz, 1H), 2.01 – 1.83 (m, 2H), 1.73 – 1.65 (m, 1H), 1.64 (d, *J* = 1.3 Hz, 3H), 1.56 (s, 3H), 1.47 – 1.39 (m, 1H), 0.91 (s, 3H); ¹³C NMR (101 MHz, CDCl₃) δ 155.5, 136.7, 135.7, 133.2, 131.9, 131.8, 129.3, 129.2, 129.2, 127.5, 127.2, 126.5, 124.2, 80.3, 77.4, 66.8, 57.4, 57.4, 49.3, 39.4, 39.1, 35.5, 29.5, 25.8, 21.9, 20.2, 17.9; HRMS (ESI⁺): *m/z*: calculated for C₂₉H₃₄ClNNaO₃: 502.2119 [M+Na]⁺; found: 502.2109; LC-MS (InfinityLab Poroshell 120 EC-C18 (2.1x50mm, 1.9 μm), Reverse phase 50% ACN, 0.5 mL/min): 2.393 min (96), 2.508 min (4); [α]_D²⁶ (*c* = 0.2 in CHCl₃) = +154 °.

(R)-4-Benzyl-3-((R)-3-((S)-methoxy(phenyl)methyl)-3,4-dihydronaphthalen-2-yl)oxazolidin-2-one (1.125m)

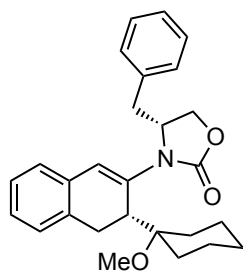
Compound **1.125m** was synthesized following the general procedure leaving the reaction during 16 h. Crude *dr* = n.d. After column chromatography (5:1 to 1: pentane:Et₂O), the product was isolated as a transparent oil (32.9 mg, 0.077 mmol, 77%) with 99:1 *dr*. ¹H NMR (400 MHz, CDCl₃) δ 7.36 – 7.14 (m, 12H), 7.12 – 7.05 (m, 2H), 7.01 (s, 1H), 3.90 – 3.84 (m, 1H), 3.80 (tdd, *J* = 8.3, 4.7, 3.3 Hz, 1H), 3.67 (dd, *J* = 8.5, 3.3 Hz, 1H), 3.42 – 3.33 (m, 1H), 3.23 (t, *J* = 8.4 Hz, 1H), 3.11 (s, 3H), 2.90 (dd, *J* = 13.9, 4.7 Hz, 1H), 2.86 – 2.73 (m, 2H), 2.46 (dd, *J* = 13.9, 8.5 Hz, 1H); ¹³C NMR (101 MHz, CDCl₃) δ 154.1, 140.2, 135.5, 133.6, 133.4, 131.9, 129.4, 129.0, 128.3, 128.1, 127.3, 127.3, 127.2, 126.9, 126.7, 119.9, 81.4, 65.3, 56.7, 56.0, 42.4, 38.9, 30.9; HRMS (ESI⁺): *m/z*: calculated for C₂₈H₂₇NNaO₃: 448.1883 [M+Na]⁺; found: 448.1885; LC-MS (InfinityLab Poroshell 120 EC-C18 (2.1x50mm, 1.9 μm), Reverse phase 50% ACN, 0.5 mL/min): 2.461 min (99), 2.885 min (1); [α]_D²⁶ (*c* = 0.2 in CHCl₃) = +251 °.

(R)-4-Benzyl-3-((R)-3-((S)-1-methoxy-1-phenylethyl)-3,4-dihydronaphthalen-2-yl)oxazolidin-2-one (1.125n)

Compound **1.125n** was synthesized following the general procedure leaving the reaction during 16 h. Crude *dr* = 98:2. After preparative TLC (CH₂Cl₂), the product was isolated as a white solid (34.8 mg, 0.079 mmol, 79%) with 98:2 *dr*. **M.p.** = 160-165 °C; ¹H NMR (400 MHz, CDCl₃) δ 7.44 – 7.36 (m, 2H), 7.36 – 7.18 (m, 6H), 7.20 – 7.10 (m, 4H), 7.14 – 7.02 (m, 2H), 6.91 (s, 1H), 3.68 – 3.58 (m, 2H), 3.51 (tdd, *J*

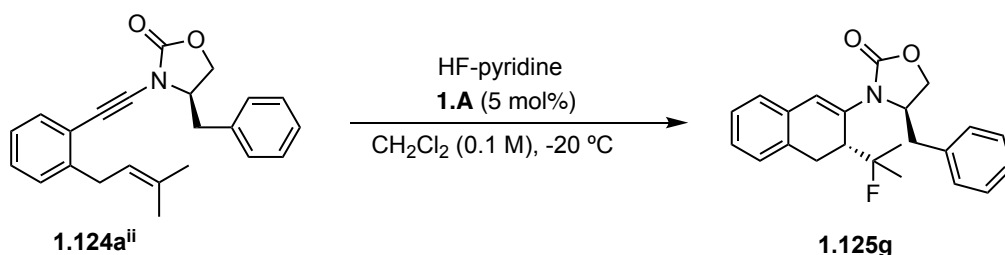
= 8.3, 4.6, 3.3 Hz, 1H), 3.06 (t, $J = 8.4$ Hz, 1H), 3.00 (s, 3H), 2.96 – 2.84 (m, 2H), 2.77 (d, $J = 8.3$ Hz, 1H), 2.51 (dd, $J = 13.9, 8.8$ Hz, 1H), 1.30 (s, 3H); ^{13}C NMR (101 MHz, CDCl_3) δ 154.4, 143.9, 135.7, 134.3, 133.3, 131.6, 129.3, 129.0, 128.1, 127.9, 127.4, 127.2, 127.0, 126.7, 126.7, 126.5, 125.9, 81.8, 65.4, 55.7, 50.2, 46.7, 39.1, 30.0, 17.4; HRMS (ESI⁺): m/z : calculated for $\text{C}_{29}\text{H}_{29}\text{NNaO}_3$: 462.2040 $[\text{M}+\text{Na}]^+$; found: 462.2039; LC-MS (InfinityLab Poroshell 120 EC-C18 (2.1x50mm, 1.9 μm), Reverse phase 50% ACN, 0.5 mL/min): 2.635 min (98), 2.852 min (2); $[\alpha]_{\text{D}}^{26}$ ($c = 0.2$ in CHCl_3) = +242 $^\circ$.

(R)-4-Benzyl-3-((R)-3-(1-methoxycyclohexyl)-3,4-dihydronaphthalen-2-yl)oxazolidin-2-one
(1.125o)

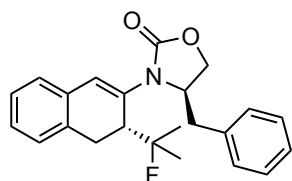


Compound **1.125o** was synthesized following the general procedure but with 10% catalyst loading leaving the reaction during 24 h. Crude $dr = nd$. After column chromatography (10:1 to 3:1 cyclohexane:EtOAc), the product was isolated as a transparent oil (22.5 mg, 0.054 mmol, 54%) with $> 99:1$ dr . ^1H NMR (400 MHz, CDCl_3) δ 7.40 – 7.31 (m, 2H), 7.29 (td, $J = 5.5, 2.4$ Hz, 1H), 7.23 – 7.17 (m, 2H), 7.18 – 7.04 (m, 4H), 6.67 (s, 1H), 4.53 (tdd, $J = 9.7, 5.8, 3.9$ Hz, 1H), 4.31 (t, $J = 8.6$ Hz, 1H), 4.14 (dd, $J = 8.8, 5.9$ Hz, 1H), 3.36 (dd, $J = 13.7, 3.9$ Hz, 1H), 3.30 (s, 1H), 3.24 (s, 3H), 3.19 (dd, $J = 16.4, 1.2$ Hz, 1H), 2.98 (dd, $J = 16.4, 8.4$ Hz, 1H), 2.74 (dd, $J = 13.8, 9.7$ Hz, 1H), 1.80 (d, $J = 13.3$ Hz, 1H), 1.52 (d, $J = 12.9$ Hz, 1H), 1.47 – 1.15 (m, 8H); ^{13}C NMR (101 MHz, CDCl_3) δ 155.5, 135.8, 134.8, 134.1, 133.2, 129.2, 129.1, 127.9, 127.5, 127.0, 126.4, 126.4, 79.6, 77.4, 66.7, 57.2, 48.2, 38.7, 38.0, 31.5, 30.3, 29.2, 25.6, 21.7, 21.6; HRMS (ESI⁺): m/z : calculated for $\text{C}_{27}\text{H}_{31}\text{NNaO}_3$: 440.2196 $[\text{M}+\text{Na}]^+$; found: 440.2198; LC-MS (InfinityLab Poroshell 120 EC-C18 (2.1x50mm, 1.9 μm), Reverse phase 50% ACN, 0.5 mL/min): 2.558 min (99), 2.797 min (1); $[\alpha]_{\text{D}}^{26}$ ($c = 0.2$ in CHCl_3) = +245 $^\circ$.

Procedure P for the gold(I)-catalyzed cyclization of 1,6-enynes followed by fluoride attack to afford
1.125g



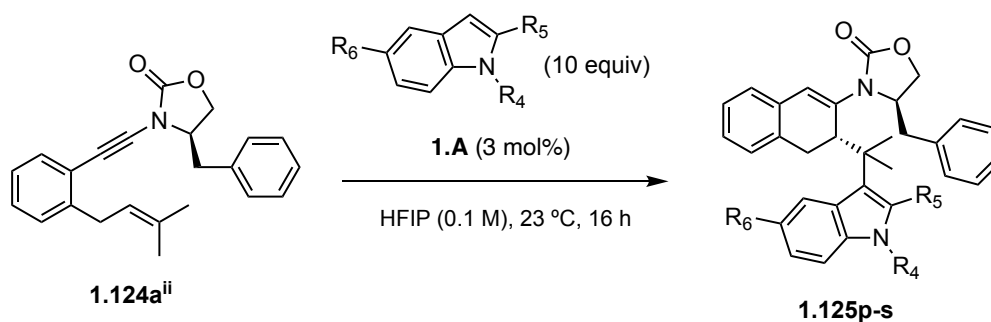
(R)-4-Benzyl-3-((R)-3-(2-fluoropropan-2-yl)-3,4-dihydronaphthalen-2-yl)oxazolidin-2-one
(1.125g)



1,6-enyne **1.124aⁱⁱ** was weighted in a microwave vial furnished with a magnet. Then, this vial was introduced in the glovebox together with a second vial containing $[\text{JohnPhosAu}(\text{MeCN})\text{SbF}_6]$ (5 mol %). The substrate was dissolved in CH_2Cl_2 as well as the catalyst (final volume of the two

combined = 0.1 M solution). Then, the vials were sealed, taken out of the glovebox, HF-pyridine (3 equiv) was added to the substrate vial and then both solutions were brought to -20 °C. Finally, the catalyst solution was added to the substrate one and the resulting mixture was left to stir at -20 °C for 36 h. The reaction mixture was quenched with triethylamine (with the reaction mixture still at -20 °C and having previously furnished the vial with a needle to release the pressure formed by the exothermic reaction). The vial was allowed to warm up to room temperature, a saturated NaHCO₃ solution was added to it and the mixture was extracted with CH₂Cl₂ (x3). Na₂SO₄ was added, then filtered and the solvent was evaporated under reduced pressure. Crude *dr* = 90:10. After column chromatography (from pure CH₂Cl₂ to 20:1 CH₂Cl₂:EtOAc), the product was isolated as a yellow oil (15.1 mg, 0.041 mmol, 41%) with 93:7 *dr*. **¹H NMR** (400 MHz, CDCl₃) δ 7.38 – 7.31 (m, 2H), 7.30 – 7.27 (m, 1H), 7.23 – 7.17 (m, 2H), 7.18 – 7.10 (m, 3H), 7.06 (dd, *J* = 7.1, 1.5 Hz, 1H), 6.81 (s, 1H), 4.58 (tt, *J* = 8.7, 5.0 Hz, 1H), 4.29 (t, *J* = 8.5 Hz, 1H), 4.13 – 4.07 (m, 1H), 3.29 – 3.16 (m, 2H), 3.05 (dd, *J* = 16.6, 8.0 Hz, 1H), 2.96 – 2.87 (m, 1H), 2.77 (dd, *J* = 13.8, 9.0 Hz, 1H), 1.39 – 1.31 (d, *J* = 22.5 Hz, 3H), 1.16 – 1.06 (d, *J* = 23.1 Hz, 3H); **¹³C NMR** (101 MHz, CDCl₃) δ 155.57, 135.78, 133.46 (d, *J* = 3.6 Hz), 133.25, 132.60, 129.33, 129.12, 127.77, 127.43, 127.03, 126.92, 126.63, 122.67, 98.70 (d, *J* = 170.1 Hz), 66.61, 56.71 (d, *J* = 1.6 Hz), 43.33 (d, *J* = 21.2 Hz), 39.18, 30.61 (d, *J* = 8.0 Hz), 25.94 (d, *J* = 24.3 Hz), 24.26 (d, *J* = 24.5 Hz); **¹⁹F NMR** (376 MHz, CDCl₃) δ -133.12; **HRMS** (ESI+): *m/z*: calculated for C₂₃H₂₄FNNaO₂: 388.1683 [M+Na]⁺; found: 388.1689; **LC-MS** (InfinityLab Poroshell 120 EC-C18 (2.1x50mm, 1.9 μm), Reverse phase 50% ACN, 0.5 mL/min): 2.012 min (93), 2.141 min (7); **[α]_D²⁶** (*c* = 0.2 in CHCl₃) = +225 °.

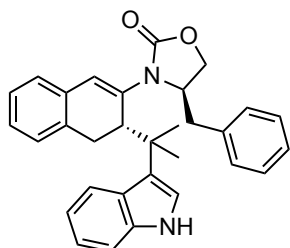
General procedure Q for gold(I)-catalyzed cyclization of 1,6-enynes followed by indoles attack to afford 1.125p-s



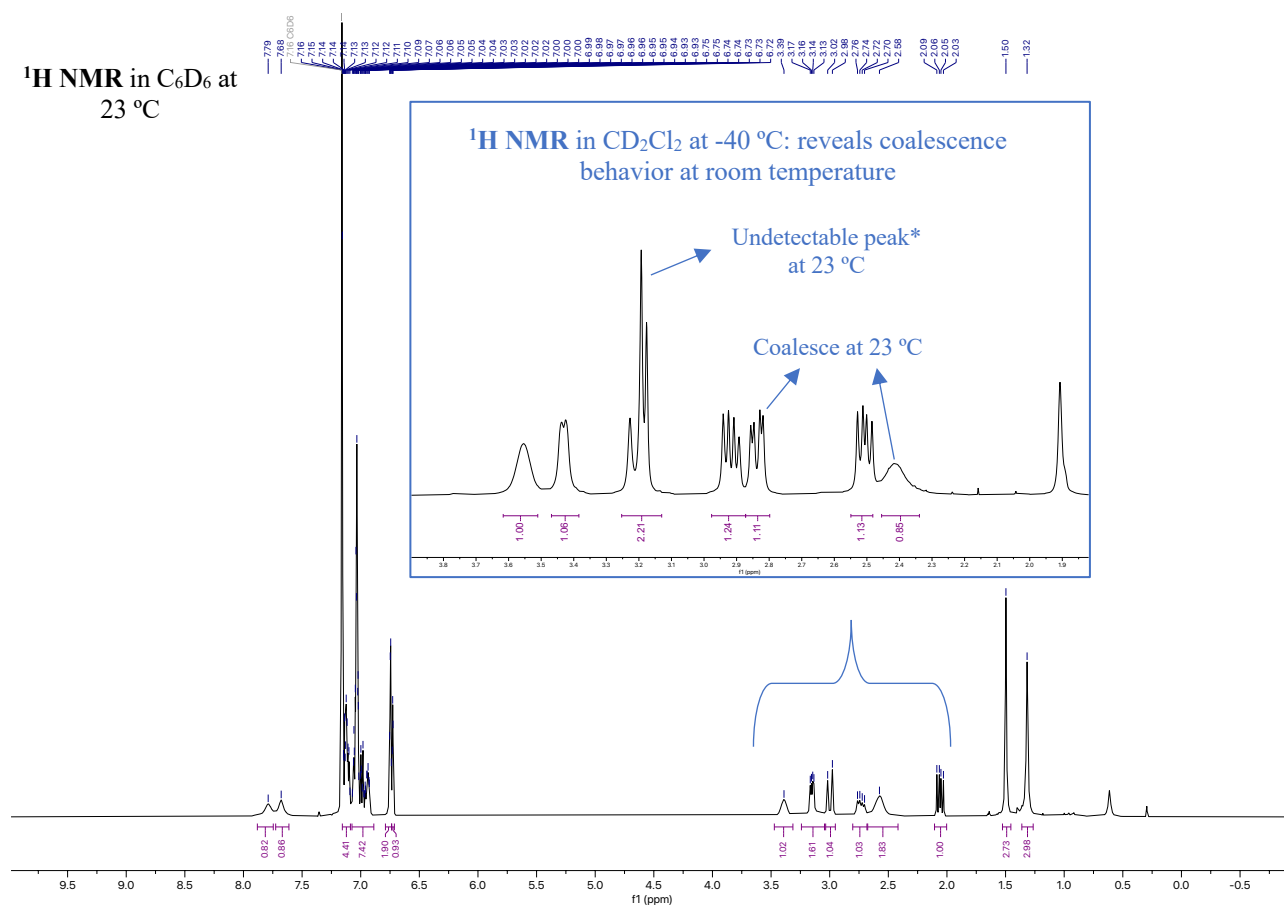
1,6-Enyne **1.124aⁱⁱ** was weighted in a microwave vial furnished with a magnet together with the corresponding indole (10 equiv) and [JohnPhosAu(MeCN)SbF₆] (3 mol%). Then, this vial was introduced in the glovebox and HFIP (previously dried over freshly activated 4Å molecular sieves) was added to it. The vial was sealed and the solution (0.1 M) was left to stir over 16 h. The reaction mixture was quenched with triethylamine, then water was added to the mixture which was subsequently extracted with CH₂Cl₂ (x3). Na₂SO₄ was added, then filtered and the solvent was evaporated under reduced pressure. The crudes were purified by flash column chromatography or preparative TLC. Since

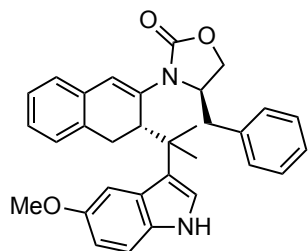
the products show slow decomposition in CDCl_3 (even if previously filtered on basic alumina), the NMR were recorded in C_6D_6 . The minor diastereomer could not be detected after purification (neither by ^1H NMR or LC-MS analysis).

(R)-3-((S)-3-(2-(1H-Indol-3-yl)propan-2-yl)-3,4-dihydronaphthalen-2-yl)-4-benzyloxazolidin-2-one (1.125p)

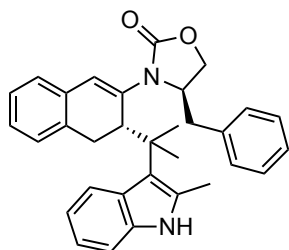


Compound **1.125p** was synthesized following the general procedure. Crude *dr* = 95:5. After column chromatography (5:1 to 3:1 cyclohexane:EtOAc), the product was isolated as a brown oil (34.6 mg, 0.075 mmol, 75%) with > 99:1 *dr* (the other diastereomer was not detected). ^1H NMR (400 MHz, C_6D_6) δ 7.79 (br. s, 1H), 7.68 (br. s, 1H), 7.19 – 7.07 (m, 4H), 7.11 – 6.89 (m, 7H), 6.78 – 6.72 (m, 2H), 6.73 (t, $J = 1.4$ Hz, 1H), 3.39 (br. s, 1H), 3.24–3.04 (m, 1 H)*, 3.15 (dd, $J = 8.4, 4.1$ Hz, 1H), 3.00 (d, $J = 16.2$ Hz, 1H), 2.73 (dd, $J = 16.1, 7.9$ Hz, 1H), 2.58 (br. s, 2H), 2.06 (dd, $J = 14.0, 8.6$ Hz, 1H), 1.50 (s, 3H), 1.32 (s, 3H); ^{13}C NMR (101 MHz, C_6D_6) δ 154.9, 137.6, 136.5, 134.7, 134.6, 129.4, 128.8, 128.2, 127.9, 127.7, 127.1, 126.9, 126.8, 126.6, 126.0, 124.3, 121.8, 121.5, 120.9, 119.1, 112.1, 65.6, 55.9, 43.3, 39.7, 39.5, 31.5, 28.0, 24.7; HRMS (ESI+): m/z : calculated for $\text{C}_{31}\text{H}_{31}\text{N}_2\text{O}_2$: 463.2380 $[\text{M}+\text{H}]^+$; found: 463.2388; LC-MS (InfinityLab Poroshell 120 EC-C18 (2.1x50mm, 1.9 μm), Reverse phase 50% ACN, 0.5 mL/min): 2.548 min (100); $[\alpha]_{\text{D}}^{26}$ ($c = 0.1$ in CHCl_3) = +193 $^\circ$.

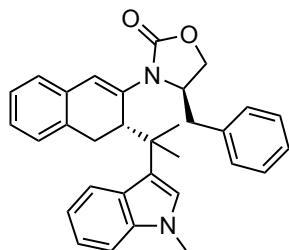


(R)-4-Benzyl-3-((S)-3-(2-(5-methoxy-1H-indol-3-yl)propan-2-yl)-3,4-dihydronaphthalen-2-yl)oxazolidin-2-one (1.125q)

Compound **1.125q** was synthesized following the general procedure. Crude *dr* = 94:6. After column chromatography (5:1 cyclohexane:EtOAc), the product was isolated as a yellow oil (20.0 mg, 0.041 mmol, 81%) with > 99:1 *dr* (the other diastereomer was not detected). ¹H NMR (400 MHz, C₆D₆) δ 7.44 (br. s, 2H), 7.11 – 6.94 (m, 8H), 6.95-6.89 (m, 2H), 6.81 – 6.75 (m, 2H), 6.72 (s, 1H), 3.66 (br. s, 2H), 3.53 (br. s, 1H), 3.20 (br. s, 1H), 2.96 (d, *J* = 16.2 Hz, 1H), 2.74 (br. s, 2H), 2.04 (dd, *J* = 13.9, 8.9 Hz, 1H), 1.49 (s, 3H), 1.35 (s, 3H); ¹³C NMR (101 MHz, C₆D₆) δ 154.2, 136.6, 134.6, 132.8, 129.3, 128.9, 128.7, 128.2, 128.1, 127.9, 127.6, 127.4, 127.1, 126.8, 126.5, 126.3, 124.2, 122.5, 112.5, 103.9, 65.8, 56.0, 55.8, 39.7, 39.7, 39.5, 31.6, 31.5, 31.4; HRMS (ESI+): *m/z*: calculated for C₃₂H₃₂N₂NaO₃: 515.2305 [M+Na]⁺; found: 515.2290; LC-MS (InfinityLab Poroshell 120 EC-C18 (2.1x50mm, 1.9 μm), Reverse phase 50% ACN, 0.5 mL/min): 2.518 min (100); [α]_D²⁶ (*c* = 0.2 in CHCl₃) = +162 °.

(R)-4-Benzyl-3-((S)-3-(2-(2-methyl-1H-indol-3-yl)propan-2-yl)-3,4-dihydronaphthalen-2-yl)oxazolidin-2-one (1.125r)

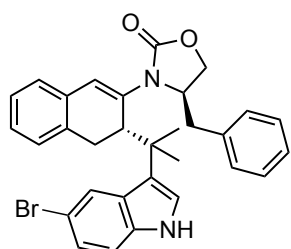
Compound **1.125r** was synthesized following the general procedure. Crude *dr* = 95:5. After column chromatography (7:1 cyclohexane:EtOAc), the product was isolated as a yellow oil (16.3 mg, 0.034 mmol, 68%) with > 99:1 *dr* (the other diastereomer was not detected). ¹H NMR (400 MHz, C₆D₆) δ 7.76 (br. s, 1H), 7.13 – 6.92 (m, 11H), 6.89 (s, 1H), 6.75 – 6.67 (m, 2H), 3.41 (br. s, 1H), 3.32 – 3.09 (m, 1H)*, 3.21 (dd, *J* = 8.4, 3.6 Hz, 1H), 3.04 – 2.96 (m, 1H), 2.82 – 2.68 (m, 1H), 2.70-2.51 (m, 2H), 2.27 (s, 3H), 2.06 (dd, *J* = 13.9, 8.8 Hz, 1H), 1.58 (s, 3H), 1.44 (s, 3H); ¹³C NMR (101 MHz, C₆D₆) δ 155.0, 136.5, 135.7, 134.9, 134.7, 131.4, 129.4, 128.8, 128.4, 128.4, 128.2, 127.9, 127.6, 127.0, 126.9, 126.7, 126.6, 121.1, 120.7, 119.0, 118.0, 111.1, 65.5, 56.1, 42.8, 41.8, 39.3, 31.6, 29.3, 26.7, 26.7, 15.7; HRMS (ESI+): *m/z*: calculated for C₃₂H₃₂N₂NaO₂: 499.2356 [M+Na]⁺; found: 499.2358; LC-MS (InfinityLab Poroshell 120 EC-C18 (2.1x50mm, 1.9 μm), Reverse phase 50% ACN, 0.5 mL/min): 2.818 min (100); [α]_D²⁶ (*c* = 0.2 in CHCl₃) = +164 °. *Undetectable proton due to coalescence, see **1.125p**.

(R)-4-Benzyl-3-((S)-3-(2-(1-methyl-1H-indol-3-yl)propan-2-yl)-3,4-dihydronaphthalen-2-yl)oxazolidin-2-one (1.125s)

Compound **1.125s** was synthesized following the general procedure. Crude *dr* = 95:5. After column chromatography (5:1 cyclohexane:EtOAc), the product was isolated as a yellow oil (19.7 mg, 0.041 mmol, 83%) with > 99:1 *dr* (the other diastereomer was not detected). ¹H NMR (400 MHz, C₆D₆) δ 7.80 (br. s, 1H), 7.16 – 7.09 (m, 2H), 7.09 – 6.91 (m, 9H), 6.75 –

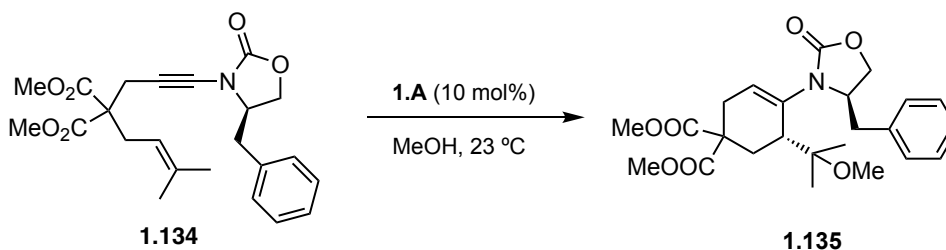
6.68 (m, 2H), 6.64 (s, 1H), 3.34 (br. s, 1H), 3.16 – 2.95 (m, 1H)*, 3.14 – 3.08 (m, 1H), 3.08 (s, 3H), 3.05 – 2.96 (m, 1H), 2.74 (dd, $J = 16.6, 7.9$ Hz, 1H), 2.58 (br. s, 1H), 2.45 (br. s, 1H), 2.01 (dd, $J = 13.9, 8.7$ Hz, 1H), 1.54 (s, 3H), 1.33 (s, 3H); ^{13}C NMR (101 MHz, C_6D_6) δ 154.4, 138.2, 136.6, 134.8, 134.6, 129.3, 128.8, 128.2, 127.9, 127.7, 127.0, 126.9, 126.8, 126.7, 126.6, 126.5, 123.0, 121.2, 121.1, 118.8, 109.9, 65.5, 55.7, 43.8, 39.8, 39.6, 31.9, 31.6, 28.0, 24.9; HRMS (ESI+): m/z : calculated for $\text{C}_{32}\text{H}_{32}\text{N}_2\text{NaO}_2$: 499.2356 $[\text{M}+\text{Na}]^+$; found: 499.2365; LC-MS (InfinityLab Poroshell 120 EC-C18 (2.1x50mm, 1.9 μm), Reverse phase 50% ACN, 0.5 mL/min): 3.009 min (100); $[\alpha]_{\text{D}}^{26}$ ($c = 0.2$ in CHCl_3) = +190 °. * Undetectable proton due to coalescence, see 1.125p.

(R)-4-Benzyl-3-((S)-3-(2-(1-methyl-1H-indol-3-yl)propan-2-yl)-3,4-dihydronaphthalen-2-yl)oxazolidin-2-one (1.125t)

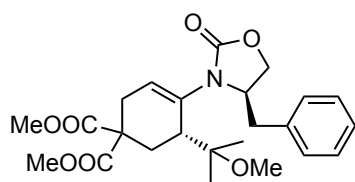


Compound 1.125t was synthesized following the general procedure. Crude $dr = 95:5$. After column chromatography (3:1 cyclohexane:EtOAc), the product was isolated as a brown oil (5.1 mg, 0.009 mmol, 19%) with 99:1 dr . ^1H NMR (400 MHz, C_6D_6) δ 8.30 (s, 1H), 8.13 (s, 1H), 7.24 – 7.19 (m, 2H), 7.07 – 6.97 (m, 5H), 6.92 – 6.81 (m, 3H), 6.72 (d, $J = 8.6$ Hz, 1H), 6.62 (s, 1H), 6.15 (s, 1H), 3.37 (br. s, 1H), 3.12 (dd, $J = 8.5, 4.5$ Hz, 1H), 2.80 (d, $J = 16.0$ Hz, 1H), 2.58 (m, 2H), 1.99 (dd, $J = 14.0, 8.8$ Hz, 1H), 1.34 (s, 3H), 1.22 (s, 3H). ^{13}C NMR (101 MHz, C_6D_6) δ 154.7, 136.3, 135.9, 134.6, 134.4, 138.7, 129.3, 129.1, 128.7, 127.7, 127.4, 127.2, 126.9, 126.7, 126.6, 124.4, 123.2, 123.1, 113.5, 112.6, 65.7, 55.8, 39.8, 39.4, 31.3, 30.2, 28.1, 24.5. HRMS (ESI+): m/z : calculated for $\text{C}_{31}\text{H}_{29}\text{BrN}_2\text{NaO}_2$: 563.1305 $[\text{M}+\text{Na}]^+$; found: 563.1310. ; LC-MS (InfinityLab Poroshell 120 EC-C18 (2.1x50mm, 1.9 μm), Reverse phase 50% ACN, 0.5 mL/min): 2.656 min (1), 2.977 min (99).

Procedure R for gold(I)-catalyzed alkoxy cyclization of 1,6-enyne 1.134 to afford 1.135



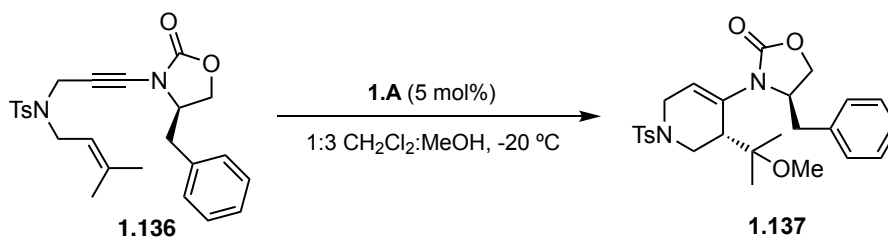
Dimethyl (R)-4-((R)-4-benzyl-2-oxooxazolidin-3-yl)-5-(2-methoxypropan-2-yl)cyclohex-3-ene-1,1-dicarboxylate (1.135)



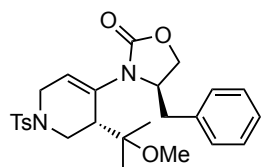
1,6-enyne 1.134 was weighted in a microwave vial furnished with a magnet. Then, this vial was introduced in the glovebox together with a second vial containing $[\text{JohnPhosAu}(\text{MeCN})\text{SbF}_6]$ (10 mol%). The catalyst was dissolved in MeOH (0.1 M) and the resulting solution was

added to the substrate vial. The vial was sealed and the reaction was left to stir in the glovebox at 23 °C over 24 h. The reaction mixture was quenched with few drops of triethylamine, and the solvent evaporated under reduced pressure. Crude *dr* = n.d. After column chromatography (5:1 to 3:1 cyclohexane:EtOAc), compound **1.135** was isolated as a transparent oil (32.8 mg mg, 0.074 mmol, 50%) with 92:8 *dr*. **¹H NMR** (400 MHz, CDCl₃) δ 7.34-7.29 (m, 2H), 7.28-7.24 (m, 1H), 7.22 – 7.13 (m, 2H), 5.06 – 4.97 (m, 1H), 4.89 – 4.83 (m, 1H), 4.27 – 4.17 (m, 1H), 4.15 – 4.01 (m, 2H), 3.72 (s, 3H), 3.71 (s, 3H), 3.57 (s, 3H), 3.19 (dd, *J* = 13.4, 3.1 Hz, 1H), 2.89 – 2.71 (m, 2H), 2.69 – 2.57 (m, 3H), 1.70 (s, 3H), 1.62 (s, 3H); **¹³C NMR** (101 MHz, CDCl₃) δ 171.8, 171.7, 156.1, 144.7, 136.0, 135.5, 129.3, 129.1, 127.4, 117.6, 104.7, 67.0, 58.0, 57.6, 56.9, 52.6, 52.5, 38.4, 31.7, 28.7, 26.2, 18.0; **HRMS** (ESI⁺): *m/z*: calculated for C₂₄H₃₁NNaO₇: 468.1993 [M+Na]⁺; found: 468.1992; **LC-MS** (InfinityLab Poroshell 120 EC-C18 (2.1x50mm, 1.9 μm), Reverse phase 50% ACN, 0.5 mL/min): 1.909 min (92), 2.093 min (8).

Procedure S for gold(I)-catalyzed alkoxy cyclization of 1,6-enyne 1.136 to afford 1.137



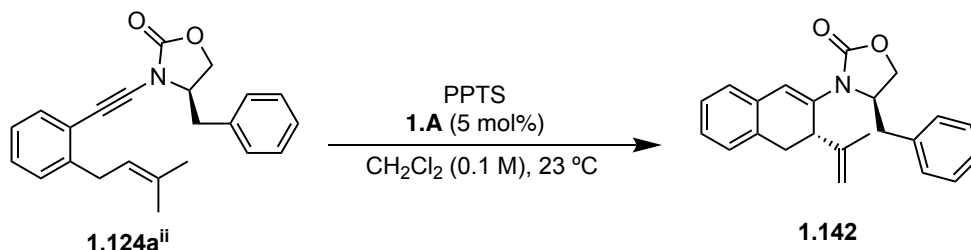
(*R*)-4-Benzyl-3-((*R*)-3-(2-methoxypropan-2-yl)-1-tosyl-1,2,3,6-tetrahydropyridin-4-yl)oxazolidin-2-one (1.137)



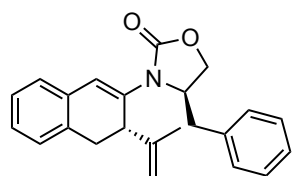
1,6-enyne **1.136** was weighted in a microwave vial furnished with a magnet. Then, this vial was introduced in the glovebox together with a second vial containing [JohnPhosAu(MeCN)SbF₆] (5 mol%). The substrate was dissolved in MeOH while the catalyst in CH₂Cl₂ (final volume = 0.1 M solution of 3:1 MeOH:CH₂Cl₂). Then, the vials were sealed, taken out of the glovebox and brought to -20 °C. Finally, the catalyst solution was added to the substrate one and the resulting mixture was left to stir at -20 °C for 24 h. The reaction mixture was then quenched with few drops of triethylamine, and the solvent evaporated under reduced pressure. Crude *dr* = 98:2. Given the fast decomposition in silica, the yield was calculated by ¹H NMR integration to be 89% by internal standard (1 equiv of 1,1,2,2-tetrachloroethane, 13.1 μl, 0.124 mmol) addition to the crude. The characterisation was also performed on the crude of **1.137**. **¹H NMR** (400 MHz, CDCl₃) δ 7.76 – 7.65 (m, 2H), 7.36 – 7.21 (m, 5H), 7.16 – 7.08 (m, 2H), 5.07 (tp, *J* = 6.8, 1.4 Hz, 1H), 4.90 (t, *J* = 7.1 Hz, 1H), 4.22 (t, *J* = 7.7 Hz, 1H), 4.11 – 4.02 (m, 1H), 4.04 – 3.87 (m, 2H), 3.82 (d, *J* = 6.9 Hz, 2H), 3.56 (s, 3H), 3.15 – 3.05 (m, 2H), 2.57 (dd, *J* = 13.5, 9.5 Hz, 1H), 2.37 (s, 3H), 1.64 (d, *J* = 1.4 Hz, 3H), 1.62 (d, *J* = 1.4 Hz, 3H); **¹³C NMR** (101 MHz, CDCl₃) δ 155.7, 145.0, 143.2, 137.4, 136.9, 135.1, 129.7, 129.2, 129.1, 127.4, 119.1, 104.3, 66.9,

57.5, 56.7, 46.5, 45.1, 42.0, 38.4, 25.9, 21.5, 17.9; **HRMS** (ESI+): m/z : calculated for $C_{26}H_{32}N_2NaO_5S$: 507.1924 $[M+Na]^+$; found: 507.1927; **LC-MS** (InfinityLab Poroshell 120 EC-C18 (2.1x50mm, 1.9 μ m), Reverse phase 50% ACN, 0.5 mL/min): 2.314 min (98), 2.460 min (2); $[\alpha]_D^{26}$ ($c = 0.21$ in $CHCl_3$) = -5.64 $^\circ$.

Procedure T for gold(I)-catalyzed cyclization-elimination of 1.124aⁱⁱ to afford 1.142

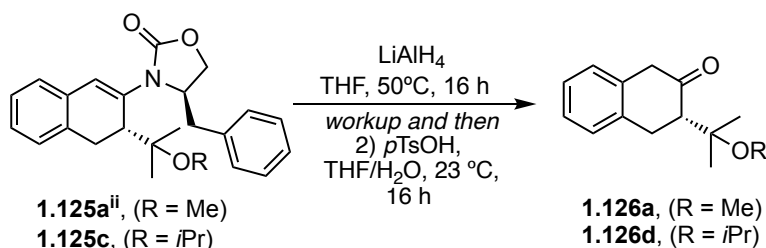


(R)-4-Benzyl-3-((S)-3-(prop-1-en-2-yl)-3,4-dihydronaphthalen-2-yl)oxazolidin-2-one (1.142)



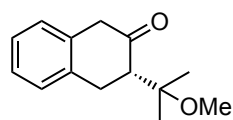
1,6-enyne **1.124aⁱⁱ** and catalyst **1.A** (5 mol%) were weighed in a microwave vial furnished with a magnet. Then, this vial was introduced in the glovebox where a solution of dry pyridinium *p*-toluenesulfonate (1 equiv) in CH_2Cl_2 (0.1 M) was prepared and added to it. The vial was sealed and the mixture was left to stir at 23 $^\circ C$ for 16 h. The reaction mixture was then quenched with few drops of triethylamine, and the solvent evaporated under reduced pressure. Crude *dr* = 91:9. After column chromatography (4:1 CH_2Cl_2 :cyclohexane to pure CH_2Cl_2) product **1.142** was isolated as a transparent oil (11.3 mg, 0.033 mmol, 65%) with 90:10 *dr*. **¹H NMR** (400 MHz, $CDCl_3$) δ 7.35 (tt, $J = 6.7, 1.1$ Hz, 2H), 7.31 – 7.27 (m, 1H), 7.22 – 7.18 (m, 2H), 7.16 – 7.05 (m, 4H), 6.67 (s, 1H), 4.79 – 4.77 (m, 1H), 4.72 (t, $J = 1.6$ Hz, 1H), 4.44 (ddt, $J = 9.6, 8.7, 4.4$ Hz, 1H), 4.24 (t, $J = 8.4$ Hz, 1H), 4.10 (dd, $J = 8.8, 4.7$ Hz, 1H), 3.79 – 3.72 (m, 1H), 3.27 (dd, $J = 13.9, 4.1$ Hz, 1H), 3.18 (dd, $J = 16.1, 8.2$ Hz, 1H), 2.93 (dd, $J = 16.1, 2.4$ Hz, 1H), 2.71 (dd, $J = 13.8, 9.5$ Hz, 1H), 1.67 (dd, $J = 1.5, 0.8$ Hz, 3H); **¹³C NMR** (101 MHz, $CDCl_3$) δ 155.3, 144.0, 135.7, 135.6, 133.2, 132.3, 129.3, 129.2, 127.6, 127.5, 127.3, 126.7, 126.4, 118.5, 112.5, 66.3, 56.7, 41.9, 38.6, 33.5, 20.5; **HRMS** (ESI+): m/z : calculated for $C_{23}H_{23}NNaO_2$: 368.1621 $[M+Na]^+$; found: 368.1619; **LC-MS** (InfinityLab Poroshell 120 EC-C18 (2.1x50mm, 1.9 μ m), Reverse phase 50% ACN, 0.5 mL/min): 2.232 min (90), 3.179 min (10); $[\alpha]_D^{26}$ ($c = 0.275$ in $CHCl_3$) = +191 $^\circ$.

General procedure U for reduction-hydrolysis sequence of 1.125aⁱⁱ and 1.125c to afford 1.126a,d



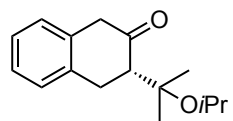
To a solution of **1.125** in dry THF (0.1 M) closed with a septum under argon, at 0 °C, lithium aluminium hydride (1 M in THF, 5 equiv) was added.⁵⁸ After 1 h at room temperature, the solution was stirred at 55 °C for 16 hours, then water, 10% aqueous sodium hydroxide, and again water (1:2:2, where the first volume of water in μl corresponds to the quantity of substrate in μmol) were added successively at 0 °C. After being stirred at rt for 30 min, the mixture presents a dark solid (sticks to the flask). More water was added and the suspension was extracted with dichloromethane (x3). The combined organic layers were washed with brine, and concentrated under reduced pressure. THF:H₂O (2:1, 0.1 M) were then added to the mixture, together with *p*-toulensulfonic acid hydrate (1.2 equiv) and the mixture was left to stir for 16 hour at 23 °C. More water was added to the mixture which was then extracted with DCM (x3) and washed with brine. Na₂SO₄ was added and the solvent evaporated. The crude was purified by column chromatography in basic alumina (2:1 cyclohexane: CH₂Cl₂). Due to decomposition of the products in CDCl₃ over time, the NMR were recorded in C₆D₆.

(S)-3-(2-Methoxypropan-2-yl)-3,4-dihydronaphthalen-2(1H)-one (1.126a)



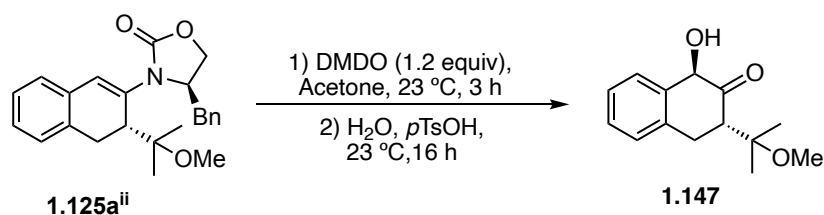
Compound **1.126a** was synthesized following the general procedure. ¹H NMR crude yield using trichloroethylene as internal standard: 65%. After column chromatography in basic alumina the product was isolated as a yellow oil (13.1 mg, 0.060 mmol, 40%) with 96:4 *er*. ¹H NMR (400 MHz, C₆D₆) δ 7.08 – 6.94 (m, 3H), 6.75 (d, *J* = 7.2 Hz, 1H), 3.39 (d, *J* = 17.4 Hz, 1H), 3.28 (d, *J* = 17.5 Hz, 1H), 2.95 – 2.88 (m, 2H), 2.88 (s, 3H), 2.21 (dd, *J* = 9.1, 7.7 Hz, 1H), 1.26 (s, 3H), 1.18 (s, 3H); ¹³C NMR (101 MHz, C₆D₆) δ 208.3, 137.5, 134.2, 128.4, 128.2, 127.9, 126.9, 76.2, 54.3, 48.6, 47.3, 30.5, 24.0, 22.2; HRMS (ESI+): *m/z*: calculated for C₁₄H₁₈NaO₂: 241.1199 [M+Na]⁺; found: 241.1202; SFC (IB N-3 (100x3 mm, 3 μm), CO₂:MeOH 95:5, 1.2 mL/min, 25 °C, BPR 150 bar; 210 nm): 1.011 min (4), 1.216 min (96); [α]_D²⁶ (*c* = 0.2 in CHCl₃) = -77.1 °.

(S)-3-(2-Isopropoxypropan-2-yl)-3,4-dihydronaphthalen-2(1H)-one (1.126d)

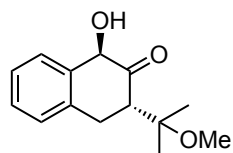


Compound **1.126d** was synthesized following the general procedure. After column chromatography in basic alumina the product was isolated as a yellow oil (13.6 mg, 0.055 mmol, 41%) with 96:4 *er*. ¹H NMR (400 MHz, C₆D₆) δ 7.08 – 6.96 (m, 3H), 6.80 – 6.73 (m, 1H), 3.53 – 3.47 (m, 1H), 3.47 – 3.39 (m, 1H), 3.34 – 3.27 (m, 1H), 3.08 – 2.88 (m, 2H), 2.15 (dd, *J* = 10.3, 6.2 Hz, 1H), 1.23 (s, 3H), 1.19 (s, 3H), 0.99 (d, *J* = 6.1 Hz, 3H), 0.94 (d, *J* = 6.1 Hz, 3H); ¹³C NMR (101 MHz, C₆D₆) δ 208.3, 137.6, 134.6, 127.9, 127.9, 127.7, 126.9, 76.8, 63.1, 55.9, 47.5, 31.0, 25.2, 25.1, 25.0, 23.2; HRMS (ESI+): *m/z*: calculated for C₁₆H₂₂NaO₂: 269.1512 [M+Na]⁺; found: 269.1507; SFC (IC-3 (100x3 mm, 3 μm), CO₂:MeOH 95:5, 1.2 mL/min, 25 °C, BPR 150 bar; 210 nm): 0.902 min (4), 1.089 min (96); [α]_D²⁶ (*c* = 0.2 in CHCl₃) = -60.8 °.

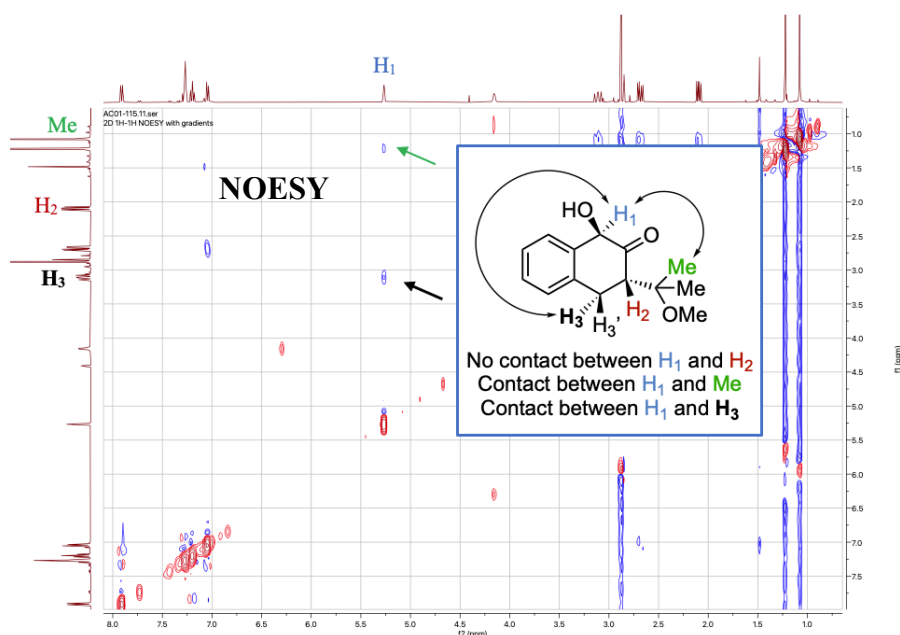
Procedure V for epoxidation-hydrolysis sequence of **1.125aⁱⁱ** to afford **1.147**

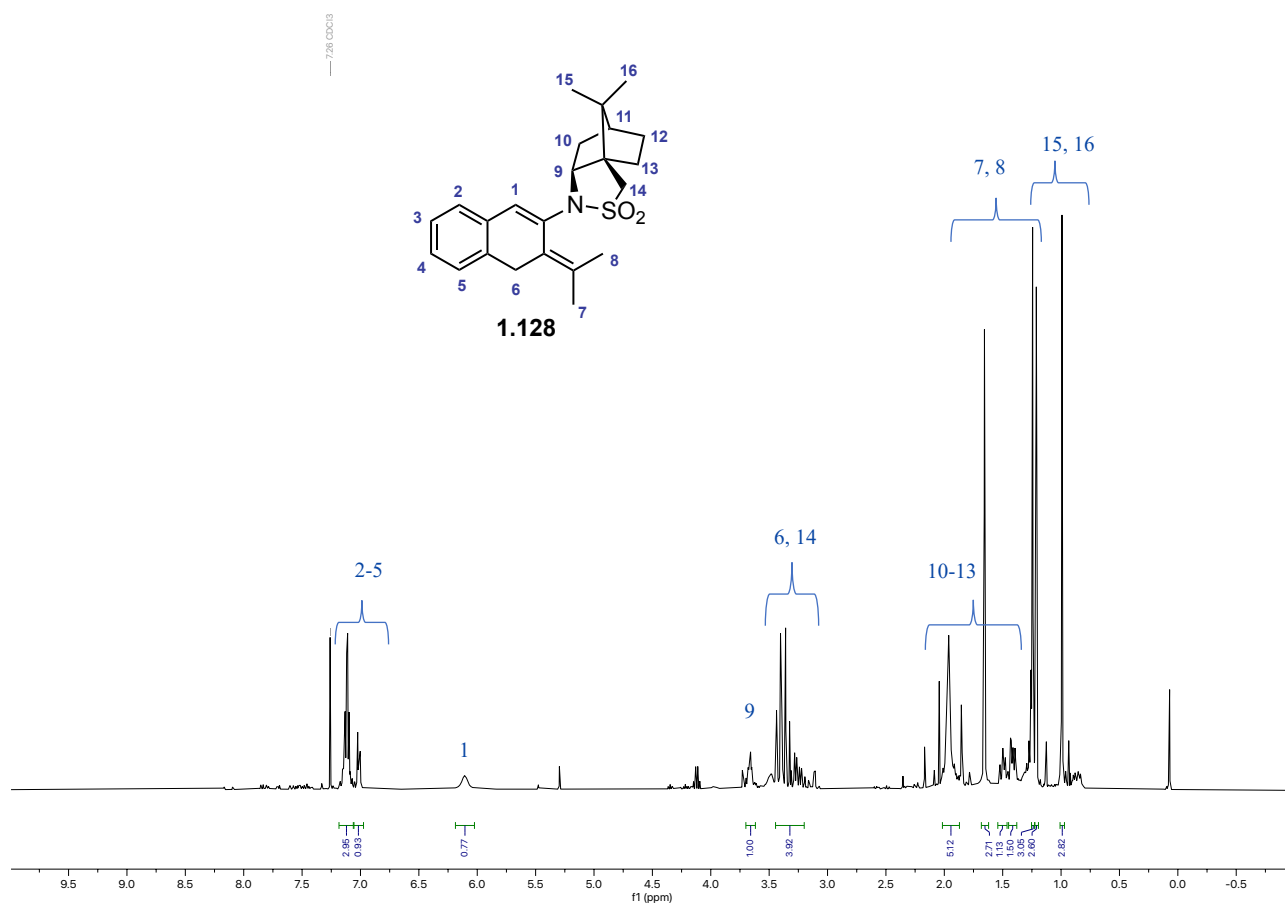
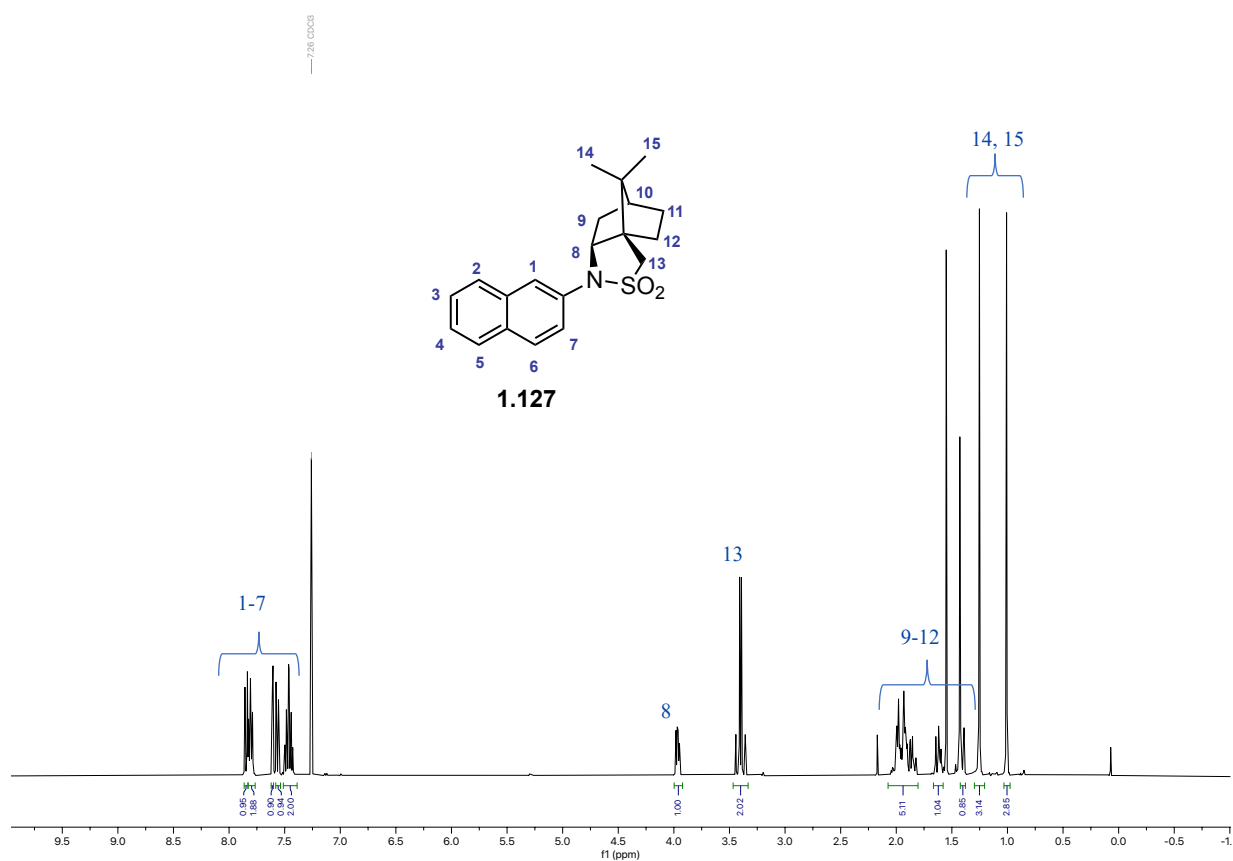


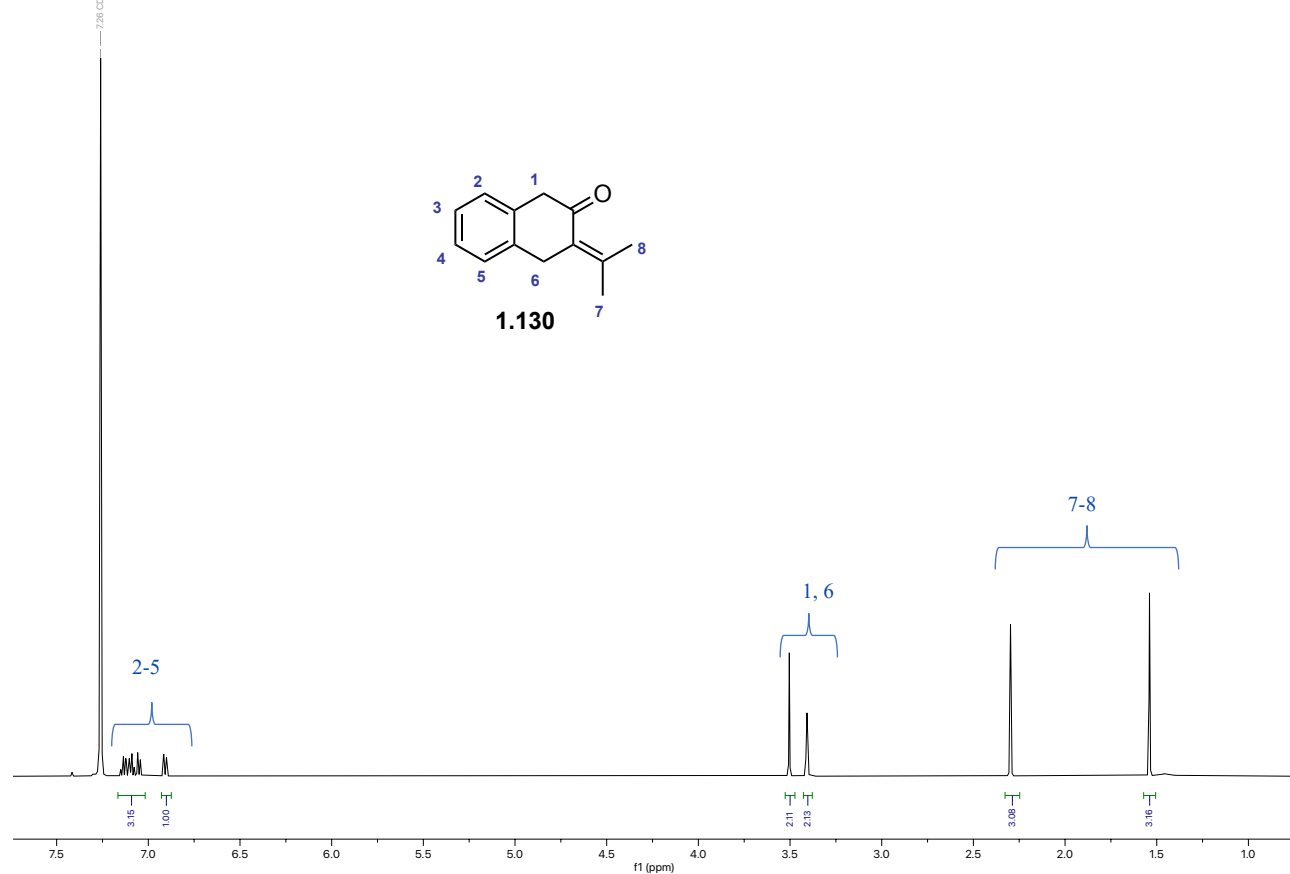
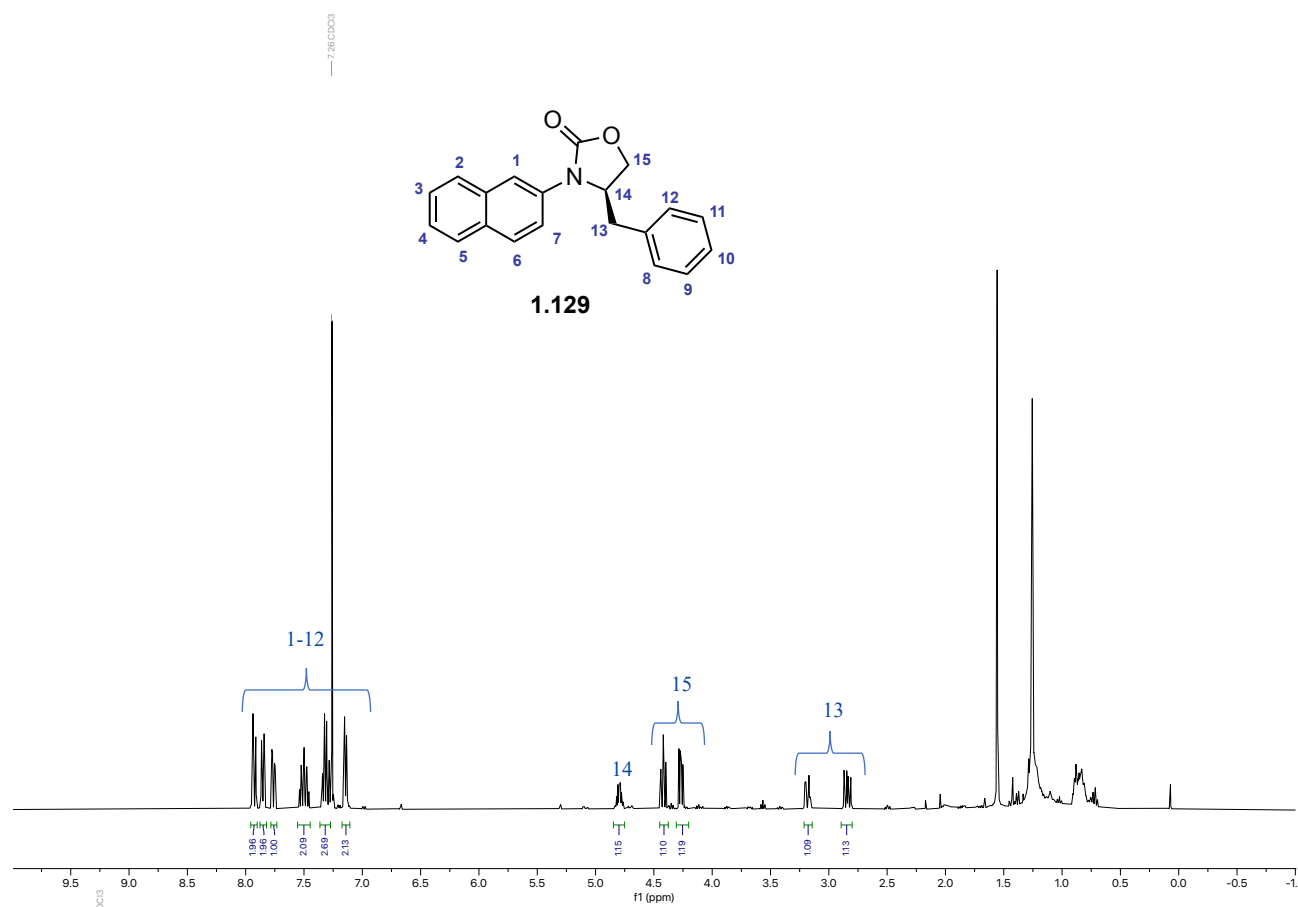
(1*R*,3*S*)-1-Hydroxy-3-(2-methoxypropan-2-yl)-3,4-dihydronaphthalen-2(1*H*)-one (1.147)

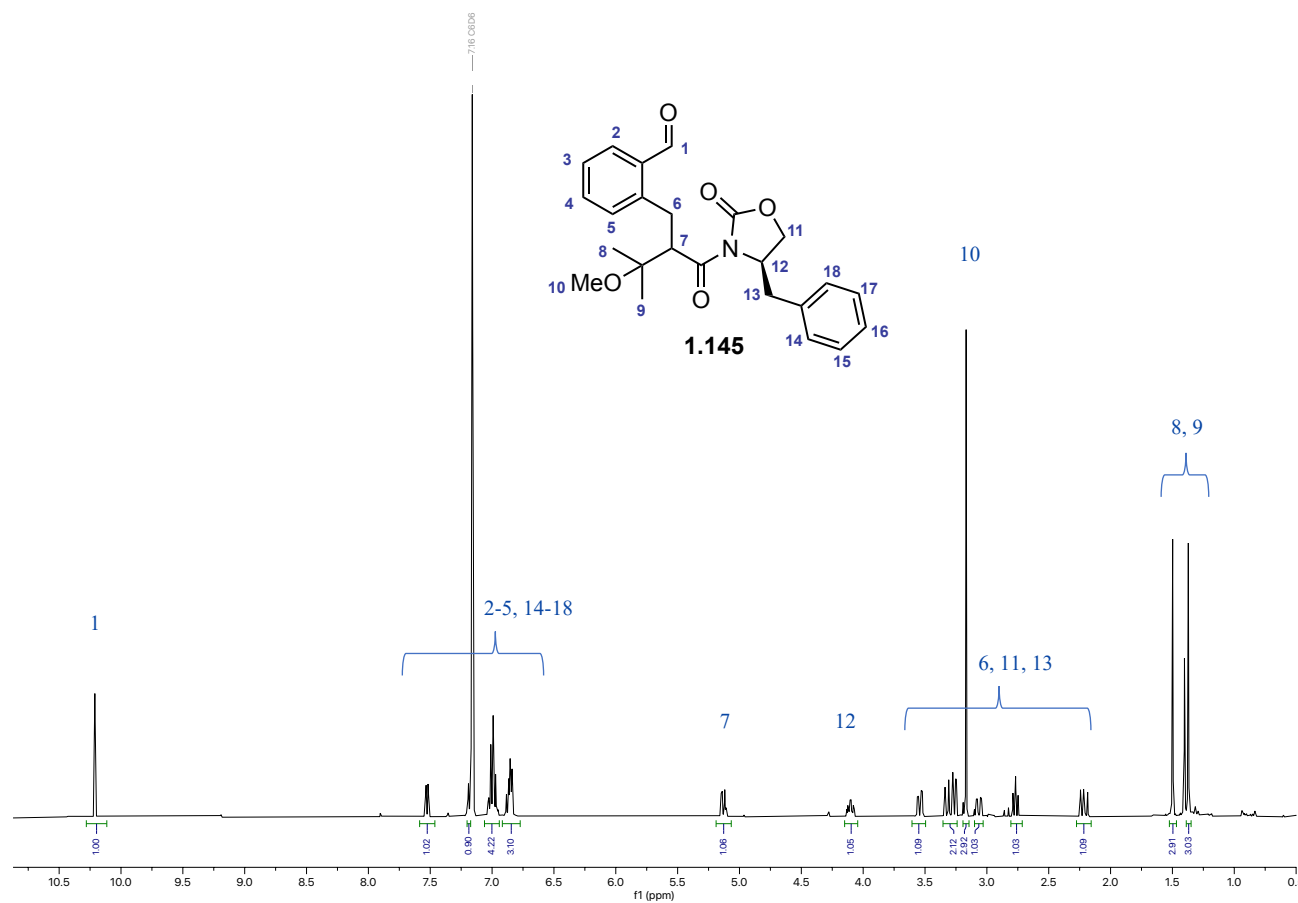
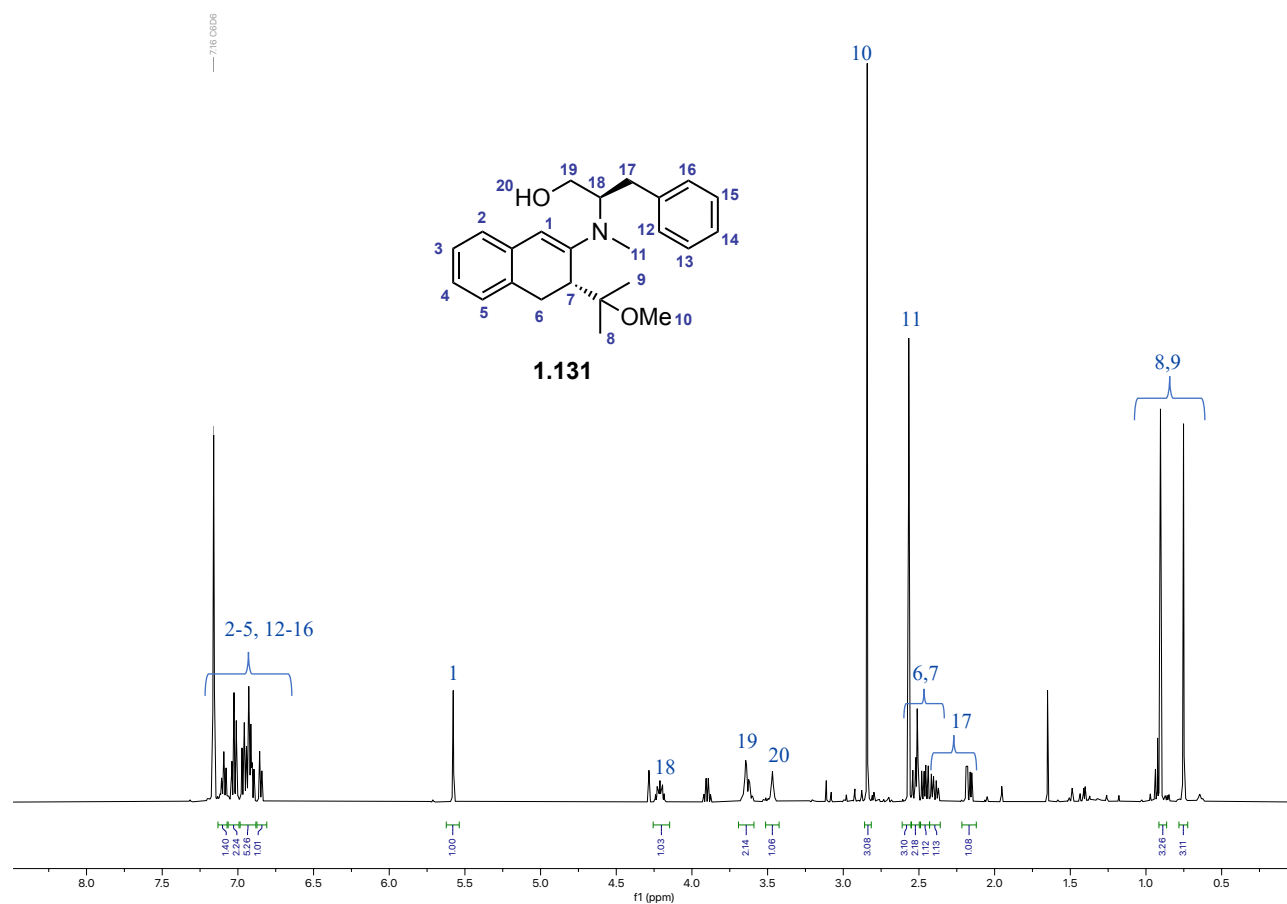


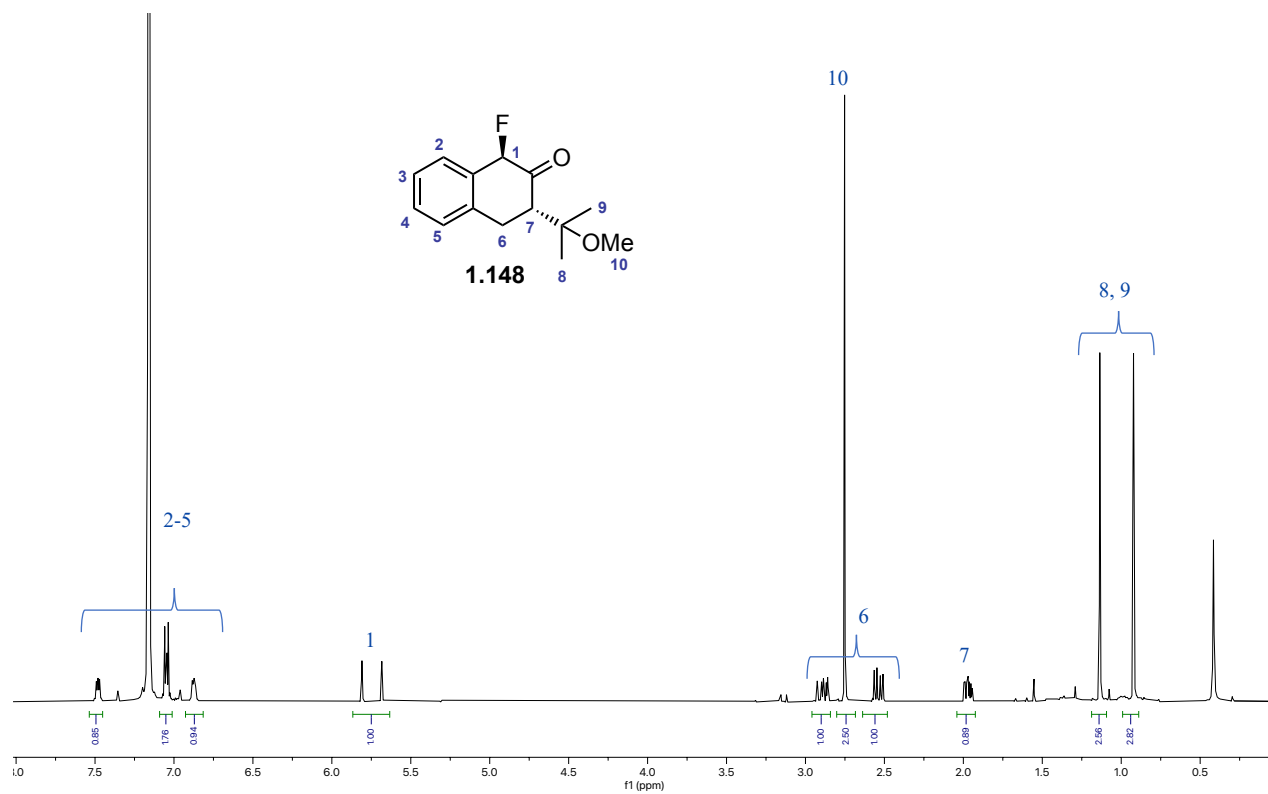
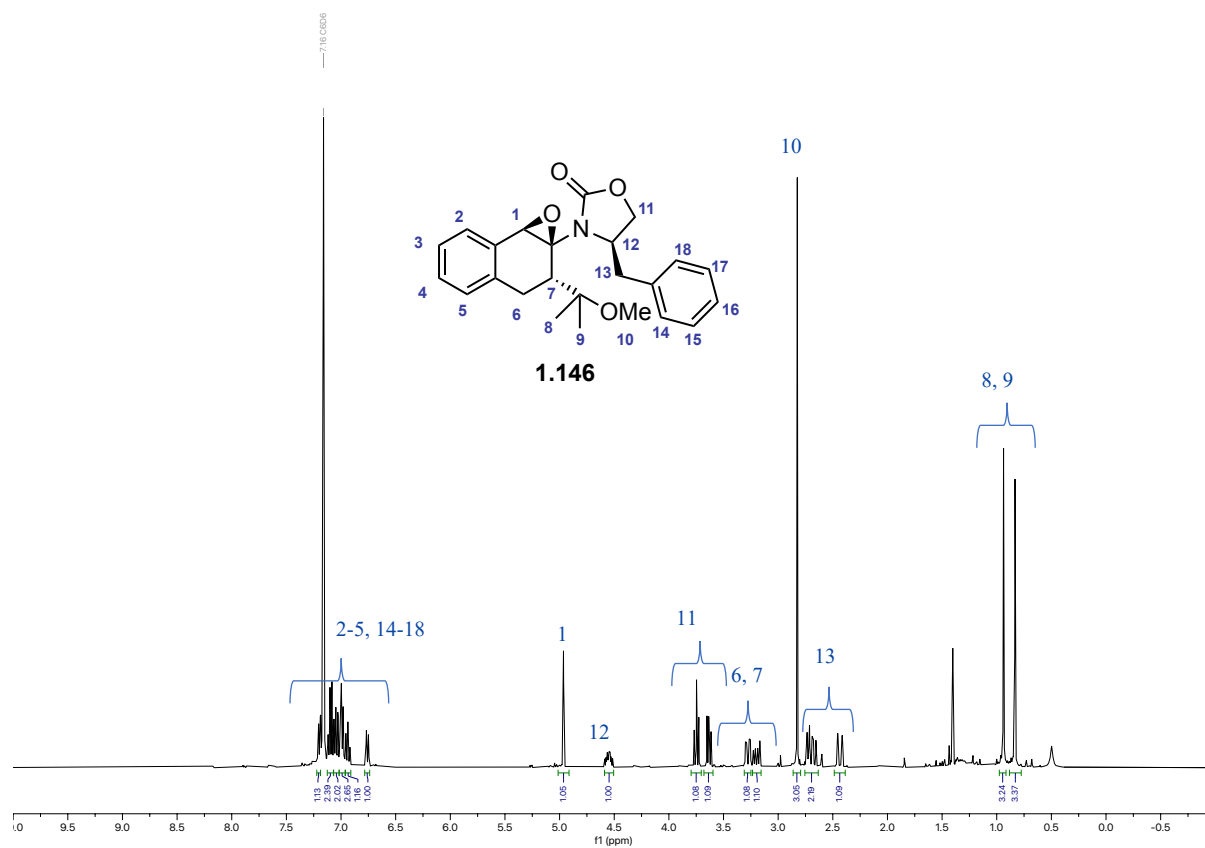
A microwave vial containing **1.125aⁱⁱ** and a stirrer bar was sealed and put under Ar atmosphere. A cold (stored at -20 °C) DMDO (3,3-dimethyldioxirane) solution in acetone (0.065 molar, 1.2 equiv)⁷² was added to the vial at 0 °C. The reaction was then left to stir at 23 °C. After 3 h water was added (half the volume of the acetone solution) followed by *p*-toluenesulfonic acid hydrate (1.2 equiv). The reaction was left to stir at 23 °C for 16 h, then water was added, the organic phase was extracted 3 times with DCM and washed with brine, dried over Na₂SO₄ and finally the solvent was evaporated under reduced pressure. ¹H NMR crude yield using trichloroethylene as internal standard: 77%. Crude *dr* = 84:16. After column chromatography in silica (7:1 cyclohexane:EtOAc) the product was isolated as a yellow oil (31.6 mg, 0.135 mmol, 54%) with 97:3 *dr* and 95:5 *er*. The configuration of the second chiral centre was assigned through NOESY. ¹H NMR (400 MHz, C₆D₆) δ 7.84 – 7.75 (m, 1H), 7.21 – 7.14 (m, 1H), 7.09 (tt, *J* = 7.4, 1.3 Hz, 1H), 7.01 – 6.88 (m, 1H), 5.16 (d, *J* = 2.8 Hz, 1H), 4.05 (d, *J* = 4.4 Hz, 1H), 3.06 – 2.94 (m, 1H), 2.77 (s, 3H), 2.58 (dd, *J* = 15.1, 6.4 Hz, 1H), 1.99 (dd, *J* = 11.2, 6.4 Hz, 1H), 1.11 (d, *J* = 0.7 Hz, 3H), 0.97 (s, 3H); ¹³C NMR (101 MHz, C₆D₆) δ 210.5, 137.0, 135.0, 127.6, 127.1, 124.1, 76.8, 76.4, 51.9, 49.1, 28.9, 23.3, 22.9; HRMS (ESI⁺): *m/z*: calculated for C₁₄H₁₈NaO₃: 257.1148 [M+Na]⁺; found: 257.1154; SFC (IC-3 (100x3 mm, 3 μm), CO₂:EtOH 90:10, 1.2 mL/min, 25 °C, BPR 150 bar; 210 nm): 1.277 min (95), 1.425 min (5). [α]_D²⁶ (*c* = 0.1 in CHCl₃) = -71.5 °.



Chiral auxiliary removal in products 1.125 and further diversification trials

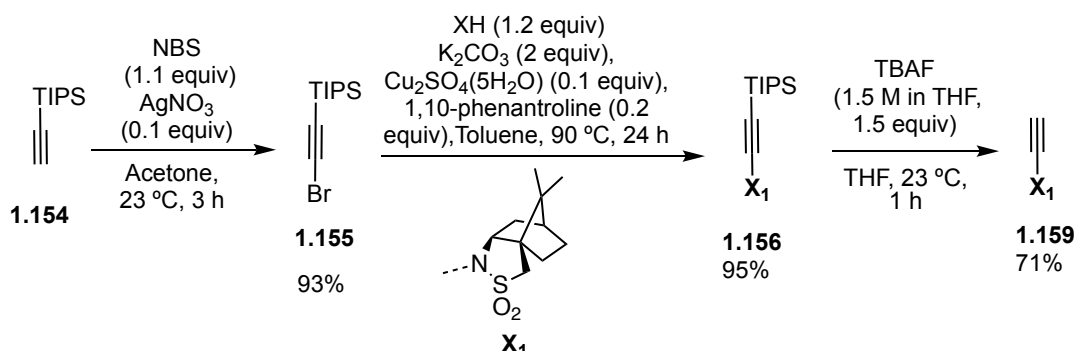




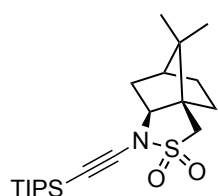


Procedure W for the synthesis of terminal ynamide 2.116

1.160^{Error! Bookmark not defined.} and **1.161**¹⁹ were reported in literature and **1.159** was synthesized following a modified literature procedure.^{Error! Bookmark not defined.}



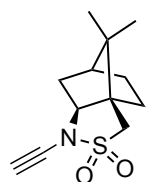
(3a*R*,6*S*,7a*S*)-8,8-Dimethyl-1-((triisopropylsilyl)ethynyl)hexahydro-3*H*-3a,6-methanobenzo[*c*]isothiazole 2,2-dioxide (1.156)



To a dried flask was added (1*R*)-(+)-2,10-Camphorsultam (577 mg, 2.68 mmol), copper(II) sulfate pentahydrate (55.7 mg, 0.223 mmol), 1,10-phenanthroline hydrate (88.5 mg, 0.446 mmol) and potassium carbonate (617 mg, 4.46 mmol), and this mixture was subsequently treated with Toluene (2.20 mL) and (bromoethynyl)triisopropylsilane (583 mg, 2.23 mmol). The reaction mixture was left under Nitrogen atmosphere for 24 hours at 85 °C. After completion, the crude reaction mixture was cooled to room temperature, filtered through Celite washing it with EtOAc, and concentrated in vacuo. Purification of the crude residue using silica column (10:1 cyclohexane:EtOAc) gave the pure ynamide a white solid after solvent evaporation (836 mg, 2.23 mmol, 95%).

¹H NMR (500 MHz, CDCl₃) δ 3.60 (dd, *J* = 8.2, 4.2 Hz, 1H), 3.23 (s, 2H), 2.23 (dtd, *J* = 13.4, 4.0, 2.8 Hz, 1H), 1.98 – 1.82 (m, 3H), 1.75 (dd, *J* = 13.4, 8.2 Hz, 1H), 1.46 – 1.38 (m, 1H), 1.36 – 1.28 (m, 1H), 1.10 (s, 3H), 1.06 (d, *J* = 1.9 Hz, 21H), 0.93 (s, 3H). ¹³C NMR (126 MHz, CDCl₃) δ 90.9, 71.9, 67.0, 51.5, 50.1, 48.1, 44.6, 34.3, 31.7, 27.2, 20.2, 20.1, 18.8 (d, *J* = 1.9 Hz), 11.4. HRMS (ESI⁺): *m/z*: calculated for C₂₁H₃₇NNaO₂Si: 418.2206 [M+Na]⁺; found: 418.2207.

(3a*R*,6*S*,7a*S*)-1-Ethynyl-8,8-dimethylhexahydro-3*H*-3a,6-methanobenzo[*c*]isothiazole 2,2-dioxide (1.159)

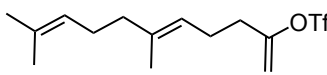


To a THF (30 mL) solution of **1.156** (828 mg, 2.09 mmol) was added TBAF (821 mg, 3.14 mL, 1 molar, 3.14 mmol) at 0 °C, and the resulting mixture was stirred at 23 °C for 1 hour. The solvent was evaporated and then water was added to the crude which was then extracted with EtOAc (x 2). The organic layer was then purified by column chromatography on a silica column (5:1 cyclohexane:EtOAc). The solvent was evaporated to give a white solid (358 mg, 1.50 mmol, 71.5 %). ¹H NMR (400 MHz, CDCl₃) δ 3.59 (dd, *J* = 8.2, 4.2 Hz, 1H), 3.25 (s, 2H), 2.80 (s, 1H), 2.21 (dtd, *J* = 13.5, 4.0, 2.7 Hz, 1H), 1.98 – 1.82 (m, 3H), 1.77 (dd, *J* = 13.4,

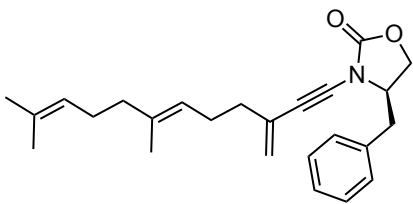
8.2 Hz, 1H), 1.49 – 1.37 (m, 1H), 1.36 – 1.27 (m, 1H), 1.09 (s, 3H), 0.93 (s, 3H). ^{13}C NMR (101 MHz, CDCl_3) δ 70.9, 66.9, 61.4, 51.4, 49.9, 48.1, 44.5, 34.4, 31.7, 27.1, 20.2, 20.0. HRMS (ESI+): m/z : calculated for $\text{C}_{12}\text{H}_{17}\text{NNaO}_2\text{S}$: 262.0872 $[\text{M}+\text{Na}]^+$; found: 262.0877

Towards the total synthesis of *hernandulcin*.

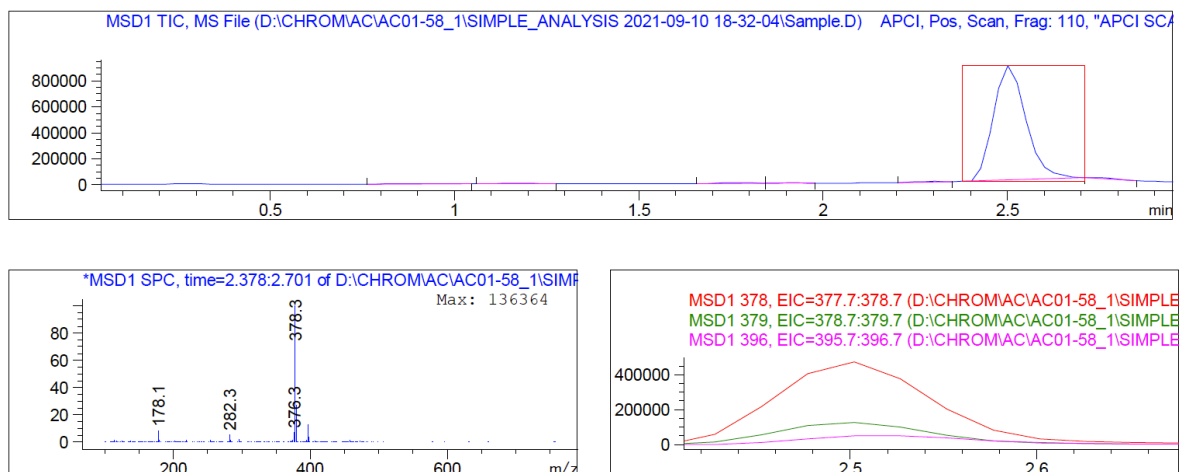
(E)-6,10-Dimethylundeca-1,5,9-trien-2-yl trifluoromethanesulfonate (1.164)

 **1.164** was synthesized following a modified literature procedure:⁸⁶ a solution of (*E*)-geranylacetone (189 mg, 0.97 mmol) in THF (0.75 mL) was added to a solution of potassium bis(trimethylsilyl)amide in toluene (252 mg, 1.26 mmol) in THF (2.00 mL) at -78 °C and the resulting solution was stirred at -78 °C for 1 h. A solution of *N*-(2-pyridyl)triflimide (497 g, 1.26 mmol) in THF (2.00 mL) was added slowly and the resulting mixture was stirred for 1 h. The mixture was quenched with NH_4Cl and warmed to 23 °C. The aqueous layer was extracted with *n*-hexane (3x 20 mL) and the combined organic layers were washed with water and brine, dried over Na_2SO_4 , filtered and all volatiles were removed in vacuo. The resulting triflate was used in the next step without any further purification. ^1H NMR (500 MHz, CDCl_3) δ 5.12 – 5.03 (m, 3H), 4.93 (dt, $J = 3.5, 1.1$ Hz, 1H), 2.41 – 2.34 (m, 2H), 2.31 – 2.17 (m, 2H), 2.09 – 2.04 (m, 2H), 2.02 – 1.92 (m, 2H), 1.69 – 1.66 (m, 3H), 1.62 – 1.61 (m, 3H), 1.60 (s, 3H).

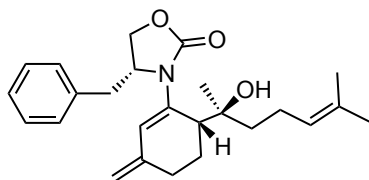
(R,E)-4-Benzyl-3-(7,11-dimethyl-3-methylenedodeca-6,10-dien-1-yn-1-yl)oxazolidin-2-one (1.165)⁵⁶

 (*R*)-4-benzyl-3-ethynyloxazolidin-2-one (235 mg, 1.17 mmol) and diisopropylamine (985 mg, 9.73 mmol) were added to a magnetically stirred mixture of **1.164** (318 mg, 0.97 mmol), copper(I) iodide (9.27 mg, 0.049 mmol), and $\text{PdCl}_2(\text{PPh}_3)_2$ (27.3 mg, 0.039 mmol) in anhydrous THF (5 mL) under nitrogen atmosphere. After stirring at 20 °C overnight, the mixture was diluted with EtOAc (30 mL) and filtered through silica. The organic phase was then washed with brine and dried over anhydrous Na_2SO_4 , filtered, and concentrated in vacuo. The product was purified by column chromatography (10:1 cyclohexane: EtOAc). **1.165** was isolated as a transparent oil (84 mg, 0.22 mmol, 23% over two steps). ^1H NMR (400 MHz, CDCl_3) δ 7.37 – 7.32 (m, 2H), 7.32 – 7.28 (m, 1H), 7.21 (dt, $J = 7.9, 1.6$ Hz, 2H), 5.34 (t, $J = 2.2$ Hz, 1H), 5.24 (d, $J = 1.8$ Hz, 1H), 5.18 – 5.04 (m, 2H), 4.38 – 4.21 (m, 2H), 4.13 (ddd, $J = 8.0, 5.3, 1.8$ Hz, 1H), 3.23 (dt, $J = 13.9, 3.2$ Hz, 1H), 2.95 (ddd, $J = 13.9, 8.1, 3.5$ Hz, 1H), 2.24 (q, $J = 6.0$ Hz, 4H), 2.06 (d, $J = 3.2$ Hz, 3H), 2.03 – 1.93 (m, 1H), 1.71 – 1.65 (m, 6H), 1.60 (d, $J = 1.3$ Hz, 3H). ^{13}C NMR and HRMS acquisition were not possible since the compound decomposed overnight.

HPLC-MS

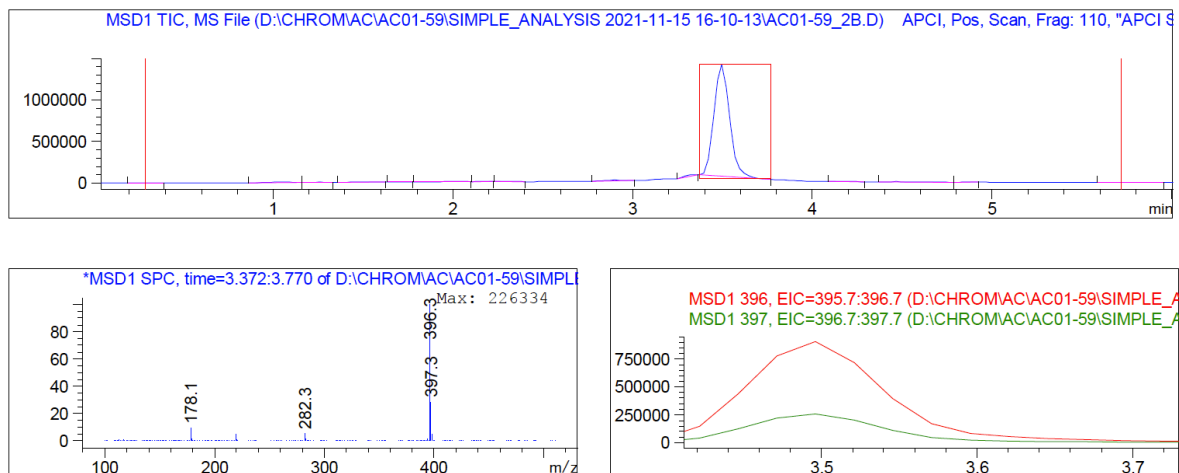


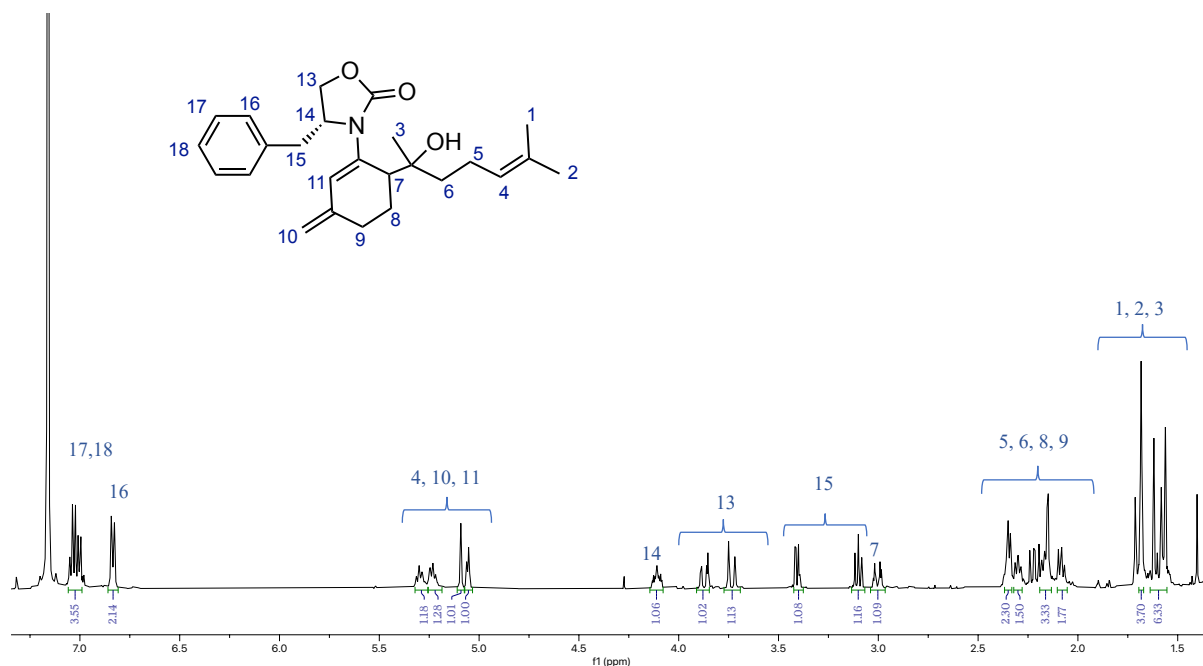
(R)-4-Benzyl-3-((R)-6-((S)-2-hydroxy-6-methylhept-5-en-2-yl)-3-methylenecyclohex-1-en-1-yl)oxazolidin-2-one (1.166a)



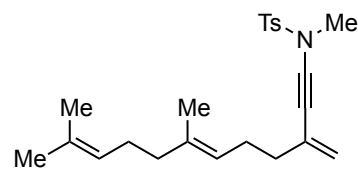
To a solution of **1.165** (21.0 mg, 0.056 mmol) in water (0.25 mL) and acetone (0.50 mL), catalyst **1.A** (2.15 mg, 0.0028 mmol) was added and the reaction was stirred at 60 °C for 3 hours. Three drops of TEA were then added, the solvent was evaporated and the crude reaction mixture was purified by column chromatography (7:1 cyclohexane:EtOAc). Among the different fraction recovered, what it is supposed to be the major diastereomer, was recovered as a transparent oil (5.5 mg, 0.014 mmol, 25%) still presenting traces of impurities. ¹H NMR (500 MHz, C₆D₆) δ 7.07 – 6.96 (m, 3H), 6.87 – 6.81 (m, 2H), 5.34 – 5.26 (m, 1H), 5.26 – 5.20 (m, 1H), 5.11 – 5.08 (m, 1H), 5.07 – 5.03 (m, 1H), 4.11 (ddt, J = 9.6, 7.8, 3.0 Hz, 1H), 3.87 (dd, J = 15.7, 3.4 Hz, 1H), 3.73 (d, J = 15.7 Hz, 1H), 3.41 (dd, J = 9.0, 2.8 Hz, 1H), 3.10 (dd, J = 9.1, 7.9 Hz, 1H), 3.00 (dt, J = 13.3, 3.4 Hz, 1H), 2.34 (d, J = 5.4 Hz, 3H), 2.33 – 2.26 (m, 1H), 2.20 – 2.13 (m, 3H), 2.12 – 2.05 (m, 1H), 1.68 (m, 3H), 1.63 – 1.55 (m, 6H).

HPLC-MS





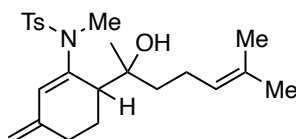
(E)-N-(7,11-Dimethyl-3-methylenedodeca-6,10-dien-1-yn-1-yl)-N,4-dimethylbenzenesulfonamide (1.167)⁵⁶



The same procedure used to synthesize **1.165** was applied for **1.167**, changing the base for piperidine (2:1 piperidine:THF, 0.33 M). The reaction crude was purified by column chromatography on silica (15:1 *n*-pentane:EtOAc) to afford **1.166** as a brown oil (351 mg, 0.91 mmol, 46% over two steps).

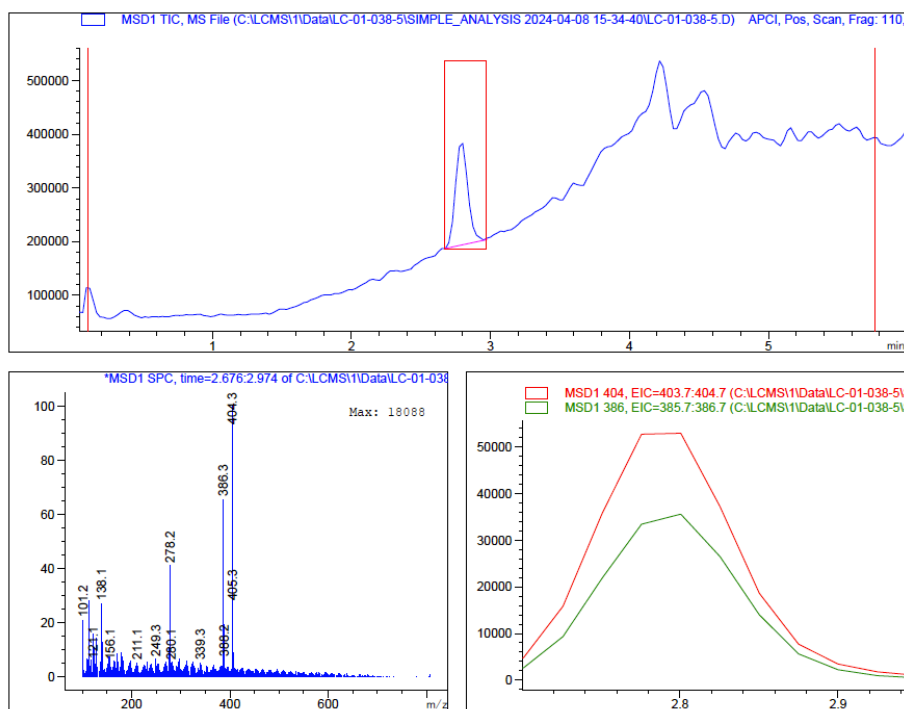
¹H NMR (500 MHz, CDCl₃) δ 7.82 – 7.76 (m, 2H), 7.38 – 7.32 (m, 2H), 5.17 (d, *J* = 1.9 Hz, 1H), 5.12 (dt, *J* = 1.9, 1.1 Hz, 1H), 5.09 (dddt, *J* = 6.9, 5.5, 2.9, 1.5 Hz, 2H), 3.09 (s, 3H), 2.45 (s, 3H), 2.23 – 2.11 (m, 4H), 2.07 (q, *J* = 7.4 Hz, 2H), 1.98 (dd, *J* = 9.1, 6.1 Hz, 2H), 1.68 (q, *J* = 1.2 Hz, 3H), 1.60 (d, *J* = 1.4 Hz, 6H). ¹³C NMR (126 MHz, CDCl₃) δ 144.8, 136.0, 133.4, 131.5, 130.8, 129.9, 128.0, 124.4, 123.3, 119.3, 84.1, 69.9, 39.8, 39.4, 37.7, 26.8, 26.8, 25.8, 21.8, 17.8, 16.2. HRMS (ESI⁺): *m/z*: calculated for C₂₃H₃₁NNaO₂S : 408.1968 [M+Na]⁺; found: 408.1966.

N-(6-(2-hydroxy-6-methylhept-5-en-2-yl)-3-methylenecyclohex-1-en-1-yl)-N,4-dimethylbenzenesulfonamide (1.168)

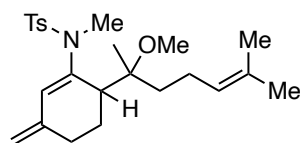


¹H NMR (400 MHz, CDCl₃) δ 7.64 (d, *J* = 8.2 Hz, 2H), 7.31 (d, *J* = 8.0 Hz, 3H), 5.52 (s, 1H), 5.12 (m, 2H), 4.81 (s, 1H), 4.66 (s, 1H), 3.06 (m, 1H), 2.95 (s, 3H), 2.58 (t, *J* = 14.6 Hz, 1H), 2.45 (s, 3H), 2.40 (m, 1H), 2.29 – 2.21 (m, 1H), 2.22 – 2.12 (m, 2H), 2.11 – 1.98 (m, 3H), 1.69 (s, 3H), 1.63 (s, 3H), 1.36 (s, 3H).

HPLC-MS

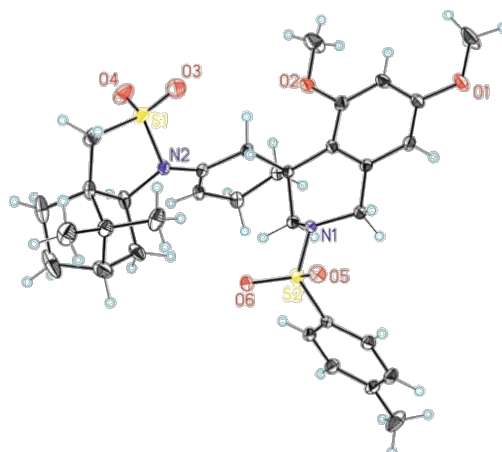


***N*-((*R*)-6-((*S*)-2-Methoxy-6-methylhept-5-en-2-yl)-3-methylenecyclohex-1-en-1-yl)-*N*,4-dimethylbenzenesulfonamide (1.169)**



¹H NMR (400 MHz, C₆D₆) δ 7.73 – 7.68 (m, 2H), 6.82 – 6.72 (m, 2H), 5.43 (s, 1H), 5.33 – 5.23 (m, 1H), 4.71 (s, 1H), 4.56 (d, *J* = 2.3 Hz, 1H), 3.60 (dd, *J* = 5.8, 2.3 Hz, 1H), 3.14 (s, 3H), 2.83 (s, 3H), 2.70 – 2.57 (m, 1H), 2.33 (dq, *J* = 12.2, 6.7 Hz, 1H), 2.18 (dd, *J* = 15.2, 4.8 Hz, 1H), 2.11 (ddd, *J* = 13.9, 5.1, 2.7 Hz, 1H), 1.87 (s, 3H), 1.86 – 1.80 (m, 1H), 1.68 (d, *J* = 1.4 Hz, 3H), 1.64 (d, *J* = 1.4 Hz, 3H), 1.27 (s, 3H).
¹³C NMR (101 MHz, C₆D₆) δ 145.0, 143.1, 143.0, 133.7, 131.1, 129.7, 129.2, 128.8, 125.5, 112.7, 79.5, 49.1, 45.0, 38.5, 38.4, 27.1, 25.9, 24.8, 23.1, 22.7, 21.2, 17.9. **HRMS** (ESI⁺): *m/z*: calculated for C₂₄H₃₅NNaO₃S :440.2230 [M+Na]⁺; found: 440.2228.

The following crystallographic data are provided free of charge by the joint Cambridge Crystallographic Data Centre and Fachinformationszentrum Karlsruhe Access Structures service www.ccdc.cam.ac.uk/structures. Programs used: data collection (Apex2 V2011.4-0), data reduction (SAINT V8.34A), structure solution (SIR2014, Burla, M. C.; Caliandro, R.; Carrozzini, B.; Cascarano, G. L.; Cuocci, C.; Giacovazzo, C.; Mallamo, M.; Mazzone, A.; Polidori, G. Crystal Structure Determination and Refinement via SIR2014. *J. Appl. Crystallogr.* **2015**, *48*, 306–309), structure refinement (SHELXTL Version 2018/3, Sheldrick, G. M. Crystal Structure Refinement with SHELXL. *Acta Crystallogr. Sect. C Struct. Chem.* **2015**, *71*, 3–81.), absorption correction (SADABS 2014/4, G. M. Sheldrick, **2008**).

Crystallographic Data**X-Ray data of 1.115a** available at CCDC 2271455**Table 1.21. Crystal data and structure refinement for mo_HS3_041_0m (compound 1.115a).**

Identification code	mo_HS3_041_0m	
Empirical formula	C ₃₃ H ₄₂ N ₂ O ₆ S ₂	
Formula weight	626.80	
Temperature	100(2) K	
Wavelength	null Å	
Crystal system	Orthorhombic	
Space group	P2(1)2(1)2(1)	
Unit cell dimensions	a = 6.8495(4)Å	α = 90°.
	b = 11.9087(9)Å	β = 90°.
	c = 39.7574(18)Å	γ = 90°.
Volume	3243.0(3) Å ³	
Z	4	
Density (calculated)	1.284 Mg/m ³	
Absorption coefficient	0.210 mm ⁻¹	
F(000)	1336	
Crystal size	0.20 x 0.10 x 0.04 mm ³	
Theta range for data collection	2.049 to 30.118°.	
Index ranges	-9<=h<=8,-16<=k<=10,-54<=l<=36	
Reflections collected	17858	
Independent reflections	8161[R(int) = 0.0352]	
Completeness to theta =30.118°	90.5%	
Absorption correction	Multi-scan	
Max. and min. transmission	0.7460 and 0.6050	
Refinement method	Full-matrix least-squares on F ²	
Data / restraints / parameters	8161/ 0/ 393	
Goodness-of-fit on F ²	1.030	
Final R indices [I>2sigma(I)]	R1 = 0.0392, wR2 = 0.0897	
R indices (all data)	R1 = 0.0446, wR2 = 0.0927	
Flack parameter	x =0.00(3)	
Largest diff. peak and hole	0.277 and -0.374 e.Å ⁻³	

X-Ray data of 1.118a available at CCDC 2271454

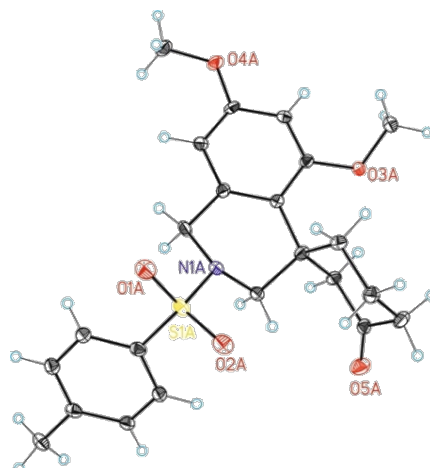
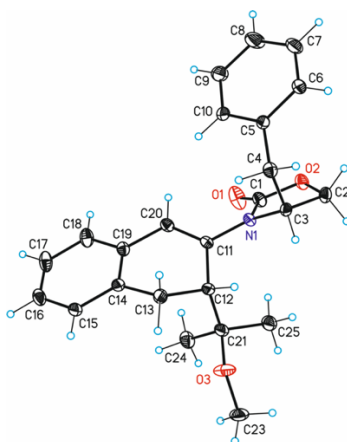


Table 1.22. Crystal data and structure refinement for mo_MPL048-b_0m (compound 1.118a).

Identification code	mo_MPL048-b_0m	
Empirical formula	C ₂₃ H ₂₇ N O ₅ S	
Formula weight	429.51	
Temperature	100(2) K	
Wavelength	0.71073 Å	
Crystal system	Monoclinic	
Space group	P2(1)	
Unit cell dimensions	a = 9.7293(5)Å	a = 90°.
	b = 16.6642(8)Å	b = 92.6452(15)°.
	c = 12.7215(7)Å	g = 90°.
Volume	2060.35(18) Å ³	
Z	4	
Density (calculated)	1.385 Mg/m ³	
Absorption coefficient	0.193 mm ⁻¹	
F(000)	912	
Crystal size	0.30 x 0.05 x 0.02 mm ³	
Theta range for data collection	1.602 to 31.051°.	
Index ranges	-13<=h<=13,-24<=k<=16,-18<=l<=17	
Reflections collected	21332	
Independent reflections	9364[R(int) = 0.0298]	
Completeness to theta =31.051°	96.200005%	
Absorption correction	Multi-scan	
Max. and min. transmission	0.996 and 0.909	
Refinement method	Full-matrix least-squares on F ²	
Data / restraints / parameters	9364/ 1/ 548	
Goodness-of-fit on F ²	1.044	
Final R indices [I>2sigma(I)]	R1 = 0.0468, wR2 = 0.1189	
R indices (all data)	R1 = 0.0558, wR2 = 0.1244	
Flack parameter	x = -0.08(11)	
Largest diff. peak and hole	0.511 and -0.374 e.Å ⁻³	

X-Ray data of 1.125aⁱⁱ available at CCDC 2271456**Table 1.23. Crystal data and structure refinement for mo_AC0142_0m (compound 1.125aⁱⁱ)**

Identification code	mo_AC0142_0m	
Empirical formula	C ₂₄ H ₂₇ N O ₃	
Formula weight	377.46	
Temperature	100(2)K	
Wavelength	0.71073 Å	
Crystal system	orthorhombic	
Space group	P 21 21 21	
Unit cell dimensions	a = 6.3012(5)Å	a = 90°.
	b = 11.8863(7)Å	b = 90°.
	c = 26.2497(17)Å	g = 90°.
Volume	1966.0(2) Å ³	
Z	4	
Density (calculated)	1.275 Mg/m ³	
Absorption coefficient	0.083 mm ⁻¹	
F(000)	808	
Crystal size	0.100 x 0.100 x 0.050 mm ³	
Theta range for data collection	1.552 to 32.676°.	
Index ranges	-7<=h<=9,-17<=k<=17,-30<=l<=39	
Reflections collected	29774	
Independent reflections	6958[R(int) = 0.0355]	
Completeness to theta =32.676°	98.7%	
Absorption correction	Multi-scan	
Max. and min. transmission	0.74 and 0.66	
Refinement method	Full-matrix least-squares on F ²	
Data / restraints / parameters	6958/ 0/ 286	
Goodness-of-fit on F ²	1.043	
Final R indices [I>2sigma(I)]	R1 = 0.0419, wR2 = 0.1047	
R indices (all data)	R1 = 0.0483, wR2 = 0.1089	
Flack parameter	x = 0.1(3)	
Largest diff. peak and hole	0.337 and -0.277 e.Å ⁻³	

DFT Calculations

Computational methods

DFT calculations were performed by the Gaussian 09 suite.¹⁰⁴ All the calculations were carried out using B3LYP¹⁰⁵ functional that has proved its efficiency in the other gold-catalyzed transformations.¹⁰⁶ The SDD basis set was used to describe Au.¹⁰⁷ The 6-31G(d) basis set¹⁰⁸ was employed for all the other atoms (C, H, O, N and P). Full geometry optimizations were carried out in CH₂Cl₂ through a polarizable continuum model (PCM).¹⁰⁹ The stationary points were characterized by vibrational analysis. Transition states were identified by the presence of one imaginary frequency while minima by a full set of real frequencies. The connectivity of the transition states was confirmed by the relaxation of each transition state towards both previous and next intermediates. All the energies are potential energies (E) and free energies (G) in solution at 298.15 K and 1 atm in Kcal·mol⁻¹. A data set collection of computational results is available in the ioChem-BD¹¹⁰ repository and can be accessed via <https://doi.org/10.19061/iochem-bd-1-281>.

¹⁰⁴ Gaussian 09, Revision B.1, Frisch, M. J., Trucks, G. W., Schlegel, H. B., Scuseria, G. E., Robb, M. A., Cheeseman, J. R., Scalmani, G., Barone, V., Mennucci, B., Petersson, G. A., Nakatsuji, H., Caricato, M., Li, X., Hratchian, H. P., Izmaylov, A. F., Bloino, J., Zheng, G., Sonnenberg, J. L., Hada, M., Ehara, M., Toyota, K., Fukuda, R., Hasegawa, J., Ishida, M., Nakajima, T., Honda, Y., Kitao, O., Nakai, H., Vreven, T., Montgomery, J. A., Peralta, Jr. J. E., Ogliaro, F., Bearpark, M., Heyd, J. J., Brothers, E., Kudin, K. N., Staroverov, V. N., Kobayashi, R., Normand, J., Raghavachari, K., Rendell, A., Burant, J. C., Iyengar, S. S., Tomasi, J., Cossi, M., Rega, N., Millam, J. M., Klene, M., Knox, J. E., Cross, J. B., Bakken, V., Adamo, C., Jaramillo, J., Gomperts, R., Stratmann, R. E., Yazyev, O., Austin, A. J., Cammi, R., Pomelli, C., Ochterski, J. W., Martin, R. L., Morokuma, K., Zakrzewski, V. G., Voth, G. A., Salvador, P., Dannenberg, J. J., Dapprich, S., Daniels, A. D., Farkas, .., Foresman, J. B., Ortiz, J. V., Cioslowski, J., Fox, D. J. Gaussian, Inc., Wallingford CT **2009**.

¹⁰⁵ a) Becke, A. D., Density-functional Thermochemistry. III. The Role of Exact Exchange, *J. Chem. Phys.* **1993**, *98*, 5648–5652. b) Becke, A. D., A New Mixing of Hartree–Fock and Local Density-functional Theories, *J. Chem. Phys.* **1993**, *98*, 1372–1377. c) Lee, C.; Yang, W.; Parr, R. G., Development of the Colle-Salvetti Correlation-Energy Formula into a Functional of the Electron Density, *Phys. Rev. B* **1988**, *37*, 785–789.

¹⁰⁶ a) Nieto-Oberhuber, C; Pérez-Galán, P; Herrero-Gómez, E.; Lauterbach, T.; Rodríguez, C.; López, S.; Bour, C.; Rosellón, A.; Cárdenas, D. J.; Echavarren, A. M., *J. Am. Chem. Soc.* **2008**, *130*, 269–279. b) García-Morales, C.; Pei, X.; Sarria Toro, J. M.; Echavarren, A. M., *Angew. Chem. Int. Ed.* **2019**, *58*, 3957–3961; *Angew. Chem.* **2019**, *131*, 3997–4001. c) García-Padilla, E.; Escofet, I.; Maseras, F.; Echavarren, A. M., Puzzling Structure of the Key Intermediates in Gold(I)-Catalyzed Cyclization Reactions of Enynes and Allenenes, *ChemPlusChem n/a*, e202300502.

¹⁰⁷ Andrae, D.; Haussermann, U.; Dolg, M.; Stoll, H.; Preuss, H., *Theor. Chim. Acta.* **1990**, *77*, 123–141.

¹⁰⁸ Hehre, W. J.; Ditchfield, R.; Pople, J. A., *J. Chem. Phys.*, **1972**, *56*, 2257–2261.

¹⁰⁹ Cancès, M. T.; Mennucci, B. B.; Tomasi, J., *J. Chem. Phys.*, **1997**, *107*, 3032–3041.

¹¹⁰ Álvarez-Moreno, M.; de Graaf, C.; Lopez, N.; Maseras, F.; Poblet, J. M.; Bo, C., *J. Chem. Inf. Model.* **2015**, *55*, 95–103.

*Computed Structures and Energies***Table 1.24.** Gold(I)-catalyzed diastereomeric cyclizations of **1.124aⁱⁱ** with L = JohnPhos.B3LYP-D3/6-31G(d)+SDD(Au), PCM (CH₂Cl₂); HLT: B3LYP-D3/6-311+G(d,p)+SDD(Au), PCM (CH₂Cl₂)

Code	E / Hartree	G / Hartree
1.A1	-2351,012596	-2350,266994
TS1.A2	-2351,009458	-2350,259814
1.A2	-2351,039162	-2350,284076
1.B1	-2351,010318	-2350,264375
TS1.B2	-2351,004657	-2350,257517
1.B2	-2351,033525	-2350,276691

Table 1.25. Gold(I)-catalyzed diastereomeric cyclizations of **1.124aⁱⁱ** with L = PMe₃.B3LYP-D3/6-31G(d)+SDD(Au), PCM (CH₂Cl₂); HLT: B3LYP-D3/6-311+G(d,p)+SDD(Au), PCM (CH₂Cl₂)

Code	E / Hartree	G / Hartree
1.A1'	-1692,310398	-1691,853453
TS1.A2'	-1692,308349	-1691,849203
1.A2'	-1692,339400	-1691,874304
1.B1'	-1692,305088	-1691,850141
TS1.B2'	-1692,301733	-1691,845259
1.B2'	-1692,328836	-1691,865681

UNIVERSITAT ROVIRA I VIRGILI

GOLD(I)-CATALYZED ASYMMETRIC CYCLIZATIONS AND CYCLOADDITIONS OF HETEROATOM-SUBSTITUTED ALKYNES WITH ALKENES

Andrea Cataffo

UNIVERSITAT ROVIRA I VIRGILI

GOLD(I)-CATALYZED ASYMMETRIC CYCLIZATIONS AND CYCLOADDITIONS OF HETEROATOM-SUBSTITUTED ALKYNES WITH ALKENES

Andrea Cataffo

Chapter II

Synthesis of Cyclobutanones by Gold(I)-Catalyzed [2+2] Cycloaddition of Ynol Ethers with Alkenes

UNIVERSITAT ROVIRA I VIRGILI

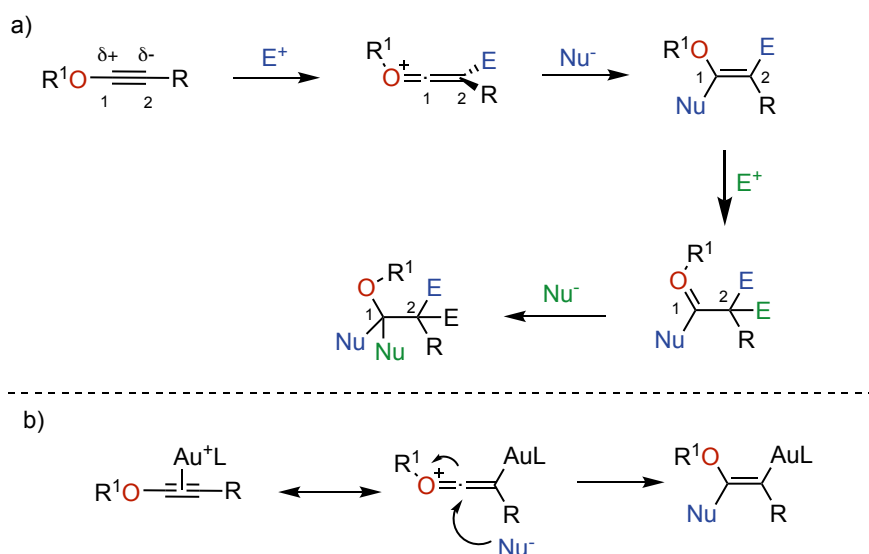
GOLD(I)-CATALYZED ASYMMETRIC CYCLIZATIONS AND CYCLOADDITIONS OF HETEROATOM-SUBSTITUTED ALKYNES WITH ALKENES

Andrea Cataffo

Introduction

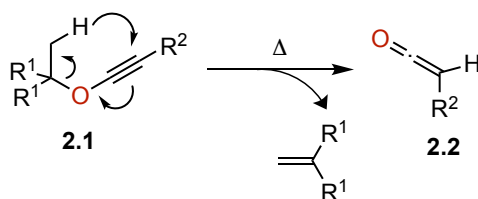
Ynol Ethers in Gold(I)-Catalysis

Oxygen-substituted alkynes, namely ynol ethers, exhibit similarities to ketenes, with a partial positive charge located on the C1 carbon attached to the oxygen and a partial negative charge on the C2 of the alkyne. Consequently, they can function as both electrophiles at C1 and nucleophiles at C2, enabling the formation of up to four new bonds in a single transformation (Scheme 2.1a). Upon coordination to gold(I) catalysts, ynol ethers can form ketenyl-gold(I) species which undergo functionalization through nucleophilic addition at the position α to the oxygen atom (Scheme 2.1b).¹



Scheme 2.1. a) General reactivity of ynol ethers with electrophiles and nucleophiles. b) General reactivity of ynol ethers under gold(I)-catalysis.

Alkyl ynol ethers, such as **2.1**, can easily undergo retro-ene reaction forming ketenes and extruding one molecule of ethylene or isobutylene (Scheme 2.2).²



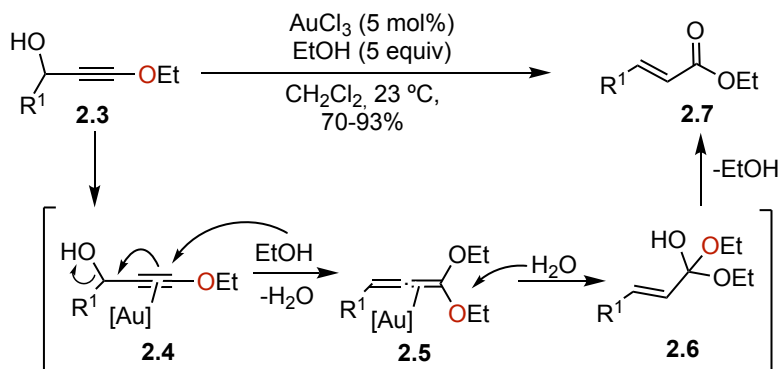
Scheme 2.2. Retro-ene as main decomposition pathway of alkyl-substituted ynol ethers

In the presence of *O*-nucleophiles, tertiary propargylic alcohols of type **2.3** were reported to react to afford α,β -unsaturated esters **2.7** following a gold(III)-catalyzed Meyer Schuster rearrangement which sees the formation of allene **2.5** as intermediate in an alternated water/alcohol-elimination/attack

¹ Campeau, D.; León Rayo, D. F.; Mansour, A.; Muratov, K.; Gagosz, F., Gold-Catalyzed Reactions of Specially Activated Alkynes, Allenes, and Alkenes, *Chem. Rev.* **2021**, *121*, 8756–8867.

² Minehan, T. G., Tandem Bond-Forming Reactions of 1-Alkynyl Ethers, *Acc. Chem. Res.* **2016**, *49*, 1168–1181.

sequence (Scheme 2.3).³ This rearrangement was eventually applied to the total synthesis of 5-deoxystrigol⁴ and stresgenin B.⁵



Scheme 2.3. Gold(III)-catalyzed Meyer Schuster rearrangement of propargylic alcohols.

The group of Aguilar reported that conjugated alkyl ynol ethers **2.8** when functionalized with a carboxylic acid (R₃ = H) can undergo *8-endo-dig* cyclization in the presence of gold(I) to afford 2,3-disubstituted phenols (Scheme 2.4, conditions A).⁶ Once formed **2.9**, a ring contraction affords **2.10** and eventually, after protodeauration, aromatic esters **2.11** are obtained. *N*-nucleophiles were also reported, by the same group, to react with similar substrates: when having an ester functionality on **2.8** (R₃ = Me) and in the presence of nitriles, a formal heterodehydro-Diels-Alder reaction occurs through the formation of the nitrilium intermediate **2.13**, which, after a cycloaromatization/protodeauration sequence, gives pyridines **2.15** (Scheme 2.4, conditions B).⁷ Due to the scarce stability of alkyl ynol ethers and the limited number of literature procedures on their synthesis, there are not so many reports involving them and most rely on silyl ynol ethers or aryl ynol ethers, which are easier to handle.

Anthranyls **2.17** were reported to act as *N*-nucleophiles with terminal aryl ynol ethers **2.16**, which, upon gold(I) activation and nucleophilic attack to form **2.19**, rearranges to the α -imino gold carbene intermediate **2.20** which is then trapped by the aryl group of the ynol ether (Scheme 2.5).⁸ The resulting aminobenzofuran derivative **2.21** undergoes an intramolecular condensation on the carbonyl group to produce the benzofuranoquinoline **2.22**.

³ a) Engel, D. A.; Dudley, G. B., Olefination of Ketones Using a Gold(III)-Catalyzed Meyer–Schuster Rearrangement, *Org. Lett.* **2006**, *8*, 4027–4029. b) Lopez, S. S.; Engel, D. A.; Dudley, G. B., The Meyer-Schuster Rearrangement of Ethoxyalkynyl Carbinols, *Synlett* **2007**, *2007*, 949–953.

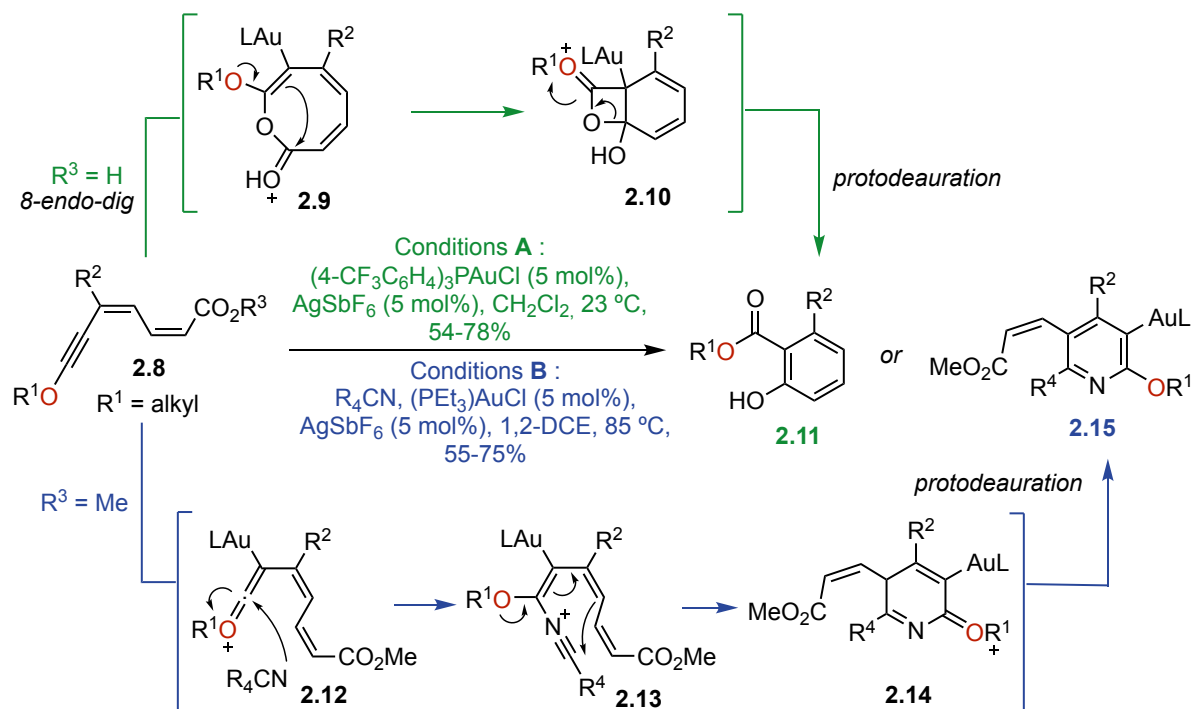
⁴ Lachia, M.; Dakas, P.-Y.; De Mesmaeker, A., Asymmetric Synthesis of the Four Stereoisomers of 5-Deoxystrigol, *Tetrahedron Lett.* **2014**, *55*, 6577–6581.

⁵ Chan, W. C.; Koide, K., Total Synthesis of the Reported Structure of Stresgenin B Enabled by the Diastereoselective Cyanation of an Oxocarbenium, *Org. Lett.* **2018**, *20*, 7798–7802.

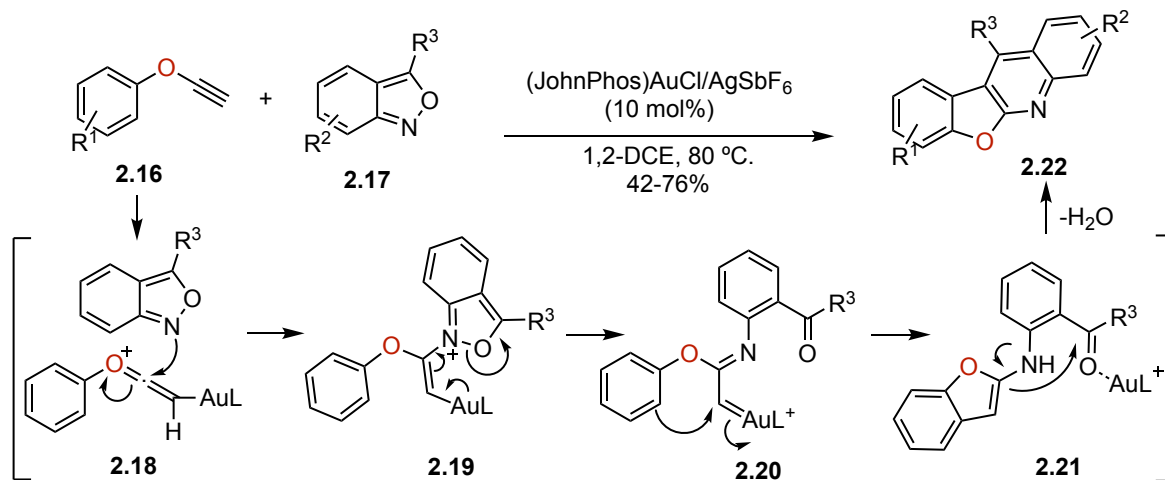
⁶ García-García, P.; Fernández-Rodríguez, M. A.; Aguilar, E., Gold-Catalyzed Cycloaromatization of 2,4-Dien-6-Yne Carboxylic Acids: Synthesis of 2,3-Disubstituted Phenols and Unsymmetrical Bi- and Terphenyls, *Angew. Chem. Int. Ed.* **2009**, *48*, 5534–5537, *Angew. Chem.* **2009**, *121*, 5642–5645.

⁷ Barluenga, J.; Fernández-Rodríguez, M. Á.; García-García, P.; Aguilar, E., Gold-Catalyzed Intermolecular Hetero-Dehydro-Diels–Alder Cycloaddition of Captodative Dienynes with Nitriles: A New Reaction and Regioselective Direct Access to Pyridines, *J. Am. Chem. Soc.* **2008**, *130*, 2764–2765.

⁸ Patil, M. D.; Liu, R.-S., Direct Access to Benzofuro[2,3-b]Quinoline and 6H-Chromeno[3,4-b]Quinoline Cores through Gold-Catalyzed Annulation of Anthranils with Arenoxyethynes and Aryl Propargyl Ethers, *Org. Biomol. Chem.* **2019**, *17*, 4452–4455.



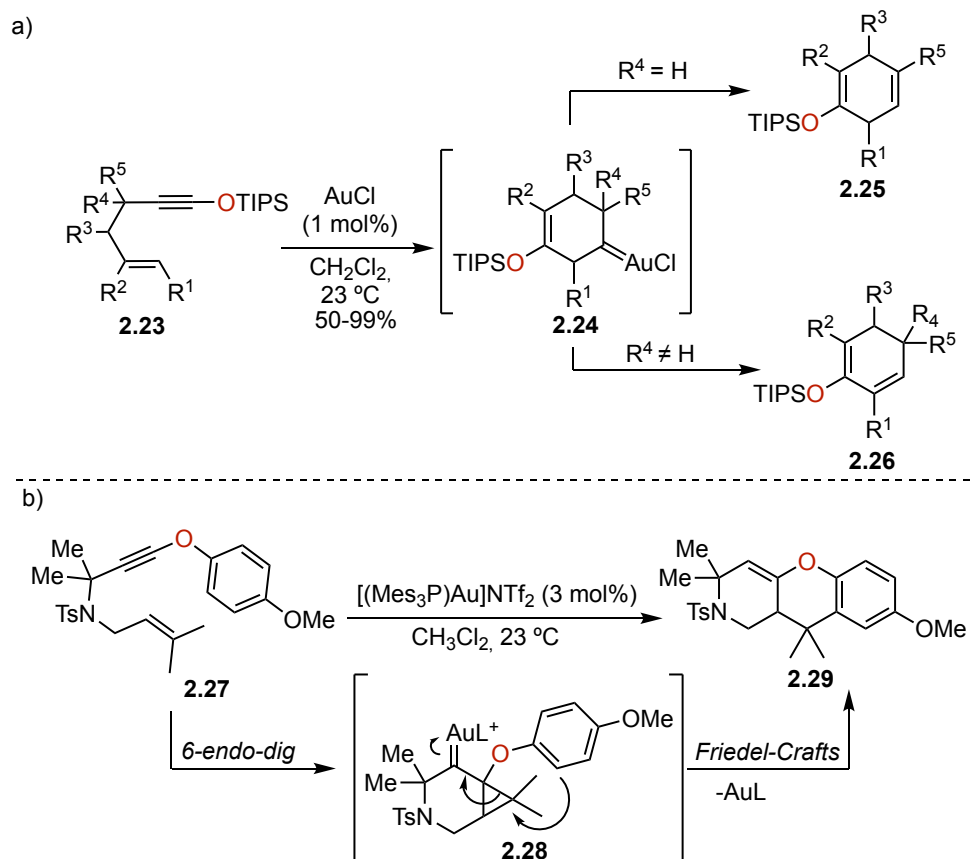
Scheme 2.4. Reactivity of conjugated alkyl ynol ethers under gold(I)-catalysis with *O*- and *N*- nucleophiles.



Scheme 2.5. Intermolecular annulation of aryl ynol ethers with anthranils.

In the case of cycloadditions with *C*-nucleophiles, 1-siloxy-1,6-enynes **2.23** were reported by Kozmin to undergo gold(I)-catalyzed cycloisomerization to form products of the type **2.25-1.26** depending on the substitution pattern of the starting material (Scheme 2.6a).⁹ 1-Aryloxy-1,6-enynes **2.27** also undergo formal [4+2] cycloaddition first via *6-endo-dig* cyclization in the presence of [(Mes₃P)Au]NTf₂ to form cyclopropyl gold(I) carbene intermediate **2.28**, which is then easily trapped by the aryloxy group to yield tricyclic **2.29** after protodeauration (Scheme 2.6b).

⁹ Zhang, L.; Kozmin, S. A., Gold-Catalyzed Cycloisomerization of Siloxy Enynes to Cyclohexadienes, *J. Am. Chem. Soc.* **2004**, *126*, 11806–11807.



Scheme 2.6. Gold(I)-catalyzed cycloisomerization of: a) 1-syloxy-1,6-enynes, b) 1-aryloxy-1,6-enynes.

The group of Hashmi applied this same methodology to furan-alkynes systems, where the double bond of the enyne belongs to a furane moiety, to eventually yield tetracycles.¹⁰

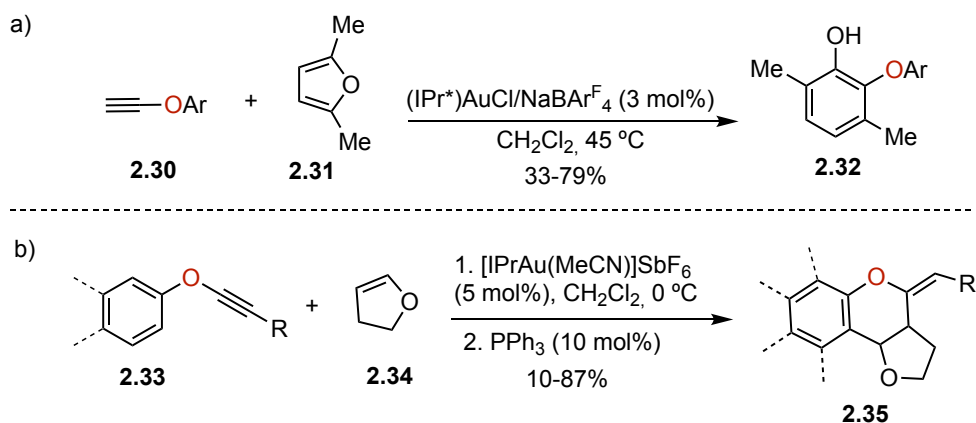
So far, reports of intermolecular cycloadditions of ynol ethers with unsaturated carbon nucleophiles are scarce. The phenol synthesis first developed by the group of Hashmi described in the **General Introduction**¹¹ could also be reproduced with ynol ethers **2.30** and 2,5-dimethylfuran **2.31** to afford phenols **2.32** (Scheme 2.7a).¹² Finally, the formal gold(I)-catalyzed [4+2] cycloaddition of ynol ethers **2.33** with alkenes was recently described, where a broad number of chromenes could be synthesized from both cyclic (**2.34**) and acyclic (not shown) alkenes (Scheme 2.7b).¹³ This approach was developed in parallel to our work discussed below and it's limited to enol ether partners. The reaction mechanism represents an intermolecular version of what has been described for 1-aryloxy-1,6-enynes (Scheme 2.6b).

¹⁰ Hashmi, A. S. K.; Rudolph, M.; Huck, J.; Frey, W.; Bats, J. W.; Hamzić, M., Gold Catalysis: Switching the Pathway of the Furan-Yne Cyclization, *Angew. Chem. Int. Ed.* **2009**, *48*, 5848–5852, *Angew. Chem.* **2009**, *121*, 5962–5966.

¹¹ Hashmi, A. S. K.; Blanco, M. C.; Kurpejović, E.; Frey, W.; Bats, J. W., Gold Catalysis: First Applications of Cationic Binuclear Gold(I) Complexes and the First Intermolecular Reaction of an Alkyne with a Furan, *Adv. Synth. Catal.* **2006**, *348*, 709–713.

¹² Zeiler, A.; Ziegler, M. J.; Rudolph, M.; Rominger, F.; Hashmi, A. S. K., Scope and Limitations of the Intermolecular Furan-Yne Cyclization, *Adv. Synth. Catal.* **2015**, *357*, 1507–1514.

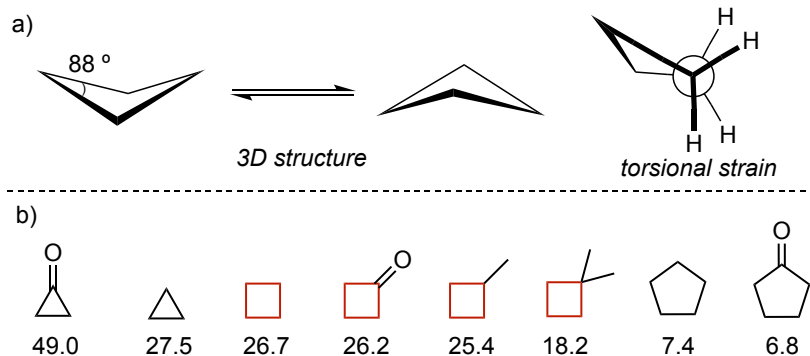
¹³ Suárez-Rodríguez, T.; Suárez-Sobrino, Á. L.; Ballesteros, A., Gold(I)-Catalyzed Intermolecular Formal [4+2] Cycloaddition of *O*-Aryl Ynol Ethers and Enol Ethers: Synthesis of Chromene Derivatives, *Chem. Eur. J.* **2021**, *27*, 13079–13084.



Scheme 2.7 Intermolecular reactions of terminal aryl ynol ethers with alkenes.

Synthesis of Cyclobutanones

Four-membered carbon rings, namely cyclobutane derivatives, adopt a folded structure, slightly reducing its bond angle to 88° from the expected 90° , thereby increasing angle strain but simultaneously alleviating torsional strain.¹⁴ Consequently, the C–C bonds exhibit slightly increased *p*-character, while the C–H bonds display more *s*-character. This elevated *s*-character, although subtle compared to cyclopropane, distinguishes cyclobutane's reactivity. As a consequence, cyclobutyl derivatives exhibit substantial ring strain, typically ranging from 18 to 27 Kcal·mol⁻¹, depending on the substituents and the hybridization of the carbons within the four-membered ring (Scheme 2.8).



Scheme 2.8. a) 3D structure of cyclobutane. b) Decreasing ring strain (Kcal·mol⁻¹) from three-membered to five-membered ring species.

This “conformational restriction” distinguishes cyclobutanes and their derivatives, cyclobutenes and cyclobutanones, in pharmacologically active compounds. The flexibility that ligands present in the binding pockets of active sites constitutes a big challenge in drug discovery and reducing the number

¹⁴ a) Dunitz, J. D.; Schomaker, V., The Molecular Structure of Cyclobutane, *J. Chem. Phys.* **1952**, *20*, 1703–1707. b) von R. Schleyer, P.; Williams, J. E.; Blanchard K. R., Evaluation of strain in hydrocarbons. The strain in adamantane and its origin. *J. Am. Chem. Soc.*, **1970**, *92*, 2377–2386. c) Ringer, A. L.; Magers, D. H., Conventional Strain Energy in Dimethyl-Substituted Cyclobutane and the *Gem*-Dimethyl Effect, *J. Org. Chem.* **2007**, *72*, 2533–2537.

of conformations with rigid¹⁵ and tridimensional¹⁶ systems is a well-known strategy. Apart from being artificially synthesized and used in medicinal chemistry,¹⁷ these compounds constitute the core of many bioactive products found in nature¹⁸ (Figure 2.1).

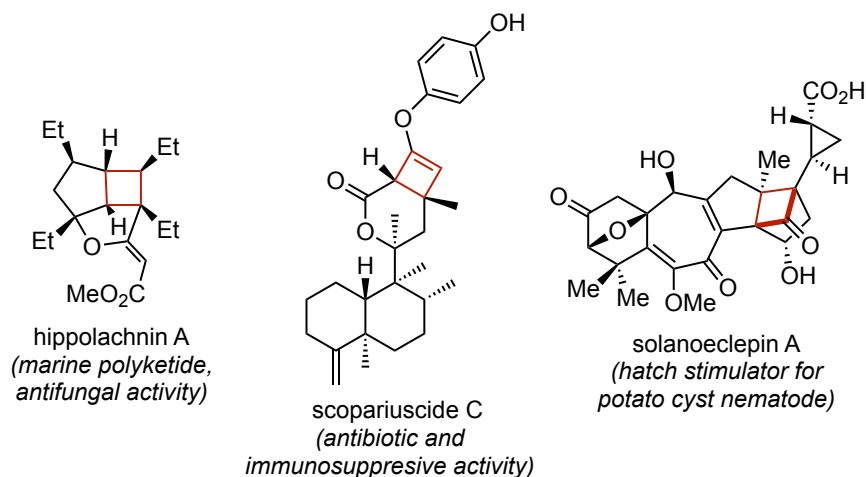


Figure 2.1. Selected examples of cyclobutane, cyclobutene and cyclobutanone motifs in natural products and pharmaceuticals.

The release of the above-mentioned ring strain serves as a potent driving force for numerous transformations (Scheme 2.9).¹⁹ The challenging α -C–C bond cleavage of cyclobutanones to afford acyclic alcohols **2.36** was achieved at high temperature through Rh catalysis in 1994.²⁰ Later in time, a series of desymmetrization strategies were developed to generate valuable enantiomerically enriched cyclic compounds.²¹ To name a few, the organocatalyzed aldol reaction to form scaffolds such as **2.37** was developed by Frongia and coworkers in 2012.²² The group of Stoltz described the asymmetric Baeyer-Villiger oxidation making use of cationic palladium catalysis with PHOX ligands to yield enantioenriched lactones **2.38**.²³

¹⁵ Fang, Z.; Song, Y.; Zhan, P.; Zhang, Q.; Liu, X., Conformational Restriction: An Effective Tactic in 'Follow-on'-Based Drug Discovery, *Future Med. Chem.* **2014**, *6*, 885–901.

¹⁶ Lovering, F.; Bikker, J.; Humblet, C., Escape from Flatland: Increasing Saturation as an Approach to Improving Clinical Success, *J. Med. Chem.* **2009**, *52*, 6752–6756.

¹⁷ a) Wishart, D. S.; Feunang, Y. D.; Guo, A. C.; Lo, E. J.; Marcu, A.; Grant, J. R.; Sajed, T.; Johnson, D.; Li, C.; Sayeeda, Z.; Assempour, N.; Iynkkaran, I.; Liu, Y.; Maciejewski, A.; Gale, N.; Wilson, A.; Chin, L.; Cummings, R.; Le, D.; Pon, A.; Knox, C.; Wilson, M., DrugBank 5.0: A Major Update to the DrugBank Database for 2018, *Nucleic Acids Res.* **2018**, *46*, D1074–D1082. b) van der Kolk, M. R.; Janssen, M. A. C. H.; Rutjes, F. P. J. T.; Blanco-Ania, D., Cyclobutanes in Small-Molecule Drug Candidates, *ChemMedChem* **2022**, *17*, e202200020.

¹⁸ a) Dembitsky, V. M., Naturally Occurring Bioactive Cyclobutane-Containing (CBC) Alkaloids in Fungi, Fungal Endophytes, and Plants, *Phytomedicine* **2014**, *21*, 1559–1581. b) Li, J.; Gao, K.; Bian, M.; Ding, H., Recent Advances in the Total Synthesis of Cyclobutane-Containing Natural Products, *Org. Chem. Front.* **2019**, *7*, 136–154.

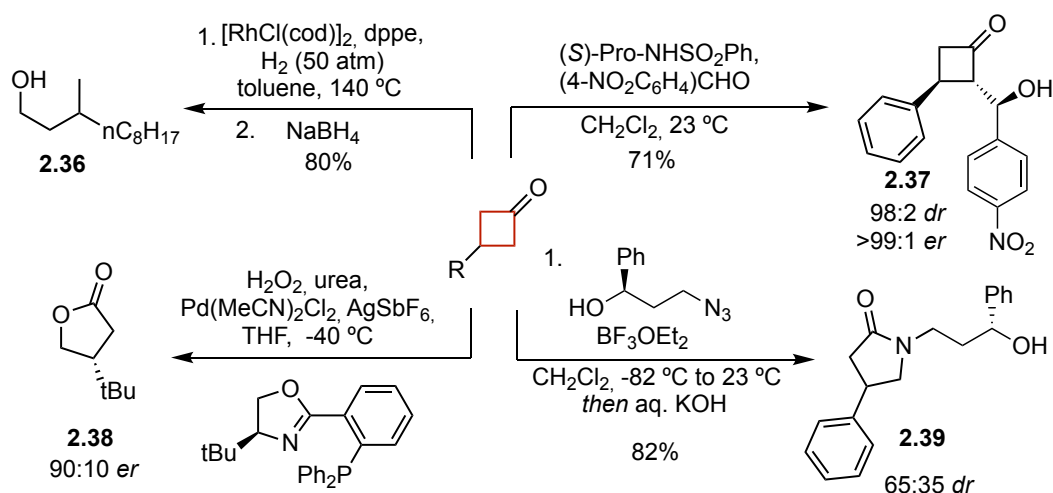
¹⁹ Seiser, T.; Saget, T.; Tran, D. N.; Cramer, N., Cyclobutanes in Catalysis, *Angew. Chem. Int. Ed.* **2011**, *50*, 7740–7752, *Angew. Chem.* **2011**, *123*, 7884–7896.

²⁰ Murakami, M.; Amii, H.; Ito, Y., Selective Activation of Carbon–Carbon Bonds next to a Carbonyl Group, *Nature* **1994**, *370*, 540–541.

²¹ Sietmann, J.; Wahl, J. M., Enantioselective Desymmetrization of Cyclobutanones: A Speedway to Molecular Complexity, *Angew. Chem. Int. Ed.* **2020**, *59*, 6964–6974, *Angew. Chem.* **2020**, *132*, 7028–7038.

²² Aitken, D. J.; Bernard, A. M.; Capitta, F.; Frongia, A.; Guillot, R.; Ollivier, J.; Piras, P. P.; Secci, F.; Spiga, M., Very High Stereoselectivity in Organocatalyzed Desymmetrizing Aldol Reactions of 3-Substituted Cyclobutanones, *Org. Biomol. Chem.* **2012**, *10*, 5045–5048.

²³ Petersen, K. S.; Stoltz, B. M., Palladium-Catalyzed, Asymmetric Baeyer–Villiger Oxidation of Prochiral Cyclobutanones with PHOX Ligands, *Tetrahedron* **2011**, *67*, 4352–4357.



Scheme 2.9 Selected examples of cyclobutanone derivatizations.

Finally, Aubé and co-workers developed an approach for an asymmetric Schmidt reaction to form lactames such as **2.39**.²⁴

The high strain that triggers cyclobutene and cyclobutanone reactivity, constitutes a challenge when coming to their construction. Among the different strategies to build cyclobutanones, some rely on ring expansion of cyclopropyl systems or ring contraction of cyclopentyls (Scheme 2.10). Pinacol-type rearrangement through acid catalysis on α -hydroxycyclopropyl carbinols **2.40** was described to afford *cis* or *trans* cyclobutanones **2.41-2.42** depending on the reaction conditions (Scheme 2.10a).²⁵ Gold(I)-catalyzed rearrangement of cyclopropanols **2.43** was reported by the group of Toste to generate alkylidene cycloalkanones of the type **2.45** in excellent yields (Scheme 2.10b).²⁶ Finally, α -carbonylated cyclobutanones **2.47** could be accessed by microwave-assisted Wolff rearrangement of cyclic 2-diazo-1,3-diketones **2.46** (Scheme 2.10c).²⁷

Another common methodology to obtain cyclobutanones simply consists in starting from their cyclobutene or cyclobutenol precursors (Scheme 2.11). Unsubstituted cyclobutenones were reported to undergo Diels-Alder cycloaddition with different dienes to afford bi- or tricyclic **2.50** (Scheme 2.11a).²⁸ The recent approach described by Tobrman sees a Suzuki-dephosphorylation sequence of phosphoenol ethers **2.51** which yields 2-substituted cyclobutanones **2.53** (Scheme 2.11b).²⁹

²⁴ Sahasrabudhe, K.; Gracias, V.; Furness, K.; Smith, B. T.; Katz, C. E.; Reddy, D. S.; Aubé, J., Asymmetric Schmidt Reaction of Hydroxyalkyl Azides with Ketones, *J. Am. Chem. Soc.* **2003**, *125*, 7914–7922.

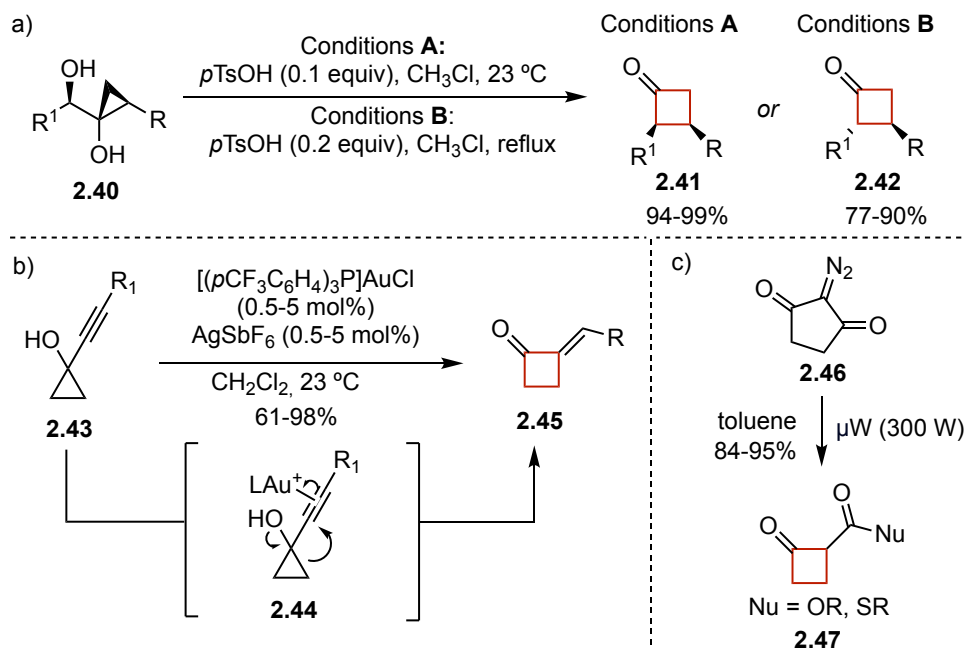
²⁵ Hussain, M. M.; Li, H.; Hussain, N.; Ureña, M.; Carroll, P. J.; Walsh, P. J., Applications of 1-Alkenyl-1,1-Heterobimetallics in the Stereoselective Synthesis of Cyclopropylboronate Esters, Trisubstituted Cyclopropanols and 2,3-Disubstituted Cyclobutanones, *J. Am. Chem. Soc.* **2009**, *131*, 6516–6524.

²⁶ Markham, J. P.; Staben, S. T.; Toste, F. D., Gold(I)-Catalyzed Ring Expansion of Cyclopropanols and Cyclobutanols, *J. Am. Chem. Soc.* **2005**, *127*, 9708–9709.

²⁷ Presset, M.; Coquerel, Y.; Rodriguez, J., Microwave-Assisted Wolff Rearrangement of Cyclic 2-Diazo-1,3-Diketones: An Eco-Compatible Route to α -Carbonylated Cycloalkanones, *J. Org. Chem.* **2009**, *74*, 415–418.

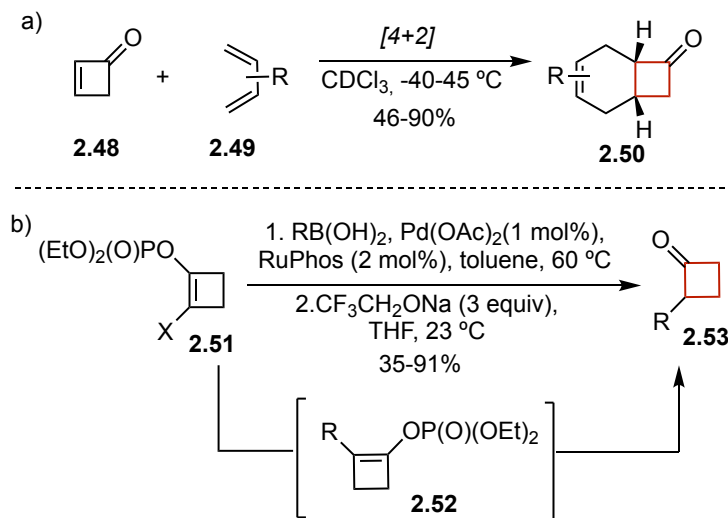
²⁸ Li, X.; Danishefsky, S. J., Cyclobutenone as a Highly Reactive Dienophile: Expanding Upon Diels–Alder Paradigms, *J. Am. Chem. Soc.* **2010**, *132*, 11004–11005.

²⁹ Koudelka, J.; Tobrman, T., Synthesis of 2-Substituted Cyclobutanones by a Suzuki Reaction and Dephosphorylation Sequence, *Eur. J. Org. Chem.* **2021**, *2021*, 3260–3269.



Scheme 2.10 Ring-expansion and ring-contraction strategies to yield cyclobutanones.

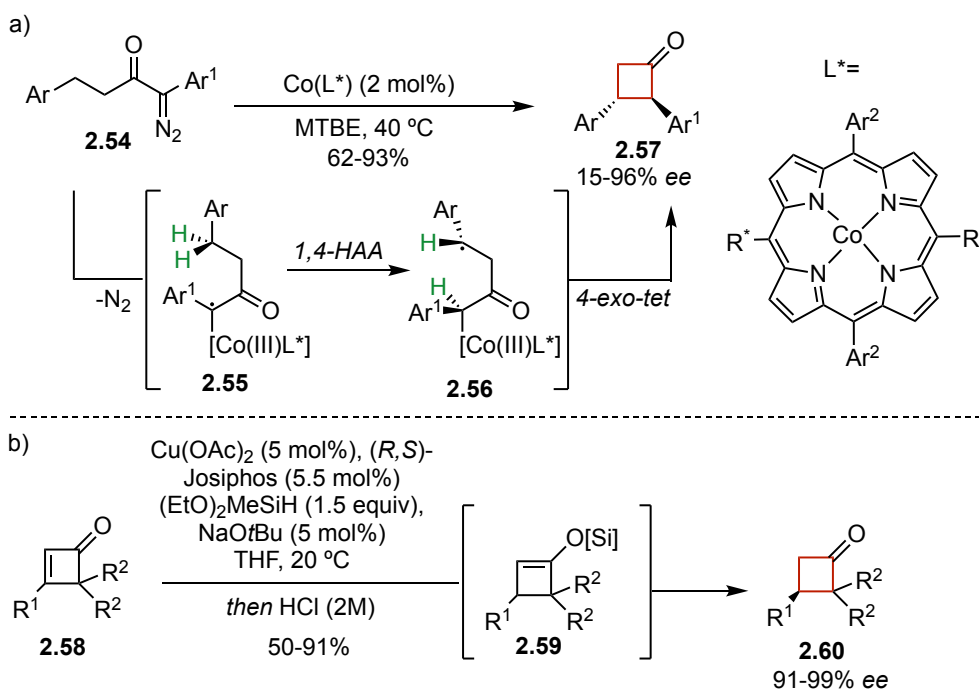
The Negishi version of the reaction which starts from alkyl-zinc precursors was also developed. In both cases the key phosphate intermediate **2.52** undergoes selective in-situ deprotection to form the desired products.



Scheme 2.11. Synthesis of cyclobutanones starting from cyclobutene precursors

Recent advances in the synthesis of enantioenriched cyclobutanones see the asymmetric metalloradical approach described by the group of Zhang, which via the use of *D*₂-symmetric chiral amidoporphyrin Co(II) complexes achieved the construction of chiral α,β -disubstituted **2.57** (Scheme 2.12a).³⁰

³⁰ Xie, J.; Xu, P.; Zhu, Y.; Wang, J.; Lee, W.-C. C.; Zhang, X. P. New Catalytic Radical Process Involving 1,4-Hydrogen Atom Abstraction: Asymmetric Construction of Cyclobutanones. *J. Am. Chem. Soc.* **2021**, *143*, 11670–11678.



Scheme 2.12. Recent asymmetric approaches to cyclobutanone synthesis

Starting from α -diazoketones **2.54**, α -Co(III)-alkyl radical **2.55** forms upon nitrogen extrusion. Then, a 1,4-hydrogen atom abstraction process (1,4-HAA) mediates the formation of **2.56** which finally yields **2.57** through a 4-*exo-tet* radical substitution. The low barrier encountered for the usually challenging 1,4-HAA³¹ was attributed to the non-covalent interactions which orient the substrate in the cavity of the catalyst and facilitate the process. Another example of asymmetric construction of cyclobutanones was reported this year by the group of Lu, who described a highly enantioselective copper-catalyzed hydrogenation of cyclobutenones using silanes as reducing agents (Scheme 2.12b).³² The reaction goes via silyl enol ether **2.59**, which is readily converted by acidic treatment to **2.60**.

Among the different strategies employed to synthesize cyclobutanones, the most atom-economical one so far consists in the [2+2] cycloadditions of ketene derivatives with alkenes (Scheme 2.13).³³ The completely unsubstituted ketene was reported to be toxic and extremely volatile, and, in general monosubstituted ketenes easily decompose or polymerize.³⁴ Disubstituted alkyl/aryl ketenes **2.62** can be generated starting from acyl chlorides **2.61** in the presence of amines and Lewis acids and in most cases can be isolated.³⁵ Monosubstituted α -aryl ketenes instead, can be generated following the same

³¹ Huang, X. L.; Dannenberg, J. J. Molecular Orbital Estimation of the Activation Enthalpies for Intramolecular Hydrogen Transfer as Functions of Size of the Cyclic Transition State and Carbon-Hydrogen-Carbon Angle. *J. Org. Chem.* **1991**, *56*, 5421–5424.

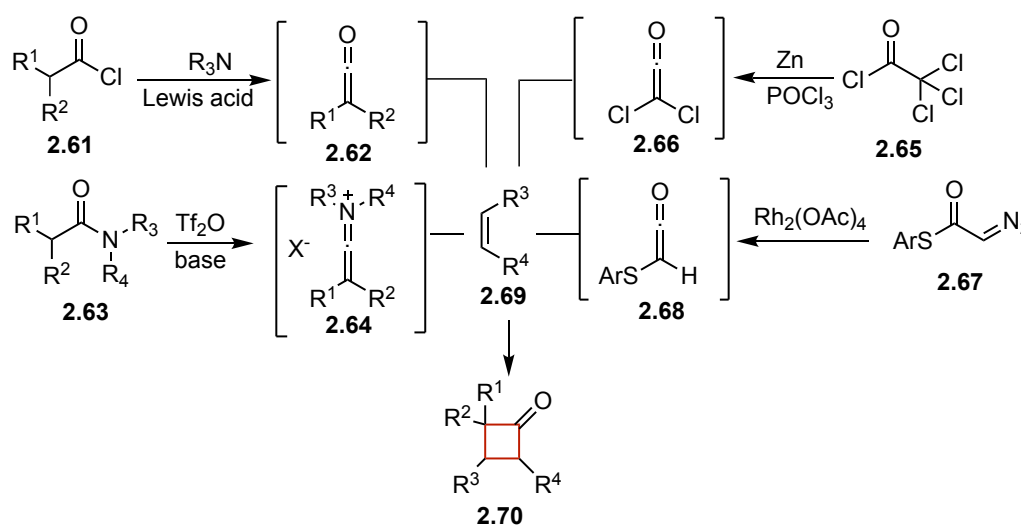
³² Wang, S.; Zhong, C.; Huang, Y.; Lu, P. Enantioselective Hydrofunctionalization of Cyclobutenones: Total Synthesis of gem-Dimethylcyclobutane Natural Products. *Angew. Chem. Int. Ed.* **2024**, e202400515, *Angew. Chem.* **2024**, e202400515.

³³ a) Snider, B. B. Intramolecular Cycloaddition Reactions of Ketenes and Keteniminium Salts with Alkenes. *Chem. Rev.* **1988**, *88*, 793–811. b) Mitzel, T. M.; Pigza, J. A. Ketene. In *Encyclopedia of Reagents for Organic Synthesis (EROS)*; John Wiley & Sons, Ltd, **2009**. c) Rasik, C. M.; Brown, M. K. Intermolecular Ketene–Alkene [2+2] Cycloadditions: The Significance of π -Lewis Acid Promoted Variants. *Synlett* **2014**, *25*, 760–765.

³⁴ Allen, A. D.; Tidwell, T. T. Ketenes and Other Cumulenes as Reactive Intermediates. *Chem. Rev.* **2013**, *113*, 7287–73421.

³⁵ Rasik, C. M.; Brown, M. K. Lewis Acid-Promoted Ketene–Alkene [2 + 2] Cycloadditions. *J. Am. Chem. Soc.* **2013**, *135*, 1673–1676.

methodology but must be combined in-situ with the alkene partner **2.69** to obtain **2.70**, given their lower stability.³⁶ An alternative protocol sees the employment of keteniminium salts **2.64** generated from amides **2.63** in the presence of triflic anhydride and a base, which combined with ethylene can give rise to α -mono or α -disubstituted cyclobutanones **2.70**.³⁷ The problems related to using, in this case, triflic anhydride and ethylene when working in big scale, were successively solved by adapting the procedure to flow reactors.³⁸ When coming to the more challenging unsubstituted ketene equivalents, dichloroketene **2.66** generated from **2.65** combined with POCl_3 and Zn,³⁹ or α -thio-substituted ketenes **2.68** accessed via rhodium catalysis on the diazo compounds **2.67**,⁴⁰ are usually generated in-situ and combined with **2.69** to generate cyclobutanones **2.70**. However, to isolate α -unsubstituted cyclobutanones, additional steps are required to remove the Cl- or the ArS- functionalities.



Scheme 2.13. Ketene precursors for the [2+2] cycloadditions with alkenes to form cyclobutanones.

³⁶ Riggsbee, E. M.; Zhou, C.; Rasik, C. M.; Spitz, A. Z.; Nichols, A. J.; Brown, M. K. Lewis Acid-Promoted [2 + 2] Cycloadditions of Alkenes with Aryl Ketenes. *Org. Biomol. Chem.* **2016**, *14*, 5477–5480.

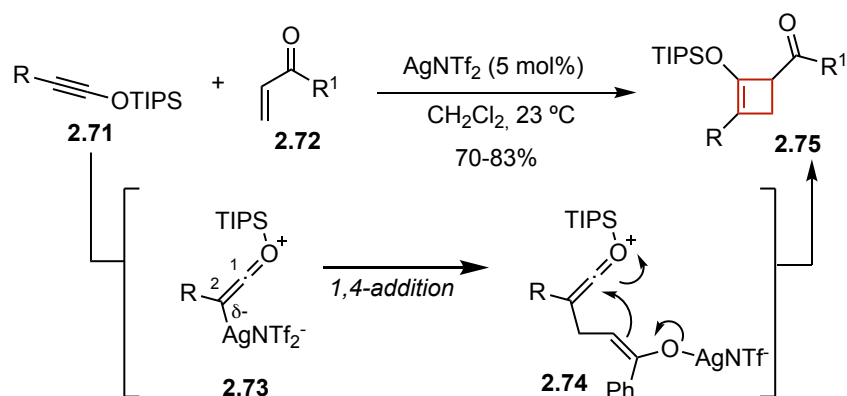
³⁷ a) Marchand-Brynaert, J.; Ghosez, L. Cycloadditions of Keteneiminium Cations to Olefins and Dienes. New Synthesis of Four-Membered Rings. *J. Am. Chem. Soc.* **1972**, *94*, 2870–2872. b) Falmagne, J.-B.; Escudero, J.; Taleb-Sahraoui, S.; Ghosez, L. Cyclobutanone and Cyclobutenone Derivatives by Reaction of Tertiary Amides with Alkenes or Alkynes. *Angew. Chem. Int. Ed. Engl.* **1981**, *20*, 879–8802. *Angew. Chem.* **1981**, *93*, 926–931. c) Lumbroso, A.; Catak, S.; Sulzer-Mossé, S.; De Mesmaeker, A. Cycloaddition of Keteniminium with Terminal Alkynes toward Cyclobuteniminium and Their Use in Diels–Alder Reactions. *Tetrahedron Lett.* **2014**, *55*, 5147–5150. d) Synthesis of Cyclobuteniminium Salts Derived from Aldo-Keteniminium Salts and Study of Their Reactivity in Diels–Alder Reaction. *Tetrahedron Lett.* **2014**, *55*, 6721–6725. e) Efficient Access to Functionalized Cyclobutanone Derivatives Using Cyclobuteniminium Salts as Highly Reactive Michael Acceptors. *Tetrahedron Lett.* **2015**, *56*, 2397–2401. e) Kolleth, A.; Lumbroso, A.; Tanriver, G.; Catak, S.; Sulzer-Mossé, S.; De Mesmaeker, A. New Access to Quaternary Aminocyclobutanes via Nucleophilic Addition on Cyclobutaniminium Salts. *Tetrahedron Lett.* **2016**, *57*, 3510–3514.

³⁸ Battilocchio, C.; Iannucci, G.; Wang, S.; Godineau, E.; Kolleth, A.; Mesmaeker, A. D.; Ley, S. V. Flow Synthesis of Cyclobutanones via [2 + 2] Cycloaddition of Keteneiminium Salts and Ethylene Gas. *React. Chem. Eng.* **2017**, *2*, 295–298.

³⁹ a) Brady, W. T.; Liddell, H. G.; Vaughn, W. L. Halogenated Ketenes. I. Dichloroketene_{1,2}. *J. Org. Chem.* **1966**, *31*, 2, 626–628. b) Ghosez, L.; Montaigne, R.; Mollet, P. Cycloadditions with Dichloroketene. *Tetrahedron Lett.* **1966**, *7*, 135–139. c) Ghosez, L.; Montaigne, R.; Roussel, A.; Vanlierde, H.; Mollet, P. Cycloadditions of Dichloroketene to Olefins and Dienes. *Tetrahedron* **1971**, *27*, 615–633. d) Bak, D. A.; Brady, W. T. Halogenated Ketenes. 31. Cycloaddition of Dichloroketene with Hindered Olefins. *J. Org. Chem.* **1979**, *44*, 107–110.

⁴⁰ Lawlor, M. D.; Lee, T. W.; Danheiser, R. L. Rhodium-Catalyzed Rearrangement of α -Diazo Thiol Esters to Thio-Substituted Ketenes. Application in the Synthesis of Cyclobutanones, Cyclobutenones, and β -Lactams. *J. Org. Chem.* **2000**, *65*, 4375–4384.

Considered what said so far, methodologies for the synthesis of stable cyclobutanone precursors are of particular interest. In 2004, Kozmin reported the silver-catalyzed cycloaddition of silyl ynol ethers **2.71** with α,β -unsaturated systems **2.72** to yield silyloxy cyclobutenes **2.75** (Scheme 2.14).⁴¹ Through mechanistic studies, it was demonstrated that upon triple bond activation, zwitterionic species **2.73** forms and acts as a C2 nucleophile towards the unsaturated system affording **2.74**. The latter finally undergoes ketene trapping to form **2.75**. Cyclobutyl enol ethers constitute stable precursors which might be readily converted to cyclobutanones by acidic hydrolysis.



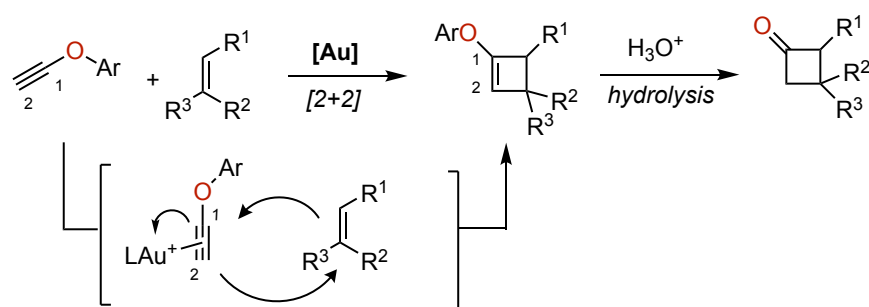
Scheme 2.14. Ag(I)-catalyzed stepwise [2+2] cycloaddition of silyl ynol ethers and α,β -unsaturated systems.

⁴¹ Sweis, R. F.; Schramm, M. P.; Kozmin, S. A. Silver-Catalyzed [2 + 2] Cycloadditions of Siloxy Alkynes. *J. Am. Chem. Soc.* **2004**, *126*, 7442–74431.

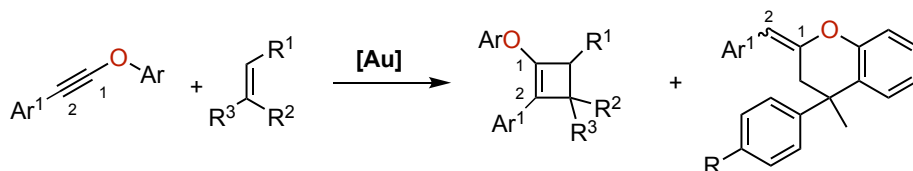
Objectives

Given the previous results from our group on [2+2] cycloadditions of alkynes with alkenes⁴² mentioned in the **General Introduction**, and our unsuccessful trials with reproducing this reactivity with *N*-substituted alkynes as described in **Chapter I**, our objective is to complement these results using *O*-substituted terminal alkynes (ynol ethers) to eventually form valuable cyclobutanone precursors.

In contrast to Kozmin's methodology using Ag(I) which relies on the formation of a C2 nucleophile,⁴¹ our Au(I)-catalyzed version envisions the formation of a C1 electrophile which will be readily attacked by electron-rich alkenes.



In the context of the same work, our aim is also to explore the reactivity of internal ynol ethers,⁴³ which, depending on the substitution pattern on the alkene partner, afford [2+2] or [4+2] cycloaddition products. This part of the work will not be discussed in the present manuscript and can be found in the related publication.⁴⁴



⁴² a) López-Carrillo, V.; Echavarren, A. M. Gold(I)-Catalyzed Intermolecular [2+2] Cycloaddition of Alkynes with Alkenes. *J. Am. Chem. Soc.* **2010**, *132*, 9292–9294. b) Elena de Orbe, M.; Echavarren, A. M. Broadening the Scope of the Gold-Catalyzed [2+2] Cycloaddition Reaction: Synthesis of Vinylcyclobutenes and Further Transformations. *Eur. J. Org. Chem.* **2018**, *2018*, 2740–2752.

⁴³ Work performed by Margherita Zanini.

⁴⁴ Zanini, M.; Cataffo, A.; Echavarren, A. M. Synthesis of Cyclobutanones by Gold(I)-Catalyzed [2 + 2] Cycloaddition of Ynol Ethers with Alkenes. *Org. Lett.* **2021**, *23*, 8989–8993.

Results and Discussion

[2+2] Cycloaddition of Ynol Ethers with Alkenes

To commence our investigation into the gold(I)-catalyzed reaction involving ynol ethers and alkenes, for practical matters, we considered using the preactivated cationic complexes **2.A-D** reported in Figure 2.2.

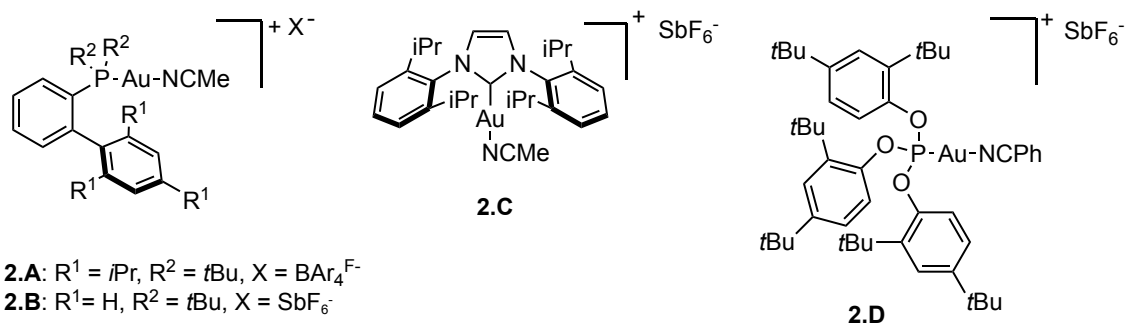
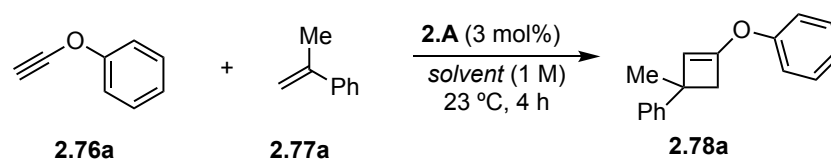


Figure 2.2. Preactivated biaryl phosphine (**2.A-2.B**), NHC (**2.C**) and phosphite (**2.D**) Au(I) catalysts used in this study.

We chose phenoxyacetylene **2.76a** for which an easy two-step synthesis was already previously described,⁴⁵ and commercially available α -methyl styrene **2.77a** as our model substrates (Table 2.1). Employing the optimal conditions established for the gold(I)-catalyzed [2+2] cycloaddition of terminal alkynes with alkenes,⁴² which see the use of the cationic XPhos gold(I) complex **2.A** as catalyst, CH₂Cl₂ as a solvent and a 1:2 alkyne:alkene ratio, the reaction proceeded with regioselectivity, yielding phenoxy-cyclobutene **2.78a** in 54% yield (Table 2.1, entry 1). Changing the solvent to toluene or 1,4-dioxane did not improve the yield (Table 2.1 entries 2-3).

Table 2.1. Solvent screening for the gold(I)-catalyzed [2+2] cycloaddition of **2.76a** with **2.77a**.^{a, 43}



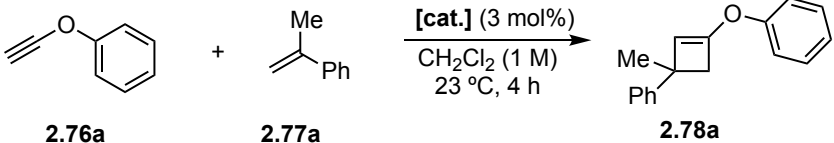
Entry	Solvent	Yield 2.78a (%) ^b
1	CH ₂ Cl ₂	54
2	PhCH ₃	50
3	1,4-Dioxane	37

^a**2.76a**:**2.77a** = 1:2. ^bYields determined by ¹H-NMR using trichloroethylene as internal standard.

⁴⁵ Graf, K.; Rühl, C. L.; Rudolph, M.; Rominger, F.; Hashmi, A. S. K. Metal-Free Oxidative Cyclization of Alkynyl Aryl Ethers to Benzofuranones. *Angew. Chem. Int. Ed.* **2013**, *52*, 12727–127311, *Angew. Chem.* **2013**, *125*, 12960–12964.

We then performed a catalyst screening, using, as anticipated, the preactivated complexes shown in Figure 2.2. Even though for the previously reported [2+2] it was shown how the use of XPhos ligand in combination with the $\text{BAr}_4^{\text{F}^-}$ counteranion would increase the yield of the cyclobutene product by avoiding the formation of a σ,π -(phenylacetylene)digold(I) complex,⁴⁶ when switching to the less bulky JohnPhos ligand and SbF_6^- counteranion, the yield increased to 71% (Table 2.2, entry 2). NHC-ligand based complex **2.C** and phosphite gold(I) species **2.D** afforded instead lower yields (Table 2.2, entries 3-4). Finally, we reproduced Kozmin conditions by using AgNTf_2 as catalyst,⁴¹ which showed to be active in catalyzing the transformation, but it afforded only 11% of **2.78a**

Table 2.2. Catalyst screening for the gold(I)-catalyzed [2+2] cycloaddition of **2.76a** with **2.77a**.^{a, 43}



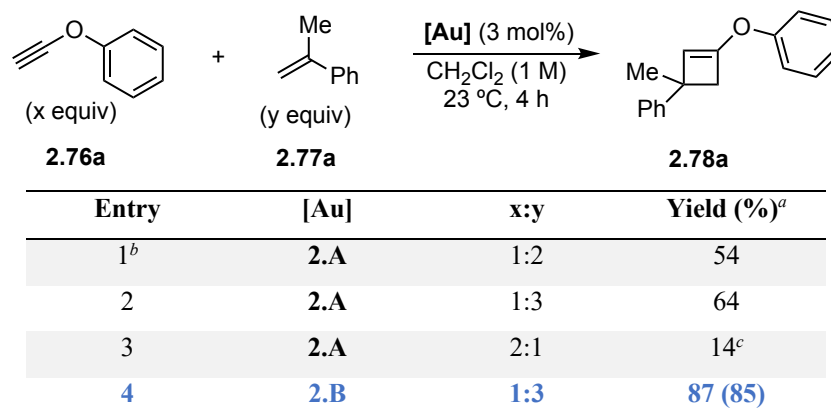
Entry	[cat.]	Yield (%) ^b
1	2.A	54
2	2.B	71
3	2.C	46
4	2.D	15
5 ^c	AgNTf_2	11

^a**2.76a:2.77a** = 1:2. ^b Yields determined by ¹H-NMR using trichloroethylene as internal standard. ^cConcentration: 0.1 M, cat. loading: 5 mol%, **2.76a:2.77a** = 1:3.

We moved then to analyze the influence of the concentration and the alkyne:alkene ratio on the reaction outcome (Table 2.3) using again catalyst **2.A**. When working with a less concentrated reaction mixture, no improvement in the yield was observed (Table 2.3, entry 1). Increasing the alkyne:alkene ratio to 1:3 had a beneficial effect on the conversion (64%, Table 2.3, entry 2) while having more alkyne than α -methyl styrene resulted in a yield drop to 14% (Table 2.3, entry 3).

Once assessed that the best x:y ratio would be 1:3, we repeated the experiment with the better performing **2.B**, which afforded product **2.78** in 85% isolated yield (Table 2.3, entry 4).

⁴⁶ Homs, A.; Obradors, C.; Lebœuf, D.; Echavarren, A. M. Dissecting Anion Effects in Gold(I)-Catalyzed Intermolecular Cycloadditions. *Adv. Synth. Catal.* **2014**, 356, 221–228.

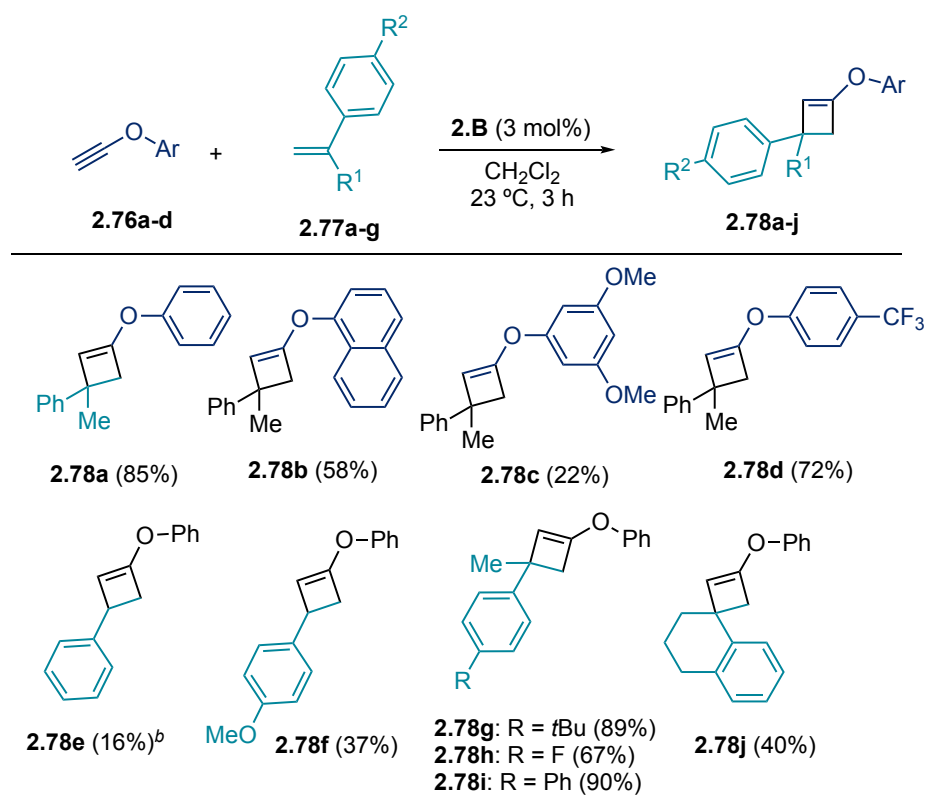
Table 2.3. Concentration and alkyne:alkene ratio variations for the gold(I)-catalyzed [2+2] cycloaddition of **2.76a** with **2.77a**.⁴³

^a Yields determined by ¹H-NMR using trichloroethylene as internal standard, isolated yields in parenthesis. ^b Reaction performed in 0.25 M concentration.

^c 22% conversion of limiting starting material.

Once having optimized the reaction for the model substrates, the scope was investigated. First, we analyzed the effect of different aryl substituents on the ynol ether in the [2+2] reaction with α -methylstyrene (Table 2.4): having the bulkier naphthyl group on **2.76b** did not have a beneficial effect on the yield of **2.78b**, nor did using the highly electron-rich **2.76c** which afforded **2.78c** in only 22% yield. Surprisingly, even for this example, no [4+2] product was detected. However, electropoor CF₃-substituted **2.76d** afforded **2.78d** in 72% yield.

Once selected **2.76a** as most efficient ynol ether, we then screened different styrene derivatives as olefin partners (Table 2.4). Unsubstituted styrene proved to be poorly reactive yielding **2.78e** in 16% internal std. yield, while more activated 4-vinylanisole afforded **2.78f** in 37% yield. Electron-poor alkenes **2.77v** and **2.77w** instead could not be reacted (Figure 2.3 below). *Para*-substituted α -methylstyrenes resulted in good to excellent yields of the corresponding cyclobutenes **2.78g** (89%), **2.78h** (67%) and **2.78i** (90%). Finally, when using the sterically hindered 1-methylene-1,2,3,4-tetrahydronaphthalene, **2.78j** could be isolated in 40% yield (Table 2.4). α -Isopropylstyrene **2.77x** and β -methylstyrene **2.77y**, probably due to steric hindrance, could not afford the desired products (Figure 2.3).

Table 2.4. Scope for the gold(I)-catalyzed [2+2] cycloaddition of terminal ynol ethers with styrene derivatives.^{a,47}

^aIsolated yields. ^bYield determined by ¹H NMR (trichloroethylene as internal standard).

Once assessed the reactivity of styrenes, we moved to aliphatic alkenes (Table 2.5). Reaction between **2.76a** and allyl trimethylsilane resulted in low 24% yield (**2.78k**). When moving to 1,1-disubstituted alkenes, only a minor amount of the opposite regioisomer was observed, and **2.78l-n** could be isolated in moderate to good yields. Apart from isoprene which afforded **2.78m** in 34% yield, other dienes did not react with the starting ynol ether (**2.77ee-gg**, Figure 2.3).

Cyclopentene **2.77cc** and cyclohexene **2.77dd** exhibited very poor reactivity towards ynol ethers (Figure 2.3), while cycloheptene, cyclooctene, and 1,5-cyclooctadiene yielded the corresponding bicyclic derivatives **2.78o-q** (Table 2.5). This result is in contrast to what was described by Houk and co-workers with Diels-Alder reactions:⁴⁸ the distortion energies to achieve the transition-state geometries in Diels-Alder reactions were computed with different dienes for cyclopropene, cyclobutene, cyclopentene and cyclohexene, observing that the value increased for bigger rings leading to a lower reactivity towards the diene, in agreement with the previously observed experimental results. Our opposite trend might be explained by the stability of the cyclobutene-containing bicyclic products which are more strained than the ones formed in the Diels-Alder, so having a more flexible bicyclic

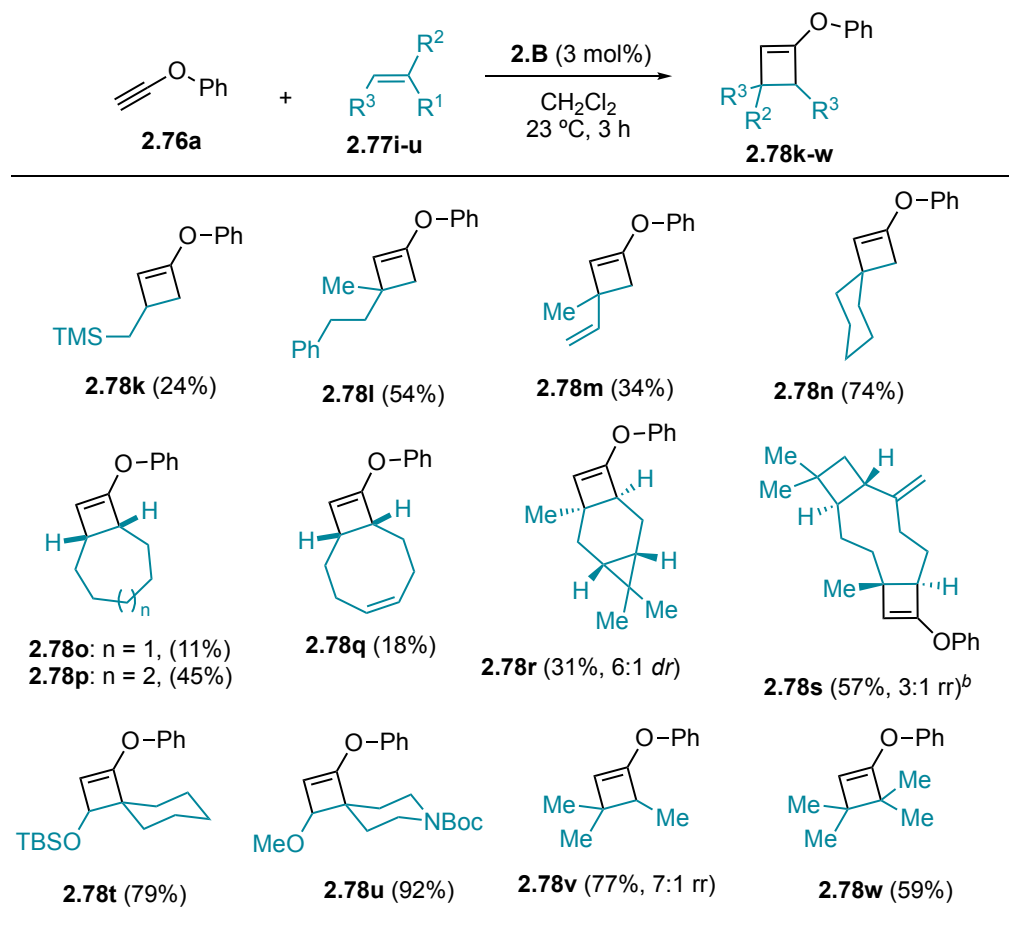
⁴⁷ Work performed in collaboration with Margherita Zanini.

⁴⁸ Liu, F.; Paton, R. S.; Kim, S.; Liang, Y.; Houk, K. N. Diels-Alder Reactivities of Strained and Unstrained Cycloalkenes with Normal and Inverse-Electron-Demand Dienes: Activation Barriers and Distortion/Interaction Analysis. *J. Am. Chem. Soc.* **2013**, *135*, 15642–15649.

system might be the driving force in our case. Furthermore, Houk's study did not include the bigger cycloheptene and cyclooctene, so we cannot draw a complete comparison. Surprisingly, even if cyclohexene exhibited insufficient reactivity, monoterpene (+)-carene successfully underwent the desired [2 + 2] cycloaddition yielding **2.78r** in 31% yield (Table 2.5). When reacting **2.76a** with sesquiterpene β -caryophyllene, only the most reactive trisubstituted double bond underwent cycloaddition, resulting in **2.78s** obtained in a 57% yield as a 3:1 mixture of regioisomers.

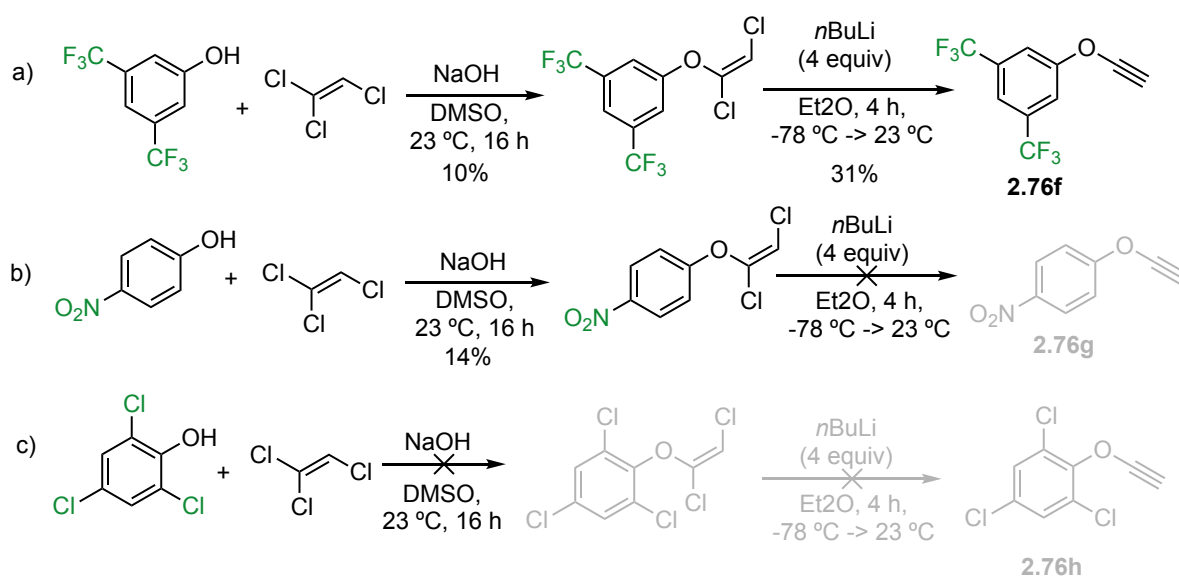
The reaction also accommodates sterically hindered enol ethers, leading to the formation of substituted cyclobutyl enol ethers **2.78t-u** in yields of 79% and 92%, respectively (Table 2.5). In contrast, smaller enol ethers (**2.77z** and **2.77aa** in Figure 2.3) experienced decomposition in the presence of the gold(I) catalyst. It is noticeable that despite the presence of an enol ether in the products of the [2+2] cycloaddition, there was never an observed further addition of the enol ether to the initial enol ether throughout the reaction. 5,6-Dihydro-2*H*-pyran-2-one **2.77bb** was also unreactive under the standard reaction conditions (Figure 2.3). To conclude, tri- and tetrasubstituted 2-methylbut-2-ene and 2,3-dimethylbut-2-ene reacted affording respectively **2.78v** (77%, presenting a 7:1 regiomic ratio) and **2.78w** (59%).

Table 2.5. Scope for the gold(I)-catalyzed [2+2] cycloaddition of terminal enol ethers with aliphatic alkenes.^{a,47}



^aIsolated yields. ^bYield determined by ¹H NMR (trichloroethylene as internal standard).

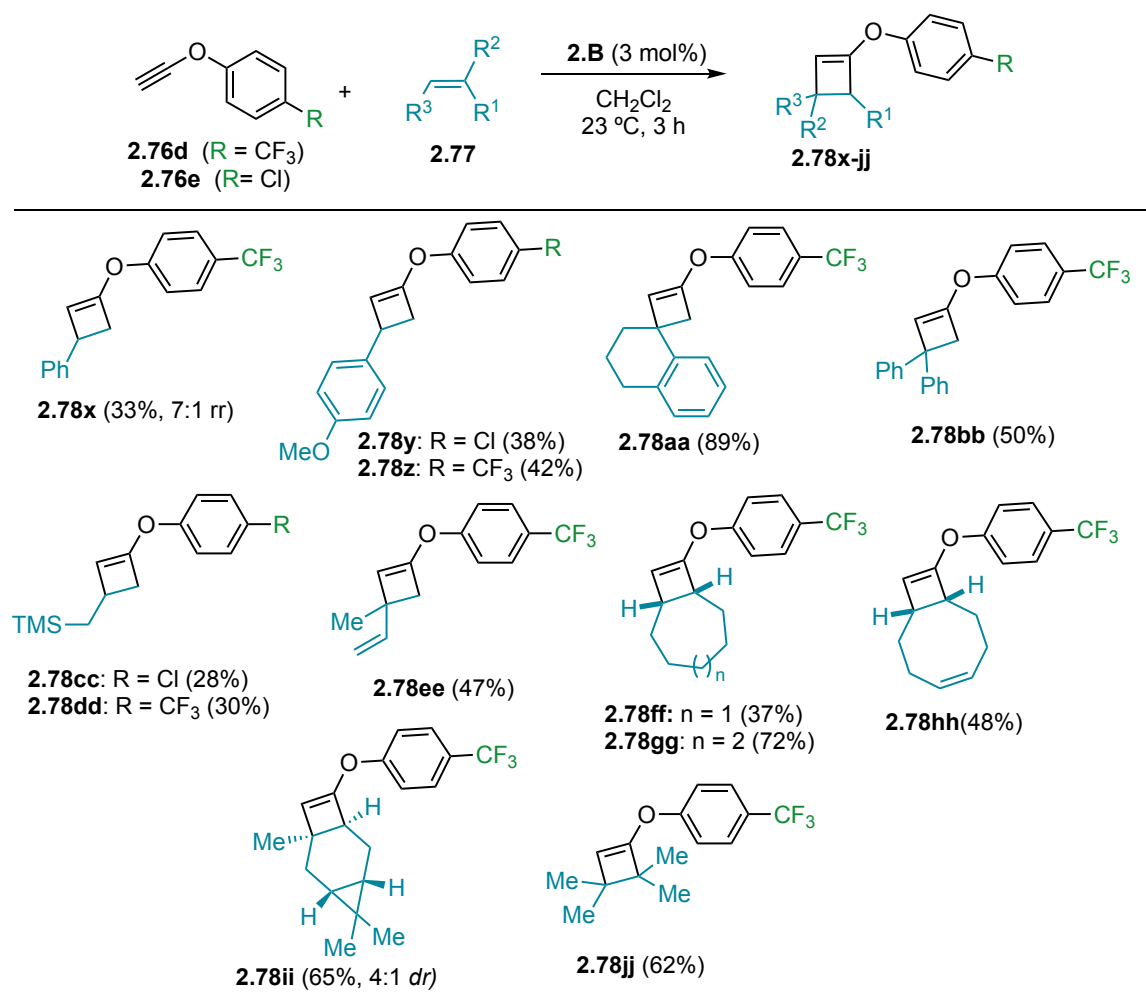
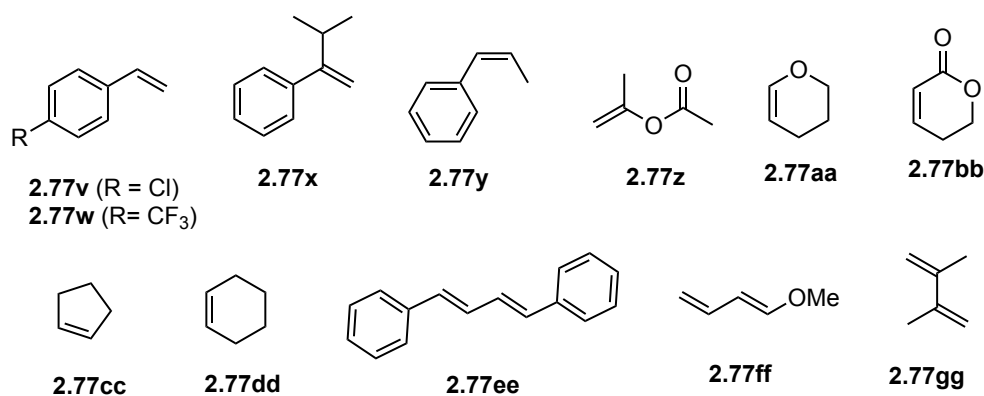
Given the low isolated yield of some of the reported examples, we were interested in improving the efficiency of the reaction and we thought we might do it by increasing the reactivity of the ynol ether partner towards nucleophilic attack. Given also the low observed yield for electron-rich **2.78c** (Table 2.4), we planned to synthesize electron-poorer variants. Apart from *p*-Cl and *p*-CF₃ aryl ynol ethers **2.76 d-e**, which synthesis is reported in literature,⁴⁵ we applied a similar procedure for the synthesis of 3,5-bis(trifluoromethyl)benzene derivative **2.76f**, which could be isolated in a very poor yield but, given its extreme volatility and instability, could not be effectively used as a substrate (Scheme 2.15a). When starting from *p*-nitrophenol, only the 1,2-dichlorovinyl precursor could be isolated in a poor 14% yield, and when subjecting the latter to *n*BuLi, it polymerized (Scheme 2.15b). Finally, 2,4,6-trichlorophenol would not react even in the first step with trichloroethylene (Scheme 2.15c).



Scheme 2.15. Attempted synthesis of highly electron-poor ynol ethers.

Given these results, we decided to repeat the reactions involving poorly reactive alkenes using this time *p*-Cl and *p*-CF₃ aryl ynol ethers **2.76d-e**. Delightfully, while in the case of α -methylstyrene no improvement was observed (**2.78d**, Table 2.4), most reactions highly benefited from the use of electron-poor alkynes (Table 2.6). For **2.78x**, **2.78aa**, **2.78ff**, **2.78gg**, **2.78hh**, **2.78ii** the yield was doubled or highly increased with respect to the products of unsubstituted ynol ethers, while **2.78bb**, which could not be formed using **2.76a** as alkyne partner, could be isolated from **2.76d** in 50% yield.

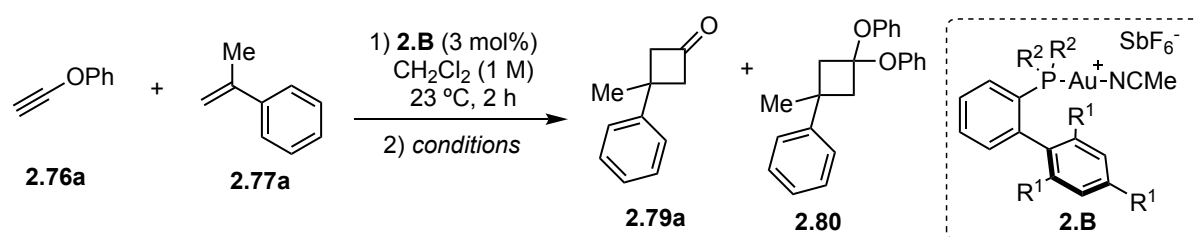
Repeating all the reactions using **2.76d** in combination with the olefins **2.77v-gg** (Figure 2.3) that were not reactive with unsubstituted **2.76a** did not result in any additional product.

Table 2.6. Scope for the gold(I)-catalyzed [2+2] cycloaddition of terminal ynol ethers presenting EWG with alkenes.^a^aIsolated yields.**Figure 2.3.** Alkenes that failed in the gold(I)-catalyzed [2+2] cycloaddition with ynol ethers.

Product Derivatization: Access to Cyclobutanones

We anticipated that by employing suitable conditions, it would be feasible to directly obtain the corresponding cyclobutanones from the starting materials **2.76** and **2.77**. To achieve this, we developed a one-pot, two-step approach, commencing with the previously optimized conditions for the [2+2] cycloaddition, succeeded by acidic hydrolysis of the enol ether moiety. Simply by adding water to the reaction mixture of **2.76a** with **2.77a** and allowing it to stir overnight at 23 °C, compound **2.78a** was recovered in a yield of 83%, with no observed hydrolysis (Table 2.7, entry 1).

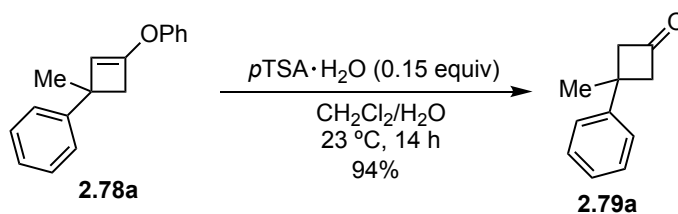
Table 2.7. Optimization of the one pot-two steps synthesis of cyclobutanone **2.79a**.^{a,47}



Entry	Conditions ^b	2.79 (%) ^c	2.80 (%) ^c
1	H ₂ O (100 equiv)	/ ^d	/ ^d
2	<i>p</i> -TSA·H ₂ O (0.15 equiv), water	37	31
3	<i>p</i>-TSA·H₂O (1 equiv), water	73 (69)	/
4 ^e	<i>p</i> -TSA·H ₂ O (1 equiv), water	43	30
5	<i>p</i> -TSA·H ₂ O (2 equiv), water	68	11
6	10% HCl in water (HCl 1 equiv)	43	43
7	1M TFA in water (TFA 1 equiv)	44	35
8	1M H ₂ SO ₄ in water (H ₂ SO ₄ 1 equiv)	/ ^d	/ ^d
9	1M AcOH in water (AcOH 1 equiv)	/ ^d	/ ^d
10 ^f	<i>p</i> -TSA·H ₂ O (1 equiv), water	40	33

^a **2.76a**:**2.77a** = 1:3. ^b reaction time 14 h, temperature = 23 °C. ^c yield determined by ¹H-NMR using trichloroethylene as internal standard. Isolated yield in parenthesis. ^d **2.78a** fully recovered. ^e The reaction was performed in CH₂Cl₂ (0.2 M). ^f The reaction was performed starting from **2.76d**.

When utilizing *p*-TSA·H₂O as a catalyst along with water as a co-solvent, the enol ether was entirely consumed. However, a 1:1 mixture of the desired ketone and acetal **2.80** was produced (Table 2.7, entry 2). Yet, subjecting pure **2.78a** to the same acidic conditions resulted in complete hydrolysis of the enol ether into the ketone, with nearly quantitative yield (Scheme 2.16).

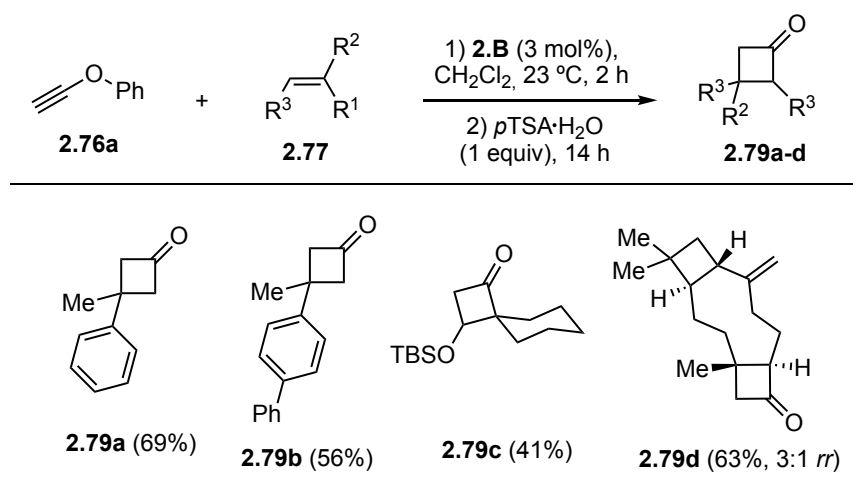


Scheme 2.16. Hydrolysis of enol ether **2.78a** to form **2.79a**.⁴³

Increasing the acid amount up to 1 equiv furnished ketone **2.79a** in a yield of 69%, with no formation of acetal **2.80** detected (Table 2.7, entry 3). When working in more diluted conditions (0.2 M) with the intention of diminishing the quantity of the acetal side product, a lower yield of **2.79a** (43%) was obtained, together with 30% of side product **2.80** (Table 2.7, entry 4). With a higher excess of acid, trace amounts of the undesired acetal were again detected in the crude ^1H NMR (Table 2.7, entry 5). Addition of an aqueous solution of HCl or TFA yielded a mixture of **2.79a** and **2.80** (Table 2.7, entries 6-7). Interestingly, after stirring for 14 hours at 23°C in the presence of H_2SO_4 (Table 2.7, entry 8) or acetic acid (Table 2.7, entry 9), the enol ether formed in the initial step was completely recovered. In the former case, the reaction likely failed due to solubility issues, while acetic acid was probably insufficiently acidic to promote the reaction. Finally, we reproduced the reaction with the best conditions found so far (1 equiv of *p*-TSA· H_2O in 1 M CH_2Cl_2) starting this time from *p*- CF_3 aryl ynol ether **2.76d**. The one-pot two-step procedure brought only to 40% of isolated **2.79a** (Table 2.7, entry 10), so **2.76a** was chosen to perform the hydrolysis scope (Table 2.8).

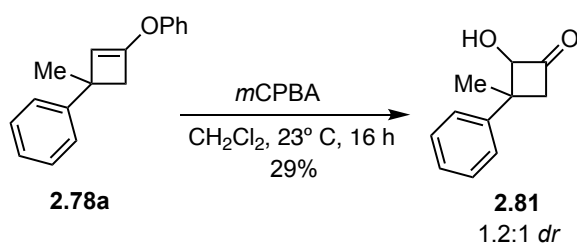
Apart from **2.79a**, also structurally similar **2.79b** could be isolated with the same procedure in 56% yield (Table 2.8). Notably, the -OTBS group of **2.79c** remained intact following the hydrolysis of the enol ether, albeit the product was obtained in a moderate yield (41%). Cyclobutanone **2.79d**, resulting from the reaction of **2.76a** and β -caryophyllene, was achieved in a yield of 63%. This product was already observed to form over time from enol ether **2.78s**. Generally, the one-pot approach for generating cyclobutanone necessitates less time and manipulation of products, however, conducting the two steps separately typically resulted in superior overall yields.

Table 2.8. Scope of the one-pot two-steps synthesis of cyclobutanones **2.79a-d**.^{a,43}



^aIsolated yields

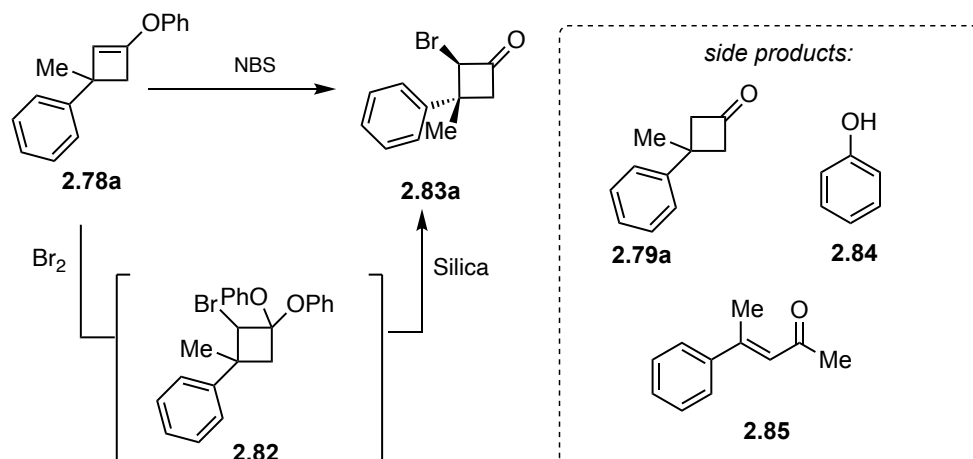
Once disclosed the acidic hydrolysis of cyclobutyl enol ethers, we were interested in exploring the functionalization of these moieties with other electrophiles. Treatment of **2.78a** with *m*CPBA afforded the α -hydroxy ketone **2.81** in low 29% yield and 1.2:1 *dr* (Scheme 2.17). Given the scarce selectivity of the reaction and the low stability of the product, no further optimization was performed.



Scheme 2.17. α -Hydroxylation-hydrolysis of **2.78a** to afford **2.81**

We then exposed **2.78a** to halogen sources with the goal of obtaining α -halogenated cyclobutanones. When using Br_2 in CCl_4 over 5 h at 23 °C, **2.83a** was obtained in 35% isolated yield after column chromatography along with the simple hydrolysis product **2.79a**, which formation is probably catalyzed by the HBr formed during the reaction, phenol **2.84** and ring-opening product **2.85** (Table 2.9, entry 1). The formation of **2.83a** together with the one of phenol hints to a bromination-hydrolysis sequence which happens presumably through to the water present in the solvent.

Table 2.9. Optimization of the α -bromination of enol ether **2.78a** to give cyclobutanone **2.83a**.



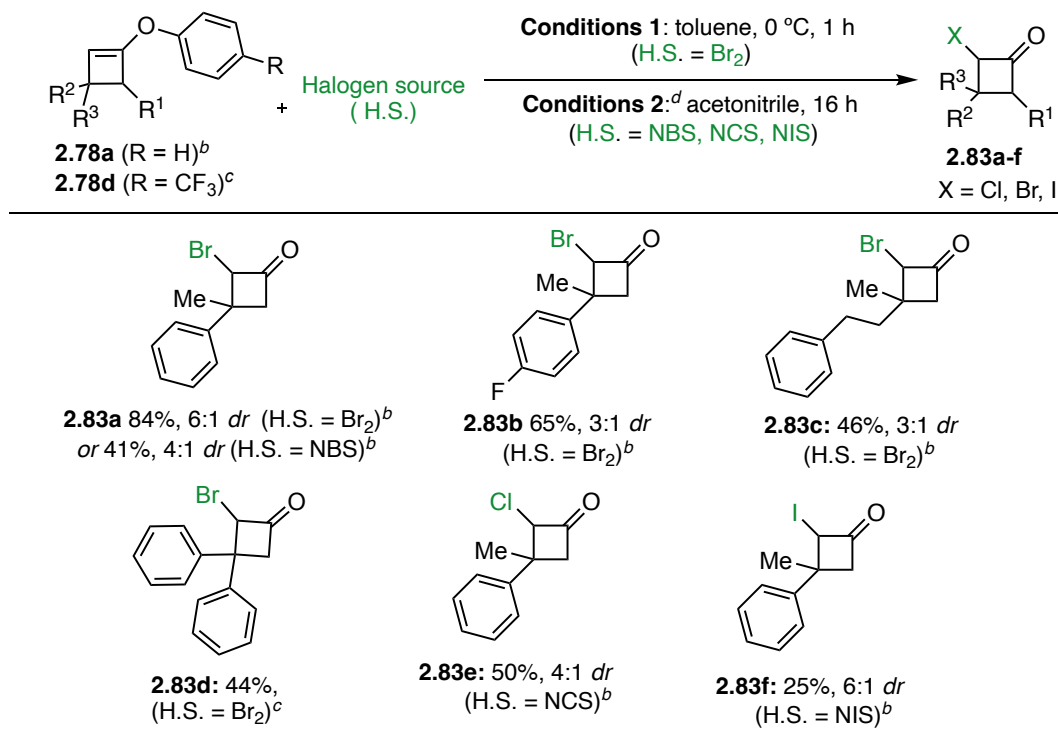
Entry	Brominating agent	Solvent ^a	T (°C)	Time (h)	Yield 2.83a (%) ^b	<i>dr</i> ^c
1	Br_2 (1.3 equiv)	CCl_4	23	5	35	n.d.
2	Br_2 (1.3 equiv)	CCl_4	0	3	58	3.5:1
3	Br_2 (1.3 equiv)	CH_2Cl_2	0	3	56	5.5:1
4^d	Br_2 (1.3 equiv)	Toluene	0	1	84	6.5:1
5	NBS (2 equiv)	CCl_4	23	24	/	n.d.
6	NBS (2 equiv)	CH_2Cl_2	23	24	20 ^e	n.d.
7	NBS (2 equiv)	Acetone	23	24	27 ^e	n.d.
8	NBS (2 equiv)	ACN	23	24	41	n.d.

^aConcentration: 0.1 M. ^bIsolated yields. ^cThe *dr* were calculated by ^1H NMR integration after purification by column chromatography. ^dWhen performing the gold(I)-catalyzed [2+2] cycloaddition under the optimized conditions followed by bromination under these conditions in a one-pot-two-step process, the isolated yield for **2.83a** went down to 18%. The isolated yield of the pure diastereomer after a second column chromatography is of 68%. ^eYield determined by ^1H NMR using trichloroethylene as internal standard.

Following a literature report where *tert*-butyl enol ethers were converted to α -bromocyclobutanones using Br_2 at 0°C ,⁴⁹ we repeated the reaction at low temperature diminishing the time to 3 hours and we isolated **2.83a** in 58% yield and 3.5:1 *dr* (Table 2.9, entry 2). By analyzing the reaction crude we could observe the main product to actually be **2.82**, which then would be converted to **2.83a** via treatment with silica gel. When switching the solvent to CH_2Cl_2 , no improvement in the yield was observed, but the *dr* grew up to 5.5:1 (Table 2.9, entry 3). Finally, reaction in toluene for 1 h revealed to be the best option affording the product in 84% yield and 6.5:1 *dr* (Table 2.9, entry 4). By performing a second purification on this diastereomeric mixture, the major diastereomer could also be isolated in 68% yield and its stereochemistry could be assigned by GOESY and NOESY NMR analysis (see Experimental Part) which matched with steric considerations, placing the newly formed C–Br bond on the opposite side of the bulkier Ph substituent. When we tried to reproduce the reaction in a one-pot two-steps sequence after the gold(I)-catalyzed [2+2] cycloaddition the final isolated yield for **2.83a** dropped down to 18%. When performing the reaction with NBS, even though **2.83a** was formed directly and no **2.82** was observed in the crude, lower yields were observed than when using Br_2 (Table 2.9, entries 5-8).

We then tested the optimized transformation on differently substituted cyclobutenes (Table 2.10).

Table 2.10. Scope for the α -halogenation-hydrolysis of cyclobutyl enol ethers **2.78** to afford **2.83a-f**.^a



^aIsolated yields. ^bStarting material: **2.78a**. ^cStarting material: **2.78d**. ^dT ($^\circ\text{C}$) specified in the Experimental Section. H.S. = Halogen source.

⁴⁹Soelch, R. R.; McNierney, E.; Tannenbaum, G. A.; Lemal, D. M. Synthesis and Chemistry of Highly Fluorinated Bicyclo[2.2.0]Hexenones. *J. Org. Chem.* **1989**, *54*, 5502–5511.

The reported yields are the ones for the isolated diastomeric mixture, but in some cases it was also possible to separate the mixture further and characterise the major diastereomer alone (see Experimental Part). β -methyl substituted **2.83b-c** were obtained following **Conditions 1** (Br_2 in toluene at 0°C) in moderate to good yields and 3:1 *dr*, while symmetric **2.83d** could be isolated starting from *p*- CF_3 aryl substituted **2.78d** in 44% yield.

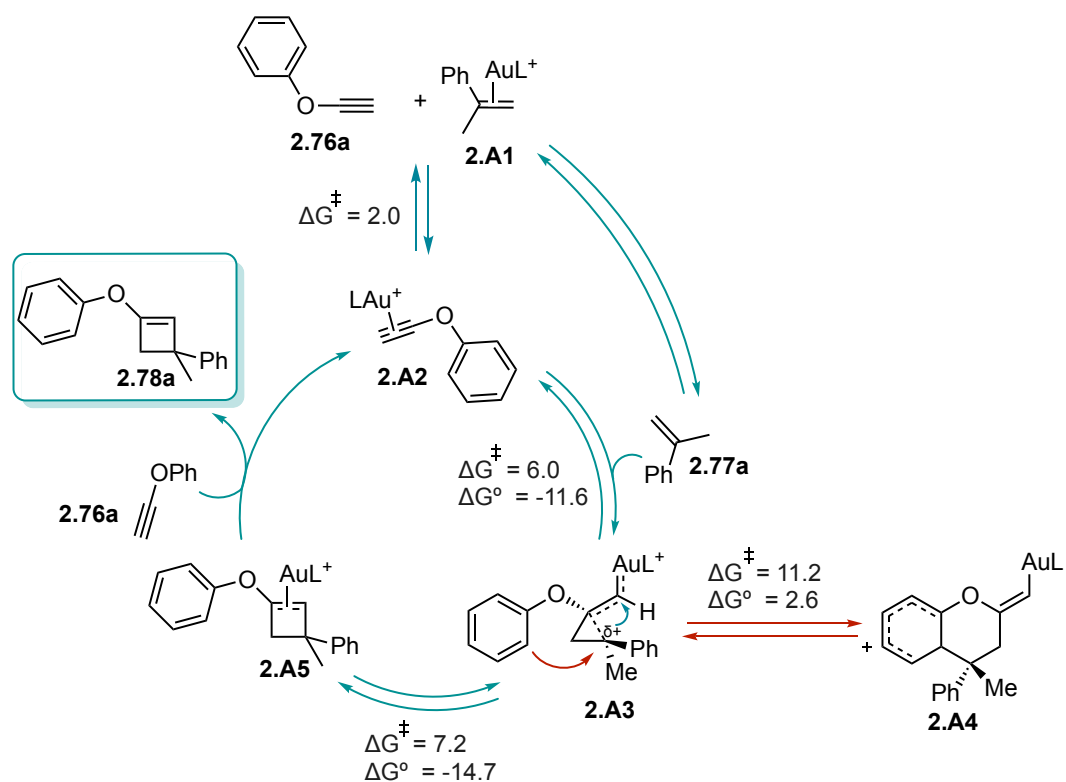
When the model substrate was exposed to NCS, NBS and NIS in acetonitrile at 23°C overnight (**Conditions 2**), products **2.83a**, **2.83e** and **2.83f** were isolated. It is possible to observe an increase of diastereoselectivity together with a decrease of yield when going from the smallest $-\text{Cl}$ to the bulkiest $-\text{I}$ substituent. In these cases, the reaction was performed again in dry acetonitrile to verify whether that could increase the yield, since the simple hydrolysis side-product was always observed in the crude. However, as expected, that shut down also the main halogenation-hydrolysis pathway since the water present in the solvent is necessary for it to happen as well.

For every product shown in Table 2.10 (except for **2.83d**, presenting only one chiral center) GOESY and NOESY NMR show that the major diastereomer is the one where the halogen and methyl groups are on the same side of the molecule.

Reaction Mechanism⁴³

We were interested in exploring the mechanism of the [2+2] cycloaddition involving terminal ynol ether **2.76a** and α -methylstyrene **2.77a**. Based on our earlier results,⁴² it seemed reasonable to suggest that the [2+2] mechanism would commence with the formation of the cyclopropyl gold(I) carbene of the type **2.A3** (Scheme 2.18). Through associative ligand exchange between $(\eta^2\text{-alkene})\text{gold(I)}$ complex **2.A1** and the ynol ether **2.76a**, the $(\eta^2\text{-alkyne})\text{gold(I)}$ complex **2.A2** is formed. Four possible cyclopropyl gold(I) carbene species (two diastereomers and two regioisomers) can be generated when the latter interacts with **2.77a**, and **2.A3** was found to be the most kinetically favored among them.^{44,50} Given the open nature of the cyclopropyl ring in this intermediate, **2.A3** was found to be closer to a homoallylic gold(I)-stabilized cation where the benzylic carbon bears a positive charge. From **2.A3**, the exothermic ring expansion ($\Delta G^\ddagger = 7.2 \text{ Kcal}\cdot\text{mol}^{-1}$) can facilitate the formation of **2.A5**, resulting in the observed product **2.78a** upon ligand exchange with another substrate molecule (blue pathway). Alternatively, the aromatic ring on the oxygen in **2.A3** might initiate a Friedel-Crafts-type reaction by attacking the benzylic carbon on the cyclopropyl ring (red pathway), leading to the formation of Wheland intermediate **2.A4** but with a higher barrier compared to ring expansion ($\Delta G^\ddagger = 11.2 \text{ Kcal}\cdot\text{mol}^{-1}$). For terminal alkynes, this secondary pathway is both kinetically and thermodynamically disfavored.

⁵⁰ Since the DFT studies were completely performed by Margherita Zanini, just the data strictly necessary to elucidate the mechanism will be discussed. Further information can be found in the cited publication.

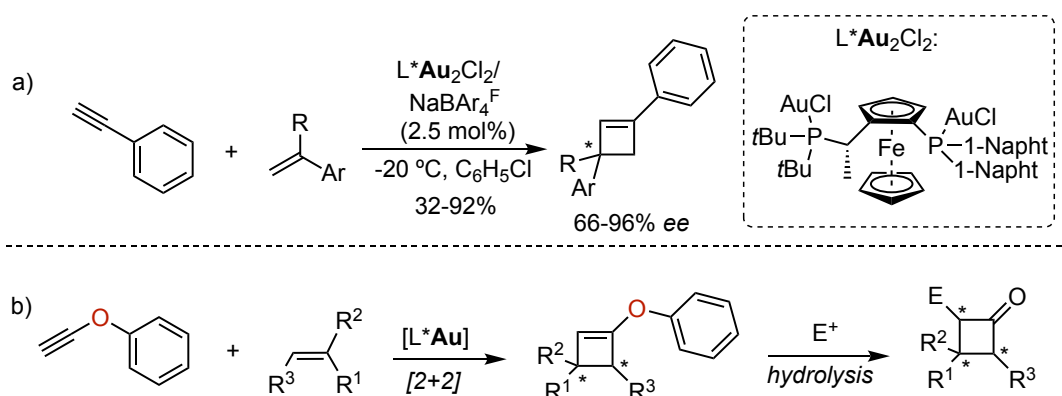


Scheme 2.18. Computed catalytic cycle of the [2+2] cycloaddition of terminal ynol ethers and alkenes. (L = PMe₃. Free energies in Kcal·mol⁻¹).

Nevertheless, we showed that for internal ynol ethers, depending on the substitution pattern of the alkene, ring expansion leading to [2+2] cycloaddition products or a Friedel-Crafts-type reaction leading to the [4+2] cycloaddition products can both happen, but for matter of brevity, it will not be discussed in the present manuscript.⁴⁴

Towards the Asymmetric [2+2] Cycloaddition

We were interested in testing whether the enantioselective [2+2] cycloaddition between ynol ethers and alkenes could be developed. As mentioned in the **General Introduction**, our group disclosed the asymmetric [2+2] between alkynes and alkenes catalyzed by a non-C₂-symmetric JosiPhos digold(I) complex (Scheme 2.19a).⁵¹ The scope is mainly limited to phenylacetylene and methylstyrene derivatives and in most cases the enantioselectivities reached are high but not excellent. We wanted to verify whether with the similar phenoxyacetylene substrate we could also achieve enantioinduction, to eventually design an asymmetric construction of cyclobutanones. (Scheme 2.19b).



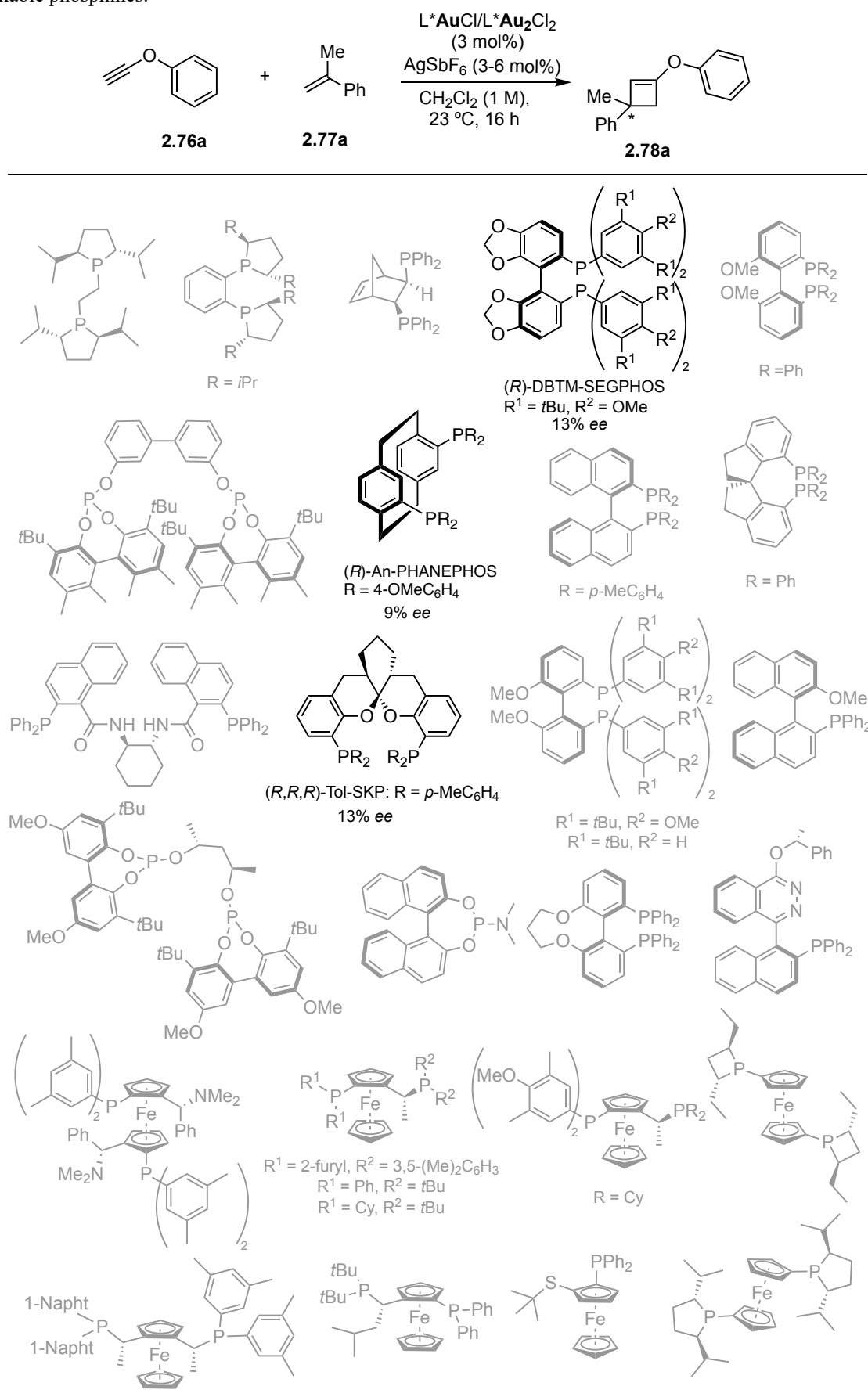
Scheme 2.19. a) Previous results on asymmetric [2+2] cycloaddition of alkynes with alkenes. b) Current strategy to synthesize enantioenriched cyclobutanones.

To start with our exploration, we first performed an HTE screening of commercially available chiral gold catalysts among our standard substrates **2.76a** and **2.77a**. (Table 2.11).

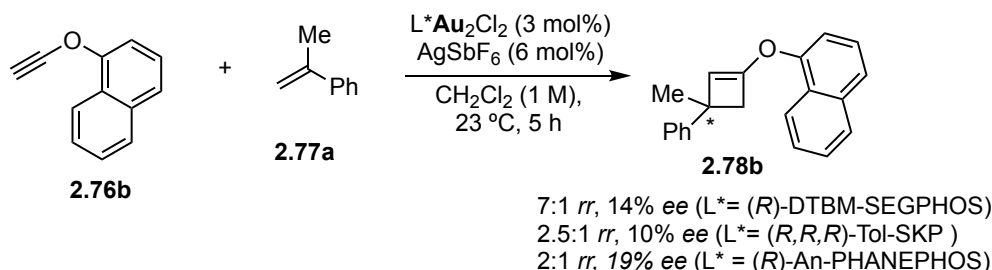
This reaction was only taken as a model for developing further studies, since, once hydrolyzed, the enantioenriched cyclobutene product **2.78a** would give rise to an achiral cyclobutanone, unless **2.78a** would be reacted with an electrophile different from a proton source, such as Br₂, which in that case would afford enantiomerically enriched diastereomers.

Unfortunately, most catalyst gave racemic products, and only dinuclear complexes (*R*)-DTBM-SEGPHOS, (*R,R,R*)-Tol-SKP and (*R*)-An-PHANEPHOS afforded slightly higher *er* (Table 2.11).

⁵¹ García-Morales, C.; Ranieri, B.; Escofet, I.; López-Suarez, L.; Obradors, C.; Konovalov, A. I.; Echavarren, A. M. Enantioselective Synthesis of Cyclobutenes by Intermolecular [2+2] Cycloaddition with Non-C₂ Symmetric Digold Catalysts. *J. Am. Chem. Soc.* **2017**, *139*, 13628–13631.

Table 2.11 HTE screening for the asymmetric [2+2] cycloaddition of ynol ethers with alkenes using commercially available phosphines.⁴³

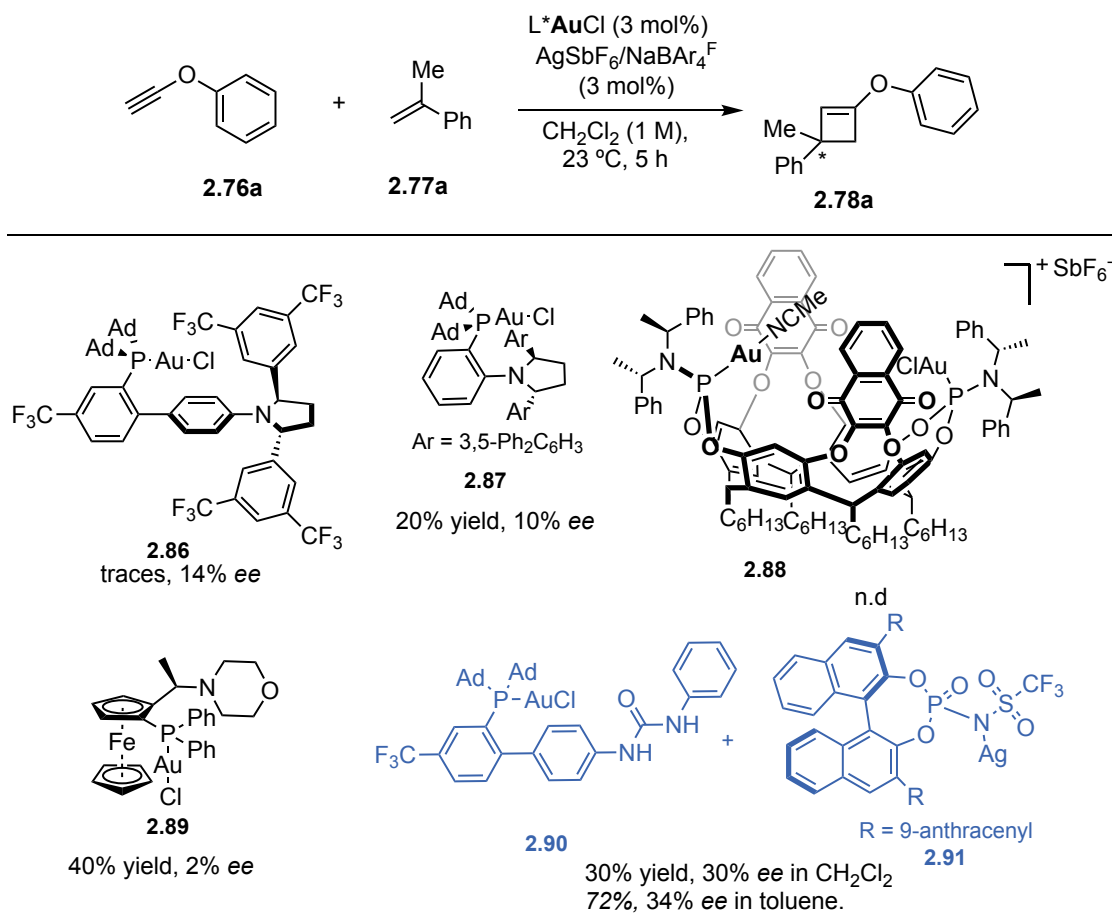
We considered that increasing the size of the phenolic part changing it for 1-naphtol might favor major level of enantioinduction. Thus, we performed the reaction among **2.76b** and **2.77a** in the presence of the three catalyst that performed best, but also in this case the observed *er* were low. Additionally, scarce regioselectivities were obtained too (Scheme 2.20).



Scheme 2.20. Asymmetric trials with naphthyl-substituted **2.76b**.⁴³

Given the disappointing results obtained with commercially available ligands, we moved to screening ligands designed in our group (Table 2.12).

Table 2.12. Screening of chiral Au(I) catalysts designed in our group for the [2+2] cycloaddition of **2.76a** and **2.77a**.⁴⁷



Pyrrolidine based catalysts **2.86-2.87**⁵² and cavitand **2.88**⁵³ performed poorly affording nearly racemic products as well as the ferrocenyl **2.89** recently developed in our group.⁵⁴ Combination of the urea-based catalyst **2.90** with the chiral Ag(I) counteranion **2.91**,⁵⁵ resulted in a 30% *ee* for product **2.78a**, the highest observed so far for this transformation, and, if the reaction was run in toluene, the *ee* went up to 34%, together with the yield which increased up to 72%.

The *ee* reached in the last case looked promising to us, given the difficulties usually encountered in gold(I)-catalyzed enantioselective reactions of alkynes performed in an intermolecular fashion.⁵⁶ We therefore decided to perform another HTE screening using this time different gold(I) complexes and silver or copper counteranions previously used to catalyze other enantioselective transformations⁵⁵ (Table 2.13). While no conversion was obtained when using **Au7** or **Ag2**, **Cu8** performed surprisingly decently when combined with **Au1** and **Au2** (= **2.90**). These last two gold complexes seem to be in general the most promising ones, and combined with **Ag5** (= **2.91**) and **Ag6**, gave the best results in terms of *ee* and yield.

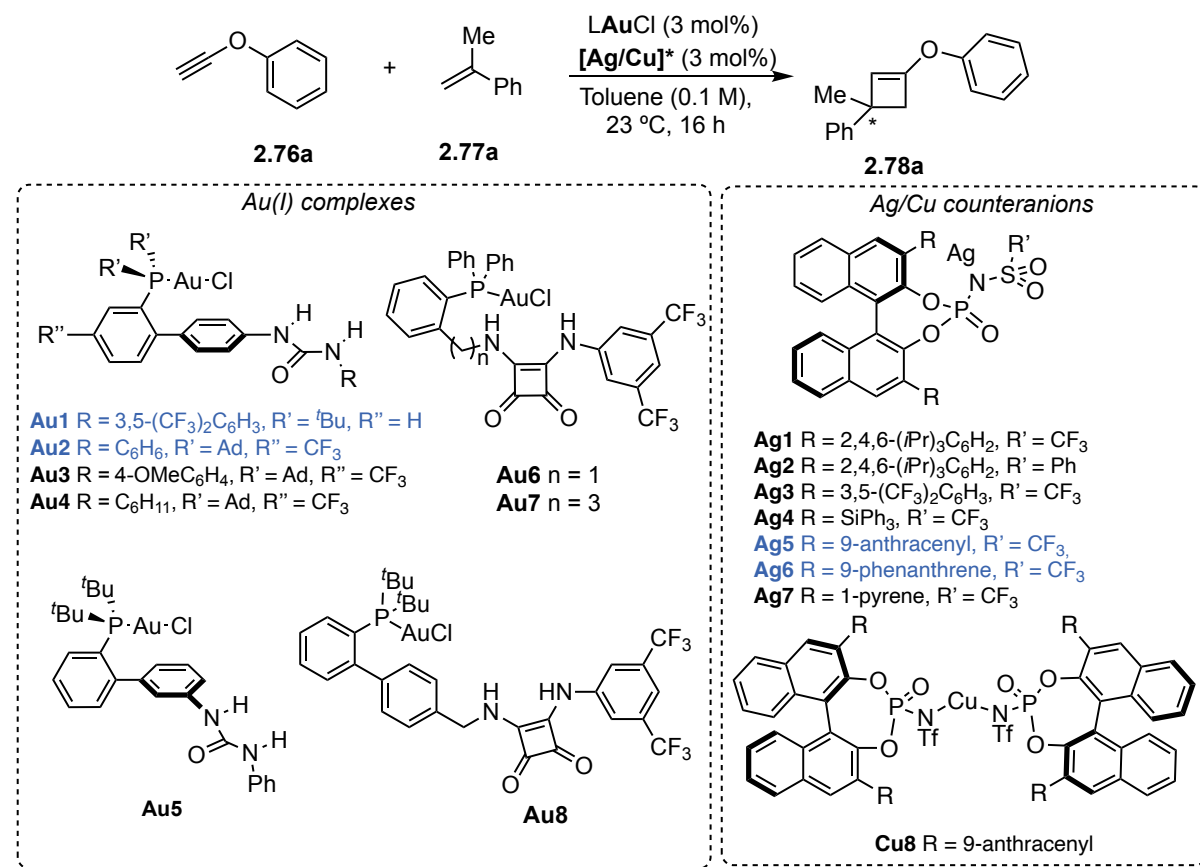
⁵² **2.87** was synthesized by Nicolas Fincias. See: a) Zuccarello, G.; Mayans, J. G.; Escofet, I.; Scharnagel, D.; Kirillova, M. S.; Pérez-Jimeno, A. H.; Calleja, P.; Boothe, J. R.; Echavarren, A. M. Enantioselective Folding of Enynes by Gold(I) Catalysts with a Remote C₂-Chiral Element. *J. Am. Chem. Soc.* **2019**, *141*, 11858–11863. b) Zuccarello, G.; Nannini, L. J.; Arroyo-Bondía, A.; Fincias, N.; Arranz, I.; Pérez-Jimeno, A. H.; Peeters, M.; Martín-Torres, I.; Sadurní, A.; García-Vázquez, V.; Wang, Y.; Kirillova, M. S.; Montesinos-Magraner, M.; Caniparoli, U.; Núñez, G. D.; Maseras, F.; Besora, M.; Escofet, I.; Echavarren, A. M. Enantioselective Catalysis with Pyrrolidinyl Gold(I) Complexes: DFT and NEST Analysis of the Chiral Binding Pocket. *JACS Au* **2023**, *3*, 1742–1754.

⁵³ **2.88** was synthesized by Inmaculada Martín-Torres and Gala Ogalla. See: Martín-Torres, I.; Ogalla, G.; Yang, J.-M.; Rinaldi, A.; Echavarren, A. M. Enantioselective Alkoxy cyclization of 1,6-Enynes with Gold(I)-Cavitands: Total Synthesis of Mafaicheenamamine C. *Angew. Chem. Int. Ed.* **2021**, *60*, 9339–9344, *Angew. Chem.* **2021**, *133*, 9425–9430.

⁵⁴ Catalyst developed by Pablo Mora.

⁵⁵ The complexes of this family were synthesized by Allegra Franchino and Àlex Martí. See: Franchino, A.; Martí, À.; Echavarren, A. M. H-Bonded Counterion-Directed Enantioselective Au(I) Catalysis. *J. Am. Chem. Soc.* **2022**, *144*, 3497–3509.

⁵⁶ Zuccarello, G.; Escofet, I.; Caniparoli, U.; Echavarren, A. M., New-Generation Ligand Design for the Gold-Catalyzed Asymmetric Activation of Alkynes, *ChemPlusChem* **2021**, *86*, 1283–1296.

Table 2.13. HTE screening of urea/squaramide Au(I) complexes in combination with chiral Ag/Cu counteranions designed in our group.^a

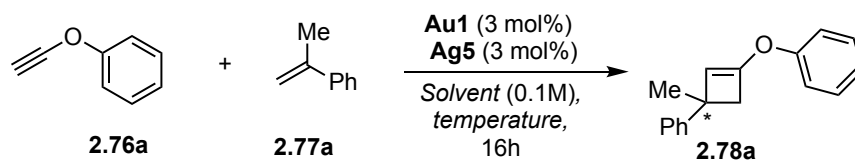
HTE	Au1	Au2	Au3	Au4	Au5	Au6	Au7	Au8
Ag1	56% yield 8% <i>ee</i>	53% yield 5% <i>ee</i>	43% yield 2% <i>ee</i>	39% yield 1% <i>ee</i>	21% yield 5% <i>ee</i>	8% yield 11% <i>ee</i>	/	20% yield -11% <i>ee</i>
Ag2	/	/	/	/	/	/	/	/
Ag3	54% yield 10% <i>ee</i>	54% yield 7% <i>ee</i>	38% yield 6% <i>ee</i>	23% yield 7% <i>ee</i>	32% yield 0% <i>ee</i>	17% yield 8% <i>ee</i>	/	16% yield -3% <i>ee</i>
Ag4	32% yield 0% <i>ee</i>	44% yield 6% <i>ee</i>	13% yield 4% <i>ee</i>	/	22% yield -6% <i>ee</i>	15% yield -5% <i>ee</i>	/	13% yield 1% <i>ee</i>
Ag5	54% yield 34% <i>ee</i>	59% yield 33% <i>ee</i>	38% yield 29% <i>ee</i>	53% yield 31% <i>ee</i>	22% yield 31% <i>ee</i>	7% yield 12% <i>ee</i>	/	15% yield 1% <i>ee</i>
Ag6	52% yield 37% <i>ee</i>	61% yield 30% <i>ee</i>	40% yield 29% <i>ee</i>	30% yield 36% <i>ee</i>	23% yield 18% <i>ee</i>	6% yield 15% <i>ee</i>	/	20% yield -4% <i>ee</i>
Ag7	50% yield 26% <i>ee</i>	60% yield 31% <i>ee</i>	39% yield 28% <i>ee</i>	40% yield 33% <i>ee</i>	16% yield 3% <i>ee</i>	7% yield 31% <i>ee</i>	/	7% yield -7% <i>ee</i>
Cu8	47% yield 31% <i>ee</i>	44% yield 30% <i>ee</i>	12% yield 26% <i>ee</i>	/	4% yield 20% <i>ee</i>	4% yield 15% <i>ee</i>	/	/

^a Yields calculated by ¹H NMR using 4,4'-dimethylbiphenyl as an internal standard.

The combination **Au1-Ag5** was chosen to perform a solvent and temperature screening in the fumehood (Table 2.14). Chloroform was assessed to be the best solvent in terms of *er*, giving product **2.78a** at 0 °C with 40% yield and 72:28 *er* (44% *ee*, Table 2.14, entry 9), so the temperature was further lowered

down to -20°C and the *er* could be increased up to 75:25 although with a low 12% yield (Table 2.14, entry 10). Starting from electron poor ynol ether **2.76d** would not increase the yield or the *er* (Table 2.14, entry 11).

Table 2.14. Solvent and temperature screening for the [2+2] of **2.76a** and **2.77a** using counteranion-directed enantioselective Au(I) catalysis.



Entry	Solvent	T ($^{\circ}\text{C}$)	Yield (%)	<i>er</i>
1	Toluene	23	62	65:35
2	CH_2Cl_2	23	48	63:37
3	$\text{C}_6\text{H}_5\text{CF}_3$	23	43	60:40
4	$\text{C}_6\text{H}_5\text{Cl}$	23	47	64:36
5	THF	23	/	/
6	<i>p</i> -Xylene	23	28	66:34
7	Benzene	23	48	70:30
8	CHCl_3	23	30	72:28
9	CHCl_3	0	40	72:28
10	CHCl_3	-20	12	75:25
11 ^b	CHCl_3	0	34	72:28

^aYields calculated by ^1H NMR using trichloroethylene as an internal std. ^bReaction performing starting from **2.76d**.

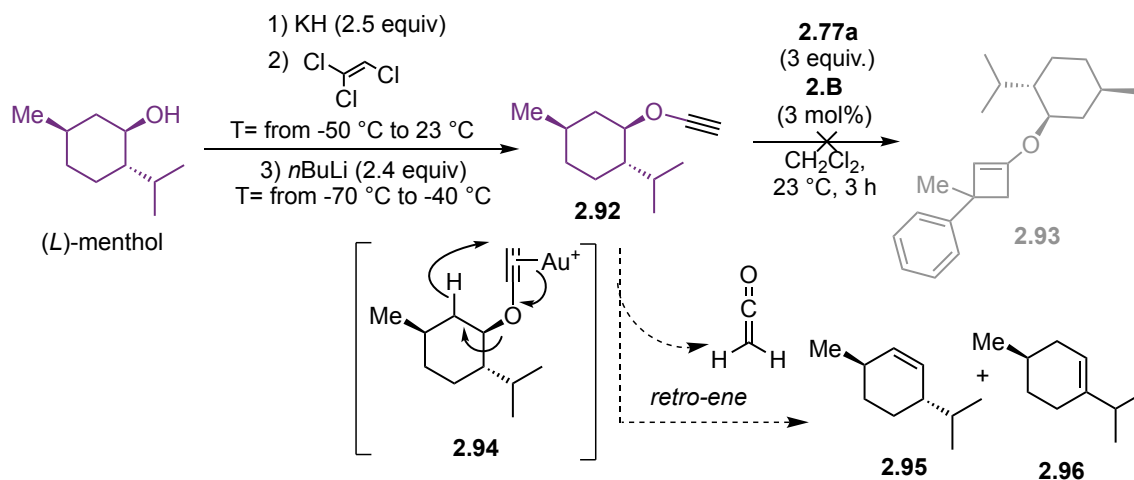
Since using catalysts designed in our group, we could reach a maximum of 75:25 *er* (50% *ee*), we wondered if by changing approach we might obtain better results.

As introduced in **Chapter I**, chiral auxiliaries are a powerful tool used in asymmetric synthesis which can substitute ligand design in a wide variety of transformations.⁵⁷ Given the failed attempts in performing the stereoselective [2+2] cycloadditions between ynamides equipped with a chiral auxiliary and alkenes, we therefore looked for commercially available chiral alcohols/phenols that we might attach to our ynol ether substrates and serve as stereoinducting moieties. We started by synthesizing **2.92** (Scheme 2.21) from (*L*)-menthol, as previously described in literature.⁵⁸ This compound resulted to be unstable in time and to silica treatment, therefore, once obtained, we subjected it immediately to gold(I) catalysis in the presence of α -methylstyrene. Unfortunately, it appears that this kind of alkyl

⁵⁷ Diaz-Muñoz, G.; Miranda, I. L.; Sartori, S. K.; de Rezende, D. C.; Alves Nogueira Diaz, M. Use of Chiral Auxiliaries in the Asymmetric Synthesis of Biologically Active Compounds: A Review. *Chirality* **2019**, *31*, 776–812.

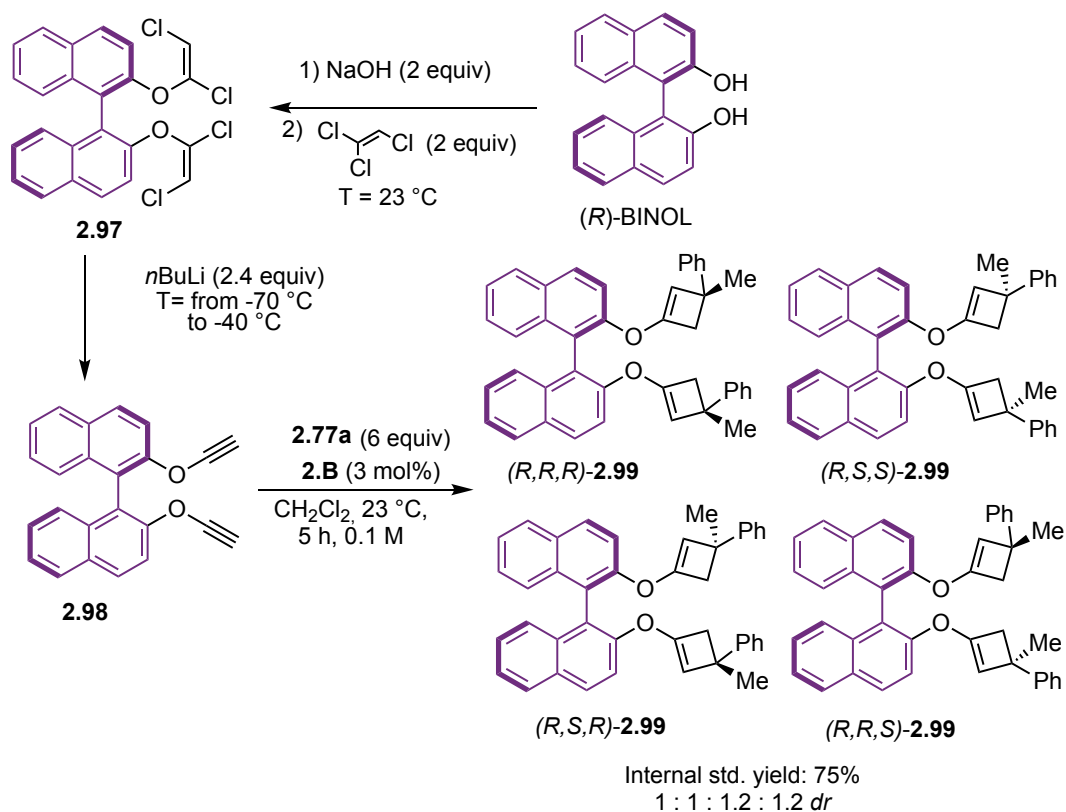
⁵⁸ Moyano, A.; Charbonnier, F.; Greene, A. E. Simple Preparation of Chiral Acetylenic Ethers. *J. Org. Chem.* **1987**, *52*, 2919–2922.

ynol ethers can undergo retro-ene reaction through **2.94**, since the mix of isomers **2.95-2.96** was identified in the crude, therefore, no desired [2+2] product **2.93** was isolated (Scheme 2.21).



Scheme 2.21. Failed attempt to use (*L*)-menthol as a chiral auxiliary for the [2+2] cycloaddition of **2.92** and **2.77a**.

To avoid retro-ene side-reactivity, we moved to select a chiral auxiliary that could not undergo this pathway, and resembled more substrate **2.76a**. Starting from (*R*)-BINOL, following the same procedure we followed for **2.76a**, **2.97** could be readily synthesized and then afford ynone ether **2.98** as a stable solid compound (Scheme 2.22). The latter underwent [2+2] cycloaddition with α -methylstyrene forming four cyclobutene diastereomers **2.99** in a total yield of 75% but with a 1:1:1.2:1.2 ratio which would not be possible to separate.



Scheme 2.22. Use of (*R*)-BINOL as chiral auxiliary for the [2+2] cycloaddition of **2.98** and **2.77a**

Conclusions

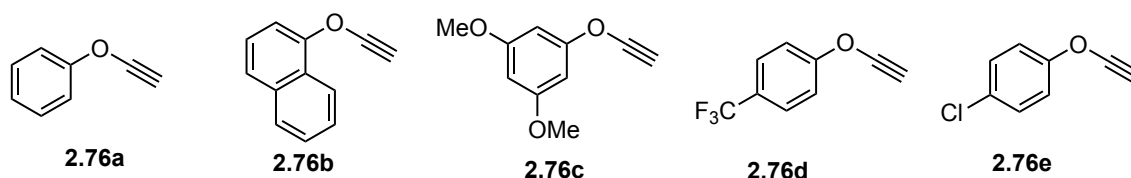
We have developed a new synthetic method that allows access to cyclobutyl enol ethers, with good yields and excellent regioselectivities, via a gold(I)-catalyzed [2+2] cycloaddition of alkenes with terminal ynol ethers. These functionalized alkynes can be considered as stable equivalents of ketenes, which are usually difficult to handle.

Hydrolysis or bromination of the [2+2] products lead to cyclobutanones. In the first case, a one-pot two-step sequence was developed to directly access the desired ketones from ynol ether precursors.

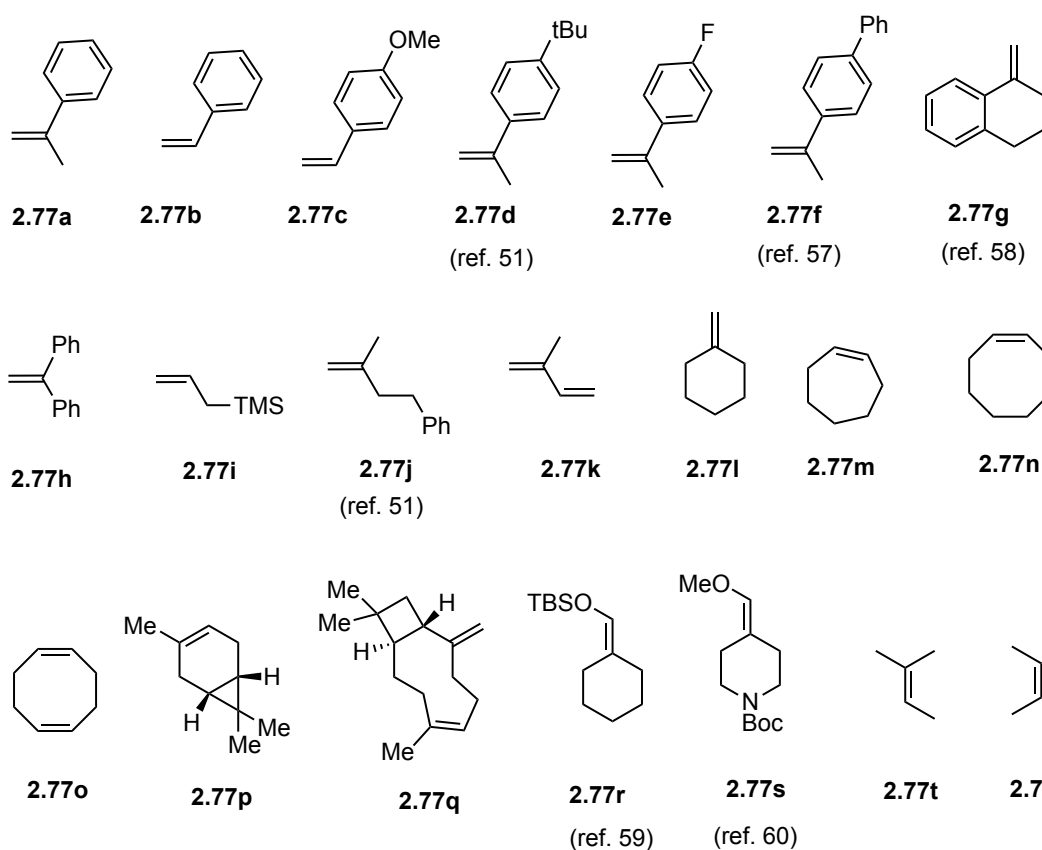
Efforts in developing the asymmetric version of the reaction were made, both via chiral auxiliary approach and enantioselective catalysis using chiral ligands. In the latter case, promising *er* were obtained using urea Au(I) catalysts presenting chiral phosphoramidate counteranions, but further optimization is required.

Experimental Part

The **General Information** is provided in the Experimental Part of **Chapter I**. All reagents were used as purchased, with no further purification. The ynol ethers used in this study and reported below were synthesized following a procedure reported in literature.⁴⁵



The alkenes that successfully yielded the products were purchased from commercial vendors or prepared according to the cited literature (see figure below).^{51,59,60,61,62}



⁵⁹ Lux, M.; Klussmann, M. Additions of Aldehyde-Derived Radicals and Nucleophilic N-Alkylindoles to Styrenes by Photoredox Catalysis. *Org. Lett.* **2020**, *22*, 3697–3701.

⁶⁰ Iwai, R.; Suzuki, S.; Sasaki, S.; Sairi, A. S.; Igawa, K.; Suenobu, T.; Morokuma, K.; Konishi, G. Bridged Stilbenes: AI-Egens Designed via a Simple Strategy to Control the Non-Radiative Decay Pathway. *Angew. Chem. Int. Ed.* **2020**, *59*, 10566–10573.

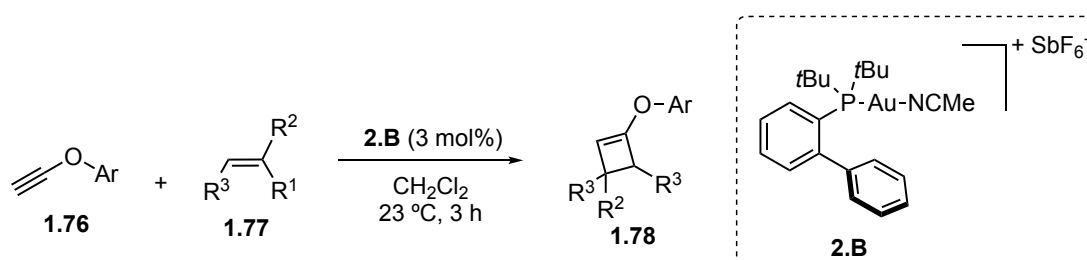
⁶¹ Song, J. J.; Tan, Z.; Reeves, J. T.; Fandrick, D. R.; Yee, N. K.; Senanayake, H. N-Heterocyclic Carbene-Catalyzed Silyl Enol Ether Formation†. *Org. Lett.* **2008**, *10*, 877–880.

⁶² Mato, M.; Garcia-Morales, C.; Echavarren, A. M. Synthesis of Trienes by Rhodium-Catalyzed Assembly and Disassembly of Non-Acceptor Cyclopropanes. *ACS Catal.* **2020**, *10*, 3564–3570.

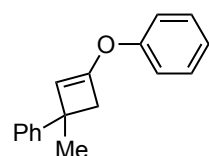
Synthetic procedures and Characterization Data

General procedure A: Gold(I)-catalyzed reaction of terminal ynol ethers with alkenes to afford **2.78**

A GC-MS vial equipped with a magnetic stirring bar was charged with the ynol ether (0.2 mmol, 1 equiv) and CH₂Cl₂ (HPLC grade, 0.2 mL, 1 M). The alkene (0.6 mmol, 3 equiv) was then added followed by [(JohnPhos)AuNCMe]SbF₆ (**2.B**, 3 mol%, 4.6 mg). The resulting mixture was stirred at 23 °C for 3 h. The reaction was monitored by GC-MS or UHPLC-MSD. Once completed, the reaction was quenched with few drops of triethylamine and the solvent evaporated. The crude product was purified by flash chromatography on silica gel (eluent = pentane:Et₂O gradient from 100:0 to 50:1, otherwise stated) to obtain the pure oxy-cyclobutene.



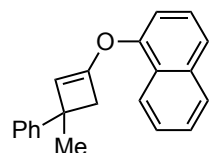
(1-Methyl-3-phenoxy-cyclobut-2-en-1-yl)benzene (**2.78a**)



Cyclobutene **2.78a** was synthesized following general procedure **A** starting from (ethynyloxy)benzene (23.6 mg, 0.2 mmol) and α -methylstyrene (78 μ L, 0.6 mmol).

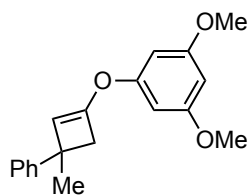
The crude product was purified by flash chromatography affording **2.78a** as a colorless oil (40 mg, 85%). ¹H NMR (400 MHz, CDCl₃) δ 7.42 – 7.30 (m, 6H), 7.25 – 7.11 (m, 4H), 5.19 (s, 1H), 2.91 (d, J = 12.6 Hz, 1H), 2.87 (d, J = 12.6 Hz, 1H), 1.61 (s, 3H). ¹³C NMR (101 MHz, CDCl₃) δ 155.0, 149.5, 148.0, 129.7, 128.2, 126.1, 125.9, 124.2, 119.5, 109.1, 47.3, 41.4, 28.4. HRMS (APCI) m/z calculated for C₁₇H₁₇O [M+H]⁺: 237.1274, found: 237.1273.

1-((3-Methyl-3-phenylcyclobut-1-en-1-yl)oxy)naphthalene (**2.78b**)

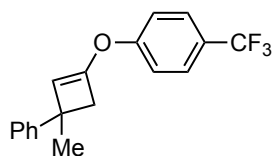


Cyclobutene **2.78b** was synthesized following general procedure **A** starting from 1-(ethynyloxy)naphthalene (34 mg, 0.2 mmol) and α -methylstyrene (78 μ L, 0.6 mmol).

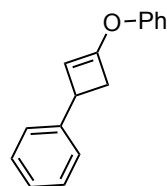
The crude product was purified by flash chromatography affording **2.78b** as a colorless oil (34 mg, 58%). ¹H NMR (400 MHz, CDCl₃) δ 8.18 (ddt, J = 6.4, 3.6, 0.8 Hz, 1H), 7.91 – 7.83 (m, 1H), 7.65 (dt, J = 8.2, 1.0 Hz, 1H), 7.57 – 7.49 (m, 2H), 7.44 (dd, J = 8.2, 7.6 Hz, 1H), 7.41 – 7.36 (m, 2H), 7.36 – 7.29 (m, 3H), 7.25 – 7.19 (m, 1H), 5.20 (s, 1H), 2.99 (d, J = 12.7 Hz, 1H), 2.95 (d, J = 12.7 Hz, 1H), 1.62 (s, 3H). ¹³C NMR (101 MHz, CDCl₃) δ 150.8, 149.7, 148.0, 135.0, 128.2, 127.9, 126.6, 126.2, 126.1, 125.9, 125.6, 124.2, 122.1, 114.4, 109.6, 47.3, 41.4, 28.4. HRMS (APCI) m/z calculated for C₂₁H₁₉O⁺ [M+H]⁺: 287.1430, found: 287.1431.

1,3-Dimethoxy-5-((3-methyl-3-phenylcyclobut-1-en-1-yl)oxy)benzene (2.78c)

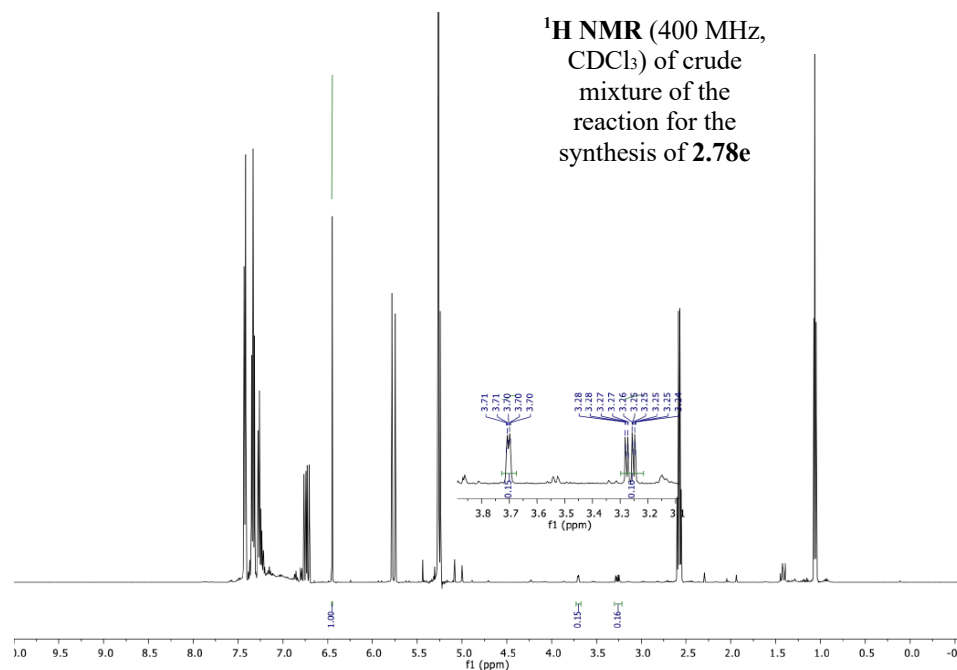
Cyclobutene **2.78c** was synthesized following general procedure **A** starting from 1-(ethynyloxy)-3,5-dimethoxybenzene (35.6 mg, 0.2 mmol) and α -methylstyrene (78 μ L, 0.6 mmol). The crude product was purified by flash chromatography affording **2.78c** as a colorless oil (13 mg, 22%). $^1\text{H NMR}$ (300 MHz, CDCl_3) δ 7.42 – 7.29 (m, 4H), 7.21 (ddt, $J = 8.5, 6.4, 1.6$ Hz, 1H), 6.36 (d, $J = 2.2$ Hz, 2H), 6.26 (t, $J = 2.2$ Hz, 1H), 5.27 (s, 1H), 3.79 (s, 6H), 2.88 (d, $J = 12.8$ Hz, 1H), 2.87 (d, $J = 12.8$ Hz, 1H), 1.60 (s, 3H). $^{13}\text{C NMR}$ (101 MHz, CDCl_3) δ 161.5, 156.7, 148.9, 147.9, 128.2, 126.1, 125.9, 109.9, 97.9, 96.3, 55.6, 47.3, 41.5, 28.4. **HRMS** (APCI) m/z calculated for $\text{C}_{19}\text{H}_{21}\text{O}_3$ $[\text{M}+\text{H}]^+$: 297.1485, found: 297.1484.

1-((3-Methyl-3-phenylcyclobut-1-en-1-yl)oxy)-4-(trifluoromethyl)benzene (2.78d)

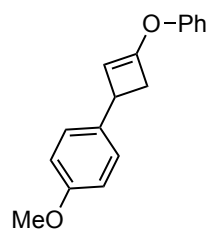
Cyclobutene **2.78d** was synthesized following general procedure **A** starting from 1-(ethynyloxy)-4-(trifluoromethyl)benzene (37.2 mg, 0.2 mmol) and α -methylstyrene (78 μ L, 0.6 mmol). The crude product was purified by flash chromatography affording **2.78d** as a colorless oil (44 mg, 72%). $^1\text{H NMR}$ (400 MHz, CDCl_3) δ 7.72 – 7.54 (m, 2H), 7.47 – 7.33 (m, 4H), 7.31 – 7.14 (m, 3H), 5.32 (s, 1H), 2.94 (d, $J = 12.7$ Hz, 1H), 2.89 (d, $J = 12.7$ Hz, 1H), 1.63 (s, 3H). $^{19}\text{F NMR}$ (376 MHz, CDCl_3) δ -62.0. $^{13}\text{C NMR}$ (101 MHz, CDCl_3) δ 157.7, 148.4, 147.5, 128.3, 127.1 (q, $J = 3.7$ Hz), 126.1, 124.2 (q, $J = 271.6$ Hz), 119.2, 111.2, 47.3, 41.7, 28.3. **HRMS** (APCI) m/z calculated for $\text{C}_{18}\text{H}_{16}\text{F}_3\text{O}$ $[\text{M}+\text{H}]^+$: 305.1148, found: 305.1156.

(3-Phenoxy)cyclobut-2-en-1-yl)benzene (2.78e)

Cyclobutene **2.78e** was synthesized following general procedure **A** starting from (ethynyloxy)benzene (23.6 mg, 0.2 mmol) and styrene (63 mg, 0.3 mmol). The diagnostic signals of product were identified in the crude mixture and quantified by $^1\text{H NMR}$ using trichloroethylene as internal standard (16%). However any attempt to isolate the product failed.

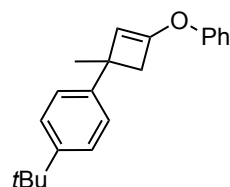


1-Methoxy-4-(3-phenoxy-cyclobut-2-en-1-yl)benzene (**2.78f**)

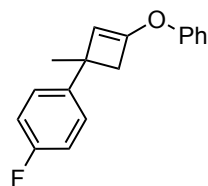


Cyclobutene **2.78f** was synthesized following general procedure **A** starting from (ethynyloxy)benzene (23.6 mg, 0.2 mmol) and 1-methoxy-4-vinylbenzene (81 mg, 0.6 mmol). The crude product was purified by flash chromatography affording **2.78f** as a yellow oil (19 mg, 37%). ¹H NMR (400 MHz, CDCl₃) δ 7.40 – 7.34 (m, 2H), 7.28 – 7.19 (m, 4H), 7.15 (ddt, *J* = 8.5, 7.0, 1.2 Hz, 1H), 6.90 – 6.84 (m, 2H), 4.97 (d, *J* = 1.0 Hz, 1H), 3.81 (s, 3H), 3.66 (dt, *J* = 4.6, 1.3 Hz, 1H), 3.24 (dd, *J* = 13.0, 4.6 Hz, 1H), 2.52 (dd, *J* = 13.0, 1.6 Hz, 1H). ¹³C NMR (101 MHz, CDCl₃) δ 158.4, 155.0, 150.1, 136.2, 129.7, 127.7, 124.2, 119.4, 113.9, 105.3, 55.5, 41.9, 36.8. HRMS (ESI) *m/z* calculated for C₁₇H₁₇O₂ [M+H]⁺: 253.1223, found: 253.1221.

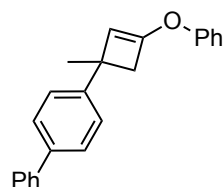
1-(*tert*-Butyl)-4-(1-methyl-3-phenoxy-cyclobut-2-en-1-yl)benzene (**2.78g**)



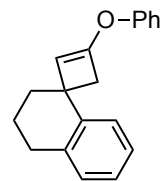
Cyclobutene **2.78g** was synthesized following general procedure **A** starting from (ethynyloxy)benzene (23.6 mg, 0.2 mmol) and 1-(*tert*-butyl)-4-(prop-1-en-2-yl)benzene (105 mg, 0.6 mmol). The crude product was purified by flash chromatography affording **2.78g** as a colorless oil (52 mg, 89%). ¹H NMR (400 MHz, CDCl₃) δ 7.40 – 7.30 (m, 6H), 7.20 (m, 2H), 7.18 – 7.12 (m, 1H), 5.18 (s, 1H), 2.91 (d, *J* = 12.6 Hz, 1H), 2.85 (d, *J* = 12.6 Hz, 1H), 1.61 (s, 3H), 1.35 (s, 9H). ¹³C NMR (101 MHz, CDCl₃) δ 155.1, 149.4, 148.6, 144.9, 129.7, 125.8, 125.1, 124.2, 119.5, 109.3, 47.3, 41.0, 34.5, 31.6, 28.3. HRMS (ESI) *m/z* calculated for C₂₁H₂₅O [M+H]⁺: 293.1900, found: 293.1898.

1-Fluoro-4-(1-methyl-3-phenoxy-cyclobut-2-en-1-yl)benzene (2.78h)

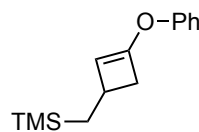
Cyclobutene **2.78h** was synthesized following general procedure **A** starting from (ethynyloxy)benzene (23.6 mg, 0.2 mmol) and 1-fluoro-4-(prop-1-en-2-yl)benzene (82 mg, 0.6 mmol). The crude product was purified by flash chromatography affording **2.78h** as a colorless oil (34 mg, 67%). **¹H NMR** (500 MHz, CDCl₃) δ 7.35 (tt, *J* = 6.8, 1.0 Hz, 2H), 7.32 – 7.28 (m, 2H), 7.19 – 7.14 (m, 2H), 7.14 – 7.11 (m, 1H), 7.02 – 6.92 (m, 2H), 5.13 (d, *J* = 0.7 Hz, 1H), 2.87 – 2.80 (m, 2H), 1.57 (s, 3H). **¹⁹F NMR** (376 MHz, CDCl₃) δ -117.87. **¹³C NMR** (126 MHz, CDCl₃) δ 162.3 (d, *J* = 243.7 Hz), 155.0, 149.6, 143.7, 143.7, 129.7, 127.6 (d, *J* = 7.8 Hz), 124.3, 119.5, 114.9 (d, *J* = 21.0 Hz), 108.9, 47.4, 40.9, 28.4. **HRMS** (APCI) *m/z* calculated for C₁₇H₁₆FO [M+H]⁺: 255.1180, found: 255.1170.

4-(1-Methyl-3-phenoxy-cyclobut-2-en-1-yl)-1,1'-biphenyl (2.78i)

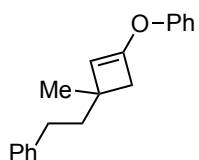
Cyclobutene **2.78i** was synthesized following general procedure **A** starting from (ethynyloxy)benzene (23.6 mg, 0.2 mmol) and 4-(prop-1-en-2-yl)-1,1'-biphenyl (117 mg, 0.6 mmol). The crude product was purified by flash chromatography affording **2.78i** as a white solid (56 mg, 90%). **¹H NMR** (500 MHz, CDCl₃) δ 7.66 – 7.61 (m, 2H), 7.61 – 7.55 (m, 2H), 7.50 – 7.44 (m, 4H), 7.42 – 7.33 (m, 3H), 7.24 – 7.21 (m, 2H), 7.17 (td, *J* = 7.3, 1.2 Hz, 1H), 5.23 (s, 1H), 2.97 (d, *J* = 12.7 Hz, 1H), 2.92 (d, *J* = 12.7 Hz, 1H), 1.67 (s, 3H). **¹³C NMR** (126 MHz, CDCl₃) δ 155.0, 149.6, 147.1, 141.2, 138.9, 129.7, 128.9, 127.2, 127.2, 127.0, 126.6, 124.3, 119.5, 109.1, 47.4, 41.2, 28.3. **HRMS** (APCI) *m/z* calculated for C₂₃H₂₁O [M+H]⁺: 313.1587, found: 313.1568.

3-Phenoxy-3',4'-dihydro-2'H-spiro[cyclobutane-1,1'-naphthalen]-2-ene (2.78j)

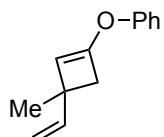
Cyclobutene **2.78j** was synthesized following general procedure **A** starting from (ethynyloxy)benzene (23.6 mg, 0.2 mmol) and 1-methylene-1,2,3,4-tetrahydronaphthalene (87 mg, 0.6 mmol). The crude product was purified by flash chromatography affording **2.78j** as a brownish oil (21 mg, 40%). **¹H NMR** (400 MHz, CDCl₃) δ 7.57 (dd, *J* = 7.5, 1.6 Hz, 1H), 7.42 – 7.34 (m, 2H), 7.28 – 7.23 (m, 2H), 7.21 – 7.06 (m, 4H), 5.00 (s, 1H), 2.84 (dd, *J* = 7.8, 4.3 Hz, 2H), 2.73 (s, 2H), 2.01 – 1.90 (m, 3H), 1.82 (dddd, *J* = 18.7, 9.1, 7.5, 4.0 Hz, 1H). **¹³C NMR** (126 MHz, CDCl₃) δ 155.1, 150.5, 141.8, 137.4, 129.7, 129.0, 126.2, 126.2, 125.7, 124.2, 119.3, 110.6, 49.6, 40.6, 36.0, 30.4, 22.1. **HRMS** (APCI) *m/z* calculated for C₁₉H₁₉O [M+H]⁺: 263.1430, found: 263.1429.

Trimethyl((3-phenoxy)cyclobut-2-en-1-yl)methylsilane (2.78k)

Cyclobutene **2.78k** was synthesized following general procedure **A** starting from (ethynyloxy)benzene (23.6 mg, 0.2 mmol) and allyltrimethylsilane (95 ml, 0.6 mmol). The crude product was purified by flash chromatography affording **2.78k** as a colorless oil (11.6 mg, 24%). ¹H NMR (500 MHz, CDCl₃) δ 7.40 – 7.25 (m, 2H), 7.15 – 7.11 (m, 2H), 7.10 (dt, *J* = 7.3, 1.2 Hz, 1H), 4.80 (d, *J* = 0.9 Hz, 1H), 2.94 (dd, *J* = 12.9, 4.2 Hz, 1H), 2.57 (tdt, *J* = 7.5, 4.2, 1.3 Hz, 1H), 2.22 (dd, *J* = 12.8, 1.5 Hz, 1H), 0.79 (d, *J* = 7.6 Hz, 2H), 0.01 (s, 9H). ¹³C NMR (126 MHz, CDCl₃) δ 155.2, 148.3, 129.6, 123.9, 119.3, 108.7, 40.9, 29.8, 23.3, -0.9. HRMS (APCI) *m/z* calculated for C₁₄H₂₁OSi [M+H]⁺: 233.1356, found: 233.1357.

(3-Methyl-3-phenethylcyclobut-1-en-1-yl)oxybenzene (2.78l)

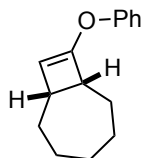
Cyclobutene **2.78l** was synthesized following general procedure **A** starting from (ethynyloxy)benzene (23.6 mg, 0.2 mmol) and (3-methylbut-3-en-1-yl)benzene (87.6 mg, 0.6 mmol). The crude product was purified by flash chromatography affording **2.78l** as a colorless oil (29 mg, 54%). ¹H NMR (500 MHz, CDCl₃) δ 7.39 – 7.32 (m, 2H), 7.29 (t, *J* = 7.5 Hz, 2H), 7.24 – 7.18 (m, 3H), 7.18 – 7.10 (m, 3H), 4.88 (s, 1H), 2.73 – 2.61 (m, 2H), 2.54 (d, *J* = 12.7 Hz, 1H), 2.44 (d, *J* = 12.7 Hz, 1H), 1.90 – 1.78 (m, 2H), 1.31 (s, 3H). ¹³C NMR (126 MHz, CDCl₃) δ 155.2, 148.7, 143.1, 129.6, 128.4, 125.8, 123.9, 119.3, 110.7, 44.3, 42.7, 37.9, 32.8, 24.8. HRMS (APCI) *m/z* calculated for C₁₉H₂₁O [M+H]⁺: 265.1587, found: 265.1585.

((3-Methyl-3-vinylcyclobut-1-en-1-yl)oxy)benzene (2.78m)

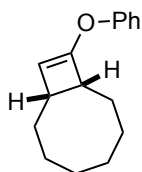
Cyclobutene **2.78m** was synthesized following general procedure **A** starting from (ethynyloxy)benzene (23.6 mg, 0.2 mmol) and isoprene (60 ml, 0.6 mmol). The crude product was purified by flash chromatography affording **2.78m** as a colorless oil (13 mg, 34%). ¹H NMR (500 MHz, CDCl₃) δ 7.38 – 7.29 (m, 2H), 7.17 – 7.14 (m, 2H), 7.14 – 7.10 (m, 1H), 6.06 (dd, *J* = 17.2, 10.4 Hz, 1H), 5.06 (dd, *J* = 17.2, 1.6 Hz, 1H), 4.94 (dd, *J* = 10.4, 1.6 Hz, 1H), 4.84 (s, 1H), 2.61 (d, *J* = 12.7 Hz, 1H), 2.55 (d, *J* = 12.7 Hz, 1H), 1.34 (s, 3H). ¹³C NMR (126 MHz, CDCl₃) δ 155.1, 148.9, 145.8, 129.7, 129.6, 124.1, 119.3, 111.2, 109.4, 45.5, 39.8, 24.1. HRMS (ESI) *m/z* calculated for C₁₃H₁₅O [M+H]⁺: 187.1117, found: 187.1122.

2-PhenoxySpiro[3.5]non-1-ene (2.78n)

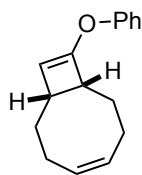
Cyclobutene **2.78n** was synthesized following general procedure **A** starting from (ethynyloxy)benzene (23.6 mg, 0.2 mmol) and methylenecyclohexane (58 mg, 0.6 mmol). The crude product was purified by flash chromatography affording **2.78n** as a colorless oil (32 mg, 74%). $^1\text{H NMR}$ (500 MHz, CDCl_3) δ 7.36 – 7.29 (m, 2H), 7.16 – 7.13 (m, 2H), 7.11 (tt, $J = 7.3, 1.2$ Hz, 1H), 4.98 (s, 1H), 2.37 (s, 2H), 1.62 – 1.38 (m, 10H). $^{13}\text{C NMR}$ (126 MHz, CDCl_3) δ 155.3, 149.9, 129.6, 123.9, 119.3, 110.8, 43.4, 39.5, 37.3, 26.0, 25.1. **HRMS** (APCI) m/z calculated for $\text{C}_{15}\text{H}_{19}\text{O}$ $[\text{M}+\text{H}]^+$: 215.1430, found: 215.1428.

8-Phenoxybicyclo[5.2.0]non-8-ene (2.78o)

Cyclobutene **2.78o** was synthesized following general procedure **A** starting from (ethynyloxy)benzene (35.4 mg, 0.3 mmol) and cycloheptene (87 mg, 0.9 mmol). The crude was purified by flash chromatography affording **2.78o** as a transparent oil (7 mg, 11%). $^1\text{H NMR}$ (500 MHz, CD_2Cl_2) δ 7.37 – 7.29 (m, 2H), 7.17 – 7.07 (m, 3H), 4.70 (d, $J = 1.0$ Hz, 1H), 3.12 (dt, $J = 11.3, 4.3$ Hz, 1H), 2.60 (dt, $J = 10.4, 4.2$ Hz, 1H), 1.87 – 1.67 (m, 5H), 1.52 – 1.21 (m, 5H). $^{13}\text{C NMR}$ (126 MHz, CD_2Cl_2) δ 155.52, 129.84, 124.14, 119.51, 104.80, 49.51, 39.75, 32.37, 31.91, 28.3, 28.3, 28.2. **HRMS** (ESI) m/z calculated for $\text{C}_{15}\text{H}_{19}\text{O}$ $[\text{M}+\text{H}]^+$: 215.1430, found: 215.1428.

9-Phenoxybicyclo[6.2.0]dec-9-ene (2.78p)

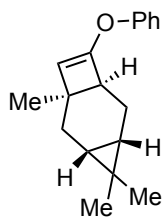
Cyclobutene **2.78p** was synthesized following general procedure **A** starting from (ethynyloxy)benzene (23.6 mg, 0.2 mmol) and (*Z*)-cyclooctene (78 mL, 0.6 mmol). The crude product was purified by flash chromatography affording **2.78p** as a yellow oil (21 mg, 45%). $^1\text{H NMR}$ (400 MHz, CDCl_3) δ 7.32 (tt, $J = 7.5, 2.2$ Hz, 2H), 7.18 – 7.12 (m, 2H), 7.12 – 7.06 (m, 1H), 4.60 (d, $J = 1.0$ Hz, 1H), 2.96 (ddd, $J = 12.0, 4.2, 2.0$ Hz, 1H), 2.48 – 2.37 (m, 1H), 1.91 (dtd, $J = 14.4, 3.9, 1.9$ Hz, 1H), 1.76 – 1.68 (m, 1H), 1.68 – 1.57 (m, 2H), 1.53 – 1.23 (m, 8H). $^{13}\text{C NMR}$ (101 MHz, CDCl_3) δ 155.1, 151.8, 129.4, 123.6, 119.0, 104.3, 48.4, 39.0, 30.4, 29.9, 28.1, 26.2, 26.1, 24.3. **HRMS** (ESI) m/z calculated for $\text{C}_{16}\text{H}_{21}\text{O}$ $[\text{M}+\text{H}]^+$: 229.1587, found: 229.1586.

(Z)-9-Phenoxybicyclo[6.2.0]deca-4,9-diene (2.78q)

Cyclobutene **2.78q** was synthesized following general procedure **A** starting from (ethynyloxy)- benzene (35.4 mg, 0.3 mmol) and 1,5-cyclooctadiene (97 mg, 0.9 mmol). The crude was purified by flash chromatography affording **2.78q** as a transparent oil (12 mg, 18%). $^1\text{H NMR}$ (500 MHz, CD_2Cl_2) δ 7.36 – 7.28 (m, 2H), 7.15 – 7.07 (m, 3H), 5.76

– 5.65 (m, 2H), 4.62 (d, $J = 1.0$ Hz, 1H), 3.27 (dt, $J = 12.3, 4.2$ Hz, 1H), 2.75 (dddd, $J = 12.1, 4.6, 3.9, 1.0$ Hz, 1H), 2.41 – 2.26 (m, 2H), 2.14 – 2.01 (m, 2H), 2.03 – 1.86 (m, 2H), 1.72 (dddd, $J = 14.4, 12.3, 7.2, 5.1$ Hz, 1H), 1.62 (dddd, $J = 14.4, 12.3, 7.3, 5.2$ Hz, 1H). ^{13}C NMR (126 MHz, CD_2Cl_2) δ 155.5, 152.8, 132.0, 131.5, 129.8, 124.2, 119.4, 104.50, 49.6, 40.4, 31.0, 27.0, 25.2, 24.7. HRMS (ESI) m/z calculated for $\text{C}_{16}\text{H}_{19}\text{O}$ $[\text{M}+\text{H}]^+$: 227.1430, found: 227.1429.

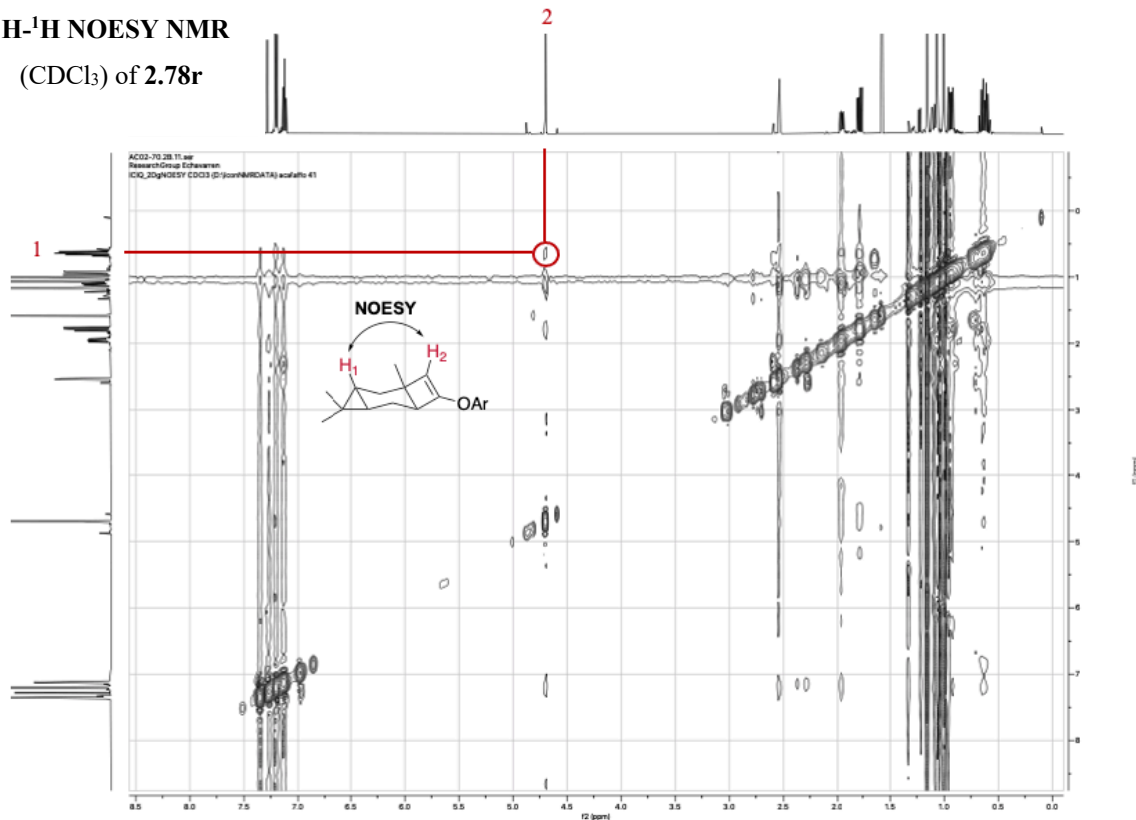
1,4,4-Trimethyl-8-(4-(trifluoromethyl)phenoxy)tricyclo[5.2.0.0^{3,5}]non-8-ene (2.78r)



Cyclobutene **2.78r** was synthesized following general procedure **A** starting from (ethynyloxy)-benzene (35.4 mg, 0.3 mmol) and (+)-3-carene (136 mg, 0.9 mmol). The crude was purified by flash chromatography affording the single diastereoisomer **2.78r** as a transparent oil (24 mg, 31%, *dr* determined by ^1H NMR of the crude mixture = 6:1). ^1H NMR (500 MHz, CDCl_3) δ 7.36 – 7.29 (m, 2H), 7.21 – 7.14 (m, 2H), 7.10 (ddt, $J = 8.5, 7.1, 1.1$ Hz, 1H), 4.68 (s, 1H), 2.51 (dd, $J = 4.0, 2.3$ Hz, 1H), 1.93 (ddd, $J = 15.1, 7.9, 2.4$ Hz, 1H), 1.76 (dd, $J = 14.7, 7.8$ Hz, 1H), 1.13 (s, 3H), 1.11 – 1.04 (m, 1H), 1.04 (s, 3H), 0.98 (s, 3H), 0.96 – 0.87 (m, 1H), 0.67 – 0.53 (m, 2H). ^{13}C NMR (126 MHz, CDCl_3) δ 155.45, 150.65, 129.56, 123.75, 119.25, 108.66, 48.41, 35.90, 28.92, 28.50, 25.84, 19.72, 18.81, 17.57, 16.84, 15.85. HRMS (ESI) m/z calculated for $\text{C}_{18}\text{H}_{23}\text{O}$ $[\text{M}+\text{H}]^+$: 255.1743, found: 255.1741. $[\alpha]^{25.9^\circ} = -3.8$ ($c = 0.55$, CHCl_3).

^1H - ^1H NOESY NMR

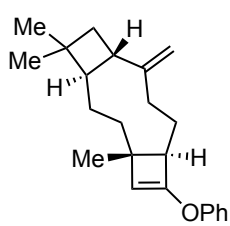
(CDCl_3) of **2.78r**



(1*R*,11*S*)-4,13,13-Trimethyl-10-methylene-6-phenoxytricyclo[9.2.0.0^{4,7}]tridec-5-ene (2.78s) and (1*R*,11*S*)-4,13,13-trimethyl-10-methylenetricyclo[9.2.0.0^{4,7}]tridecan-6-one (2.79d)

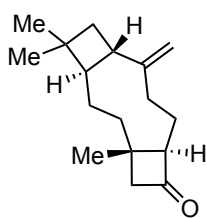
The cyclobutene **2.78s** and the cyclobutanone **2.79d** were synthesized following general procedure **A** starting from (ethynyloxy)benzene (23.6 mg, 0.2 mmol) and β -Caryophyllene (170 ml, 0.6 mmol). The yield (57%, 3:1 r.r.) of **2.78s** was determined by ^1H NMR analysis of the crude reaction mixture using trichloroethylene as the internal standard. The crude product was purified by flash chromatography affording a mixture of **2.78s** and **2.79d** in a ratio changing during time. Few fractions of pure **2.78s** as 1:1 mixture of regioisomers were separated (8 mg, 10%) and used to assign the structure by ^1H NMR and ^{13}C NMR, however **2.78s** was fully converted into **2.79d** overnight, and no HRMS was measured. A second purification by flash chromatography afforded **2.79d** as a yellow oil, 3:1 mixture of regioisomers (21 mg, 43%).

(1*R*,11*S*)-4,13,13-Trimethyl-10-methylene-6-phenoxytricyclo[9.2.0.0^{4,7}]tridec-5-ene (2.78s)



(Mr = major regioisomer, mr = minor regioisomer). ^1H NMR (400MHz, CDCl_3) δ 7.36–7.30(m,4H,Mr+mr), 7.16 (dq, $J=7.9$, 1.3Hz, 4H, Mr+mr), 7.13– 7.08 (m, 2H, Mr + mr), 4.95 (t, $J=1.3$ Hz, 1H, mr), 4.93 (s, 1H, Mr), 4.86 (d, $J=1.5$ Hz, 1H, mr), 4.85 (s, 1H, Mr), 4.66 (s, 1H, Mr), 4.48 (d, $J=1.1$ Hz, 1H, mr), 2.86 (dd, $J=12.9$, 2.7 Hz, 1H, Mr), 2.54 – 2.38 (m, 6H, Mr + mr), 2.09 – 2.00 (m, 1H, mr), 1.95 – 1.86 (m, 3H, Mr + mr), 1.86 – 1.69 (m, 5H, Mr + mr), 1.63 (m, 6H, Mr + mr), 1.56 – 1.40 (m, 3H, Mr + mr), 1.41 – 1.25 (m, 2H, Mr + mr), 1.23 (s, 3H, mr), 1.14 (s, 3H, Mr), 1.04 (s, 3H, mr), 1.02 (s, 3H, Mr), 1.00 (s, 6H, Mr + mr). ^{13}C NMR (101 MHz, CDCl_3) δ 155.3, 153.2, 152.6, 151.7, 129.5, 123.8, 119.3, 119.2, 110.4, 109.5, 101.0, 54.8, 50.2, 49.3, 49.2, 43.1, 41.9, 40.6, 39.7, 36.9, 34.4, 34.0, 34.0, 33.9, 32.9, 30.1, 30.1, 29.2, 26.9, 26.3, 25.7, 24.8, 24.5, 21.8, 19.3.

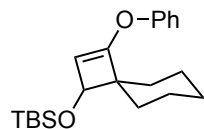
(1*R*,11*S*)-4,13,13-Trimethyl-10-methylenetricyclo[9.2.0.0^{4,7}]tridecan-6-one (2.79d)



(Mr = major regioisomer, mr = minor regioisomer) ^1H NMR (400MHz, CDCl_3) δ 4.95 (d, $J=1.2$ Hz, 1H, Mr), 4.92 (t, $J=1.3$ Hz, 0.3H, mr) 4.85 (d, $J=1.6$ Hz, 0.3H, mr), 4.84 (q, $J=1.1$ Hz, 1H, Mr), 3.15 – 3.07 (m, 0.3H, mr), 3.06 – 2.99 (m, 1H, Mr), 2.78 (dd, $J=16.8$, 2.9 Hz, 1H, Mr), 2.69 (dd, $J=18.0$, 8.1 Hz, 0.3H, mr), 2.55 (dd, $J=16.8$, 2.1 Hz, 1H, Mr), 2.49 – 2.33 (m, 2H, Mr + mr), 2.33 – 2.22 (m, 1H, Mr), 2.05 – 1.97 (m, 1H, Mr), 1.96 – 1.80 (m, 3H, Mr + mr), 1.69 – 1.51 (m, 8H, Mr + mr), 1.51 – 1.33 (m, 2H, Mr + mr), 1.12 (s, 1H, mr), 1.12 (s, 3H, Mr), 1.00 (s, 6H, Mr), 0.99 (s, 1H, mr), 0.98 (s, 1H, mr). ^{13}C NMR (126 MHz, CDCl_3) δ 216.3(mr), 211.6 (Mr), 152.6 (mr), 152.2 (Mr), 110.6 (Mr), 109.3 (mr), 63.9 (mr), 62.9 (Mr), 60.1 (Mr), 55.6 (Mr), 54.9 (mr), 49.6, 48.2, 45.5, 44.8, 38.1, 37.0, 36.9, 34.4, 34.3 (mr), 34.2, 33.9, 33.5, 32.9, 32.4, 30.1 (mr), 30.1 (Mr), 25.7, 24.8 (mr), 24.5 (Mr), 21.9

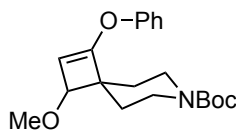
(Mr), 21.7 (mr), 20.1 (Mr), 14.1 (mr). **HRMS** (ESI) m/z calculated for $C_{17}H_{26}NaO$ $[M+Na]^+$: 269.1876, found: 269.1867.

***tert*-Butyldimethyl((3-phenoxyspiro[3.5]non-2-en-1-yl)oxy)silane (2.78t)**



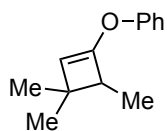
Cyclobutene **2.78t** was synthesized following general procedure **A** starting from (ethynyloxy)benzene (23.6 mg, 0.2 mmol) and *tert*-butyl(cyclohexylidenemethoxy)dimethylsilane (136 mg, 0.6 mmol). The crude product was purified by flash chromatography affording **2.78t** as a yellow oil (54 mg, 79%). **¹H NMR** (400 MHz, $CDCl_3$) δ 7.37–7.28 (m, 2H), 7.18–7.09 (m, 3H), 4.58 (d, $J = 0.8$ Hz, 1H), 4.12 (d, $J = 0.8$ Hz, 1H), 1.82 – 1.70 (m, 2H), 1.70 – 1.61 (m, 2H), 1.61 – 1.45 (m, 2H), 1.44 – 1.32 (m, 2H), 1.32 – 1.12 (m, 2H), 0.90 (s, 9H), 0.07 (s, 3H), 0.06 (s, 3H). **¹³C NMR** (101 MHz, $CDCl_3$) δ 162.0, 155.2, 129.6, 124.4, 119.8, 100.8, 72.8, 55.5, 33.8, 30.4, 26.1, 26.1, 24.4, 23.5, 18.4, -4.2, -4.5. **HRMS** (ESI) m/z calculated for $C_{21}H_{33}O_2Si$ $[M+H]^+$: 345.2244, found: 345.2249.

***tert*-Butyl 3-methoxy-1-phenoxy-7-azaspiro[3.5]non-1-ene-7-carboxylate (2.78u)**



Cyclobutene **2.78u** was synthesized following general procedure **A** starting from (ethynyloxy)benzene (23.6 mg, 0.2 mmol) and *tert*-butyl 4-(methoxymethylene)piperidine-1-carboxylate (136 mg, 0.6 mmol). The crude product was purified by flash chromatography affording **2.78u** as a colorless oil (64 mg, 92%). **¹H NMR** (400 MHz, $CDCl_3$) δ 7.39–7.30 (m, 2H), 7.20–7.11 (m, 3H), 4.78 (d, $J = 0.8$ Hz, 1H), 3.77 (d, $J = 0.8$ Hz, 1H), 3.70 – 3.47 (m, 4H), 3.33 (s, 3H), 1.93 – 1.79 (m, 3H), 1.72 (ddd, $J = 12.7, 7.8, 3.9$ Hz, 1H), 1.47 (s, 9H). **¹³C NMR** (101 MHz, $CDCl_3$) δ 161.8, 155.2, 154.7, 129.7, 124.8, 119.7, 98.7, 80.1, 79.4, 56.9, 53.2, 28.6, 28.6. **HRMS** (ESI) m/z calculated for $C_{20}H_{27}NNaO_4^+$ $[M+H]^+$: 368.1832, found: 368.1831.

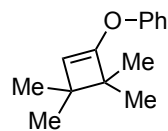
((3,3,4-Trimethylcyclobut-1-en-1-yl)oxy)benzene (2.78v)



Cyclobutene **2.78v** was synthesized following general procedure **A** starting from (ethynyloxy)benzene (23.6 mg, 0.2 mmol) and 2-methylbut-2-ene (64 mL, 0.6 mmol). The crude product was purified by flash chromatography affording **2.78v** as a yellow oil 7:1 mixture of regioisomers (29 mg, 77%). Major regioisomer (Mr), minor regioisomer (mr). **¹H NMR** (400 MHz, $CDCl_3$) δ 7.36–7.29 (m, 3H, Mr+mr), 7.19–7.12 (m, 2H, Mr+mr), 7.09 (td, $J = 7.3, 1.2$ Hz, 1H, Mr), 7.06 – 6.96 (m, 0.15H, mr), 4.73 (s, 1H, Mr), 4.56 (d, $J = 1.0$ Hz, 0.15H, mr), 2.69 (q, $J = 7.1$ Hz, 1H, Mr), 2.21 – 2.14 (m, 0.15H, mr), 1.19 (s, 3H, Mr), 1.18 (s, 0.7H, mr), 1.12 (s, 0.7H, mr), 1.09 (d, $J = 7.2$ Hz, 3H, Mr), 1.07 (s, 3H, Mr), 1.03 (d, $J = 6.8$ Hz, 1H, mr). **¹³C NMR** (101 MHz, $CDCl_3$) δ 155.4 (mr), 152.6 (Mr), 129.5 (Mr), 129.5 (Mr), 123.8 (Mr), 122.7 (mr), 119.4 (mr), 119.2

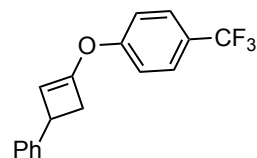
(Mr), 117.9 (mr), 110.0 (Mr), 102.2 (mr), 48.8 (Mr), 45.1 (mr), 40.4 (mr), 37.3 (mr), 28.1 (Mr), 24.8 (Mr), 22.7 (Mr), 19.6 (mr), 15.6 (mr), 12.6 (Mr). **HRMS** (ESI) m/z calculated for $C_{13}H_{17}O$ $[M+H]^+$: 189.1274, found: 189.1273.

(3,3,4,4-Tetramethylcyclobut-1-en-1-yl)oxy)benzene (2.78w)



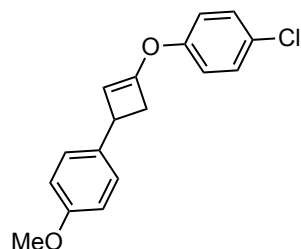
Cyclobutene **2.78w** was synthesized following general procedure **A** starting from (ethynyloxy)benzene (23.6 mg, 0.2 mmol) and 2,3-dimethylbut-2-ene (72 mL, 0.6 mmol). The crude product was purified by flash chromatography affording **2.78w** as a colorless oil (24 mg, 59%). **¹H NMR** (400 MHz, $CDCl_3$) δ 7.36 – 7.28 (m, 2H), 7.19 – 7.14 (m, 2H), 7.09 (ddt, $J = 7.7, 7.0, 1.2$ Hz, 1H), 4.60 (s, 1H), 1.19 (s, 6H), 1.10 (s, 6H). **¹³C NMR** (101 MHz, $CDCl_3$) δ 156.5, 155.5, 129.5, 123.8, 119.4, 107.4, 48.8, 40.5, 24.3, 21.5. **HRMS** (ESI) m/z calculated for $C_{14}H_{19}O$ $[M+H]^+$: 203.1430, found: 203.1432.

1-((3-Phenylcyclobut-1-en-1-yl)oxy)-4-(trifluoromethyl)benzene (2.78x)



Cyclobutene **2.78x** was synthesized following general procedure **A** starting from 1-(ethynyloxy)-4-(trifluoromethyl)benzene (37.2 mg, 0.2 mmol) and styrene (63 mg, 0.3 mmol). The crude was purified by flash chromatography affording **2.78x** as a transparent oil, 7:1 mixture of regioisomers (19 mg, 33%). **¹H NMR** (400 MHz, $CDCl_3$) δ 7.68 – 7.57 (m, 2.4 H, Mr + mr), 7.37 – 7.27 (m, 6.6 H, Mr + mr), 7.29 – 7.19 (m, 1.1H, Mr + mr), 5.12 (m, 1H, Mr), 5.03 (s, 0.1 H, mr), 4.26 (dd, $J = 4.6, 1.5$ Hz, 0.1H, mr), 3.74 (dt, $J = 4.6, 1.3$ Hz, 1H, Mr), 3.29 (dd, $J = 13.07, 4.57$ Hz, 1H, Mr), 2.71 (ddd, $J = 10.7, 4.6, 1.0$ Hz, 0.1H, mr), 2.61 (dd, $J = 13.1, 1.6$ Hz, 1H, Mr), 2.09 (ddd, $J = 10.7, 1.5, 1.0$ Hz, 0.1H, mr). **¹⁹F NMR** (376 MHz, $CDCl_3$) δ -62.03. **¹³C NMR** (101 MHz, $CDCl_3$) δ 157.6 (Mr + mr), 149.8 (mr), 149.0 (Mr), 143.5 (Mr), 140.2 (mr), 128.8 (mr), 128.6 (Mr), 127.2 (q, $J = 3.8$ Hz, Mr + mr), 127.0 (mr), 126.9 (mr), 126.8 (Mr), 126.7 (Mr), 126.3 (q, $J = 32.9$ Hz, Mr), 124.2 (q, $J = 271.5$ Hz, Mr), 119.2 (Mr), 118.7 (mr), 107.2 (Mr), 103.8 (mr), 49.5 (mr), 41.8 (Mr), 37.6 (Mr), 31.6 (mr). Two aromatic ¹³C signals of the mr were not detected because of low intensity. **HRMS** (ESI) m/z calculated for $C_{17}H_{14}F_3O$ $[M+H]^+$: 291.0991, found: 291.0986.

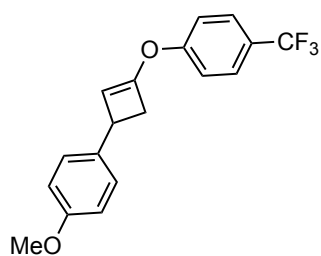
1-Chloro-4-((3-(4-methoxyphenyl)cyclobut-1-en-1-yl)oxy)benzene (2.78y)



Cyclobutene **2.78y** was synthesized following general procedure **A** starting from 1-chloro-4-(ethynyloxy)benzene (45.8 mg, 0.3 mmol) and 1-methoxy-4-vinylbenzene (121 mg, 0.9 mmol). The crude was purified by flash chromatography affording **2.78y** as a transparent oil (33 mg, 38%). **¹H NMR** (400 MHz, $CDCl_3$) δ 7.36 – 7.27 (m, 2H), 7.27 – 7.19 (m, 2H), 7.19 – 7.10

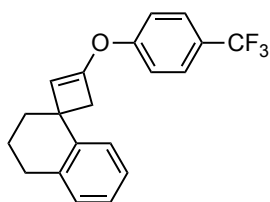
(m, 2H), 6.92 – 6.80 (m, 2H), 4.96 (dd, $J = 1.0, 0.4$ Hz, 1H), 3.80 (s, 3H), 3.65 (dt, $J = 4.4, 1.3$ Hz, 1H), 3.22 (dd, $J = 13.0, 4.5$ Hz, 1H), 2.51 (ddd, $J = 13.0, 1.6, 0.4$ Hz, 1H). $^{13}\text{C NMR}$ (101 MHz, CDCl_3) δ 158.4, 153.5, 149.8, 135.8, 129.7, 129.4, 120.7, 113.9, 105.7, 55.45, 41.8, 36.8. **HRMS** (ESI) m/z calculated for $\text{C}_{17}\text{H}_{16}\text{ClO}_2$ $[\text{M}+\text{H}]^+$: 287.0833, found: 287.0832.

1-Methoxy-4-(3-(4-(trifluoromethyl)phenoxy)cyclobut-2-en-1-yl)benzene (2.78z)



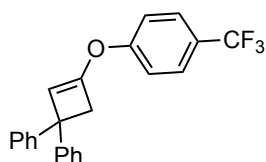
Cyclobutene **2.78z** was synthesized following general procedure **A** starting from 1-(ethynyloxy)-4-(trifluoromethyl)benzene (55.8 mg, 0.3 mmol) and 1-methoxy-4-vinylbenzene (121 mg, 0.9 mmol). The crude was purified by flash chromatography affording **2.78z** as a transparent oil (40 mg, 42%). $^1\text{H NMR}$ (500 MHz, CDCl_3) δ 7.65 – 7.59 (m, 2H), 7.32 – 7.27 (m, 2H), 7.25 – 7.22 (m, 2H), 6.89 – 6.85 (m, 2H), 5.11 – 5.07 (d, 1H), 3.81 (s, 3H), 3.69 (dt, $J = 4.6, 1.3$ Hz, 1H), 3.25 (dd, $J = 13.1, 4.6$ Hz, 1H), 2.55 (ddd, $J = 13.1, 1.6, 0.4$ Hz, 1H). $^{19}\text{F NMR}$ (376 MHz, CDCl_3) δ -62.03 $^{13}\text{C NMR}$ (126 MHz, CDCl_3) δ 158.5, 157.6, 148.9, 135.5, 127.7, 127.2 (q, $J = 3.7$ Hz), 126.2 (q), 125.6 (q, $J = 272.2$ Hz), 119.1, 114.0, 107.4, 55.5, 42.0, 37.0. **HRMS** (ESI) m/z calculated for $\text{C}_{18}\text{H}_{16}\text{F}_3\text{O}_2$ $[\text{M}+\text{H}]^+$: 321.1097, found: 321.1101.

3-(4-(Trifluoromethyl)phenoxy)-3',4'-dihydro-2'H-spiro[cyclobutane-1,1'-naphthalen]-2-ene (2.78aa)



Cyclobutene **2.78aa** was synthesized following general procedure **A** starting from 1-(ethynyloxy)-4-(trifluoromethyl)benzene (37.4 mg, 0.2 mmol) and 1-methylene-1,2,3,4-tetrahydronaphthalene (87 mg, 0.6 mmol). The crude was purified by flash chromatography affording **2.78aa** as a yellow solid (59 mg, 89%). **M.p.** = 61–69 °C. $^1\text{H NMR}$ (500 MHz, CDCl_3) δ 7.69 – 7.63 (m, 2H), 7.55 (dd, $J = 7.6, 1.7$ Hz, 1H), 7.35 (d, $J = 8.5$ Hz, 2H), 7.23 – 7.09 (m, 3H), 5.14 (d, $J = 0.7$ Hz, 1H), 2.86 (dd, $J = 8.0, 4.2$ Hz, 2H), 2.78 (p, $J = 1.3$ Hz, 2H), 2.08 – 1.93 (m, 3H), 1.91 – 1.79 (m, 1H). $^{19}\text{F NMR}$ (376 MHz, CDCl_3) δ -62.01. $^{13}\text{C NMR}$ (126 MHz, CDCl_3) δ 157.71, 149.35, 141.26, 137.41, 129.14, 127.18 (q, $J = 3.7$ Hz), 126.39, 126.24, 126.18 (q, $J = 32.8$ Hz), 125.51, 124.21 (q, $J = 271.5$ Hz), 112.61, 49.70, 40.89, 35.83, 30.33, 22.02. **HRMS** (ESI) m/z calculated for $\text{C}_{20}\text{H}_{18}\text{F}_3\text{O}$ $[\text{M}+\text{H}]^+$: 331.1304, found: 331.1302.

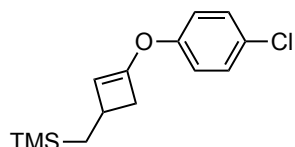
(3-(4-(Trifluoromethyl)phenoxy)cyclobut-2-ene-1,1-diyl)dibenzene (2.78bb)



Cyclobutene **2.78bb** was synthesized following general procedure **A** starting from 1-(ethynyloxy)-4-(trifluoromethyl)benzene (18.6 mg, 0.1 mmol) and ethene-1,1-diyl dibenzene (54 mg, 0.3 mmol). The crude was purified by flash

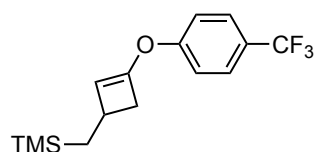
chromatography affording **2.78bb** as a yellow solid (18 mg, 50%). **M.p.** = 110-122 °C. **¹H NMR** (400 MHz, CDCl₃) δ 7.67 – 7.59 (m, 2H), 7.38 – 7.25 (m, 10H), 7.22 (ddt, *J* = 7.3, 5.9, 2.0 Hz, 2H), 5.59 (s, 1H), 3.39 (s, 2H). **¹⁹F NMR** (376 MHz, CDCl₃) δ -61.66. **¹³C NMR** (101 MHz, CDCl₃) δ 157.4, 149.8, 146.1, 128.4, 127.3, 127.2 – 127.1 (m), 126.6 (q, *J* = 32.7 Hz), 126.3, 124.2 (q, *J* = 271.6 Hz), 119.5, 109.4, 49.0, 47.9. **HRMS** (ESI) *m/z* calculated for C₂₃H₁₈F₃O [M+H]⁺: 367.1304, found: 367.1304.

((3-(4-Chlorophenoxy)cyclobut-2-en-1-yl)methyl)trimethylsilane (**2.78cc**)



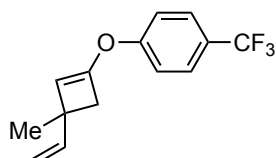
Cyclobutene **2.78cc** was synthesized following general procedure **A** starting from 1-chloro-4-(ethynyloxy)benzene (45.8 mg, 0.3 mmol) and allyltrimethylsilane (103 mg, 0.9 mmol). The crude was purified by flash chromatography affording **2.78cc** as a transparent oil (22 mg, 28%). **¹H NMR** (500 MHz, CDCl₃) δ 7.30 – 7.26 (m, 2H), 7.08 – 7.03 (m, 2H), 4.79 (d, *J* = 0.9 Hz, 1H), 2.92 (dd, *J* = 12.9, 4.2 Hz, 1H), 2.56 (tdt, *J* = 7.6, 4.2, 1.3 Hz, 1H), 2.20 (dd, *J* = 12.9, 1.4 Hz, 1H), 0.78 (d, *J* = 7.6 Hz, 2H), 0.01 (s, 9H). **¹³C NMR** (101 MHz, CDCl₃) δ 153.7, 148.0, 129.6, 129.0, 120.6, 109.1, 40.9, 29.8, 23.2, -0.92. **HRMS** (ESI) *m/z* calculated for C₁₄H₂₀ClOSi [M+H]⁺: 267.0966, found: 267.0962.

Trimethyl((3-(4-(trifluoromethyl)phenoxy)cyclobut-2-en-1-yl)methyl)silane (**2.78dd**)



Cyclobutene **2.78dd** was synthesized following general procedure **A** starting from 1-(ethynyloxy)-4-(trifluoromethyl)benzene (55.8 mg, 0.3 mmol) and allyltrimethylsilane (103 mg, 0.9 mmol). The crude was purified by flash chromatography affording **2.78dd** as a transparent oil (27 mg, 30%). **¹H NMR** (500 MHz, CDCl₃) δ 7.62 – 7.56 (m, 2H), 7.24 – 7.18 (m, 2H), 4.94 (d, *J* = 1.0 Hz, 1H), 2.97 (dd, *J* = 12.9, 4.2 Hz, 1H), 2.65 – 2.57 (m, 1H), 2.25 (dd, *J* = 12.9, 1.4 Hz, 1H), 0.81 (d, *J* = 7.6 Hz, 2H), 0.02 (s, 9H). **¹⁹F NMR** (376 MHz, CDCl₃) δ -61.99. **¹³C NMR** (126 MHz, CDCl₃) δ 157.9, 147.1, 127.1 (q, *J* = 3.8 Hz), 125.8 (q), 125.3 (q, *J* = 272.3 Hz), 118.9, 111.0, 41.1, 30.1, 23.1, -0.9. **HRMS** (ESI) *m/z* calculated for C₁₅H₂₀F₃OSi [M+H]⁺: 301.1230, found: 301.1225.

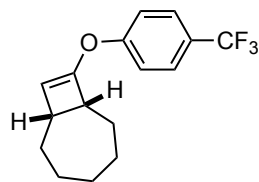
((3-Methyl-3-vinylcyclobut-1-en-1-yl)oxy)-4-(trifluoromethyl)benzene (**2.78ee**)



Cyclobutene **2.78ee** was synthesized following general procedure **A** starting from 1-(ethynyloxy)-4-(trifluoromethyl)benzene (37.7 mg, 0.2 mmol) and isoprene (41 mg, 0.6 mmol). The crude was purified by flash chromatography affording **2.78ee** as a transparent oil (24 mg, 47%). **¹H NMR** (500 MHz, CDCl₃) δ 7.63 – 7.57 (m, 2H), 7.27 – 7.21 (m, 2H), 6.06 (dd, *J* = 17.3, 10.4 Hz, 1H), 5.08 (dd, *J* = 17.2, 1.5 Hz, 1H), 4.97 (s, 1H), 4.97 (dd, *J* = 10.4, 1.5 Hz, 1H), 2.63 (d, *J* = 12.8 Hz, 1H), 2.58 (d, *J* = 12.8 Hz, 1H), 1.36 (s, 3H). **¹⁹F NMR** (376 MHz, CDCl₃) δ -61.64. **¹³C NMR** (126 MHz, CDCl₃) δ 157.7,

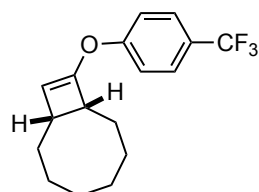
147.8, 145.3, 127.1 (q, $J = 3.7$ Hz), 126.1 (q, $J = 32.7$ Hz), 124.2 (q, $J = 271.4$ Hz), 119.0, 111.6, 111.5, 45.6, 40.1, 24.0. **HRMS** (ESI) m/z calculated for $C_{14}H_{14}F_3O$ $[M+H]^+$: 255.0991, found: 255.0986.

8-(4-(Trifluoromethyl)phenoxy)bicyclo[5.2.0]non-8-ene (2.78ff)



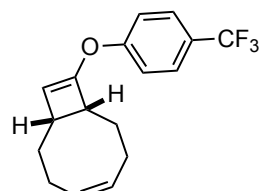
Cyclobutene **2.78ff** was synthesized following general procedure **A** starting from 1-(ethynyloxy)-4-(trifluoromethyl)benzene (37.2 mg, 0.2 mmol) and cycloheptene (58 mg, 0.6 mmol). The crude was purified by flash chromatography affording **2.78ff** as a transparent oil (21 mg, 37%). **1H NMR** (500 MHz, $CDCl_3$) δ 7.62 – 7.55 (m, 2H), 7.27 – 7.21 (m, 2H), 4.84 (d, $J = 1.0$ Hz, 1H), 3.15 (dt, $J = 11.4, 4.4$ Hz, 1H), 2.64 (dt, $J = 10.4, 4.2$ Hz, 1H), 1.92 – 1.64 (m, 5H), 1.54 – 1.18 (m, 5H). **^{19}F NMR** (376 MHz, $CDCl_3$) δ -61.58. **^{13}C NMR** (126 MHz, $CDCl_3$) δ 158.0, 151.7, 127.0 (q, $J = 3.8$ Hz), 125.8 (q, $J = 32.6$ Hz), 124.3 (q, $J = 271.7$ Hz), 119.0, 106.8, 49.4, 39.6, 32.0, 31.4, 28.0. **HRMS** (ESI) m/z calculated for $C_{16}H_{16}F_3O$ $[M+H]^+$: 283.1304, found: 283.1304.

9-(4-(Trifluoromethyl)phenoxy)bicyclo[6.2.0]dec-9-ene (2.78gg)



Cyclobutene **2.78gg** was synthesized following general procedure **A** starting from 1-(ethynyloxy)-4-(trifluoromethyl)benzene (55.8 mg, 0.3 mmol) and (*Z*)-cyclooctene (99 mg, 0.9 mmol). The crude was purified by flash chromatography affording **2.78gg** as a transparent oil (64 mg, 72%). **1H NMR** (500 MHz, $CDCl_3$) δ 7.62 – 7.55 (m, 2H), 7.26 – 7.20 (m, 2H), 4.74 (d, $J = 1.0$ Hz, 1H), 2.98 (ddd, $J = 12.0, 4.2, 2.0$ Hz, 1H), 2.48 (dddd, $J = 11.5, 4.1, 1.8, 1.0$ Hz, 1H), 1.88 (dtd, $J = 14.5, 3.9, 2.0$ Hz, 1H), 1.74 (dtd, $J = 12.5, 3.1, 1.9$ Hz, 1H), 1.64 (dddd, $J = 14.2, 13.0, 6.5, 3.9$ Hz, 2H), 1.54 – 1.27 (m, 8H). **^{19}F NMR** (376 MHz, $CDCl_3$) δ -61.98. **^{13}C NMR** (126 MHz, $CDCl_3$) δ 158.0, 150.7, 127.0 (q, $J = 3.8$ Hz), 125.7 (q, $J = 32.9$ Hz), 124.3 (q, $J = 271.4$ Hz), 118.8, 106.7, 48.7, 39.4, 30.5, 30.0, 28.1, 26.4, 26.2, 24.4. **HRMS** (ESI) m/z calculated for $C_{17}H_{20}F_3O$ $[M+H]^+$: 297.1461, found: 297.1455.

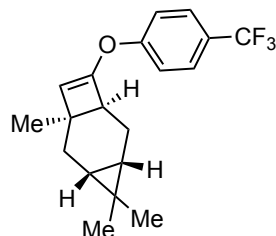
(*Z*)-9-(4-(Trifluoromethyl)phenoxy)bicyclo[6.2.0]deca-4,9-diene (2.78hh)



Cyclobutene **2.78hh** was synthesized following general procedure **A** starting from 1-(ethynyloxy)-4-(trifluoromethyl)benzene (37.2 mg, 0.2 mmol) and 1,5-cyclooctadiene (65 mg, 0.6 mmol). The crude was purified by flash chromatography affording **2.78hh** as a transparent oil (28 mg, 48%). **1H NMR** (400 MHz, $CDCl_3$) δ 7.63 – 7.54 (m, 2H), 7.22 (dt, $J = 7.8, 0.9$ Hz, 2H), 5.78 – 5.64 (m, 2H), 4.76 (d, $J = 1.0$ Hz, 1H), 3.29 (dt, $J = 12.3, 4.2$ Hz, 1H), 2.83 – 2.73 (m, 1H), 2.43 – 2.26 (m, 2H), 2.17 – 2.00 (m, 2H), 2.04 – 1.87 (m, 2H), 1.82 – 1.57 (m, 2H). **^{19}F NMR** (376 MHz, $CDCl_3$) δ -61.99. **^{13}C NMR** (101 MHz, $CDCl_3$) δ 157.9, 151.2, 131.7, 131.2, 127.0 (q, $J = 3.7$ Hz), 125.8 (q, $J = 32.7$

Hz), 124.3 (q, $J = 271.7$ Hz), 118.9, 106.5, 49.4, 40.1, 30.4, 26.6, 24.9, 24.5. **HRMS** (ESI) m/z calculated for $C_{17}H_{18}F_3O$ $[M+H]^+$: 295.1304, found: 295.1304.

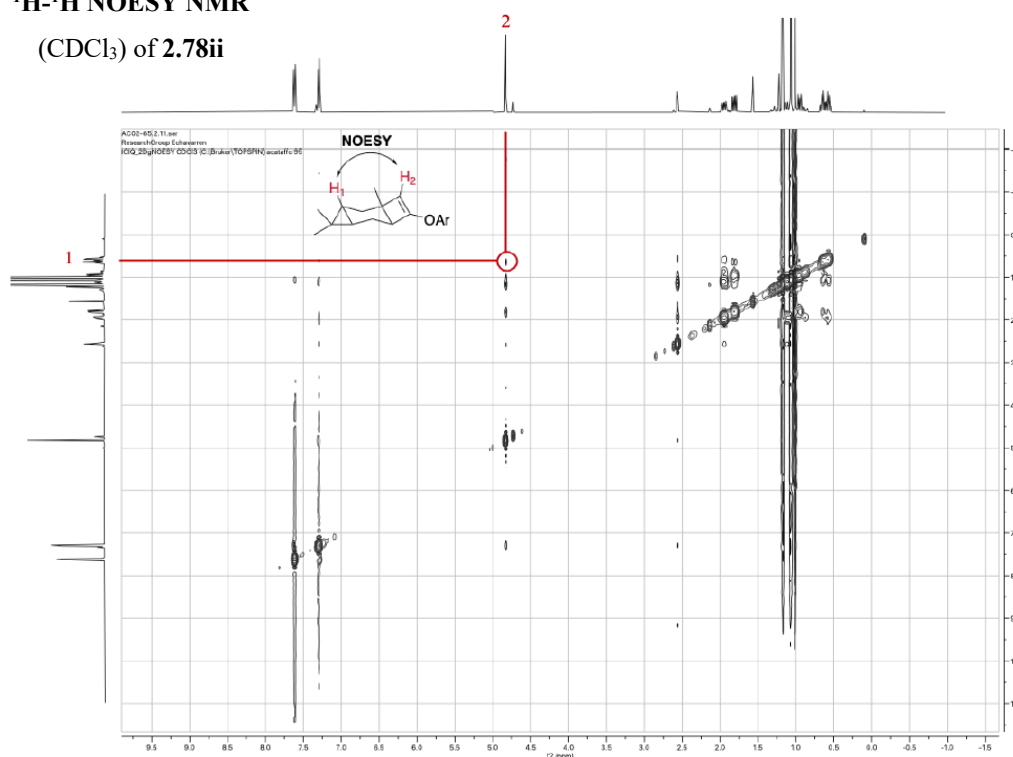
1,4,4-Trimethyl-8-(4-(trifluoromethyl)phenoxy)tricyclo[5.2.0.0^{3,5}]non-8-ene (**2.78ii**)

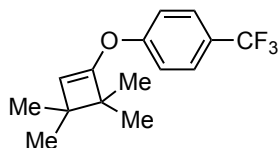


Cyclobutene **2.78ii** was synthesized following general procedure **A** starting from 1-(ethynyloxy)-4-(trifluoromethyl)benzene (18.6 mg, 0.1 mmol) and (+)-3-carene (41 mg, 0.3 mmol). The crude was purified by flash chromatography affording **2.78ii** as a transparent oil, 6:1 mixture of diastereomers (21 mg, 65%, *dr* determined by 1H NMR of the crude mixture = 4:1). **1H NMR** (400 MHz, $CDCl_3$) δ 7.59 – 7.51 (m, 2.4H, Md + md), 7.22 (dt, $J = 9.0, 0.9$ Hz, 2.4H, Md + md), 4.76 (s, 1H, Md), 4.66 (d, $J = 0.9$ Hz, 0.2H, md), 2.49 (dd, $J = 4.0, 2.3$ Hz, 1H, Md), 2.07 (t, $J = 3.0$ Hz, 0.2H, md), 1.93 – 1.77 (m, 1.2H, Md + md), 1.74 (dd, $J = 14.7, 7.9$ Hz, 1.2H, Md + md), 1.11 (s, 3.6H, Md + md), 1.10 – 1.00 (m, 1.2H, Md + md), 0.99 (s, 3.6H, Md + md), 0.94 (s, 3.6H, Md + md), 0.94 – 0.78 (m, 1.2H, Md + md), 0.63 – 0.44 (m, 2.4H, Md + md). **^{19}F NMR** (376 MHz, $CDCl_3$) δ -61.96. **^{13}C NMR** (101 MHz, $CDCl_3$) δ 158.2 (Md + md), 153.7 (md), 149.5 (Md), 127.0 (q, $J = 3.7$ Hz Md + md), 125.7 (q, $J = 33.0$ Hz, Md), 124.3 (q, $J = 271.5$ Hz, Md), 119.1 (md), 118.9 (Md), 110.8 (Md), 103.2 (md), 48.7 (Md), 46.2 (md), 40.0 (md), 36.3 (Md), 28.9 (Md + md), 28.4 (Md), 26.1 (md), 25.7 (Md), 22.5 (md), 21.0 (md), 19.67 (Md), 19.4 (md), 18.8 (Md), 17.5 (Md + md), 16.9 (Md), 15.8 (Md + md). Two aromatic ^{13}C signals of the *mr* were not detected because of low intensity. **HRMS** (ESI) m/z calculated for $C_{19}H_{22}F_3O$ $[M+H]^+$: 323.1617, found: 323.1614.

1H - 1H NOESY NMR

($CDCl_3$) of **2.78ii**

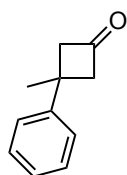


1-((3,3,4,4-Tetramethylcyclobut-1-en-1-yl)oxy)-4-(trifluoromethyl)benzene (2.78jj)

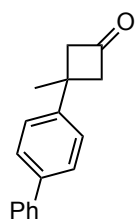
Cyclobutene **2.78jj** was synthesized following general procedure **A** starting from 1-(ethynyloxy)-4-(trifluoromethyl)benzene (55.8 mg, 0.3 mmol) and 2,3-dimethylbut-2-ene (76 mg, 0.9 mmol). The crude was purified by flash chromatography affording **2.78jj** as a transparent oil (50 mg, 62%). **¹H NMR** (500 MHz, CDCl₃) δ 7.58 (dt, *J* = 8.4, 0.7 Hz, 2H), 7.28 – 7.23 (m, 2H), 4.73 (s, 1H), 1.19 (s, 6H), 1.12 (s, 6H). **¹⁹F NMR** (376 MHz, CDCl₃) δ -61.98. **¹³C NMR** (126 MHz, CDCl₃) δ 158.3, 155.2, 127.0 (q, *J* = 3.8 Hz), 125.8 (q, *J* = 33.5 Hz), 124.3 (q, *J* = 271.6 Hz), 119.1, 109.3, 49.1, 40.8, 24.2, 21.4. **HRMS** (ESI) *m/z* calculated for C₁₅H₁₈F₃O [M+H]⁺: 271.1304, found: 271.1307.

General procedure B: one-pot synthesis of cyclobutanones 2.79 starting from ynol ethers 2.76

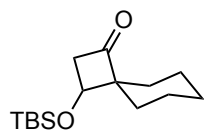
A GC-MS vial equipped with a magnetic stirring bar was charged with the ynol ether (0.2 mmol, 1 equiv) and CH₂Cl₂ (HPLC grade, 0.2 mL, 1 M). The alkene (0.6 mmol, 3 equiv) was added followed by [(JohnPhos)AuNCMe]SbF₆ (**2.B**, 3 mol%, 4.6 mg). The resulting mixture was stirred at 23 °C for 3 h. The reaction was monitored by GC-MS or UHPLC-MSD. Once completed, *p*-TSA·H₂O (38 mg, 0.2 mmol, 1 equiv) was added. The reaction was stirred overnight and then diluted with CH₂Cl₂ and the organic phases was washed three times with H₂O. The collected organic phase was dried over Na₂SO₄ and the solvent removed under reduced pressure. The crude product was purified by flash chromatography on silica gel using a pentane:Et₂O 20:1 as eluent and affording cyclobutanone **2.79**.

3-Methyl-3-phenylcyclobutan-1-one (2.79a)

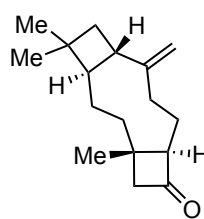
Cyclobutanone **2.79a** was obtained synthesized following general procedure **B** starting from (ethynyloxy)benzene (23.6 mg, 0.2 mmol) and α-methylstyrene (78 μL, 0.6 mmol). The crude product was purified by flash chromatography affording **2.79a** as a colorless oil (22 mg, 69%). The same reaction was performed also on 1.0 mmol scale starting from (ethynyloxy)benzene (118 mg, 1 mmol) and α-methylstyrene (390 μL, 3 mmol) and using *p*-TSA·H₂O (323 mg, 1.7 mmol, 1.7 equiv). and 106 mg of **2.79a** were obtained (66% yield). **¹H NMR** (300 MHz, CDCl₃) δ 7.42 – 7.29 (m, 3H), 7.29 – 7.21 (m, 2H), 3.58 – 3.39 (m, 2H), 3.25 – 3.00 (m, 2H), 1.61 (s, 3H). **¹³C NMR** (101 MHz, CDCl₃) δ 206.9, 148.4, 128.7, 126.4, 125.8, 59.4, 34.1, 31.2. **IR** (selected frequency): 1783 cm⁻¹. Data in agreement with the one reported in literature.²³

3-([1,1'-Biphenyl]-4-yl)-3-methylcyclobutan-1-one (2.79b)

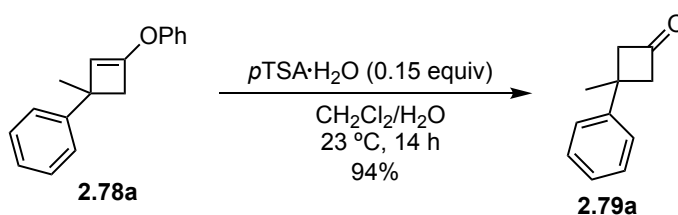
Cyclobutanone **2.79b** was obtained synthesized following general procedure **B** starting from (ethynyloxy)benzene (23.6 mg, 0.2 mmol) and 4-(prop-1-en-2-yl)-1,1'-biphenyl (117 mg, 0.6 mmol). The crude product was purified by flash chromatography affording **2.79b** as a white solid (26 mg, 56%). ¹H NMR (400 MHz, CDCl₃) δ 7.65 – 7.56 (m, 4H), 7.50 – 7.43 (m, 2H), 7.43 – 7.39 (m, 2H), 7.39 – 7.32 (m, 1H), 3.62 – 3.39 (m, 2H), 3.26 – 3.04 (m, 2H), 1.67 (s, 3H). ¹³C NMR (101 MHz, CDCl₃) δ 206.7, 147.4, 140.8, 139.4, 128.9, 127.4, 127.2, 126.3, 59.5, 33.9, 31.1. HRMS (ESI) *m/z* calculated for C₁₇H₁₆NaO [M+Na]⁺: 259.1093, found: 259.1091. IR (selected frequency): 1771 cm⁻¹.

3-((tert-Butyldimethylsilyloxy)spiro[3.5]nonan-1-one (2.79c)

Cyclobutanone **2.79c** was obtained synthesized following general procedure **B** starting from (ethynyloxy)benzene (12 mg, 0.1 mmol) and tert-butyl(cyclohexylidenemethoxy)dimethylsilane (68 mg, 0.3 mmol). The crude product was purified by flash chromatography affording **5d** as a brown oil (11 mg, 41%). ¹H NMR (400 MHz, CDCl₃) δ 4.14 (dd, *J* = 6.9, 4.7 Hz, 1H), 3.22 (dd, *J* = 17.8, 6.9 Hz, 1H), 2.86 (dd, *J* = 17.8, 4.7 Hz, 1H), 1.76 – 1.58 (m, 5H), 1.58 – 1.48 (m, 1H), 1.44 (dt, *J* = 9.1, 2.0 Hz, 2H), 1.34 – 1.21 (m, 2H), 0.90 (s, 9H), 0.09 (s, 3H), 0.07 (s, 3H). ¹³C NMR (101 MHz, CDCl₃) δ 214.4, 68.2, 67.5, 52.8, 31.7, 26.5, 25.9, 25.8, 22.8, 22.6, 18.2, -4.6, -4.9. HRMS (ESI) *m/z* calculated for C₁₅H₂₈NaO₂Si [M+Na]⁺: 291.1751, found: 291.1744.

(1*R*,11*S*)-4,13,13-Trimethyl-10-methylenetricyclo[9.2.0.0^{4,7}]tridecan-6-one (2.79d)

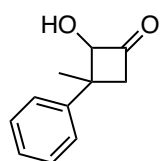
Cyclobutanone **2.79d** was obtained synthesized following general procedure **B** starting from (ethynyloxy)benzene (23.6 mg, 0.2 mmol) and b-Caryophyllene (170 ml, 0.6 mmol) The crude product was purified by flash chromatography affording **2.79d** as a yellow oil 3:1 mixture of regioisomers (31 mg, 68%). See above for the characterization.

Procedure C for the hydrolysis of 2.78a o form cyclobutanone 2.79a

Cyclobutene **2.78a** (47 mg, 0.2 mmol) was dissolved in CH₂Cl₂ (0.2 mL) and water (0.1 mL). *p*-toluenesulfonic acid monohydrate (5.7 mg, 0.03 mmol) was then added and the biphasic mixture was vigorously stirred at 23°C until complete conversion was observed by monitoring the reaction by TLC. The reaction was then diluted with CH₂Cl₂ and the organic phases was washed three times with H₂O. The collected organic phase was dried over Na₂SO₄ and the solvent removed under reduced pressure. The crude product was purified by flash chromatography on silica gel using a pentane:Et₂O 20:1 as eluent and affording **2.79a** as a colorless oil (30 mg, 94%).

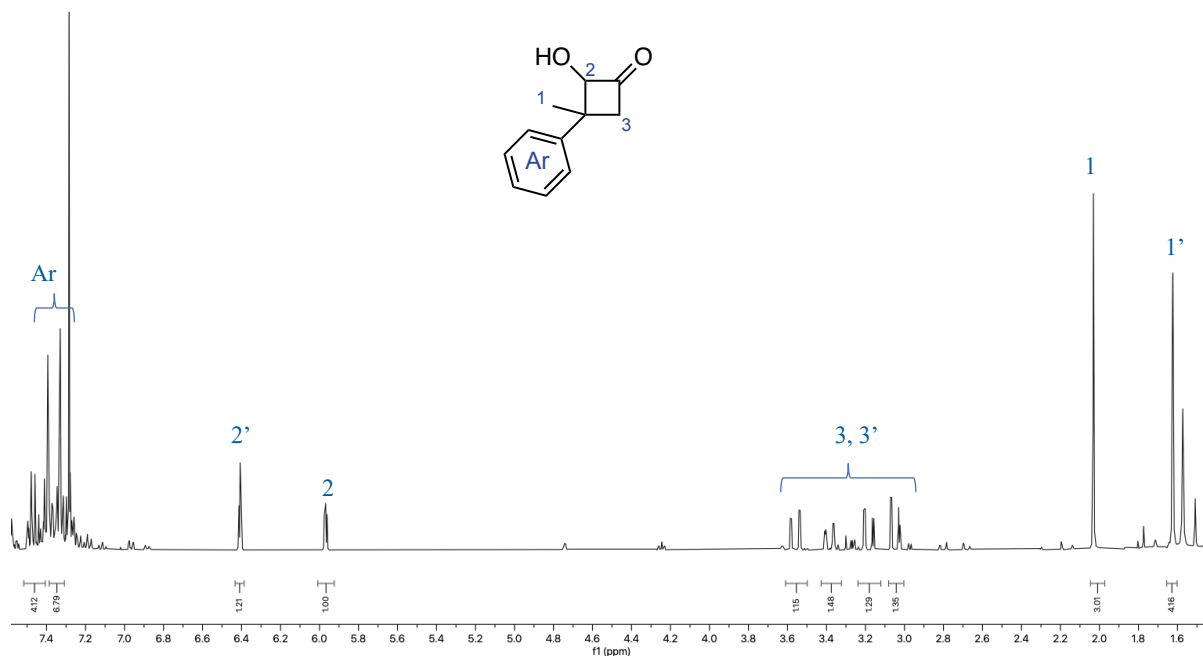
*Procedure D for the synthesis of α -hydroxycyclobutanone **2.81** starting from cyclobutene **2.78a**.*

2-Hydroxy-3-methyl-3-phenylcyclobutan-1-one (**2.81**)

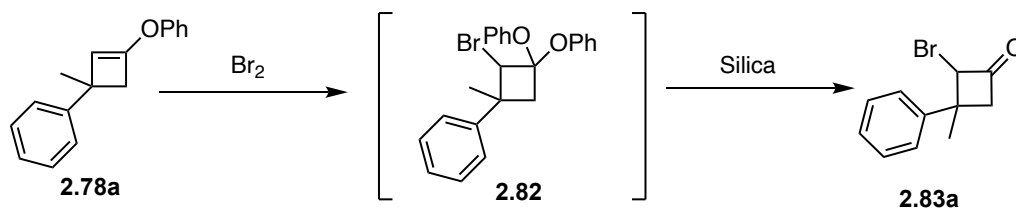


*m*CPBA (18.0 mg, 0.1 mmol) was added to a solution of (1-methyl-3-phenoxy)cyclobut-2-en-1-yl)benzene (19.0 mg, 0.080 mmol) in CH₂Cl₂ (0.80 mL). The reaction was left to stir over 16 h. NaSO₃ aq. was added to the mixture and the organic layer separated and washed with NaHCO₃. The crude product was purified by flash chromatography in 50:1 Pentane:Et₂O affording **2.81** as a transparent oil (4.1 mg, 29%) as a 1.2:1 diastereomeric mixture. Given the instability of the product over time, just the ¹H NMR of the product was recorded.

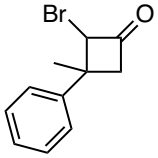
¹H NMR of **2.81** (diastereomeric mixture + impurities)

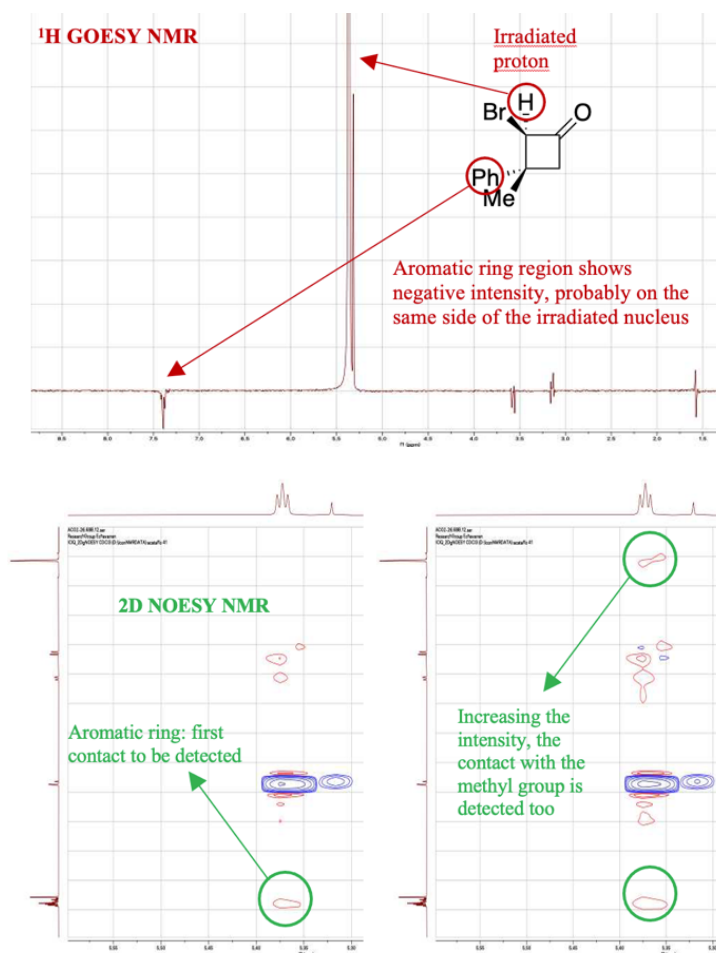


*Procedure E for the synthesis of α -halocyclobutanones **2.83** starting from cyclobutenes **2.78**.*

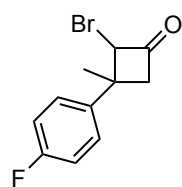


2-Bromo-3-methyl-3-phenylcyclobutan-1-one (**2.83a**)

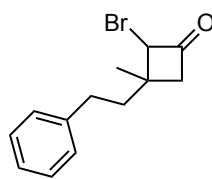
 Br_2 (62 mg, 0.39 mmol, 1.3 equiv) was added dropwise to a solution of (1-methyl-3-phenoxycyclobut-2-en-1-yl)benzene (70.9 mg, 0.30 mmol, 1 equiv.) in dry toluene (3.00 mL, 0.1 M) at 0 °C and the reaction mixture was left to stir for 1h at the same temperature. The solvent was then evaporated and the crude redissolved in CH_2Cl_2 , silica gel was added and the solvent evaporated again. The crude product absorbed on silica was purified by flash chromatography (2:1 CH_2Cl_2 :cyclohexane) on silica gel delivering cyclobutanone **2.83a**. in a 6:1 diastereomeric ratio (60 mg, 84%). A second column (30:1 pentane:Et₂O) afforded the major diastereomer as a transparent oil (49 mg, 68%). **Notes:** After the evaporation of toluene, **2.82** was detected as the only product of the reaction. This intermediate completely hydrolyzes over purification on silica gel delivering the final product **2.83a**. *Diastereomeric mixture + impurity:* $^1\text{H NMR}$ (500 MHz, CDCl_3) δ 7.52 (dddd, $J = 6.7, 4.1, 2.8, 1.6$ Hz, 0.2H, md), 7.44 – 7.33 (m, 4.4H Md + md), 7.35 – 7.27 (m, 1H, Md), 7.29 – 7.23 (m, 0.4H, md), 5.35 (t, $J = 2.2$ Hz, 1H, Md), 4.95 (dd, $J = 4.9, 2.2$ Hz, 0.2H, md), 3.80 (dd, $J = 17.1, 2.1$ Hz, 0.2 H, md), 3.55 (ddq, $J = 16.4, 2.5, 0.8$ Hz, 1H, Md), 3.20 (dd, $J = 17.1, 4.9$ Hz, 0.2H, md), 3.13 (dd, $J = 16.4, 1.9$ Hz, 1H, Md), 1.84 (s, 0.6H, md), 1.55 (d, $J = 0.8$ Hz, 3H, Md). *Major diastereomer:* $^1\text{H NMR}$ (400 MHz, CDCl_3) δ 7.44 – 7.32 (m, 4H), 7.36 – 7.26 (m, 1H), 5.35 (t, $J = 2.2$ Hz, 1H), 3.55 (ddd, $J = 16.4, 2.6, 0.9$ Hz, 1H), 3.12 (dd, $J = 16.4, 1.9$ Hz, 1H), 1.55 (s, $J = 0.8$ Hz, 3H). $^{13}\text{C NMR}$ (126 MHz, CDCl_3) $^{13}\text{C NMR}$ (126 MHz, CDCl_3) δ 197.76, 146.55, 128.93, 127.24, 125.19, 60.54, 54.59, 39.67, 28.17. **HRMS** (ESI) m/z calculated for $\text{C}_{11}\text{H}_{11}\text{BrNaO}$ $[\text{M}+\text{Na}]^+$: 260.9885, found: 260.9881. **IR (selected frequency):** 1787 cm^{-1} . The relative configuration of the major diastereomer was assigned by **GOESY** and **NOESY** NMR (See below).



2-Bromo-3-(4-fluorophenyl)-3-methylcyclobutan-1-one (**2.83b**)

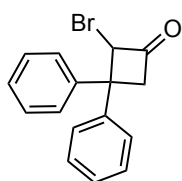


Cyclobutanone **2.83b** was prepared following the same procedure reported for **2.83a**, starting from 2-bromo-3-(4-fluorophenyl)-3-methylcyclobutan-1-one (42.8 mg, 0.17 mmol) and Br₂ (32 mg, 0.20 mmol). The crude product absorbed on silica was purified by flash chromatography (2:1 CH₂Cl₂:cyclohexane) on silica gel delivering cyclobutanone **2.83b** in a 3:1 diastereomeric ratio (28 mg, 65%). A second column (30:1 pentane:Et₂O) afforded the major diastereomer as a yellow solid (20 mg, 46%). *Diastereomeric mixture*: ¹H NMR (500 MHz, CDCl₃) δ 7.36 – 7.28 (m, 2H, Md), 7.25 – 7.18 (m, 0.8H, md), 7.11 – 7.03 (m, 2.8H, Md + md), 5.30 (t, *J* = 2.2 Hz, 1H, Md), 4.94 (dd, *J* = 4.8, 2.2 Hz, 0.4H, md), 3.74 (dd, *J* = 17.1, 2.1 Hz, 0.4H, md), 3.52 (ddq, *J* = 16.4, 2.6, 0.9 Hz, 1H, Md), 3.22 (dd, *J* = 17.1, 4.8 Hz, 0.4H, md), 3.12 (dd, *J* = 16.3, 1.9 Hz, 1H, Md), 1.82 (s, 1.2H, md), 1.53 (d, *J* = 0.9 Hz, 3H, Md). *Major diastereomer*: **M.p.** = 58–62 °C. ¹H NMR (500 MHz, CDCl₃) δ 7.36 – 7.28 (m, 2H), 7.11 – 7.03 (m, 2H), 5.30 (t, *J* = 2.2 Hz, 1H), 3.52 (ddt, *J* = 16.4, 2.6, 0.9 Hz, 1H), 3.12 (dd, *J* = 16.3, 1.9 Hz, 1H), 1.53 (d, *J* = 0.8 Hz). ¹⁹F NMR (376 MHz, CDCl₃) δ -114.88. ¹³C NMR (126 MHz, CDCl₃) δ 197.30, 161.89 (d, *J* = 246.2 Hz), 142.35 (d, *J* = 3.3 Hz), 126.95 (d, *J* = 8.0 Hz), 115.83 (d, *J* = 21.6 Hz), 60.54, 54.72, 39.29, 28.29. **HRMS** (ESI) *m/z* calculated for C₁₁H₁₁BrFO [M+H]⁺: 256.9972, found: 256.9968.

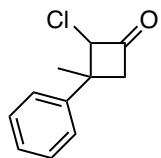
2-Bromo-3-methyl-3-phenethylcyclobutan-1-one (2.83c)

Cyclobutanone **2.83c** was prepared following the same procedure reported for **2.83a**, starting from ((3-methyl-3-phenethylcyclobut-1-en-1-yl)oxy)benzene (34.8 mg, 0.13 mmol) and Br₂ (25 mg, 0.16 mmol). The crude product absorbed on silica was purified by flash chromatography (2:1 CH₂Cl₂:cyclohexane) on silica gel delivering cyclobutanone **2.83c** as a transparent oil in a 3:1 diastereomeric ratio (16.2 mg, 46%) which could not be separated further.

Diastereomeric mixture: ¹H NMR (500 MHz, CDCl₃) δ 7.33 – 7.28 (m, 2.6H, Md + md), 7.24 – 7.18 (m, 3.9H, Md + md), 4.88 (t, J = 2.4 Hz, 1H, Md), 4.86 (d, J = 1.0 Hz, 0.3H, md), 2.97 (ddd, J = 16.8, 2.7, 0.7 Hz, 1H, Md), 2.82 – 2.66 (m, 3.6H, Md + md), 2.58 (ddd, J = 13.5, 12.0, 4.9 Hz, 0.3H, md), 2.16 – 2.03 (m, 2.3H, Md + md), 2.00 – 1.89 (m, 0.3H, md), 1.74 (ddd, J = 14.0, 12.2, 4.9 Hz, 0.3H, md), 1.54 (s, 0.9H, md), 1.32 (s, 3H, Md). ¹³C NMR (126 MHz, CDCl₃) δ 199.2 (md), 198.7 (Md), 141.5 (md), 141.2 (Md), 128.7 (Md), 128.7 (md), 128.4 (md), 128.4 (Md), 126.4 (Md), 126.3 (md), 61.3 (md), 59.9 (Md), 54.8 (Md), 53.9 (md), 43.4 (Md), 39.9 (md), 35.7 (Md), 35.5 (md), 32.1 (Md), 31.6 (md), 25.1 (md), 22.6 (Md). **HRMS** (ESI) m/z calculated for C₁₃H₁₅BrNaO [M+Na]⁺: 289.0198, found: 289.0194.

2-Bromo-3,3-diphenylcyclobutan-1-one (2.83d)

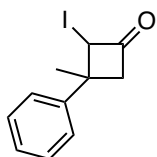
Cyclobutanone **2.83d** was prepared following the same procedure reported for **2.83a**, starting from (3-(4-(trifluoromethyl)phenoxy)cyclobut-2-ene-1,1-diyl)dibenzene (16.7 mg, 0.046 mmol) and Br₂ (8.7 mg, 0.054 mmol). The crude product absorbed on silica was purified by flash chromatography (2:1 CH₂Cl₂:cyclohexane) on silica gel delivering cyclobutanone **2.83d** as a transparent oil (6.1 mg, 44%). ¹H NMR (400 MHz, CDCl₃) δ 7.49 – 7.42 (m, 2H), 7.42 – 7.34 (m, 3H), 7.33 – 7.21 (m, 3H), 7.03 – 6.96 (m, 2H), 5.76 (dd, J = 2.8, 1.4 Hz, 1H), 3.97 – 3.70 (m, 2H), 1.55 (s, 3H). ¹³C NMR (101 MHz, CDCl₃) δ 198.0, 145.7, 142.6, 129.0, 128.3, 127.9, 127.6, 127.4, 127.2, 60.8, 56.7, 48.1. **HRMS** (ESI) m/z calculated for C₁₆H₁₃BrNaO [M+Na]⁺: 323.0042, found: 323.0055.

2-Chloro-3-methyl-3-phenylcyclobutan-1-one (2.83e)

NCS (53.4 mg, 0.4 mmol) was added to a solution of (1-methyl-3-phenoxy)cyclobut-2-en-1-yl)benzene (47.3 mg, 0.2 mmol) in acetonitrile (2.00 mL) and the mixture was left to stir at 60°C for 72 h. The solvent was evaporated and the crude mixture was purified by flash chromatography on silica gel (2:1 CH₂Cl₂:cyclohexane) affording product **2.83e** as a 4.6:1 diastereomeric mixture (20 mg, 51%, *dr* determined by ¹H NMR of the crude mixture = 1.3:1). A second column (30:1 pentane:Et₂O) afforded the major diastereomer as a transparent oil (15 mg, 39%). *Diastereomeric mixture:* ¹H NMR (500 MHz, CDCl₃) δ 7.43 – 7.36 (m, 2.4 H Md + md), 7.37 – 7.32 (m, 2H, Md), 7.34 – 7.26 (m, 1.6H, Md + md), 5.16 (t, J = 2.2 Hz, 1H, Md), 4.83 (dd, J =

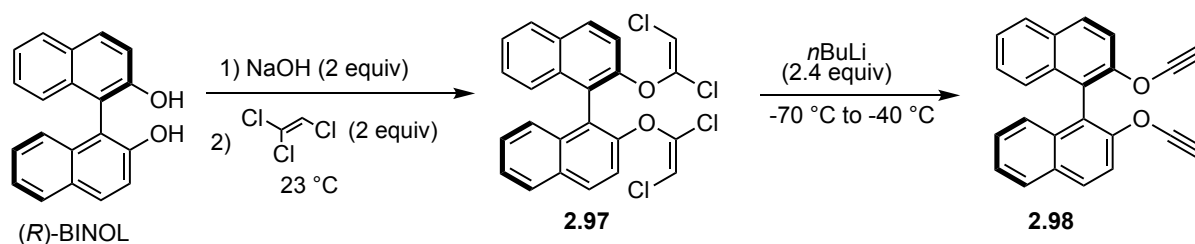
4.1, 2.2 Hz, 0.2H, md), 3.70 (dd, $J = 17.3, 2.2$ Hz, 0.2H, md), 3.47 (ddq, $J = 16.4, 2.5, 0.9$ Hz, 1H, Md), 3.20 (dd, $J = 17.3, 4.1$ Hz, 0.2H, md), 3.08 (dd, $J = 16.4, 2.1$ Hz, 1H, Md), 1.86 (s, 0.6H, md), 1.51 (d, $J = 0.9$ Hz, 3H, Md). *Major diastereomer*: $^1\text{H NMR}$ (500 MHz, CDCl_3) δ 7.43 – 7.36 (m, 2H), 7.38 – 7.31 (m, 2H), 7.34 – 7.27 (m, 1H), 5.16 (t, $J = 2.2$ Hz, 1H), 3.51 – 3.43 (m, 1H), 3.08 (dd, $J = 16.4, 2.0$ Hz, 1H), 1.51 (d, $J = 0.9$ Hz, 3H). $^{13}\text{C NMR}$ (126 MHz, CDCl_3) δ 198.4, 146.6, 129.0, 127.3, 125.3, 70.3, 54.5, 40.7, 25.9. **HRMS** (ESI) m/z calculated for $\text{C}_{11}\text{H}_{11}\text{ClNaO}$ $[\text{M}+\text{Na}]^+$: 217.0391, found: 217.0386.

2-Iodo-3-methyl-3-phenylcyclobutan-1-one (2.83f)

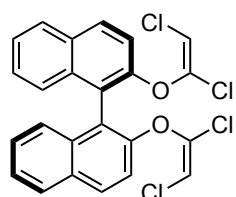


NIS (58.5 mg, 0.26 mmol) was added to a solution of (1-methyl-3-phenoxy-cyclobut-2-en-1-yl)benzene (47.3 mg, 0.2 mmol) in acetonitrile (2.00 mL) and the mixture was left to stir at 23 °C for 16 h. NaSO_3 aq. was added to the mixture and the organic layer separated from the aqueous one which was afterwards washed with Et_2O (x2). The combined organic layers were then washed with brine. The solvent was evaporated and the crude mixture was purified by flash chromatography on silica gel (2:1 CH_2Cl_2 :cyclohexane) affording product **2.83f** as a 6:1 diastereomeric mixture (14.5 mg, 25%) which was not possible to separate further. *Diastereomeric mixture*: $^1\text{H NMR}$ (500 MHz, CDCl_3) δ 7.42 – 7.34 (m, 4.8H Md + md), 7.33 – 7.27 (m, 1H, Md), 7.24 – 7.20 (m, 0.2H, md), 5.73 (dd, $J = 2.7, 1.7$ Hz, 1H, Md), 5.30 – 5.25 (m, 0.2H, md), 3.80 (dd, $J = 16.8, 2.1$ Hz, 0.2H, md), 3.76 – 3.68 (m, 1H, Md), 3.21 (dd, $J = 16.9, 5.6$ Hz, 0.2H, md), 3.01 (dd, $J = 16.4, 1.8$ Hz, 1H, Md), 1.85 (d, $J = 0.6$ Hz, 0.6H, md), 1.58 (d, $J = 0.8$ Hz, 3H, Md). $^{13}\text{C NMR}$ (126 MHz, CDCl_3) δ 200.7 (md), 198.5 (Md), 146.7 (md), 128.9 (Md), 128.4 (md), 127.2 (Md), 126.7 (md), 125.1 (Md), 54.3 (md), 53.9 (Md), 42.0 (md), 39.6 (Md), 37.8 (Md), 32.4 (Md), 28.9 (md), 27.1 (md). **HRMS** (APCI) m/z calculated for $\text{C}_{11}\text{H}_{12}\text{IO}$ $[\text{M}+\text{H}]^+$: 286.9927, found: 286.9924.

Procedure F for a symmetric [2+2] cycloaddition of ynol ethers with alkenes.

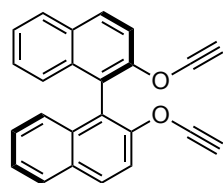


2,2'-Bis(((E)-1,2-dichlorovinyl)oxy)-1,1'-binaphthalene (2.97)

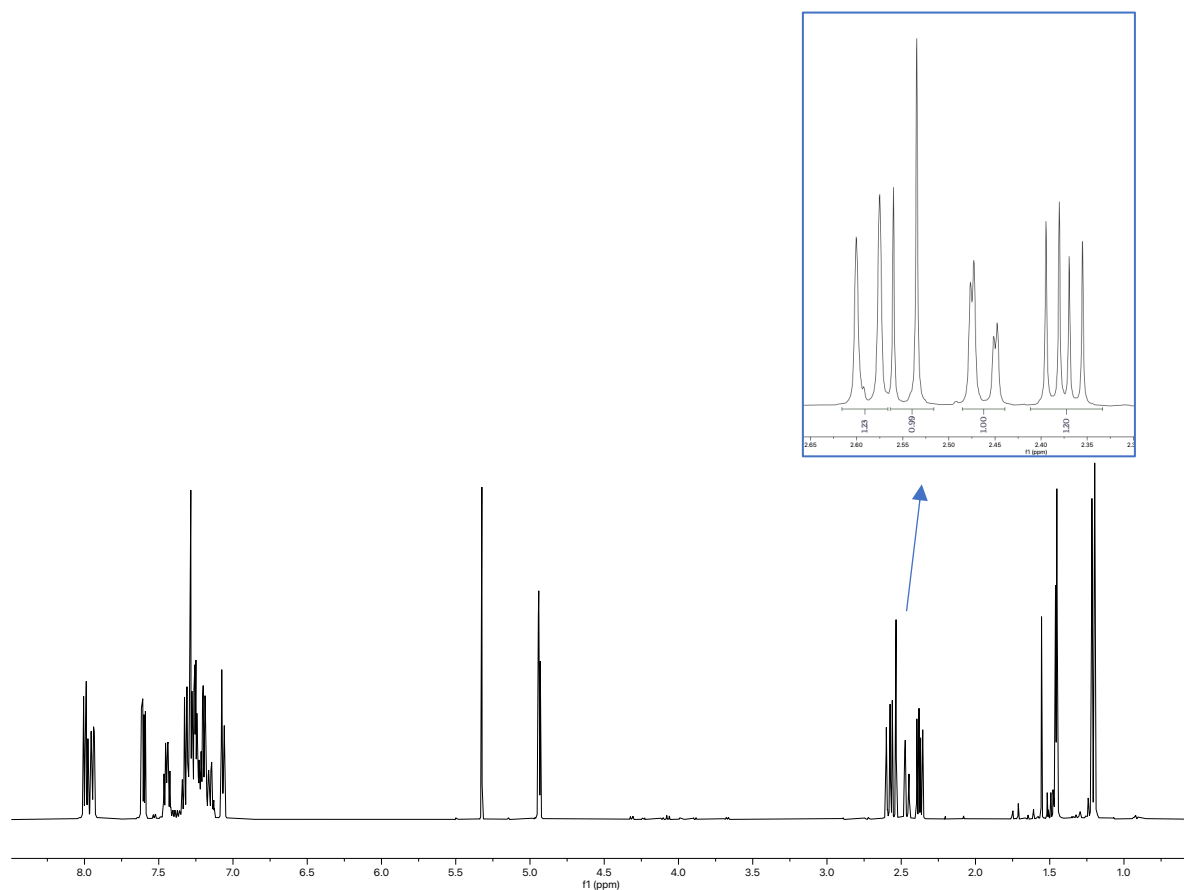
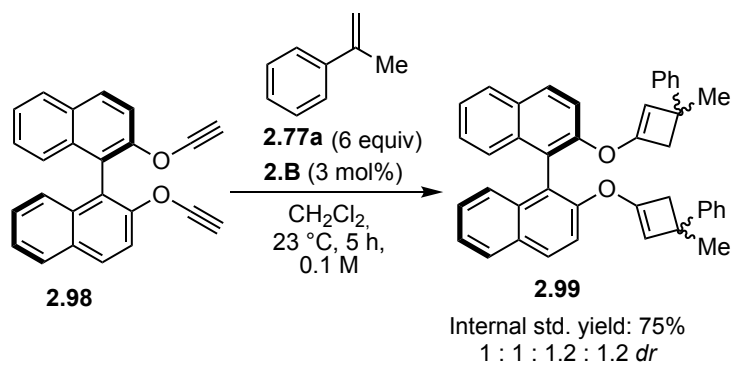


A round bottom flask was charged with a solution of the [1,1'-binaphthalene]-2,2'-diol (859 mg, 3.00 mmol) derivative in DMSO (3 mL). To this solution NaOH (240 mg, 6.00 mmol) was added and the resulting mixture was stirred at room temperature for 2 hours. Afterwards trichloroethylene (788 mg, 540 μL , 6.00 mmol) was slowly added and the resulting mixture was stirred for the given amount of time (monitor by TLC). After completion the reaction was quenched with water. The phases were separated and aqueous phase was extracted with CH_2Cl_2 . The combined organic layers were washed with brine, dried over magnesium sulphate and concentrated under reduced pressure. The crude mixture was purified by flash chromatography on silica gel in pentane affording **2.97** as a transparent oil (956 mg, 67%). $^1\text{H NMR}$ (500 MHz, CDCl_3) δ 8.01 (d, $J = 8.9$ Hz, 2H), 7.91 (dt, $J = 8.3, 0.9$ Hz, 2H), 7.43 (ddd, $J = 8.1, 6.5, 1.4$ Hz, 2H), 7.39 (d, $J = 9.0$ Hz, 2H), 7.29 (ddd, $J = 7.9, 6.6, 1.3$ Hz, 2H), 7.24 (s, 2H), 5.74 (s, 2H).

2,2'-Bis(ethynyloxy)-1,1'-binaphthalene (2.98)



A flame dried Schlenk tube under an inert gas atmosphere was charged with a solution of the 2,2'-bis(((E)-1,2-dichlorovinyl)oxy)-1,1'-binaphthalene (615 mg, 1.3 mmol) in dry Et_2O (13 mL) and cooled to -78 $^\circ\text{C}$. At this temperature $n\text{BuLi}$ (662 mg, 4.1 mL, 2.5 M, 10.3 mmol) was dropwise added. The resulting solution was stirred at maintained temperature for 1 h before it was allowed to warm to -40 $^\circ\text{C}$ in the course of 1 h. The mixture was stirred at this temperature for another 2 h before being quenched with water. The phases were separated and the aqueous layer was extracted with Et_2O . The combined organic layers were washed with a saturated ammonium chloride solution and brine, dried over magnesium sulphate and concentrated under reduced pressure affording **2.98** as an orange solid (248 mg, 57%). $^1\text{H NMR}$ (400 MHz, C_6D_6) δ 7.91 (d, $J = 9.1$ Hz, 2H), 7.67 – 7.53 (m, 4H), 7.21 (dq, $J = 8.5, 0.9$ Hz, 2H), 7.10 (ddd, $J = 8.1, 6.8, 1.2$ Hz, 2H), 6.94 (ddd, $J = 8.3, 6.8, 1.3$ Hz, 2H), 1.63 (s, 2H). $^{13}\text{C NMR}$ (101 MHz, C_6D_6) δ 151.4, 133.8, 131.5, 131.1, 128.6, 125.8, 125.6, 118.0, 114.5, 85.1, 33.6. **HRMS** (ESI) m/z calculated for $\text{C}_{24}\text{H}_{14}\text{NaO}_2$ $[\text{M}+\text{Na}]^+$: 357.0886, found: 357.0881.



UNIVERSITAT ROVIRA I VIRGILI

GOLD(I)-CATALYZED ASYMMETRIC CYCLIZATIONS AND CYCLOADDITIONS OF HETEROATOM-SUBSTITUTED ALKYNES WITH ALKENES

Andrea Cataffo

Chapter III

Enantioselective Cyclizations of Bromoenynes: A New Mechanistic Understanding of Gold(I)-Catalyzed Alkoxy cyclizations

UNIVERSITAT ROVIRA I VIRGILI

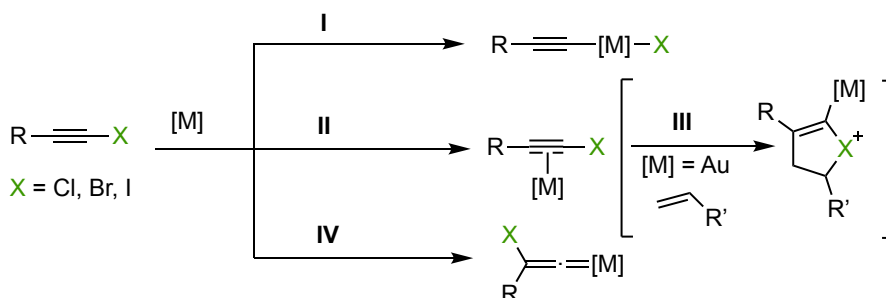
GOLD(I)-CATALYZED ASYMMETRIC CYCLIZATIONS AND CYCLOADDITIONS OF HETEROATOM-SUBSTITUTED ALKYNES WITH ALKENES

Andrea Cataffo

Introduction

Haloalkynes in gold(I)-catalysis

Halogen-substituted alkynes present a significant polarization, which makes them essential building blocks in organic synthesis. Their dual reactivity in transition metal catalysis is pivotal: the π -system enables functionalization with nucleophiles, while the halogen moiety provides opportunities for additional diversification.¹ They can be activated by transition metals giving rise to different intermediates (Scheme 3.1) via: σ -activation (**I**), π -activation (**II**), metal vinylidene formation (**IV**). Furthermore, when combined with another unsaturated system in the presence of a gold(I) catalyst, they have been reported to generate cyclic halonium intermediates (**III**).²



Scheme 3.1. Different modes of activation of haloalkynes with transition metals.

Their reactivity under gold(I)-catalysis allows for various inter- and intramolecular functionalization with nucleophiles (Scheme 3.2a).³ Very common is their use in hydrofunctionalization reaction with heteroatom-nucleophiles to generate highly functionalized alkenes. As shown in Scheme 3.2b, the hydration⁴ and hydroalkoxylation⁵ of haloalkynes to respectively form ketones **3.1** and (*Z*)-enol ethers **3.2** were both described to happen under mild conditions. As another example of oxygen nucleophiles, the Markovnikov addition of carboxylic acids⁶ or diphenyl phosphates⁷ affords (*Z*)- β -iodoenol esters **3.3** and phosphorylated (*Z*)- β -haloenol ethers **3.4**. *S*- and *N*-nucleophiles can also be attached to chloro-

¹ Wu, W.; Jiang, H. Haloalkynes: A Powerful and Versatile Building Block in Organic Synthesis. *Acc. Chem. Res.* **2014**, *47*, 2483–2504.

² a) De Orbe, M. E.; Zanini, M.; Quinonero, O.; Echavarren, A. M. Gold- or Indium-Catalyzed Cross-Coupling of Bromoalkynes with Allylsilanes through a Concealed Rearrangement. *ACS Catal.* **2019**, *9*, 7817–7822. b) Kreuzahler, M.; Haberhauer, G., Gold(I)-Catalyzed Haloalkynylation of Aryl Alkynes: Two Pathways, One Goal, *Angew. Chem. Int. Ed.* **2020**, *59*, 9433–9437, *Angew. Chem.* **2020**, *132*, 9519–9524. c) Kreuzahler, M.; Haberhauer, G. Cyclopropenylmethyl Cation: A Concealed Intermediate in Gold(I)-Catalyzed Reactions. *Angew. Chem. Int. Ed.* **2020**, *59*, 17739–17749., *Angew. Chem.* **2020**, *132*, 17892–17902. d) García-Fernández, P. D.; Iglesias-Sigüenza, J.; Rivero-Jerez, P. S.; Díez, E.; Gómez-Bengoña, E.; Fernández, R.; Lassaletta, J. M. Au^I-Catalyzed Hydroalkynylation of Haloalkynes. *J. Am. Chem. Soc.* **2020**, *142*, 16082–16089.

³ a) 6/10/24 11:40:00 AM

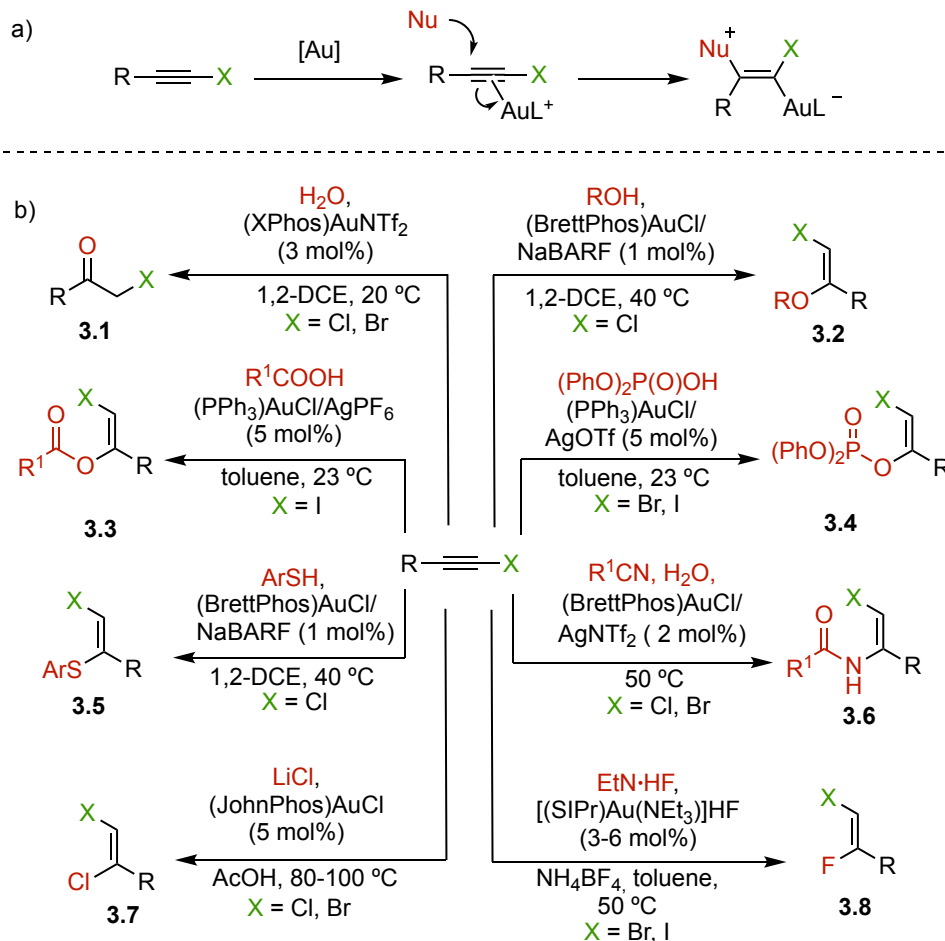
⁴ Xie, L.; Wu, Y.; Yi, W.; Zhu, L.; Xiang, J.; He, W. Gold-Catalyzed Hydration of Haloalkynes to α -Halomethyl Ketones. *J. Org. Chem.* **2013**, *78*, 9190–9195.

⁵ Liu, C.; Xu, J.; Ding, L.; Zhang, H.; Xue, Y.; Yang, F. Au-Catalyzed Tandem Intermolecular Hydroalkoxylation/Claisen Rearrangement between Allylic Alcohols and Chloroalkynes. *Org. Biomol. Chem.* **2019**, *17*, 4435–4439.

⁶ González-Liste, P. J.; León, F.; Arribas, I.; Rubio, M.; García-Garrido, S. E.; Cadierno, V.; Pizzano, A., Highly Stereoselective Synthesis and Hydrogenation of (*Z*)-1-Alkyl-2-Arylvinyl Acetates: A Wide Scope Procedure for the Preparation of Chiral Homobenzylic Esters, *ACS Catal.* **2016**, *6*, 3056–3060.

⁷ Chary, B. C.; Kim, S.; Shin, D.; Lee, P. H. A Regio- and Stereoselective Synthesis of Trisubstituted Alkenes via gold(I)-Catalyzed Hydrophosphoryloxylation of Haloalkynes. *Chem. Commun.* **2011**, *47*, 7851–7853.

and bromoalkynes to form hydrothiolation products **3.5**⁸ and enamides **3.6**.⁹ The latter could be obtained through Ritter reaction of the haloalkynes with nitriles. Finally, the formal *anti*-addition of hydrogen chloride¹⁰ and hydrogen fluoride¹¹ to haloalkynes could be obtained by treating the substrate with LiCl to obtain **3.7** in the first case and Et₃NHF to obtain **3.8** in the second case.



Scheme 3.2. Gold(I)-catalyzed intermolecular nucleophilic additions to haloalkynes.

Regarding the reactivity with carbon-based nucleophiles, the group of Fürstner reported the formation of gold(I) vinylidene intermediates in the intramolecular hydroarylation of *ortho*-alkynylbiaryls **3.9** (Scheme 3.3a).¹² The products generated via this transformation were proposed to be formed by an initial 1,2-halogen migration to form gold vinylidenes **3.10** followed by electrophilic aromatic substitution to form halophenanthrenes **3.11**. As a key example of this vinylidene-mediated chemistry,

⁸ Liu, C.; Xue, Y.; Ding, L.; Zhang, H.; Yang, F. Au-Catalyzed Addition of Nucleophiles to Chloroalkynes: A Regio- and Stereoselective Synthesis of (*Z*)-Alkenyl Chlorides. *Eur. J. Org. Chem.* **2018**, *2018*, 6537–6540.

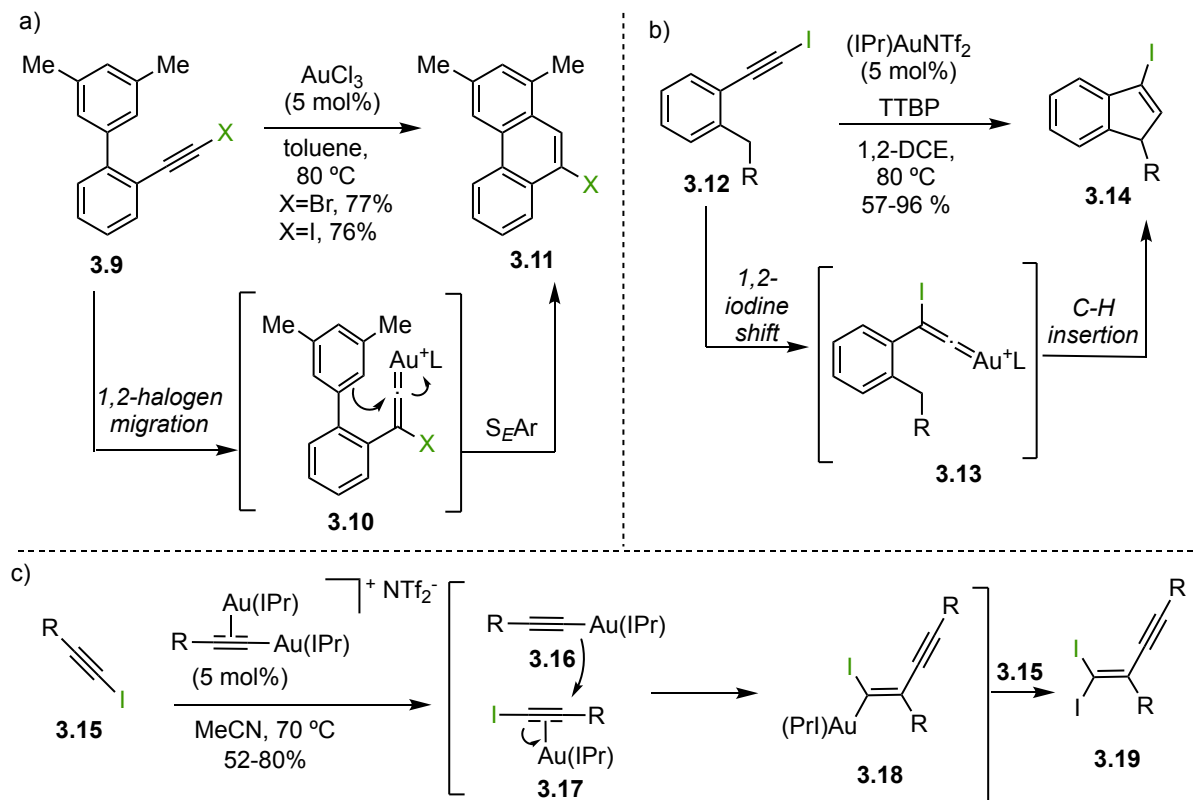
⁹ Liu, C.; Yang, F. Au-Catalyzed Stereoselective Ritter Reaction of Haloalkynes with Nitriles for (*Z*)- β -Halogenated Enamides. *Eur. J. Org. Chem.* **2019**, *2019*, 6867–6870.

¹⁰ Zeng, X.; Liu, S.; Hammond, G. B.; Xu, B., Hydrogen-Bonding-Assisted Brønsted Acid and Gold Catalysis: Access to Both (*E*)- and (*Z*)-1,2-Haloalkenes via Hydrochlorination of Haloalkynes, *ACS Catal.* **2018**, *8*, 904–909.

¹¹ Gómez-Herrera, A.; Nagra, F.; Brill, M.; Nolan, S. P.; Cazin, C. S. J. Sequential Functionalization of Alkynes and Alkenes Catalyzed by Gold(I) and Palladium(II) N-Heterocyclic Carbene Complexes. *ChemCatChem* **2016**, *8*, 3381–3388.

¹² Mamane, V.; Hannen, P.; Fürstner, A., Synthesis of Phenanthrenes and Polycyclic Heteroarenes by Transition-Metal Catalyzed Cycloisomerization Reactions, *Chem. Eur. J.* **2004**, *10*, 4556–4575.

González harnessed their reactivity to synthesize 3-iodoindenes **3.14** from aryl iodoalkynes **3.12** through a benzylic C–H bond insertion validated by deuterium labeling experiments (Scheme 3.3b).¹³ While gold(I)-catalyzed hydroarylations of iodoalkynes result vastly explored in literature,¹⁴ scarce are the reports concerning the reaction of these species with alkenes or triple bonds.



Scheme 3.3. a) First case of gold(I)-vinylidene through activation of haloalkynes. b) Gold(I)-vinylidene mediated C–H insertion starting from iodoalkynes. c) Head-to-tail dimerization of iodoalkynes.

Hashmi described the gold(I)-catalyzed cyclization of 1,2-bis(2-iodoethynyl)benzenes which again proceeds by the 1,2-halogen migration to form gold vinylidenes.¹⁵ The same group described the head-to-tail dimerization of iodoalkynes under dual gold catalysis (Scheme 3.3c).¹⁶ It was suggested that the

¹³ Morán-Poladura, P.; Rubio, E.; González, J. M., Intramolecular C–H Activation through Gold(I)-Catalyzed Reaction of Iodoalkynes, *Angew. Chem. Int. Ed.* **2015**, *54*, 3052–3055, *Angew. Chem.* **2015**, *127*, 3095–3098.

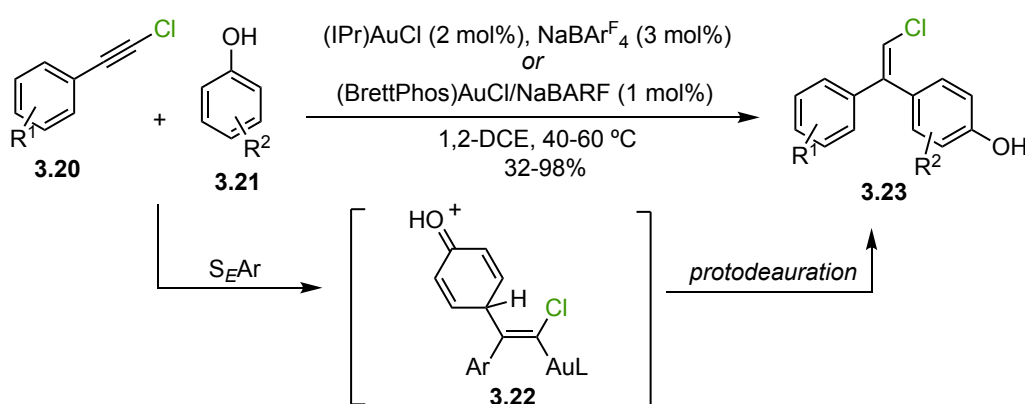
¹⁴ Staben, S. T.; Kennedy-Smith, J. J.; Toste, F. D., Gold(I)-Catalyzed 5-Endo-Dig Carbocyclization of Acetylenic Dicarboxyl Compounds, *Angew. Chem. Int. Ed.* **2004**, *43*, 5350–5352, *Angew. Chem.* **2004**, *116*, 5464–5466. b) Shibata, T.; Ueno, Y.; Kanda, K., Cationic Au(I)-Catalyzed Cycloisomerization of Aromatic Enynes for the Synthesis of Substituted Naphthalenes, *Synlett* **2006**, *2006*, 411–414. c) Walker, D. B.; Howgego, J.; Davis, A. P., Synthesis of Regioselectively Functionalized Pyrenes via Transition-Metal-Catalyzed Electrocyclization, *Synthesis* **2010**, *2010*, 3686–3692. d) Morán-Poladura, P.; Suárez-Pantiga, S.; Piedrafita, M.; Rubio, E.; González, J. M., Regiocontrolled Gold(I)-Catalyzed Cyclization Reactions of *N*-(3-Iodoprop-2-Ynyl)-*N*-Tosylanilines, *J. Organomet. Chem.* **2011**, *696*, 12–15. e) Nakae, T.; Ohnishi, R.; Kitahata, Y.; Soukawa, T.; Sato, H.; Mori, S.; Okujima, T.; Uno, H.; Sakaguchi, H., Effective Synthesis of Diiodinated Picene and Dibenz[*a,h*]Anthracene by AuCl-Catalyzed Double Cyclization, *Tetrahedron Lett.* **2012**, *53*, 1617–1619. f) Morán-Poladura, P.; Rubio, E.; González, J. M., Gold(I)-Catalyzed Hydroarylation Reaction of Aryl (3-Iodoprop-2-Yn-1-Yl) Ethers: Synthesis of 3-Iodo-2H-Chromene Derivatives, *Beilstein J. Org. Chem.* **2013**, *9*, 2120–2128. g) Nösel, P.; Lauterbach, T.; Rudolph, M.; Rominger, F.; Hashmi, A. S. K., Gold-Catalyzed Synthesis of Iodofulvenes, *Chem. Eur. J.* **2013**, *19*, 8634–8641. h) Johannsen, T.; Golz, C.; Alcarazo, M., α -Cationic Phospholes: Synthesis and Applications as Ancillary Ligands, *Angew. Chem. Int. Ed.* **2020**, *59*, 22779–22784, *Angew. Chem.* **2020**, *132*, 22969–22975.

¹⁵ Nösel, P.; Müller, V.; Mader, S.; Moghimi, S.; Rudolph, M.; Braun, I.; Rominger, F.; Hashmi, A. S. K. Gold-Catalyzed Hydroarylation Cyclization of 1,2-Bis(2-Iodoethynyl)Benzenes. *Adv. Synth. Catal.* **2015**, *357*, 500–506.

¹⁶ Mader, S.; Molinari, L.; Rudolph, M.; Rominger, F.; Hashmi, A. S. K., Dual Gold-Catalyzed Head-to-Tail Coupling of Iodoalkynes, *Chem. Eur. J.* **2015**, *21*, 3910–3913.

reaction proceeds via gold acetylide **3.16** which attacks on the π -activated **3.17** leading to vinyl gold species **3.18** and eventually to **3.19** after reacting with another molecule of **3.15** which regenerates the catalytic cycle.

Chloroalkynes instead were reported to react with phenols in a stereoselective hydroarylation reaction by both the groups of Yang⁸ and Hashmi¹⁷ (Scheme 3.4). This transformation, conducted under mild conditions, demonstrated high versatility with various chloroalkynes **3.20** and phenols **3.21**. After the *para*-oriented electrophilic aromatic substitution to form **3.22**, follows a protodeauration-rearomatization step which brings to the formation of alkenyl chlorides **3.23**. This methodology was successfully extended to indoles and aryloxyethers as coupling partners, along with alkyl-substituted chloroalkynes.⁸



Scheme 3.4. Gold(I)-catalyzed hydroarylation of chloroalkynes with phenols.

Meanwhile, Zhang described the intermolecular [2+2] cycloadditions of chloroalkynes with unactivated 1,2-disubstituted alkenes, resulting in the formation of cyclobutenes (Scheme 3.5a).¹⁸ The reaction exhibited versatility across cycloalkenes of varying sizes, furthermore, it demonstrated compatibility with aryl-substituted chloroalkynes **3.24** bearing different functionalities. The proposed mechanism coincides with the one mentioned in the **General Introduction**¹⁹ which sees a nucleophilic attack-cyclopropyl gold(I) carbene formation-ring expansion sequence to afford the target four-membered rings **3.28**.

The group of Haberhauer studied in detail the intricate mechanism of chloroalkynylation reactions,²⁰ reported different mechanisms when combining aryl-substituted alkynes with 1,1-disubstituted alkenes

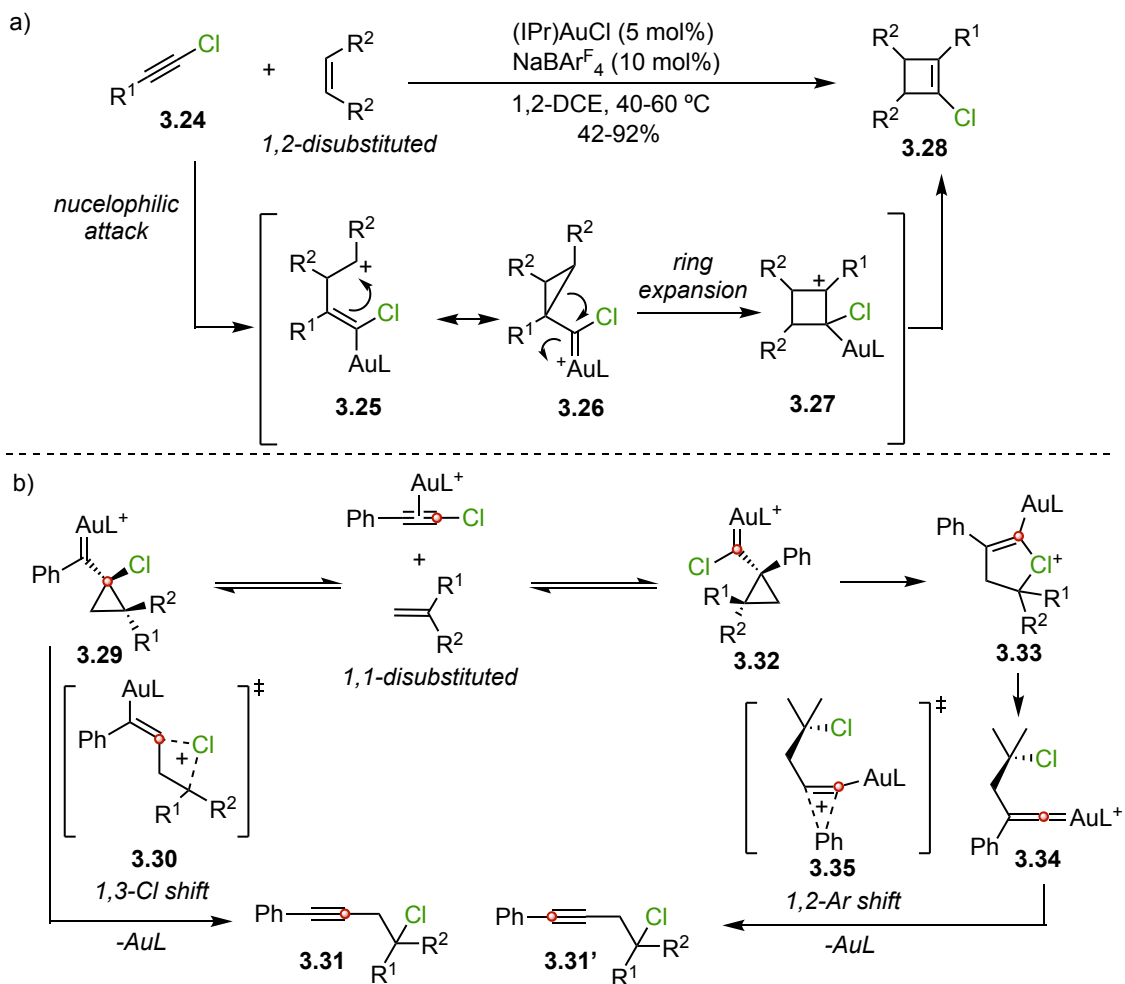
¹⁷ Adak, T.; Schulmeister, J.; Dietl, M. C.; Rudolph, M.; Rominger, F.; Hashmi, A. S. K. Gold-Catalyzed Highly Chemo- and Regioselective C–H Bond Functionalization of Phenols with Haloalkynes. *Eur. J. Org. Chem.* **2019**, 2019, 3867–3876.

¹⁸ Bai, Y.-B.; Luo, Z.; Wang, Y.; Gao, J.-M.; Zhang, L. Au-Catalyzed Intermolecular [2+2] Cycloadditions between Chloroalkynes and Unactivated Alkenes. *J. Am. Chem. Soc.* **2018**, 140, 5860–5865.

¹⁹ López-Carrillo, V.; Echavarren, A. M. Gold(I)-Catalyzed Intermolecular [2+2] Cycloaddition of Alkynes with Alkenes. *J. Am. Chem. Soc.* **2010**, 132, 9292–9294.

²⁰ a) Kreuzahler, M.; Haberhauer, G., Metal-Catalyzed Haloalkynylation Reactions, *Chem. Eur. J.* **2022**, 28, e202103046. More work from the group on chloroalkynes: b) Semleit, N.; Kreuzahler, M.; Haberhauer, G. Gold(I)-Catalyzed Allene–Diene–Alkyne Coupling Reaction to Polycycles. *Eur. J. Org. Chem.* **2020**, 2020, 6629–6634. c) Siera, H.; Semleit, N.; Kreuzahler, M.; Wölper, C.; Haberhauer, G. Gold Catalysis of Non-Conjugated Haloacetylenes. *Synthesis* **2021**, 53, 1457–1470.

(Scheme 3.5b).²¹ Through thorough mechanistic studies^{2c} it was rationalized that depending on the catalyst and on the substituents on the alkyne, a 1,3-Cl shift (**3.30**) or cyclic halonium (**3.33**) followed by 1,2-Ar shift (**3.35**) can mediate the chloroalkynylation, affording two products (respectively **3.31** and **3.31'**) that differ only by the positions of the two carbons on the alkyne which could be differentiated by isotopic labeling experiments.



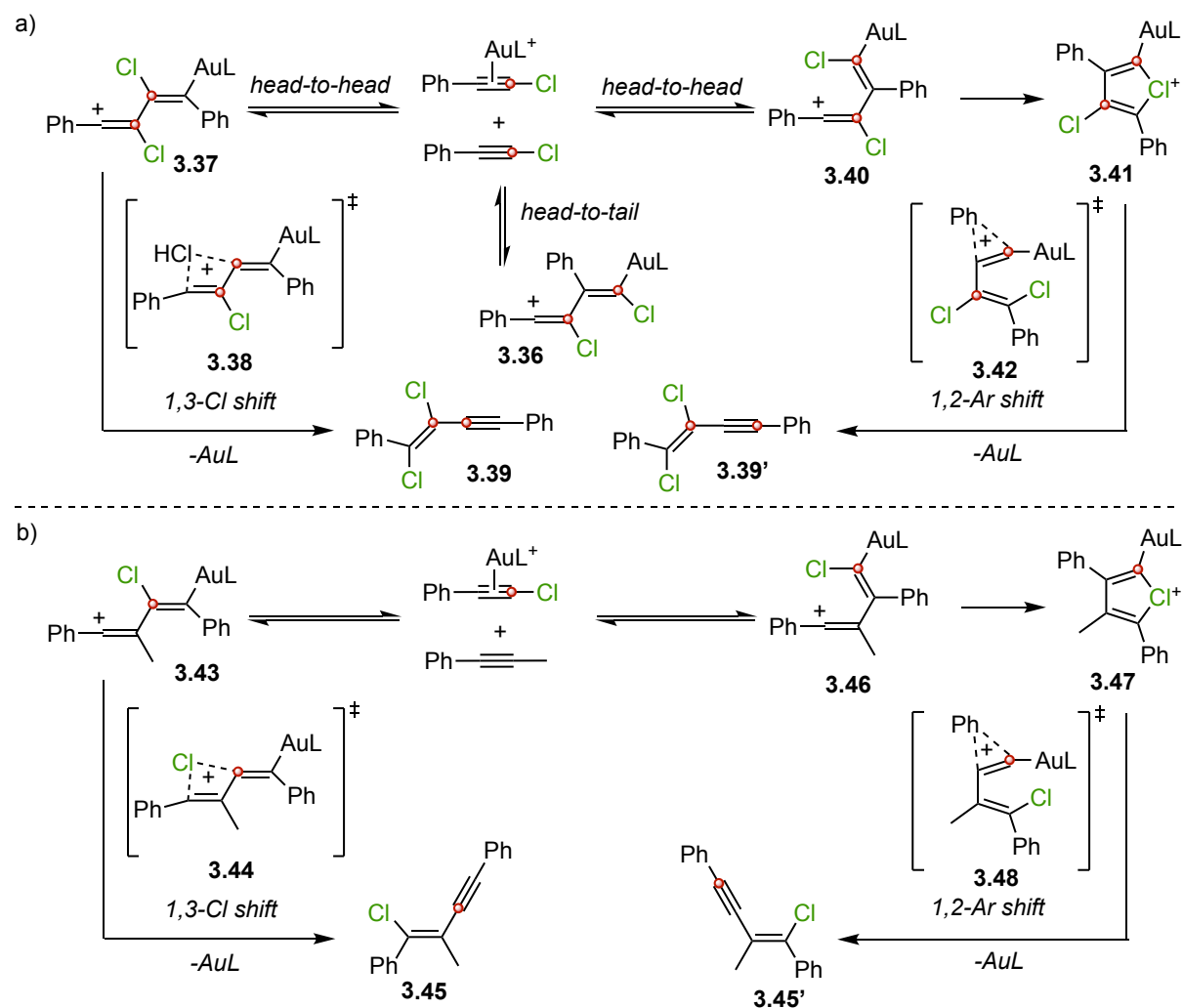
Scheme 3.5. a) Gold(I)-catalyzed [2+2] cycloadditions of chloroalkynes with 1,2-disubstituted alkenes. b) Gold(I)-catalyzed chloroalkynylation of 1,1-disubstituted alkenes. The carbon highlighted in red represents ¹³C-labeling.

A similar mechanism was postulated for the head-to-head dimerization of chloroalkynes (Scheme 3.6a).²² Given the stronger nature of the C–Cl bond compared to C–I, no gold(I) acetylide species is formed (Scheme 3.3c), instead, the reaction commences with the direct attack of one chloroalkyne on another activated by π -coordination with gold(I). In accordance with experimental results, the head-to-

²¹ Kreuzahler, M.; Haberhauer, G. Gold(I)-Catalyzed Chloroalkynylation of 1,1-Disubstituted Alkenes via 1,3-Chlorine Shift: A Combined Experimental and Theoretical Study. *J. Org. Chem.* **2019**, *84*, 8210–8224.

²² Kreuzahler, M.; Daniels, A.; Wölper, C.; Haberhauer, G. 1,3-Chlorine Shift to a Vinyl Cation: A Combined Experimental and Theoretical Investigation of the *E*-Selective Gold(I)-Catalyzed Dimerization of Chloroacetylenes. *J. Am. Chem. Soc.* **2019**, *141*, 1337–1348.

head pathways were corroborated, by DFT calculations, to be energetically favored compared to the head-to-tail one (**3.36**). Also in this case, an irreversible 1,3-chloride shift in the vinyl cation **3.37** or a cyclic chloronium intermediate **3.41** followed by 1,2-Ar shift **3.42** mediate the formation of the products **3.39** and **3.39'** which always differ only in the position of the carbon labeled in red (Scheme 3.6a). Finally, the haloalkynylation of aryl alkynes has also been reported. As for the previous cases, the presence of two possible pathways was demonstrated to bring to products **3.45** and **3.45'**, also here distinguishable only by ^{13}C labeling (Scheme 3.6b).^{2b}

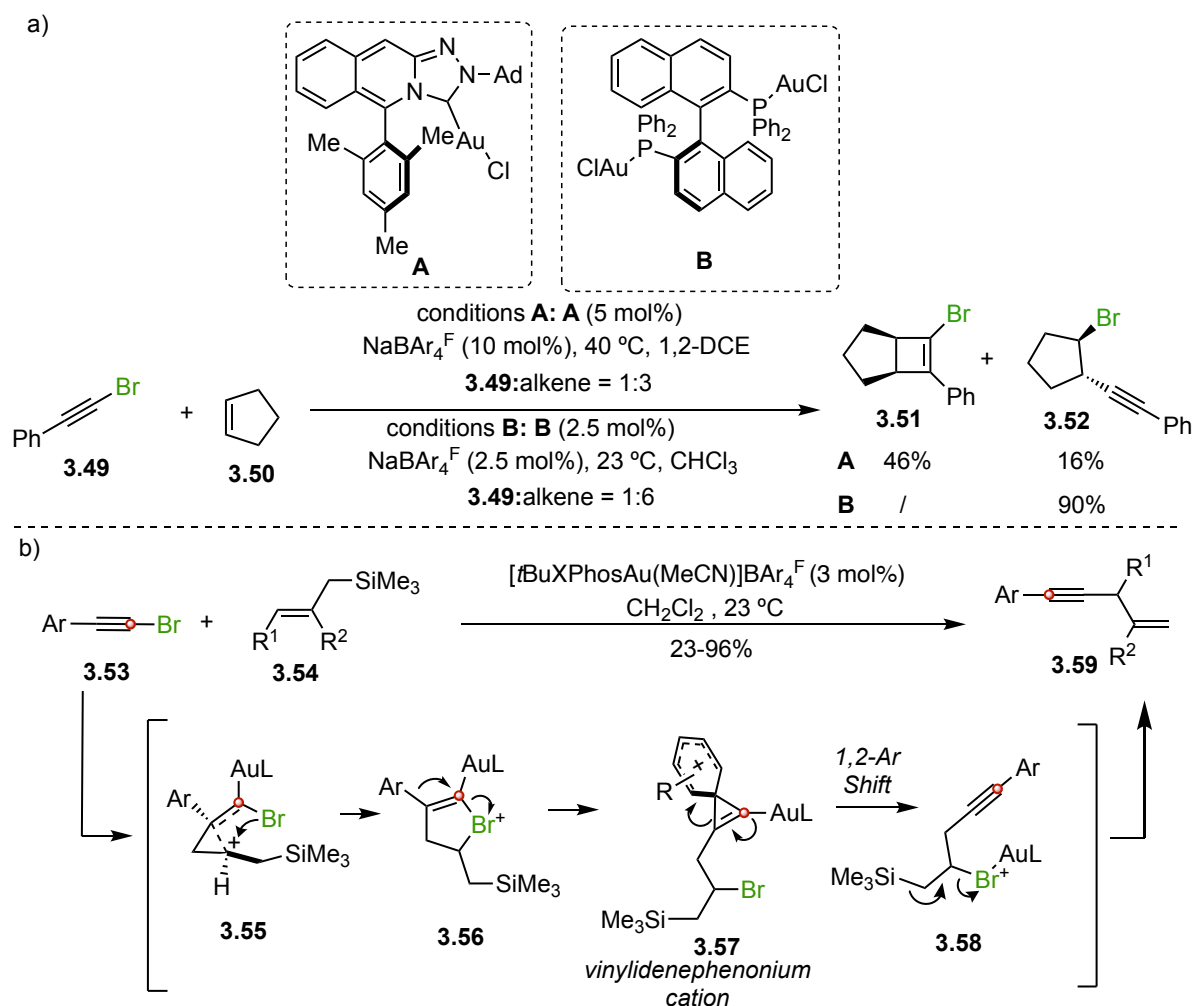


Scheme 3.6. a) Gold(I)-catalyzed dimerization of chloroalkynes. b) Gold(I)-catalyzed chloroalkynylation of aryl alkynes. The carbons highlighted in red represents ^{13}C -labeling.

In terms of reactivity of carbon nucleophiles with bromoalkynes,²³ cyclic and terminal alkenes were described by Fernández and Lassaletta to react with bromoalkynes **3.49** (Scheme 3.7a) in the presence

²³ For further literature on the topic which was not discussed in the present manuscript: a) Bellavance, G.; Barriault, L., Total Syntheses of Hyperforin and Papuaforins A–C, and Formal Synthesis of Nemorosone through a Gold(I)-Catalyzed Carbocyclization, *Angew. Chem. Int. Ed.* **2014**, *53*, 6701–6704, *Angew. Chem.* **2014**, *126*, 6819–6822. b) Qin, X.-Y.; Meng, F.-T.; Wang, M.; Tu, S.-J.; Hao, W.-J.; Wang, J.; Jiang, B., Gold-Catalyzed Skeletal Rearrangement of Alkenes: Regioselective Synthesis of Skeletally Diverse Tricyclic Heterocycles and Mechanistic Investigations, *ACS Catal.* **2021**, *11*, 6951–6959. c) Wei, C.; Wu, J.; Zhang, L.; Xia, Z., Gold(I)-Catalyzed Selective Hydroarylation of Indoles with Haloalkynes,

of cationic gold catalysts, yielding [2+2] cycloaddition products **3.51** or haloalkynylation **3.52** depending on the reaction conditions.²⁴ In both cases, the reaction mechanisms correlate to the ones described for chloroalkynes (see Scheme 3.5a for the [2+2] cycloaddition^{8,17} and Scheme 3.5b for the haloalkynylation^{2b,c,21}). The haloalkynylation was demonstrated to also happen through cyclic halonium formation via ¹³C-labeling studies performed by our group when describing the cross-coupling between bromoalkynes **3.53** and allylsilanes **3.54** (Scheme 3.7b).^{2a}

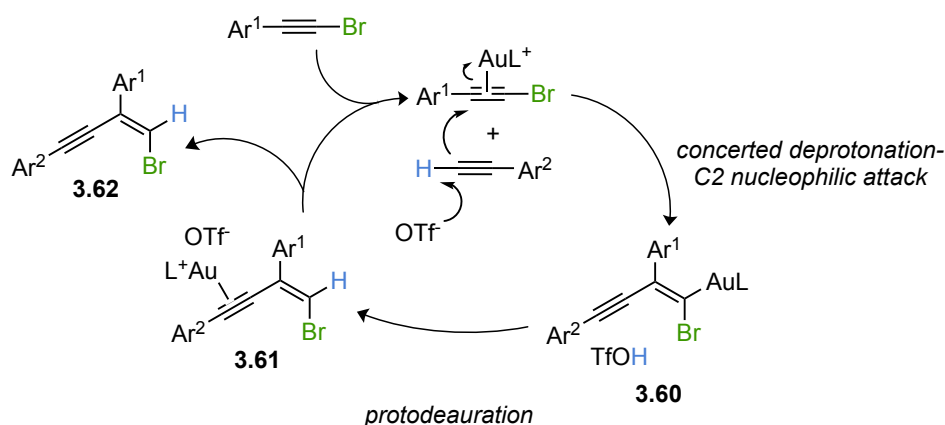


Scheme 3.7. a) Gold(I)-catalyzed [2+2] cycloaddition vs bromoalkynylation of alkenes. b) Gold(I)-catalyzed cross-coupling of bromoalkynes with allylsilanes. The carbon highlighted in red represents ¹³C-labeling. In the course of this study, 1,4-enynes **3.59** could be synthesized through two different mechanisms which see the involvement of gold vinylidenes in the case of alkyl-alkynes (as well as for chloroalkynes: intermediate **3.34** in Scheme 3.5b) and vinylidene phenonium cations **3.57** in case of aryl-alkynes (Scheme 3.7b).

Org. Lett. **2022**, *24*, 4689–4693. d) Miguélez, R.; Semleit, N.; Rodríguez-Arias, C.; Mykhailiuk, P.; González, J. M.; Haberhauer, G.; Barrio, P., C–H Activation of Unbiased C(Sp³)–H Bonds: Gold(I)-Catalyzed Cycloisomerization of 1-Bromoalkynes, *Angew. Chem. Int. Ed.* **2023**, *62*, e202305296, *Angew. Chem.* **2023**, *135*, e202305296.

²⁴ García-Fernández, P. D.; Izquierdo, C.; Iglesias-Sigüenza, J.; Díez, E.; Fernández, R.; Lassaletta, J. M., Au^I-Catalyzed Haloalkynylation of Alkenes, *Chem. Eur. J.* **2020**, *26*, 629–633.

Complementing the work of Haberhauer on chloroalkynes^{2b,c,21,22} and ours on bromoalkynes,^{2a} Lassaletta also studied thoroughly the gold(I)-catalyzed reactions of terminal alkynes and aromatic haloalkynes^{2d} which can be shifted towards the bromoalkynylation of terminal alkynes when employing SIPrAuCl/NaBARF₄ (mechanism equivalent to the chloroalkynylation shown in Scheme 3.6b^{2b}) vs the unprecedented hydroalkynylation of haloalkynes, using a SIPrAuCl/AgOTf catalytic system (Scheme 3.8). In this latter case, the triflate counteranion serves as an ideal proton shuttle, sufficiently basic to facilitate a concerted C–C bond formation with simultaneous deprotonation of the terminal alkyne which brings to species **3.60**. The latter then undergoes protodeauration and gold decoordination to deliver 1,3-enynes **3.62**.



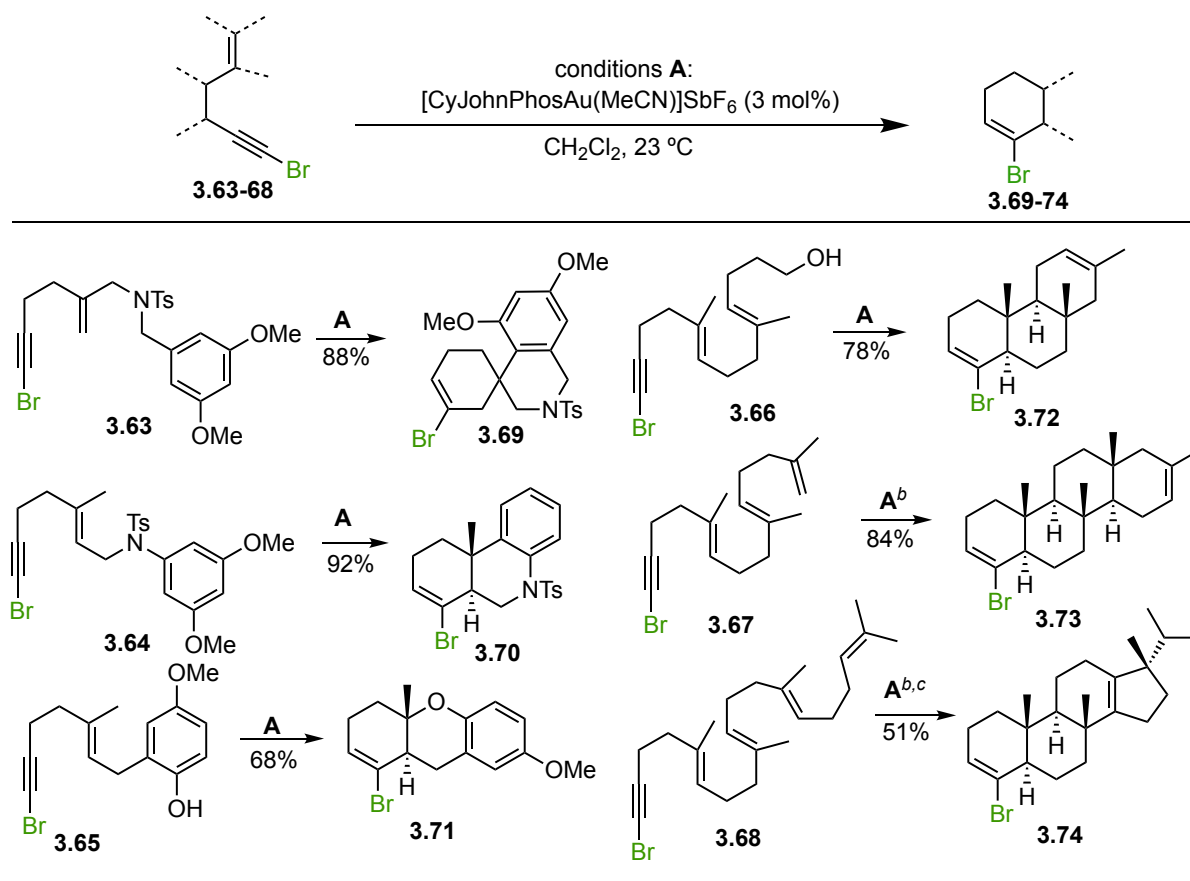
Scheme 3.8. Gold(I)-catalyzed hydroalkynylation of haloalkynes.

When it comes to bromoenynes,²⁵ our group disclosed that 1-bromo-1,5-enyne derivatives **3.63-68** could undergo cascade cyclizations, yielding complex polycyclic structures **3.69-74** (Table 3.1).²⁶ Notably, tetracyclic compound **3.74** could be formed by a cyclization-Wagner–Meerwein 1,2-H and Me migrations, followed by proton elimination and protonolysis of the alkenylgold(I) bond starting from **3.68**.

Table 3.1. Gold(I)-catalyzed polyenyne cyclizations: selected examples starting from 1-bromoalkynes.^a

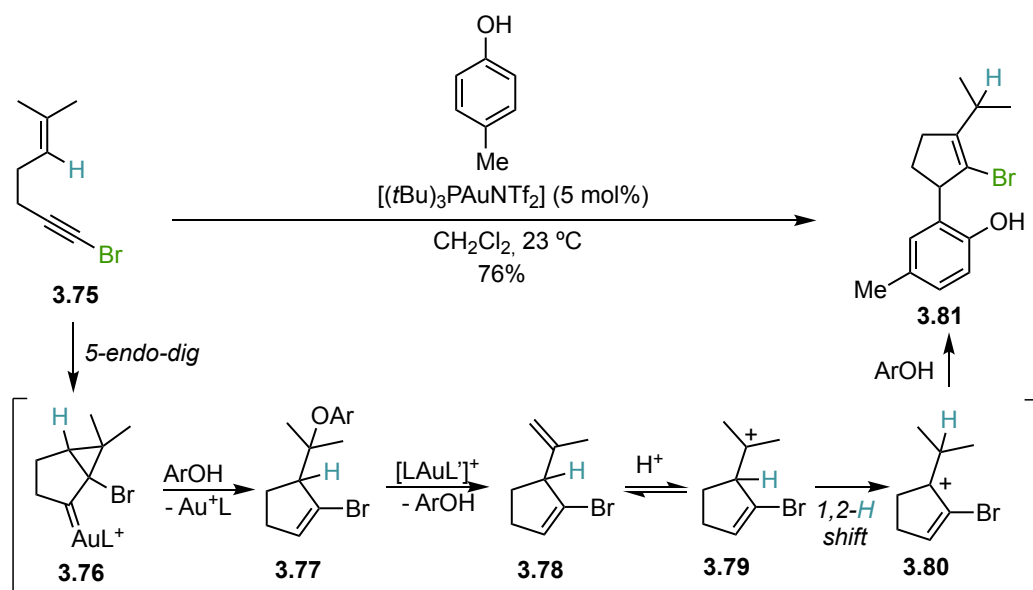
²⁵ For further literature on the topic which was not discussed in the present manuscript: a) Lim, C.; Kang, J.-E.; Lee, J.-E.; Shin, S., Gold-Catalyzed Tandem C–C and C–O Bond Formation: A Highly Diastereoselective Formation of Cyclohex-4-Ene-1,2-Diol Derivatives, *Org. Lett.* **2007**, *9*, 3539–3542. b) Matsuda, T.; Kadowaki, S.; Yamaguchi, Y.; Murakami, M., Gold-Catalysed Intramolecular Trans-Allylsilylation of Alkynes Forming 3-Allyl-1-Silaindenes, *Chem. Commun.* **2008**, No. 24, 2744.

²⁶ Rong, Z.; Echavarren, A. M. Broad Scope Gold(I)-Catalysed Polyenyne Cyclisations for the Formation of up to Four Carbon–Carbon Bonds. *Org. Biomol. Chem.* **2017**, *15*, 2163–2167.



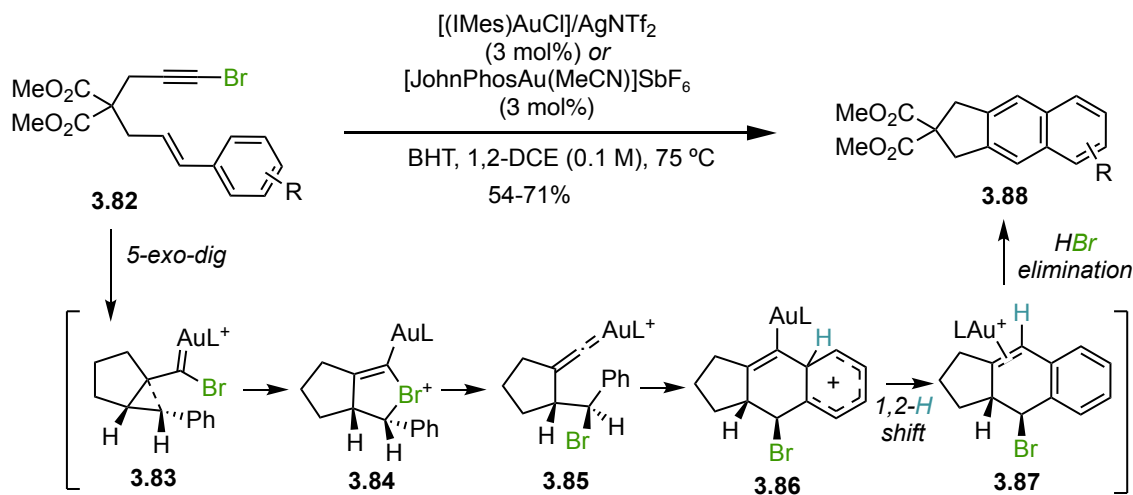
Magauer's group achieved the synthesis of (2-bromocyclopent-2-en-1-yl)phenols **3.81** through gold(I)-catalyzed cycloisomerization of 1-bromo-1,5-enynes **3.75** (Scheme 3.9).²⁷ Through deuterium labeling studies and trapping of intermediates at low temperature, the authors proposed that after the *5-endo-dig* cyclization and nucleophilic attack of the *p*-cresol's oxygen to the newly formed cyclopropyl-gold(I) carbene **3.76**, protodeauration affords product **3.77** (which could only be isolated when working at -30 °C). Then, a gold-promoted *p*-cresol elimination brings to the formation of **3.78**, which in the slightly acidic medium of the reaction, is in equilibrium with cationic species **3.79**. From this intermediate, an irreversible 1,2-H shift, possibly driven by the formation of a tertiary carbocation and its further stabilization by interaction with the bromine atom, occurs to form **3.80**. To conclude, the attack of the aryl group of the phenol to the allylic system affords **3.81** as only product.

²⁷ Speck, K.; Karaghiosoff, K.; Magauer, T. Sequential O–H/C–H Bond Insertion of Phenols Initiated by the Gold(I)-Catalyzed Cyclization of 1-Bromo-1,5-Enynes. *Org. Lett.* **2015**, *17*, 1982–1985.



Scheme 3.9. Gold(I)-catalyzed cyclization of 1-bromo-5-enynes followed by a 1,2-H shift-nucleophilic attack sequence.

Finally, our group described the gold(I)-catalyzed formal [4+2] cycloaddition of 1-bromo-1,6-enynes (Scheme 3.10).^{2a} Also in this case, the transformation is mediated by the cyclic bromonium intermediate **3.84** which evolves in gold vinylidene **3.85**. Subsequent hydroarylation to afford **3.86**, followed by formal 1,2-H shift to **3.87** and final HBr elimination, yield tricyclic 2,3-dihydro-1*H*-cyclopenta[*b*]naphthalenes **3.88**.

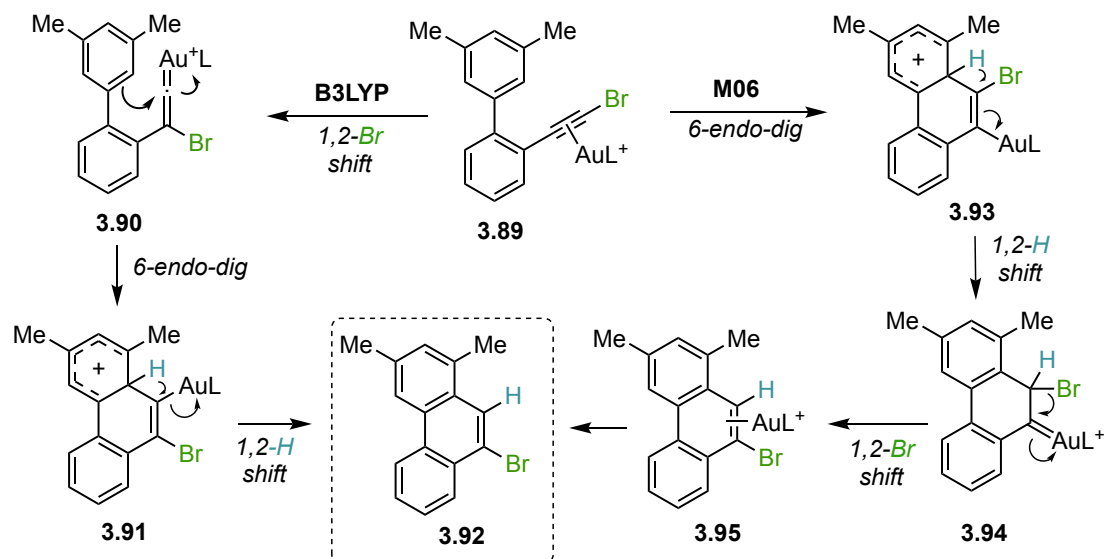


Scheme 3.10. Gold(I)-catalyzed cyclization of 1-bromo-1,6-enynes.

1,2-H Shift in Gold(I)-Catalysis

As just introduced above in Schemes 3.9-3.10, within the various processes involved in gold(I)-catalyzed cyclizations, 1,2-hydride shifts (1,2-H) have been often proposed to explain product formation.^{2a,27} When studying computationally the hydroarylation of *ortho*-alkynylbiaryls originally described by Fürstner (Scheme 3.3a)¹², two different pathways were then proposed depending on the

DFT functional used (Scheme 3.11). When using B3LYP, Soriano and Marco-Contelles reported a first 1,2-halogen migration followed by the formation of gold(I) vinylidene **3.90**, which would then undergo a *6-endo-dig* step yielding **3.91**. This intermediate would eventually evolve to product **3.92** through a formal 1,2-H shift.²⁸ However, subsequent calculations performed by the group of Xia employing the M06 functional indicated a different preferred pathway, wherein *6-endo-dig* cyclization precedes, leading to the formation of **3.93**, followed by a 1,2-H shift resulting in carbene **3.94**, and ultimately, a 1,2-Br shift and demetallation affords product **3.92**.²⁹



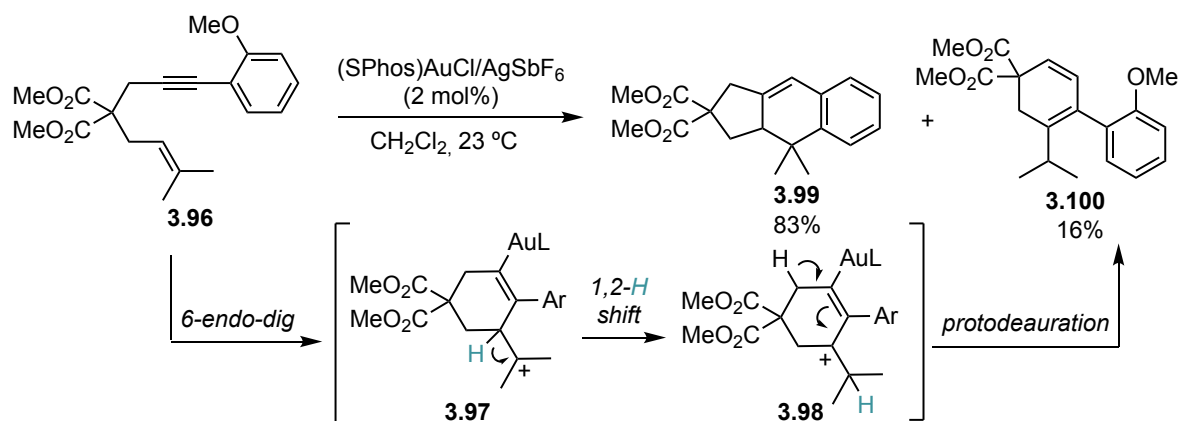
Scheme 3.11. 1,2-H Shifts mediating two different mechanisms for the gold(I)-catalyzed hydroarylation of *ortho*-alkynylbiaryls.

When exploring the scope of the first gold(I)-catalyzed intramolecular [4+2] cycloaddition of arylalkynes our group found that, for some substrates, together with the formation of tricyclic **3.99** occurring via a *5-exo-dig* cyclization followed by a Friedel-Crafts-type reaction (as mentioned in the **General Introduction**), product **3.100** was also observed (Scheme 3.12)³⁰. The latter has to originate from a *6-endo-dig* cyclization to form **3.97** which would then undergo 1,2-H shift to produce the more stable **3.98**, and finally, protodeauration.

²⁸ Soriano, E.; Marco-Contelles, J. Mechanisms of the Transition Metal-Mediated Hydroarylation of Alkynes and Allenes. *Organometallics* **2006**, *25*, 4542–4553.

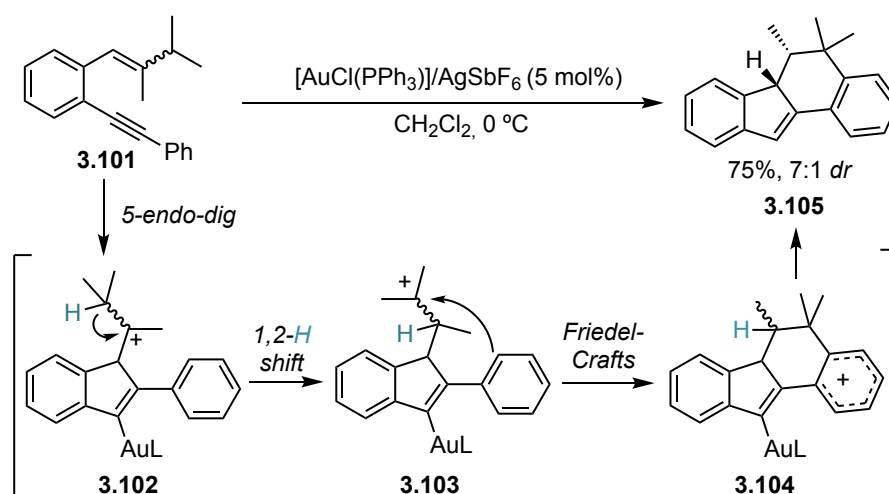
²⁹ Huang, G.; Cheng, B.; Xu, L.; Li, Y.; Xia, Y., Mechanism of the Transition-Metal-Catalyzed Hydroarylation of Bromo-Alkynes Revisited: Hydrogen versus Bromine Migration, *Chem. Eur. J.* **2012**, *18*, 5401–5415.

³⁰ Nieto-Oberhuber, C.; Pérez-Galán, P.; Herrero-Gómez, E.; Lauterbach, T.; Rodríguez, C.; López, S.; Bour, C.; Rosellón, A.; Cárdenas, D. J.; Echavarren, A. M. Gold(I)-Catalyzed Intramolecular [4+2] Cycloadditions of Arylalkynes or 1,3-Enynes with Alkenes: Scope and Mechanism. *J. Am. Chem. Soc.* **2008**, *130*, 269–279.



Scheme 3.12. Experimental evidence for a 1,2-H shift occurring after 6-endo-dig cyclization of **3.96**.

Sanz and co-workers also suggested the involvement of 1,2-H shift in the gold(I)-catalyzed formation of dihydrobenzo[*a*]fluorenes (Scheme 3.13).³¹ After an initial 5-endo-dig cyclization of 1-phenyl-5-enynes **3.101** to form cationic **3.102**, a 1,2-hydride shift followed by Friedel-Crafts-type reaction brings to Wheland intermediate **3.104** which eventually protodemetalates to tetracyclic **3.105**.



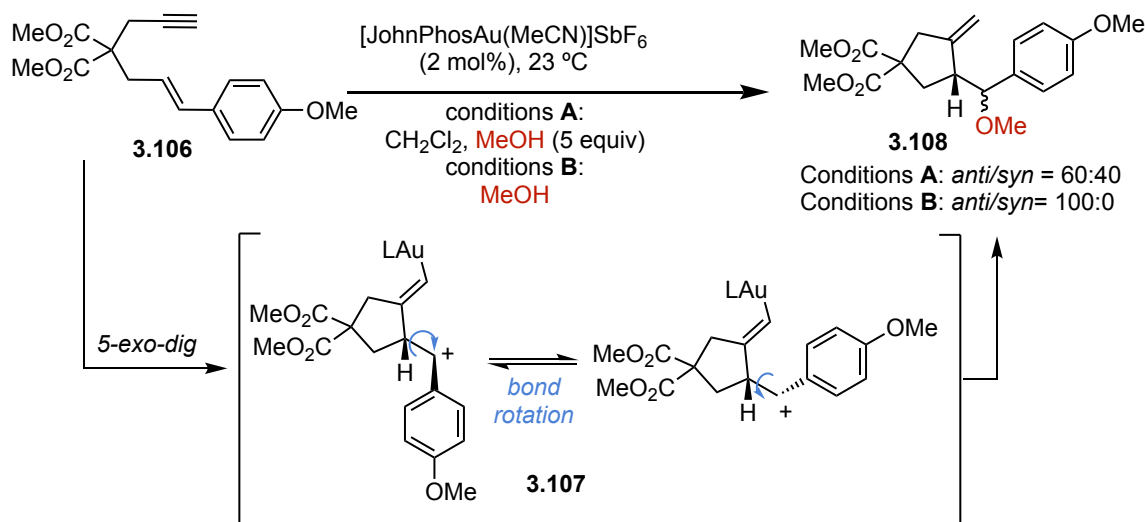
Scheme 3.13. Gold(I)-catalyzed synthesis of dihydrobenzo[*a*]fluorenes via 5-endo-dig-1,2-H shift sequence.

Enantioselective Alkoxy cyclizations of Enynes

As mentioned in the general introduction, the alkoxy cyclization of enynes envisions a metal-catalyzed cyclization step which generates a cationic species that will then be subjected to intermolecular nucleophilic attack from an alcohol. In 2008, our group observed varying stereospecificity in racemic 1,6-enyne alkoxy cyclizations when changing the quantity of alcohol in the reaction mixture (Scheme

³¹ a) García-García, P.; Rashid, M. A.; Sanjuán, A. M.; Fernández-Rodríguez, M. A.; Sanz, R., Straightforward Synthesis of Dihydrobenzo[*a*]Fluorenes through Au(I)-Catalyzed Formal [3 + 3] Cycloadditions, *Org. Lett.* **2012**, *14*, 4778–4781. b) Sanjuán, A. M.; Rashid, M. A.; García-García, P.; Martínez-Cuezva, A.; Fernández-Rodríguez, M. A.; Rodríguez, F.; Sanz, R., Gold(I)-Catalyzed Cycloisomerizations and Alkoxy cyclizations of Ortho-(Alkynyl)Styrenes, *Chem. Eur. J.* **2015**, *21*, 3042–3052.

3.14).³² When using only 5 equiv of MeOH (conditions **A**) low stereospecificity was observed, while when using the nucleophile as a solvent (conditions **B**) the product preserved the *E-anti* stereospecificity which usually characterizes these transformations (**General Introduction**, Scheme 4).³³ This phenomenon was attributed to the bond rotation of the carbocationic intermediate **3.107** formed after the *5-exo-dig* cyclization of 1,6-enynes of the type **3.106**, which, at high concentrations of nucleophile, is readily trapped before this rotation can occur. This behavior was only observed in enynes presenting electron-donating groups on the aryls attached to the alkene which could stabilize the open form of the carbocationic intermediate of the type **3.107** over the closed cyclopropyl gold(I) carbene ones (not shown), for which the barriers for bond rotation were calculated to be too high.³⁴



Scheme 3.14. Loss of stereospecificity given by bond rotation on cationic intermediate **3.107** in gold(I)-catalyzed alkoxylation of 1,6-enynes.

The first enantioselective alkoxylation of 1,6-enynes was reported by Genêt's group (Scheme 3.15a) using a Pt(II) catalyst,³⁵ and our group achieved a similar outcome with gold(I) shortly after (Scheme 3.15b).³⁶ At that time, no attention was devoted to the effect that the quantity of alcohol (or water) could have, and the reactions were mostly run in the pure nucleophile (like in the case of **3.111**) or in mixtures containing a substantial amount of it (like in the case of **3.109**).

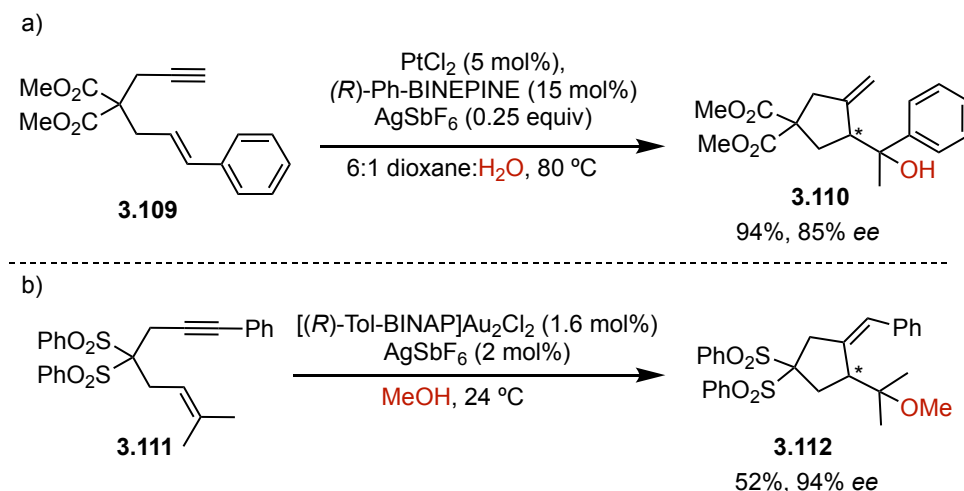
³² Jiménez-Núñez, E.; Claverie, C. K.; Bour, C.; Cárdenas, D. J.; Echavarren, A. M., Cis-Selective Single-Cleavage Skeletal Rearrangement of 1,6-Enynes Reveals the Multifaceted Character of the Intermediates in Metal-Catalyzed Cycloisomerizations, *Angew. Chem. Int. Ed.* **2008**, *47*, 7892–7895, *Angew. Chem.* **2008**, *120*, 8010–8013.

³³ a) Nieto-Oberhuber, C.; Muñoz, M. P.; Buñuel, E.; Nevado, C.; Cárdenas, D. J.; Echavarren, A. M., Cationic Gold(I) Complexes: Highly Alkynophilic Catalysts for the Exo- and Endo-Cyclization of Enynes, *Angew. Chem. Int. Ed.* **2004**, *43*, 2402–2406, *Angew. Chem.* **2004**, *116*, 2456–2460. b) Nieto-Oberhuber, C.; Muñoz, M. P.; López, S.; Jiménez-Núñez, E.; Nevado, C.; Herrero-Gómez, E.; Raducan, M.; Echavarren, A. M., Gold(I)-Catalyzed Cyclizations of 1,6-Enynes: Alkoxylation and Exo/Endo Skeletal Rearrangements, *Chem. Eur. J.* **2006**, *12*, 1677–1693.

³⁴ For a recent in-depth mechanistic study on the topic: García-Padilla, E.; Maseras, F.; Echavarren, A. M. Gold(I)-Catalyzed 1,6-Enyne Single-Cleavage Rearrangements: The Complete Picture. *ACS Org. Inorg. Au* **2023**, *3*, 312–320.

³⁵ Charruault, L.; Michelet, V.; Taras, R.; Gladiali, S.; Genêt, J.-P. Functionalized Carbo- and Heterocycles via Pt-Catalyzed Asymmetric Alkoxylation of 1,6-Enynes. *Chem. Commun.* **2004**, No. 7, 850–851.

³⁶ Muñoz, M. P.; Adrio, J.; Carretero, J. C.; Echavarren, A. M. Ligand Effects in Gold- and Platinum-Catalyzed Cyclization of Enynes: Chiral Gold Complexes for Enantioselective Alkoxylation. *Organometallics* **2005**, *24*, 1293–1300.

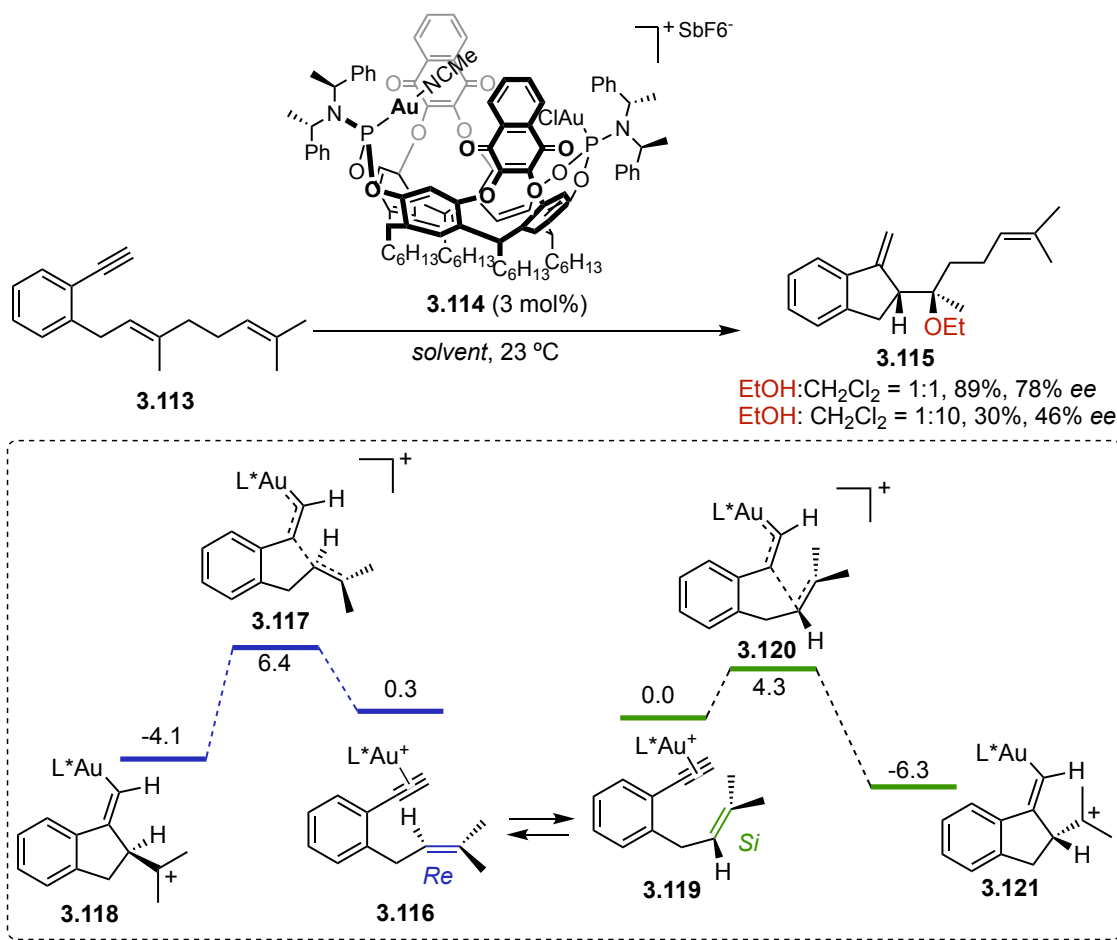


Scheme 3.15. First a) platinum(II) and b) gold(I)-catalyzed enantioselective alkoxycyclizations.

More recently, our group has developed chiral gold(I)-cavitand complexes of the type **3.114** that mediate the alkoxymercuration of aryl-tethered terminal enynes **3.113** (Scheme 3.16).³⁷ When having a 1:1 ratio of EtOH:CH₂Cl₂ the product **3.115** was isolated in 89% yield and 78% *ee*, while when decreasing the nucleophile amount to a 1:10 ratio, the product was obtained with reduced yield (30%, probably due to the cavity effect: the nucleophile can't easily reach the substrate) and a lower 46% *ee*. The enantiodetermining step was calculated to be the *5-exo-dig* cyclization from the *Si* face of the alkene (**3.119-121**), which is energetically favored over the competing *Re* face cyclization (**3.116-3.118**). The subsequent nucleophilic attack step should not affect the newly formed chiral center in terms of *ee*. Therefore, it is reasonable to think that in this case, the different observed *ee* might be connected to the different polarity of the solvent when changing the alcohol:CH₂Cl₂ ratio, which can affect the enantiodetermining cyclization step *before* the nucleophilic attack happens. The DFT calculations brought on in the context of this work, as well as in other examples in literature,³⁸ stop at the cyclization step, and the nucleophilic attack was not modeled.

³⁷ Martín-Torres, I.; Ogalla, G.; Yang, J.-M.; Rinaldi, A.; Echavarren, A. M., Enantioselective Alkoxymercuration of 1,6-Enynes with Gold(I)-Cavitands: Total Synthesis of Mafaicheenamine C, *Angew. Chem. Int. Ed.* **2021**, *60*, 9339–9344, *Angew. Chem.* **2021**, *133*, 9425–9430.

³⁸ a) Virumbrales, C.; Suárez-Pantiga, S.; Marín-Luna, M.; Silva López, C.; Sanz, R., Unlocking the 5-Exo Pathway with the AuI-Catalyzed Alkoxymercuration of 1,3-Dien-5-Ynes, *Chem. Eur. J.* **2020**, *26*, 8443–8451. b) Martí, À.; Ogalla, G.; Echavarren, A. M., Hydrogen-Bonded Matched Ion Pair Gold(I) Catalysis, *ACS Catal.* **2023**, *13*, 10217–10223.



Scheme 3.16. Gold(I)-cavitand-catalyzed alkoxy cyclization of aryl-tethered 1-*H*-1,6-enynes.

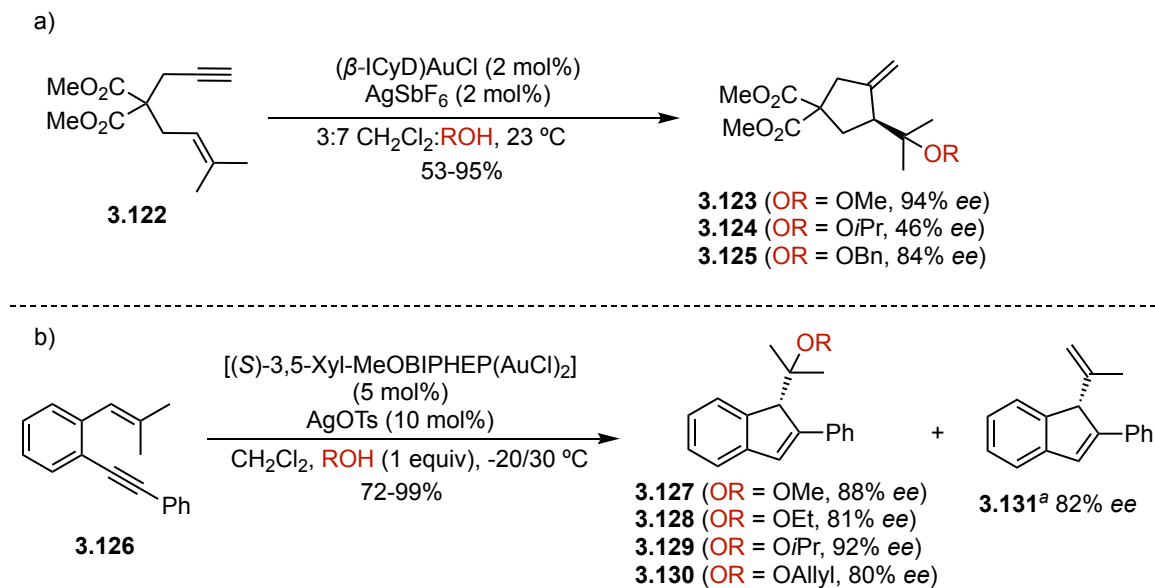
Apart from the amount, also the nature of the nucleophile was observed to influence the selectivity of these transformations. Enyne **3.122** was described to cyclize using cyclodextrin complex (β -ICyD)AuCl in the presence of different alcohols, always in a 7:3 ratio with CH_2Cl_2 (Scheme 3.17a).³⁹ It is possible to see here how the enantiomeric excess varies from a 46% *ee* value when using isopropanol (**3.124**) to 84% *ee* with benzyl alcohol (**3.125**), finally reaching an excellent 94% *ee* with methanol (**3.123**). Also in this case, these different values might be attributed, as mentioned above, to the different polarity of the selected alcohols, given their use as co-solvents.

However, Sanz and co-workers reported that in the context of the 5-*endo-dig* cyclizations of 1,5-enyne **3.126**, maintaining the amount of alcohol to 1 equiv in a 0.25 M solution of CH_2Cl_2 , the *ee* of the alkoxy cyclized product varied from 80% (**3.130**, ROH = allyl alcohol) to 92% (**3.129**, ROH = isopropanol) (Scheme 3.17b).⁴⁰

³⁹ Tugny, C.; Del Rio, N.; Koohgard, M.; Vanthuynne, N.; Lesage, D.; Bijouard, K.; Zhang, P.; Mejjide Suárez, J.; Roland, S.; Derat, E.; Bistri-Aslanoff, O.; Sollogoub, M.; Fensterbank, L.; Mouriès-Mansuy, V. β -Cyclodextrin–NHC–Gold(I) Complex (β -ICyD)AuCl: A Chiral Nanoreactor for Enantioselective and Substrate-Selective Alkoxy cyclization Reactions. *ACS Catal.* **2020**, *10*, 5964–5972.

⁴⁰ Martínez, A.; García-García, P.; Fernández-Rodríguez, M. A.; Rodríguez, F.; Sanz, R., Gold(I)-Catalyzed Enantioselective Synthesis of Functionalized Indenes, *Angew. Chem. Int. Ed.* **2010**, *49*, 4633–4637, *Angew. Chem.* **2010**, *122*, 4737–4741.

In the absence of an alcohol partner, the cycloisomerization product **3.131** was isolated with a 82% *ee*, comparable to the one obtained for the ethoxycyclization product **3.128** (81% *ee*).



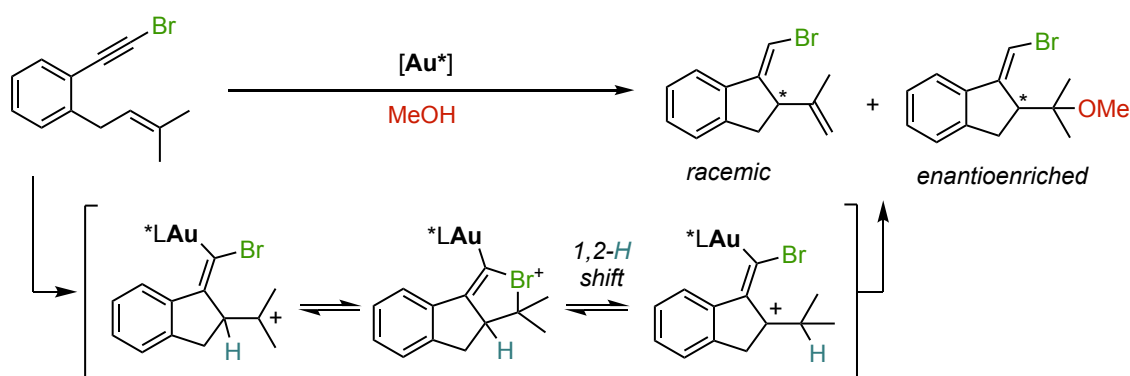
Scheme 3.17. a) Alcohol effect in gold(I)-cyclodextrin-catalyzed alkoxy cyclization of malonate-tethered 1-H-1,6-enynes. b) Alcohol effect in gold(I)-catalyzed alkoxy cyclization of aryl-tethered 1-phenyl-1,5-enynes.

^a Reaction performed in the absence of ROH.

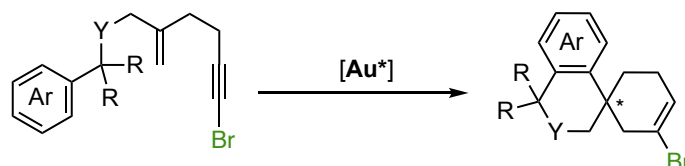
Objectives

Given the limited number of examples of enantioselective gold(I)-catalyzed transformations involving halogen-substituted alkynes, our objective is to develop enantioselective alkoxy cyclizations of 1-*Br*-1,6-enynes, precursors of the enynamide substrates described in **Chapter I**. To mediate the transformation, we envision the use of modified JohnPhos ligands with a distal C₂-2,5-diarylpyrrolidine developed in our group.⁴¹

Through the study of a racemization pathway operated by an unprecedented reversible 1,2-H shift, we aim to better understand the mechanism of gold(I)-catalyzed alkoxy cyclizations experimentally and computationally.⁴²



In the context of the same work, the enantioselective cascade cyclization of 1-bromo-5-enynes shown below was also explored⁴³, but it will not be discussed in the present manuscript.



⁴¹ a) Zuccarello, G.; Mayans, J. G.; Escofet, I.; Scharnagel, D.; Kirillova, M. S.; Pérez-Jimeno, A. H.; Calleja, P.; Boothe, J. R.; Echavarren, A. M., Enantioselective Folding of Enynes by Gold(I) Catalysts with a Remote C₂-Chiral Element, *J. Am. Chem. Soc.* **2019**, *141*, 11858–11863. b) Zuccarello, G.; Nannini, L. J.; Arroyo-Bondía, A.; Fincias, N.; Arranz, I.; Pérez-Jimeno, A. H.; Peeters, M.; Martín-Torres, I.; Sadurní, A.; García-Vázquez, V.; Wang, Y.; Kirillova, M. S.; Montesinos-Magraner, M.; Caniparoli, U.; Núñez, G. D.; Maseras, F.; Besora, M.; Escofet, I.; Echavarren, A. M., Enantioselective Catalysis with Pyrrolidinyl Gold(I) Complexes: DFT and NEST Analysis of the Chiral Binding Pocket, *JACS Au* **2023**, *3*, 1742–1754.

⁴² Work performed in collaboration with Eduardo García-Padilla.

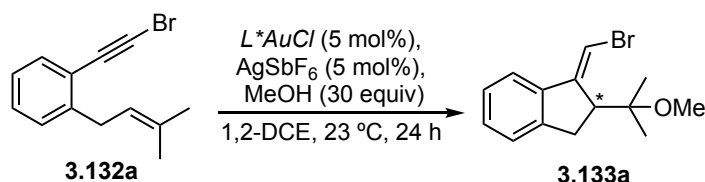
⁴³ Work performed by Giuseppe Zuccarello and Guilong Tian.

Results and Discussion

Reaction Optimization, Scope and Product Diversification

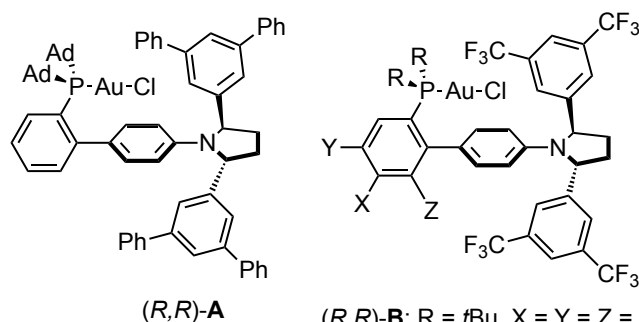
After having developed the diastereoselective alkoxy cyclizations of ennamides as described in **Chapter I**, we decided to explore the reactivity of their *Br*-substituted precursors under enantioselective catalysis. We selected 1-bromo-1,6-enyne **3.132a** as a model substrate for our study⁴⁴ (compound **1.123** in **Chapter I**). First, a catalyst screening at room temperature was performed over 24 h using AgSbF₆ as a chloride scavenger and 30 equiv of MeOH. We envisioned that the diarylpyrrolidine catalysts (*R,R*)-**A-G** synthesized in our group, which performed in an excellent manner for enantioselective alkoxy cyclizations of 1-aryl-6-enynes,^{41a} could also perform well with these substrates (Table 3.2).

Table 3.2. Catalyst screening for the 1-bromo-1,6-enyne alkoxy cyclization.



Entry	L*AuCl	Yield (%) ^a	<i>er</i>
1	(<i>R,R</i>)- A	80	81:19
2	(<i>R,R</i>)- B	74	63:33
3	(<i>R,R</i>)- C	59	72:28
4	(<i>R,R</i>)- D	62	74:26
5	(<i>R,R</i>)- E	78	71:29
6	(<i>R,R</i>)- F	81	73:27
7	(<i>R,R</i>)- G	84	74:26
8^b	(<i>R,R</i>)-A	80	81:19

^aIsolated yields. ^bCat. loading = 3 mol%.



(*R,R*)-**A**

(*R,R*)-**B**: R = *t*Bu, X = Y = Z = H

(*R,R*)-**C**: R = Ad, X = Y = Z = H

(*R,R*)-**D**: R = Ad, X = Z = H, Y = CF₃

(*R,R*)-**E**: R = Ad, X = CH₃, Y = Z = H

(*R,R*)-**F**: R = Ad, X = H, Y = Z = F

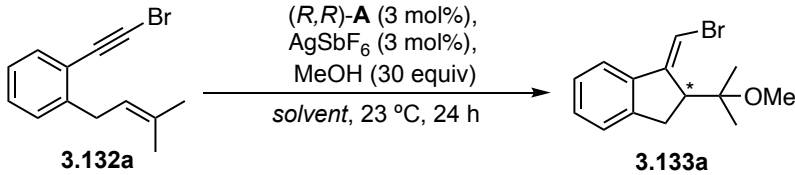
(*R,R*)-**G**: R = Ad, X = H, Y = Z = CF₃

Unexpectedly, given previous results reported in the group obtained with similar substrates, catalyst (*R,R*)-**A** performed the best affording 80% yield and 81:19 *er* (Table 3.2, entry 1), while the more

⁴⁴ All the reported yields in this section are isolated yields after preparative TLC in 2:1 CH₂Cl₂:cyclohexane.

electron-poor (*R,R*)-**B-G** led to lower enantioselectivity (Table 3.2, entries 2-7). When the catalyst loading was then lowered from 5 mol% to 3 mol%, no change in yield or enantioselectivity was observed (Table 3.2, entry 8). We moved then to screening different solvents for the transformation. No big changes were observed when switching from chlorinated solvents to aromatic ones (Table 3.3, entries 1-4). When using THF, the worst yields and *er* were obtained, (Table 3.3, entry 5), while α,α,α -trifluorotoluene afforded the products in 81% yield and 81:19 *er* (Table 3.3, entry 6) and lowering the quantity of methanol to 10 equiv had a slight beneficial effect on the *er* (83:17 *er*, Table 3.3, entry 7).

Table 3.3. Solvent screening for the 1-bromo-1,6-enyne alkoxy cyclization.

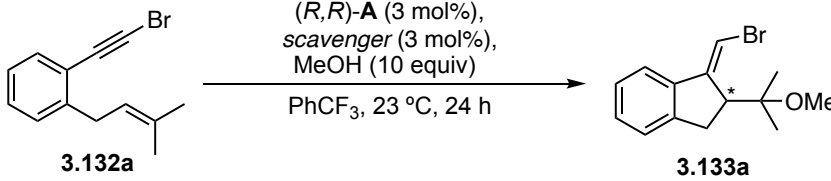


Entry	Solvent	<i>n</i> MeOH	Yield (%) ^a	<i>er</i>
1	DCE	30	80	81:19
2	CH ₂ Cl ₂	30	73	80:20
3	toluene	30	74	78:22
4	C ₆ H ₅ Cl	30	64	80:20
5	THF	30	54	77:23
6	PhCF ₃	30	81	81:19
7	PhCF ₃	10	81	83:17

^aIsolated yields.

Once selected the solvent, we performed a chloride scavenger screening (Table 3.4). Low conversions were observed with NaBAR^F₄, AgBF₄ and AgTFA (14-24% yield, Table 3.4, entries 2,4,5) probably due to solubility issues, even though the enantioselectivities were comparable to those observed with the better performing AgSbF₆ (89% yield, 83:17 *er*, Table 3.4, entry 1) and AgPF₆ (72% yield, 81:19 *er*, Table 3.4, entry 3).

Table 3.4 Screening of chloride scavengers for the 1-bromo-1,6-enyne alkoxy cyclization.

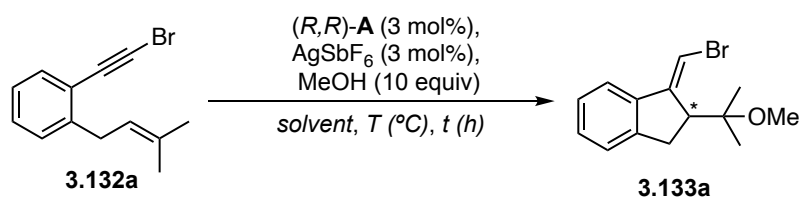


Entry	Scavenger	Yield (%) ^a	<i>er</i>
1	AgSbF ₆	80	83:17
2	NaBAR ^F ₄	24	82:18
3	AgPF ₆	72	81:19
4	AgBF ₄	14	81:19
5	AgTFA	16	79:21

^aIsolated yields.

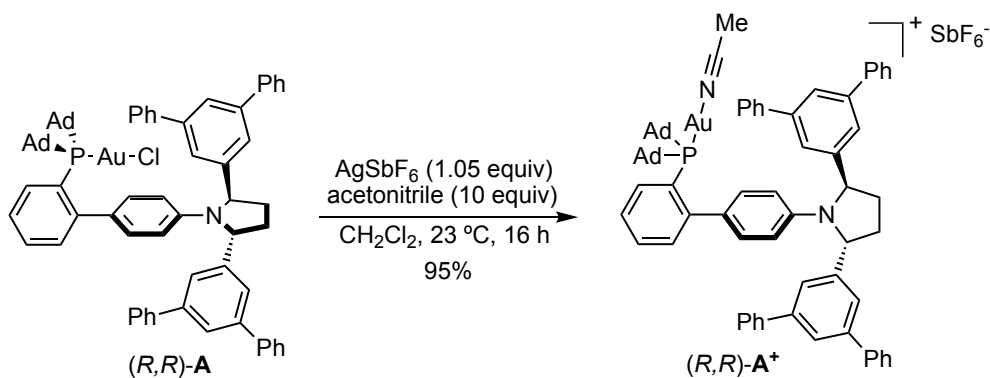
Once assessed that AgSbF_6 was the best option, the temperature was varied (Table 3.5). Given the beneficial effect in terms of enantioselectivity that was observed with this family of catalysts when lowering the temperatures,^{41b} we run the reaction at -20°C to indeed observe an increase in *er* to 85:15 as well as in yield (83%, Table 3.5, entry 1). To lower the temperature further to -40°C , the solvent was changed again to $\text{C}_6\text{H}_5\text{Cl}$, which afforded the product in 72% yield and 88:12 *er* (Table 3.5, entry 2). To get to -60°C , the solvent was switched to CH_2Cl_2 , and, after 4 days, full conversion was observed with 90:10 *er* (Table 3.5, entry 3). We then wanted to test the preactivated complex $(R,R)\text{-A}^+$, synthesized by mixing the chloride precursor $(R,R)\text{-A}$ with AgSbF_6 in CH_2Cl_2 and 10 equiv of acetonitrile overnight and then by filtering the resulting solution in Celite, as shown in Scheme 3.18 below. This would avoid the presence of silver in the reaction mixture and might have beneficial effect on the enantioselectivity. Since no improvement was observed (Table 3.3, entry 4) and given the short-term stability of $(R,R)\text{-A}^+$, we preferred to continue our studies with the stable chloride precursor. A trial in toluene was performed too, but even though the *er* resulted to be higher (92:8 *er*), the product was isolated only in traces after 7 days (Table 3.4, entry 5).

Table 3.5. Temperature screening for the 1-bromo-1,6-enyne alkoxy cyclization.



Entry	Solvent	T (°C)	Time	Yield (%) ^a	<i>er</i>
1	PhCF_3	-20	24 h	83	85:15
2	$\text{C}_6\text{H}_5\text{Cl}$	-40	24 h	72	88:12
3	CH_2Cl_2	-60	4 d	99	90:10
4 ^b	CH_2Cl_2	-60	4 d	99	90:10
5	toluene	-60	7 d	3	92:8
6	CH_2Cl_2	-80	14 d	43	93:7

^aIsolated yields. ^b Preactivated $(R,R)\text{-A}^+$ was used instead of $(R,R)\text{-A}$.



Scheme 3.18. Synthesis of preactivated complex $(R,R)\text{-A}^+$

Reaction in CH₂Cl₂ at -80 °C resulted in an increased 93:7 *er* but with an isolated yield of just 43% after 14 days (Table 3.4, entry 6), so we decided to keep the temperature no lower than -60° C when exploring the substrate scope.

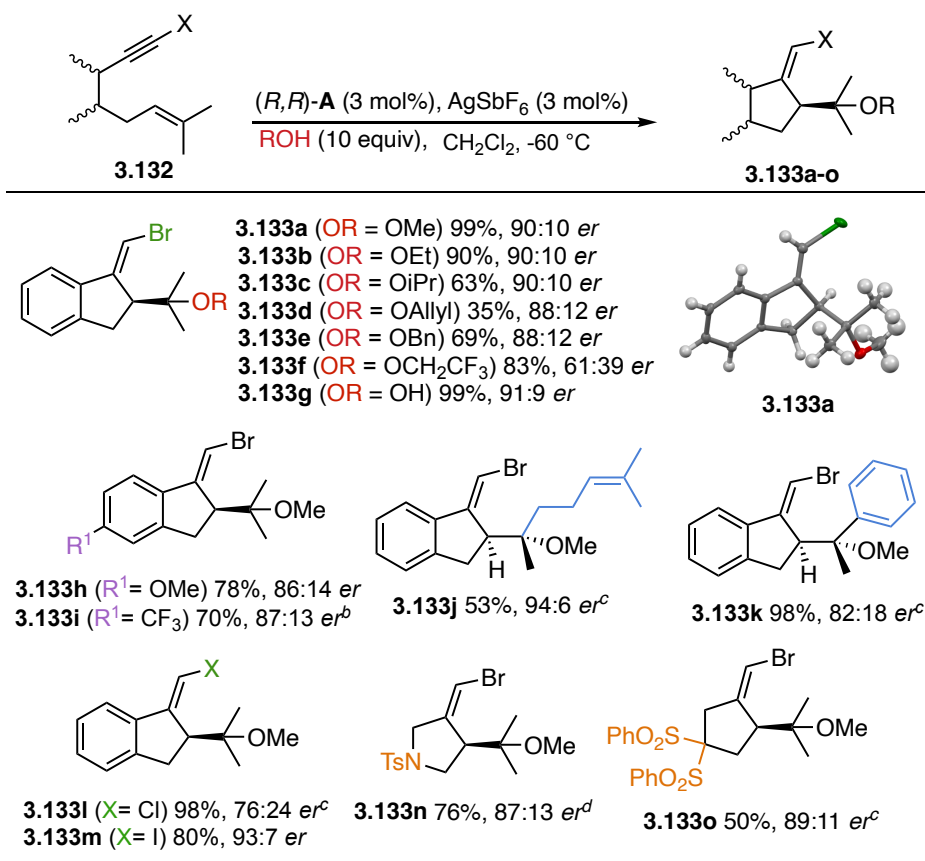
Substrate **3.132a** underwent cyclization with various alcohols (Table 3.6). In most cases, after 5 days, we observed good to excellent conversion and enantiomeric ratios (*er*) ranging from 88:12 to 90:10 for products **3.133a-e**. X-Ray diffraction analysis of **3.133a** confirmed that **3.132a** undergoes 5-*exo-dig* cyclization, and allowed to assign the absolute configuration of the newly formed chiral center as *S*. Remarkably, even electron-poor trifluoroethanol acted as a nucleophile, yielding **3.133f** with good overall yield albeit low enantioselectivity. Water also served as a nucleophile, providing **3.133g** in a 99% yield with a 91:9 *er*.

The aryl tether tolerated both electron-donating (**3.133h**) and electron-withdrawing groups (**3.133i**), although the *er* values were slightly worse. When 1-bromo-1,6-enyne presenting a geranyl chain was cyclized, **3.133j** was obtained with a moderate yield but a surprisingly high 94:6 *er*. Introducing a phenyl group instead of one of the methyls resulted in excellent yield and a good 82:18 *er* for **3.133k**. For these last two examples, we assume the major diastereomer to be the ones reported in the picture, based again on the aforementioned literature reports which show that the cyclizations starting from *E* alkenes afford in a stereospecific manner the *anti* products.³³

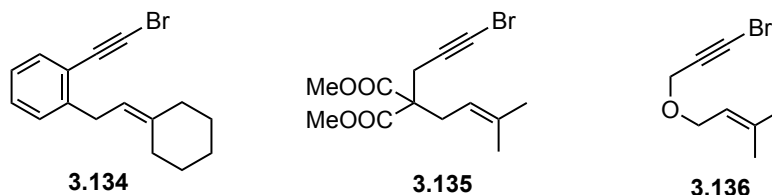
We wanted then to compare the different reactivity of *Br*-enynes with their Cl- and I-substituted analogues. Vinyl chloride **3.133l** was isolated in excellent yields but low enantioselectivity (similar to results obtained at room temperature, as later indicated in Table 3.9 below), while vinyl iodide **3.133m** was obtained with a high yield (80%) and excellent 93:7 *er*: the enantioselectivity appears to improve with the size of the halogen substituent, possibly due to the chiral pocket of the catalyst that might become tighter and therefore more effective with a bulkier substituent on the alkyne.

Expanding our exploration to different enyne tethers, *N*-heterocyclic **3.133n** and sulphone-tethered **3.133o** were isolated with respective *er* values of 87:13 and 89:11. For the former, lowering the temperature did not enhance the *er*, prompting us to run the reaction at room temperature.

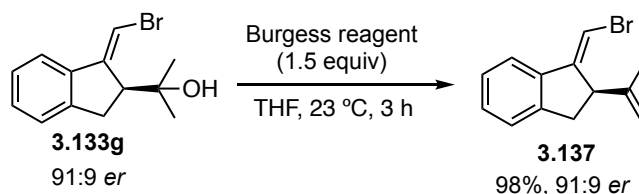
The substrates that afforded poor yield or did not react at all in the selected transformation are listed in Figure 3.1. While **3.134** afforded the product in 30% isolated yield over 5 days at -60 °C with a discrete 75:25 *er*, **3.135** and **3.136** did not react even when working at 23 °C.

Table 3.6. Substrate scope for the 1-bromo-1,6-enyne alkoxycyclization.^a

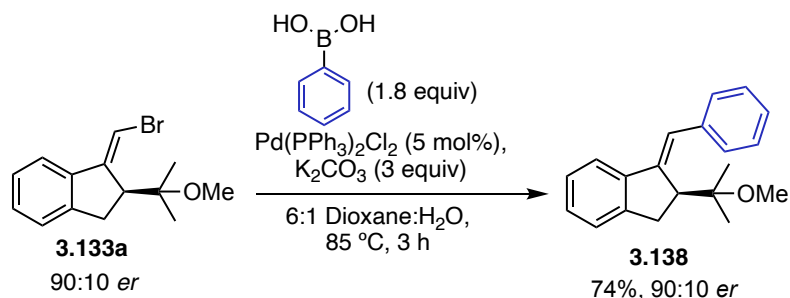
^aIsolated yields. ^bThe reaction was run using 5% of cat. loading. ^cT = -40 °C. ^dT = 23 °C.

**Figure 3.1.** Unsuccessful substrates for the 1-bromo-1,6-enyne alkoxycyclization.

Compound **3.137**, product of the formal cycloisomerization of **3.132a**, could be successfully isolated with excellent 98% yield and an *er* of 91:9 (Scheme 3.19). This was achieved reacting enantiomerically enriched **3.133g** with the Burgess reagent in THF during 3 hours.

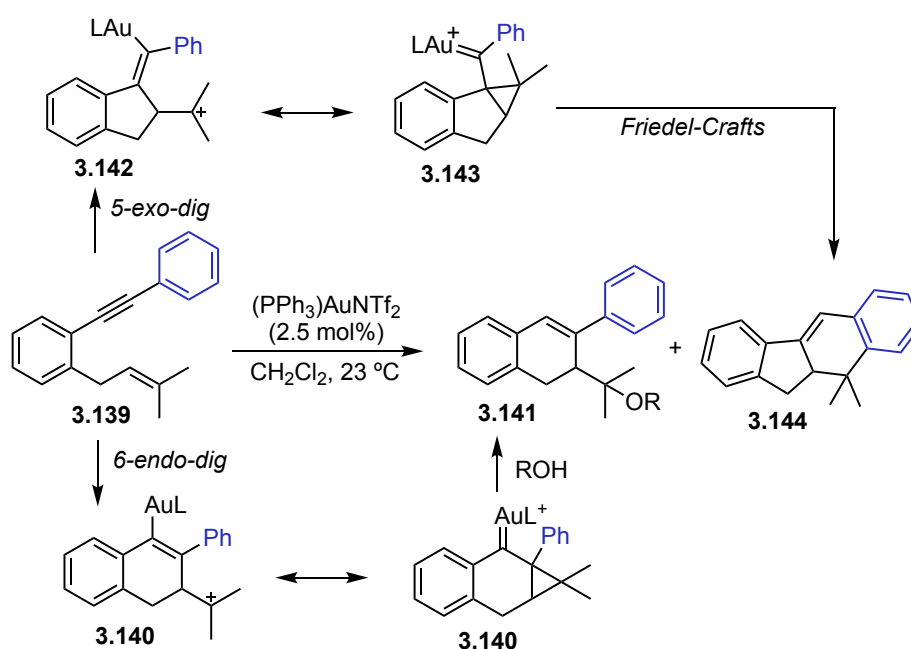
**Scheme 3.19.** Water elimination from **3.133g** obtain enantioenriched **3.137**.

Compound **3.133a** could be functionalized to form the product **3.138** of formal 5-*exo-dig* cyclization of 1-phenyl-1,6-enynes through Suzuki coupling with phenylboronic acid (Scheme 3.20).



Scheme 3.20. Pd-catalyzed Suzuki coupling to obtain the product of formal *5-exo-dig* cyclization of 1-phenyl-1,6-enynes.

It is worth noting that, in the presence of nucleophiles, 1-phenyl-1,6-enynes **3.139** are reported to preferentially yield *6-endo-dig* cyclization products **3.141**, since the *5-exo-dig* cyclization mainly affords [4+2] cycloaddition products **3.144** via Friedel-Crafts arylation (Scheme 3.21).⁴⁵

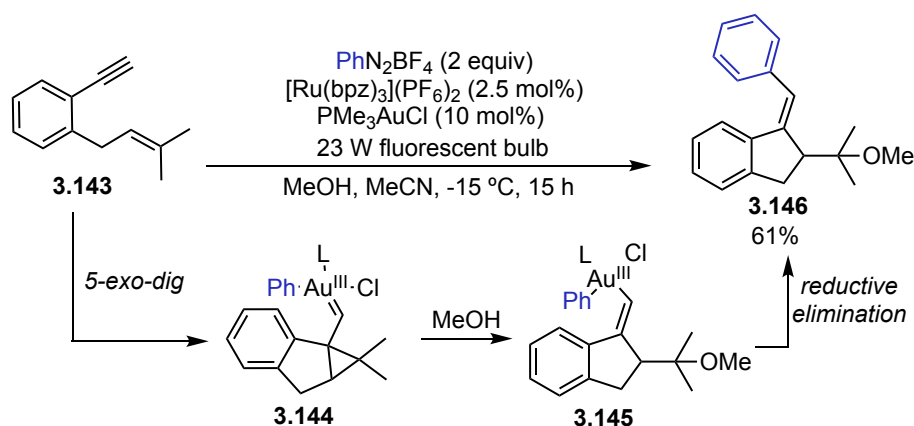


Scheme 3.21. Gold(I)-catalyzed *5-exo-dig* vs *6-endo-dig* cyclization of 1-phenyl-1,6-enynes.

The 5-membered ring variant was obtained selectively only with an opposite configuration at the alkene: this was achieved through a photoredox procedure recently developed in our group (Scheme 3.22).⁴⁶ This strategy envisions the use of diazonium salts and a ruthenium photocatalyst to generate the Au(III) species which then operates the *5-exo-dig* cyclization of **3.143** to form **3.144**, followed by nucleophilic attack and reductive elimination to yield compounds of the type **3.146** with a *Z* configuration at the exocyclic alkene.

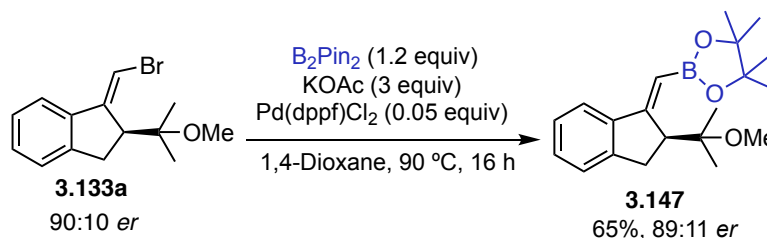
⁴⁵ Sanjuán, A. M.; Martínez, A.; García-García, P.; Fernández-Rodríguez, M. A.; Sanz, R. Gold(I)-Catalyzed 6-*Endo* Hydroxycyclization of 7-Substituted-1,6-Enynes. *Beilstein J. Org. Chem.* **2013**, *9*, 2242–2249.

⁴⁶ Mayans, J. G.; Suppo, J.-S.; Echavarren, A. M. Photoredox-Assisted Gold-Catalyzed Arylative Alkoxylation of 1,6-Enynes. *Org. Lett.* **2020**, *22*, 3045–3049.



Scheme 3.22. Photoredox-Assisted Gold-Catalyzed Arylative Alkoxy cyclization of 1,6-Enynes.

To conclude the alkoxy cyclization product functionalization study, a C–B bond was successfully formed again through Pd catalysis in the presence of B_2Pin_2 , affording product **3.147** in 65% yield without relevant loss in enantiomeric ratio (Scheme 3.23).

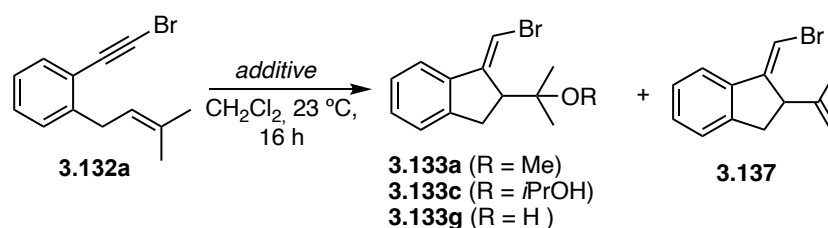


Scheme 3.23. C–B bond formation by Pd-catalyzed cross coupling of **3.133a** with B_2Pin_2 .

Experimental Mechanistic Studies

As previously mentioned, limited attention has been given to describe enyne alkoxy cyclizations with an accurate model. To delve into this aspect, we conducted control experiments using 1-bromo-1,6-enyne substrate **3.132a** (Table 3.7).

When the reaction was run without a chloride scavenger, no product was formed (Table 3.7, entry 1). A 15% yield of the methoxycyclization product **3.133a** was detected by ^1H NMR when working in the absence of gold catalyst, indicating partial activity of the silver salt towards the transformation (Table 3.7, entry 2). In the absence of alcohol and using a wet solvent, a 1.4:1 ratio of the hydroxycyclization product **3.133g** to the cycloisomerization product **3.137** was detected (Table 3.7, entry 3). The surprising discrepancy in enantiomeric ratios for these two products was notable: while **3.133g** presented a 82:18 *er*, **3.137** was obtained in a racemic form (51:49 *er*). Since AgSbF_6 might also partially serve as a catalyst, the reaction was repeated in the absence of silver using the preactivated complex $(R,R)\text{-A}^+$, which, in dry conditions and without a nucleophile, resulted in **3.137** being formed again in a racemic manner (Table 3.7, entry 4). Using 1 equiv of MeOH (Table 3.7, entry 5) also afforded the cycloisomerization product **3.137** consistently less enantioenriched (54:36 *er*) than the methoxycyclization product **3.133a** (80:20 *er*).

Table 3.7. Mechanistic experiments for the 1-bromo-1,6-enyne alkoxy cyclization.

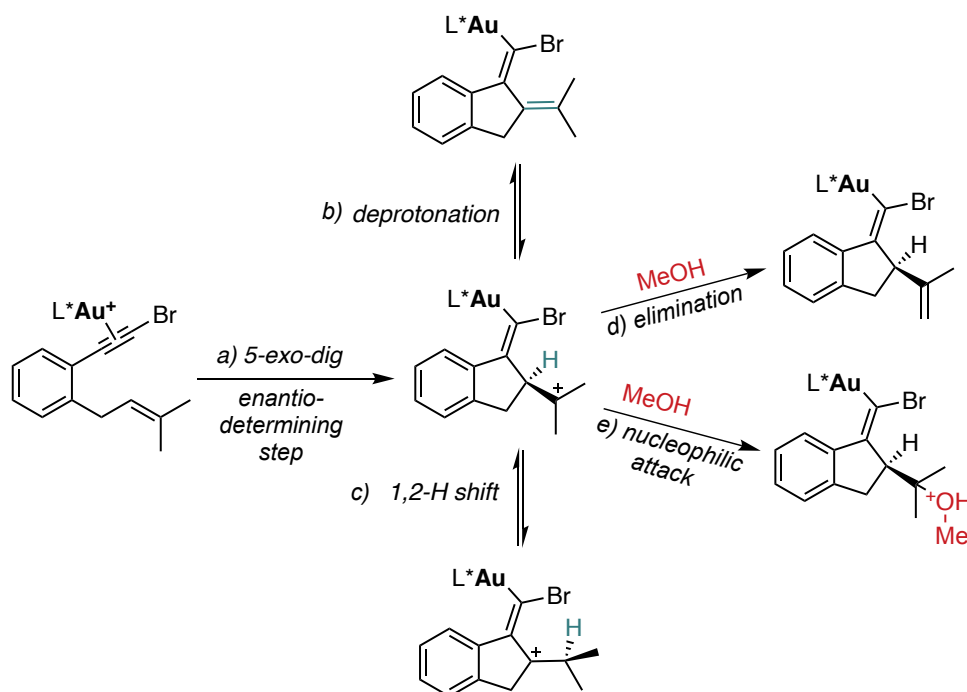
Entry	[Au] ^a	[Ag]	Alcohol	Products ^b
1	(<i>R,R</i>)- A	/	MeOH (10 equiv)	/
2	/	AgSbF ₆ ^c	MeOH (10 equiv)	3.133a (15%)
3^d	(<i>R,R</i>)- A	AgSbF ₆ ^a	/	3.133g (45%, 82:18 <i>er</i>) + 3.137 (32%, 51:49 <i>er</i>)
4^e	(<i>R,R</i>)- A ⁺	/	/	3.137 (8%, 50:50 <i>er</i>)
5^e	(<i>R,R</i>)- A ⁺	/	MeOH (1 equiv)	3.133a (92%, 80:20 <i>er</i>) + 3.137 (9%, 54:46 <i>er</i>)
6^e	(<i>R,R</i>)- A ⁺	/	MeOH (10 equiv)	3.133a (65%, 80:20 <i>er</i>) + 3.137 (3%, 60:40 <i>er</i>)
7^e	(<i>R</i>)- L ^{c,f}	AgSbF ₆ ^c	/	3.137 (12%, 61:39 <i>er</i>)
8^e	(<i>R</i>)- L ^{c,f}	AgSbF ₆ ^c	MeOH (1 equiv)	3.133a (20%, 71:29 <i>er</i>) + 3.137 (37%, 70:30 <i>er</i>)
9^e	(<i>R,R</i>)- A ⁺	/	<i>i</i> PrOH (1 equiv)	3.133c (55%, 81:19 <i>er</i>) + 3.137 (28%, 70:30 <i>er</i>)
10^e	(<i>R,R</i>)- A ⁺	/	<i>i</i> PrOH (10 equiv)	3.133c (76%, 80:20 <i>er</i>) + 3.137 (22%, 75:25 <i>er</i>)
11^e	(<i>R,R</i>)- A	AgSbF ₆ ^c	HFIP (10 equiv)	3.137 (59%, 76:24 <i>er</i>)

^a 3 mol%. ^b The reported yields were calculated by ¹H NMR integration using 1,1,2,2-tetrachloroethane or trichloroethylene as internal standards. The *er* were measured on the pure isolated products. ^c 5 mol%. ^d The reaction was run in α,α,α -trifluorotoluene. ^e Dry CH₂Cl₂ and alcohols from the glovebox were used to perform these reactions. ^f **L** = DTBM-segphos(AuCl)₂.

Increasing the quantity of MeOH to 10 equiv (Table 3.7, entry 6) afforded **3.137** in a slightly more enantioenriched manner (60:40 *er*) but still more racemic than **3.133a** (80:20 *er*). To discard the possibility that this phenomenon would be catalyst-dependent, we tested the commercially available ligand (*R*)-DTBM-segphos ((*R*)-**L**) previously employed in gold(I)-catalyzed alkoxy cyclizations.⁴⁰ This catalyst resulted to be more selective for the cycloisomerization product **3.137** compared to (*R,R*)-**A**⁺ (compare yields in Table 3.7, entry 7-8 with entry 4-5). However, under dry conditions (Table 3.7, entry 7), the *er* for **3.137** remained reduced (61:39 *er*) compared to when using 1 equiv of methanol (Table 3.7, entry 8, 70:30 *er*). In the presence of 1 equiv of the more basic and less nucleophilic isopropanol, more cycloisomerization product **3.137** was formed compared to when using methanol (Table 3.7, entry 9). Although this resulted in a lower *er* (70:30 *er*) compared to the alkoxy cyclization product **3.133c** (81:19 *er*), the difference was less pronounced than in the previous cases. This discrepancy further diminished (75:25 *er* vs 80:20 *er*) with the use of 10 equiv of isopropanol (Table 3.7, entry 10).

These findings suggest the occurrence of a racemization event after the enantiodetermining gold(I)-catalyzed 5-*exo-dig* cyclization (Scheme 3.24a) or propose the potential involvement of an entirely different mechanism for the cycloisomerization product compared to the alkoxy cyclization one.

Concerning the first hypothesis, we considered two plausible racemization pathways following the cyclization step: a reversible elimination/protonation at the chiral carbon center (Scheme 3.24b) or a reversible 1,2-H shift (Scheme 3.24c). Due to the C_{sp^3} - C_{sp^2} equilibrium, both pathways would result in a loss of enantiomeric excess. In these scenarios, elements that can promote faster elimination at one of the isopropyl methylenes (Scheme 3.24d), such as a higher alcohol concentration (10 equiv vs 1 equiv), the use of a stronger base (*i*PrOH) or a different catalyst ((*R*)-**L**), would also lead to an increased enantiomeric ratio for the final cycloisomerization product, as observed in the experimental results.



Scheme 3.24. Working hypothesis for plausible in-cycle racemization pathways.

We therefore decided to conduct the reaction in the presence of HFIP, relatively known for its positive effects on reaction rates in gold(I)-catalysis.^{10,47} and which, as shown in **Chapter I**, may facilitate the cycloisomerization reaction by providing a proton shuttle to the system.⁴⁸ **3.137** was indeed isolated in 59% yield and with nearly the same enantioselectivity (76:24 *er*) as the alkoxy cyclization products **3.133a**, **3.133c**, and **3.133g** (Table 3.7, entry 11). The higher value of *er* encountered in this case compared to when working in fully dry conditions (Table 3.7, entry 4), constitutes a further proof that a decreased racemization can be obtained by facilitating *path d* over *path b* or *path c* (Scheme 3.24)

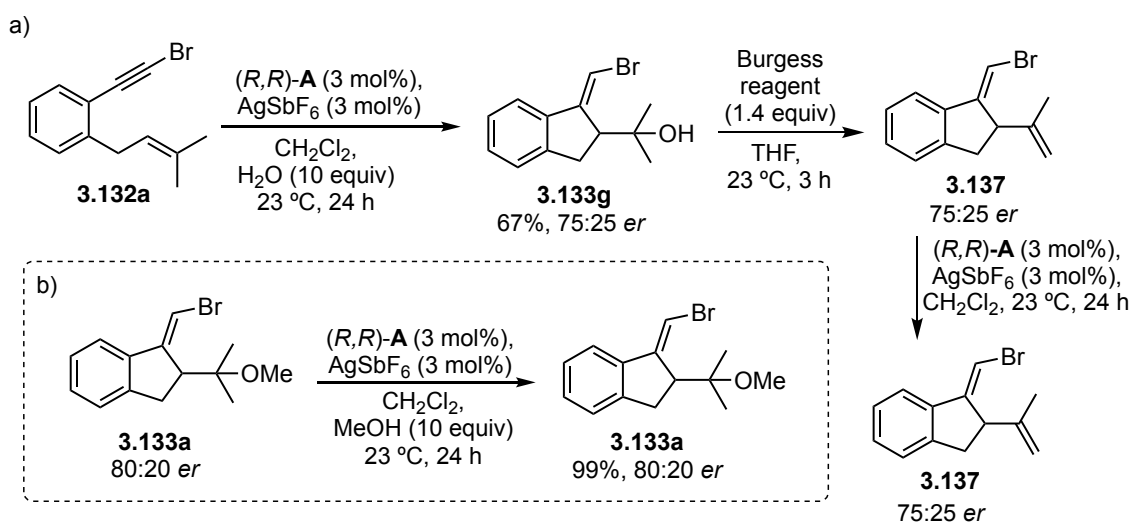
However, so far, it remains unclear why following one of the two proposed racemization pathways, the alkoxy cyclization product (Scheme 3.24e) would not also be isolated in a racemic manner.

⁴⁷ a) Tzouras, N. V.; Gobbo, A.; Pozsoni, N. B.; Chalkidis, S. G.; Bhandary, S.; Van Hecke, K.; Vougioukalakis, G. C.; Nolan, S. P., Hydrogen Bonding-Enabled Gold Catalysis: Ligand Effects in Gold-Catalyzed Cycloisomerizations in Hexafluoroisopropanol (HFIP), *Chem. Commun.* **2022**, 58, 8516–8519. b) Tzouras, N. V.; Zorba, L. P.; Kaplanai, E.; Tsoureas, N.; Nelson, D. J.; Nolan, S. P.; Vougioukalakis, G. C., Hexafluoroisopropanol (HFIP) as a Multifunctional Agent in Gold-Catalyzed Cycloisomerizations and Sequential Transformations, *ACS Catal.* **2023**, 13, 8845–8860.

⁴⁸ Cataffo, A.; Peña-López, M.; Pedrazzani, R.; Echavarren, A. M., Chiral Auxiliary Approach for Gold(I)-Catalyzed Cyclizations, *Angew. Chem. Int. Ed.* **2023**, 62, e202312874, *Angew. Chem.* **2023**, 135, e202312874.

In pursuit of deeper insights, we first conducted additional experiments to rule out potential alternative mechanisms leading to similar outcomes.

We wanted to discard the possibility of racemization occurring on product **3.137** post-protodeauration, via a reversible double bond isomerization initiated by gold itself⁴⁹ or Brønsted acids generated in the presence of gold within the reaction mixture.⁵⁰ With this purpose, the enantioselective hydroxycyclization of **3.132a** was conducted using complex (*R,R*)-**A** to form enantioenriched **3.133g** (75:25 *er*) (Scheme 3.25a). Then, alcohol elimination was promoted with the Burgess reagent to yield **3.137** presenting a preserved *er* (75:25). Finally, exposing this product to the standard reaction conditions did not alter its enantiomeric ratio. Similarly, when product **3.133a** underwent treatment with (*R,R*)-**A**, AgSbF₆, and MeOH, it was fully recovered with unchanged *er* (Scheme 3.25b).

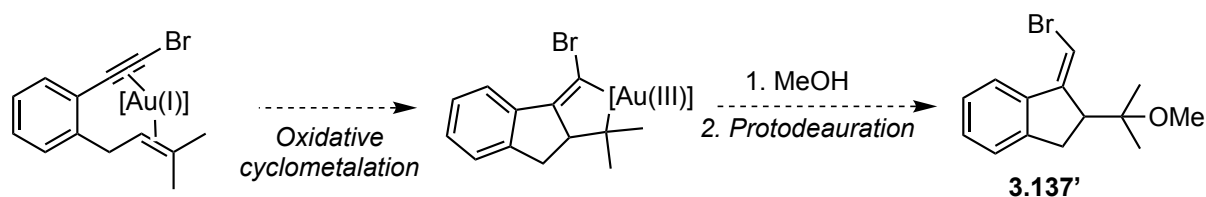


Scheme 3.25. Exposure to standard reaction conditions for a) enantioenriched elimination product **3.137** and b) enantioenriched alkoxycyclization product **3.133a**.

Another hypothesis considers the formation of **3.137'** via oxidative cyclometallation of substrate **3.132a** which would eventually yield the racemic product with an opposite configuration at the bromoalkene (*Z* instead of *E*) compared to the alkoxycyclization products **3.137** (Scheme 3.26).

⁴⁹ a) Ito, H.; Harada, T.; Ohmiya, H.; Sawamura, M. Intramolecular Hydroamination of Alkynic Sulfonamides Catalyzed by a Gold–Triethynylphosphine Complex: Construction of Azepine Frameworks by 7-Exo-Dig Cyclization. *Beilstein J. Org. Chem.* **2011**, *7*, 951–959. b) Pflästerer, D.; Schumacher, S.; Rudolph, M.; Hashmi, A. S. K., Mechanistic Insights into the Post-Cyclization Isomerization in Gold-Catalyzed 7-Exo-Dig-Hydroarylations, *Chem. Eur. J.* **2015**, *21*, 11585–11589. c) Bhoyare, V. W.; Tathe, A. G.; Gandon, V.; Patil, N. T., Unlocking the Chain-Walking Process in Gold Catalysis, *Angew. Chem. Int. Ed.* **2023**, *62*, e202312786, *Angew. Chem.* **2023**, *135*, e202312786.

⁵⁰ a) Kanno, O.; Kuriyama, W.; Wang, Z. J.; Toste, F. D., Regio- and Enantioselective Hydroamination of Dienes by Gold(I)/Menthol Cooperative Catalysis, *Angew. Chem. Int. Ed.* **2011**, *50*, 9919–9922, *Angew. Chem.* **2011**, *123*, 10093–10096. b) Brooner, R. E. M.; Robertson, B. D.; Widenhofer, R. A. Mechanism of 1,3-Hydrogen Migration in a Gold Bicyclo[3.2.0]Heptene Complex: The Role of Brønsted Acid in the Gold-Catalyzed Cycloisomerization of 7-Aryl-1,6-Enynes. *Organometallics* **2014**, *33*, 6466–6473.



This kind of transformation while already described for other transition metals,⁵¹ was never reported for gold. To rule out this unlikely possibility, NOESY spectroscopy was conducted on enantioenriched **3.133g** (82:18 *er*) and racemic **3.137** (51:49 *er*) both generated from **3.132a** during the course of the same reaction (Table 3.7, entry 3). As depicted in Figure 3.2, in both products a contact between the aromatic protons and the bromoalkene was observed, indicating an *E* configuration for both.

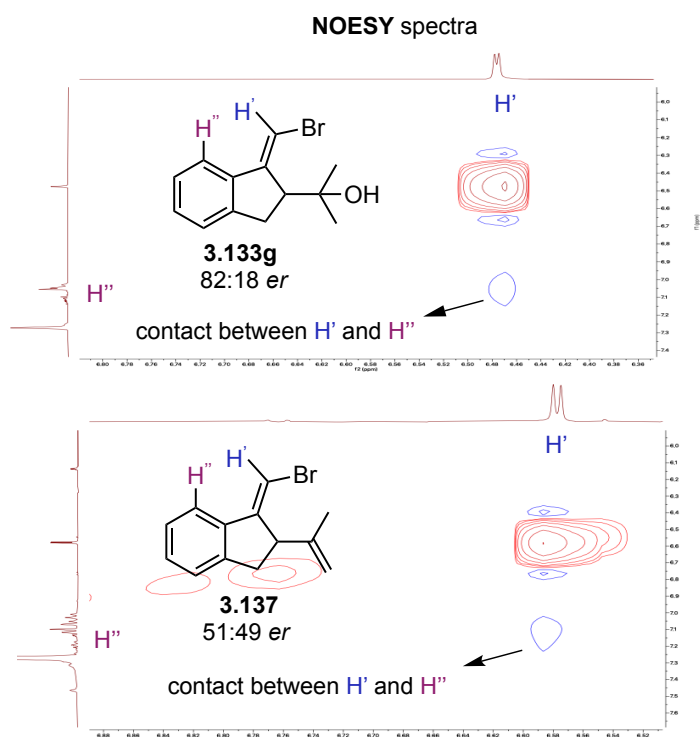
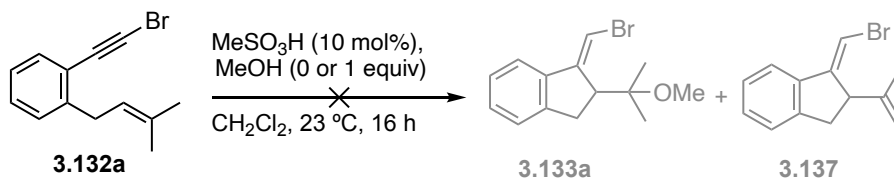


Figure 3.2. NOESY NMR contact between vinylic proton H' and aromatic H'' in **3.133g** and **3.137**.

We continued our studies by considering the possibility that racemic **3.137** might be formed through a proton-catalyzed pathway, which, in dry conditions, could potentially compete with the gold-catalyzed cyclization.

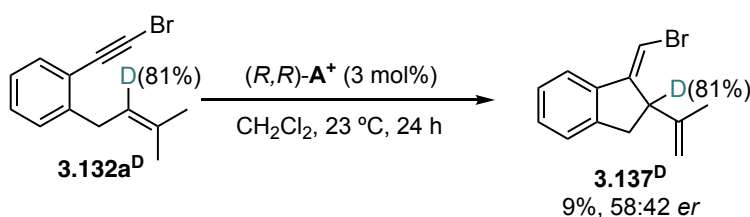
⁵¹ Michelet, V.; Toullec, P. Y.; Genêt, J.-P., Cycloisomerization of 1,*n*-Enynes: Challenging Metal-Catalyzed Rearrangements and Mechanistic Insights, *Angew. Chem. Int. Ed.* **2008**, *47*, 4268–4315, *Angew. Chem.* **2008**, *120*, 4338–4386. b) Zhang, X.-S.; Han, Y.-P.; Liang, Y.-M., Recent Advances in the Cascade Cyclization Reactions of 1,7-Enynes, *Adv. Synth. Catal.* **2024**, *366*, 324–356.

We hypothesized that the protodeauration step, lacking alcohol or water residues which can serve as proton shuttles, might prove challenging^{48,52} However, upon the introduction of methanesulfonic acid to **3.132a** no reaction happened, regardless of the presence or absence of MeOH (Scheme 3.27). Additionally, DFT calculations revealed that no such competition is feasible (see below).



Scheme 3.27. Full recovery of starting material when exposing **3.132a** to MeSO₃H.

Finally, to demonstrate that the mechanism under observation is an in-cycle racemization, we synthesized deuterium-labeled substrate **3.132a^D** and then we run the reaction with (*R,R*)-**A**⁺ under dry conditions (Scheme 3.28). The absence of proton scrambling excludes the hypothesis of a reversible deprotonation contributing to the experimentally observed racemization (Scheme 3.24b). Moreover, the slightly reduced racemization observed for product **3.137^D** (58:42 *er*) compared to **3.137** (51:49 *er*) suggests the involvement of the 1,2-H shift as the operating racemization mechanism (Scheme 3.24c) since this aligns with a higher energetic barrier associated with deuterium migration, as discussed in the Computational Studies section below.



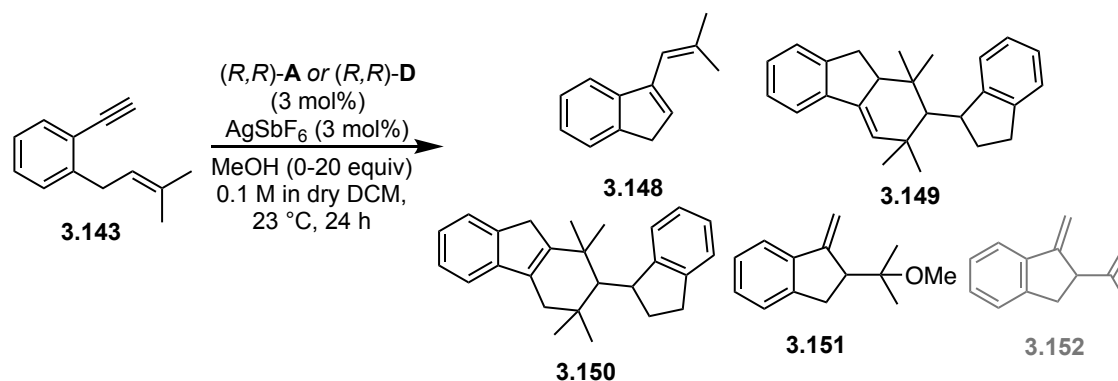
Scheme 3.28. (*R,R*)-**A**⁺ catalyzed cycloisomerization of deuterium-labeled **3.132a^D**.

Once excluded experimentally the possible competing pathways, we were interested in understanding whether the same trend would manifest in substrates bearing different substitutions on the alkyne.

Upon testing terminal enyne **3.143**, as expected, diene **3.148** was formed, together with dimerization products **3.149-150** (Scheme 3.29).⁵³ Furthermore, methoxycyclization product **3.151** formed. However, no trace of the cycloisomerization product **3.152** was observed. Therefore, this enyne was discarded from the present study.

⁵² a) Barrio, P.; Kumar, M.; Lu, Z.; Han, J.; Xu, B.; Hammond, G. B., Acidic Co-Catalysts in Cationic Gold Catalysis, *Chem. Eur. J.* **2016**, *22*, 16410–16414. a) Stylianakis, I.; Faza, O. N.; López, C. S.; Kolocouris, A. The Key Role of Protodeauration in the Gold-Catalyzed Reaction of 1,3-Diynes with Pyrrole and Indole to Form Complex Heterocycles. *Org. Chem. Front.* **2020**, *7*, 997–1005. b) Gubler, J.; Radić, M.; Stöferle, Y.; Chen, P. 2-Aminoalkylgold Complexes: The Putative Intermediate in Au-Catalyzed Hydroamination of Alkenes Does Not Protodemetalate. *Chem. Eur. J.* **2022**, *28*, e202200332. c) Pedrazzani, R.; Kiriakidi, S.; Monari, M.; Lazzarini, I.; Bertuzzi, G.; López, C. S.; Bandini, M. Fluorinated Biphenyl Phosphine Ligands for Accelerated [Au(I)]-Catalysis. *ACS Catal.* **2024**, *14*, 6128–6136.

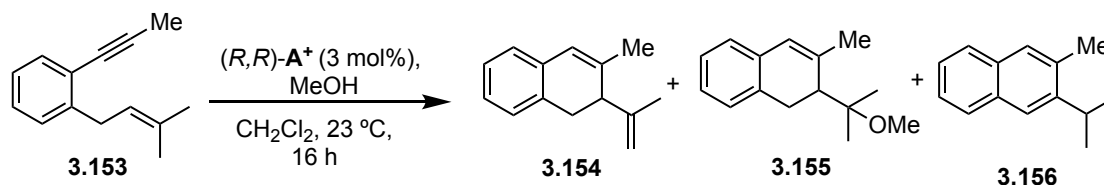
⁵³ Álvarez-Pérez, M.; Frutos, M.; Viso, A.; Fernández de la Pradilla, R.; de la Torre, M. C.; Sierra, M. A.; Gornitzka, H.; Hemmert, C. Gold(I)-Catalyzed Cycloisomerization–Dimerization Cascade of Benzene-Tethered 1,6-Enynes. *J. Org. Chem.* **2017**, *82*, 7546–7554.



Scheme 3.29. Products of $(R,R)\text{-A}$ or $(R,R)\text{-D}$ catalyzed cyclization of 1-H-1,6-enynes.

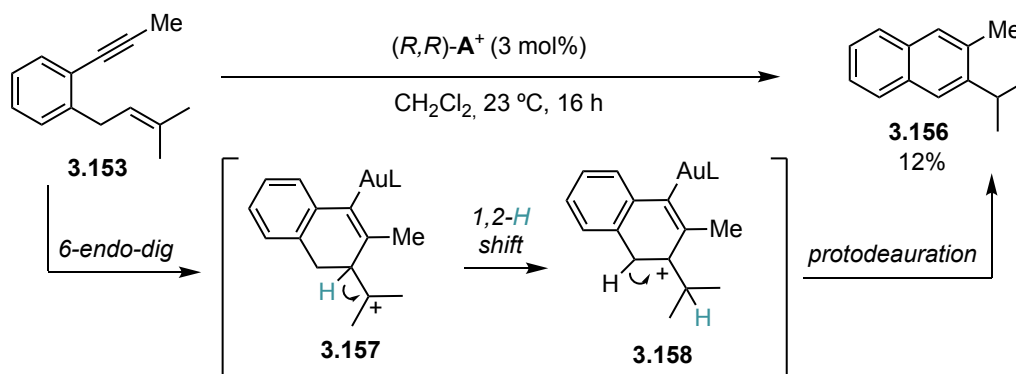
Testing 1-methyl-1,6-enyne **3.153** in the presence of $(R,R)\text{-A}^+$ presented challenges due to the high instability of formal cycloisomerization product **3.154** on silica which could be isolated only in very low yields, preventing accurate measurement of its enantiomeric ratio (Table 3.8). Enyne **3.153** was therefore considered not suitable for our racemization studies. Nevertheless, under anhydrous conditions, 2-isopropyl-3-methylnaphthalene **3.156** was detected. (Table 3.8, entry 1). This compound constitutes a first experimental evidence in the context of this work for an irreversible 1,2-H shift starting from *6-endo-dig* intermediate **3.157** (similar to the one discussed in Scheme 3.12), which subsequently protodeaurates to form the thermodynamically favored naphthalene compound (Scheme 3.30). Ultimately, in the presence of 1 equiv of MeOH , previously unknown **3.155** was obtained with a 65% isolated yield (preparative TLC utilizing a 50:1 hexane:EtOAc mixture) and a remarkable 91:9 *er* (Table 3.8, entry 2).

Table 3.8. *6-endo-dig* cyclizations of 1-methyl-1,6-enyne **3.153**.^a



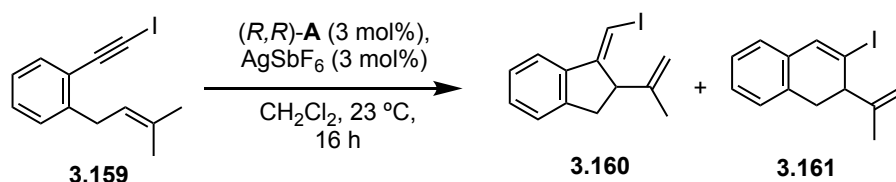
Entry	MeOH (equiv)	3.154	3.155	3.156
1	0	6%, ~ 78:22 <i>er</i>	/	12%
2	1	1%, <i>er</i> n.d.	77% (65%), 91:9 <i>er</i>	/

^aAll the reactions were performed under dry conditions using glovebox solvents. The reported yields were calculated by ^1H NMR integration using 1,1,2,2-tetrachloroethane as internal standard. Isolated yields in parenthesis. The *er* were measured on the pure isolated products.



Scheme 3.30. Proposed mechanism for the formation of naphthalene derivative **3.156**.

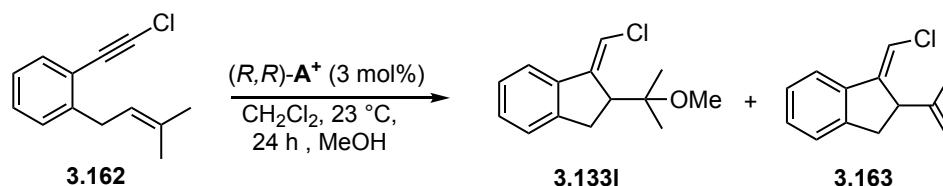
Iodoenynes **3.159** was also excluded from this study due to the formation of a mixture of *5-exo-dig* and *6-endo-dig* cycloisomerization products when working in the absence of methanol (Scheme 3.31). Unfortunately, these products were inseparable by column chromatography.



Scheme 3.31. *(R,R)*-A-catalyzed cyclization of 1-iodo-1,6-enynes under dry conditions.

When working with 1-chloro-1,6-enyne **3.162**, finally, we found that we could well study the system under the standard reaction conditions. Being **3.162** structurally very similar to 1-bromo-1,6-enyne **3.132a**, we expected it to behave similarly. From 0 to 10 equiv of alcohol, we consistently isolated the cycloisomerization product **3.163** with a reduced enantiomeric ratio (*er*) compared to the alkoxy cyclization product **3.133I** (Table 3.9, entries 1-3). Increasing the quantity of nucleophile had no impact on the *er* of the alkoxy cyclization product, as observed previously, but did negatively affect its yield.

Table 3.9. *5-exo-dig* cyclizations of 1-chloro-1,6-enyne **3.162**.

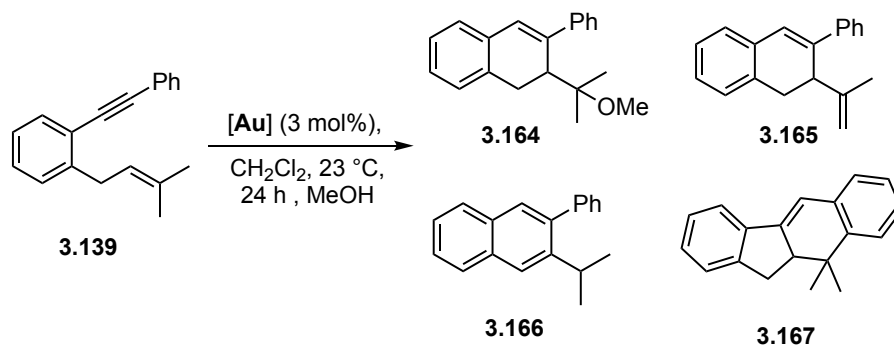


Entry	MeOH (equiv)	3.133I	3.163
1	0	/	16%, 55:45 <i>er</i>
2	1	74%, 74:26 <i>er</i>	8%, 53:47 <i>er</i>
3	10	48%, 75:25 <i>er</i>	10% 51:40 <i>er</i>

^aAll the reactions were performed under dry conditions using glovebox solvents. The reported yields were calculated by ¹H NMR integration using 1,1,2,2-tetrachloroethane as internal standard. The *er* were measured on the pure isolated products.

When we moved to the electronically distinct 1-phenyl-1,6-enyne **3.139**, no elimination product was observed if working in dry conditions (Table 3.10, entry 1). 2-isopropyl-3-phenylnaphthalene product **3.166**, resulting from a *6-endo-dig* cyclization/1,2-H shift sequence, as in the case of 1-methyl-1,6-enynes (Scheme 3.30), and product **3.167**, formed via a [4+2] cycloaddition, were instead detected in the reaction mixture. With 1 equiv of MeOH, alkoxy cyclization product **3.164** was obtained in excellent yield with an exceptionally high 98:2 *er* (Table 3.10, entry 2). Unfortunately, cycloisomerization product **3.165** was formed only in 2% NMR yield, insufficient for *er* measurement. We replicated the experiments using catalyst (*R,R*)-**D** previously employed in our group for cyclizing this type of 1-phenyl-1,6-enynes,^{41a} with the hope of getting more insights. Due to the instability of its cationic version, we conducted the studies using the gold(I)-chloride precursor together with AgSbF₆, as it has been established that the observed racemization in 1-bromo-1,6-enyne **3.132a** is not catalyst or silver-dependent (Table 3.7). In dry conditions and without methanol, again, **3.166** and **3.167** were the sole identified products (Table 3.10, entry 3). Raising the equiv of alcohol to 1 or 5 equiv, both **3.164** and **3.165** were isolated, exhibiting identical *er*: no discrepancy was observed in this case.

Table 3.10. *6-endo-dig* cyclizations of 1-phenyl-1,6-enynes **3.153**.



Entry	[Au]	[Ag]	MeOH (equiv)	3.164	3.165	3.166	3.167
1	(<i>R,R</i>)- A ⁺	/	/	/	/	37% (28%)	35%
2	(<i>R,R</i>)- A ⁺	/	1	76%, 98:2 <i>er</i>	2%	/	/
3	(<i>R,R</i>)- D	AgSbF ₆	/	/	/	56%	14%
4	(<i>R,R</i>)- D	AgSbF ₆	1	3%, 89:11 <i>er</i>	42%, 89:11 <i>er</i>	/	/
5	(<i>R,R</i>)- D	AgSbF ₆	5	39%, 89:11 <i>er</i>	20%, 89:11 <i>er</i>	/	/

^aAll the reactions were performed under dry conditions using glovebox solvents. The reported yields were calculated by ¹H NMR integration using 1,1,2,2-tetrachloroethane as internal standard. The *er* were measured on the pure isolated products.

This suggests and confirms that for carbon-based enynes, the 1,2-H shift operates in an irreversible manner, as seen experimentally by the formation of stable naphthalene species and as opposed to the reversible 1,2-H shift hypothesized for the 1-halo-1,6-enynes object of this study. Further elaboration on the topic will be furnished in the Computational Studies section below.

Computational Studies

With the aim of investigating the aforementioned effects and comprehending the processes leading to racemization, loss of enantioselectivity, or other forms of enantiomeric scrambling, we conducted Density Functional Theory (DFT) calculations⁵⁴ to elucidate the unusual alcohol dependence.

We used Gaussian09⁵⁵ with the B3LYP⁵⁶ functional, incorporating Grimme's D3 dispersion correction.⁵⁷ Solvent modeling employed the polarizable continuum model (PCM)⁵⁸ with CH₂Cl₂ as the implicit solvent. Gold was modeled using the Stuttgart-Dresden basis set and effective core potential,⁵⁹ bromine with LANL2TZ(f)⁶⁰, and all other non-metal atoms with the Pople⁶¹ basis set 6-311+G(d,p). This level of theory had previously demonstrated efficacy in DFT calculations of gold(I)-catalyzed transformations.⁶² While previous research in gold(I)-catalyzed cycloisomerization of *ortho*-(alkynyl)styrenes highlighted the participation of the counteranion in the mechanism, to the point that its choice could affect the outcome of the reaction,⁶³ we suspect that ion pair effects in those cases were exaggerated by geometry optimizations performed in a vacuum, therefore the hexafluoroantimonate counteranion was excluded from our computational model. In fact, when we tried to reproduce the calculations with our PCM approach, it resulted in the disappearance of short contacts.

Since enantioenriched compounds **3.133a** and **3.137** exhibited no racemization under the standard reaction conditions (Scheme 3.25), any discrepancies in enantiomeric ratio observed must stem from the reaction process itself, particularly within the reactive intermediates. We therefore investigated

⁵⁴ A dataset collection of computational results is available in the ioChem-BD repository and can be accessed via <https://doi.org/10.19061/iochem-bd-1-307>. Álvarez-Moreno, M.; De Graaf, C.; López, N.; Maseras, F.; Poblet, J. M.; Bo, C. Managing the Computational Chemistry Big Data Problem: The **ioChem-BD** Platform. *J. Chem. Inf. Model.* **2015**, *55*, 95–103.

⁵⁵ Gaussian 09, Revision B.1, Frisch, M. J.; Trucks, G. W.; Schlegel, H. B.; Scuseria, G. E.; Robb, M. A.; Cheeseman, J. R.; Scalmani, G.; Barone, V.; Mennucci, B.; Petersson, G. A.; Nakatsuji, H.; Caricato, M.; Li, X.; Hratchian, H. P.; Izmaylov, A. F.; Bloino, J.; Zheng, G.; Sonnenberg, J. L.; Hada, M.; Ehara, M.; Toyota, K.; Fukuda, R.; Hasegawa, J.; Ishida, M.; Nakajima, T.; Honda, Y.; Kitao, O.; Nakai, H.; Vreven, T.; Montgomery, J. A.; Peralta, Jr. J. E.; Ogliaro, F.; Bearpark, M.; Heyd, J. J.; Brothers, E.; Kudin, K. N.; Staroverov, V. N.; Kobayashi, R.; Normand, J.; Raghavachari, K.; Rendell, A.; Burant, J. C.; Iyengar, S. S.; Tomasi, J.; Cossi, M.; Rega, N.; Millam, J. M.; Klene, M.; Knox, J. E.; Cross, J. B.; Bakken, V.; Adamo, C.; Jaramillo, J.; Gomperts, R.; Stratmann, R. E.; Yazyev, O.; Austin, A. J.; Cammi, R.; Pomelli, C.; Ochterski, J. W.; Martin, R. L.; Morokuma, K.; Zakrzewski, V. G.; Voth, G. A.; Salvador, P.; Dannenberg, J. J.; Dapprich, S.; Daniels, A. D.; Farkas, ..; Foresman, J. B.; Ortiz, J. V.; Cioslowski, J.; Fox, D. J. Gaussian, Inc., Wallingford CT, **2009**.

⁵⁶ a) Becke, A. D., Density-functional Thermochemistry. III. The Role of Exact Exchange, *J. Chem. Phys.* **1993**, *98*, 5648–5652. b) Becke, A. D., A New Mixing of Hartree-Fock and Local Density-functional Theories, *J. Chem. Phys.* **1993**, *98*, 1372–1377. c) Lee, C.; Yang, W.; Parr, R. G., Development of the Colle-Salvetti Correlation-Energy Formula into a Functional of the Electron Density, *Phys. Rev. B* **1988**, *37*, 785–789.

⁵⁷ Grimme, S. Density Functional Theory with London Dispersion Corrections. *WIREs Comput. Mol. Sci.* **2011**, *1*, 211–228.

⁵⁸ Cancès, E.; Mennucci, B.; Tomasi, J. A New Integral Equation Formalism for the Polarizable Continuum Model:

Theoretical Background and Applications to Isotropic and Anisotropic Dielectrics. *J. Chem. Phys.* **1997**, *107*, 3032–3041.

⁵⁹ Andrae, D.; Häußermann, U.; Dolg, M.; Stoll, H.; Preuß, H. Energy-Adjusted *ab Initio* Pseudopotentials for the Second and Third Row Transition Elements. *Theor. Chim. Acta* **1990**, *77*, 123–141.

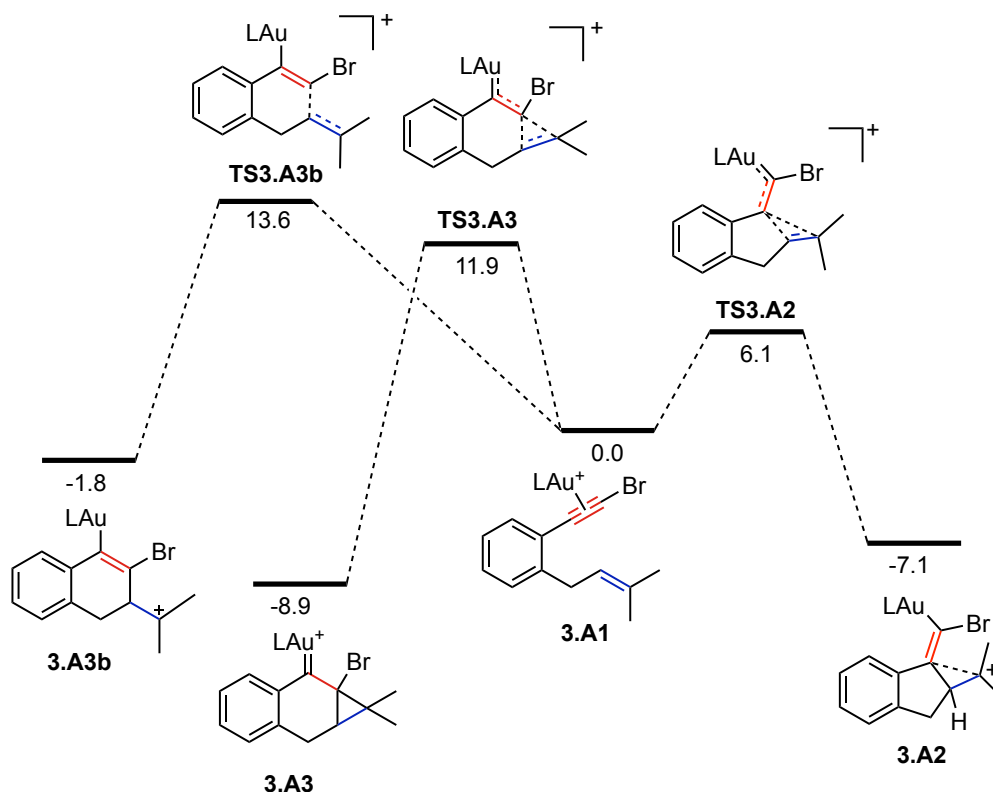
⁶⁰ Wadt, W. R.; Hay, P. J. *Ab Initio* Effective Core Potentials for Molecular Calculations. Potentials for Main Group Elements Na to Bi. *J. Chem. Phys.* **1985**, *82*, 284–298.

⁶¹ Hehre, W. J.; Ditchfield, R.; Pople, J. A., Self-Consistent Molecular Orbital Methods. XII. Further Extensions of Gaussian-Type Basis Sets for Use in Molecular Orbital Studies of Organic Molecules, *J. Chem. Phys.* **1972**, *56*, 2257–2261.

⁶² García-Padilla, E.; Escofet, I.; Maseras, F.; Echavarren, A. M. Puzzling Structure of the Key Intermediates in Gold(I)-Catalyzed Cyclization Reactions of Enynes and Allenenes. *ChemPlusChem*, e202300502.

⁶³ Zhou, L.; Zhang, Y.; Fang, R.; Yang, L. Computational Exploration of Counterion Effects in Gold(I)-Catalyzed Cycloisomerization of *Ortho*-(Alkynyl)Styrenes. *ACS Omega* **2018**, *3*, 9339–9347.

potential pathways that could facilitate interconversion between the two chiral products. Since the hypothesis deals with a case of racemization, in which the ligand doesn't play a role, enantioselectivity determination was not necessary, thus we simplified the modeled ligand on gold to trimethylphosphine. We started by modelling the competition between the *5-exo-dig* and *6-endo-dig* pathways starting from gold(I)-coordinated intermediate **3.A1** (Scheme 3.32). Transition states **TS3.A3** and **TS3.A3b** yielded *6-endo-dig* products, while transition state **TS3.A2** resulted in the *5-exo-dig* product **3.A2**. The energy disparity exceeds 5 Kcal·mol⁻¹, aligning with the experimentally observed preference towards **3.A2** and thereby validating our model.



Scheme 3.32. Competition between *5-exo-dig* and *6-endo-dig* barriers with gold(I) bromoalkyne complex **3.A1**, consistent with the experimental observations. Free energy in Kcal·mol⁻¹ at B3LYP-D3/6-311G+(d,p) + SDD, PCM.

Subsequent racemization steps were expected after this initial cyclization. To model the productive pathways from intermediate **3.A2**, including alkoxy cyclization and elimination, we considered the alcohol dependence and its activity as nucleophile or base. As mentioned above, previous calculations of alkoxy cyclizations or related eliminative cyclizations (formal cycloisomerizations) had stopped at carbocationic precursors,^{37,38} considering the subsequent steps not important for the mechanistic understanding of the reactions. This led us to start drawing the first model for alcohol participation in alkoxy cyclizations. We started from evaluating whether methanol would arrange in a monomeric form, or in higher order clusters, in dichloromethane. After calculating several neutral and protonated clusters,

we found the neutral monomer **3.m1** and a protonated tetramer **3.pm4** to be the most stable.⁶⁴ To diminish the complexity of our calculations, protonated methanol dimer **3.pm2** which was comparable in energy, was chosen to model alcohol-mediated deprotonations.

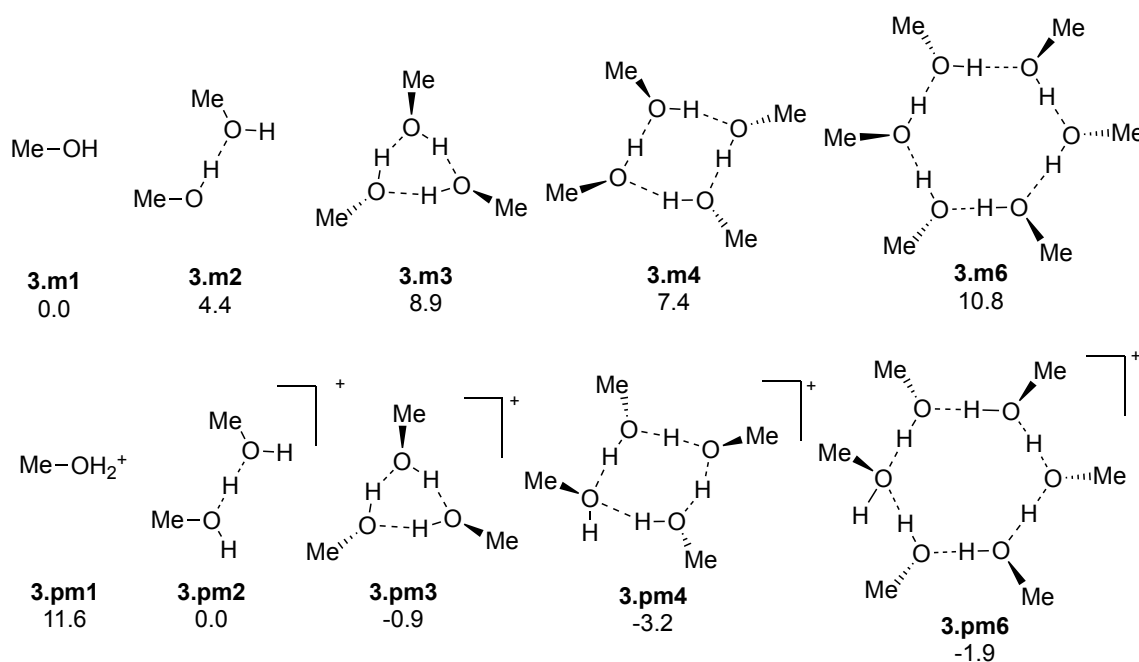


Figure 3.3. Most stable calculated neutral and protonated methanol clusters for each molecularity (in dichloromethane modelled with PCM). Free energy in $\text{Kcal}\cdot\text{mol}^{-1}$.⁶⁴

We found that intermediate **3.A2**, formed by *5-exo-dig* cyclization, is an intermediate structure between an open carbocation and a more closed cyclopropyl-gold(I)-carbene which is in equilibrium with cyclic bromonium **3.A2b** as observed previously with gold(I)-catalyzed cycloadditions of haloalkynes with alkenes² (Figure 3.4). In this case, no vinylidene intermediate was found to mediate the subsequent transformations (see Scheme 3.10).

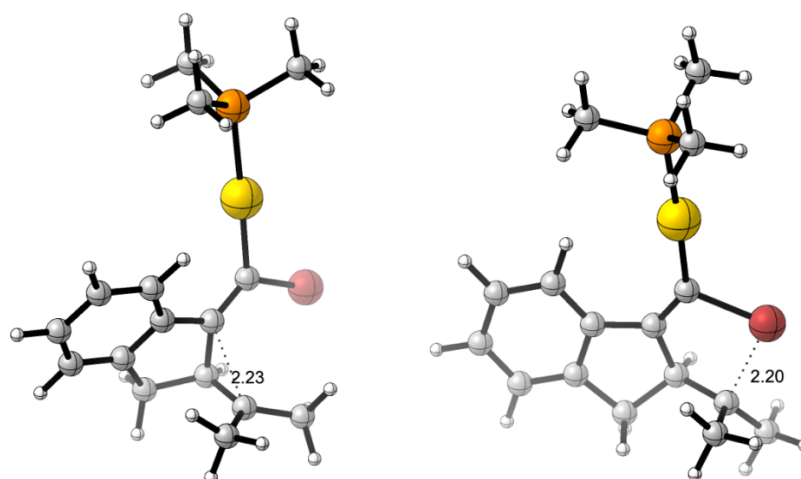
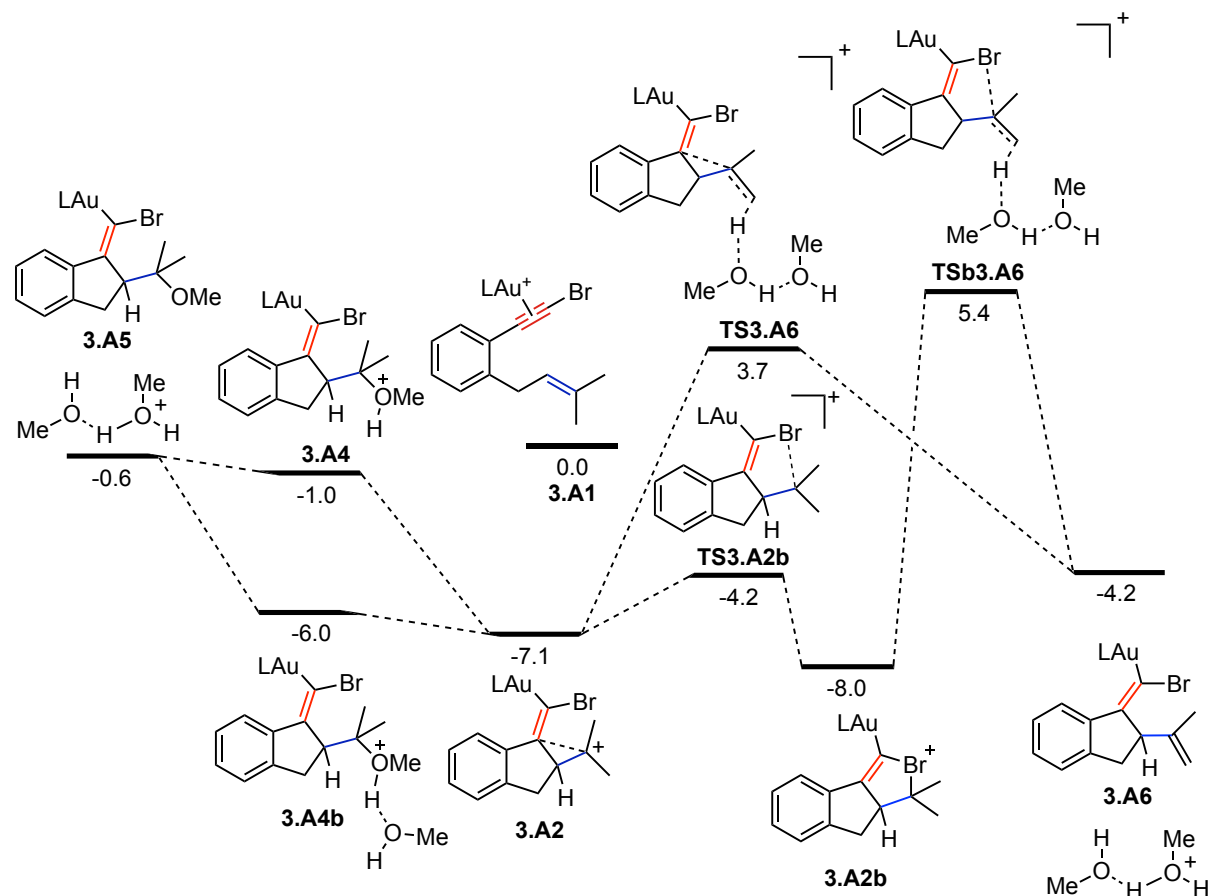


Figure 3.4. Structures of intermediate **3.A2** (left) and **3.A2b** (right). Bond distances in Å.

⁶⁴ Calculations performed by Eduardo García-Padilla

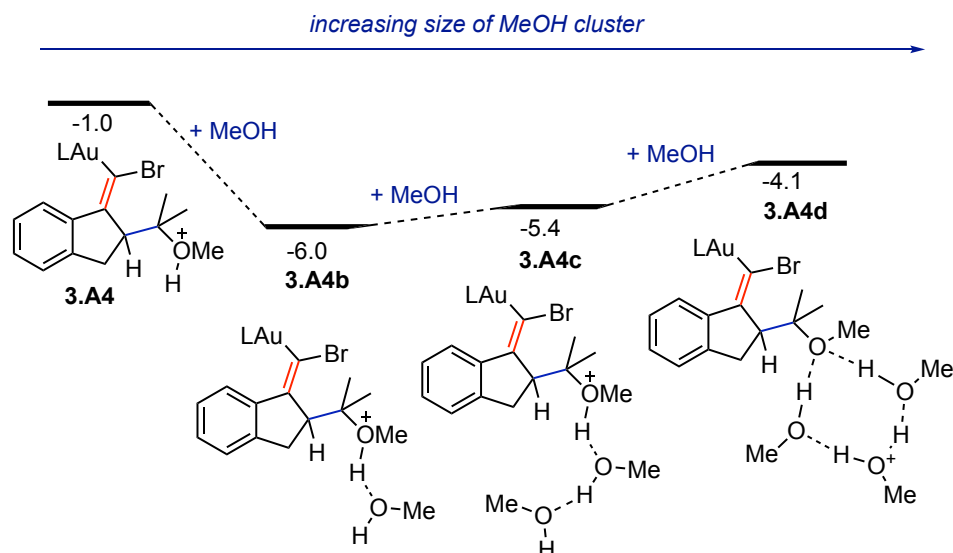
Two elimination processes can now originate which give rise to the same cycloisomerization product **3.A6**: a direct elimination from **3.A2** through transition state **TS3.A6** or E2 elimination (only type of allowed elimination due to sterics) from bromonium **3.A2b**, through **TSb3.A6**, the former being more favored than the latter (Scheme 3.33). As for the nucleophilic attack, methanol, if treated as a monomer, would attack **3.A2** to form **3.A4** but this high energy intermediate would immediately dissociate a molecule of methanol to form the cation back in a barrierless way (Scheme 3.33). This might happen due to a charge build-up on the oxygen atom of the alcohol, so we evaluated higher order clusters in which the positive charge could be more delocalized.



Scheme 3.33. Methanol-mediated nucleophilic attack vs elimination starting from cyclopropyl gold(I) carbene **3.A2** to afford **3.A5** and **3.A6**. Free energy in Kcal·mol⁻¹ at B3LYP-D3/6-311G+(d,p) + SDD, PCM.

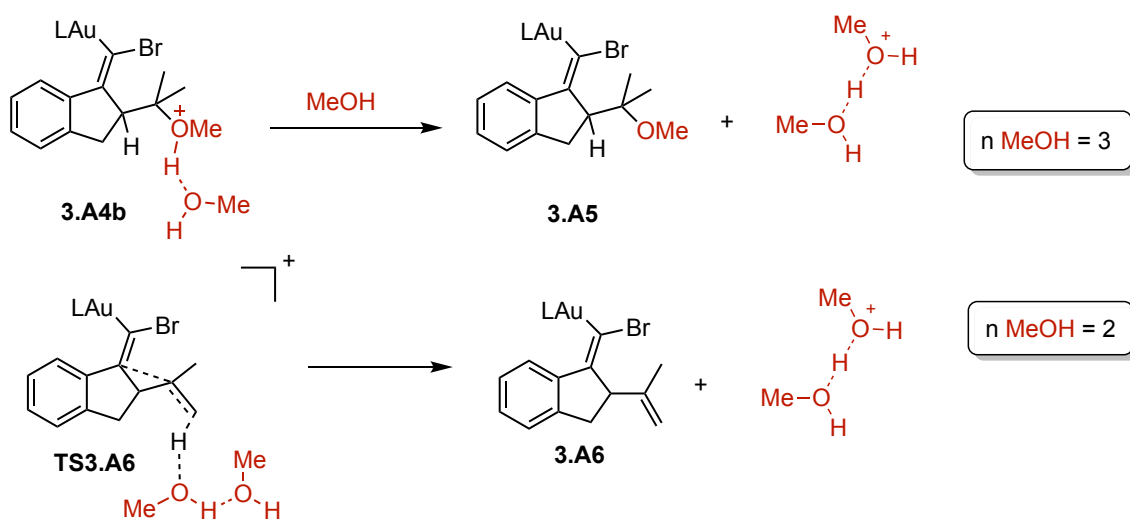
As shown in Scheme 3.34 below, having methanol dimer attacking **3.A2** resulting in intermediate **3.A4b**, appeared to be the most favored option. Despite efforts, we could not find the transition state to deprotonate alkoxy cyclization intermediate **3.A4b** to give **3.A5** (Scheme 3.33) pointing to the possibility of a barrierless transformation.

Given the diverse array of methanol-containing entities available, numerous almost isoenergetic pathways likely coexist. Having only a simple dimer of methanol involved in the transition state towards **3.A5**, would imply the strongly disfavored decoordination of [MeOH₂]⁺. As we saw that protonated methanol primarily exists in CH₂Cl₂ as a tetramer, we assume that higher-order clusters are required for the complete alkoxy cyclization pathway compared to elimination.



Scheme 3.34. Comparison of the relative stability of alkoxyacyclization intermediates depending on the number of coordinated methanol molecules. Free energy in $\text{Kcal}\cdot\text{mol}^{-1}$ at B3LYP-D3/6-311G+(d,p) + SDD, PCM.⁴²

This would, at a minimum, involve a trimer, where one methanol forms the methyl ether product and two more solvate the residual proton. In contrast, elimination only requires a minimum of two molecules to stabilize the proton from deprotonation. (Scheme 3.35)

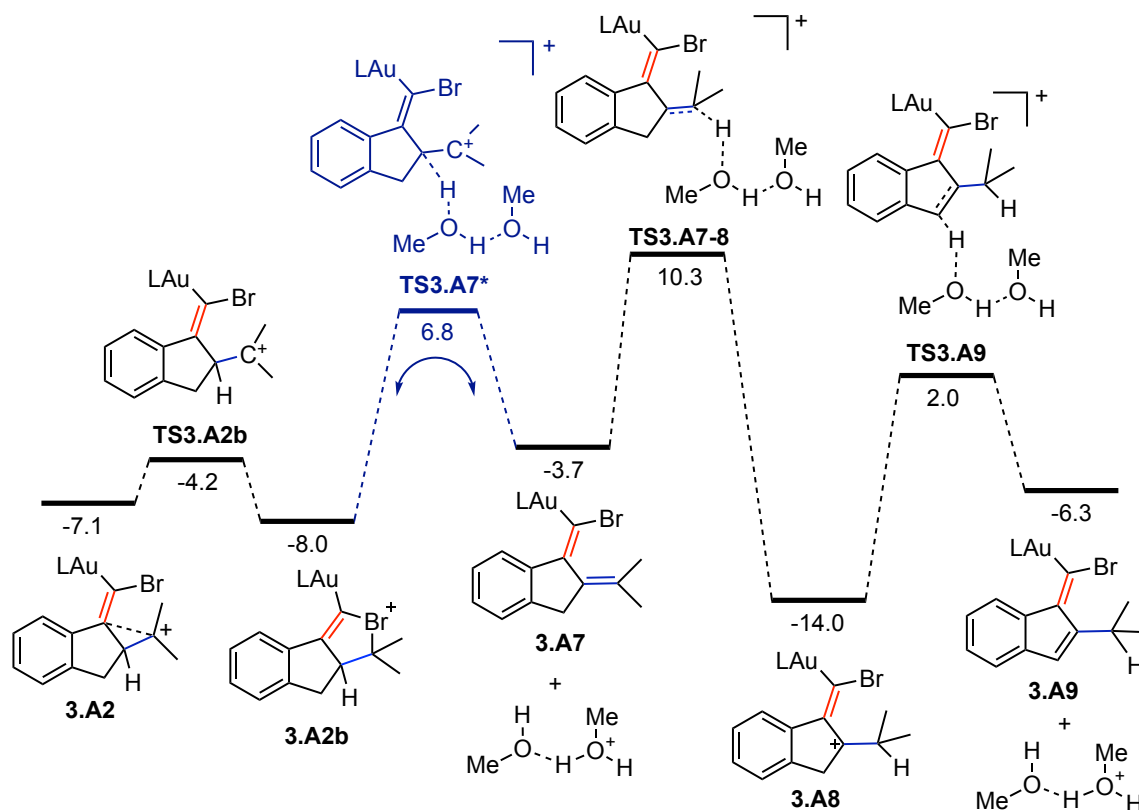


Scheme 3.35. Minimum number of methanol molecules required to mediate the nucleophilic attack to afford **3.A5** and elimination to afford **3.A6** according to our model.

Once assessed the model for nucleophilic attack to form alkoxyacyclization product **3.133a** and alcohol-mediated deprotonation to form cycloisomerization product **3.137**, our goal was to rationalize the the difference found in enantiomeric ratios for these two species.

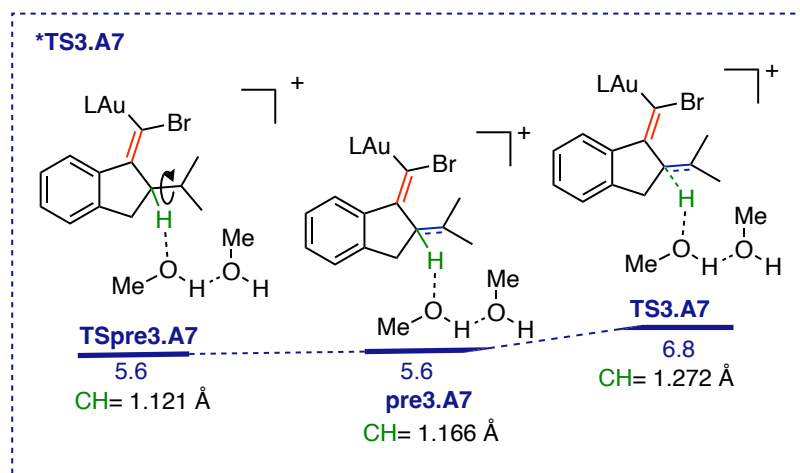
As anticipated (Scheme 3.24) two initial possibilities were considered: a reversible deprotonation at the chiral carbon center or a 1,2-H shift from this carbon to newly formed carbocation as a result of the 5-*exo-dig* cyclization.

We started ruling out the deprotonation pathway with the first experimental evidence given by deuterium labeling: the absence of deuterium scrambling is already a first strong proof that no such mechanism can operate (Scheme 3.28). We then decided to corroborate with result with calculations, modeling the deprotonation pathway (Scheme 3.36).



Scheme 3.36. Discarded racemization pathway through reversible deprotonation in the bromoenyne cyclization. Free energy in $\text{Kcal}\cdot\text{mol}^{-1}$ at B3LYP-D3/6-311G+(d,p) + SDD, PCM.

We found that deprotonation **TS3.A7** is actually constituted by a multistep process consisting of **TSpre3.A7** that leads to high-energy intermediate **pre3.A7**, which after rotation around the isopropyl bond affords **pre3.A7** and finally **TS3.A7** (Scheme 3.37 below). Since overall **TS3.A7** is $3.1 \text{ Kcal}\cdot\text{mol}^{-1}$ higher than the direct elimination from **3.A2** (**TS3.A6**, Scheme 3.33) and since both the direct elimination and deprotonation pathway need two molecules of methanol to happen, **TS3.A7** results to be disfavored thermodynamically and entropically not advantageous with respect to **TS3.A6** (Scheme 3.36). Furthermore, even if formed, **3.A7** would undergo rapid protodeauration, a barrierless process for a neutral intermediate, yet the resulting diene product was never observed experimentally. Alternatively, **3.A8** could be generated from **3.A7**, but the deprotonation **TS3.A9** would be significantly more favorable than the reverse reaction (by $8.3 \text{ Kcal}\cdot\text{mol}^{-1}$), as both processes involve a methanol dimer. Also in this case, the diene resulting from **3.A9** was never detected experimentally. All these considerations, exclude from our hypothesis the reversible deprotonation as a racemization pathway.



Scheme 3.37. Dissection of **TS3.A7** in two additional species. Free energy in $\text{Kcal}\cdot\text{mol}^{-1}$ at B3LYP-D3/6-311G+(d,p) + SDD, PCM.

We then moved to considering the other hypothesized pathway, the 1,2-H shift through **TS3.A2b-8** (Scheme 3.38a). We found this shift to originate from the cyclic bromonium **3A2b** through a so called “hidden” intermediate^{62,65} which was found by analysis of the IRC (Figure 3.5) and is common to both **TS3.A2b** and **TS3.A2b-8**. This hidden intermediate is a non-stationary geometry which varies from **TS3.A2b** essentially just by the angle labeled as α in Scheme 3.38, which needs to be wider to favor the 1,2-H shift. Confronting Figure 3.5 (right) with Figure 3.4 (left) it is in fact possible to notice the rotation of the isopropyl group which occurred to allow the hydride migration by orbital alignment. This species doesn’t correspond to a downhill bifurcation point, but rather to an intermediate geometry that relaxes in a barrierless manner. **TS3.A2b-8** lies about $3 \text{ Kcal}\cdot\text{mol}^{-1}$ higher in energy than the elimination transition states **TS3.A6** and **TSb3.A6** (Scheme 3.33), making it energetically accessible at lower methanol concentrations. Furthermore, since this intramolecular shift operates without the need for methanol, it is entropically more likely than intermolecular deprotonation **TS3.A7** and every other quenching pathway that requires alcohol participation (Scheme 3.36).

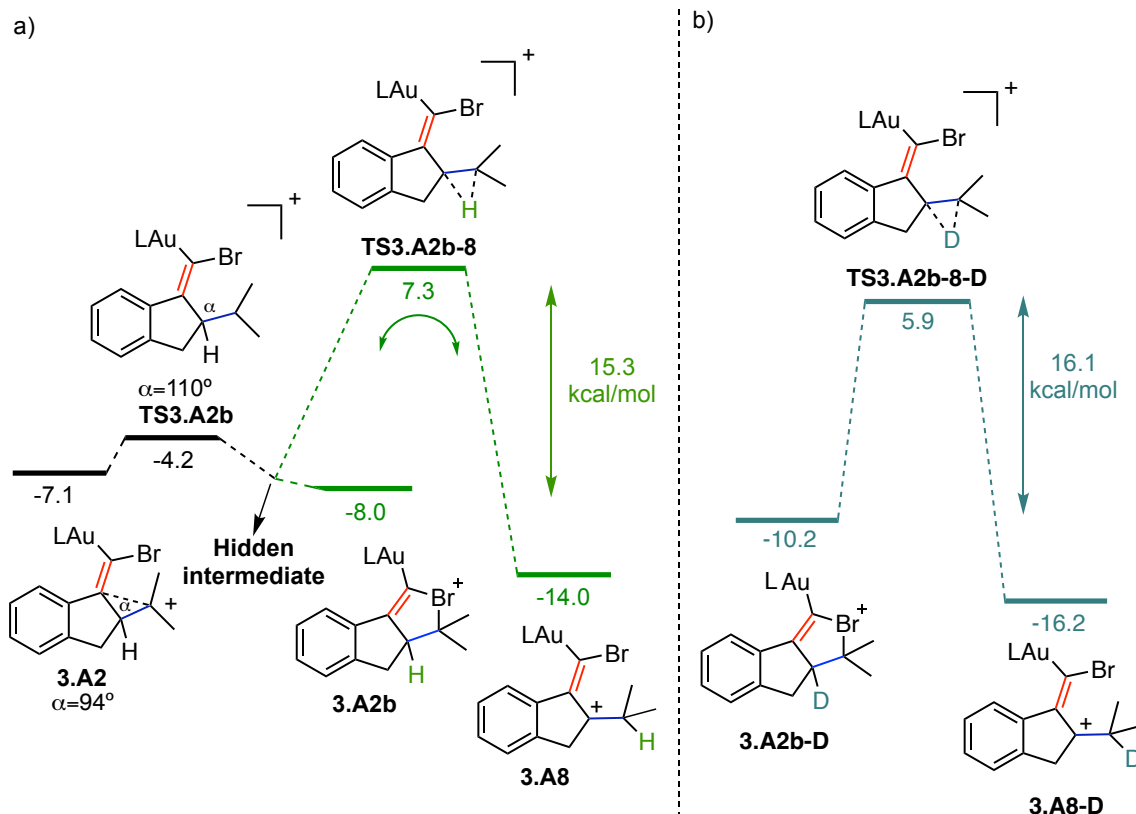
While 1,2-H shifts are typically irreversible processes, some instances of reversible hydride shifts exist,⁶⁶ including the racemization of a stereogenic sp^3 carbon atom.⁶⁷ This would be in accordance with experimental results with the deuterated substrate, showing a slight diminished racemization in the cyclization of **3.132a^D** (Scheme 3.28), consistent with the slower rate in the migration of the heavier deuterium atom. We therefore calculated the 1,2-hydride shift racemization barrier for the deuterium-labeled bromoenyne by modeling **TS3A2b-8-D** (Scheme 3.38b). The ΔG^\ddagger , at $16.1 \text{ Kcal}\cdot\text{mol}^{-1}$, results

⁶⁵ a) Kraka, E.; Cremer, D., Computational Analysis of the Mechanism of Chemical Reactions in Terms of Reaction Phases: Hidden Intermediates and Hidden Transition States, *Acc. Chem. Res.* **2010**, *43*, 591–601. b) Roca-López, D.; Polo, V.; Tejero, T.; Merino, P., Understanding Bond Formation in Polar One-Step Reactions. Topological Analyses of the Reaction between Nitrones and Lithium Ynolates, *J. Org. Chem.* **2015**, *80*, 4076–4083.

⁶⁶ Hudson, H. R.; Koplick, A. J.; Poulton, D. J. Competitive 1,2- and 1,3-Hydride Shifts in the Thermal Decomposition of N-Alkyl Chloroformates. *Tetrahedron Lett.* **1975**, *16*, 1449–145299.

⁶⁷ Shapirot, S.S.; Dennis, D. Lactic Acid Racemization in Clostridium butylicum. Evidence for a Direct Internal Hydride Shift, *Biochemistry*, **1965**, *4*, 2283–2288

0.8 Kcal·mol⁻¹ higher than with ¹H (15.3 Kcal·mol⁻¹), consistent with the slower racemization observed experimentally.



Scheme 3.38 a) Racemization pathway for **3.A2** through a reversible 1,2-H shift. b) Comparison with 1,2-D shift. Free energy in Kcal mol⁻¹ at B3LYP-D3/6-311G+(d,p) + SDD, PCM.

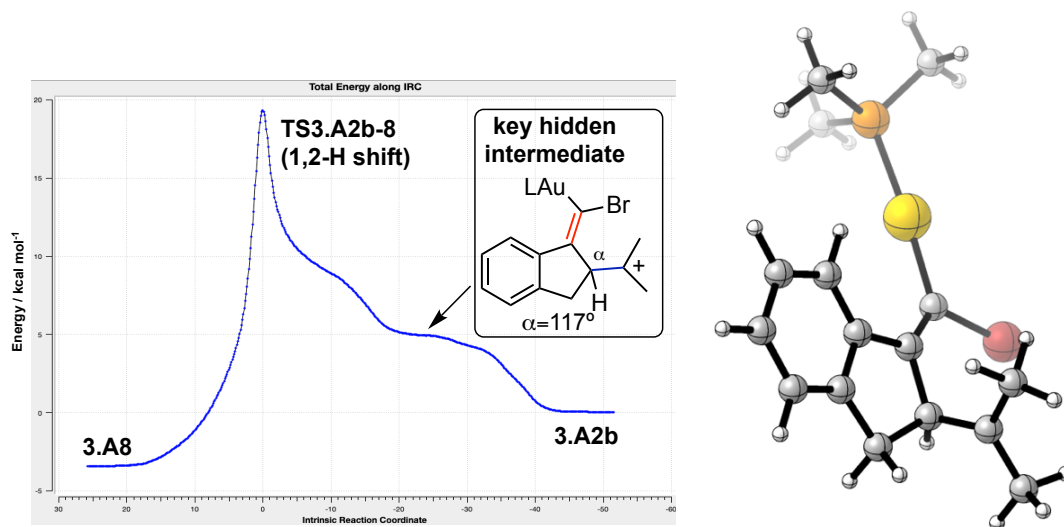
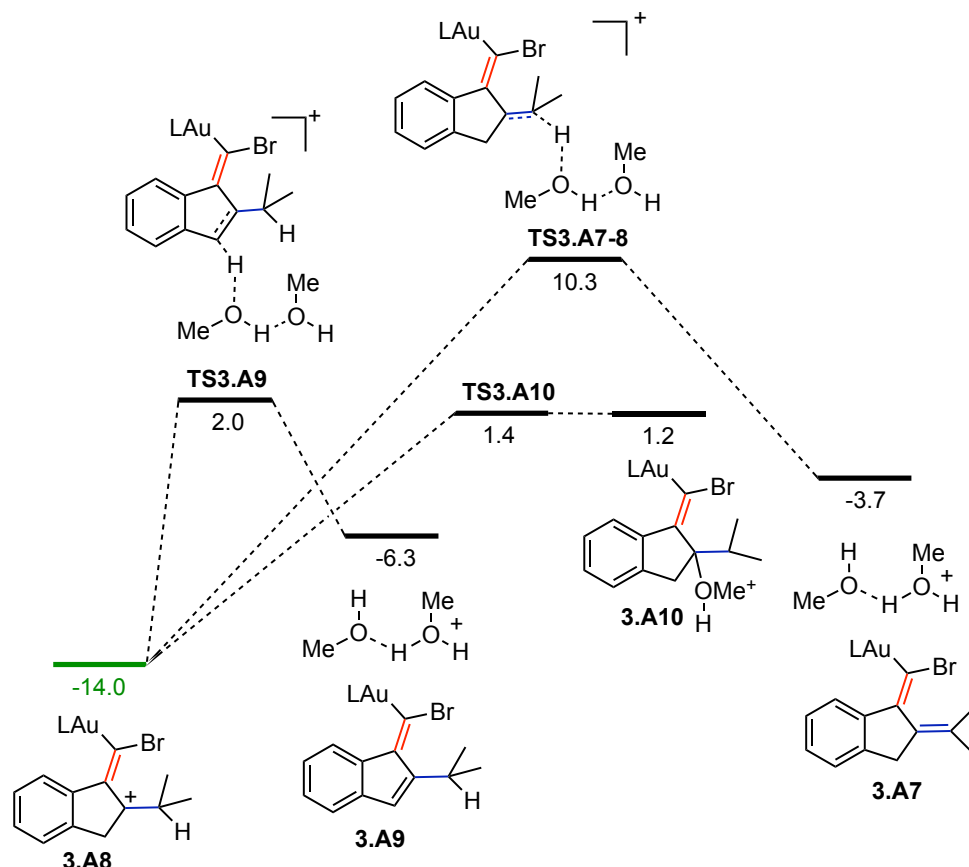


Figure 3.5 IRC plot for **TS3A2b-8**. (left). Computed structure for the hidden intermediate (right).

After having established the feasibility of the 1,2-H shift process, it was important to study what pathways could arise from intermediate **3.A8** once formed (Scheme 3.39). Deprotonation at the stereogenic center to form diene **3.A7** presents a 24.3 Kcal·mol⁻¹ barrier when starting from **3.A8**, which is higher than the reverse shift to give **3.A2b** back (21.3 Kcal·mol⁻¹, Scheme 3.38a). Nucleophilic attack

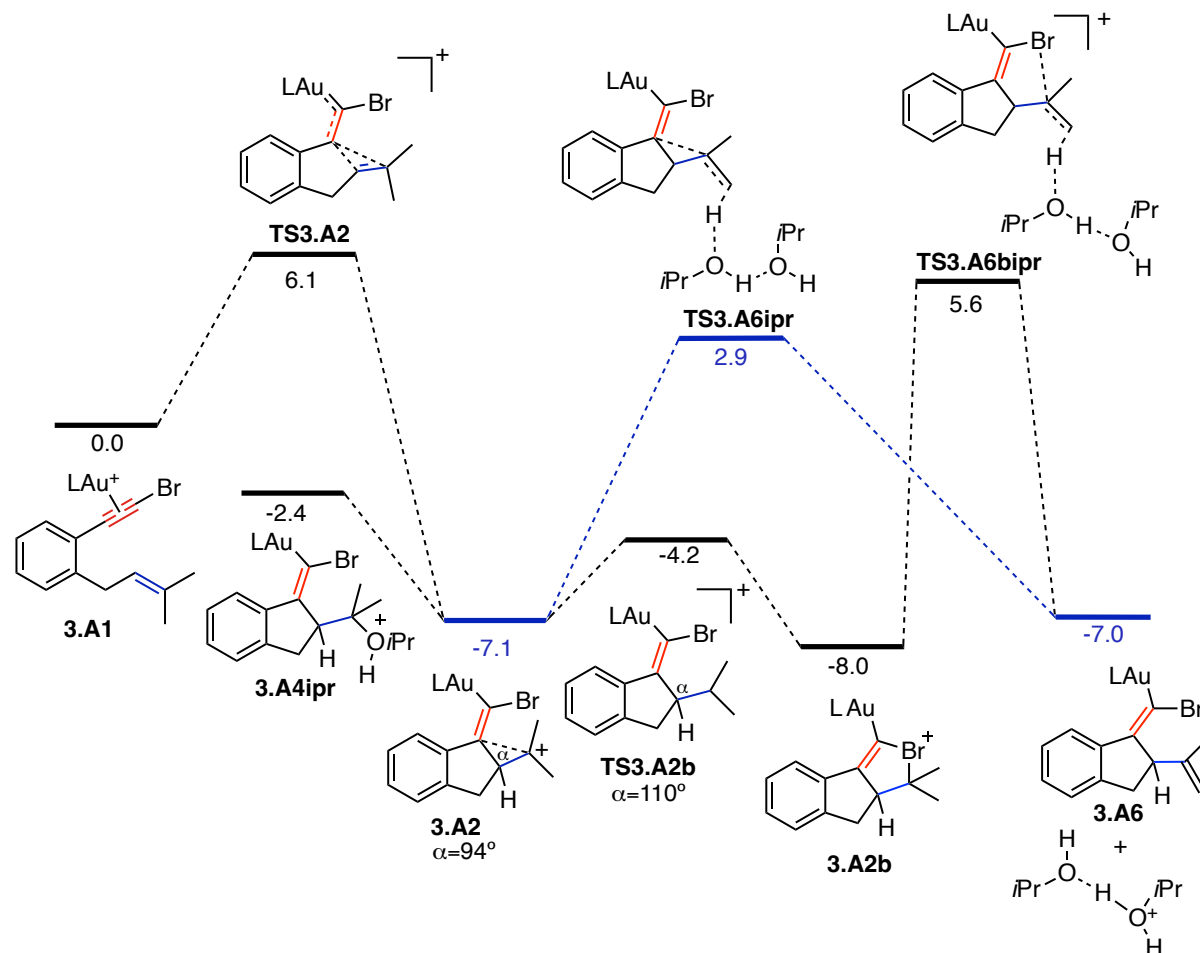
on the tertiary carbocation to afford **3.A10** through **TS3.A10** presents a nearly inexistent barrier for methanol dissociation to form **3.A8** again. Finally, benzylic deprotonation may appear competitive initially, but at low enough methanol concentrations where **TSA2b-8** is accessed and entropically favored, the reversibility of the intramolecular hydride shift becomes plausible. Additionally, we never detected experimentally any of the products that could be generated from the intermediates shown in Scheme 3.39.



Scheme 3.39. Outcompeted quenching pathways that require methanol. Free energy in Kcal·mol⁻¹ at B3LYP-D3/6-311G+(d,p) + SDD, PCM.

The disparity in enantiomeric ratios between products **3.133a** and **3.137** (modeled through the precursors **3.A5** and **3.A6**) can now be fully understood. At lower concentrations of methanol, elimination is favored because it requires few molecules of methanol to complete the catalytic cycle (as opposed to the alkoxyxycyclization which need higher-order methanol oligomers). Simultaneously, the 1,2-hydride shift becomes competitive resulting in the observed racemization. At higher concentration of methanol, alkoxyxycyclization happens at a much faster rate than 1,2-hydride shift or than elimination (lower energetic barrier) leading to fully enantioenriched compounds. The alkoxyxycyclized product **3.A5** can undergo methanol dissociation in a barrierless process, whereas this reversibility is less facile for the elimination one **3.A6**. This racemization has a more pronounced impact on the elimination products, as at lower methanol concentrations, the alkoxyxycyclization products are less likely to reform. These results align with experiments in the presence of HFIP (Table 3.7, entry 11), which yielded

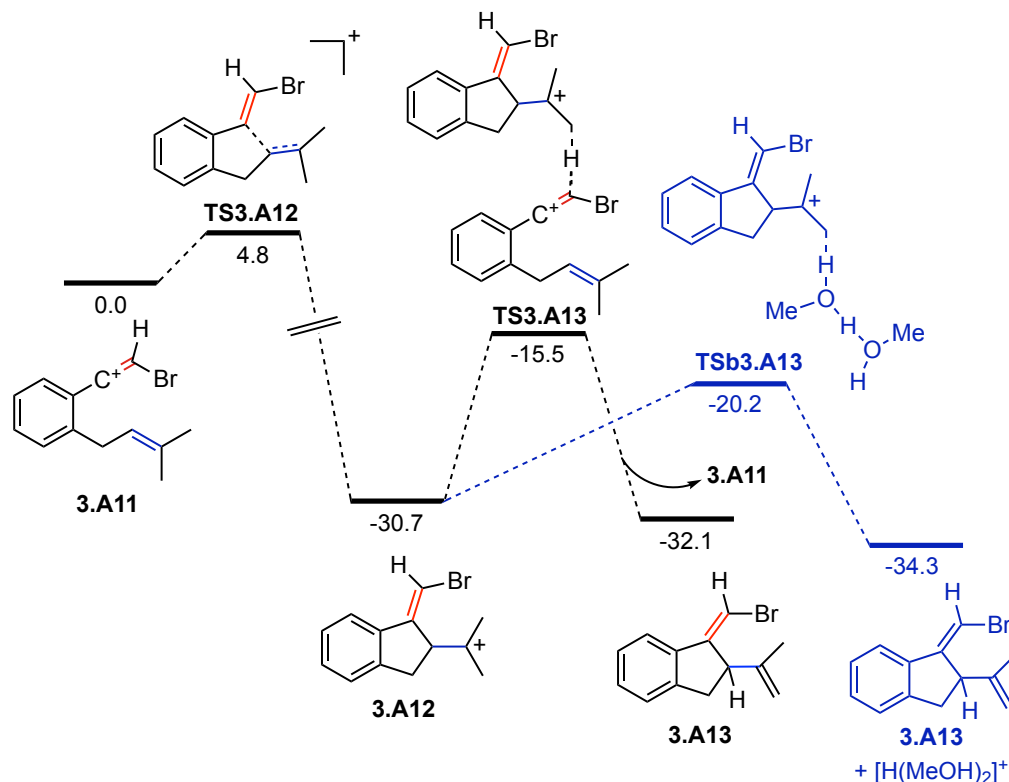
enantioenriched elimination products by outcompeting the 1,2-H shift with an alternative proton shuttle. Additionally, the use of more basic isopropanol, favoring elimination, resulted in higher enantiomeric ratios (Table 3.7, entries 9-10). This observed pattern was supported by additional computational studies which see a lower (0.8 Kcal·mol⁻¹) barrier for the elimination step **TS3.A6ipr** compared to **TS3.A6** (Scheme 3.40).



Scheme 3.40. Gold(I)-catalyzed alkoxy cyclization and cycloisomerization pathways of bromoenyne complex **3.A1** with isopropanol-mediated nucleophilic attack or elimination. Free energy in Kcal·mol⁻¹ at B3LYP-D3/6-311G+(d,p) + SDD, PCM.

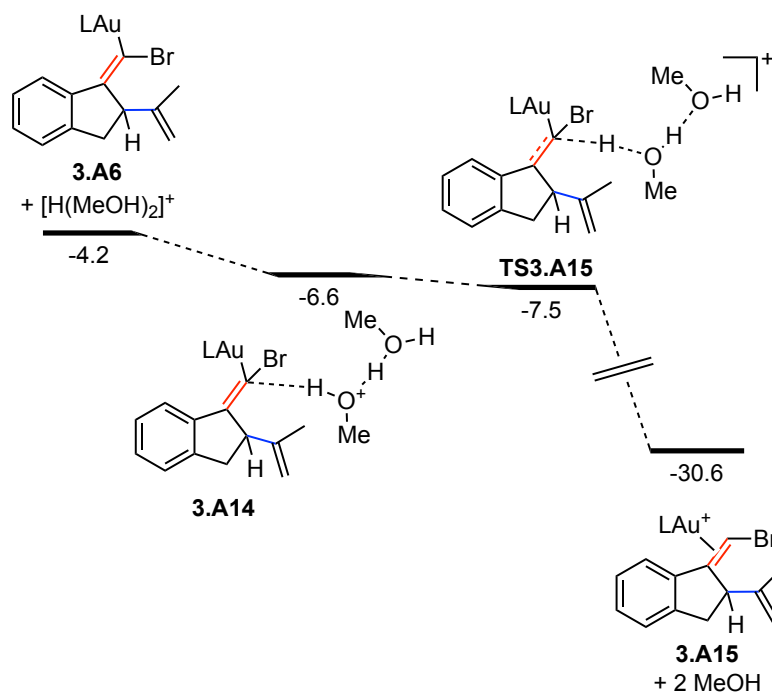
As anticipated in the experimental session, we also wanted to exclude the possibility of a proton-catalyzed pathway which could coexist with the gold(I)-catalyzed transformation and serve as an explication for the observed racemic product formation. Brønsted acid participation has been identified in the isomerization process of gold(I)-catalyzed products: the acidic protons involved are well-known to originate from cationic intermediates like **3.A2** or **3.A2b**.^{50b} However, it remained unclear whether these protons could catalyze cycloisomerizations similar to gold(I). Calculations for the Brønsted acid-catalyzed cyclization revealed low barriers for cyclization (**TS3.A12**) and moderately high barriers for proton transfer to the next enyne (**TSA13**) (Scheme 3.41).⁶⁴ Nevertheless, the viability of this catalytic cycle does not solely hinge on the accessibility of transition states at room temperature, since the reaction medium has the ability to intercept most of these extremely acidic intermediates. The presence

of trace amounts of water, alcohol or any suitable proton shuttles that could preferentially undergo protonation can halt the catalytic cycle (Scheme 3.41, pathway depicted in blue). According to relative energies, as little as 10 mol% of methanol (or water) would completely deprotonate these structures. Moreover, proton catalysis would likely result also in the formation of the *Z* isomer of **3.A13**, apart from the *E*. This is because no significant steric or electronic factors would hinder *Z*-type reactivity compared to gold(I) catalysis. However, experimentally, this product was never observed.



Scheme 3.41. Mechanism of the proton-catalyzed cyclization of bromoenynes. In blue, methanol model for side-deprotonations. Free energy in Kcal·mol⁻¹ at B3LYP-D3/6-311G+(d,p) + SDD, PCM.⁶⁴

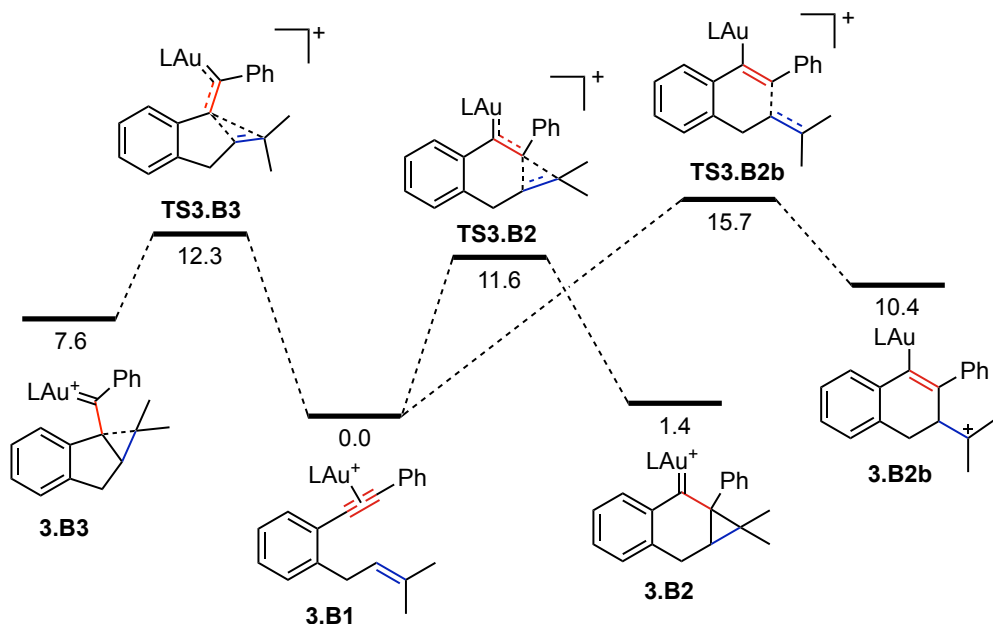
Another aspect to take in consideration is that if **3.A12** should ever form, its extreme acidity or the one of other protonated organic fragments/traces of methanol or water, would easily facilitate the protodeauration of the catalyst, as the process lacks any barriers, and therefore always favor the gold(I)-catalyzed pathway over the proton catalyzed one (Scheme 3.42). Following these computational results together with our experimental evidence (Scheme 3.27) we can deduce that the Brønsted acid-catalyzed pathway is not in competition under the given reaction conditions and cannot be attributed as a cause to the racemized product formation.



Scheme 3.42. Mechanism of protodemetalation of a model vinylgold(I) intermediate. The potential energy of intermediate **3.A14** is lower than that of **TS3.A15**. Free energy in Kcal·mol⁻¹ at B3LYP-D3/6-311G+(d,p) + SDD, PCM.⁶⁴

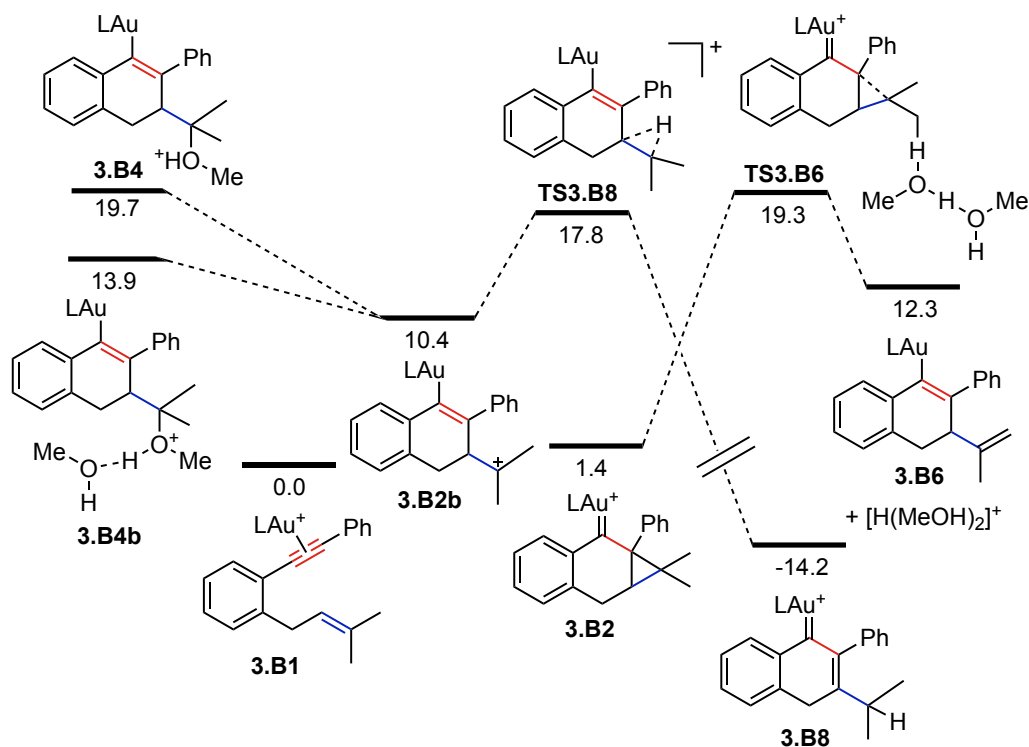
We subsequently investigated analogous reactions with 1-phenyl-1,6-enyne **3.139**.⁶⁴ This substrate experimentally showed to be selective towards the *6-endo-dig* cyclization (Table 3.10), which was confirmed by DFT calculations (Scheme 3.43) where we can see **TS3.B2** as the most favored pathway (the small preference seen computationally against the full selectivity seen experimentally can be reconducted to stereoelectronic effects of the ligand). **TS3.B2b** provides access to open vinylgold(I) **3.B2b**, which is possibly in direct equilibrium with the more favored cyclopropyl-gold(I) carbene **3.B2**, but this pathway was not investigated.

As anticipated, when operating in the absence of nucleophiles, the isolation of the naphthalene compound **3.166**, in this case, and **3.156** in the case of methyl-1,6-enyne **3.153**, hint to the involvement of a 1,2-H shift process in the mechanism, presumably starting from intermediate **3.B2b**. However, by cyclizing 1-phenyl-1,6-enyne **3.139** under the standard reaction conditions in the presence of methanol, we could see that no racemization was observed for the cycloisomerization product **3.165** compared to the alkoxy cyclization **3.164** (Table 3.10, entries 4-5). The 1,2-H shift pathway should therefore be inaccessible or be irreversible and therefore not result in racemization.



Scheme 3.43. Competition between 5-*exo*-dig and 6-*endo*-dig barriers with gold(I) phenylacetyne complex **3.B1**. Free energy in Kcal·mol⁻¹ at B3LYP-D3/6-311G+(d,p) + SDD, PCM.⁶⁴

In contrast to haloenynes, the 1,2-H shift through **TS3.B8** results to be indeed irreversible, requiring 32 Kcal·mol⁻¹ to return from **3.B8** (Scheme 3.44).



Scheme 3.44. Methanol-mediated nucleophilic attack/elimination and 1,2-H shift originating from 6-*endo*-dig cyclization products **3.B2-3.B2b**. Free energy in Kcal·mol⁻¹ at B3LYP-D3/6-311G+(d,p) + SDD, PCM.⁶⁴

The barrier for 1,2-H shift is comparable to the one for elimination **TS3.B6**, therefore, under dry conditions, **3.B8** can be easily formed and its deprotonation-protodeauration would, as observed

experimentally, afford 2-phenyl-3-isopropyl-naphthalene **3.166**. This provides further evidence supporting the involvement of 1,2-H shifts in gold(I)-catalyzed cyclizations.

The same racemization pathways, involving deprotonation (**TS3.A7** of the bromoenyne), were also calculated for the phenyl-enyne, as well as deprotonations from open-form **3.B2b**. However, these pathways were determined to be non-competitive. Additionally, the competitive and non-competitive mechanisms were examined for chloroenyne and methylenyne substrates, behaving similarly to their analogs, and are excluded from the present discussion.⁶⁴

Conclusions

The first enantioselective gold(I)-catalyzed alkoxy cyclization of 1-bromo-1,6-enynes has been developed using a modified JohnPhos ligands with a distal C₂-2,5-diarylpyrrolidine. Different haloenynes could be cyclized in the presence of alcohols and the synthetic utility of the bromide functionality in the 5-membered-ring products was demonstrated by further functionalization.

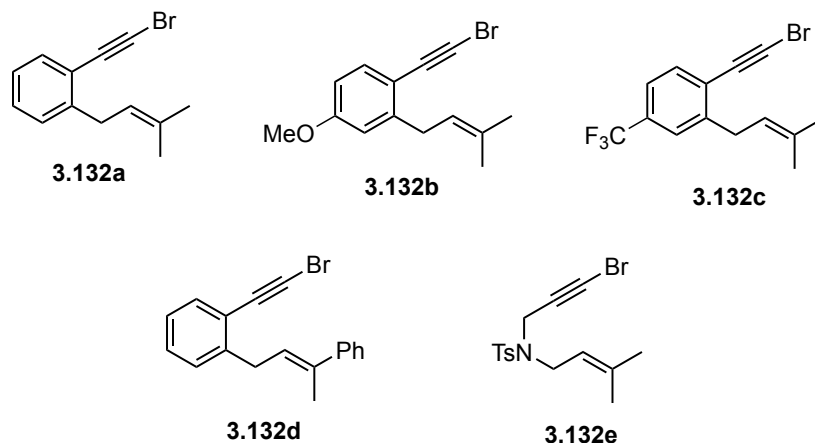
Experimental and computational studies highlight an unprecedented reversible 1,2-H shift as a key racemization process for the cycloisomerization product formed during the reaction. At lower methanol concentrations, elimination is favoured due to the fewer methanol molecules required to complete the catalytic cycle. Concurrently, the 1,2-H shift becomes competitive, resulting in observed racemization. Conversely, at higher methanol concentrations, alkoxy cyclization occurs at a much faster rate than the 1,2-H shift or elimination, given its lower energetic barrier, leading to fully enantioenriched compounds.

While Cl-substituted enynes behave as the *Br*-substituted analogues, methyl- or phenyl-enynes exhibit an irreversible 1,2-H shift, preventing racemization. This is consistent with the experimentally detected naphthalenes formed under anhydrous conditions.

These findings provide a new comprehensive understanding of gold(I)-catalyzed alkoxy cyclizations, presenting an accurate model for the first time.

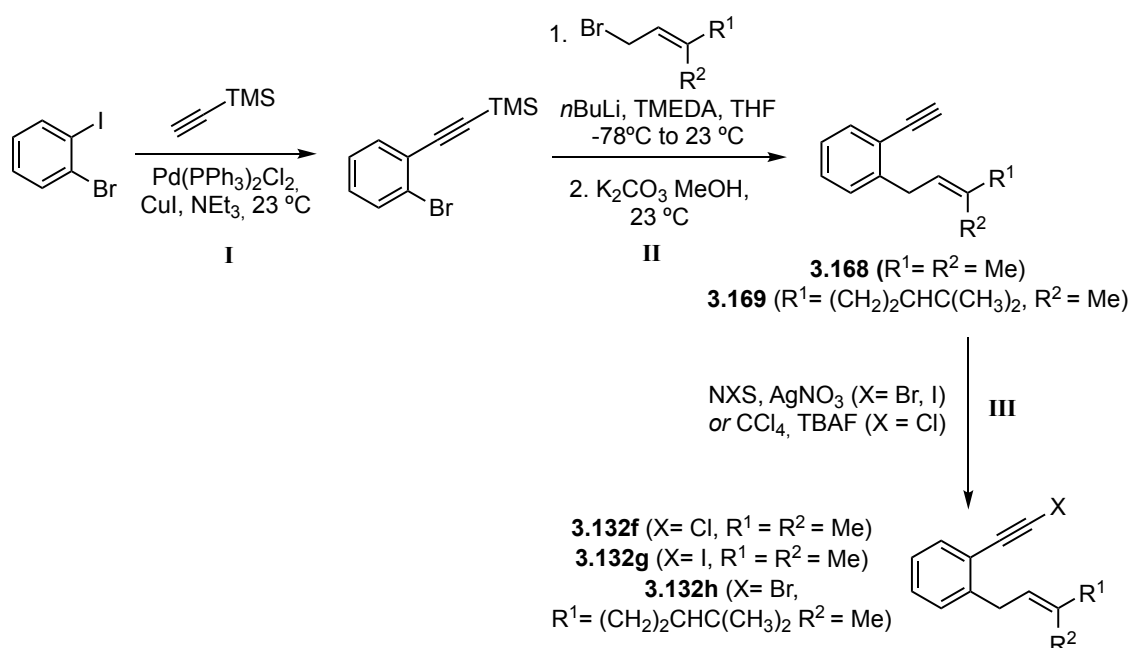
Experimental Part

The **General Information** is provided in the Experimental Part of **Chapter I**. All reagents were used as purchased, with no further purification. The characterization of **3.132a-e** listed below is reported in **Chapter I**.⁴⁸ The spectral analysis is in accordance with the reported data.



Synthetic Procedures and Characterization Data

General procedure A for the synthesis of 1-halo-6-enynes 3.132f-h



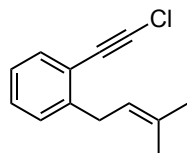
Step I-II: Precursors **3.168-3.169** were prepared according to literature procedure.³⁷

Step III: **3.132f** was prepared by adding TBAF·3H₂O (0.1 equiv) to a solution of **3.168** (equiv) in CCl₄ (1.7 M)⁶⁸ which was then left to stir 6 h at 23 °C and quenched by the addition of water. **3.132g,h** were instead prepared by dissolving **3.168-3.169** (1 equiv) in acetone (0.05 M) and by adding NXS ($X = \text{Cl}$, Br; 1.1 equiv) and AgNO₃ (0.2 equiv) to the resulting solution which was then stirred for 2 h at 23 °C

⁶⁸ Zeng, X.; Tu, Y.; Zhang, Z.; You, C.; Wu, J.; Ye, Z.; Zhao, J. Transition-Metal-Free One-Step Synthesis of Ynamides. *J. Org. Chem.* **2019**, *84*, 4458–4466.

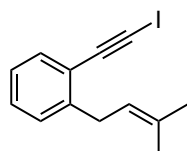
and quenched by the addition of water. For **3.132f-h** extraction of the aqueous phase in pentane (x3) was followed by the addition of brine to the organic phase which was finally dried with anhydrous Na₂SO₄. The crudes were purified by flash column chromatography.

1-(Chloroethynyl)-2-(3-methylbut-2-en-1-yl)benzene (3.132f)



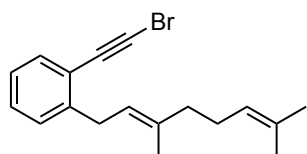
3.132f was synthesized following general procedure A. The pure product was isolated by flash column chromatography purification on silica gel (pentane), as a yellow oil (750 mg, 6.00 mmol, 61%). ¹H NMR (500 MHz, CDCl₃) δ 7.45 (dt, *J* = 7.7, 1.3 Hz, 1H), 7.33 – 7.26 (m, 1H), 7.22 (dd, *J* = 7.6, 1.4 Hz, 1H), 7.16 (td, *J* = 7.5, 1.4 Hz, 1H), 5.32 (ddq, *J* = 8.8, 5.8, 1.4 Hz, 1H), 3.53 (d, *J* = 7.4 Hz, 2H), 1.79 (d, *J* = 4.7 Hz, 6H). ¹³C NMR (126 MHz, CDCl₃) δ 144.5, 133.1, 132.8, 128.9, 128.6, 125.9, 122.3, 121.6, 71.3, 68.5, 33.1, 25.9, 18.0. HRMS (APCI+): *m/z*: calculated for C₁₃H₁₂Cl: 203.0622 [M-H]⁺; found: 203.0617.

1-(Iodoethynyl)-2-(3-methylbut-2-en-1-yl)benzene (3.132g)



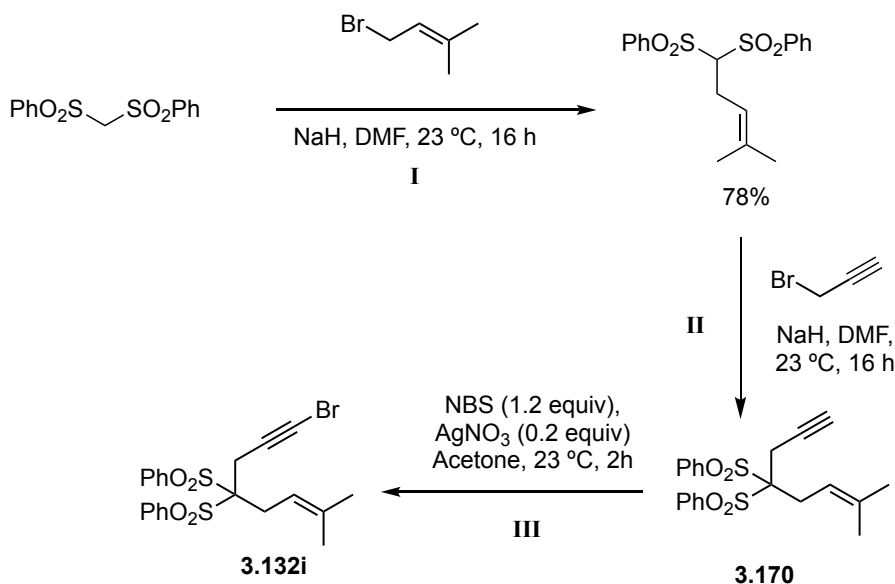
3.132g was synthesized following general procedure A. The pure product was isolated by flash column chromatography purification on silica gel (pentane), as a yellow oil (450 mg, 2.11 mmol, 72%). ¹H NMR (500 MHz, CDCl₃) δ 7.41 (dd, *J* = 7.7, 1.4 Hz, 1H), 7.29 – 7.22 (m, 1H), 7.19 (dd, *J* = 7.8, 1.4 Hz, 1H), 7.13 (td, *J* = 7.5, 1.5 Hz, 1H), 5.29 (ddq, *J* = 8.8, 5.9, 1.5 Hz, 1H), 3.51 (d, *J* = 7.4 Hz, 2H), 1.76 (s, 6H). ¹³C NMR (126 MHz, CDCl₃) δ 144.9, 133.2, 129.1, 128.5, 125.7, 122.9, 122.3, 93.3, 77.4, 33.1, 26.0, 18.2, 9.0. HRMS (APCI+): *m/z*: calculated for C₁₃H₁₄I: 297.0135 [M+H]⁺; found: 297.0138.

(E)-1-(Bromoethynyl)-2-(3,7-dimethylocta-2,6-dien-1-yl)benzene (3.132h)



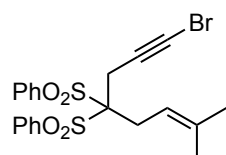
3.132h was synthesized following general procedure A. The pure product was isolated by flash column chromatography purification on silica gel (pentane), as a transparent oil (190 mg, 0.599 mmol, 55%). ¹H NMR (400 MHz, C₆D₆) δ 7.35 (dd, *J* = 7.7, 1.4 Hz, 1H), 7.12 – 7.01 (m, 1H), 6.99 (td, *J* = 7.6, 1.4 Hz, 1H), 6.82 (td, *J* = 7.5, 1.4 Hz, 1H), 5.36 (tq, *J* = 7.3, 1.3 Hz, 1H), 5.17 (ddq, *J* = 8.4, 5.5, 1.4 Hz, 1H), 3.54 (d, *J* = 7.3 Hz, 2H), 2.13 (q, *J* = 7.5 Hz, 2H), 2.09 – 2.02 (m, 2H), 1.66 (s, 3H), 1.62 (s, 3H), 1.52 (s, 3H); ¹³C NMR (101 MHz, C₆D₆) δ 144.8, 136.7, 133.1, 131.3, 129.1, 128.8, 127.9, 126.0, 124.8, 122.7, 79.8, 53.5, 40.1, 33.3, 27.0, 25.9, 17.8, 16.3. HRMS (APCI+): *m/z*: calculated for C₁₈H₂₂Br: 317.0899 [M+H]⁺; found: 317.0894.

Procedure B for the synthesis of 1-bromo-1,6-enyne 3.132i



Step I-II: Precursor **3.170** was synthesized according to literature procedure.⁶⁹

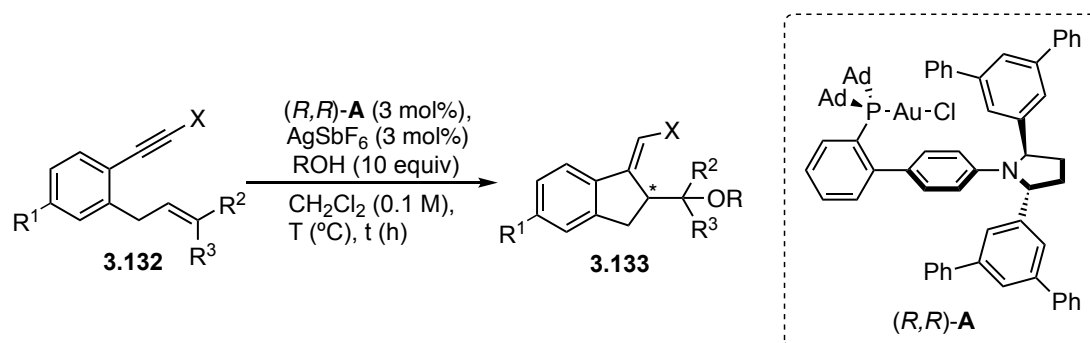
(1-Bromo-7-methyloct-6-en-1-yne-4,4-diyl-disulfonyl)dibenzene (3.132i)



NBS (1.2 equiv) was added to a solution of **3.S3** (1 equiv) in acetone (0.05 M) and the resulting solution was left to stir over 2 h at 23 °C. The reaction was quenched by the addition of water, then, the aqueous phase was extracted in pentane (x3), the organic phase washed with brine and finally dried with anhydrous Na₂SO₄.

The pure product was isolated by flash column chromatography purification of the crude on silica gel (5:1 cyclohexane:EtOAc), as a white solid (229 mg, 0.648 mmol, 73%). **M.p.** 135-143 °C. **¹H NMR** (500 MHz, CDCl₃) δ 8.13 – 8.03 (m, 4H), 7.75 – 7.66 (m, 2H), 7.64 – 7.53 (m, 4H), 5.39 (ddt, *J* = 6.8, 5.4, 1.4 Hz, 1H), 3.22 (s, 2H), 2.99 (d, *J* = 1.3 Hz, 2H), 1.76 (d, *J* = 1.4 Hz, 3H), 1.57 (s, 3H). **¹³C NMR** (126 MHz, CDCl₃) δ 137.7, 136.8, 134.8, 131.6, 128.7, 114.9, 89.1, 77.4, 72.5, 44.5, 28.5, 26.3, 21.9, 18.4. **HRMS** (ESI⁺): *m/z*: calculated for C₂₁H₂₁BrNaO₄S₂: 502.9957 [M+Na]⁺; found: 502.9972.

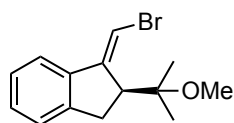
General Procedure C for the enantioselective gold(I)-catalyzed alkoxy-cyclization of 1-bromo-1,6-enynes to afford 3.133



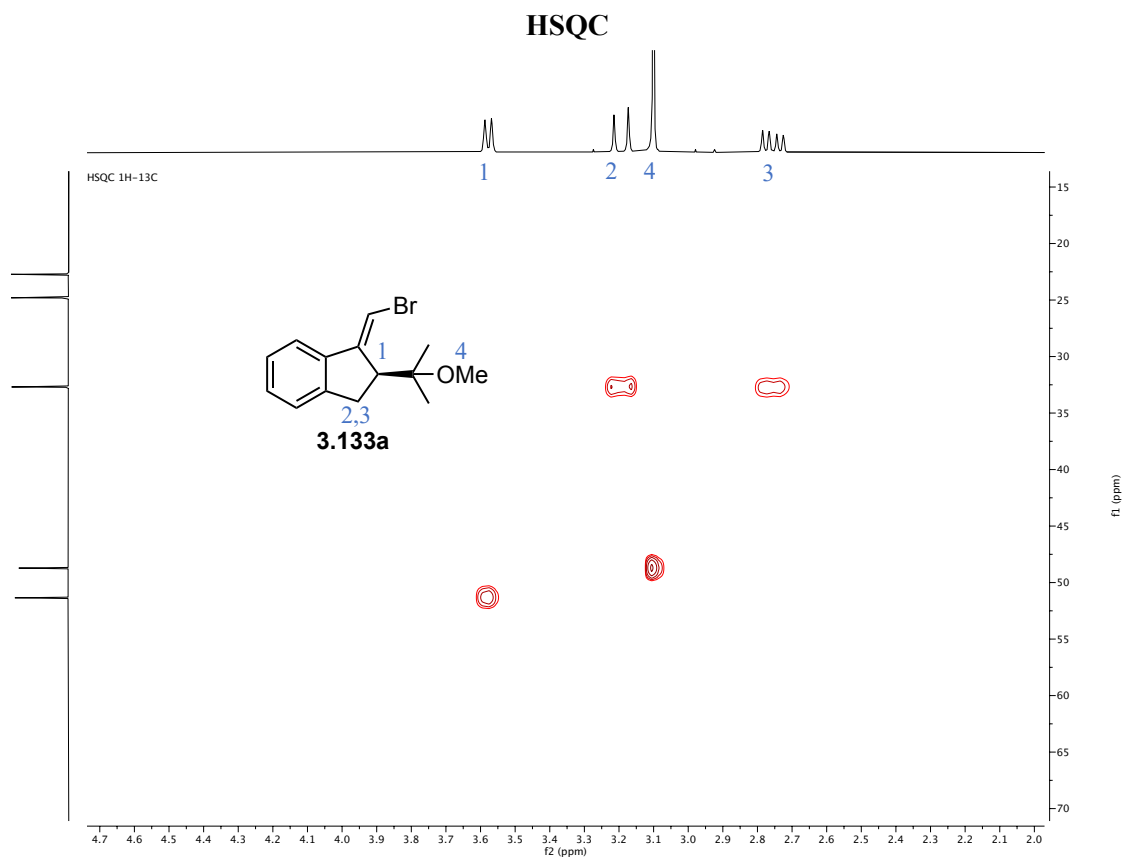
⁶⁹ Muñoz, M. P.; Méndez, M.; Nevado, C.; Cárdenas, D. J.; Echavarren, A. M., Hydroxy- and Alkoxy-cyclizations of Enynes Catalyzed by Platinum(II) Chloride, *Synthesis* **2003**, 2898–2902.

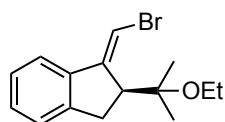
1-Halo-6-enynes of type **3.132** (1 equiv) were weighted in a microwave vial together with gold catalyst (*R,R*)-**A** (3 mol%) and a magnet. The vial was tapped and introduced in the glovebox where dry CH₂Cl₂ (0.1 M) and ROH (10 equiv) were added to it. AgSbF₆ (3 mol%) was weighted in the glovebox in a second vial and dissolved in the minimum quantity of dry CH₂Cl₂. Then, the two vials were taken out of the glovebox, they were both brought to the required temperature (specified below) and finally the solution of AgSbF₆ was added to the first vial. The reaction was left over the time specified below and, once completed (monitored by TLC), three drops of NEt₃ were added to quench it. The crude products were purified by flash column chromatography purification on silica gel or preparative TLC. Some of the NMR of these products were measured in C₆D₆ due to long-term instability in CDCl₃.

(*S,E*)-1-(Bromomethylene)-2-(2-methoxypropan-2-yl)-2,3-dihydro-1*H*-indene (3.133a)

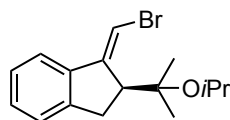


3.133a was synthesized following general procedure **C** performing the reaction at -60 °C for 4 days. The pure product was isolated by preparative TLC (2:1 CH₂Cl₂: cyclohexane), as a transparent oil (27.8 mg, 99.0 μmol, 99%). ¹H NMR (400 MHz, C₆D₆) δ 7.05 – 6.96 (m, 1H), 6.99 – 6.91 (m, 3H), 6.38 (d, *J* = 1.4 Hz, 1H), 3.47 (d, *J* = 7.7 Hz, 1H), 3.08 (d, *J* = 16.4 Hz, 1H), 2.99 (s, 3H), 2.64 (dd, *J* = 16.2, 7.6 Hz, 1H), 1.33 (s, 3H), 0.76 (s, 3H). ¹³C NMR (101 MHz, C₆D₆) δ 149.6, 145.7, 141.7, 128.8, 126.8, 125.1, 120.0, 101.3, 78.5, 51.6, 49.0, 32.9, 25.1, 23.0. HRMS (ESI⁺): *m/z*: calculated for C₁₄H₁₇BrNaO: 303.0355 [M+Na]⁺; found: 303.0348. SFC (OD-3 (100x3 mm, 3 μm), CO₂:MeOH 90:10, 1.2 mL/min, 25 °C, BPR 150 bar; 230 nm): 0.945 min (90), 1.064 min (10); [α]_D²⁶ (*c* = 0.24 in CH₂Cl₂) = 75.9°.

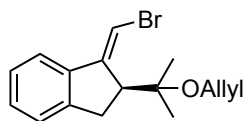


(*S,E*)-1-(Bromomethylene)-2-(2-ethoxypropan-2-yl)-2,3-dihydro-1*H*-indene (3.133b)

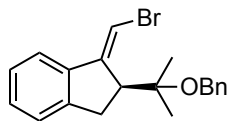
3.133b was synthesized following general procedure C performing the reaction at $-60\text{ }^{\circ}\text{C}$ for 4 days. The pure product was isolated by preparative TLC (pentane) as a transparent oil (26.6 mg, 0.090 mmol, 90%). **$^1\text{H NMR}$** (400 MHz, CDCl_3) δ 7.31 (dt, $J = 7.3, 1.1$ Hz, 1H), 7.24 – 7.19 (m, 2H), 7.19 – 7.13 (m, 1H), 6.64 (d, $J = 1.4$ Hz, 1H), 3.51 (dt, $J = 7.6, 1.2$ Hz, 1H), 3.45 (q, $J = 7.0$ Hz, 2H), 3.17 (d, $J = 16.5$ Hz, 1H), 2.94 (dd, $J = 16.4, 7.5$ Hz, 1H), 1.38 (s, 3H), 1.15 (t, $J = 7.0$ Hz, 3H), 0.75 (s, 3H) ppm. **$^{13}\text{C NMR}$** (101 MHz, CDCl_3) δ 149.4, 145.5, 141.5, 128.7, 126.7, 125.1, 119.8, 100.8, 56.8, 51.3, 32.9, 25.9, 23.7, 16.2 ppm. **HRMS** (ESI+): m/z : calculated for $\text{C}_{15}\text{H}_{19}\text{BrNaO}$: 317.0511 $[\text{M}+\text{Na}]^+$; found: 317.0513. **SFC** (OD-3 (100x3 mm, 3 μm), CO_2 :MeOH 95:5, 1.2 mL/min, $25\text{ }^{\circ}\text{C}$, BPR 150 bar; 254 nm): 1.409 min (90), 1.598 min (10); $[\alpha]_{\text{D}}^{26}$ ($c = 0.44$ in CH_2Cl_2) = 97.4° .

(*S,E*)-1-(Bromomethylene)-2-(2-isopropoxypropan-2-yl)-2,3-dihydro-1*H*-indene (3.133c)

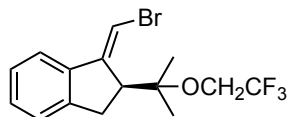
3.133c was synthesized following general procedure C performing the reaction at $-60\text{ }^{\circ}\text{C}$ for 4 days. The pure product was isolated by preparative TLC (pentane) as a transparent oil (19.5 mg, 0.063 mmol, 63%). **$^1\text{H NMR}$** (500 MHz, C_6D_6) δ 7.01 (m, 1H), 6.99 – 6.91 (m, 3H), 6.38 (d, $J = 1.4$ Hz, 1H), 3.67 (hept, $J = 6.1$ Hz, 1H), 3.47 (dt, $J = 7.6, 1.2$ Hz, 1H), 3.19 (d, $J = 16.5$ Hz, 1H), 2.68 (dd, $J = 16.3, 7.6$ Hz, 1H), 1.38 (s, 3H), 1.05 (dd, $J = 13.9, 6.1$ Hz, 6H), 0.75 (s, 3H). **$^{13}\text{C NMR}$** (126 MHz, C_6D_6) δ 149.6, 145.8, 141.8, 128.7, 126.7, 125.0, 120.0, 101.4, 79.1, 63.4, 52.8, 33.8, 26.4, 25.3, 25.0, 23.7. **HRMS** (ESI+): m/z : calculated for $\text{C}_{16}\text{H}_{21}\text{BrNaO}$: 331.0668 $[\text{M}+\text{Na}]^+$; found: 331.0666. **SFC** (IG (4.6 mm x 150 mmL, 3 μm), CO_2 :IPA 97:3, 2 mL/min, $25\text{ }^{\circ}\text{C}$, 2000 psi; 290 nm): 2.140 min (10), 2.390 min (90); $[\alpha]_{\text{D}}^{26}$ ($c = 0.45$ in CH_2Cl_2) = 61.3° .

(*S,E*)-2-(2-(Allyloxy)propan-2-yl)-1-(bromomethylene)-2,3-dihydro-1*H*-indene (3.133d)

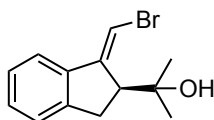
3.133d was synthesized following general procedure C performing the reaction at $-60\text{ }^{\circ}\text{C}$ for 4 days. The pure product was isolated by preparative TLC (pentane) as a transparent oil (10.9 mg, 0.035 mmol, 35%). **$^1\text{H NMR}$** (500 MHz, C_6D_6) δ 7.00 (ddd, $J = 8.1, 5.5, 2.5$ Hz, 1H), 6.98 – 6.92 (m, 3H), 6.37 (d, $J = 1.4$ Hz, 1H), 5.83 (ddt, $J = 17.2, 10.5, 4.9$ Hz, 1H), 5.21 (dq, $J = 17.2, 1.9$ Hz, 1H), 5.02 (dq, $J = 10.5, 1.8$ Hz, 1H), 3.71 (qdt, $J = 12.7, 5.0, 1.7$ Hz, 2H), 3.45 (d, $J = 7.6$ Hz, 1H), 3.13 (d, $J = 16.5$ Hz, 1H), 2.64 (ddd, $J = 16.5, 7.7, 1.1$ Hz, 1H), 1.34 (s, 3H), 0.82 (s, 3H). **$^{13}\text{C NMR}$** (126 MHz, C_6D_6) δ 149.6, 145.7, 141.7, 136.5, 128.7, 126.7, 125.1, 120.0, 114.6, 101.3, 78.8, 62.6, 52.1, 33.0, 25.8, 23.4. **HRMS** (APCI+): m/z : calculated for $\text{C}_{13}\text{H}_{14}\text{Br}$: 249.0273 $[\text{M}-\text{OAllyl}]^+$; found: 249.0271. **SFC** (OD-3 (100x3mm,3 μm), CO_2 :MeOH 95:5, 1.2 mL/min, $25\text{ }^{\circ}\text{C}$, BPR 150 bar; 254 nm): 1.411 min (88), 1.627 min (12); $[\alpha]_{\text{D}}^{26}$ ($c = 0.19$ in CH_2Cl_2) = 95.3° .

(*S,E*)-2-(2-(Benzyloxy)propan-2-yl)-1-(bromomethylene)-2,3-dihydro-1*H*-indene (3.133e)

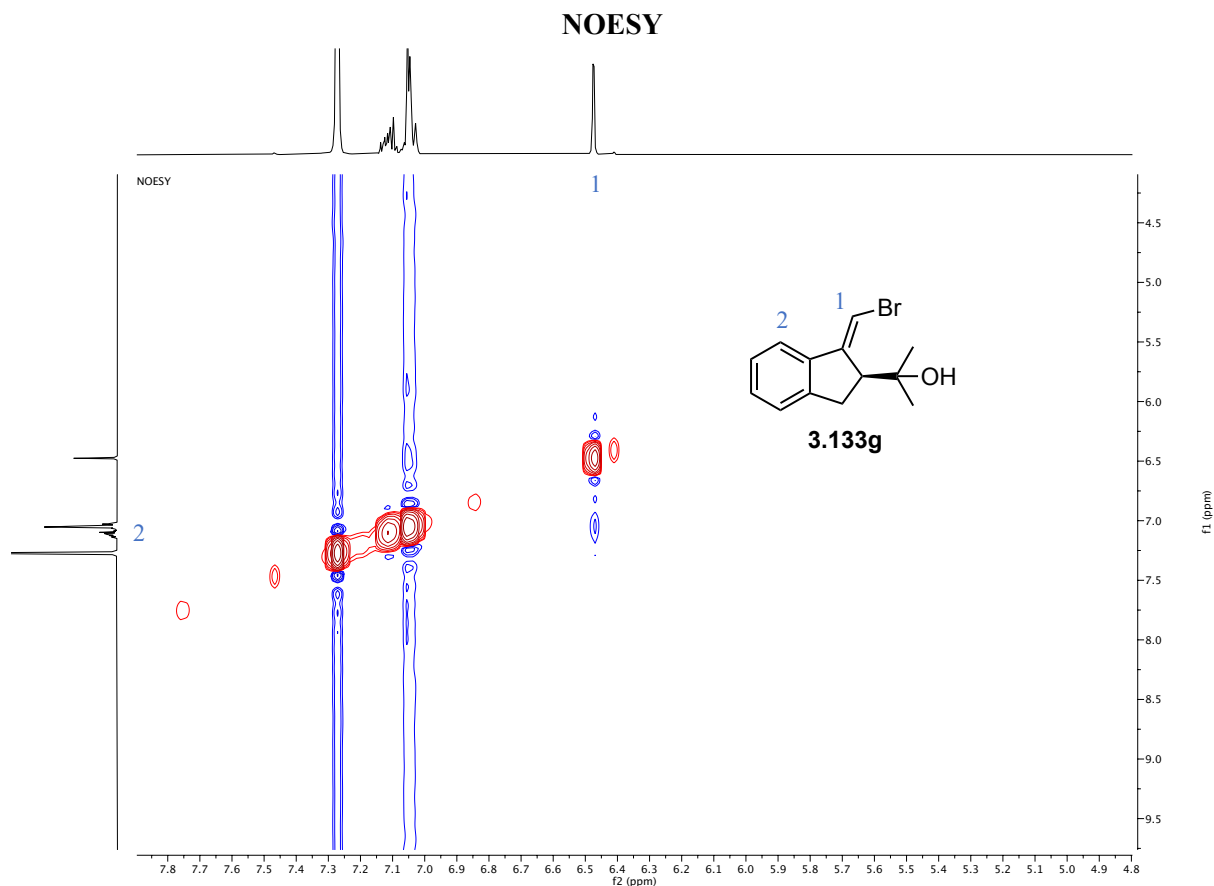
3.133e was synthesized following general procedure **C** performing the reaction at $-60\text{ }^{\circ}\text{C}$ for 4 days. The pure product was isolated by preparative TLC (pentane) as a transparent oil (24.7 mg, 0.069 mmol, 69%). $^1\text{H NMR}$ (400 MHz, C_6D_6) δ 7.24 – 7.18 (m, 4H), 7.14 – 7.09 (m, 1H), 7.01 (ddd, $J = 7.2, 5.8, 2.6$ Hz, 1H), 6.98 – 6.91 (m, 3H), 6.39 (d, $J = 1.4$ Hz, 1H), 4.33 – 4.20 (m, 2H), 3.52 (dt, $J = 7.6, 1.2$ Hz, 1H), 3.16 (d, $J = 16.5$ Hz, 1H), 2.65 (ddd, $J = 16.4, 7.6, 1.2$ Hz, 1H), 1.41 (s, 3H), 0.88 (s, 3H) ppm. $^{13}\text{C}\{^1\text{H}\}$ NMR (101 MHz, C_6D_6) δ 149.6, 145.7, 141.7, 140.2, 128.7, 128.4, 127.4, 127.2, 126.7, 125.1, 120.0, 101.3, 79.1, 63.8, 52.3, 33.1, 25.8, 23.5 ppm. **HRMS** (ESI+): m/z : calculated for $\text{C}_{20}\text{H}_{21}\text{BrNaO}$: 379.0668 $[\text{M}+\text{Na}]^+$; found: 379.0683. **SFC** (OD-3 (100x3mm,3 μm), CO_2 :MeOH 80:20, 1.2 mL/min, $25\text{ }^{\circ}\text{C}$, BPR 150 bar; 254 nm): 1.274 min (88), 1.541 min (12); $[\alpha]_{\text{D}}^{26}$ ($c = 0.38$ in CH_2Cl_2) = 92.8° .

(*S,E*)-1-(Bromomethylene)-2-(2-(2,2,2-trifluoroethoxy)propan-2-yl)-2,3-dihydro-1*H*-indene (3.133f)

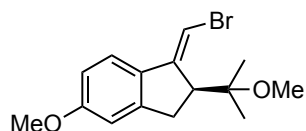
3.133f was synthesized following general procedure **C** performing the reaction at $-60\text{ }^{\circ}\text{C}$ for 4 days. The pure product was isolated by preparative TLC (pentane) as a yellow oil (10.9 mg, 0.035 mmol, 35%). $^1\text{H NMR}$ (400 MHz, C_6D_6) δ 6.99 (m, 1H), 6.95 – 6.87 (m, 3H), 6.30 (d, $J = 1.4$ Hz, 1H), 3.34 – 3.21 (m, 3H), 2.98 (d, $J = 16.6$ Hz, 1H), 2.55 (dd, $J = 16.6, 7.6$ Hz, 1H), 1.13 (s, 3H), 0.61 (s, 3H) ppm. $^{13}\text{C NMR}$ (101 MHz, C_6D_6) δ 148.7, 145.2, 141.2, 129.0, 126.9, 125.1, 120.0, 101.7, 80.4, 60.4 (q, $J = 34.1$ Hz), 51.7, 32.8, 25.3, 22.5 ppm. $^{19}\text{F NMR}$ (376 MHz, C_6D_6) δ -74.1 ppm. **HRMS** (APCI+): m/z : calculated for $\text{C}_{15}\text{H}_{16}\text{BrF}_3\text{O}$: 348.0331 $[\text{M}]^+$; found: 348.0333. **SFC** (OD-3 (100x3mm,3 μm), CO_2 :MeOH 98:2, 1.2 mL/min, $25\text{ }^{\circ}\text{C}$, BPR 150 bar; 254 nm): 1.204 min (61), 1.605 min (39); $[\alpha]_{\text{D}}^{26}$ ($c = 0.17$ in CH_2Cl_2) = 13.0° .

(*S,E*)-2-(1-(Bromomethylene)-2,3-dihydro-1*H*-inden-2-yl)propan-2-ol (3.133g)

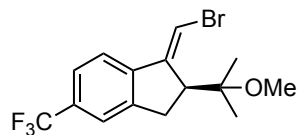
3.133g was synthesized following general procedure **C** performing the reaction at $-60\text{ }^{\circ}\text{C}$ for 4 days. The pure product was isolated by flash column chromatography purification on silica gel (10:1 cyclohexane:EtOAc), as a transparent oil (35.4 mg, 0.099 mmol, 99%). $^1\text{H NMR}$ (400 MHz, C_6D_6) δ 7.06 – 6.95 (m, 1H), 6.98 – 6.89 (m, 3H), 6.36 (d, $J = 1.4$ Hz, 1H), 3.16 (dt, $J = 7.5, 1.3$ Hz, 1H), 2.80 – 2.71 (m, 1H), 2.63 (ddd, $J = 16.5, 7.5, 1.1$ Hz, 1H), 1.07 (s, 3H), 0.96 (s, 3H). $^{13}\text{C NMR}$ (101 MHz, C_6D_6) δ 149.2, 145.5, 141.2, 128.8, 126.9, 125.1, 120.1, 101.6, 74.4, 55.1, 33.9, 28.7, 27.5. **HRMS** (ESI+): m/z : calculated for $\text{C}_{13}\text{H}_{15}\text{BrNaO}$: 289.0198 $[\text{M}+\text{Na}]^+$; found: 289.0195. **SFC** (IG-3 (100x3mm,3 μm), CO_2 :MeOH 80:20, 1.2 mL/min, $25\text{ }^{\circ}\text{C}$, BPR 150 bar; 254 nm): 1.322 min (91), 2.790 min (9); $[\alpha]_{\text{D}}^{26}$ ($c = 0.3$ in CH_2Cl_2) = 94.0° .



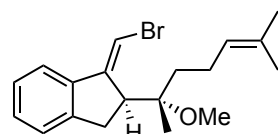
**(*S,E*)-1-(Bromomethylene)-5-methoxy-2-(2-methoxypropan-2-yl)-2,3-dihydro-1*H*-indene
(3.133h)**



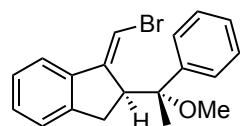
3.133h was synthesized following general procedure **C** performing the reaction at $-60\text{ }^{\circ}\text{C}$ for 5 days. The pure product was isolated by flash column chromatography purification on silica gel (100:1 pentane:Et₂O), as a transparent oil (24.4 mg, 0.078 mmol, 78%). ¹H NMR (400 MHz, C₆D₆) δ 6.89 (d, $J = 8.4$ Hz, 1H), 6.63 (dd, $J = 8.4, 2.4$ Hz, 1H), 6.56 (br s, 1H), 6.28 (d, $J = 1.4$ Hz, 1H), 3.52 (dt, $J = 7.6, 1.2$ Hz, 1H), 3.27 (s, 3H), 3.08 (d, $J = 16.5$ Hz, 1H), 3.02 (s, 3H), 2.65 (dd, $J = 16.5, 7.6$ Hz, 1H), 1.39 (s, 3H), 0.82 (s, 3H) ppm. ¹³C NMR (101 MHz, C₆D₆) δ 161.1, 149.0, 147.7, 134.6, 121.0, 113.7, 109.6, 98.7, 78.7, 54.9, 51.9, 49.0, 33.1, 25.2, 23.0 ppm. HRMS (APCI⁺): m/z : calculated for C₁₄H₁₆BrO: 279.0379 [M-OMe]⁺; found: 279.0380. SFC (IG-3 (100x3mm,3 μ m), CO₂:EtOH 90:10, 1.2 mL/min, 25 $^{\circ}\text{C}$, BPR 150 bar; 254 nm): 1.161min (14), 1.418 min (86); $[\alpha]_{\text{D}}^{26}$ ($c = 0.21$ in CH₂Cl₂) = 84.6 $^{\circ}$.

(*S,E*)-1-(Bromomethylene)-2-(2-methoxypropan-2-yl)-5-(trifluoromethyl)-2,3-dihydro-1*H*-indene (3.133i)

3.133i was synthesized following general procedure **C** performing the reaction at -60 °C for 5 days and using 5 mol% of (*R,R*)-**A** and of AgSbF₆. The pure product was isolated by preparative TLC (2:1 cyclohexane:CH₂Cl₂) followed by flash column chromatography in silica gel (20:1 cyclohexane:CH₂Cl₂), as a transparent oil (24.3 mg, 0.070 mmol, 70%). ¹H NMR (400 MHz, C₆D₆) δ 7.18 (m, 2H), 6.70 (d, *J* = 7.9 Hz, 1H), 6.30 (d, *J* = 1.4 Hz, 1H), 3.34 (dt, *J* = 7.8, 1.2 Hz, 1H), 2.92 (s, 3H), 2.88 (m, 1H), 2.42 (dd, *J* = 16.8, 7.7 Hz, 1H), 1.21 (s, 3H), 0.65 (s, 3H). ¹³C NMR (101 MHz, C₆D₆) δ 148.29, 146.23, 144.94, 128.18, 127.94, 123.95 (q, *J* = 3.8 Hz), 122.11 (q, *J* = 3.8 Hz), 120.12, 104.09, 78.31, 52.00, 48.95, 32.69, 24.69, 22.66. ¹⁹F NMR (376 MHz, C₆D₆) δ -61.73. HRMS (APCI+): *m/z*: calculated for C₁₄H₁₃BrF₃: 317.0147 [M-OMe]⁺; found: 317.0150. SFC (IG (4.6 mm x 150 mmL, 3 μm), CO₂:IPA 97:3, 2 mL/min, 25 °C, 2000 psi; 291 nm): 1.820 min (13), 2.080 min (87); [α]_D²⁶ (*c* = 0.24 in CH₂Cl₂) = 74.2°.

(*S,E*)-1-(bromomethylene)-2-((*S*)-2-methoxy-6-methylhept-5-en-2-yl)-2,3-dihydro-1*H*-indene (3.133j)

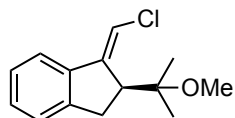
3.133j was synthesized following general procedure **C** performing the reaction at -40 °C for 5 days. The pure product was isolated by preparative TLC (100:1 pentane:Et₂O), as a transparent oil (18.5 mg, 0.053 mmol, 53%) and as a single diastereomer. ¹H NMR (500 MHz, C₆D₆) δ 7.05 – 6.97 (m, 1H), 6.98 – 6.92 (m, 3H), 6.36 (d, *J* = 1.4 Hz, 1H), 5.37 – 5.30 (m, 1H), 3.48 (d, *J* = 7.7 Hz, 1H), 3.13 (d, *J* = 16.4 Hz, 1H), 2.97 (s, 3H), 2.62 (ddd, *J* = 16.3, 7.6, 1.2 Hz, 1H), 2.36 – 2.21 (m, 1H), 2.15 – 2.02 (m, 2H), 1.84 – 1.71 (m, 1H), 1.70 (s, 3H), 1.60 (s, 3H), 0.81 (s, 3H). ¹³C NMR (126 MHz, C₆D₆) δ 149.7, 145.7, 142.0, 131.0, 128.8, 126.8, 125.6, 125.0, 120.0, 101.3, 80.2, 50.3, 48.8, 37.2, 32.5, 25.9, 22.7, 20.7, 17.8. HRMS (APCI+): *m/z*: calculated for C₁₈H₂₂Br: 317.0899 [M-OMe]⁺; found: 317.0900. SFC (IG-3 (100x3mm,3um), CO₂:MeOH 97:3, 1.2 mL/min, 25 °C, BPR 150 bar; 254 nm): 1.461 min (6), 2.275 min (94); [α]_D²⁶ (*c* = 0.21 in CH₂Cl₂) = 61.1°.

(*S,E*)-1-(Bromomethylene)-2-((*R*)-1-methoxy-1-phenylethyl)-2,3-dihydro-1*H*-indene (3.133k)

3.133k was synthesized following general procedure **C** performing the reaction at -40 °C for 4 days. The pure product was isolated by preparative TLC (7:1 cyclohexane:CH₂Cl₂), as a white solid (33.7 mg, 0.098 mmol, 98%) and as a single diastereomer. **M.p.** 64-72 °C. ¹H NMR (400 MHz, C₆D₆) δ 7.40 – 7.33 (m, 2H), 7.24 – 7.16 (m, 2H), 7.16 – 7.07 (m, 1H), 7.04 – 6.89 (m, 5H), 6.40 (d, *J* = 1.4 Hz, 1H), 3.62 (dt, *J* = 7.8, 1.2 Hz, 1H), 3.23 (d, *J* = 16.6 Hz, 1H), 2.84 (s, 3H), 2.70 (dd, *J* = 16.6, 7.7 Hz, 1H), 1.26 (s, 3H). ¹³C NMR (101

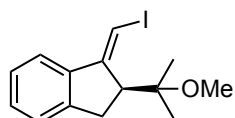
MHz, C₆D₆) δ 148.0, 145.5, 144.2, 142.0, 128.5, 127.3, 126.6, 125.0, 119.9, 102.9, 81.9, 56.3, 50.3, 33.9, 30.2, 19.6, 1.4. **HRMS** (APCI+): m/z : calculated for C₁₈H₁₆Br: 311.0430 [M-OMe]⁺; found: 311.0425. **SFC** (OJ-3 (100x3mm,3 μ m), CO₂:MeOH 95:5, 1.2 mL/min, 25 °C, BPR 150 bar; 280 nm): 2.609 min (18), 3.641 min (82); $[\alpha]_D^{26}$ ($c = 0.23$ in CH₂Cl₂) = 74.4°.

(S,E)-1-(Chloromethylene)-2-(2-methoxypropan-2-yl)-2,3-dihydro-1H-indene (3.133l)



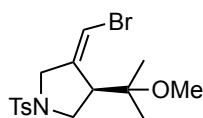
3.133l was synthesized following general procedure C performing the reaction at -40 °C for 24 h. The pure product was isolated by preparative TLC (pentane), as a yellow oil (23.1 mg, 0.098 mmol, 98%). **¹H NMR** (500 MHz, C₆D₆) δ 7.04 – 6.91 (m, 4H), 6.25 (d, $J = 1.5$ Hz, 1H), 3.51 (dt, $J = 7.8, 1.3$ Hz, 1H), 3.10 (d, $J = 16.5$ Hz, 1H), 2.99 (s, 3H), 2.66 (dd, $J = 16.5, 7.7$ Hz, 1H), 1.31 (s, 3H), 0.76 (s, 3H). **¹³C NMR** (126 MHz, C₆D₆) δ 146.6, 145.6, 141.2, 128.7, 126.7, 125.0, 119.8, 112.3, 78.6, 49.9, 49.0, 33.1, 24.8, 22.8. **HRMS** (APCI+): m/z : calculated for C₁₃H₁₄Cl: 205.0779 [M-OMe]⁺; found: 205.0777. **SFC** (IG-3 (100x3mm,3 μ m), CO₂:MeOH 97:3, 1.2 mL/min, 25 °C, BPR 150 bar; 254 nm): 1.115 min (76), 1.256 min (24); $[\alpha]_D^{26}$ ($c = 0.22$ in CH₂Cl₂) = 63.0°.

(S,E)-1-(Iodomethylene)-2-(2-methoxypropan-2-yl)-2,3-dihydro-1H-indene (3.133m)



3.133m was synthesized following general procedure C performing the reaction at -60 °C for 6 days. The pure product was isolated by preparative TLC (pentane), as a yellow oil (26.3 mg, 0.080 mmol, 80%). **¹H NMR** (500 MHz, C₆D₆) δ 7.00 (ddd, $J = 7.2, 6.0, 2.5$ Hz, 1H), 6.97 – 6.90 (m, 3H), 6.45 (d, $J = 1.3$ Hz, 1H), 3.35 (dt, $J = 7.5, 1.1$ Hz, 1H), 3.04 (d, $J = 16.4$ Hz, 1H), 2.99 (s, 3H), 2.63 (ddd, $J = 16.3, 7.5, 1.2$ Hz, 1H), 1.34 (s, 3H), 0.76 (s, 3H). **¹³C NMR** (126 MHz, C₆D₆) δ 155.6, 145.8, 142.3, 128.7, 126.7, 125.1, 120.3, 78.8, 73.0, 54.4, 48.9, 32.7, 25.2, 23.2. **HRMS** (APCI+): m/z : calculated for C₁₃H₁₄I: 297.0135 [M-OMe]⁺; found: 297.0125. **SFC** (IBN-3 (100x3mm,3 μ m), CO₂:MeOH 95:5, 1.2 mL/min, 25 °C, BPR 150 bar; 280 nm): 1.367 min (93), 1.530 min (7); $[\alpha]_D^{26}$ ($c = 0.20$ in CH₂Cl₂) = -97.0°.

(R,E)-3-(Bromomethylene)-4-(2-methoxypropan-2-yl)-1-tosylpyrrolidine (3.133n)

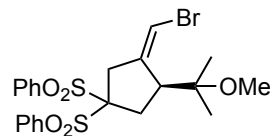


3.133n was synthesized following general procedure C performing the reaction at 23 °C for 24 h. The pure product was isolated by preparative TLC (10:1 cyclohexane:EtOAc), as a yellow oil (29.4 mg, 0.076 mmol, 76%). **¹H NMR** (500 MHz, C₆D₆) δ 7.73 (d, $J = 8.2$ Hz, 2H), 6.82 – 6.76 (m, 2H), 5.55 (s, 1H), 3.71 (dd, $J = 10.1, 2.2$ Hz, 1H), 3.66 (d, $J = 1.6$ Hz, 2H), 3.21 (dd, $J = 10.1, 7.8$ Hz, 1H), 2.79 – 2.71 (m, 1H), 2.55 (s, 3H), 1.89 (s, 3H), 0.87 (s, 3H), 0.84 (s, 3H). **¹³C NMR** (126 MHz, C₆D₆) δ 142.80, 142.44, 135.44, 129.54, 103.68, 77.47, 53.66, 51.51, 48.85, 48.64, 34.44, 23.66, 22.73, 22.31, 21.10, 14.28. **HRMS** (ESI+): m/z : calculated for C₁₆H₂₂BrNNaO₃S: 410.0396 [M+Na]⁺; found: 410.0396. **SFC** (IA-3 (100x3mm,3 μ m),

CO₂:MeOH 85:15, 1.2 mL/min, 25 °C, BPR 150 bar; 210 nm): 1.584 min (87), 2.022 min (13); [α]_D²⁶ ($c = 0.21$ in CH₂Cl₂) = -6.2°.

(*S,Z*)-(3-(Bromomethylene)-4-(2-methoxypropan-2-yl)cyclopentane-1,1-disulfonyl)dibenzene

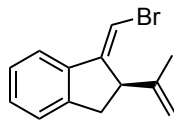
(3.133o)



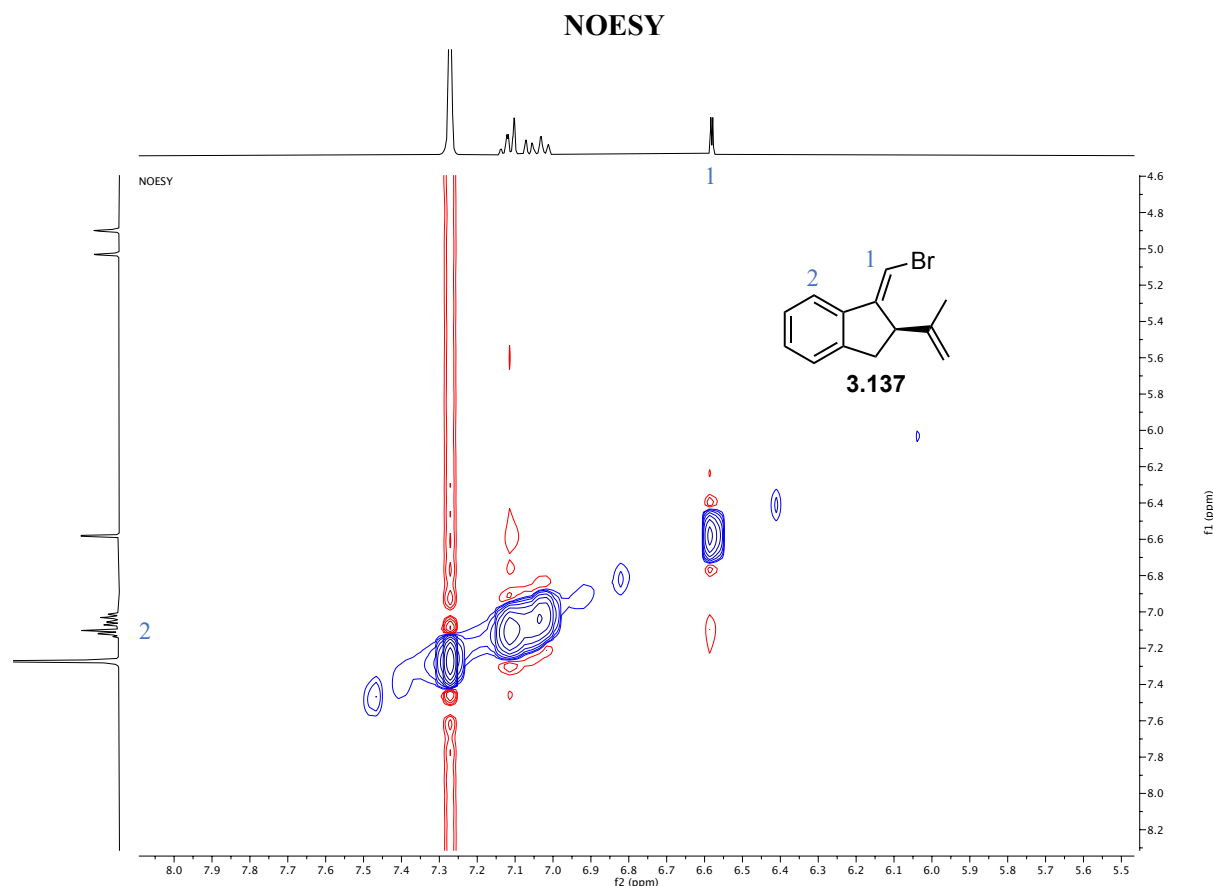
3.133o was synthesized following general procedure C performing the reaction at -40 °C for 48 h. The pure product was isolated by preparative TLC (3:1 CH₂Cl₂:cyclohexane), as a transparent oil (25.9 mg, 0.050 mmol, 50%). ¹H NMR (400 MHz, CDCl₃) δ 8.11 – 7.99 (m, 4H), 7.76 – 7.66 (m, 2H), 7.66 – 7.55 (m, 4H), 6.05 (dd, $J = 2.4, 1.5$ Hz, 1H), 3.51 (ddd, $J = 15.7, 2.7, 1.4$ Hz, 1H), 3.05 (s, 3H), 3.02 – 2.92 (m, 2H), 2.80 – 2.68 (m, 2H), 1.25 (s, 3H), 1.20 (s, 3H). ¹³C NMR (101 MHz, CDCl₃) δ 143.6, 137.4, 136.3, 134.9, 134.6, 131.3, 131.1, 129.0, 128.9, 103.2, 91.8, 78.5, 50.6, 49.4, 41.7, 32.4, 24.7, 23.5. HRMS (ESI⁺): m/z : calculated for C₂₂H₂₅BrNaO₅S₂: 535.0219 [M+Na]⁺; found: 535.0238. SFC (OJ-3 (100x3mm,3um), CO₂:MeOH 80:20, 1.2 mL/min, 25 °C, BPR 150 bar; 230 nm): 1.057 min (11), 1.433 min (89); [α]_D²⁶ ($c = 0.21$ in CH₂Cl₂) = -22.6°.

Alkoxy cyclization products derivatization to afford 3.137, 3.138 and 3.147

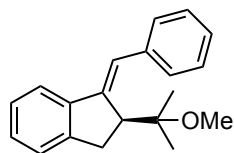
(*R,E*)-1-(Bromomethylene)-2-(prop-1-en-2-yl)-2,3-dihydro-1H-indene (3.137)



Under Ar atmosphere, **3.133g** (10.9 mg, 0.041 mmol) and Burgess reagent (14.6 mg, 0.061 mmol, 1.5 equiv) were dissolved in anhydrous THF (0.41 mL) and the mixture was stirred for 16 h at 23°C. The reaction was quenched with the addition of 2 mL of H₂O and 2 mL of EtOAc. After that, the aqueous phase was extracted with EtOAc (x3) and the combined organic layers were joined, washed with brine and dried with Na₂SO₄. The pure product was isolated by preparative TLC (pentane), as a yellow oil (10.0 mg, 0.040 mmol, 98%). ¹H NMR (400 MHz, C₆D₆) δ 7.05 – 6.87 (m, 4H), 6.47 (d, $J = 2.0$ Hz, 1H), 4.92 (dp, $J = 1.7, 0.8$ Hz, 1H), 4.79 (p, $J = 1.5$ Hz, 1H), 3.67 (dtd, $J = 8.8, 2.2, 0.8$ Hz, 1H), 2.90 (dd, $J = 16.7, 8.8$ Hz, 1H), 2.52 (dd, $J = 16.8, 2.3$ Hz, 1H), 1.54 (dd, $J = 1.5, 0.8$ Hz, 3H). ¹³C NMR (101 MHz, C₆D₆) δ 149.4, 145.5, 144.9, 140.1, 129.0, 127.1, 125.7, 120.5, 111.8, 100.6, 51.4, 37.5, 19.8. HRMS (APCI⁺): m/z : calculated for C₁₃H₁₄Br: 249.0273 [M+H]⁺; found: 249.0270. SFC (OJ-3 (100x3mm,3um), CO₂:MeOH 98:2, 1.2 mL/min, 25 °C, BPR 150 bar; 254 nm): 1.586 min (9), 1.768 min (91); [α]_D²⁶ ($c = 0.24$ in CH₂Cl₂) = 103.3°.

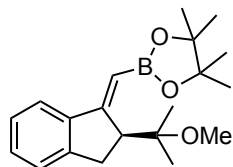


(*S,E*)-1-Benzylidene-2-(2-methoxypropan-2-yl)-2,3-dihydro-1*H*-indene (3.138)



Phenylboronic acid (17.2 mg, 0.141 mmol, 1.8 equiv), Pd(PPh₃)₂Cl₂ (2.76 mg, 0.0039 mmol, 0.05 equiv) and K₂CO₃ (32.6 mg, 0.236 mmol, 3 equiv) were added to a solution of **3.133a** (22.1 mg, 0.076 mmol) in 1,4-dioxane (1.25 mL) and water (0.21 mL). The mixture was stirred for 3 h at 85 °C. Water was then added, the aqueous phase was extracted with Et₂O (x3) and the combined organic layers were joined, washed with brine and dried with Na₂SO₄. The product was purified by preparative TLC (20:1 cyclohexane:EtOAc) as a white solid (16.2 mg, 0.058 mmol, 74%). **M.p.** 75-83 °C. **¹H NMR** (500 MHz, C₆D₆) δ 7.46 – 7.42 (m, 2H), 7.42 – 7.38 (m, 1H), 7.24 – 7.14 (m, 2H), 7.17 – 7.03 (m, 5H), 4.01 (d, *J* = 7.9 Hz, 1H), 3.23 (d, *J* = 16.6 Hz, 1H), 2.97 – 2.91 (m, 1H), 2.91 (s, 3H), 0.86 (s, 3H), 0.75 (s, 3H). **¹³C NMR** (126 MHz, C₆D₆) δ 145.7, 145.7, 144.2, 139.5, 129.2, 128.6, 128.4, 128.4, 126.8, 124.9, 123.2, 120.0, 79.1, 48.8, 48.0, 33.6, 23.4, 22.1. **HRMS** (ESI⁺): *m/z*: calculated for C₂₀H₂₂NaO: 301.1563 [M+Na]⁺; found: 301.1552. **SFC** (OJ-3 (100x3mm,3um), CO₂:MeOH 90:10, 1.2 mL/min, 25 °C, BPR 150 bar; 210 nm): 1.299 min (10), 1.542 min (90); [α]_D²⁶ (*c* = 0.1 in CH₂Cl₂) = -175.0°

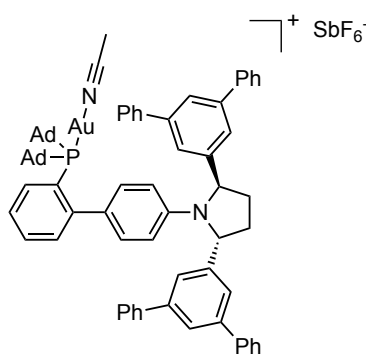
(*S,E*)-2-((2-(2-Methoxypropan-2-yl)-2,3-dihydro-1*H*-inden-1-ylidene)methyl)-4,4,5,5-tetramethyl-1,3,2-dioxaborolane (3.147)



Following a modified procedure found in literature,⁷⁰ to a solution of dry 1,4-dioxane (0.35 mL) in a oven-dried flask were added **3.133a** (20.0 mg, 0.071 mmol), B₂Pin₂ (21.7 mg, 0.085 mmol, 1.2 equiv), and KOAc (20.9 mg, 0.213 mmol, 3 equiv). The solution was purged with N₂, and Pd(dppf)Cl₂ (2.60 mg, 0.0036 mmol, 0.05 equiv) was added. The mixture was stirred at 90 °C for 24 h. The solvent was removed under vacuo, and of Et₂O was added. The crude mixture was filtered through a pad of Celite® and the pad washed with Et₂O. Then, water was added to the filtrate, and the mixture was extracted with Et₂O. The organic phase was washed with brine, dried with Na₂SO₄, and concentrated in vacuo. The product was purified by preparative TLC (15:1 cyclohexane:EtOAc) as a yellow oil (15.2 mg, 0.046 mmol, 65%). ¹H NMR (400 MHz, C₆D₆) δ 7.39 (dd, *J* = 7.6, 1.2 Hz, 1H), 7.04 (dd, *J* = 3.9, 1.0 Hz, 2H), 6.98 (dq, *J* = 8.2, 4.3 Hz, 1H), 6.24 (d, *J* = 1.3 Hz, 1H), 4.07 (d, *J* = 7.5 Hz, 1H), 3.21 (d, *J* = 16.6 Hz, 1H), 3.16 (s, 3H), 2.83 (dd, *J* = 16.5, 7.6 Hz, 1H), 1.38 (s, 3H), 1.14 (s, 6H), 1.14 (s, 6H), 0.82 (s, 3H). ¹³C NMR (101 MHz, C₆D₆) δ 165.7, 147.0, 144.1, 129.4, 126.8, 125.0, 120.8, 82.9, 77.7, 50.8, 49.0, 33.3, 25.3, 24.9, 23.1, 22.5. HRMS (ESI⁺): *m/z*: calculated for C₂₀H₂₉NaO₃B: 350.2138 [M+Na]⁺; found: 350.2133. SFC (IG-3 (100x3mm,3um), CO₂:MeOH 96:4, 1.2 mL/min, 25 °C, BPR 150 bar; 280 nm): 1.191 min (89), 1.512 min (11); [α]_D²⁶ (*c* = 0.16 in CH₂Cl₂) = 34.3°.

Experimental mechanistic studies

Synthesis of pre-activated catalyst (*R,R*)-A⁺



A solution of AgSbF₆ (5.95 mg, 0.0173 mmol, 1.05 equiv) in CH₂Cl₂ (0.25 mL) was added to a mixture of complex (*R,R*)-A (20.0 mg, 0.0165 mmol) in acetonitrile (8.6 μL, 0.165 mmol, 10 equiv) and CH₂Cl₂ (0.50 mL) under an atmosphere of argon. The reaction was stirred at 24 °C for 16 h. The mixture was filtered through a path of Celite®, washed with CH₂Cl₂ and concentrated to yield complex (*R,R*)-A⁺ (22.7 mg, 0.0156 mmol, 95% yield) as a yellow solid. **M.p.** 243-280 °C.

¹H NMR* (400 MHz, CD₂Cl₂) δ 7.73 (s, 1H), 7.68-7.60 (m, 8H), 7.54-7.45 (m, 15H), 7.44-7.38 (m, 4H), 7.21 (s, 1H), 7.05 – 6.94 (m, 2H), 6.78 (s, 1H), 6.68 (s, 1H), 5.41 (s, 2H), 2.78 (s, 2H), 2.25 (s, 3H), 2.18 – 1.90 (m, 20H), 1.72 (s, 6H), 1.63 (s, 6H). ¹³C NMR* (101 MHz, CD₂Cl₂) δ 145.7, 144.8, 142.7, 141.4, 134.4, 131.5, 131.2, 129.3, 128.2, 127.8, 127.0, 125.4, 124.3, 121.6, 114.9, 64.5, 43.2, 42.4, 36.4, 33.3, 30.1, 29.2 (d, *J* = 9.9 Hz), 28.9 (d, *J* = 9.9 Hz), 2.1. ³¹P NMR (162 MHz, CD₂Cl₂) δ

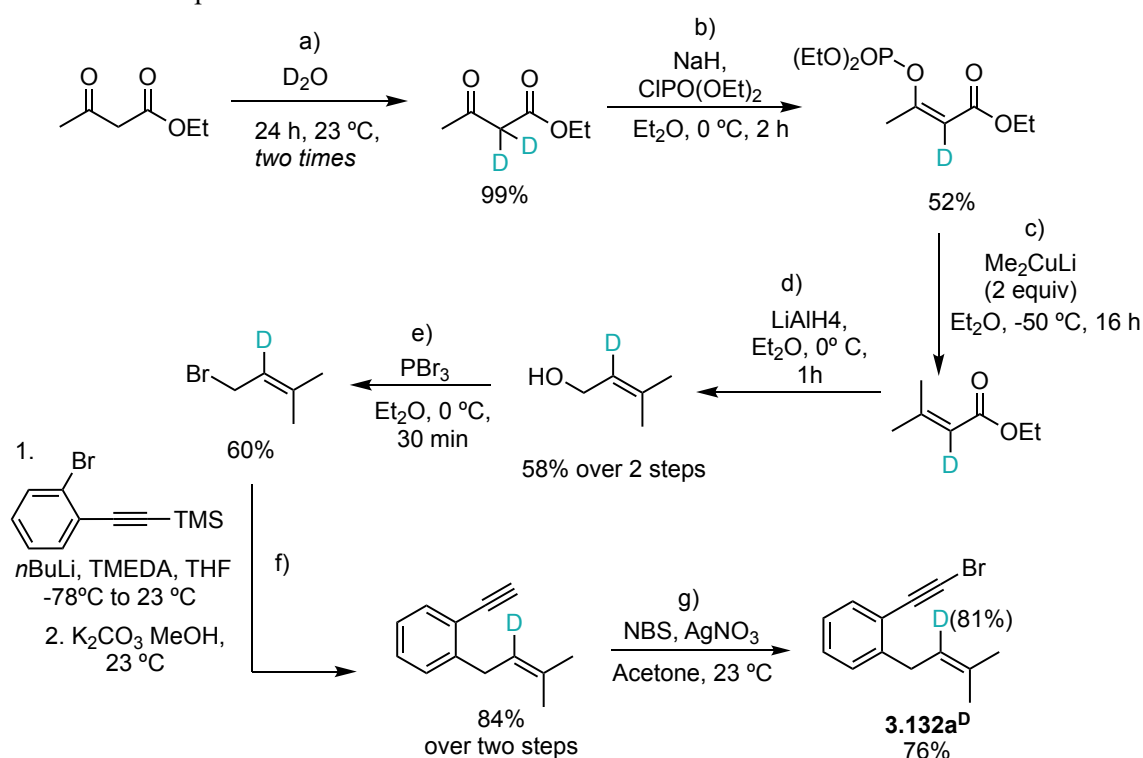
⁷⁰ Cruché, C.; Neiderer, W.; Collins, S. K. Heteroleptic Copper-Based Complexes for Energy-Transfer Processes: *E* → *Z* Isomerization and Tandem Photocatalytic Sequences. *ACS Catal.* **2021**, *11*, 8829–8836.

62.7. **HRMS** (ESI+): m/z : calculated for $C_{72}H_{70}AuNP$: 1176.4906 $[M-MeCN-SbF_6]^+$; found: 1176.4869. $[\alpha]_D^{26}$ ($c = 0.2$ in CH_2Cl_2) = 74.5°.

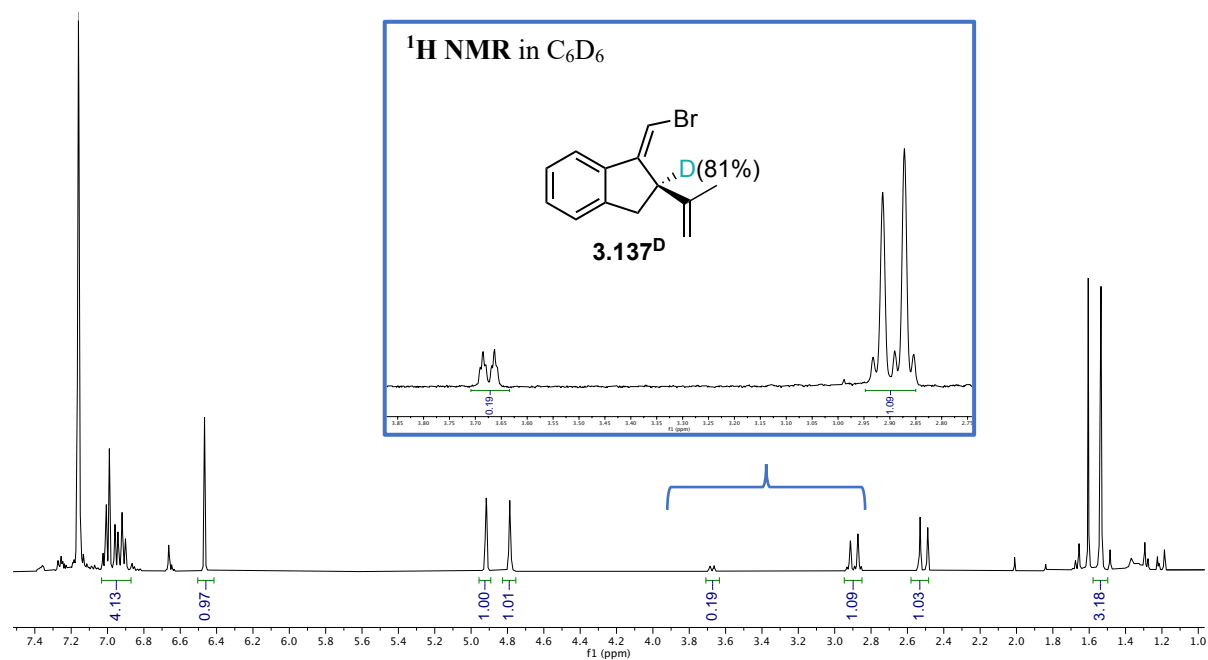
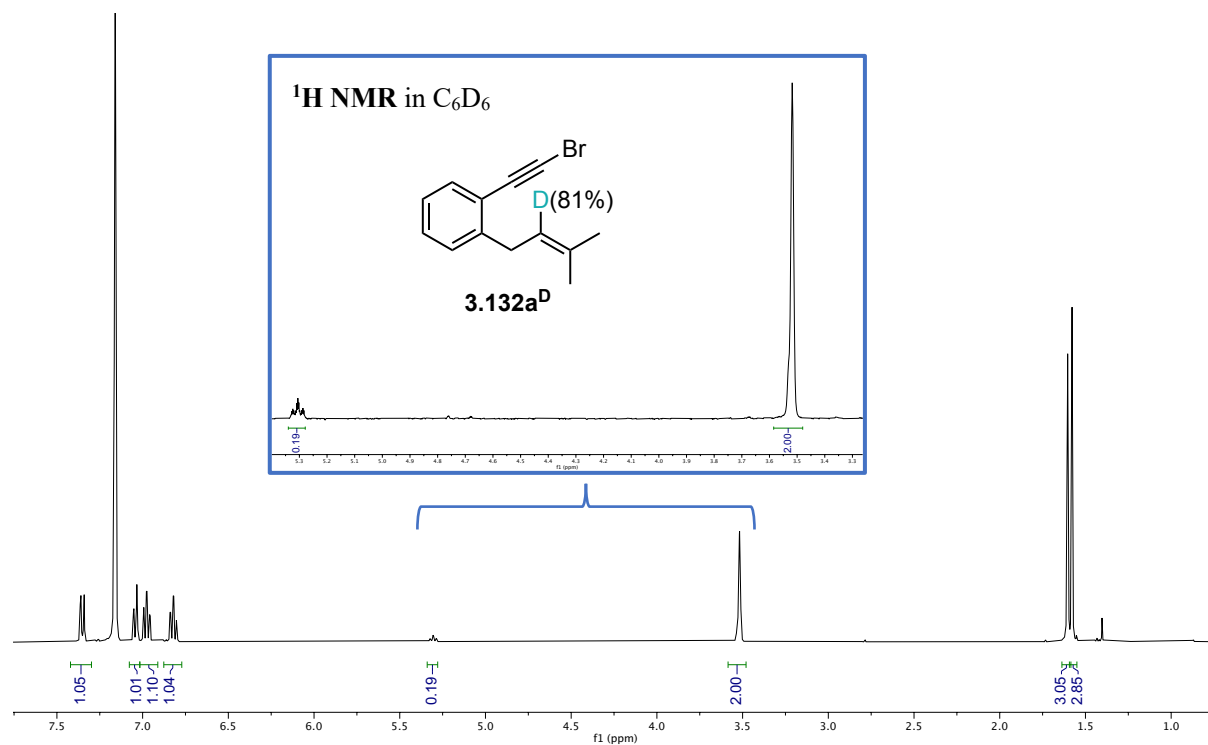
* Due to the cationic nature of this species, both the 1H NMR and the ^{13}C NMR are not as clear as the neutral species' one.^{41a} Nevertheless, the presence of a single signal in the ^{31}P NMR which results shifted compared to the neutral complex (δ 65.3)^{41a} combined with the **HRMS**, and its catalytic activity in the absence of chloride scavenger, demonstrate that we have indeed isolated complex $(R,R)-A^+$.

Deuterated substrate **3.132a^D** and product **3.137^D**

Substrate **3.132a^D** was synthesized following the route depicted below which was adapted from different literature procedures.^{48,71}

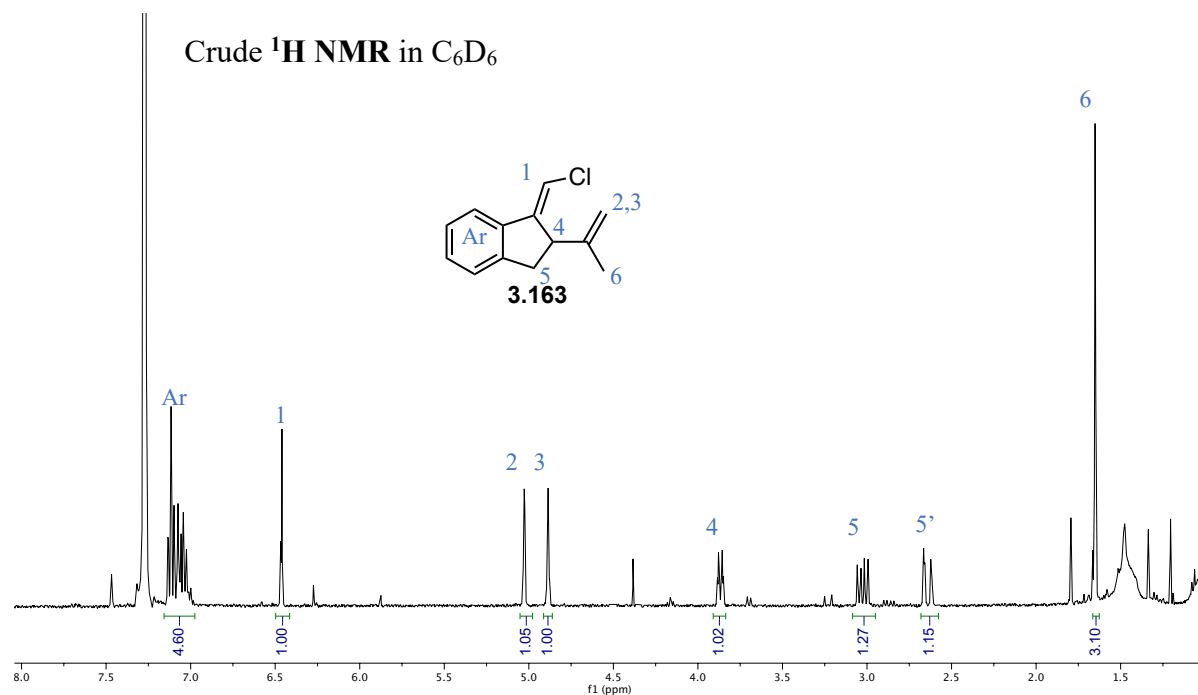


⁷¹ Steps a, b, e) Thulasiram, H. V.; Phan, R. M.; Rivera, S. B.; Poulter, C. D., Synthesis of Deuterium-Labeled Derivatives of Dimethylallyl Diphosphate, *J. Org. Chem.* **2006**, *71*, 1739–1741. Step c) Sum, F. W.; Weiler, L., Synthesis of Isoprenoid Natural Products from β -Keto Esters, *Tetrahedron* **1981**, *37*, 303–317. Step d) Citron, C. A.; Rabe, P.; Barra, L.; Nakano, C.; Hoshino, T.; Dickschat, J. S., Synthesis of Isotopically Labeled Oligoprenyl Diphosphates and Their Application in Mechanistic Investigations of Terpene Cyclases, *Eur. J. Org. Chem.* **2014**, *2014*, 7684–7691. Steps f-g) ref. 48.



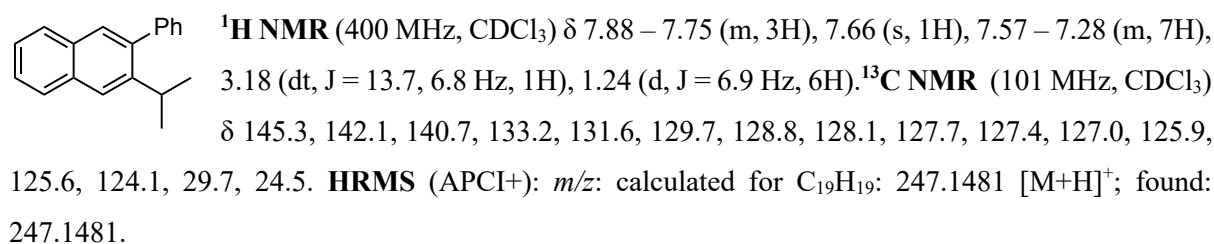
Cl-, Me- and Ph- substituted enynes

In the case of chloroenyne **3.162**, the cycloisomerization product **3.163** was never purified since it would decompose in silica (Table 3.9).



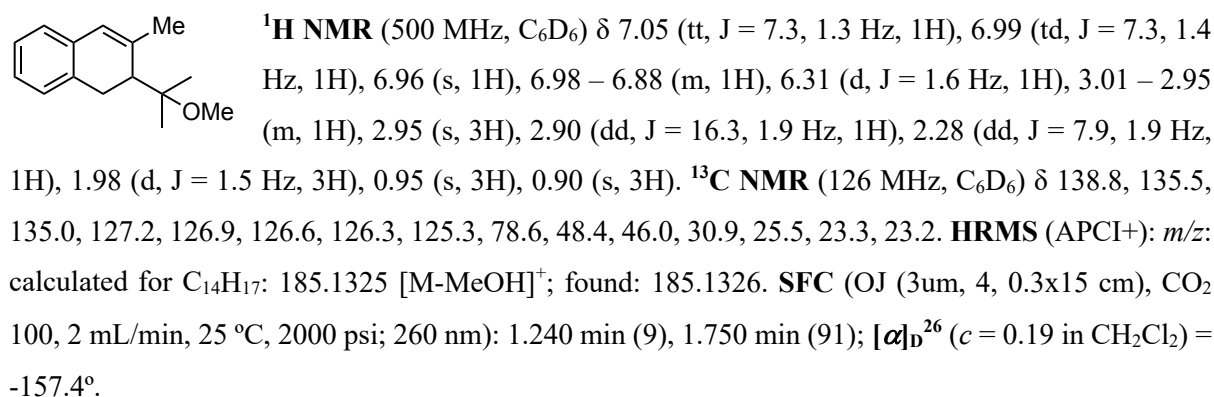
While products **3.164**, **3.165**⁷² and **3.167**⁴⁵ are reported in literature, when using $(R,R)\text{-A}^+$ under anhydrous conditions, phenylenyne **3.139** afforded **3.166** in a 28% isolated yield (flash chromatography in pentane) for the first time (Table 3.10, entry 1).

2-Isopropyl-3-phenylnaphthalene (**3.166**)



Enyne **3.153** afforded **3.155** in 65% isolated yield (flash chromatography in pentane) when using 1 equiv of MeOH (Table 3.8, entry 2).

2-(2-Methoxypropan-2-yl)-3-methyl-1,2-dihydronaphthalene (**3.155**)



⁷² Franchino, A.; Martí, À.; Echavarrén, A. M. H-Bonded Counterion-Directed Enantioselective Au(I) Catalysis. *J. Am. Chem. Soc.* **2022**, *144*, 3497–35091.

Crystallographic Data

X-Ray⁷³ data of **3.133a** available at CCDC 2337764

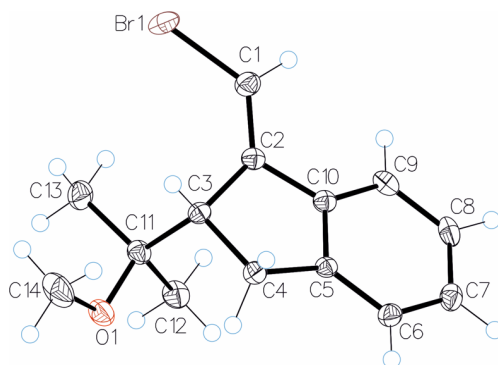


Table 3.11. Crystal data and structure refinement for mo_AC013061B_0m (compound 3.133a).

Identification code	mo_AC013061B_0m
Empirical formula	C ₁₄ H ₁₇ BrO
Formula weight	281.18
Temperature/K	100.40
Crystal system	orthorhombic
Space group	P2 ₁ 2 ₁ 2 ₁
a/Å	7.2267(12)
b/Å	11.976(2)
c/Å	14.973(3)
α/°	90
β/°	90
γ/°	90
Volume/Å ³	1295.9(4)
Z	4
ρ _{calc} /cm ³	1.441
μ/mm ⁻¹	3.150
F(000)	576.0
Crystal size/mm ³	0.3 × 0.2 × 0.1
Radiation	MoKα (λ = 0.71073)
2θ range for data collection/°	4.356 to 61.224
Index ranges	-10 ≤ h ≤ 8, -14 ≤ k ≤ 17, -21 ≤ l ≤ 18
Reflections collected	14021
Independent reflections	3880 [R _{int} = 0.0303, R _{sigma} = 0.0283]
Data/restraints/parameters	3880/0/148
Goodness-of-fit on F ²	1.042
Final R indexes [I ≥ 2σ (I)]	R ₁ = 0.0249, wR ₂ = 0.0634
Final R indexes [all data]	R ₁ = 0.0298, wR ₂ = 0.0653
Largest diff. peak/hole / e Å ⁻³	0.44/-0.40
Flack parameter	-0.007(4)

⁷³ These data are provided free of charge by the joint Cambridge Crystallographic Data Centre and Fachinformationszentrum Karlsruhe Access Structures service www.ccdc.cam.ac.uk/structures. Single crystal was measured on a **Bruker APEX-II CCD** diffractometer. The crystal was kept at 100.40 K during data collection. Programs used: Olex2 (O.V. Dolomanov, L.J. Bourhis, R. J. Gildea, J. A. K. Howard and H. Puschmann, *J. Appl. Cryst.* **2009**, *42*, 339-341), data collection (Apex2 V2011.4-0), data reduction (SAINT V8.34A), structure solution (SIR2014, M. C. Burla, R. Caliandro, B. Carrozzini, G. L. Casciaro, C. Cuocci, C. Giacovazzo, M. Mallamo, A. Mazzone, G. Polidori, *J. Appl. Cryst.* **2015**, *48*, 306), structure refinement (SHELXTL Version 2018/3, G. M. Sheldrick, *Acta Crystallographica Section C-Structural Chemistry* **2015**, *71*, 3), absorption correction (SADABS 2014/4, G. M. Sheldrick, **2008**).

DFT Calculations

Computational methods

The calculations were performed in Gaussian09⁵⁵ with B3LYP⁵⁶ using Grimme's D3 empirical dispersion correction,⁵⁷ modelling the solvent (CH₂Cl₂) with implicit solvation using the polarizable continuum model.⁵⁸ Gold was modelled with the Stuttgart-Dresden basis set and effective core potential,⁵⁹ bromine with LANL2TZ(f)⁶⁰ and all other non-metal atoms with Pople⁶¹ basis set 6-311+G(d,p). Single-point energy calculations were performed with the 6-311+G(d,p) basis set for non-metal atoms and SDD basis set and ECP for gold.

The stationary points were characterized by vibrational analysis. Transition states were identified by the presence of one imaginary frequency while minima by a full set of real frequencies. The connectivity of the transition states was confirmed by the relaxation of each transition state towards both previous and next intermediates. All the energies are potential energies (E) and free energies (G) in solution at 298.15 K and 1 atm in Kcal·mol⁻¹. A data set collection of computational results is available in the ioChem-BD⁵⁴ repository and can be accessed via <https://doi.org/10.19061/iochem-bd-1-307>.

Computed structures and energies

Table 3.12. Bromoenyne alkoxy cyclizations and eliminations. B3LYP-D3/6-31G(d)+SDD(Au), PCM (CH₂Cl₂); HLT: B3LYP-D3/6-311+G(d,p)+SDD(Au), PCM (CH₂Cl₂).

Code	E / Hartree	G / Hartree	E _{HLT} / Hartree
3.A1	-1113.13464	-1112.85505	-1113.33394
3.A3	-1113.16085	-1112.87697	-1113.35242
3.A3b	-1113.14297	-1112.86204	-1113.33814
3.A2	-1113.15203	-1112.87100	-1113.34666
3.A2b	-1113.15711	-1112.87231	-1113.35191
3.A4	-1228.89794	-1228.56056	-1229.13569
3.A4b	-1344.65133	-1344.26485	-1344.93511
3.A4c	-1460.39336	-1459.95976	-1460.72359
3.A4d	-1576.14378	-1575.65734	-1576.51668
3.A6	-1112.73494	-1112.46477	-1112.93629
3.A8	-1113.16513	-1112.88273	-1113.35902
3.A10	-1228.89361	-1228.55740	-1229.13103
Pre3.A7	-1344.61378	-1344.23986	-1344.90405
3.A7	-1112.73530	-1112.46582	-1112.93477
3.A9	-1112.74134	-1112.47004	-1112.94073
3.A5	-1228.48931	-1228.16490	-1228.72711
3.A14	-1344.63822	-1344.25738	-1344.93044
3.A15	-1113.19126	-1112.90672	-1113.38766

TS3.A2	-1113.12555	-1112.84759	-1113.32251
TS3.A2b	-1113.14676	-1112.86582	-1113.34196
TS3.A6	-1344.61714	-1344.24224	-1344.90804
TSb3.A6	-1344.61393	-1344.24070	-1344.90529
TS3.A32b-8	-1113.12629	-1112.84641	-1113.32258
TS3.A10	-1228.89154	-1228.55600	-1229.13003
TS3.A7-8	-1344.60842	-1344.23315	-1344.89776
TS3.A9	-1344.62047	-1344.24575	-1344.91058
TS3.A3	-1113.11694	-1112.83725	-1113.31510
TS3.A3b	-1113.11387	-1112.83520	-1113.31128
TS3.A15	-1344.63477	-1344.26039	-1344.92535
TSpre3.A7	-1344.61275	-1344.23918	-1344.90365
TS3.A7	-1344.61311	-1344.23834	-1344.90298
3.A2b-D	-1113.15711	-1112.87585	-1113.35191
3.A8-D	-1113.16513	-1112.88630	-1113.35902
TS3.A2b-8-D	-1113.12629	-1112.84871	-1113.32258
pre3.A7ipr	-1501.90603	-1501.42256	-1502.23841
3.A4ipr	-1307.54328	-1307.15276	-1307.80304
TS3.A7ipr	-1501.90518	-1501.42174	-1502.23782
TSpre3.A7ipr	-1501.90382	-1501.42212	-1502.23722
TS3.A6bipr	-1501.90414	-1501.42030	-1502.23777
TS3.A6ipr	-1501.90939	-1501.42551	-1502.24222
TS3.A7-8ipr	-1501.89894	-1501.41483	-1502.23054

Table 3.13. Protonated bromoenyne intermediates and Brønsted acid-mediated transition states. B3LYP-D3/6-31G(d) + SDD(Au), PCM (CH₂Cl₂); HLT: B3LYP-D3/6-311+G(d,p) + SDD(Au), PCM (CH₂Cl₂).

Code	E / Hartree	G / Hartree	E_{HLT} / Hartree
3.A16	-516.31696	-516.14242	-516.45851
3.A17	-516.72082	-516.53590	-516.85712
3.A11	-516.72827	-516.54188	-516.86144
3.A18	-516.37653	-516.19633	-516.51479
3.A19	-516.79350	-516.60236	-516.92398
3.A20	-516.73515	-516.54532	-516.86982
3.A18b	-516.37763	-516.19733	-516.51546
3.A19b	-516.79434	-516.60182	-516.92502
3.A12	-516.78248	-516.59236	-516.91401
TS3.A12	-516.72587	-516.53840	-516.85840
TS3.A13	-1033.10169	-1032.71809	-1033.37085
TSb3.A13	-748.25503	-747.96901	-748.48143

Table 3.14. Phenylenyne alkoxy cyclizations and eliminations. B3LYP-D3/6-31G(d) + SDD(Au), PCM (CH₂Cl₂); HLT: B3LYP-D3/6-311+G(d,p) + SDD(Au), PCM (CH₂Cl₂).

Code	E / Hartree	G / Hartree	E _{HLT} / Hartree
3.B1	-1331.64504	-1331.27826	-1331.90458
3.B3	-1331.64125	-1331.27105	-1331.89583
3.B2	-1331.65775	-1331.28456	-1331.90880
3.B2b	-1331.63523	-1331.26629	-1331.89011
3.B8	-1331.67977	-1331.30850	-1331.93166
3.B4	-1447.37601	-1446.95076	-1447.67393
3.B4b	-1563.13038	-1562.65696	-1563.47366
3.B6_cisoid	-1331.21994	-1330.86035	-1331.48095
3.B6_transoid	-1331.22127	-1330.86192	-1331.48298
3.B7	-1331.22638	-1330.86796	-1331.48606
3.B5	-1446.96615	-1446.55378	-1447.26415
3.TSB3	-1331.62799	-1331.26163	-1331.88449
3.TSB2	-1331.63013	-1331.26334	-1331.88611
3.TSB2b	-1331.62457	-1331.25726	-1331.88005
3.TSB2b-8	-1331.62122	-1331.25306	-1331.87751
3.TSB6_cisoid	-1563.10236	-1562.63992	-1563.45354
3.TSB6_transoid	-1563.10346	-1562.64033	-1563.45480
3.TSbB6	-1562.63848	-1562.63848	-1563.44953
3.TSB7-8	-1562.64878	-1562.64878	-1563.46140
3.TSB7	-1562.63887	-1562.63887	-1563.45150

Table 3.15. Methanol and isopropanol clusters, neutral and protonated. B3LYP-D3/6-31G(d) + SDD(Au), PCM (CH₂Cl₂); HLT: B3LYP-D3/6-311+G(d,p) + SDD(Au), PCM (CH₂Cl₂). Methanol clusters named as (p)mNX, where p = protonated, N = number of methanol units, X is a specific conformation or bonding arrangement.

Code	E / Hartree	G / Hartree	E _{HLT} / Hartree
iPrOH	-194.36003	-194.27882	-194.43549
H(iPrOH) ₂	-389.15998	-388.96869	-389.29922
m1	-115.71753	-115.68892	-115.77095
m2a	-231.44894	-231.37568	-231.55089
m3Aa	-347.18581	-347.06447	-347.33398
m3Ab	-347.18621	-347.06409	-347.33379
m3Ba	-347.19120	-347.06844	-347.33560
m4Aa	-462.91964	-462.75266	-463.11603
m4Ab	-462.91704	-462.75296	-463.11435
m4Ac	-462.92175	-462.75309	-463.11616

m4Ad	-462.92134	-462.75161	-463.11660
m4Ae	-462.91962	-462.75287	-463.11618
m4Ba	-462.92093	-462.74893	-463.11537
m4Ca	-462.93417	-462.76548	-463.12630
m4Cb	-462.93455	-462.76452	-463.12622
m4Cc	-462.93485	-462.76428	-463.12651
m6	-694.40525	-694.14719	-694.69483
pm1	-116.11177	-116.07015	-116.16045
pm2a	-231.86924	-231.78377	-231.96507
pm2b	-231.86908	-231.78287	-231.96504
pm3Aa	-347.61601	-347.48003	-347.75928
pm3Ab	-347.61657	-347.48011	-347.75989
pm3Ba1	-347.61374	-347.48034	-347.75549
pm3Ba2	-347.61320	-347.47791	-347.75495
pm4Aa1	-463.35503	-463.17494	-463.54641
pm4Aa2	-463.34621	-463.16431	-463.53760
pm4Ab1	-463.35576	-463.17747	-463.54614
pm4Ab2	-463.35748	-463.17519	-463.54711
pm4Ac1	-463.35554	-463.17566	-463.54653
pm4Ac2	-463.34644	-463.16171	-463.53742
pm4Ad1	-463.35676	-463.17462	-463.54672
pm4Ad2	-463.32905	-463.14892	-463.52242
pm4Ae1	-463.35834	-463.17867	-463.54821
pm4Ba	-463.34349	-463.16137	-463.53559
pm4Ca	-463.36402	-463.17992	-463.55165
pm4Cb1	-463.36299	-463.17870	-463.55030
pm4Cb2	-463.36399	-463.18046	-463.55162
pm4Cc	-463.36431	-463.18178	-463.55191
pm6	-694.84076	-694.56696	-695.12572

UNIVERSITAT ROVIRA I VIRGILI

GOLD(I)-CATALYZED ASYMMETRIC CYCLIZATIONS AND CYCLOADDITIONS OF HETEROATOM-SUBSTITUTED ALKYNES WITH ALKENES

Andrea Cataffo

General Conclusions

UNIVERSITAT ROVIRA I VIRGILI

GOLD(I)-CATALYZED ASYMMETRIC CYCLIZATIONS AND CYCLOADDITIONS OF HETEROATOM-SUBSTITUTED ALKYNES WITH ALKENES

Andrea Cataffo

General Conclusions

This Doctoral Thesis discusses the study of new asymmetric reactions catalyzed by gold(I) involving heteroatom-substituted alkynes. In particular, both cyclizations and cycloadditions with alkene partners were explored to yield four-, five-, and six-membered rings. In every case, the heteroatom functionality allowed for useful product derivatization, otherwise inaccessible starting from unsubstituted substrates.

N-Substituted alkynes: We have developed the first chiral-auxiliary-based gold(I)-catalyzed cyclization of enynes with ynamides bearing chiral *N*-groups. Two classes of diastereoselective cyclizations were developed to form enantioenriched six-membered ring ketones: 1,5-enynamide cascade cyclizations to afford spirocyclic ketones and 1,6-enynamide alkoxy cyclization for the synthesis of enantioenriched β -tetralones.

O-Substituted alkynes: We have demonstrated that ynol ethers react in intermolecular gold(I)-catalyzed [2+2] cycloaddition with alkenes to afford oxygen-substituted four-membered rings (phenoxy cyclobutenes). Acidic hydrolysis or α -halogenation of the cyclobutenes gave access to valuable cyclobutanone scaffolds. This reaction corresponds to a formal [2+2] cycloaddition of a ketene equivalent to an alkene.

Br-Substituted alkynes: We have developed the enantioselective gold(I)-catalyzed alkoxy cyclization of 1-bromo-1,6-enynes to yield enantioenriched 5-membered-ring-vinyl bromides. In addition, by both experimental and computational means, we have discovered that a reversible 1,2-H shift takes place after the enantio-determining cyclization step leading to partial racemization of products of formal cycloisomerization. These results led us to draw a wider general picture of gold(I)-catalyzed alkoxy cyclizations.

UNIVERSITAT ROVIRA I VIRGILI

GOLD(I)-CATALYZED ASYMMETRIC CYCLIZATIONS AND CYCLOADDITIONS OF HETEROATOM-SUBSTITUTED ALKYNES WITH ALKENES

Andrea Cataffo

UNIVERSITAT ROVIRA I VIRGILI

GOLD(I)-CATALYZED ASYMMETRIC CYCLIZATIONS AND CYCLOADDITIONS OF HETEROATOM-SUBSTITUTED ALKYNES WITH ALKENES

Andrea Cataffo

UNIVERSITAT ROVIRA I VIRGILI

GOLD(I)-CATALYZED ASYMMETRIC CYCLIZATIONS AND CYCLOADDITIONS OF HETEROATOM-SUBSTITUTED ALKYNES WITH ALKENES

Andrea Cataffo